Optimization of enantioselective halocyclizations via BAM catalysis, and investigation of aryl triflamides as achiral modifiers in organocatalysis

By

Jenna L. Payne

Dissertation

Submitted to the Faculty of the

Graduate School of Vanderbilt University

in partial fulfillment of the requirements

for the degree of

DOCTOR OF PHILOSOPHY

in

CHEMISTRY

August 31, 2021

Nashville, Tennessee

Approved:

Jeffrey N. Johnston, Ph.D.

Carmelo J. Rizzo, Ph.D.

Steven D. Townsend, Ph.D.

Sean B. Seymore, Ph.D.

Table of Contents

Table of Figures

Table of Tables

Acknowledgements

I am indebted to a massive community for the support and education I have received during my time at Vanderbilt. While I am incredibly proud of this accomplishment, it would be foolish to think of it as an individual accomplishment. When I arrived at Vanderbilt, I didn't fully understand how much I would grow as both a scientist and as a person. This growth is a direct result of the time and dedication given to me by my mentors and peers.

I would like to first thank Dr. Johnston for the opportunity to work in his lab. Dr Johnston has been a phenomenal mentor, always taking the time to ensure that I had both the knowledge and resources to work effectively. What initially impressed me by this lab was the clear attention to education and mentorship, while also never shaming a student for making mistake. Dr Johnston developed a lab environment that was both rigorous and team-oriented, which is a testament to his leadership.

I am indebted to some wonderful professors from my time and the University of Detroit Mercy. Being a first-generation college student, I was not familiar with graduate school as an opportunity for STEM students. Dr. Benvenuto, Dr. Mio, and Dr. Evans all took the time to cultivate my interest in chemistry. The countless hours I spent in their office hours gave me the tools I needed to go to graduate school and their continued support has been a true blessing.

I would also like to thank my committee Dr. Rizzo, Dr. Townsend, and Dr. Seymore for their commitment to my education and scientific development. Thank you for giving your time, for giving me feedback on my projects, and advising me.

One of the best parts about working in MRB IV is that there were excellent neighbors in both the Lindsley and Sulikowski labs. I would like to specifically thank Jason, Alex, Zach, and Quinn for sharing their chemistry expertise and being excellent teammates in the Merck Synthesis Challenge.

The postdoctoral fellows that have work in the Johnston lab have also served as excellent mentors. While I never had the opportunity to work with Dr. Roozbeh Yousefi, I was grateful to the organized notes he left behind. I would also like to thank Dr. Mahesh Vishe, whose attentive instruction helped me improve my laboratory skills and gain a broader understanding of synthetic chemistry. Mahesh was also a great teammate on the carbamation project. Dr. Rashanique Quarels was also instrumental in my understanding of chemistry. Additionally, Rashanique was a true friend – always available to help or to just listen.

Dr. Thomas Struble and Dr. Matthew Knowe were senior students when I joined the lab and were by my side helping me every day. They spent hours helping me with presentations, documents, laboratory skills, etc. Their time and dedication to mentorship was instrumental to my personal development, but also benefited the entire lab. They showed me what it means to be a team player in a lab environment, which is a mentality I hope to carry with me for the rest of my life.

The two other senior graduate students present when I joined the lab were Dr. Jade Bing and Dr. Michael Crocker. While Jade and I worked on different projects, her assistance with my documents and presentations was incredibly helpful. Jade always took an interest in the chemistry going on around her, asking thought provoking questions and making the people

around her feel heard. Michael Crocker became one of my closest friends in graduate school. Michael is incredibly detail oriented, with a broad knowledge of chemistry. After he left, I have had to work tirelessly to find an equally-willing snack buddy.

As I've work in the Johnston lab, we've had a number of new additions. Zihang Deng has proven to be a great partner in catalysis and I have learned so much from work with him. Paige Thorpe has shown true resilience in graduate school, working tirelessly on her project. Additionally, Paige has a sense of humor and wit that makes everyone around her laugh. This past year we had a great group of first years join the lab – Preston, Corri, Scott, Kyle, and Melanie. All of them are excellent chemists in their own right and I look forward to watching them grow.

The last group members I would like to thank are Jade Izaguirre, Jade Williams, and Abby Smith. We all joined the program at the same time and they proved to be great colleagues and friends. Jade W. is an incredibly passionate and creative chemist, and I have learned so much working with her. Jade I. was great colleague, friend, and teacher.

The amazing thing about working with Abby is that, while trying to grow as an individual, she also makes the people around her better. Her rigor and attention to detail is infectious. She is also incredibly team-oriented, always working to improve the lab around her for generations to come. She's rebuilt instruments, organized cabinets, written lab manuals, etc. She's not afraid to get her hands dirty if it will help the people around her. Thanks for challenging with me, teaching me about peptides, and being a great friend.

In addition to all of my peers at Vanderbilt, I would like to thank my friends and family. I have made a ton of friends in Nashville, far too many to list. I would like to specifically thank Megan for being my running buddy and true friend. Thank you to Martha for being my roommate in Detroit and FaceTime buddy from Chicago. We went through graduate school together, albeit remotely. John and Sydney have also proved to be great friends, opening their home to us often.

I would also like to thank my Paynegang for all their love and support. My parents cultivated my interest in STEM from a young age, buying microscopes from garage sales and sending me to math camp. Their dedication to my education laid the foundation for my future goals.

The last person I need to thank is my husband, Dominic. Your love and support have never wavered. I can't wait to go on more adventures with you.

Chapter 1 – Optimization of an enantioselective synthesis of cyclic carbamates via CO_2-capture

1.1 Introduction

Synthetic chemists have an ongoing need to prepare chiral molecules.[1] Whether the interest is based in large natural products or small molecules, there is an unremitting need to control the formation of chiral centers in organic compounds. Biological systems are chiral environments, therefore enantiomers of a given compound may have different activities *in vivo*.[2,3] Because of this increasing demand, the development of new, highly selective reactions is important. These new reactions enable chemists to access molecules with unique functionalities, which generates new applications.[4] There are many ways to approach this problem, organocatalysis being one of great interest.[5,6]

Organocatalysis is a critical area of enantioselective catalysis because it is more accessible than transition metal catalysis. Many organocatalysts are prepared from chiral molecules that are made naturally in the biological world, making them inexpensive and often available in large amounts. Cinchona alkaloids are a great example of this phenomenon, these are natural products that are often employed in chiral catalysis.[7] In addition, amino-acids have a wide application in organocatalysis.[8,9] Peptide catalysis is a growing field in part because these chiral ligands are easy to prepare, and the functional diversity of peptides provides chemists with a large structural field to explore. Organocatalysts are typically insensitive to water and oxygen, making them easy to use in a laboratory setting without expensive equipment. These practical aspects of organocatalysis are important because all of these variables converge to lower the barrier to entry. The need for single-enantiomer materials is ubiquitous, and straightforward approaches that rely on accessible catalysts are likely to have the greatest overall impact.

---

[1] Lovering, F.; Bikker, J.; Humblet, C. *J. Med. Chem.* **2009**, *52*, 6752.
[2] Mannschreck, A.; Kiesswetter, R.; von Angerer, E. *J. Chem. Educ.* **2007**, *84*, 2012.
[3] McMorris, T. C.; Staake, M. D.; Kelner, M. J. *J. Org. Chem.* **2004**, *69*, 619.
[4] Brown, D. G.; Boström, J. *J. Med. Chem.* **2016**, *59*, 4443.
[5] Alemán, J.; Cabrera, S. *Chem. Soc. Rev.* **2013**, *42*, 774.
[6] Han, B.; He, X.-H.; Liu, Y.-Q.; He, G.; Peng, C.; Li, J.-L. *Chem. Soc. Rev.* **2021**, *50*, 1522.
[7] Marcelli, T.; Hiemstra, H. *Synthesis* **2010**, *2010*, 1229.
[8] Jarvo, E. R.; Miller, S. J. *Tetrahedron* **2002**, *58*, 2481.
[9] Wennemers, H. *Chem. Commun.* **2011**, *47*, 12036.

Figure 1: Comparison of early organocatalytic reactions to modern approaches.

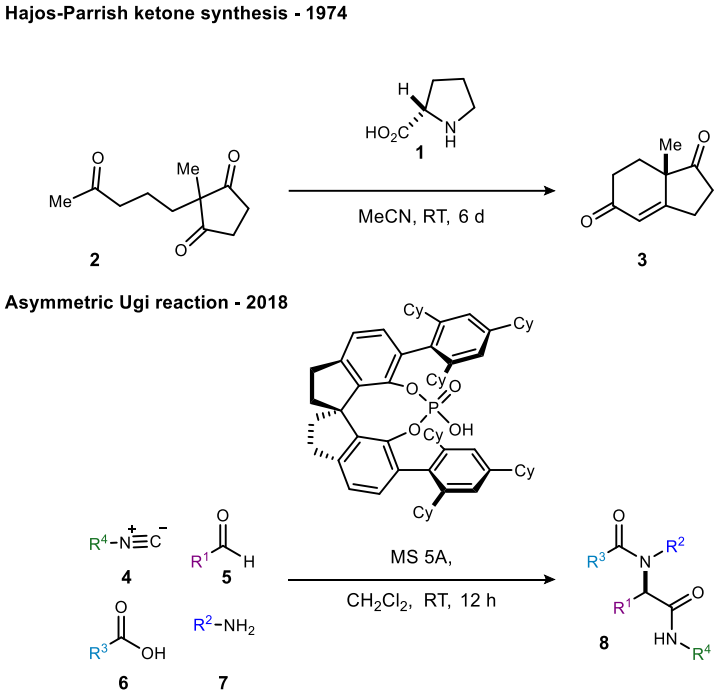

While the field of organocatalysis only grew in popularity in this century, it originated in the 1970's with proline catalysis. The value of proline in organocatalysis was first highlighted in aldol chemistry by scientists at Hoffman-La-Roche in what has become known as the Hajos-Parrish ketone synthesis.[10] Since then, organocatalytic scaffolds have grown beyond simple amino acids where hypothesis-driven ligand design is the predominant approach (Figure 1). As the complexity of these ligands grow, so does the complexity of the synthetic transformations. For example, in 2018 Tan published the first asymmetric Ugi reaction using a chiral phosphoric acid catalyst. The Ugi reaction is a four-component reaction that assembles peptide-like α-acylaminoamides in a one pot reaction using an amine, an acid, a carbonyl, and an isocyanide.[11] To successfully control the facial selectivity of four components illustrates the remarkable potential of organocatalysis. It is imaginable that one day these catalysts will truly rival the enzymes from which many of these reagents borrow features of substrate activation.

To reduce the field of organocatalysis to two examples is utterly insufficient. A myriad of scientists has worked in the field, leveraging a wide variety of organocatalysts. Some key

[10] Hajos, Z. G.; Parrish, D. R. *J. Org. Chem.* **1974**, *39*, 1615.
[11] Zhang, J.; Yu, P.; Li, S.-Y.; Sun, H.; Xiang, S.-H.; Wang, J.; Houk, K. N.; Tan, B. *Science* **2018**, *361*, eaas8707.

examples being cinchona alkaloids,[7] thiourea catalysts,[12] chiral guanidines,[13] imminium catalysis,[14] chiral phosphoric acids,[15] bisamidines,[16] and many more. What unites these approaches is their ability to use chiral ligands to activate organic molecules through hydrogen bonding. The steric influence of these chiral ligands restricts the flexibility of these molecules to ultimately stabilize a single, diastereomeric transition state.

1.1.1 Chiral proton catalysis

Bisamidine chiral ligands have emerged as key tools within a novel approach to Brønsted acid/base catalysis. These chiral ligands are both easy to prepare[17] and easy to modify because they are typically C_2-symmetric (see Figure 2). The first variable pursued during initial optimization efforts is the diamine backbone. Different diamines have different N-C-C-N dihedral angles, which controls the cavity size of the chiral ligand.[18] The bifunctionality is generated by protonating one of the quinoline rings, with the protonated quinoline serving as the Brønsted acid, or chiral proton donor. If one is careful to avoid over-protonating the chiral ligand, the unprotonated aminoquinoline is a Brønsted base and accessible as well. In previous studies over many years, the monoprotonated Brønsted acid salt of the BAM ligand is almost always a more selective catalyst. In development, the proton source is evaluated because it has been shown that the acidic counterion may have a significant effect on enantioselection.[19] The basicity of the ligand is modified by adding electron donating groups to the quinoline ring. The 4-position of the quinoline ring can be rapidly derivatized with a wide variety of heteroatom-based nucleophiles through a nucleophilic aromatic substitution reaction. Modifying the quinoline ring substitution enables one to modify the basicity of the chiral ligands. When developing an organocatalyst, the acidity of these chiral ligands must match with the substrate for optimal acid/base chemistry and hydrogen bonding.

---

[12] Serdyuk, O. V.; Heckel, C. M.; Tsogoeva, S. B. *Org. Biomol. Chem.* **2013**, *11*, 7051.
[13] Dong, S.; Feng, X.; Liu, X. *Chem. Soc. Rev.* **2018**, *47*, 8525.
[14] Erkkilä, A.; Majander, I.; Pihko, P. M. *Chem. Rev.* **2007**, *107*, 5416.
[15] Maji, R.; Mallojjala, S. C.; Wheeler, S. E. *Chem. Soc. Rev.* **2018**, *47*, 1142.
[16] Nugent, B. M.; Yoder, R. A.; Johnston, J. N. *J. Am. Chem. Soc.* **2004**, *126*, 3418.
[17] Davis, T. D., M.; Schwieter, K.; Chun, A.; Johnston, J. *Org. Synth.* **2012**, *89*, 380.
[18] Kim, H.; Yen, C.; Preston, P.; Chin, J. *Org. Lett.* **2006**, *8*, 5239.
[19] Dobish, M. C.; Johnston, J. N. *J. Am. Chem. Soc.* **2012**, *134*, 6068.

Figure 2: BisAmidine (BAM) catalyst structure.

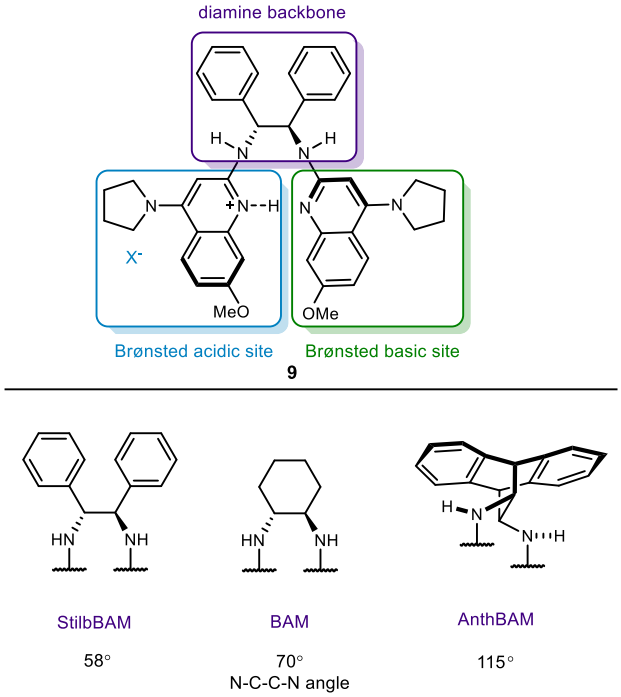

BAM catalysis has been applied to a wide variety of substrates, with the three main pillars of reactivity being the aza-Henry reaction, iodolactonizations, and asymmetric Michael additions to nitroalkenes. The first BAM catalyzed reaction was an aza-Henry reaction.[16] The stereoselective addition of nitroalkanes to imines is an essential carbon-carbon bond forming reaction that prepares two chiral β-amino nitroalkanes in high ee and dr. These chiral β-amino nitroalkanes can be reduced to chiral diamines, or they can be derivatized to amide products using Umpolung Amide Synthesis (UmAS).[20] The initial reaction was highly selective, but reactivity was poor. In order to achieve high conversion, the nitroalkane was used as solvent. As shown in Figure 3, Davis and coworkers developed a new BAM catalyst that was significantly more reactive, while maintaining high stereoselectivity.[21] This work illustrates the matched Brønsted acid/base relationship between the organocatalyst and the substrates. The Dudding group investigated the role of the BAM ligand in this aza-Henry chemistry computationally, illustrating how the charge-assisted hydrogen bond governed the relative orientation of substrate bonding.[22]

[20] Shen, B.; Makley, D. M.; Johnston, J. N. *Nature* **2010**, *465*, 1027.
[21] Davis, T. A.; Wilt, J. C.; Johnston, J. N. *J. Am. Chem. Soc.* **2010**, *132*, 2880.
[22] Belding, L.; Taimoory, S. M.; Dudding, T. *ACS Catalysis* **2015**, *5*, 343.

Figure 3: Evaluation of ligand basicity in the aza-Henry reaction.

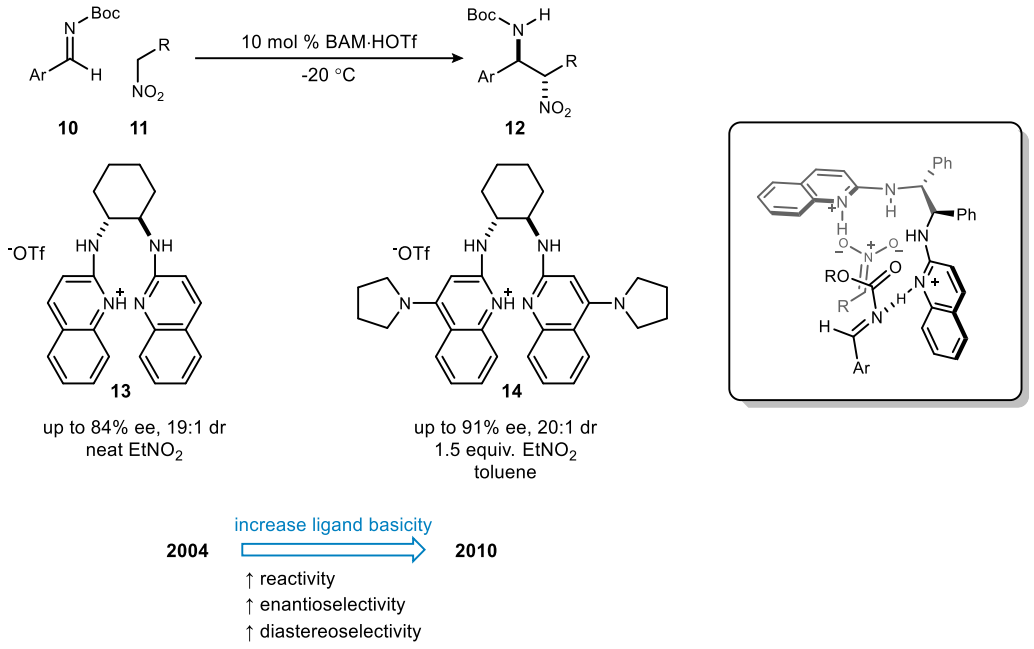

BAM catalysis proved to be a general approach to the aza-Henry reaction and was successfully applied to a wide variety of substrates including nitroacetic acid derivatives[23], α-nitrophosphonates[24], and secondary nitroalkanes[25]. The wide scope of the aza-Henry chemistry makes it broadly applicable. Additionally, a divergent approach to access to the syn- and anti-diastereomers of the aza-Henry products was developed (Figure 4).[26,27] This provides an efficient synthesis of α,β-diamino acid derivatives, where all stereoisomers may be prepared in high selectivity. It is an unusual example of diastereodivergence where by modifying the substitution of the BAM diamine, the syn-diastereomer is accessed over the previously favored anti-diastereomer. Computation studies are currently underway with the Dudding group to better understand this diastereodivergent phenomenon.

[23] Singh, A.; Yoder, R. A.; Shen, B.; Johnston, J. N. *J. Am. Chem. Soc.* **2007**, *129*, 3466.
[24] Wilt, J. C.; Pink, M.; Johnston, J. N. *Chem. Commun.* **2008**, 4177.
[25] Davis, T. A.; Danneman, M. W.; Johnston, J. N. *Chem. Commun.* **2012**, *48*, 5578.
[26] Singh, A.; Johnston, J. N. *J. Am. Chem. Soc.* **2008**, *130*, 5866.
[27] Sprague, D. J.; Singh, A.; Johnston, J. N. *Chem. Sci.* **2018**, *9*, 2336.

Figure 4: Diastereodivergent approach to aza-Henry additions via BAM catalysis.

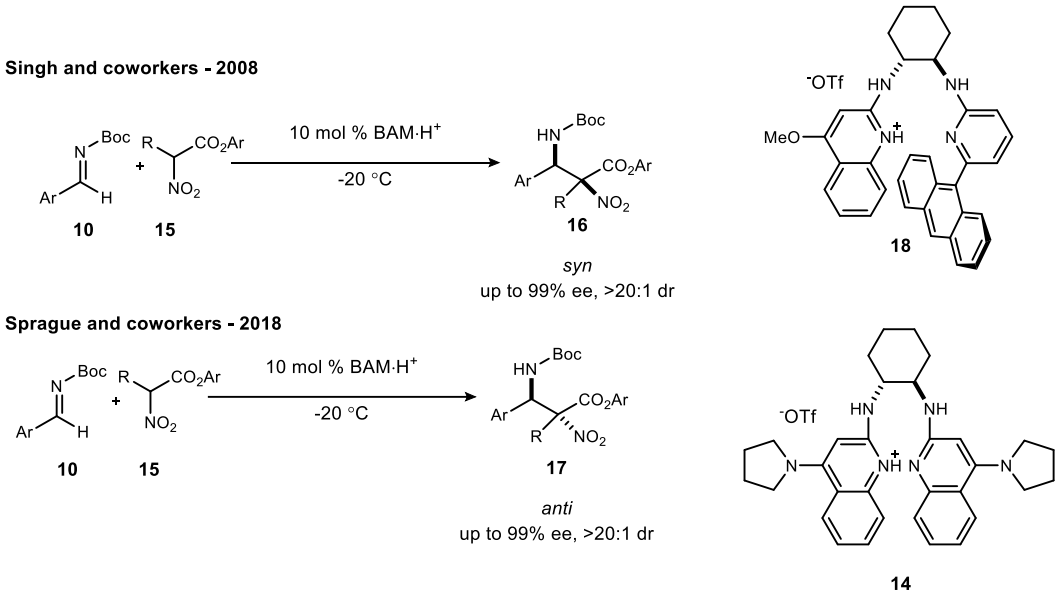

Another proven application of BAM catalysis is in halolactonization reactions.[19] When investigating this cyclization, it was noted that the halogen source needed to have a hydrogen bond acceptor such as a carbonyl. This enabled Brønsted acid activation of the iodine source, which served to activate the olefin. The observed high facial selectivity is a result of the hydrogen bond between NIS and the amidine ion, as illustrated in Figure 5.

In addition to preparing lactones in high ee, this iodocyclization demonstrated an interesting relationship between the proton source and BAM catalyst. The proton source generates the amidinium ion, but the nature of the resulting counterion was largely unexplored. It was unclear if the counterion was associated with the BAM ligand, or largely dissociated. To investigate this question, Dobish screened a number of acids that varied in both sterics and electronics (Figure 5). Enantioselection generally increased with the acidity of the proton source, which indicates that a more dissociated counterion is more effective. Notably, the fluorinated cyclic triflimide provided similar selectivity as the bistriflimide. Observing the effect of sterically robust counterions on reactivity and selectivity illustrates that these counterions do more than provide a resting state for the catalyst – they also play an active role in the reactive catalyst structure as it relates to the substrate.

BAM catalysis has been applied to a number of other halocyclizations to prepare various heterocycles, including the synthesis of chiral phosphoramidates,[28] ureas,[29] carbonates,[30] and bridged lactones.[31] The synthesis of phosphoramidates and bridged lactones both posed an interesting problem mechanistically, where high π-carbon facial selectivity and oxygen-atom differentiation would have to be well-controlled in order to develop a highly selective cyclization. Mechanistically, the halonium source must be trans to the oxygen nucleophile for cyclization to occur. To achieve π-carbon selectivity, the catalyst must control the orientation of the substrate, as this will dictate which face of the olefin is activated by the iodine source.

Figure 5: Evaluation of proton sources in enantioselective lactonization.

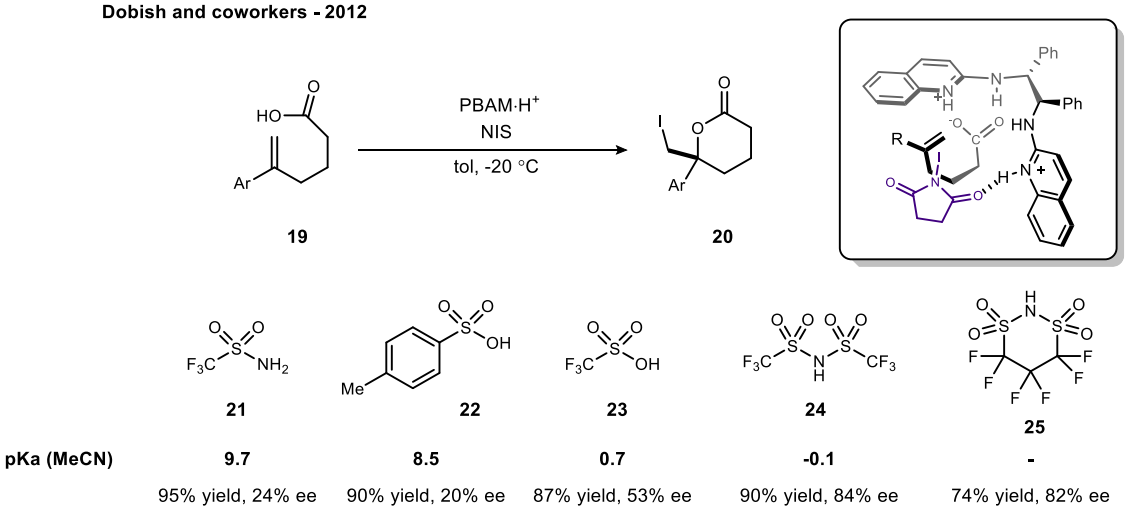

The cyclic structure imposes a conformational restriction such that the organocatalyst may only bind to the nucleophile or electrophile. This deviates from previous BAM catalyzed reactions, where bifunctional control was the proposed mode of activation. Even if the substrate orientation is well controlled, the oxygen atoms of the carboxylic acid must be differentiated for enantioselection. Knowe used an X-ray cocrystal structure of his acid and StilbPBAM catalyst to redesign his catalyst, as shown in Figure 6. After visualizing the co-crystal, he hypothesized that installing a large aryl amine substituent at carbon-4 of the quinoline ring, in lieu of pyrrolidine, would produce a steric influence. To strengthen this effect, carbon-6 of the quinoline ring was

[28] Toda, Y.; Pink, M.; Johnston, J. N. *J. Am. Chem. Soc.* **2014**, *136*, 14734.
[29] Struble, T. J.; Lankswert, H. M.; Pink, M.; Johnston, J. N. *ACS Catalysis* **2018**, *8*, 11926.
[30] Vara, B. A.; Struble, T. J.; Wang, W.; Dobish, M. C.; Johnston, J. N. *J. Am. Chem. Soc.* **2015**, *137*, 7302.
[31] Knowe, M. T.; Danneman, M. W.; Sun, S.; Pink, M.; Johnston, J. N. *J. Am. Chem. Soc.* **2018**, *140*, 1998.

functionalized with a *tert*-butyl group, to orient the aniline ring toward the substrate. This modification greatly improved enantioselectivity from 62% ee with StilbPBAM, to 94% ee.

Knowe's work is important for a number of reasons. This is the first cocrystal structure of a substrate bound to a BAM ligand, which is an impressive feat. In addition, he illustrated a new approach to desymmetrization reactions using BAM catalysis. This story highlights some excellent problem solving, while highlighting how steric modifications of BAM ligands can have a profound effect on selectivity. This work is reminiscent of Dobish's lactonization chemistry – both reactions illustrate a unique approach to catalyst optimization, where steric effects had a profound effect on selectivity.

Figure 6: Analysis of X-ray cocrystal structure of StilbPBAM and *meso*-acid, and its impact on ligand design.

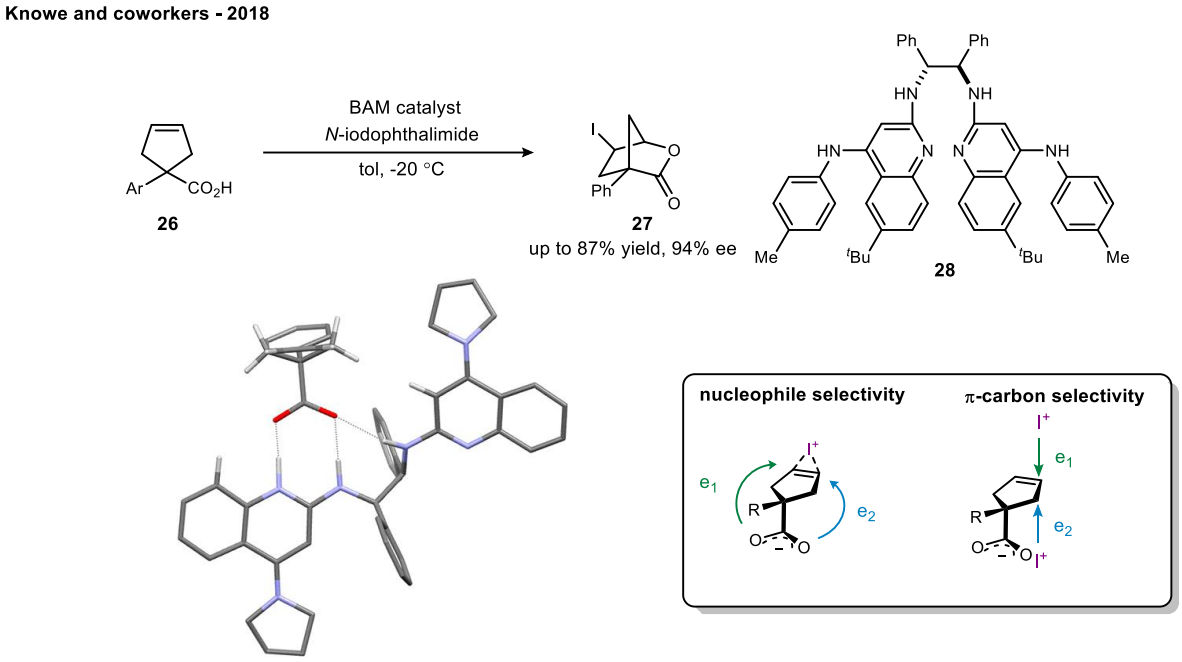

Recent catalysis work with BAM ligands focused on β-functionalization of nitroalkenes via Michael addition chemistry. As shown in Figure 7, Vishe and coworkers developed conditions to direct the addition of nitroalkanes to nitroalkenes in high dr and ee.[32] These products were derivatized using UmAS to prepare *anti*-β[2,3]-amino amides. Deng expanded this work to develop conditions to reduce nitroalkenes via β-hydride addition. To catalyze this reaction in high ee, Deng developed a new asymmetrical BAM ligand, as shown in Figure 8. In Deng's work, the

[32] Vishe, M.; Johnston, J. N. *Chem. Sci.* **2019**, *10*, 1138.

modification to the BAM ligand played a key role in selectivity. Deng's work is the first BAM catalyzed enantioselective reduction, and the conditions employ a novel, MAM ligand.

Figure 7: Enantioselective addition of nitroalkanes to nitroalkenes.

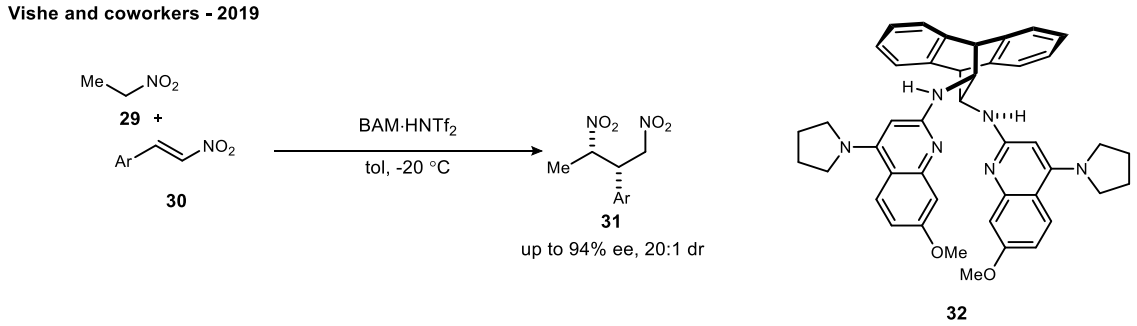

BAM ligands have been applied to three main areas of catalysis: 1) aza-Henry reactions, 2) halocyclizations, and 3) β-functionalization of nitroalkenes. A wide variety of chiral scaffolds were prepared for these reaction types, which speaks to the broad utility and applicability of these chiral ligands. Because the synthesis of BAM ligands is so straightforward, they could be employed in both academia and industry research settings. To highlight this broad application potential, Tsukanov collaborated with Eli Lilly to illustrate the successful application of BAM catalyzed aza-Henry reactions in flow.[33]

Figure 8: Enantioselective hydride addition to nitroalkenes.

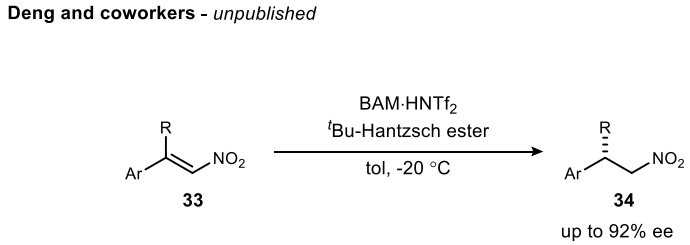

1.1.2 Organocatalytic asymmetric halocyclizations

Halocyclizations are an important transformation because lactones are a prevalent scaffold in both natural products and small-molecule therapeutics.[34] Additionally, lactonization may be used in the preparation of chiral carbon centers, with a halogenated handle for further structural

[33] Tsukanov, S. V.; Johnson, M. D.; May, S. A.; Kolis, S. P.; Yates, M. H.; Johnston, J. N. *Org. Process Res. Dev.* **2018**, *22*, 971.
[34] Kristianslund, R.; Tungen, J. E.; Hansen, T. V. *Org. Biomol. Chem.* **2019**, *17*, 3079.

modifications. The concerted intramolecular ring-opening/ring-closing reaction is anti-stereospecific, and thus forms two new carbon-heteroatom bonds. Asymmetric variants are of

Figure 9: Evaluation of chiral auxiliaries in the preparation of chiral lactones.

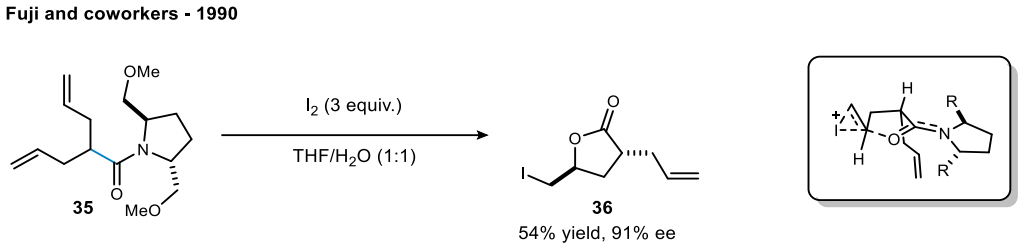

interest to increase the utility of these scaffolds. Initial efforts to access enantioenriched lactonization products utilized chiral auxiliaries, an early example being Fuji's work shown in Figure 9.[35] Notably, a C_2-symmetric auxiliary was optimal for selection, which provides the rationale for the mode of induction. The two R-groups restrict the rotation of the C-C bond highlighted in blue. The carbon chain interacts with the pyrrolidine substituents, leading to a favored diastereomeric conformation.

While auxiliaries can serve as powerful agents in stereoselective synthesis, they are not ideal. Auxiliaries must be both installed and removed from a substrate of interest. While Fuji's work is an interesting example where the auxiliary is removed in the cyclization conditions, this is not typically the case. Reagent-controlled conditions are ideal because they reduce the number of synthetic transformations. A catalytic reagent is even better, improving atom economy and reducing chemical waste. However, controlling the stereochemistry at the newly formed sp^3 center using a catalyst would be quite difficult for a number of reasons. The stereocontrolled cyclization must outcompete the noncatalyzed background reactions, which is expected to be difficult considering there are plenty of non-catalyzed variants. In addition, the catalyst must coordinate and/or activate the halogenating agent without oxidizing to an inactive catalyst form. Most reported reactions cyclize onto a chiral halonium species. However, if that chiral halonium opens to the carbocation, facial selection is most likely dictated via nucleophile control.

[35] Kaoru, F.; Manabu, N.; Yoshimitsu, N.; Takeo, K. *Tetrahedron Lett.* **1990**, *31*, 3175.

There are three primary modes of activation in these catalyzed lactonizations: 1) acid-catalyzed, 2) base-catalyzed, or 3) bifunctional acid-base catalysis. General depictions of these modes of activations are shown in Figure 10. Lewis acid catalysts enhance the reactivity of an electrophilic species by decreasing their electron density. In Brønsted acid catalysis, a proton serves as this electron acceptor, typically via hydrogen bonding.[36] Lewis base catalysis is defined

Figure 10: Primary modes of activation in organocatalyzed lactonizations.

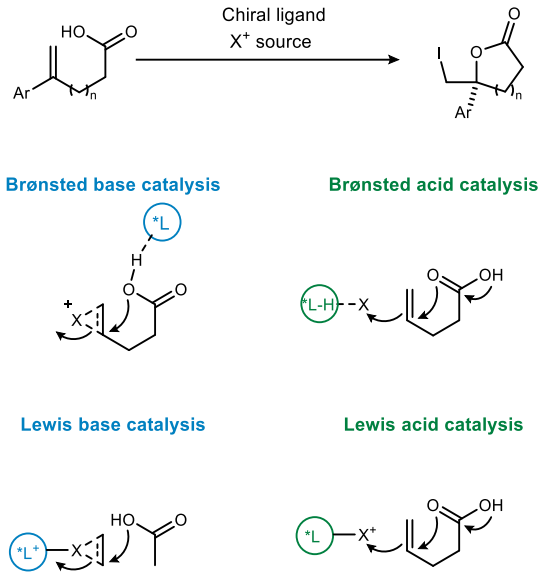

as a process by which an electron-pair donor (the catalyst) increases the rate of a given reaction by interacting with an acceptor atom (the substrate or reagent).[37] In Brønsted base catalysis, the same principle applies, but the acceptor atom is a hydrogen. Most Brønsted-base catalyzed reactions proceed via nucleophile control. In bifunctional catalysis, the orientations of both the nucleophile and electrophile are controlled by the active catalyst. In all cases, a combination of both steric and electronic effects dictates the orientation of the substrate and halogen source.

[36] Merad, J.; Lalli, C.; Bernadat, G.; Maury, J.; Masson, G. *Chem. Eur. J.* **2018**, *24*, 3925.
[37] Denmark, S. E.; Beutner, G. L. *Angew. Chem. Int. Ed.* **2008**, *47*, 1560.

Figure 11 shows a number of interesting chiral ligands that were successfully applied to enantioselective iodolactonization reactions of alkenoic acids. Prior to 2009, more of the reported lactonizations were not highly selective.[34] Goa and coworkers investigated salen complexes as

Figure 11: Evaluation of chiral ligands applies to iodolactonization reactions of unsaturated acids.

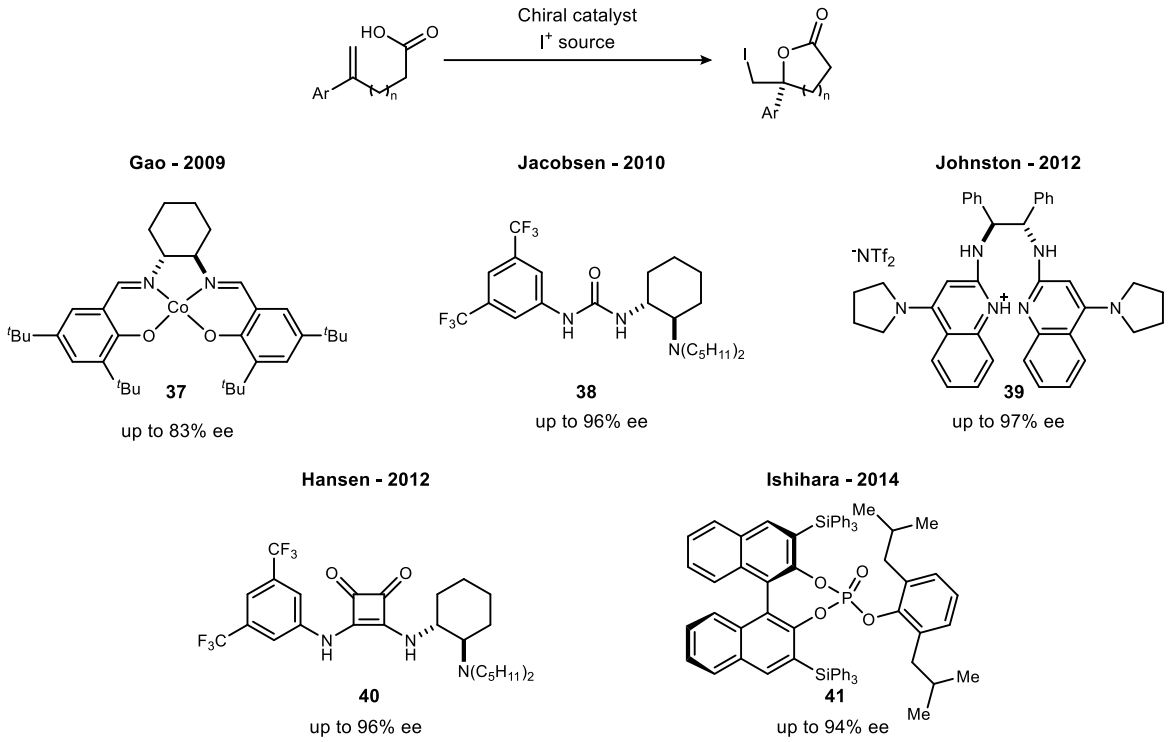

catalysts in this lactonization chemistry and found that cobalt-(II) was applied successfully, producing the 5-membered lactone in up to 83% ee.[38] This work was a significant contribution to the literature, but wasn't practical in application with limited substrate scope tolerance and high catalyst loadings (40 mol %). The Jacobsen group applied their bifunctional urea organocatalyst to this reaction, producing cyclic lactones in unprecedented yield and ee.[39] Their scope was impressive, tolerating a variety of substrates. Electron-rich olefins displayed reduced selectivity (48% ee), however, alkyl-substituted olefins were moderately tolerated (76% ee). This cyclization utilized a unique oxidant system, where I_2 was used as an additive in addition to the *N*-iodoimide oxidant. In their proposed mechanism, the tertiary-amine group of their ligand is

[38] Ning, Z.; Jin, R.; Ding, J.; Gao, L. *Synlett* **2009**, *2009*, 2291.
[39] Veitch, G. E.; Jacobsen, E. N. *Angew. Chem. Int. Ed.* **2010**, *49*, 7332.

oxidized to the halamine as an example of Lewis-base catalysis. The halamine serves as the active catalyst species, activating the olefin via halonium formation.

Figure 12: Analysis of *syn*-selective chlorolactonization.

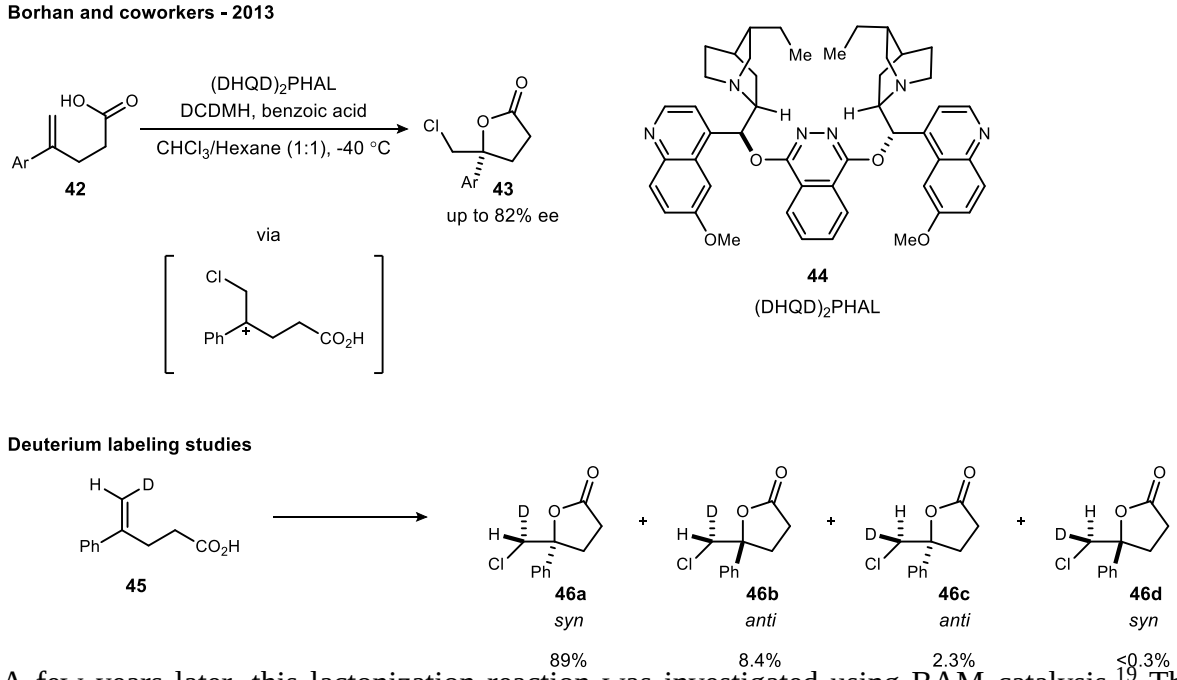

A few years later, this lactonization reaction was investigated using BAM catalysis.[19] These ligands were an improvement over thiourea catalysis, employing only 2 mol % of the BAM ligand as opposed to 15 mol %. In addition, *N*-iodosuccinimide is a sufficient oxidant, with no iodine needed. The Hansen lab also published work with their squaramide organocatalyst, though it should be noted that their ligand and conditions are quite similar to Jacobsen's work with diminished selectivity observed.[40] The work illustrates that both squaramides and ureas may serve to activate carboxylic acids via hydrogen bonding.

In 2014, Ishihara prepared 5-membered cyclic lactones using their chiral triaryl phosphate catalyst.[41] Their work is an interesting example of the chiral ligand acts as a nucleophilic promotor. The oxidant system oxidizes the ligand to the hypoiodite form. The hypoiodite serves as the chiral oxidant, whereby the cyclization turns over the catalyst and produces the lactone in up to 94% ee.

[40] Tungen, J. E.; Nolsøe, J. M. J.; Hansen, T. V. *Org. Lett.* **2012**, *14*, 5884.
[41] Nakatsuji, H.; Sawamura, Y.; Sakakura, A.; Ishihara, K. *Angew. Chem. Int. Ed.* **2014**, *53*, 6974.

In addition to these impressive iodolactonization examples, there has been a plethora of work done to expand the scope of these lactonizations. The Borhan group published a chlorolactonization that was *syn* selective, as opposed to the established *anti*-cyclizations.[42] Previous work indicated a halonium activation of the olefin, whereby the cyclization is *trans*-stereospecific. The mechanism of this cyclization reaction was probed via deuterium labeling studies, as shown in Figure 12. Using a mono-deuterated 1,1-disubstituted olefin, Borhan was able to study the stereochemical relationship between the quaternary carbon and deuterated center. The *syn* products were greatly favored over the *anti* (91.3:8.7). The formation of both diastereomers indicates that the reaction does not proceed via a single, stereospecific pathway, instead requiring an overall sequence capable of multiple stereochemical outcomes. A likely possibility is that the cyclization proceeds via a carbocation intermediate. This means the high enantioselectivity of the lactone must be a result of high selectivity in the ring-closing step, presumably as a result of hydrogen bonding to the catalyst.

Figure 13: Potential pitfalls of basic nucleophiles in organocatalyzed cyclizations.

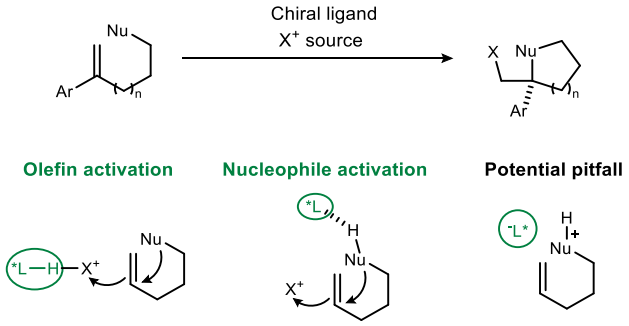

Enantioselective lactonizations have served as a foundational approach to the functionalization of unactivated olefins. Through their development, a variety of conditions and organocatalysts were developed to catalyze these lactonizations. Chemists have expanded the scope of lactonizations beyond iodine. In addition, the scope of these reactions was extended to include enynes and alkynes[43]. This work has enabled scientists to expand their work beyond lactone to prepare other cyclic products.[44] Expanding the scope of these cyclizations to include more basic nucleophiles is a notable challenge because most organocatalysts impart nucleophile control via

[42] Yousefi, R.; Ashtekar, K. D.; Whitehead, D. C.; Jackson, J. E.; Borhan, B. *J. Am. Chem. Soc.* **2013**, *135*, 14524.
[43] Wilking, M.; Mück-Lichtenfeld, C.; Daniliuc, C. G.; Hennecke, U. *J. Am. Chem. Soc.* **2013**, *135*, 8133.
[44] Tripathi, C. B.; Mukherjee, S. *Synlett* **2014**, *25*, 163.

hydrogen bonding. As these nucleophiles increase in basicity, they are more likely to deactivate the Lewis or Brønsted acid in lieu of coordination. (Figure 13)

Figure 14: Evaluation of chiral ligands employed in halocyclizations of basic nucleophiles.

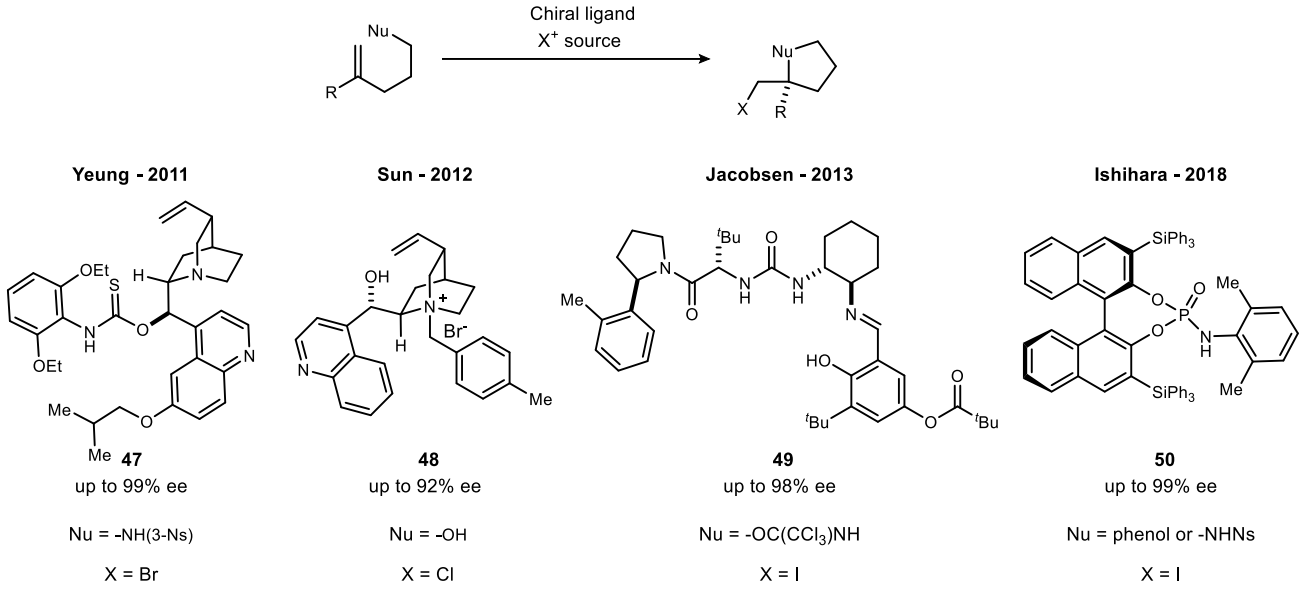

Enantioenriched heterocycles garner attention because they are essential units of many natural products and pharmaceuticals. Yeung and coworkers applied their amino-thiocarbamate catalyst to effect this enantioselective bromocyclization to prepare enantioenriched pyrrolidines.[45] To obtain product in high ee, they were limited to Nosyl-protected amines. Sun and coworkers applied a cinchonine catalyst to an enantioselective chlorocyclization reaction to prepare tetrahydrofurans.[46] Jacobsen and coworkers developed an iodocyclization to prepare trichloroacetimidates using their urea organocatalyst.[47] Similar to the Nosyl protecting groups Yeung's work, the trichloroacetimidate makes the nitrogen more acidic and therefore more amenable to hydrogen bond catalysis. These chiral trichloroacetimidates are interesting products because they may serve as precursors to chiral C-N bonds and chiral amino alcohols. Ishihara's chiral amidophosphate catalyst was applied to both phenol and unsaturated amide nucleophiles. Two similar chiral ligands were used to catalyze both cyclizations, which illustrates the impressive versatility of these chiral ligands.

[45] Zhou, L.; Chen, J.; Tan, C. K.; Yeung, Y.-Y. *J. Am. Chem. Soc.* **2011**, *133*, 9164.
[46] Zeng, X.; Miao, C.; Wang, S.; Xia, C.; Sun, W. *Chem. Commun.* **2013**, *49*, 2418.
[47] Brindle, C. S.; Yeung, C. S.; Jacobsen, E. N. *Chem. Sci.* **2013**, *4*, 2100.

Figure 15: Preparation of chiral ureas via BAM catalysis.

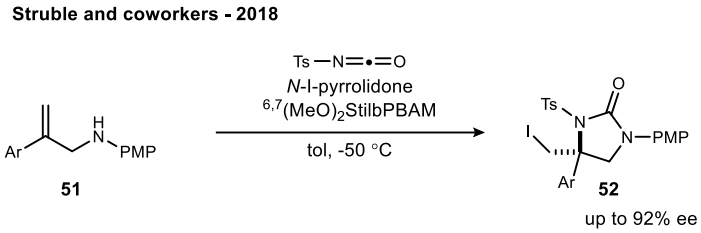

As illustrated in these previous examples, in order to use basic nucleophiles such as amine in hydrogen bond catalysis, an electron-withdrawing protecting group is used to reduce the basicity of the amine. An interesting approach utilized BAM catalysis to prepare enantioenriched heterocycles via multi-component cyclization reactions. The nucleophilic atoms are deactivated in the reaction conditions, in lieu of additional synthetic steps. For example, Vara and coworkers prepared cyclic carbonates from linear carbonic acids, which were generated *in situ* from homoallylic alcohols and carbon dioxide.[30] Struble expanded the Johnston lab's work in multicomponent reactions using allylic amine substrates and isocyanates (Figure 15).[29] This approach to heterocycle synthesis is interesting because it enables chemists to rapidly construct complex molecules from simple materials.

Figure 16: The first organocatalyzed polycyclization reaction.

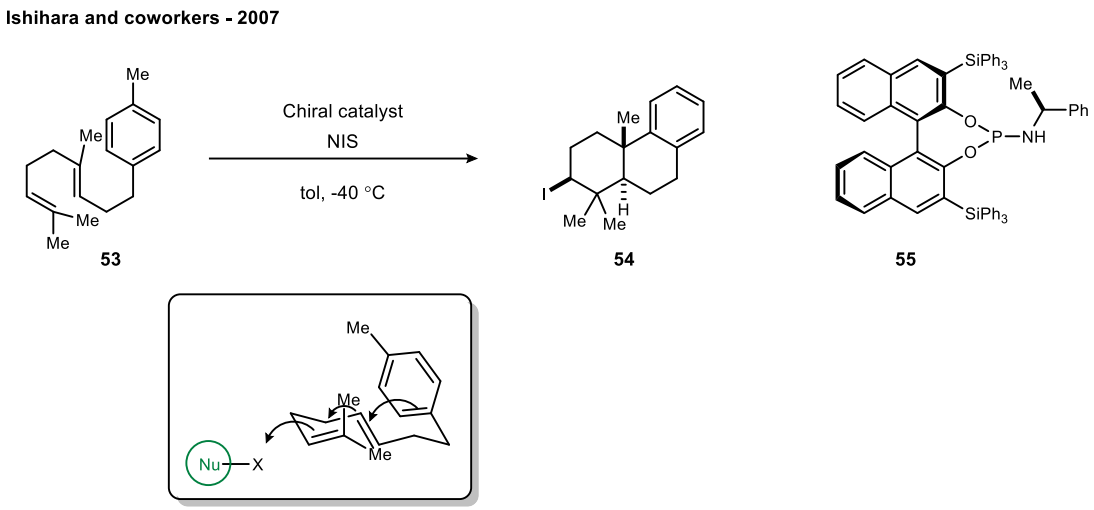

The Ishihara lab developed a nucleophilic phosphoramidite chiral reagent to catalyze an enantioselective polycyclization. (Figure 16)[48] This nucleophilic promotor is an interesting

[48] Sakakura, A.; Ukai, A.; Ishihara, K. *Nature* **2007**, *445*, 900.

deviation from chiral Lewis acid catalysis. Conventionally, a chiral Lewis acid activates the halogenating agent via hydrogen bonding, as shown in BAM catalysis. However, Ishihara used a nucleophilic promoter as the chiral ligand. Similar to the previous Ishihara example, the phosphoramide is oxidized to halamine by NIS and serves to activate the olefin directly. This increases the proximity of the chiral ligand and the substrate, which better facilitates the cyclization. Unlike the previous examples in this document, the nucleophile is not a heteroatom, rather an electron rich aryl ring. This polycyclization is an impressive accomplishment, being the first enantioselective organocatalyzed polycyclization, a reaction where an enantioselective variant had remained elusive for many years.

These examples capture a small portion of the halocyclization chemistry that is published in the literature. Many scientists have chosen to study these halocyclization reactions because these heterocycles are commonly used in a variety of synthetic applications. Additionally, preparing chiral quaternary carbon centers is an arduous task.[49] As the field of enantioselective catalysis grows, synthetic routes to complex molecules will become more efficient.

1.1.3 The application of carbon dioxide as a reagent in enantioselective synthesis

In chemical synthesis, the ideal of sustainability could be advanced by replacing unfavorable reagents like phosgene with CO_2 to achieve a similar goal. Carbon dioxide ($0.000066/mol) is an inexpensive and environmentally friendly C1 building block and an excellent alternative to triphosgene ($533/mol) and CDI ($233/mol). Phosgene and its surrogates are highly reactive electrophiles but present safety issues.[50] CO_2 addresses these practical issues, but its poor electrophilicity has limited its use, particularly in enantioselective synthesis. However, recently the field of CO_2 capture has grown as chemists developed a number of approaches to address these issues.

[49] Christoffers, J.; Baro, A. *Adv. Synth. Catal.* **2005**, *347*, 1473.
[50] Niemi, T.; Perea-Buceta, J. E.; Fernández, I.; Alakurtti, S.; Rantala, E.; Repo, T. *Chem. Eur. J.* **2014**, *20*, 8867.

Figure 17: Common methods employed in the activation of CO_2.

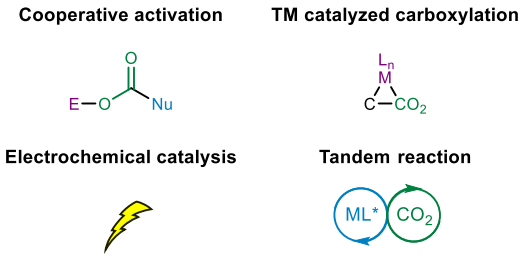

Scientists activate carbon dioxide through four main areas of reactivity: 1) cooperative activation, 2) transition-metal catalyzed carboxylation, 3) electrochemical catalysis, and 4) tandem reactions. (Figure 17)[51] In cooperative activation, a nucleophile engages with the carbon atom of CO_2, whereby the resulting carboxylate intermediate may engage an electrophile via nucleophilic attack. This carboxylate intermediate may be intercepted by a chiral ligand, which

Figure 18: Preparation of cyclic carbonates via CO_2 capture.

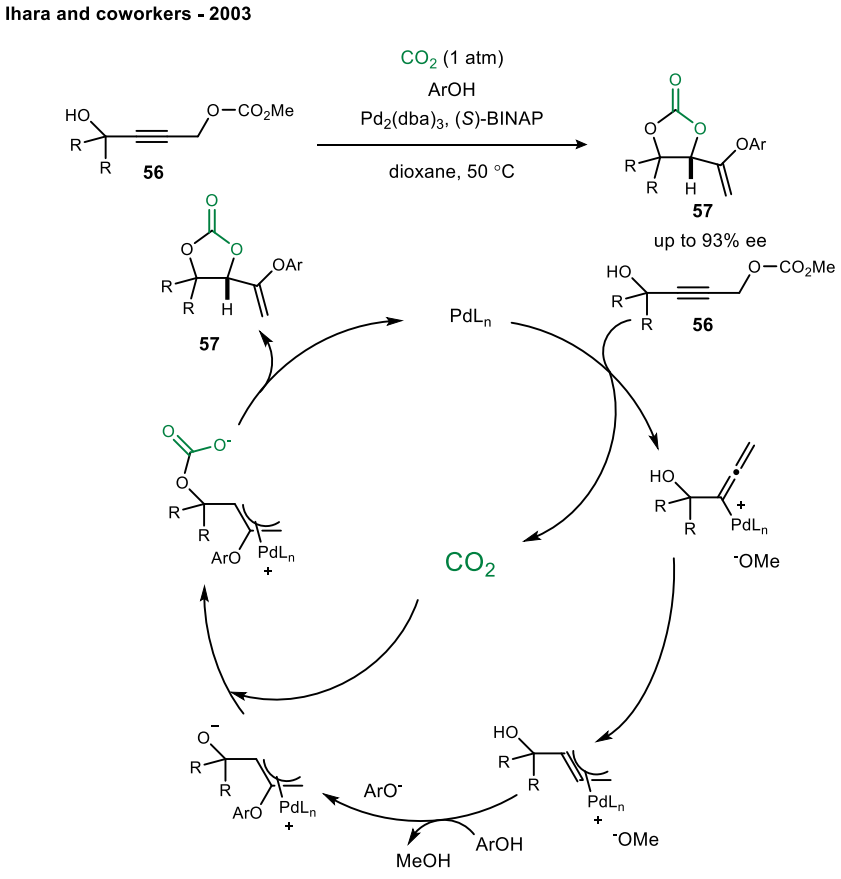

[51] Shi, Y.; Pan, B.-W.; Zhou, Y.; Zhou, J.; Liu, Y.-L.; Zhou, F. *Org. Biomol. Chem.* **2020**, *18*, 8597.

results in the formation a new C-O bond and chiral product. Cooperative activation will be the primary focus of this section, as it is most relevant to the experimental work featured in this chapter. Transition metal-catalyzed carboxylations engage both unsaturated compounds and CO_2 to prepare a new enantioselective C-C bond. Electrochemical catalysis utilizes similar reactivity approaches, but uses redox reagents to access less reactive compounds. Tandem reactions are a combination of CO_2 fixation with an advanced catalytic process. CO_2 reacts directly with already generated chiral intermediates, thus enabling the construction of chiral products with high stereoselectivity.

One of the first examples of CO_2 capture in enantioselective catalysis originates from the Ihara lab to prepare cyclic carbonates.[52] As shown in Figure 18, the CO_2 byproduct from a decarboxylation step is recycled in the cyclization sequence. The chiral π-allyl palladium intermediate dictates facial selectivity of the carbonate nucleophile. Mechanistic studies support this recycling mechanism because using a CO_2 atmosphere increased the overall yield of this reaction, though it was not necessary for reactivity. Notably, to obtain good enantioselectivity, molecular sieves were used as an additive. This work is significant because it illustrates the potential application of CO_2 as an oxygen- and carbon-atom donor. Prior work indicated that harsh conditions, utilizing elevated temperatures and strong bases, were required to activate CO_2.[50,53] However, Ihara and coworkers used a weakly basic nucleophile and atmospheric conditions, making this reaction an excellent proof of concept that CO_2 may be utilized under mild conditions.

Figure 19: Example of desymmetrization reaction to prepare cyclic carbonates.

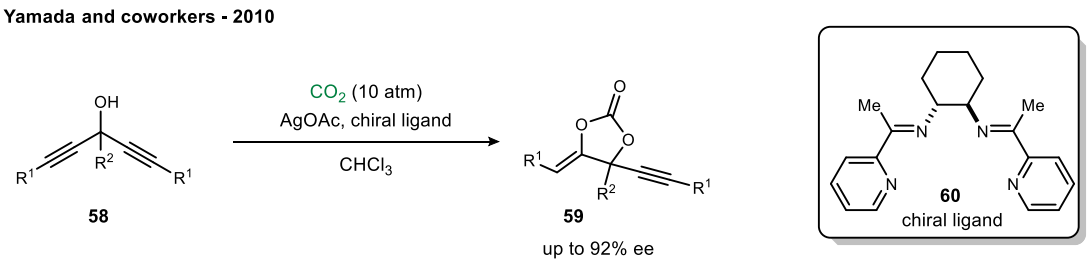

[52] Yoshida, M.; Fujita, M.; Ishii, T.; Ihara, M. *J. Am. Chem. Soc.* **2003**, *125*, 4874.
[53] Kielland, N.; Whiteoak, C. J.; Kleij, A. W. *Adv. Synth. Catal.* **2013**, *355*, 2115.

Yamada and coworkers published a desymmetrization reaction to prepare cyclic carbonates from propargyl alcohols, as shown in Figure 19.[54] A chiral Lewis acid catalyst was prepared from silver acetate and a Schiff-base ligand. As is common with CO_2 capture, elevated pressures were required for reactivity. A variety of alkyl groups were tolerated at the R^2 position, including a -CH_2F group. A variety of aryl substituents at the alkyne were tolerated as well, however, electron deficient arenes showed diminished enantioselectivity and required extended reaction times. The Zhou groups applied a similar approach to the kinetic resolution of oxindole-based racemic propargyl alcohols.[55] Like Yamada, silver acetate was used with a Shiff-base ligand. This reaction resolved the *(S)*-propargylic alcohol in up to 60% ee and produced the *(R)*-spirocarbonate in up to 43% ee.

Zhao and coworkers developed an impressive intermolecular domino reaction to prepare enantioenriched allylic carbamates (Figure 20).[56] Using iridium catalysis, they engaged weakly nucleophilic carbamic acid molecules, formed *in situ*, with an activated allyl π-complex. This creative approach activates electron-rich olefins, which would otherwise be weakly electrophilic, and thus unreactive. The substrate scope showed good yields and selectivity, however, a broad scope of substrates was not investigated. The starting halides used were all styrene derivatives except for one alkyl substrate, which produced the carbamate in only 41% yield and 38% ee. Additionally, electron-rich alkyl amines were necessary for reactivity; aniline rings did not show any reactivity. This is not surprising because aniline is significantly less basic than alkyl amines, which disfavors carbamic acid formation.

Figure 20: Multicomponent reaction to prepare enantioenriched allylic carbamates.

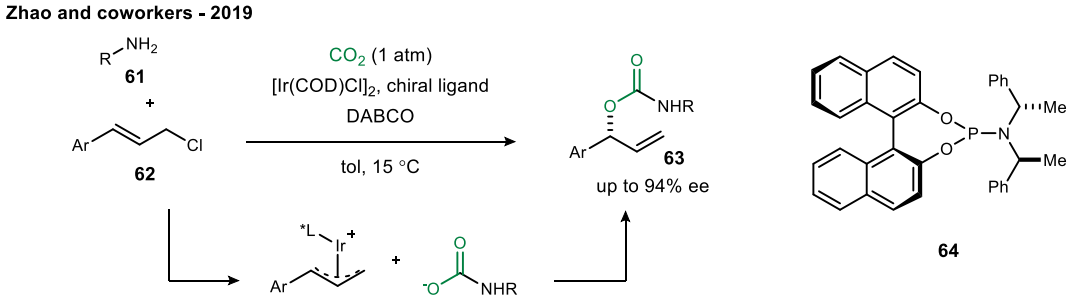

[54] Yoshida, S.; Fukui, K.; Kikuchi, S.; Yamada, T. *J. Am. Chem. Soc.* **2010**, *132*, 4072.
[55] Xie, S.; Gao, X.; Zhou, F.; Wu, H.; Zhou, J. *Chin. Chem. Lett.* **2020**, *31*, 324.
[56] Zhang, M.; Zhao, X.; Zheng, S. *Chem. Commun.* **2014**, *50*, 4455.

Figure 21: Activation of epoxides to prepare cyclic carbonates via CO_2 capture.

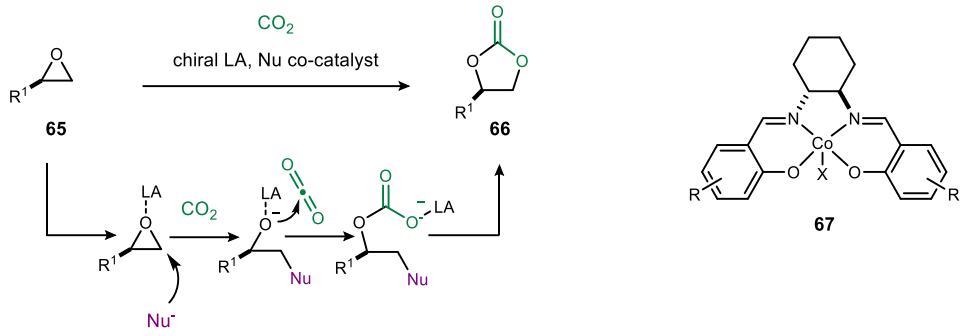

One of the most common approaches to cooperative activation of CO_2 is the activation of epoxides and aziridine rings to prepare cyclic carbonates and polycarbonates. (Figure 21) This transformation has been approached in a number of different ways, including the kinetic resolution of racemic epoxides[57] or desymmetrization of *meso*-epoxides[58]. A bifunctional catalyst is typically employed, with a Lewis acid component to activate the oxygen or nitrogen atom, along with a nucleophilic component to open the strained ring.[51] The most investigated system for this transformation is a chiral Schiff-base metal complex, with cobalt often the applied metal.[59] While the chiral cobalt catalyst is robust, scientists have focused their investigation on the nucleophilic co-catalyst, which affects both reactivity and selectivity.[55] These co-catalysts vary greatly in structure have been studied broadly.

There are relatively few examples of cooperative CO_2 activation using organocatalaysis. The Johnston lab has successfully demonstrated the use of homoallylic alcohols[30] and amines[60] in halocyclization chemistry, as detailed in other portions of this chapter. Additionally, there are a number of organocatalyzed reactions where cyclic carbonates are prepared from epoxides. Selectivity for these resolutions was modest (47-83% ee) in the organocatalyzed examples published to date.[58,61] Other than this work, the only other example of organocatalysis comes from the Shi lab in the form of a kinetic resolution.[62] A bifunctional phosphine ligand was used to resolved propargylic alcohols in high ee, with a reported selectivity factor (s) of 24.6. (Figure

[57] Tokunaga, M.; Larrow, J. F.; Kakiuchi, F.; Jacobsen, E. N. *Science* **1997**, *277*, 936.
[58] Ema, T.; Yokoyama, M.; Watanabe, S.; Sasaki, S.; Ota, H.; Takaishi, K. *Org. Lett.* **2017**, *19*, 4070.
[59] Lu, X.-B.; Liang, B.; Zhang, Y.-J.; Tian, Y.-Z.; Wang, Y.-M.; Bai, C.-X.; Wang, H.; Zhang, R. *J. Am. Chem. Soc.* **2004**, *126*, 3732.
[60] Yousefi, R.; Struble, T. J.; Payne, J. L.; Vishe, M.; Schley, N. D.; Johnston, J. N. *J. Am. Chem. Soc.* **2019**, *141*, 618.
[61] Takaishi, K.; Okuyama, T.; Kadosaki, S.; Uchiyama, M.; Ema, T. *Org. Lett.* **2019**, *21*, 1397.
[62] Sun, Y.-L.; Wei, Y.; Shi, M. *Organic Chemistry Frontiers* **2019**, *6*, 2420.

22) The scope was limited to ynones, which limits the applicability of this chemistry. This

Figure 22: Resolution of propargylic alcohols via CO_2 capture.

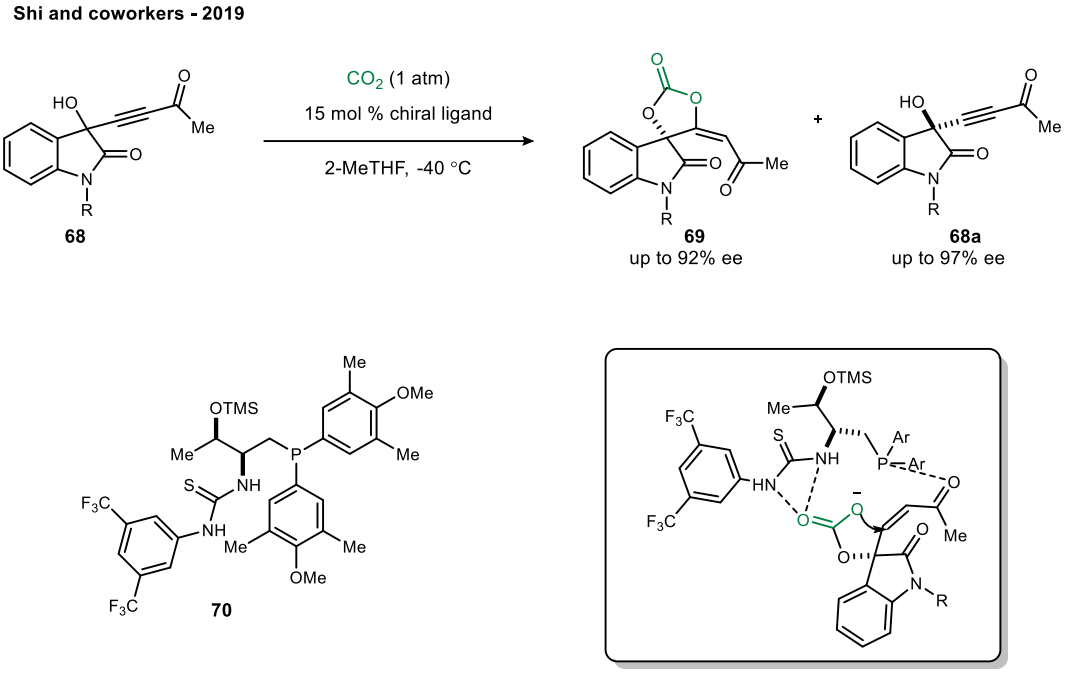

chemistry is a significant contribution to the literature because carbon dioxide was activated under relatively mild conditions – atmospheric pressure and low temperature. A similar resolution was published by Zhou in 2020 using a silver-(I) catalyst and BOX ligand system, though selectivity was modest.[55] The work of Johnston and Shi will serve as a template for future CO_2 activation chemistry, as they established that bifunctional organocatalysts may serve as an alternative to transition metals.

Transition metals may activate organic molecules through unique modes of activation, expanding synthetic chemists' ability to form new bonds. Because of this, transition metal catalysis has expanded the utility of carbon dioxide in synthesis greatly. Metal catalysis affected CO_2 fixation through two main reaction types: 1) oxidative cycloadditions and 2) hydrocarboxylations. Oxidative cycloadditions in this context are a reaction between an extensive π-system and carbon dioxide. An example of an oxidative cycloaddition is shown in Figure 23 in the first enantioselective nickel-catalyzed carboxylative cyclization reaction of bis-

1,3-dienes.[63] The conditions were somewhat mild, employing atmospheric CO_2 and reduced temperatures, however over 4 equivalents of dialkyl zinc was needed for complete conversion. In this reaction, zinc served as both an alkylating reagent and served to reduce the nickel (II) pre-catalyst to the active nickel-(0) species. This cyclization is impressive because three

Figure 23: Oxidative cyloaddition to prepare enantioenriched allylic esters.

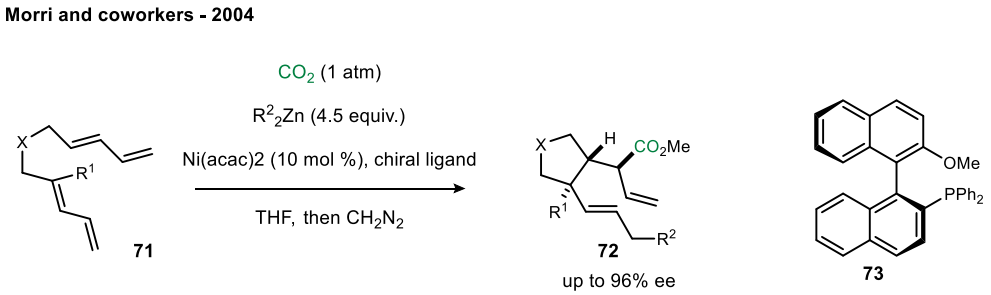

stereocenters were set in a single step in high ee (up to 96%). While the reported scope is rather small, this cyclization remains an impressive transformation to build up molecular complexity. This example is also significant because most reactions that engage CO_2 utilize a heteroatom nucleophile, while this reaction uses a carbon nucleophile to prepare an enantioenriched ester substrate.

Figure 24: Copper-catalyzed hydrocarboxylation via CO_2 capture.

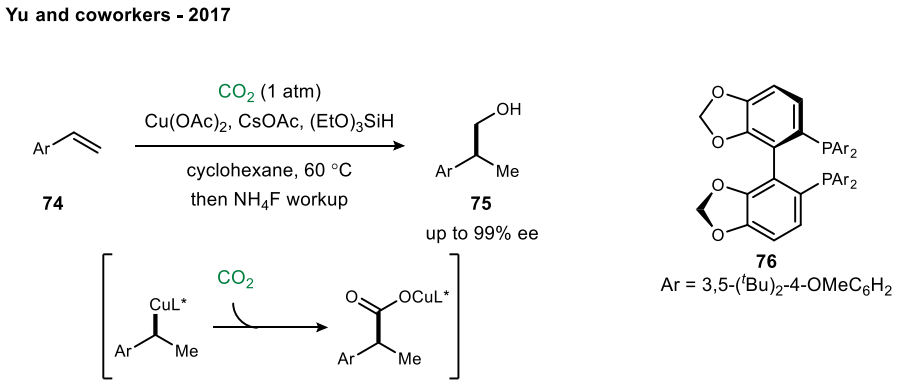

Figure 24 illustrates an example of hydrocarboxylation via CO_2 capture. The Yu lab developed a copper catalyzed Markovnikov functionalization of olefins using silane reducing agents. In addition to functionalizing styrene derivatives, the authors also successfully functionalized dienes. A large excess of silane (8 equiv.), presumably because silyl formate was obtained from

[63] Takimoto, M.; Nakamura, Y.; Kimura, K.; Mori, M. *J. Am. Chem. Soc.* **2004**, *126*, 5956.

$(EtO)_3SiH$ and CO_2 via copper catalysis. (Figure 24) The author's studies indicated that this silyl formate is not an active species in the catalytic cycle, making this byproduct a non-productive process that lowers the active hydride concentration. The olefin inserts into the Cu-H bond with high regioselectivity and enantioselectivity to form a carbon-copper bond. Carbon dioxide inserts into this bond to produce the copper alkoxide, which is ultimately reduced via σ-bond metathesis with hydrosilane. Copper plays a critical role mechanistically, engaging both the olefin and carbon dioxide via insertion. While this reaction is interesting mechanistically, these products are also synthetically useful. Primary alcohols are easily derivatized via oxidation and displacement type chemistry, making this chemistry a viable method to prepare chiral alkyl halides and carboxylic acids. A similar transformation was developed by the Ding group to functionalize allenes.[64]

Figure 25: Examples of asymmetric electrochemical carboxylation reactions.

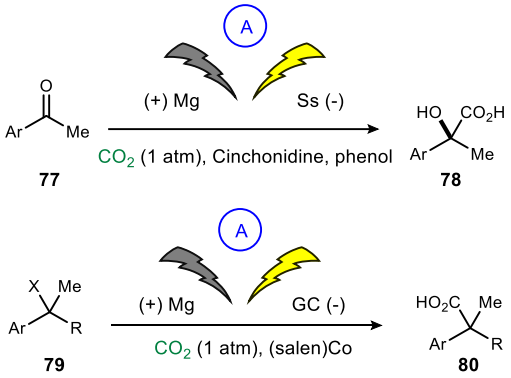

Electrochemistry has proved to be a powerful technique in CO_2 chemical fixation chemistry. While a number of impressive transformations have been published, the field is still relatively new. In these transformations, CO_2 reacts with chiral intermediates, but does not participate in the enantiodetermining step. Because CO_2 is not playing an active role in the enantiodetermining step, it was hypothesized that established electrochemistry procedures may be applied to produce products in high ee without too much optimization; the primary hurdle to overcome is associated with reactivity. Because this chapter primary focuses on engaging CO_2 in the enantiodetermining step, this work will not be discussed with as much depth as previous examples; these electrochemistry examples are also an example of tandem reactions. Cinchonidine has proved to

[64] Qiu, J.; Gao, S.; Li, C.; Zhang, L.; Wang, Z.; Wang, X.; Ding, K. *Chem. Eur. J.* **2019**, *25*, 13874.

be an effective chiral ligand asymmetric electrochemical carboxylations of ketones, as shown in Figure 25. The Lu group has published a number of asymmetric carboxylation conditions for ketones, though selectivity for these transformations has been moderate (up to 48% ee).[65,66] Enantioselective carboxylation of benzyl halides proved to be more selective with a (salen)Co-(II) complex for chiral induction.[67] The Mei group has worked to expand this work to the include asymmetric carboxylations of allyl esters.[68] Selectivity was modest, only up to 67% ee. The application of CO_2 chemical fixation in electrochemical synthesis only began recently and these approaches illustrate the untapped potential of this field.

Figure 26: Tandem CO_2 capture reaction to prepare enantioenriched cyclic carbamates.

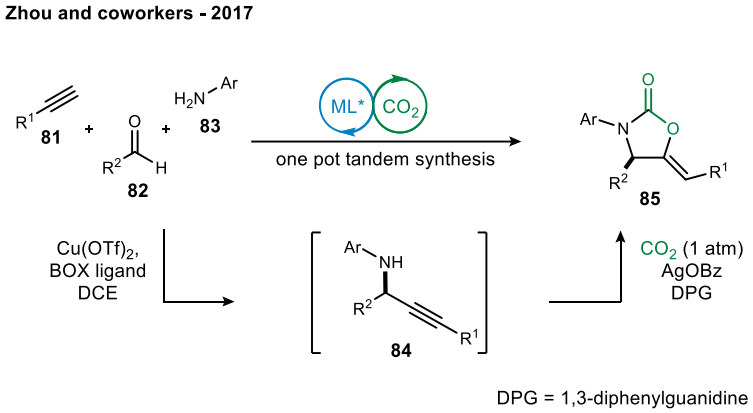

As illustrated in the examples of CO_2 fixation in electrochemistry, tandem reactions are another growing area in multi-component reaction development. In these reactions, carbon dioxide does not affect the enantiodetermining step, but it is incorporated into the final product. For this reason, tandem reactions will not be discussed broadly in this section. A strong example of a tandem reaction comes from Zhou and coworkers in their synthesis of enantioenriched cyclic carbamates. (Figure 26)[69] This cyclization is an impressive reaction where four simple molecules are brought together in one pot. The synthesis of the enantioenriched propargylamine intermediate is a copper catalyzed alkyne addition to an imine, followed by a silver catalyzed CO_2 capture and subsequent cyclization to give the carbamate. Because the amine is

[65] Zhao, S.-F.; Zhu, M.-X.; Zhang, K.; Wang, H.; Lu, J.-X. *Tetrahedron Lett.* **2011**, *52*, 2702.
[66] Chen, B.-L.; Tu, Z.-Y.; Zhu, H.-W.; Sun, W.-W.; Wang, H.; Lu, J.-X. *Electrochim. Acta* **2014**, *116*, 475.
[67] Chen, B.-L.; Zhu, H.-W.; Xiao, Y.; Sun, Q.-L.; Wang, H.; Lu, J.-X. *Electrochem. Commun.* **2014**, *42*, 55.
[68] Jiao, K.-J.; Li, Z.-M.; Xu, X.-T.; Zhang, L.-P.; Li, Y.-Q.; Zhang, K.; Mei, T.-S. *Organic Chemistry Frontiers* **2018**, *5*, 2244.
[69] Gao, X.-T.; Gan, C.-C.; Liu, S.-Y.; Zhou, F.; Wu, H.-H.; Zhou, J. *ACS Catalysis* **2017**, *7*, 8588.

enantioenriched, the cyclization produces chiral cyclic products. Chiral oxazolidinones are known ton be utilized greatly in synthetic chemistry, making the products of this reaction widely employable.

Utilizing carbon dioxide as an alternative to other C1 donors is an exciting area of exploration. It would be naïve to imply that these transformations would have a positive impact on global CO_2 levels, however, it seems obvious to use a resource that is so abundant, safe, and inexpensive. The study of CO_2 capture is focused on improving atom economy of synthetic transformations, much like catalysis. This opportunity has empowered chemists to be creative, utilizing carbon dioxide to prepare complex molecules.

1.1.4 The effect of water as an additive in organic reactions

The development of high-performing synthetic transformations is the pursuit of organic chemists. To achieve this goal, scientists investigate various parameters to optimize the reaction, such as catalyst optimization, temperature, solvents, etc. In addition to these well-developed parameters, additives may be employed to improve reactivity and stereoselectivity.[70,71] In general, the mechanistic role of an additive is to activate substrates, stabilize a high energy intermediate, or regenerate the active catalyst. There is a wide variety of additive effects reported in the literature, making it difficult to summarize the role of additives generally. Though additives can be ambiguous, it is important to study their effects because understanding their role in synthetic transformations provides key information regarding reaction development. By understanding the effect of an additive, one could imagine tailoring the reaction conditions accordingly, to ultimately design a more effective set of conditions that may or may not employ the studied additive.

[70] Hong, L.; Sun, W.; Yang, D.; Li, G.; Wang, R. *Chem. Rev.* **2016**, *116*, 4006.
[71] Ribe, S.; Wipf, P. *Chem. Commun.* **2001**, 299.

Water has served as an additive in a wide variety of synthetic transformations.[72,73] The application of water in organic chemistry is often counterintuitive because the compounds are often far too hydrophobic to dissolve in water. Indeed, it is for this reason that water is rarely used as a solvent. While water may not serve as an ideal solvent, its multifaceted chemical properties make it an ideal additive. Water may participate in hydrogen bonding, acting as a hydrolyzing agent, or promote Lewis acid activation.[71,74] Because there is a variety of potential modes of reactivity, it can be difficult to identify the mechanistic role of water as additive in synthetic transformations. Luckily, some chemists have risen to the challenge and have expanded

Figure 27: Role of water in CH_2-extrusion reaction.

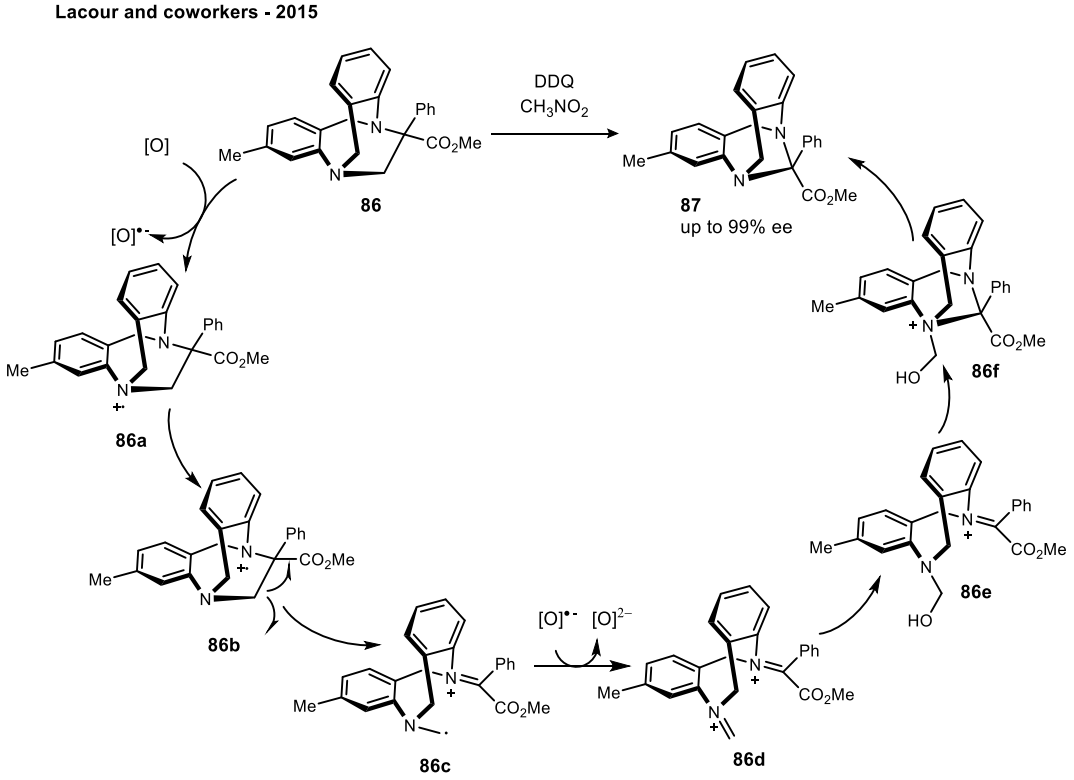

% mol H_2O	time (h)	yield (%)	ee (%)
0	24	81	98
1.3	8	85	98

[72] Hayashi, Y. *Angew. Chem. Int. Ed.* **2006**, *45*, 8103.
[73] Narayan, S.; Muldoon, J.; Finn, M. G.; Fokin, V. V.; Kolb, H. C.; Sharpless, K. B. *Angew. Chem. Int. Ed.* **2005**, *44*, 3275.
[74] Evans, D. A.; Willis, M. C.; Johnston, J. N. *Org. Lett.* **1999**, *1*, 865.

our understanding of this phenomenon.

The Lacour group reported a CH_2-extrusion reaction that displays an example of water having an additive effect by acting as a hydrolyzing agent.[75] While the reported extrusion reaction proceeded in high selectivity in a DDQ oxidation system, reaction times were long at 30 hours. However, with 1.3% water present in the nitromethane solvent, full conversion was realized at only 8 hours. After looking at the crude NMR of the accelerated reaction, the authors noted that significantly amount of formaldehyde was formed in the cyclization. This observation supports the mechanism shown below in Figure 27. The α-aminomethyl radical species was rapidly oxidized to the iminium. This is where water is critical because the iminium species is not nucleophilic, however the resulting hemiaminal may undergo cyclization. The final step is the subsequent elimination of the ammonium intermediate, producing formaldehyde and the final Tröger base derivative.

The Muñiz lab reported a cooperative light-activated iodine catalyzed amination reaction of $C_{sp}{}^3$-H bonds[76], reminiscent to the Hofmann-Löffler-Freytag reaction (Figure 28). They observed that trace amounts of water were required to initiate the reaction. They hypothesized that iodine was not a sufficient oxidant for the amine. However, iodine may react with water to form

Figure 28: 1,5-HAT amination reaction accelerated by hypoiodite formation.

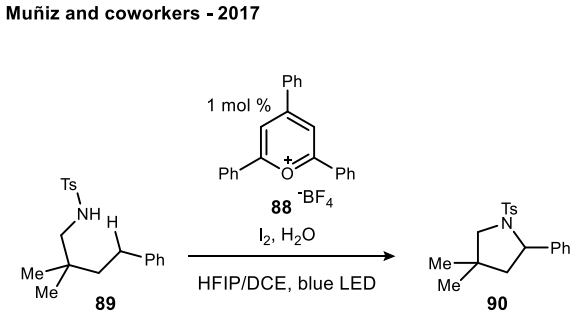

procedural modifications	yield (%)
O_2 free/anhydrous	trace
under air	20
HFIP/under air	80

[75] Pujari, S. A.; Besnard, C.; Bürgi, T.; Lacour, J. *Angew. Chem. Int. Ed.* **2015**, *54*, 7520.
[76] Becker, P.; Duhamel, T.; Stein, C. J.; Reiher, M.; Muñiz, K. *Angew. Chem. Int. Ed.* **2017**, *56*, 8004.

hypoiodite, a more reactive oxidant source.[77] The authors investigated this phenomenon using Raman spectroscopy, where they observed the formation of hypoiodite in the reaction. This indicated that there is an equilibrium between molecular iodine, iodide, and hypoiodite. Water is reacting with iodine to form a more reactive oxidant source. A similar additive effect was observed the Zhang group in an oxidative amidation of terminal alkenes.[78] In this chemistry, an electrophilic bromine source (1,3-dibromo-5,5-dimethylhydantoin) reacted with an olefin to prepare a halohydrin intermediate. Oxidation of the halohydrin and subsequent haloform displacement with ammonium produced the amide type product. The authors noted that the halohydrin intermediate was inaccessible in anhydrous conditions. Similar to Muñiz's work, they proposed that hypobromite is the active oxidant in this chemistry.

The Johnston lab studied the conversion of an electron deficient olefin to a β-amino oxazolidine dione using an electron-rich azide source and triflic acid.[79] The mechanism of this

Table 1: Water catalyzed triazoline fragmentation to oxazolidine.

Johnston and coworkers - 2008

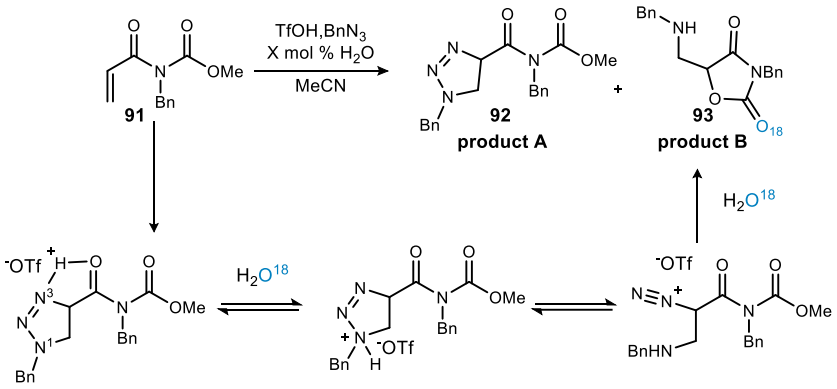

entry	mol % H_2O	t (°C)	product ratio (A:B)
1	0	-20 °C → RT	5:95
2	0	-20 °C	95:5
3	10	-20 °C	29:71
4	100	-20 °C	10:90
5	200	-20 °C	5:95

[77] Uyanik, M.; Hayashi, H.; Ishihara, K. *Science* **2014**, *345*, 291.
[78] Ma, C.; Fan, G.; Wu, P.; Li, Z.; Zhou, Y.; Ding, Q.; Zhang, W. *Org. Biomol. Chem.* **2017**, *15*, 9889.
[79] Hong, K. B.; Donahue, M. G.; Johnston, J. N. *J. Am. Chem. Soc.* **2008**, *130*, 2323.

transformation illustrates a [3+2] azide-olefin cycloaddition, and subsequent decomposition of the triazoline cleanly to oxazolidine dione. Notably, in anhydrous conditions the authors primarily isolated product A. The reaction was studied using *in situ* reaction IR, where the authors observed a secondary acceleration effect by molecular water in the triazoline ring opening. Johnston and coworkers proposed two roles for water in this reaction. Following the final cyclization where the ester displaces N_2^+, water serves to hydrolyze the result oxonium intermediate. Through H_2O^{18} labeling studies, the authors observed O^{18} labeling at the carbamate. Additionally, the evidence suggests that water accelerates the triazoline fragmentation by catalyzing the preceding isomerization (a non-hydrolytic process). This is proposed because N^3 protonation is ten times preferred to the protonation of N^1. However, water lowers the barrier of isomerization, possibly through acting as a proton shuttle. The protonation of N^1 leads to an irreversible triazole decomposition, which is the driving force. The authors suggest a secondary catalysis effect based on these observations. To further support this work, the authors note that if water is added at the beginning of the reaction, conversion diminishes. (Table 1) This aligns with their proposal, because the cycloaddition reaction to the triazole is Lewis acid catalyzed; triflic acid is a superior Lewis acid to hydronium, so one would expect triflic acid to accelerate the cycloaddition. The multifaceted roles water exhibits in this chemistry is novel and illustrates water's unique potential as an additive in synthetic chemistry.

Figure 29: The effect of water on a proline-catalyzed aldol reaction.

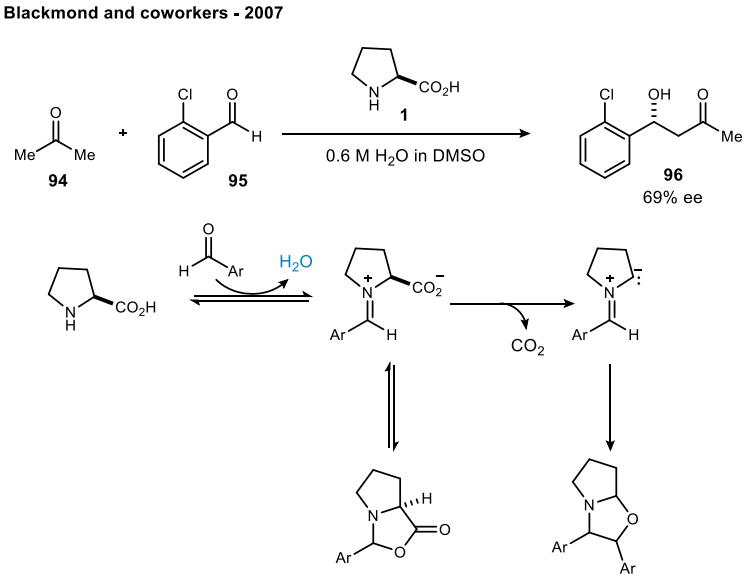

Another effect water can have as an additive is as an internal quenching agent, serving to drive chemical equilibria toward the desired products. The application of proline catalysis in aldol chemistry is well-precedented, dating to the 1970's in the Hajos-Parrish-Ketone synthesis.[10] Since then, a number of groups have expanded the application of proline catalysis beyond Robinson-annulation chemistry. Aldol reactions were studied, producing product in good yields and selectivities.[80] Notably, an excess of ketone was required for good reactivity. As proline catalysis was investigated further, it was reported that a rate acceleration was observed in the presence of water.[81] In the presence of water, catalyst loading was reduced and only a stoichiometric amount of water was required for reactivity. The Blackmond group investigated the effect of water in proline catalyzed aldol reactions. (Figure 29)[82] Blackmond observed decomposition of the organocatalyst through non-productive reactivity between the aryl aldehyde and proline catalysis. Proline rapidly condenses on the aldehyde, which can result in oxazolidinone formation. Additionally, this iminium formation promotes decarboxylation to form the azomethine ylide, which may react with an addition equivalent of aldehyde to form 1-oxapyrrolizidine. Water shifts the equilibrium to favor proline in the monomeric form, which serves to increase the active catalyst concentration. It is counterintuitive to see a rate acceleration in the presence of water in aldol chemistry because it also serves to disfavor proline condensation on the ketone, a step that is critical to product formation. Blackmond notes that because water may both disfavor product formation and byproduct formation, this rate acceleration affect may not be observed in all proline catalyzed aldol reactions. Nonetheless, this is still an interesting example of water as an additive, serving as an internal quenching agent.

The role of water as an internal quenching agent, in addition to being observed in organocatalysis, has also been observed in metal catalysis. The Umani-Ronchi group found that the application of water as an additive in their allylzinc addition to chiral imines had a positively affected diastereoselectivity.[83] While the initial addition to the imine occurred with high dr, the authors noted that selectivity diminished over the course of the reaction. When conversion was incomplete, dr was 99:1. However, if the reaction was left to run for extended reaction times, product was observed at nearly 1:1 dr. This erosion in selectivity was due to retroallylation.

[80] List, B.; Lerner, R. A.; Barbas, C. F. *J. Am. Chem. Soc.* **2000**, *122*, 2395.
[81] Pihko, P. M.; Laurikainen, K. M.; Usano, A.; Nyberg, A. I.; Kaavi, J. A. *Tetrahedron* **2006**, *62*, 317.
[82] Zotova, N.; Franzke, A.; Armstrong, A.; Blackmond, D. G. *J. Am. Chem. Soc.* **2007**, *129*, 15100.
[83] Basile, T.; Bocoum, A.; Savoia, D.; Umani-Ronchi, A. *J. Org. Chem.* **1994**, *59*, 7766.

Through the addition of 0.7 equivalents of water, the authors were able to quench the resulting zinc bromide that was produced in the reaction overtime. (Table 2) This hydrolysis inhibited the retroallylation process because zinc bromide that was serving as a Lewis acid. A similar additive effect was observed in a copper catalyzed addition to electron-deficient acetylenes.[84] The authors found that the organocuprate intermediate, if not quenched *in situ*, would decompose the addition product. Similar to Umani-Ronchi, the addition of 2 mol% of water inhibited these degradation procuresses by acting as an internal quenching agent. These reactions are an interesting example of water as an additive because water does not deactivate the active metal species that is required for reactivity.

Table 2: Improved selectivity observed in diastereoselective allylation reaction using protic additive.

Umani-Ronchi and coworkers - 1994

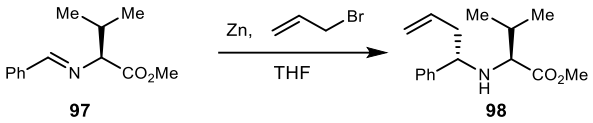

97 98

time (h)	equiv. of H_2O	yield (%)	dr
0.5	0	80	99:1
1.5	0	100	94:6
32	0	100	52:48
7	0.7	60	100:0
24	0.7	100	100:0

Despite water's Lewis basicity, it may also acts as an activator or coactivator to produce more Lewis-acidic species. This effect is most commonly observed in transition metal catalysis, so it will only be covered briefly in this chapter. An example of this additive effect was published by the Buono group in their enantioselective copper catalyzed Et_2Zn addition to enones.[85] The authors observed that adding 0.5 equivalents of water to the reaction improvement enantioselection dramatically. The authors proposed that $Zn(OH)_2$ was generated *in situ* by hydrolysis of the IZnEt intermediate. To probe this hypothesis, they used $Zn(OH)_2$ as an additive and observed a similar improvement in selectivity. The authors proposed that $Zn(OH)_2$ was a

[84] Ryu, I.; Matsumoto, K.; Kameyama, Y.; Ando, M.; Kusumoto, N.; Ogawa, A.; Kambe, N.; Murai, S.; Sonoda, N. *J. Am. Chem. Soc.* **1993**, *115*, 12330.
[85] Delapierre, G.; Constantieux, T.; Brunel, Jean M.; Buono, G. *Eur. J. Org. Chem.* **2000**, *2000*, 2507.

more effective activator than Et_2Zn because the hydrolyzed zinc species may provide assistance to the approaching copper species via chelation. Unlike Et_2Zn, $Zn(OH)_2$ may activate both the enone and cuprate species. This is an example of water acting as a coactivator, making zinc a more effective Lewis acid.

Table 3: The effect on water on facial selectivity in cuprate adddition to enones.

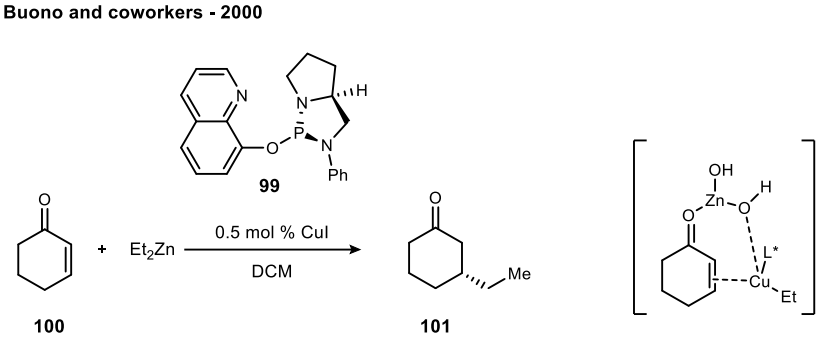

procedural modifications	yield (%)	ee (%)
anhydrous	55	7
0.5 eq. H2O	76	61
anhydrous, 0.25 eq. $Zn(OH)_2$	81	53

Prior to Umani-Ronchi's work, Corey reported a different cuprate addition to enones where diastereoselectivity improved greatly through the addition of water.[86] In anhydrous conditions,

Figure 30: Rate acceleration observed in cuprate addition to enones.

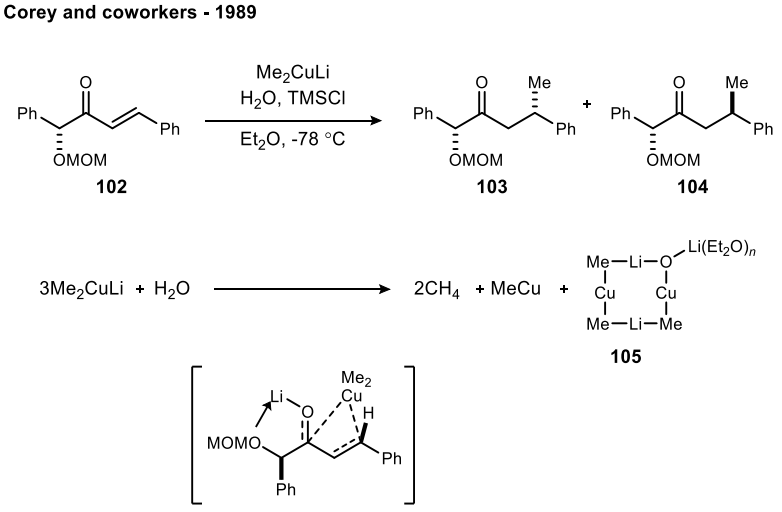

[86] Corey, E. J.; Hannon, F. J.; Boaz, N. W. *Tetrahedron* **1989**, *45*, 545.

the product was isolated in 2:1 dr. However, through the addition of 30 mol % of water, the product ratio improved to 33:1. The authors proposed that a planar mixed cuprate structure formed, as shown in Figure 30. This structure is suited for chelate formation, which stabilizes the diastereomeric transition state. In this reaction, water makes the cuprate more electron-rich, which accelerates the rate of this addition reaction. Additionally, chelation from the Lewis acid ($Zn(OH)_2$) to the cuprate improves facial selectivity.

Additive effects are observed widely in synthetic chemistry. More specifically, water has been utilized as an additive in a variety of reactions, where it may serve as a hydrolyzing agent, an internal quenching agent, or a Lewis acid activator. At first glance, it is surprising to see water have such a profound effect on reactivity and selectivity because bulk water will deactivate most catalysts. This is true in both organocatalysis and transition metal catalysis. As indicated in these examples, most of these additive effects are observed at a specific amount of water. For this reason, some scientists choose to employ terminology to describe the amount of water. "In water" is used if water is used as a reaction solvent, while "on water" is used to describe biphasic reactions.[73] Hayashi proposed the term "in the presence of water" to describe water effects where water is not employed as a bulk solvent.[72] This terminology serves as a useful tool to describe the effect of water. However, rather than employing terminology, it is more important that the effect of water on a reaction is quantified so that the chemistry is consistent and reproducible. As we understand the effect of additives on reactivity, we better understand how to develop new reactions.

1.2 Development of enantioselective carbamation reaction via CO_2 capture

1.2.1 Proposal for an enantioselective CO_2 capture halocyclization reaction

The carbamate functional group is commonly used in medicinal chemistry because of its hydrolytic stability *in vivo* and ability to permeate cell membranes.[87] The polarity and ability to both donate and accept hydrogen bonds contributes to a molecule's ability to cross cell

[87] Ghosh, A. K.; Brindisi, M. *J. Med. Chem.* **2015**, *58*, 2895.

membranes via active transport.[88] Carbamates possess similar hydrogen-bonding abilities to amides, with improved hydrolytic stability, making them ideal peptide bond surrogates. Linezolid[89] and efavirenz[90] are two examples of enantioenriched carbamates used in therapeutic applications (Figure 31). Cyclic carbamates are conventionally prepared by reacting amino-alcohols with toxic C1 donors, such as phosgene gas. Phosgene and its surrogates are highly reactive electrophiles but present safety issues and are expensive. Carbon dioxide ($0.000066/mol) is an inexpensive and relatively benign C1 building block and an excellent alternative to triphosgene ($533/mol) and CDI ($233/mol). However, previous CO_2 capture procedures with amines required forcing conditions for reactivity, such as high temperatures, supercritical conditions, or excessive amounts of base.[50,91]

The preparation of cyclic carbamates from amino-alcohols is relatively straightforward, however, the preparation of chiral amino-alcohols is a known challenge. 5-membered cyclic carbamates are accessible from reduced amino acid scaffolds, which means the chiral pool serves as the source of chirality. Preparing enantioenriched carbamates at other ring sizes, however, is more laborious synthetically. The development of new reactions will play a critical role in expanding the utility and application of small molecules in medicinal chemistry. More specifically, new enantioselective methods will play a critical role in the development of carbamate-derived therapeutics.

Figure 31: Examples of cyclic carbamates in pharmaceuticals.

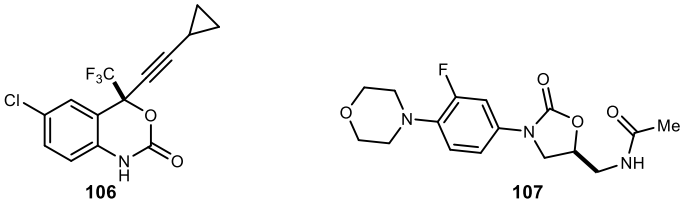

[88] van der Sandt, I. C. J.; Vos, C. M. P.; Nabulsi, L.; Blom-Roosemalen, M. C. M.; Voorwinden, H. H.; de Boer, A. G.; Breimer, D. D. *AIDS* **2001**, *15*.
[89] Lohray, B. B.; Baskaran, S.; Srinivasa Rao, B.; Yadi Reddy, B.; Nageswara Rao, I. *Tetrahedron Lett.* **1999**, *40*, 4855.
[90] Pierce, M. E.; Parsons, R. L.; Radesca, L. A.; Lo, Y. S.; Silverman, S.; Moore, J. R.; Islam, Q.; Choudhury, A.; Fortunak, J. M. D.; Nguyen, D.; Luo, C.; Morgan, S. J.; Davis, W. P.; Confalone, P. N.; Chen, C.-y.; Tillyer, R. D.; Frey, L.; Tan, L.; Xu, F.; Zhao, D.; Thompson, A. S.; Corley, E. G.; Grabowski, E. J. J.; Reamer, R.; Reider, P. J. *J. Org. Chem.* **1998**, *63*, 8536.
[91] Seayad, J.; Seayad, A. M.; Ng, J. K. P.; Chai, C. L. L. *ChemCatChem* **2012**, *4*, 774.

Figure 32: Examples of BAM-catalyzed halocyclizations.

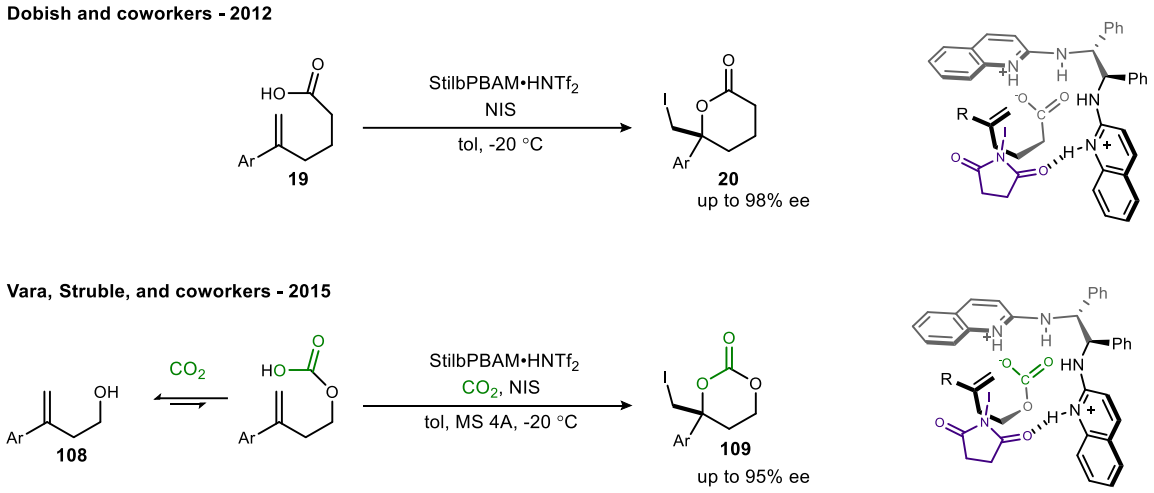

Using the lactonization chemistry[19] as precedent, it was envisioned that a variety of different scaffolds could be accessed through a similar mode of reactivity. (Figure 32) Two scaffolds of interest were carbonic and carbamic acids, both of which readily form when alcohols and amines are exposed to carbon dioxide respectively. In 2015, the Johnston lab published a new enantioselective approach in which an alcohol captures CO_2 at atmospheric pressure, and the resulting carbonic acid adduct undergoes alkene functionalization with high enantiomeric excess.[30] Weak hydrogen bond donor-acceptor interactions are responsible for activation and

Figure 33: Potential pitfalls in BAM catalyzed carbamation reaction using homoallylic amines.

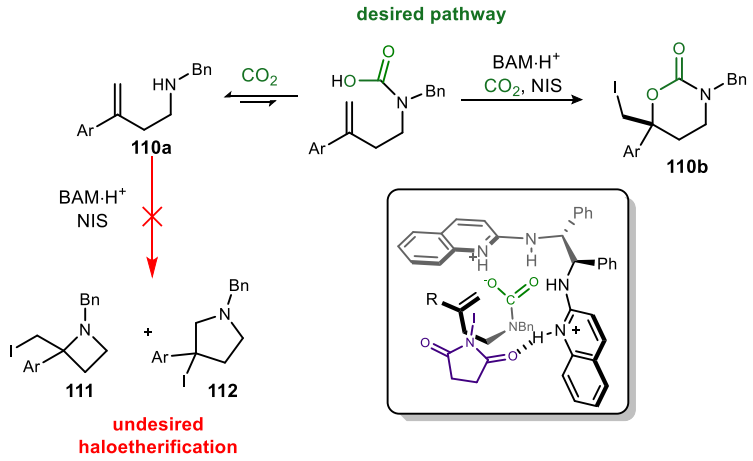

stereocontrol, this approach represents a new paradigm for small molecule catalysis of CO_2-fixation reactions.

Carbamic acids are similar in structure and acidity (pka ~ 5) to carboxylic acids[92], making them analogous to previous functional groups used in BAM catalysis. It was envisioned that these multi-component intermediates could be intercepted for lactonization chemistry. This carbamation reaction is an interesting application of Brønsted-acid catalysis because basic amine substrates are used without deprotonating the acidic BAM·$HNTf_2$ salt.

Using established lactonization chemistry developed in the Johnston lab, we set out to develop an enantioselective iodocarbamation reaction using bifunctional Brønsted acid/base catalysis. Carbon dioxide served as both a carbon and oxygen atom donor, which is an unconventional and inexpensive approach to carbamate synthesis. The objective was to develop a reaction that was both high yielding and highly selective for the carbamate product. Given the nucleophilicity of the amine substrates, there was concern for undesired haloamination byproducts, as shown in Figure 33. Additionally, there was concern that the Brønsted acid catalyst would engage in proton transfer with the amine substrates, forming a potential achiral ammonium catalyst.

1.2.2 Initial reaction optimization

Initial work on this iodocarbamation reaction was completed by Dr. Roozbeh Yousefi, a post-doctoral researcher in the Johnston lab. He completed a huge amount of work, including catalyst design, reaction optimization, investigation of a substrate scope, and developed derivations of the carbamate scaffold. His work provided a strong foundation for this project.

Initial results of this chemistry were promising. A variety of bisamidine catalysts were evaluated, including StilbPBAM, ^{7}MeStilbPBAM, and ^{7}MeOStilbPBAM, which increased in basicity respectively. The free base of all the catalyst backbones showed some reactivity, but the bifunctional catalyst with a triflimide anion showed much higher enantioselection. (Table 4)

While the initial studies may have required the typical problem-solving, attempts to reproduce the results were met with a new challenge. Specifically, the simultaneous observation of high

[92] Masuda, K.; Ito, Y.; Horiguchi, M.; Fujita, H. *Tetrahedron* **2005**, *61*, 213.

yield and high enantioselection was rare. Instead, high enantioselection and low yield was a typical result. Interestingly, attempts to purify the catalyst by HPLC and recrystallization led to low yield/high ee product. An occasional high yield/high ee result fueled optimism that a solution could be found. In a representative example, Yousefi observed full conversion, isolating substrate **113b** in 86% yield and 92% ee. Struble, along with other lab members, isolated **113b** in a 30% yield and 83% ee. While the diminished selectivity was concerning, the biggest hurdle to overcome was the lack of reactivity.

Table 4: The effect of ligand basicity on iodocarbamation reaction.

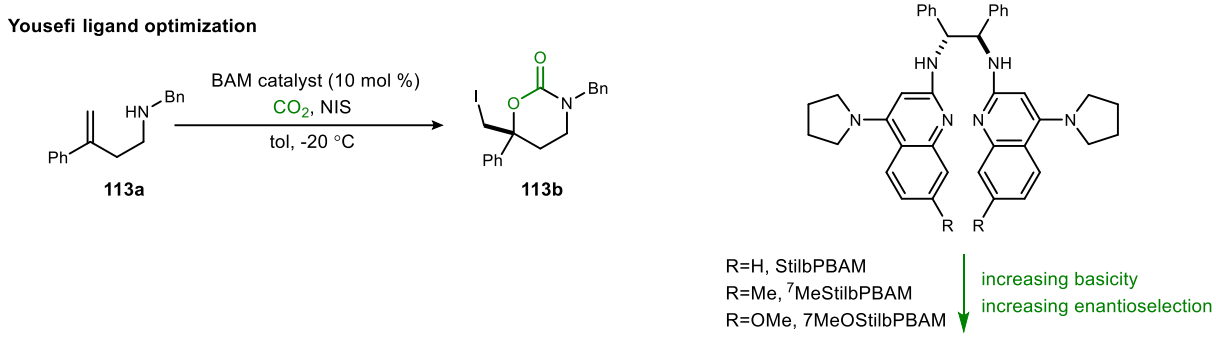

entry	ligand	acid	yield (%)	ee (%)
1	-	-	0	-
2	triazabicyclodecene	-	79	-
3	StilbPBAM	-	35	30
4	StilbPBAM	$HNTf_2$	15	50
5	^{7}MeStilbPBAM	$HNTf_2$	31	81
6	^{7}MeOStilbPBAM	$HNTf_2$	86	92

The operating hypothesis for the observed poor conversion was the large amount of precipitation that formed over the course of the reaction. The NMR spectrum of the dark brown precipitate showed that it was a mixture of the homoallylic amine substrate and *N*-iodosuccinimide (NIS). NIS is not soluble in toluene, so it was expected in the spectrum. However, the homoallylic amine substrate was initially soluble in the reaction conditions. It was not understood why the amine substrate became less soluble over the course of the reaction. In addition, it was reported that Yousefi did not have solubility problems while running these cyclizations.

An interesting finding was that the catalyst and amine substrate prepared by Yousefi always performed better than the material prepared by Struble. To be more specific, both batches of amine substrate and BAM catalyst prepared by Yousefi showed improved solubility, yield, and enantioselectivity relative to material prepared by other Johnston lab members. Based on these findings, it was hypothesized that there was some type of additive effect at play. To probe this hypothesis, the NMR spectra of the substrates and chiral ligand were analyzed for impurities. However, all materials were found to be greater than 95% pure, which meant if indeed there was an additive effect, the additive was present in a very small amount. This made identifying the nature of the additive quite difficult. It was at this point that I joined the Johnston lab and was able to contribute to this iodocarbamation project. The objective going forward was to identify conditions for this reaction that were both highly reactive and reproducible. Given Yousefi's success developing this chemistry, it was known that highly reactive conditions were already discovered.

Figure 34: Preparation of both substrate and catalyst for iodocarbamation reaction.

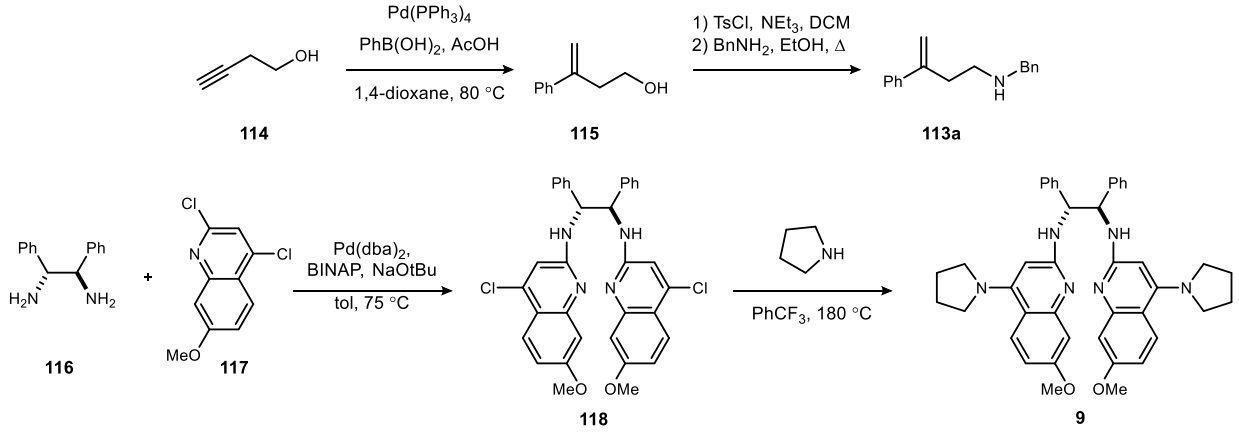

While the nature of the additive was not identified in Yousefi's NMR spectra, it was hypothesized that the additive was introduced to the iodocarbamation reaction by the starting materials. Because many of these additives are capable of hydrogen bonding, it was thought that they may accelerate the rate of the reaction. Routes to the amine substrate and BAM ligand are shown in Figure 34. We screened all the starting materials, reagents, and intermediates shown in Figure 35 for additive effects. In addition, a variety of additives were screened as that were capable of hydrogen bonding to the BAM ligand such as 2-nitroproane and tetrabutyl ammonium bromide. It was hypothesized that the additive was serving to accelerate the rate of reactivity by

interacting with the catalyst. As shown in Figure 35, improved conversion and selectivity was observed occasionally. However, these positive results were never repeatable. In should be noted that while reactivity varied greatly in these screens, enantioselectivity did not deviate greatly from 83% ee. Because the main objective was to develop consistent chemistry, none of these hits were pursued further. If anything, the occasional successes only further strengthened our conviction that an additive effect was at play that was not well understood.

Figure 35: Evaluation of the effect additives had on yield in iodocarbamation reaction.

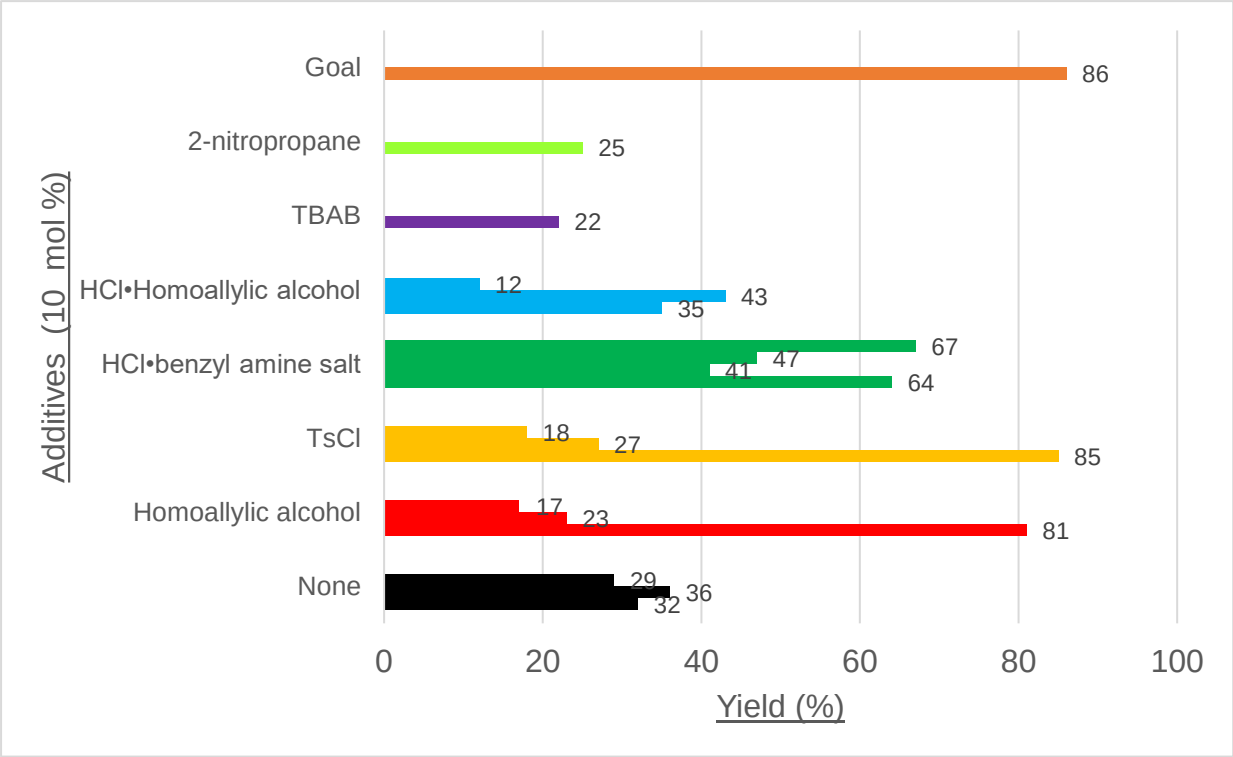

After an unsuccessful investigation of additives, other reagents were evaluated for their ability to accelerate the cyclization reaction. While it was understood that these conditions would differ from Yousefi's initial conditions, a different additive may be identified that had a similar effect. In addition, the cyclization was run with a large excess of NIS and the concentration was increased in order to improve reactivity. Looking at Yousefi's optimization table, it was observed that the free-base BAM ligand was more reactive than ^{7}MeOStilbPBAM·HNTf$_2$ salt. It was hypothesized that weakly basic additives may accelerate the cyclization, without diminishing ee. Cesium carbonate increased conversion greatly, without diminishing ee. While

these conditions were an improvement, 82% ee was still considerably lower than the initial work. (Figure 36)

Figure 36: Evaluation of Cs_2CO_3 as an additive relative to previous work.

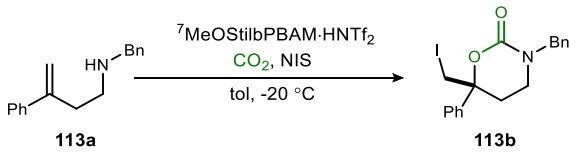

113a 113b

initial conditions	Cs_2CO_3 conditions
0.13 M	0.33 M
1.1 eq. NIS	1.8 eq. NIS
86% yield, 92% ee	**80% yield, 82% ee**

These cesium carbonate conditions were not a publishable because selectivity was moderate at best. While not optimal, these conditions were studied and used to probe the additive effect further. It was still unclear why cesium carbonate accelerated this cyclization reaction. Initially, it was proposed that cesium carbonate was a basic additive. The observed selectivity was significantly higher than observed with free-base catalyst, which indicated that the protonation state of the BAM ligand was conserved. Based on this hypothesis, the role of cesium carbonate in the cyclization was investigated.**Error! Bookmark not defined.**,[93] Notably, other basic additives were not as prolific as cesium carbonate. For example, Cesium hydroxide, potassium carbonate, and cesium hydroxide did not improve reactivity relative to the control reaction where no basic additives were used. Another use of cesium carbonate is as a drying agent. With this in mind, the role of drying agents and water were evaluated in this iodocyclization reaction.

1.2.3 Observed rate acceleration in wet toluene

With the role of cesium carbonate in question, other additives were evaluated to probe this effect. The hypothesis was that cesium carbonate was acting as a drying agent, as opposed to the expected basic reactivity. To probe this, a few common drying agents were tested and compared

[93] Salvatore, R. N.; Nagle, A. S.; Jung, K. W. *J. Org. Chem.* **2002**, *67*, 674.

to the cesium carbonate results (as shown in Table 5). To our delight, sodium sulfate successfully improved both yield and enantioselectivity. More importantly, we achieved results similar to Yousefi's work and these results were repeated several times. Because sodium sulfate improved conversion, similarly to cesium carbonate, it was hypothesized that both reagents were acting as drying agents. Therefore, water must have a deleterious effect on this reaction.

While these results were exciting, some of the data we collected didn't quite align with the operating hypothesis. Molecular sieves diminished conversion greatly, which contradicted previous work completed by the Johnston lab.[30] In the carbonation chemistry, molecular sieves played a critical role in developing a reaction that was high yielding and highly reproducible. If indeed water was having a deleterious effect, why did molecular sieves diminish conversion in the carbamation chemistry, but not the carbonation chemistry? To probe this effect, sodium sulfate was activated using a drying pistol. If sodium sulfate was indeed acting as a drying agent, conversion and ee should either improve or be conserved after activating it. We were surprised to see that the activated sodium sulfate reduced conversion and enantioselectivity. These contradictory pieces of data indicated that indeed water was affecting this carbamation reaction, however, the nature of this effect remained unclear.

Table 5: The effect of various drying agents on both yield and selectivity.

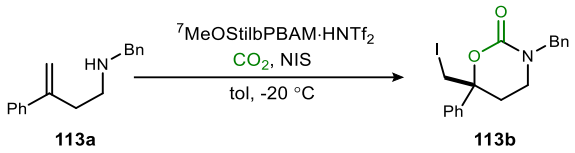

113a **113b**

Drying agent	yield (%)	ee (%)
Cs_2CO_3	58	78
MS 4Å	28	73
Na_2SO_4	72	89
activated Na_2SO_4	54	82

After investigating the application of various additives in this iodocarbamation reaction, a novel high-yielding result was observed. A control experiment (ran without an additive) furnished the carbamate in 60% yield and 90% ee. After evaluating the materials used for this reaction, it was noted that a sure-seal bottle of toluene was employed. All previous work

employed toluene that was removed from the solvent system and stored over molecular sieves. In this novel result, a bottle of toluene used was a sure-seal bottle, opened 6 months prior. More importantly, the result was repeatable by multiple scientists when this specific sure-seal bottle of toluene was used for the cyclization. However, when other toluene sources were employed, incomplete conversion was observed.

Based on this data, the new operating hypothesis was water was having an effect on this carbamation reaction, however, the effect was only observed at a narrow range. After evaluating both sources of toluene using a Karl-Fischer titrator, the amount of water present in those bottles were 90 ppm in the sure-seal bottle and 0 ppm when stored over sieves. These results indicate that a small amount of water accelerated the cyclization, however the optimal amount of water was still unknown.

Figure 37: The effect on water on both reactivity and selectivity.

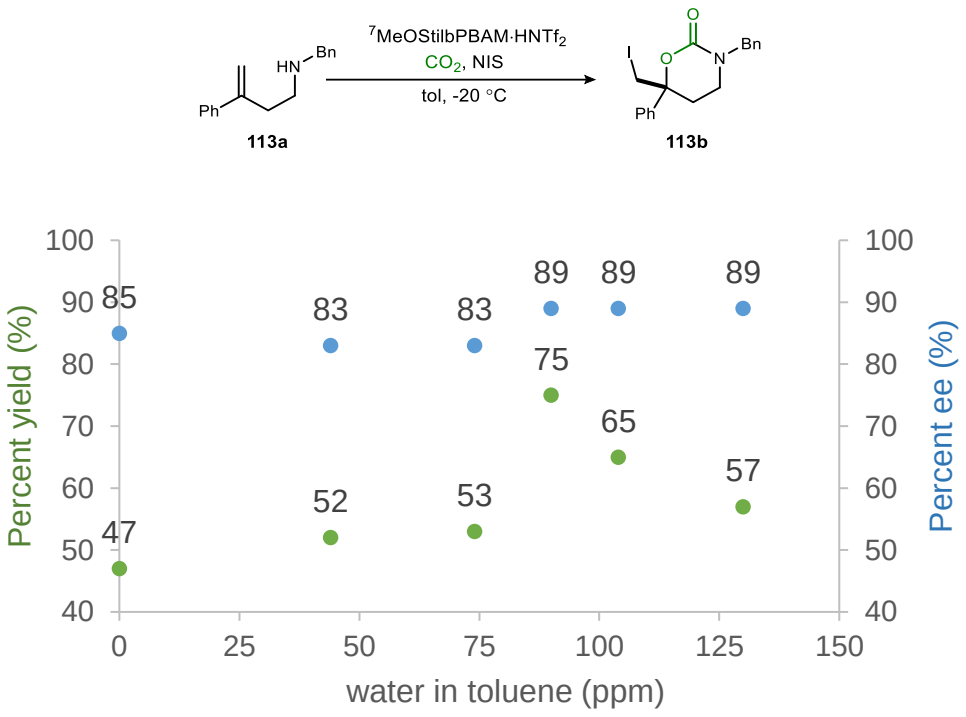

To quantify this effect, a number of wet toluene solutions were prepared and evaluated for their effect on conversion and enantioselectivity (Figure 37). Conversion increased as the amount of water increased up to 90 ppm of water in toluene, and then conversion diminished again as the amount of water increased. Enantioselection increased up to 90 ppm, and leveled off from there.

This water effect was affectionately referred to as the "Goldilock's Effect" because too little or too much water had a deleterious effect on the reaction. This cyclization operates at 10 mol % catalyst loading, making the concentration of water present in this chemistry a significant amount. While the amount of water in this chemistry may seem like a negligible amount, 90 ppm of water at 0.13 M is about 4 mol %. In order to verify this effect, a similar screen was performed with a different amine substrate that was notably less-reactive than other substrates in the scope (Figure 38). Substrate **114a** was less soluble than substrate **113a**, and it was observed that additional water had a positive effect on both yield and ee. It is proposed that water may enhance the solubility of **114a**, which ultimately improved reactivity. Substrate **114a** is another good example of the rate-acceleration of this iodocarbamation reaction in wet toluene.

Figure 38: Confirmation of the "Goldilock's Effect" on an addition substrate.

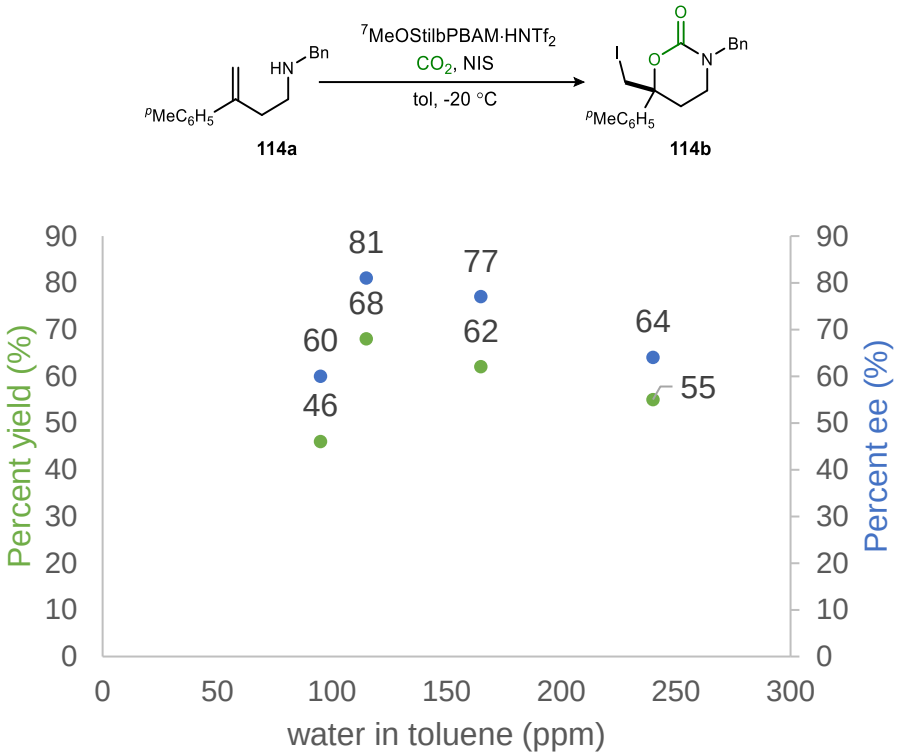

While the exact role of water in this reaction is not fully understood, Struble performed ^{19}F DOSY (Diffusion-ordered spectroscopy) NMR experiments for mechanistic insights. These studies provided a better understanding of the reaction mechanism and revealed several complexes that formed in the reaction conditions. Before the role of water is further investigated, it should be noted that the authors evaluated water in this chemistry numerous times. The results

were inconsistent, at times water would result in a rate acceleration. However, as with the other additives screened, the results were not reproducible. Most of the time, water had a deleterious effect on the reaction. In hindsight, water was typically employed in stoichiometric quantities, which is why the rate acceleration was not observed. This negative result aligned with previous work collected in the Johnston lab while optimizing the carbonation chemistry. Like this project, during optimization the carbonation chemistry was plagued with conversion and consistency issues. At times high yields were observed, but conversion was typically poor with high enantioselectivity. Vara and Struble observed a large amount of precipitate forming over the course of the reaction. After a variety of additives were screen, they found that molecular sieves addressed issues associated with conversion and consistency. The operating hypothesis was that carbonic acid formed as residual water reacted with carbon dioxide. The carbonic acid molecules were acidic enough to over-protonate the BAM ligand, rendering the BAM ligand insoluble in toluene. In this reaction, carbonic acid lowered the active catalyst concentration, which explained the conversion issues. Through the application of molecular sieves as an additive, water was sequestered, which ultimately stopped the formation of carbonic acid molecules (Figure 39).[30] To support this hypothesis, *in situ* IR was employed to study this reaction. It was observed that water inhibited the formation of the linear carbonic acid intermediate, which was necessary for reactivity.

Figure 39: The deleterious effect on water on iodocarbonation reaction.

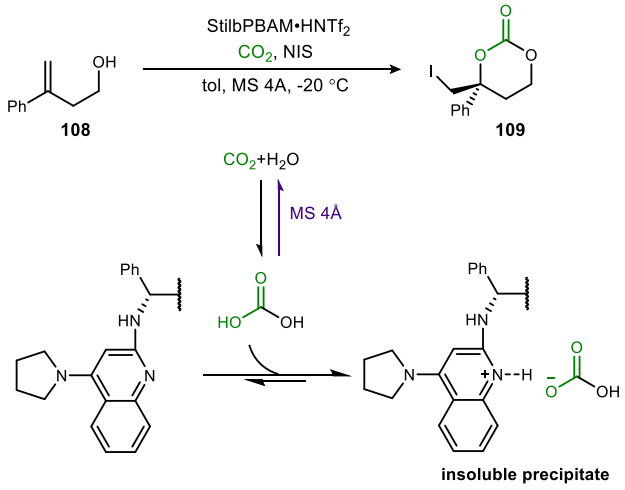

1.2.4 Mechanistic proposal based on DOSY NMR experiments

The mechanism of this carbamation reaction was investigated using DOSY NMR. Diffusion-ordered NMR spectroscopy is a 2D NMR experiment developed to measure diffusion coefficients of molecules in solution. In this technique, one dimension represents chemical shift information, and the second dimension distinguishes species by diffusion coefficient, which is inversely related to their particle sizes.[94] The procedure used was developed by Sibi and coworkers[95], who developed a protocol to determine formula weights for acid-base complex in solution using ^{19}F DOSY NMR. The sensitivity of ^{19}F NMR yields sharp peaks over a wide chemical-shift range simplified the spectral analysis greatly. A number of fluorinated internal standards were prepared of various weights, which were used to determine the linear relationship between formula weight and diffusion rate in the carbamation conditions. By using a fluorinated amine substrate and $HNTf_2$ salt of the BAM catalyst, he was able to analyze the diffusion rate of various fluorinated complexes that formed in the carbamation reaction conditions.

Figure 40: The proposed complexes observed in DOSY NMR studies.

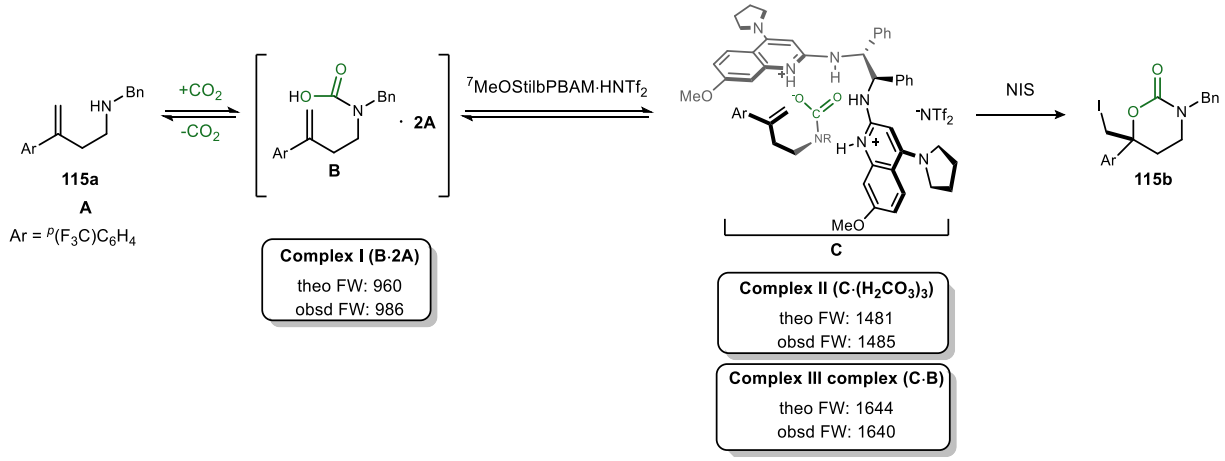

Using the linear relationship between the formula weight and diffusion rate, the molecular weights of these complexes were determined. Figure 40 shows the observed formula weights and the proposed complexes associated with them. When the amine substrate was exposed to carbon

[94] Li, D.; Kagan, G.; Hopson, R.; Williard, P. G. *J. Am. Chem. Soc.* **2009**, *131*, 5627.
[95] Subramanian, H.; Jasperse, C. P.; Sibi, M. P. *Org. Lett.* **2015**, *17*, 1429.

dioxide (without BAM catalyst), complex I was observed. Upon the addition of ^{7}MeOStilbPBAM·HNTf$_2$, complex I is replaced with complexes II and III. It was observed that both complexes II and III contained substrate **A** and Tf$_2$NH. Because NIS was omitted from these NMR experiments, the Brønsted acid portion of the ligand was unsatisfied, coordinating to both intermediate **B** and carbonic acid molecules. Residual water molecules would readily react with carbon dioxide in solution, making the presence of carbonic acid molecules presumed.

Figure 41: Proposed mechanism of BAM catalyzed carbamation reaction.

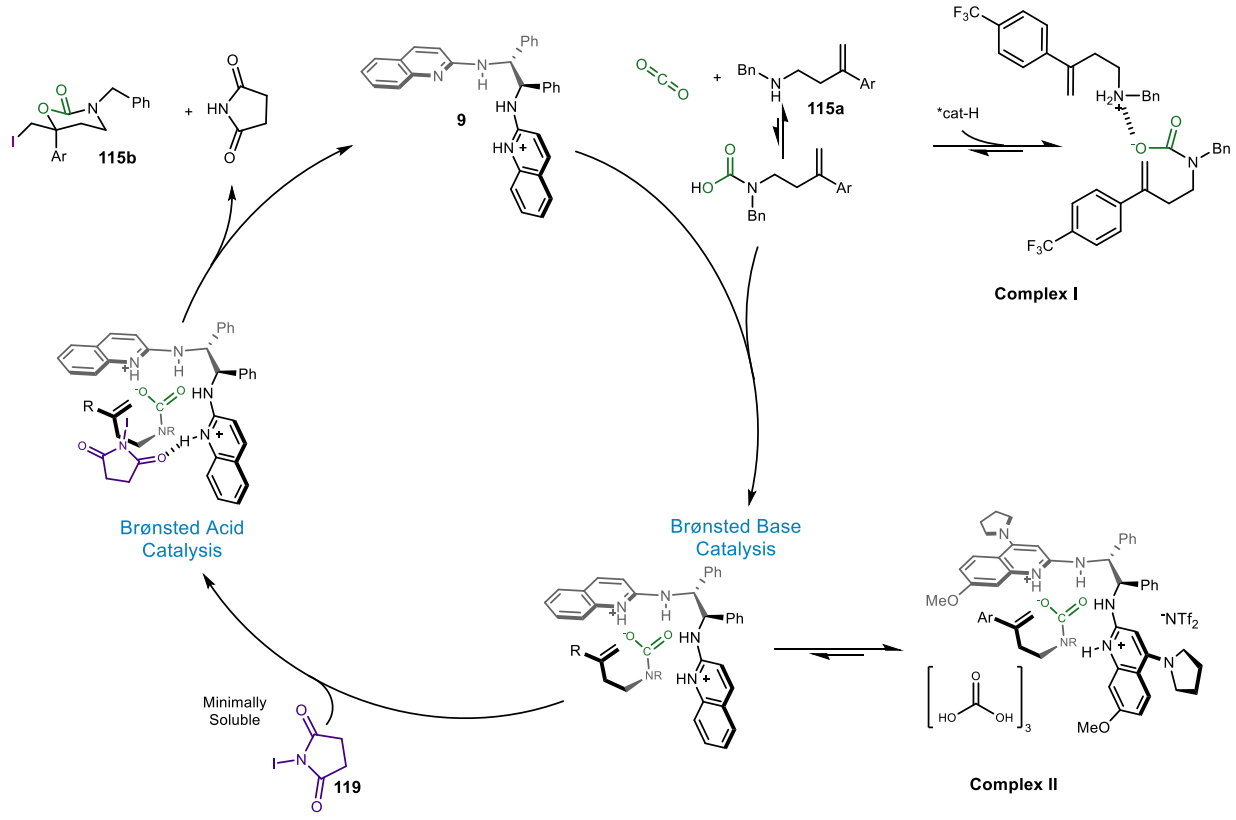

Based on these findings, a mechanism was proposed for this iodocarbamation reaction. The proposed mechanism is shown in Figure 41. Under a carbon dioxide atmosphere at atmospheric pressure, the amine is in equilibrium with a carbamic acid form. The catalytic starts with the mono-protonated BAM ligand, which deprotonates the carbamic acid intermediate via Brønsted base catalysis, which serves to control the nucleophilic approach. NIS is activated by the protonated portion of the BAM ligand, with the halamine activating the olefin. It is the Brønsted

acidic interaction that controls orientation of the olefin. It is this bifunctional control which provides high facial selectivity, furnishing the cyclic carbamate in high ee.

In addition, to acquiring mechanistic support, the observed complexes were used to better understand the effect of water in this reaction. As noted during initial optimization efforts, large amounts of precipitation were associated with incomplete conversion. Further inspection of the precipitate indicated that the amine substrate was crashing out over the course of the reaction. This finding was surprising given the substrate's complete dissolution at the start of the reaction. The DOSY NMR studies highlight the formation of complex I, which is a salt of the amine substrate with a carbamic acid molecules. It is assumed that this ionic complex is insoluble in toluene, which would explain the issues associated with reactivity. One hypothesis for the role of water in this reaction is that it helps activate complex I by either improving its solubility in the cyclization conditions, or it acts as a proton shuttle. As a proton shuttle, water could return the carbamic acid to its most active, monomer form.

Another complex observed in the DOSY studies that may help identify the role of water in this chemistry is complex II, where a number of carbonic acid molecules bound to the ionic complex between the BAM ligand and carbamic acid molecule. It is known that water readily reacts with carbon dioxide to form carbonic acid molecules, making the formation of these acidic molecules unsurprising. While the role of the carbonic acid in this complex is not well understood, there is potential for hydrogen bonding, which may help stabilize this complex. With NIS being

Figure 42: Comparison of proposed hypoiodate complex with organocatalyst.

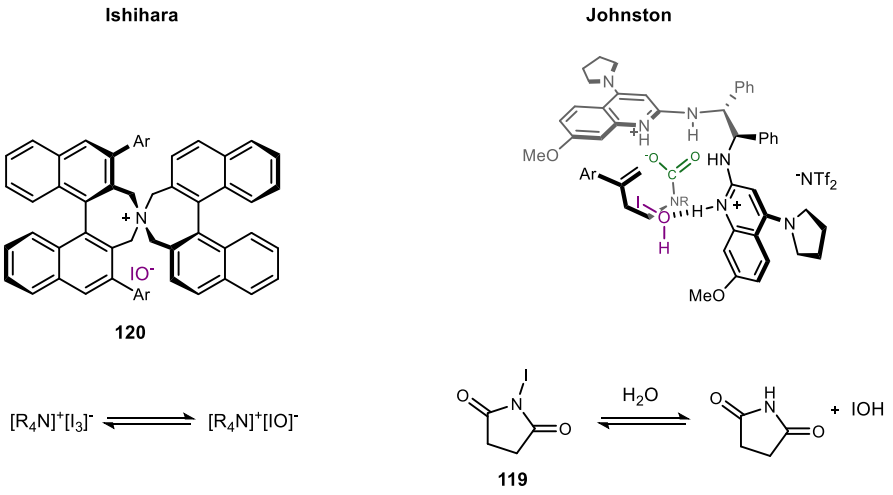

minimally soluble, this stabilization may stabilize this complex until NIS is solubilized for reactivity.

While water may be playing a role in the formation or dispersion of these complexes, there is a third hypothesis for the role of water in this chemistry. Scientists have observed the formation of hypoiodite when electrophilic iodine sources are exposed to water.[76] The Muñiz group observed the formation of hypoiodite using Raman spectroscopy in their photoredox-catalyzed pyrrolidine synthesis, where iodine acted as a catalyst. Residual water in their solvent bottle was necessary for reaction initiation. A similar hypoiodite formation was observed by the Ishihara group in their tocopherol synthesis.[77] Ishihara proposed that their chiral quaternary ammonium catalyst formed a salt with hypoiodite, which served as a chiral electrophilic halogen source. (Figure 42) Hypoiodite is thought to be a more active halogen donor, which served to accelerate the reaction rate. In this CO_2 capture chemistry, it's possible that hypoiodite is more reactive because it is a homogenous iodine source, while NIS is minimally soluble in the conditions. For a more detailed explanation on the effect of water in these examples, please reference section 1.1.4.

In spite of our best efforts, the experimental data we collected does not clearly define the role of water in this chemistry. The observed rate acceleration, however, was undeniable. Through the application of these wet toluene conditions, along with an additional procedural modification, a substrate scope was successfully completed and a manuscript was published.

1.2.5 Modification of ligand purification to improve catalyst performance

While conversion was an issue in this chemistry, an additional issue was the inconstancy observed across different batches of ^{7}MeOStilbPBAM. Some batches of the chiral catalyst performed well, while some were unreactive. While the catalyst showed poor reactivity, similar enantioselection was observed. Even after the water effect was clarified, these catalyst issues persisted. It was hypothesized that the preparation of the chiral ligand effected the ligand's reactivity. To probe the effect of purification, a large batch of ligand was prepared. The crude material was purified in two different ways: 1) recrystallization from dichloromethane/hexanes and 2) precipitation from dichloromethane/hexanes. Notably, both batches of material were indistinguishable by NMR and MS but performance differently in the carbamation reaction. The

catalyst purified via precipitation produced the carbamate in full conversion and 90% ee. However, the batch of recrystallized catalyst gave product in 15% yield and 86% ee. This was surprising because one would expect recrystallized catalyst to be higher in purity, and therefore product the product in higher yield. Because the catalyst batches were very similar in purity, it was not thought that residual impurities had an effect on reactivity.

To probe the role of ligand purification further, crystals of ^{7}MeOStilbPBAM were analyzed via X-Ray crystallography by Dr. Nathan Schley. The XRD data showed the chiral ligand formed a well-organized structure in the solid state. As shown in Figure 43, two chiral ligand molecules were interlocked through complementary hydrogen bonds, with N-N distances measured 3.022-3.093 Å for each hydrogen bond donor-acceptor interaction. Alongside, N-H-N angles ranging from 167-176°. In addition to the formation of ligand dimers, a total of eight molecules in the form of interlocked pairs fill the unit cell, as shown in Figure 44. These dimeric structures are coordinated to a number of dichloromethane molecules. Based on hydrogen bonding, it is thought that these ligand molecules may be readily solubilized to their dimeric form. However, further solvation to the monomeric form might occur less readily due to the highlight stabilizing hydrogen bonding between the two ligand molecules.

Crystallized ligand has been used often in BAM catalysis in the past. After the chiral ligand is purified, the ligand salt is prepared by mixing the ligand in dichloromethane with the strong acid

Figure 43: X-ray crystal structure of ^{7}MeOStilbPBAM.

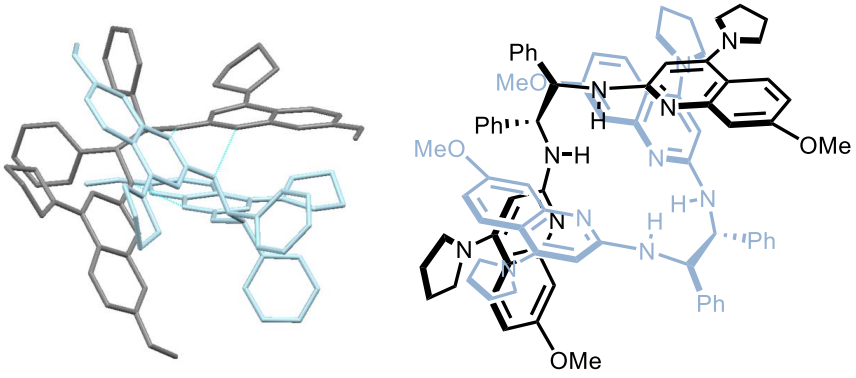

for 30 minutes at room temperature. It was always thought by mixing the ligand in solvent with a strong hydrogen bond donor, any artifacts of the crystallization process would be interrupted, returning the chiral ligand to its most active monomer form. Notably, ^{7}MeOStilbPBAM is one of

the most electron rich BAM ligands, which would only strengthen the hydrogen bond network of the BAM ligand. It is hypothesized that because ^{7}MeOStilbPBAM coordinates so strongly with itself, its crystals are more difficult to solvate compared to other BAM ligands. It is hypothesized that the tightly packed crystalline structure made crystallized catalyst slow to solubilize, and therefore, lowered the active catalyst concentration.

While this phenomenon was the most problematic in this chemistry, with a 60% difference in conversion, similar issues were observed in Knowe's lactonization chemistry.[31] Knowe was able to recover his catalyst's reactivity by refluxing the ligand in ethyl acetate for several hours. Unfortunately, this same procedure was not successful in the carbamation reaction. By adopting the trituration procedure, the BAM catalyst could be repaired multiple times with consistency across catalyst batches. By modifying the ligand procedure and using water as an additive, the substrate scope was repeated with confidence. These procedure modifications produced a novel method to prepare cyclic carbamates in high yield and ee using CO_2 capture.

Figure 44: The highly-ordered solid state structure of ^{7}MeOStilbPBAM observed via XRD.

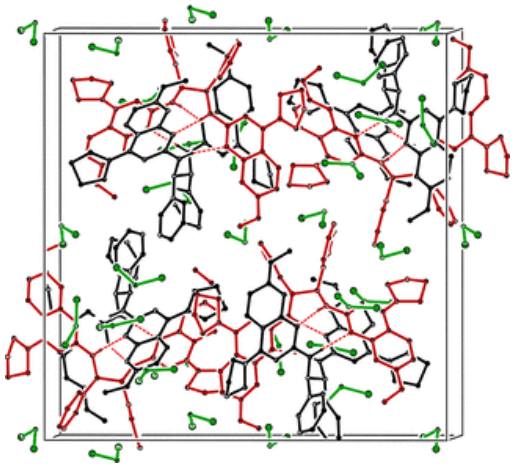

1.2.6 Analysis of scope and limitations

With the help of Dr. Mahesh Vishe, the modified conditions were applied to a substrate scope. To ensure the chemistry reported in the final manuscript was highly reactive and reproducible, both Vishe and myself tested every substrate multiple times. The reported results were analyzed rigorously and the authors reported the median results of every substrate. Figure 45 shows the

full scope, which illustrated the broad steric and electronic tolerance of this cyclization. These procedure modifications were investigated in order to develop conditions that were highly

Figure 45: Evaluation of iodocarbamation reaction via substrate scope.

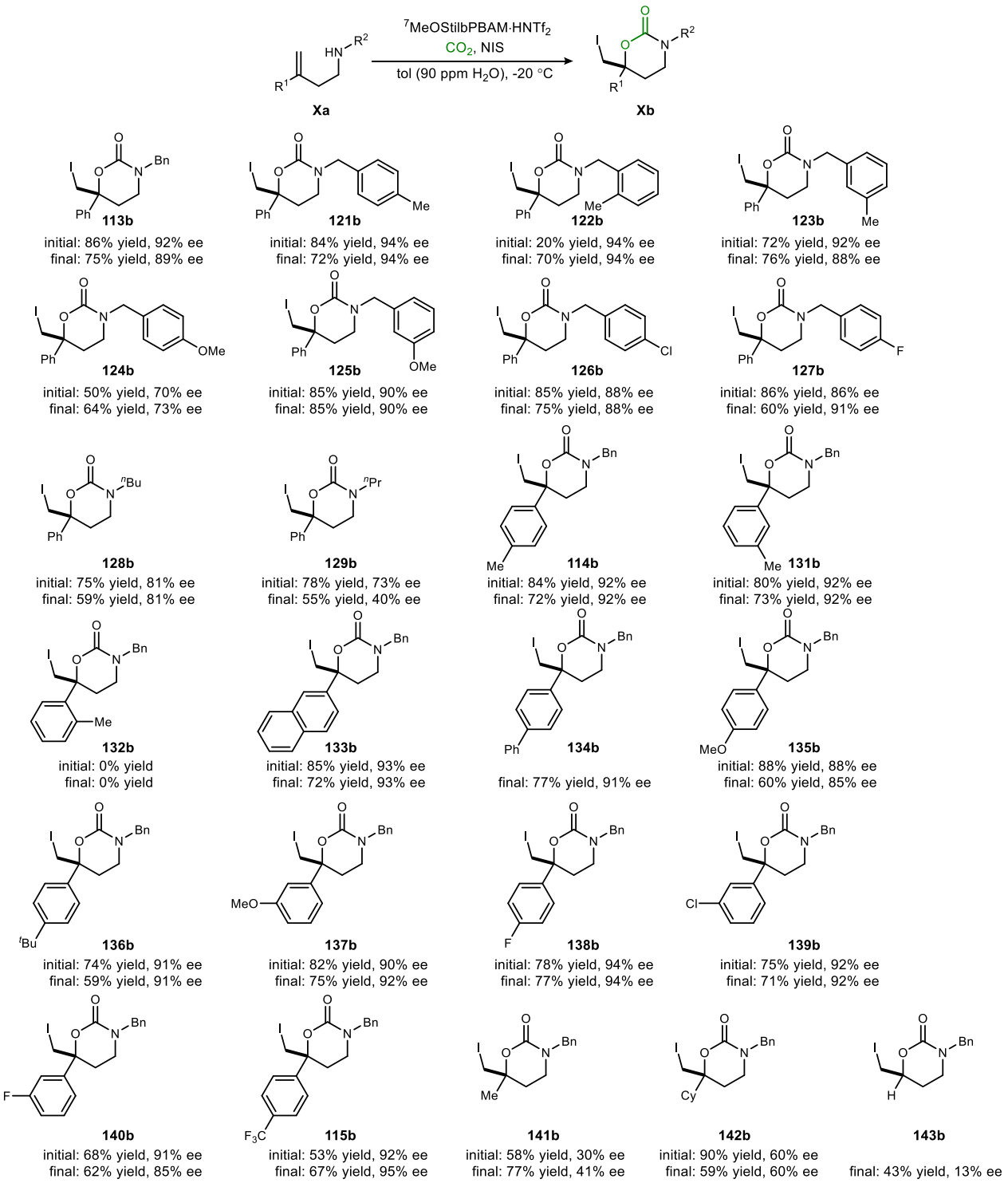

reactive and selective, hoping to reproduce the results collected by Yousefi. To illustrate how successful we were in this venture, the substrate scope shows both initial and final results. The initial results are the results Yousefi reported initially, while the final results were verified by both myself and Vishe and published in the final manuscript.[60] Most the reported results are very similar, which indicates that Yousefi's procedure was presumably quite similar in practice to the modified conditions.

Figure 45 illustrated how the employment of the triturated ligand and wet toluene were broadly effective. A variety of substitutions at the nitrogen protecting group were well tolerated (Figure, **1b**-**10b**). Electronic modifications of the benzyl substituent were largely left selectivity unaffected. Notably, *ortho*-substitution was tolerated, but the reaction time was extended to 5 days (Figure 45, **3b**). The steric nature of the nitrogen has a greater impact on reactivity compared to selectivity, perhaps affecting the rate of CO_2 capture. This illustrates that sterics does not affect the enantiodetermining step. Substituents at the alkene affected the results more significantly, consistent with the preferences for an unhindered π-nucleophile to engage NIS. As expected, electron donating groups (Figure 45, **11b**-**20b**) lead to carbamates in high yield and enantioselectivity (85-93% ee). Highly electron rich *para*-methoxy (**18b**) and sterically demanding 2-napthalene (**16b**) gave the desired product in 85% and 93% ee respectively. Unfortunately, substitution in close proximity to the olefin was not tolerated, as illustrated by substrate **15b**, which was unreactive. Electron deficient aryl rings were prepared in high enantioselectivity (85-95% ee), but longer reaction times were needed for some substrates (5 d for **22b**-**24b**). Olefins bearing aliphatic substituents, as opposed to styrene derivatives, were converted to desired carbamates with moderate selectivity, as shown with substrates **25b** and

Figure 46: Evaluation of trisubstituted alkene in carbamation reaction.

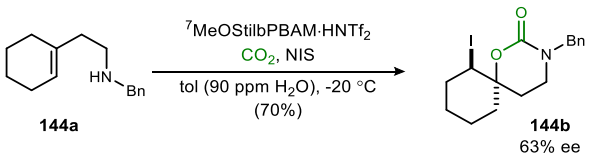

26b. These substrates were produced in 41 and 60% ee respectively. Allylic amines showed moderate reactivity and poor selectivity, as shown in **27b**, where the product was prepared in a 43% yield and 13% ee. Substrate **28a** was prepared to probe trisubstituted alkanes in this chemistry. Despite its increased steric demands and aliphatic substituents, an encouraging level

of reactivity and selectivity was observed. Spirocycle **28b** was produced in 70% yield in 63% ee, as shown in Figure 46. While other trisubstituted olefins weren't evaluated, this result illustrates their potential in this chemistry.

1.2.7 Derivation of cyclic carbamates and target synthesis

Substrate scopes play a critical role in illustrating the broad utility of a new reaction. In addition to developing an enantioselective method to prepare cyclic carbamates, this enantioenriched product can be derivatized to other useful chiral scaffolds. (Figure 47) Importantly, all of these transformations proceed with full retention of stereochemistry. Nucleophilic displacement of the primary halide was carried out with both sodium azide and

Figure 47: Derivations of cyclic carbamate scaffold.

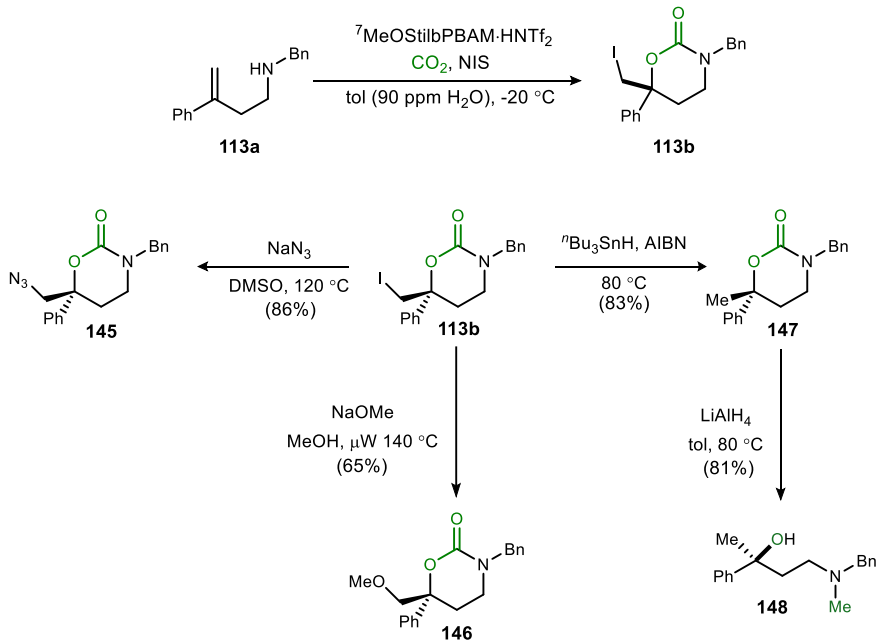

sodium methoxide. The primary halide may also be reduced to remove the halogen functionality. With iodine removed, a reduction with lithium aluminum hydride produces a chiral amino alcohol. The product of the reduction is actually a methylamine, which is an interesting application of carbon dioxide. Carbon dioxide is acting as both a carbon- and oxygen-atom donor.

To illustrate the utility of this reaction, a target molecule was synthesized in good yields and >99% ee on a gram scale. The chiral amino alcohol shown in Figure 48 is a σ_1 inhibitor, with the (*S*)-enantiomer being the most biologically active in the biological investigation.[96-97] the σ_1 receptor is a type of opioid receptor that is closely related to the central nervous system and is involved in neuroprotection.[98] At the behavioral level, this receptor is involved in antipsychotic activity, response to stress and depression, and marked anti-amnesic properties against several modes of amnesia. Because of its critical role in mental health at the physiochemical level, a σ_1 agonist is a potential therapeutic tool in several pathological conditions.

Figure 48: Preparation of σ_1-inhibitor.

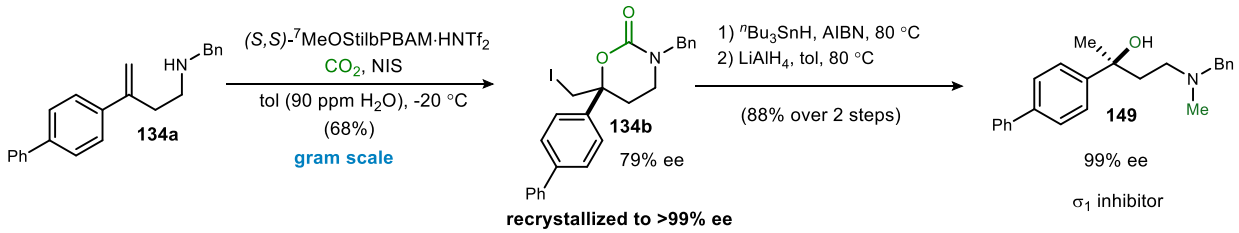

1.2.8 Conclusions

In conclusion, we have developed conditions to prepare enantioenriched cyclic carbamates via CO_2 capture. Optimization of the bisamidine organocatalyst indicated that pK_a had a profound effect on selectivity, which indicates that the basicity of the catalyst may be tuned to the substrate. Additionally, the purification of the chiral ligand had an effect on reactivity. It was proposed that recrystallized ligand formed a well-ordered solid-state structure, which was slow to solubilize and therefore lowered the active catalyst concentration. A rate acceleration was observed in wet toluene, notably this effect was limited to an exact concentration (approximately 4 mol % water). These procedural modifications ultimately made this reaction high yielding, highly repeatable, and scalable. This work simplified the preparation of chiral 6-membered cyclic carbamates. These products may be modified via nucleophilic displacement of the primary

[96] Rossi, D.; Rui, M.; Di Giacomo, M.; Schepmann, D.; Wünsch, B.; Monteleone, S.; Liedl, K. R.; Collina, S. *Bioorg. Med. Chem.* **2017**, *25*, 11.
[97] Quesada-Romero, L.; Mena-Ulecia, K.; Zuñiga, M.; De-la-Torre, P.; Rossi, D.; Tiznado, W.; Collina, S.; Caballero, J. *J. Chemom.* **2015**, *29*, 13.
[98] Alonso, G.; Phan, V. L.; Guillemain, I.; Saunier, M.; Legrand, A.; Anoal, M.; Maurice, T. *Neuroscience* **2000**, *97*, 155.

halides or may be reduced to a chiral amino alcohol. This reduction is an interesting example of CO_2 acting as both an oxygen and carbon donor, as this reduction sequence produced the *N*-Me amine. This carbamation reaction illustrates an interesting alternative to phosgene equivalents, and may be applied to the preparation of small molecule scaffolds.

1.3 Future directions

The work detailed in this chapter is an interesting example an enantioselective multicomponent functionalization of an olefin. Carbon dioxide is utilized as an oxygen and carbon donor. One area of future study that would be interesting is utilizing other C1 donors in this chemistry, such carbon disulfide, isocyanates[29], ketenes, formaldehyde, etc. Each of these donors are dissimilar from carbon dioxide electronically, though sterically they are relatively similar. Developing methods to intercept these various C1 donors would expand the utility of this chemistry to prepare a wide variety of chiral scaffolds. Because the conditions for this carbamation are metal-free and ran at atmospheric pressure, this chemistry would be easy to implement in both academic and industrial settings.

Figure 49: Proposed intermolecular CO_2 capture reaction.

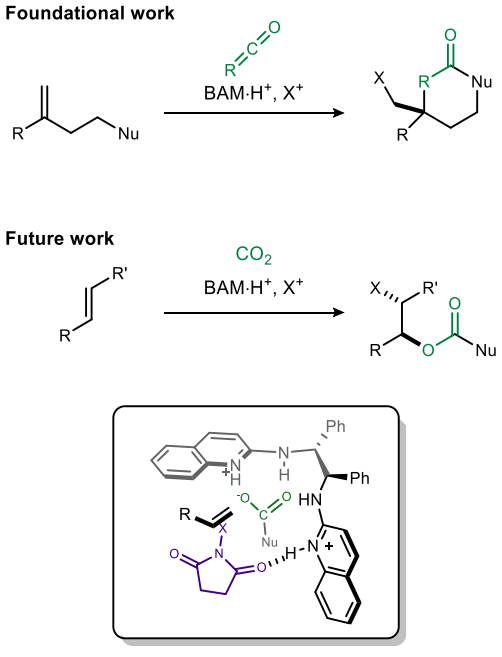

While there are practical applications for this chemistry, it would also be an interesting area of study. Because these electrophiles are so different electronically, ligand development may not be straightforward. As Yousefi illustrated in catalyst optimization, the Brønsted basicity of the catalyst is tuned to match the substrate. Most examples of BAM catalysis report the activation of acidic, O- or N-, or C-atom nucleophiles. Employing other nucleophiles that are basic would be a challenge, however, a carbonyl may be a sufficient H-bond acceptor for activation. Carbon disulfide would be an interesting area of study because S-nucleophiles have not been studied in BAM catalysis. While capable of intramolecular coordination, sulfur is not an equivalent hydrogen bond acceptor to oxygen. It is unclear how a BAM ligand would be modified to activate a sulfur atom. One hypothesis is that a more acidic ligand would be required to activate the less-basic sulfur atom.

An additional area to study would be an intermolecular activation of carbamic acids. The chemistry detailed in this document is an intramolecular functionalization of a halonium species. This intramolecular cyclization is a faster process than the intermolecular variant because the transition state is preorganized by the substrate, which provides an entropic advantage. While this intermolecular variant would be more difficult to develop, it would also be widely applicable as an alternative to dihydroxylation and aminohydroxylation procedures, which often employ toxic transition metals.[99]

The Johnston lab has illustrated that BAM catalysts may be used to intercept multicomponent nucleophiles generated by CO_2 in their reported carbonation[30] and carbamation[60] chemistry. This interaction brings the olefin in close proximity to the activated halogen source, shown as NIS in Figure 49. It is unclear high facial specificity could be obtained in this intermolecular chemistry because all BAM-catalyzed halofunctionalizations are intramolecular. The coordination of the nucleophile via Brønsted base activation adds rigidity to the overall transition state, which means it plays a role in facial selection. Additionally, the use of heterogenous halogen sources such as NIS makes the formation of the halonium intermediate slow.

Developing conditions to affect the functionalization of olefins intermolecularly would be a challenging, but ultimately rewarding, area to study BAM catalysis. Established methods to functionalize unactivated olefins often employs transition metals. The application of

[99] O'Brien, P. *Angew. Chem. Int. Ed.* **1999**, *38*, 326.

organocatalysis poses an interesting challenge because, while olefin activation may be more difficult with non-metallic catalysts, bisamidine catalysts have successfully been employed to activate electron-rich alkenes. Given the wide application of olefin functionalization, it is no doubt that this chemistry would be synthetically useful. Additionally, developing this chemistry would increase our understanding of BAM ligand design. While olefin activation would require a highly Brønsted acidic site, it has been established that a strongly basic ligand accelerates CO_2 capture. This may be a good application of a nonsymmetrical BAM ligand to ensure that both electronic requirements are met. An asymmetrical BAM ligand was successfully developed to affect selective aza-Henry reactions.[26]

Chapter 2 – investigation of aryl triflamides as achiral modifiers in BAM catalysis

2.1 Introduction

The preparation of substituted nitroalkanes is significant because they may be described as "synthetic chameleons", serving as masked functionality to be transformation in future synthetic work.[100] Nitroalkanes are a versatile synthetic handle because they may undergo a Nef reaction[101], nucleophilic displacement[102], reduction to an amino group, or conversion to a nitrile oxide[103]. This broad synthetic utility has generated an interest in the preparation of enantioenriched nitroalkanes as a means to prepare chiral small molecules. Asymmetric conjugate addition reactions are a useful method to prepare chiral molecules because nitroalkenes are strongly electrophilic, receiving various carbon and heteroatom nucleophiles to the β-carbon of the nitroalkene, and then using these addition products in the construction of highly functionalized building blocks.

2.1.1 Organocatalyzed additions to nitroalkenes

[100] Berner, Otto M.; Tedeschi, L.; Enders, D. *Eur. J. Org. Chem.* **2002**, *2002*, 1877.
[101] Noland, W. E. *Chem. Rev.* **1955**, *55*, 137.
[102] Tamura, R.; Kamimura, A.; Ono, N. *Synthesis* **1991**, *1991*, 423.
[103] Mukaiyama, T.; Hoshino, T. *J. Am. Chem. Soc.* **1960**, *82*, 5339.

Asymmetric conjugated additions to nitroalkenes have been broadly studied using chiral auxiliaries[104], metal catalysts[105], and organocatalysis.[100] This section will focus on the development of chiral ligands to affect the addition of various nucleophiles to nitroalkenes. A prominent area of focus has been on the addition of carbonyl-based nucleophiles, with an emphasis on aldehydes, ketones, and 1,3-dicarbonyls. (Figure 50) The predominating mode of activation for aldehyde-based nucleophiles is via enamine catalysis. The Han group developed rigid bicyclic proline-like compounds that catalyze the addition of aldehydes to nitroalkenes.[106]

Figure 50: Evaluation of organocatalysis employed in asymmetric additions to nitroalkenes.

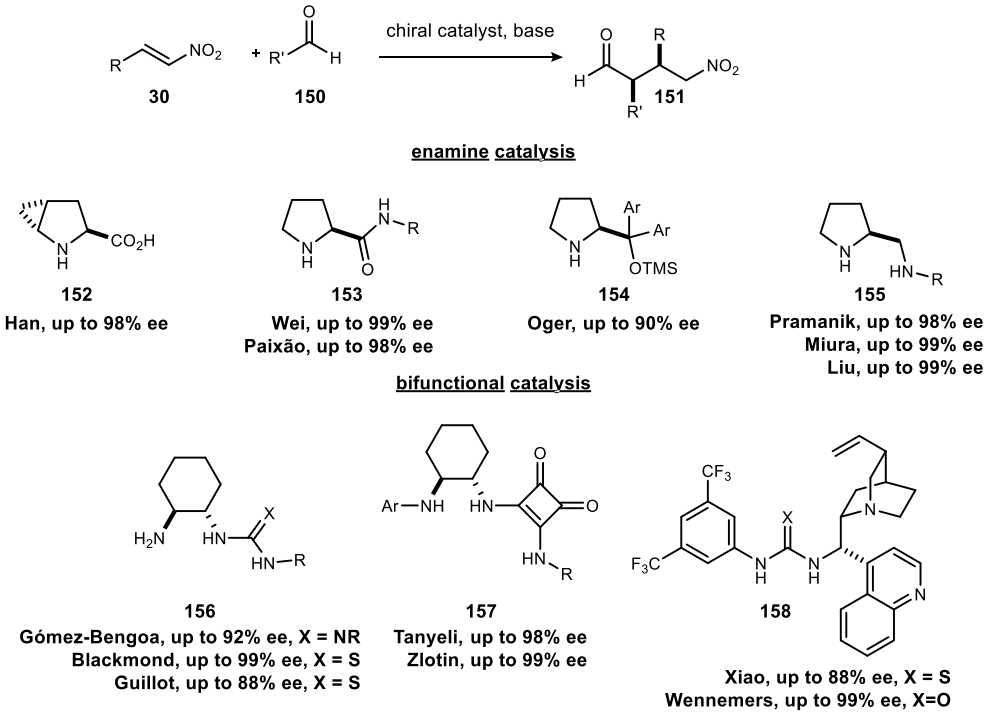

L-Proline only furnished the nitroalkane in 25% ee, but this bicyclic catalyst was highly reactive at 5 mol % catalyst loadings and furnished the product in up to 94% ee and high dr. Another approach for proline catalysis was well-illustrated by the Wei, Lin[107], and the Paixão[108] groups. Both labs found that derivatizing the acid of L-proline via amide-bond forming reactions enabled them to develop highly selective catalysts. Wei prepared sterically encumbered amides, installing

[104] Fernández, R.; Gasch, C.; Lassaletta, J.-M.; Llera, J.-M. *Tetrahedron Lett.* **1994**, *35*, 471.
[105] Hayashi, T.; Senda, T.; Ogasawara, M. *J. Am. Chem. Soc.* **2000**, *122*, 10716.
[106] Yu, H.; Liu, M.; Han, S. *Tetrahedron* **2014**, *70*, 8380.
[107] Wang, Y.; Li, D.; Lin, J.; Wei, K. *RSC Adv.* **2015**, *5*, 5863.
[108] de la Torre, A. F.; Rivera, D. G.; Ferreira, M. A. B.; Corrêa, A. G.; Paixão, M. W. *J. Org. Chem.* **2013**, *78*, 10221.

an N-adamantly group. They observed a clear trend that as the amide substituent increased in size, selectivity improved. The Paixão group ligand development showcased a similar trend, however, small peptide chains were investigated instead of substituted amines. Another common proline catalyst derivative is the Jørgensen-Hayashi catalyst, utilized by Oger and coworkers.[109] Some have sought to move beyond proline catalysis, using bifunctional Brønsted acid/base activation. The Gómez-Bengoa[110] and Blackmond[111] groups both used hydrogen-bond activation to impart facial selectivity. The Gómez-Bengoa utilized a chiral quinidine scaffold to activate the nitroalkene via hydrogen bonding, while the Blackmond group applied a thiourea ligand.

Similar approaches to catalyze the addition of ketones to nitroalkenes were employed, using both enamine[112,113,114] and bifunctional catalysis[115]. Because ketones are less-electrophilic than aldehydes, hydrogen-bonding is a more broadly studied area of catalysis for these substrates. Additionally, a variety of bifunctional catalysts have been developed for 1,3-dicarbonyls.[116,117,118] These additions have served as a method to prepare carbon-carbon bonds in high ee, with both the carbonyl and nitroalkane groups serving as synthetic handles for further modification.

Because there have been a number of successful additions of enols to nitroalkenes to prepare carbon-carbon bonds, many have used these reactions as a template for future work with other strong carbon acids (pKa ~ 10). Nitroalkanes are strong carbon acids, owing to the strong electron-withdrawing effect of the nitro group. For this reason, nitroalkanes may undergo similar addition reactions as carbonyls, while also introducing different functionality. A number of labs have investigated the addition of nitroalkanes to nitroalkenes to prepare 1,3-dinitroalkanes in high ee and dr. (Figure 51) The Wang lab developed a bifunctional amine-thiourea ligand with

[109] Candy, M.; Durand, T.; Galano, J.-M.; Oger, C. *Eur. J. Org. Chem.* **2016**, *2016*, 5813.
[110] Fernandes, T. d. A.; Vizcaíno-Milla, P.; Ravasco, J. M. J. M.; Ortega-Martínez, A.; Sansano, J. M.; Nájera, C.; Costa, P. R. R.; Fiser, B.; Gómez-Bengoa, E. *Tetrahedron: Asymmetry* **2016**, *27*, 118.
[111] Ji, Y.; Blackmond, D. G. *Catal. Sci. Technol.* **2014**, *4*, 3505.
[112] Mahato, C. K.; Kundu, M.; Pramanik, A. *Tetrahedron: Asymmetry* **2017**, *28*, 511.
[113] Nakashima, K.; Hirashima, S.-i.; Kawada, M.; Koseki, Y.; Tada, N.; Itoh, A.; Miura, T. *Tetrahedron Lett.* **2014**, *55*, 2703.
[114] Liu, F.-L.; Chen, J.-R.; Feng, B.; Hu, X.-Q.; Ye, L.-H.; Lu, L.-Q.; Xiao, W.-J. *Org. Biomol. Chem.* **2014**, *12*, 1057.
[115] Capitta, F.; Frongia, A.; Ollivier, J.; Aitken, D. J.; Secci, F.; Piras, P. P.; Guillot, R. *Synlett* **2015**, *26*, 123.
[116] Işık, M.; Unver, M. Y.; Tanyeli, C. *J. Org. Chem.* **2015**, *80*, 828.
[117] Kastl, R.; Arakawa, Y.; Duschmalé, J.; Wiesner, M.; Wennemers, H. *Chimia* **2013**, *67*, 279.
[118] Tukhvatshin, R. S.; Kucherenko, A. S.; Nelyubina, Y. V.; Zlotin, S. G. *ACS Catalysis* **2017**, *7*, 2981.

multiple hydrogen bond donors.[119] These hydrogen bond donors served to activate both -NO_2 groups, for activation of both nucleophile and electrophile to control facial selectivity. To verify this, it was observed that if the sulfonamide residue is methylated, no addition product is observed. Notably, to achieve full conversion, a large excess of nitroalkane was used as a solvent. The Tanyeli group published the same reaction using a quinine squaramide chiral ligand. Similarly, a large excess of nitroalkane was employed. The Johnston lab developed conditions for this reaction using one of their bisamidine ligands.[32] This catalyst proved to be highly efficient, necessitating only five equivalents of nitroalkane to achieve full conversion. To illustrate the broad utility of these addition products, the authors prepared *anti*-$\beta^{2,3}$-amino amides in two steps.

Figure 51: Evaluation of organocatalyzed nitroalkanes additions to nitroalkenes.

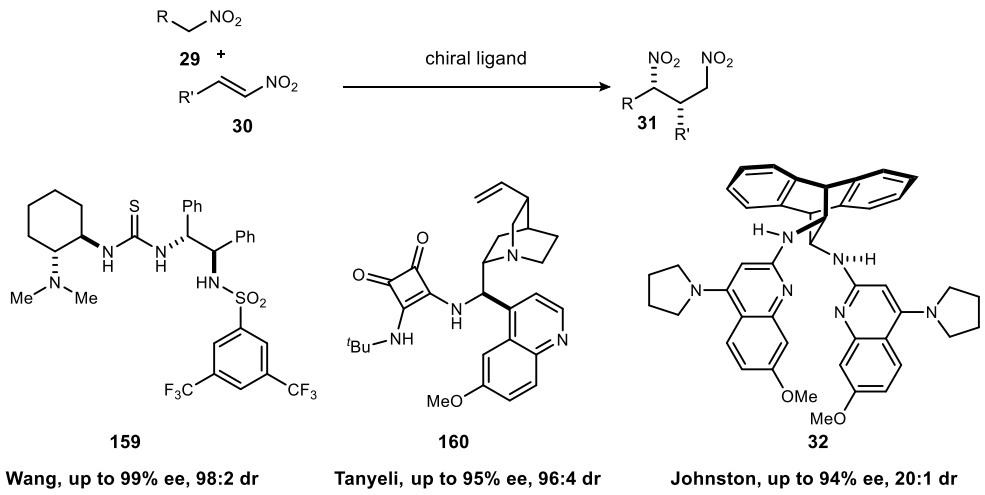

The derivation of nitroalkanes via asymmetric Michael additions has primarily focused on carbon-carbon bond forming reactions. Because these transformations are an efficient method to introduce stereochemical complexity, expanding the scope of this work to include the formation of carbon-heteroatoms is an important and underdeveloped area of study. A number of bifunctional organocatalysts have been investigated in the addition of heteroatom-based nucleophiles, as shown below in Figure 52. It can be difficult to influence heteroatom-derived nucleophiles using hydrogen bond catalysts because the basicity of the substrate can deactivate the chiral ligand. To mitigate these potential issues, most nucleophiles are deactivated by an

[119] Dong, X.-Q.; Teng, H.-L.; Wang, C.-J. *Org. Lett.* **2009**, *11*, 1265.

electron-deficient protecting group. As shown in previous examples, thioureas proved to be an effective hydrogen bond donor.[120] The Herrera lab carried out an aza-Michael addition to prepare β-nitrohydrazides. This served as an interesting alternative to established methods, such as aza-Henry reactions. They propose that the hyrazide is directed via Brønsted base catalysis, where the trisubstituted amine of the ligand hydrogen bonds with the hydrazide. The Wang group utilized a thiourea ligand derived from cinchonine to direct the addition of phthalimide to nitrolefins.[121] The products of this transformation are useful because the phthalimide is a known precursor to amines, making this transformation a useful method to prepare enantioenriched benzylic amines.

Figure 52: Evaluation of various nucleophiles in nitroalkene additions.

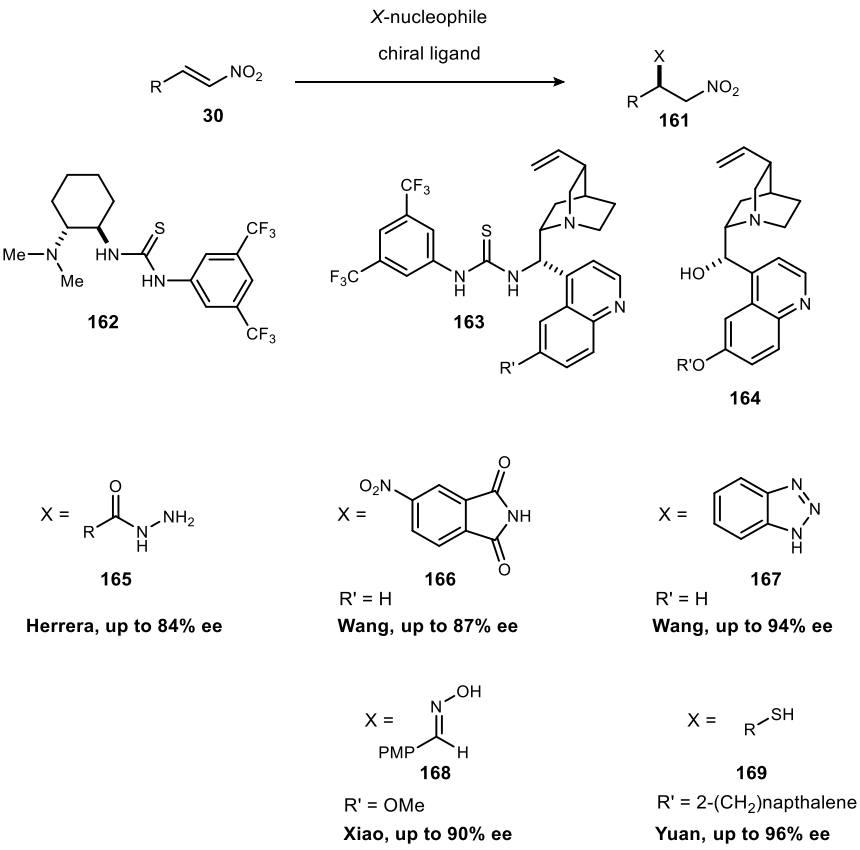

The Xiao group illustrated the application of the same thiourea ligand to affect the addition of oximes to nitroalkenes as a method to prepare enantioenriched amino alcohols.[114] Both the oxime and the nitroalkane may be selectively deprotected, making selective functionalization of the

[120] Alcaine, A.; Marqués-López, E.; Herrera, R. P. *RSC Adv.* **2014**, *4*, 9856.
[121] Ma, S.; Wu, L.; Liu, M.; Huang, Y.; Wang, Y. *Tetrahedron* **2013**, *69*, 2613.

respective heteroatoms relatively straightforward. The Wang group employed a cinchona alkaloid catalyst to direct the addition of triazoles to nitroalkenes.[122] A few other heterocycles were investigated in this reaction, though extended reaction times were required for reactivity. The Yuan group sought to control the addition of thiophenols to trisubstituted nitroalkenes to prepare tertiary thioethers in high ee.[114] The products of this reaction may be derivatized to $\beta^{2,2}$-amino acids. Similar to the hydrazide chemistry published by the Herrera lab, the thiourea serves to activate the nitroalkene while the trisubstituted amine residue activates the thiophenol via hydrogen bonding.

The preparation of enantioenriched nitroalkanes is an active field since they may be derivatized to a wide variety of small molecule scaffolds. Many groups have studied asymmetric Michael additions to nitroalkenes, though most have focused on the formation of carbon-carbon bond forming reactions. There is much to study in the addition of heteroatoms to nitroalkenes, where only a small number of catalysts and nucleophiles have been studied. The work detailed in this chapter seeks to expand the scope of these reactions to include azide nucleophiles. Additionally, we explored the application of bisamidine catalysis to functionalize nitroalkanes. This work is the first example of BAM catalysis effecting azide additions to nitroalkenes to form chiral carbon-nitrogen bonds using hydrazoic acid.

2.1.2 Organocatalyzed nucleophilic azidation reactions

Enantioselective nucleophilic azidation is a prominent strategy to prepare α-chiral azides. The most common nucleophilic sources of azides are azidosilanes, hydrazoic acid, and sodium azides. Though the use of azide as a nucleophile is well precedented in synthesis, there are only two types of enantioselective reactions based on this strategy: ring opening of epoxides or aziridines and conjugate addition to electron-deficient olefins. Most of the established work in this area has utilized transition metal catalysis, though recent work has focused on the developing metal-free conditions.

Using azide as a nucleophile to open enantioenriched epoxides is well-established[123], however, there are not any known enantioselective epoxide opening reactions using azide as a nucleophile.

[122] Wang, J.; Li, H.; Zu, L.; Wang, W. *Org. Lett.* **2006**, *8*, 1391.
[123] Jacobsen, E. N. *Acc. Chem. Res.* **2000**, *33*, 421.

The established chemistry to open epoxides with high facial selectivity use chiral Lewis acids, such as chromium[124], zirconium[125], and zinc[126]. Similar Lewis acids have been applied to the enantioselective ring opening reaction of *meso*- or racemic aziridines. Some notable examples being ytterbium[127], chromium[128], and magnesium[129]. This work showcased the ability of chiral Lewis acids to impart facial selectivity in nucleophilic ring openings of strained ring systems.

The Antilla lab established that chiral Brønsted acid catalysis is effective in the activation of aziridine rings toward nucleophilic ring opening with selectivity.[130] Using a chiral phosphoric acid (CPA) catalyst to activate aziridine rings, they were able to control the addition of $TMSN_3$. Initial mechanistic studies indicated that trimethylsilyl group was critical for facial selectivity, as sodium azide was not reactive in the presence of CPA catalyst. Notably, when the CPA ligand was not employed, sodium azide successfully opened the aziridine ring. Because it is known that basic atoms may activate silane compounds into donating a nucleophile, the Antilla group proposed the transition state shown below in Figure 53. Notably, this mechanism has been disputed by the Della Sala group.[131] Because commercially available phosphoric acids contain variable amounts of metallic impurities, Della Sala proposed that trace impurities may play a role in the catalytic cycle. It was observed that when the CPA ligand was washed with acid prior to its use in this ring opening, racemic product was isolated. This work indicates that a chiral Lewis acid may still be required in aziridine addition reactions.

[124] Martinez, L. E.; Leighton, J. L.; Carsten, D. H.; Jacobsen, E. N. *J. Am. Chem. Soc.* **1995**, *117*, 5897.
[125] McCleland, B. W.; Nugent, W. A.; Finn, M. G. *J. Org. Chem.* **1998**, *63*, 6656.
[126] Hiroyuki, Y. *Bull. Chem. Soc. Jpn.* **1988**, *61*, 1213.
[127] Fukuta, Y.; Mita, T.; Fukuda, N.; Kanai, M.; Shibasaki, M. *J. Am. Chem. Soc.* **2006**, *128*, 6312.
[128] Li, Z.; Fernández, M.; Jacobsen, E. N. *Org. Lett.* **1999**, *1*, 1611.
[129] Nakamura, S.; Hayashi, M.; Kamada, Y.; Sasaki, R.; Hiramatsu, Y.; Shibata, N.; Toru, T. *Tetrahedron Lett.* **2010**, *51*, 3820.
[130] Rowland, E. B.; Rowland, G. B.; Rivera-Otero, E.; Antilla, J. C. *J. Am. Chem. Soc.* **2007**, *129*, 12084.
[131] Della Sala, G. *Tetrahedron* **2013**, *69*, 50.

Figure 53: Evaluation of enantioselective aziridine opening using $TMSN_3$ nucleophile.

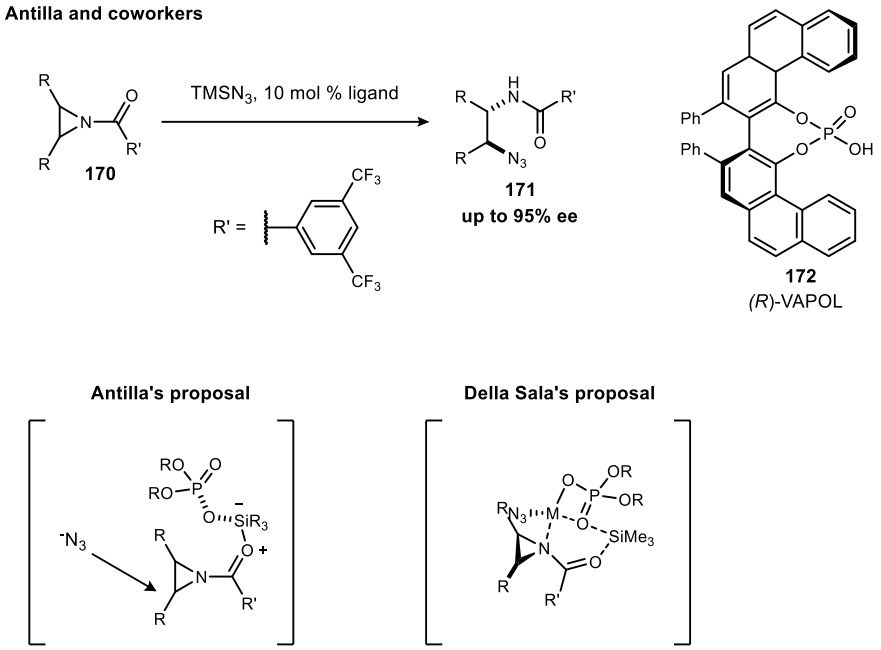

The other primary field of study in enantioselective nucleophilic azide additions is the conjugate addition to electron deficient alkenes, such as α,β-unsaturated carbonyl compounds, nitroalkenes, and allenes. Most examples of enantioselective allene functionalization utilize transition-metal catalysis,[132,133,134] however, there are a number of organocatalyzed azide additions to other electron deficient olefins. The Miller group investigated *β*-peptides as organocatalysts to direct the addition of hydrazoic acid to unsaturated imides (Figure 54).[135] The mechanism of activation is unclear with these catalysts, however they did not observe any non-linear effects, so they propose that the ligand operates as a monomeric form.[136,137] A subsequent investigation into this reaction found that selectivity could be improved by employing a *β*-substituted His derivative.[138] This modification improved ee on their test substrate from 63% ee to 85% ee. Additionally, they were able to improve reactivity at reduced temperatures and expand their substrate scope to include a more diverse library of unsaturated imides.

---

[132] Myers, J. K.; Jacobsen, E. N. *J. Am. Chem. Soc.* **1999**, *121*, 8959.
[133] Zhou, P.; Lin, L.; Chen, L.; Zhong, X.; Liu, X.; Feng, X. *J. Am. Chem. Soc.* **2017**, *139*, 13414.
[134] Khrakovsky, D. A.; Tao, C.; Johnson, M. W.; Thornbury, R. T.; Shevick, S. L.; Toste, F. D. *Angew. Chem. Int. Ed.* **2016**, *55*, 6079.
[135] Horstmann, T. E.; Guerin, D. J.; Miller, S. J. *Angew. Chem. Int. Ed.* **2000**, *39*, 3635.
[136] Satyanarayana, T.; Abraham, S.; Kagan, H. B. *Angew. Chem. Int. Ed.* **2009**, *48*, 456.
[137] Guillaneux, D.; Zhao, S.-H.; Samuel, O.; Rainford, D.; Kagan, H. B. *J. Am. Chem. Soc.* **1994**, *116*, 9430.
[138] Guerin, D. J.; Miller, S. J. *J. Am. Chem. Soc.* **2002**, *124*, 2134.

The Alemán group employed a quinine-derived squaramide ligand to direct $TMSN_3$ to enones in high ee.[139] Unlike most examples of azide additions in organocatalysis, the authors did not generate hydrazoic acid *in situ*. This is an interesting deviation from established work, where authors noted that a hydrogen bond acceptor was needed for nucleophilic control. After investigating the role of water as an additive, the authors observed a rate acceleration in the presence of water. Computation studies supported a mechanistic hypothesis wherein water served to activate $TMSN_3$ via hydrolysis, and in further support of this hypothesis, the formation of trimethylsilanol was noted by ^1H and ^{29}Si NMR. The work of both Miller and Alemán is a significant addition to the field, despite their limited scope. The Miller group's conditions were only applied to imides and the Alemán group was limited to aryl ketones. The identification of a chiral ligand, and its development into a catalyst that is both highly selective and widely applicable would greatly increase the utility of this chemistry.

Figure 54: Evaluation of asymmetric azide additions to enones.

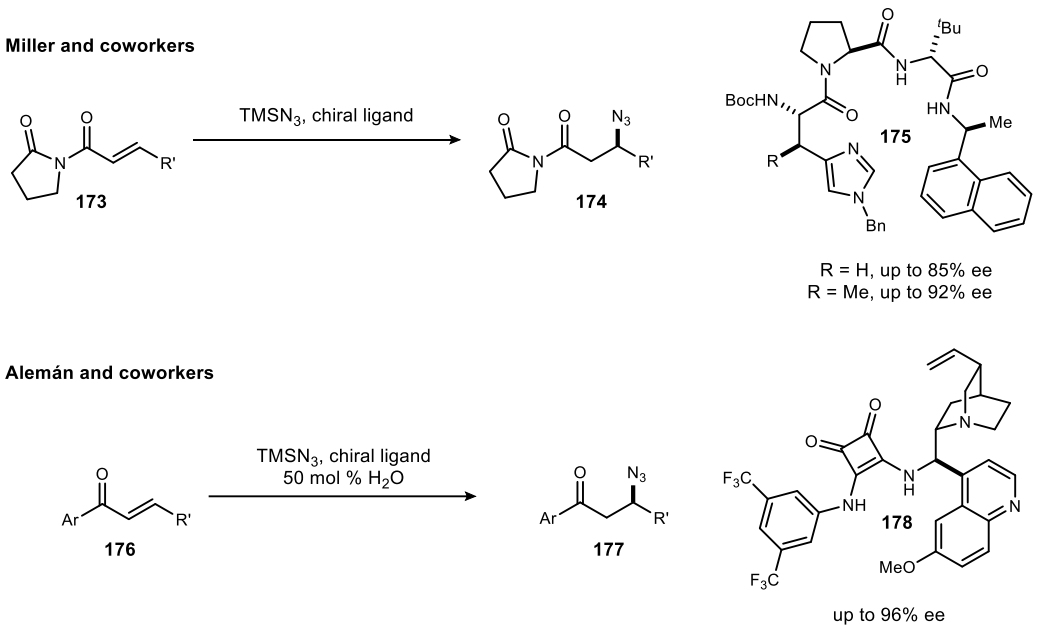

Nitroalkanes are pronucleophiles that have been investigated in the functionalization of electron-poor alkenes. Nitroalkanes are synthetically versatile, and the nitro group is often considered a 'protected' form of amine. The enantioselective addition of azide to nitroalkenes

[139] Humbrías-Martín, J.; Pérez-Aguilar, M. C.; Mas-Ballesté, R.; Dentoni Litta, A.; Lattanzi, A.; Della Sala, G.; Fernández-Salas, J. A.; Alemán, J. *Adv. Synth. Catal.* **2019**, *361*, 4790.

was discovered by the Jørgensen group using a ligand derived from cinchonine.[140] While selectivity was modest, their work served as a proof of concept. They investigated the role of acidic additives in this chemistry and observed a profound effect on selectivity. Despite a large investigation, a single acid could not be identified to be applied broadly. Different substrates required different acids for optimal results. Della Sala applied a bifunctional thiourea ligand to direct the addition of hydrazoic acid to nitroalkenes.[141] This work was an improvement over previous work, showing moderate selectivity in a variety of substrates. However, neither Della Sala nor Jørgensen found conditions to direct the azide to nitrostyrenes. (Figure 55)

There is a clear need to develop better conditions to catalyze the addition of azides to electron-deficient alkenes. We proposed that BAM catalysis could be adapted to additions of this type, with the overall goal to broaden the scope to include azide nucleophiles and nitroalkene electrophiles with an expanded tolerance while remaining highly selective.

Figure 55: Evaluation of asymmetric azide additions to nitroalkenes.

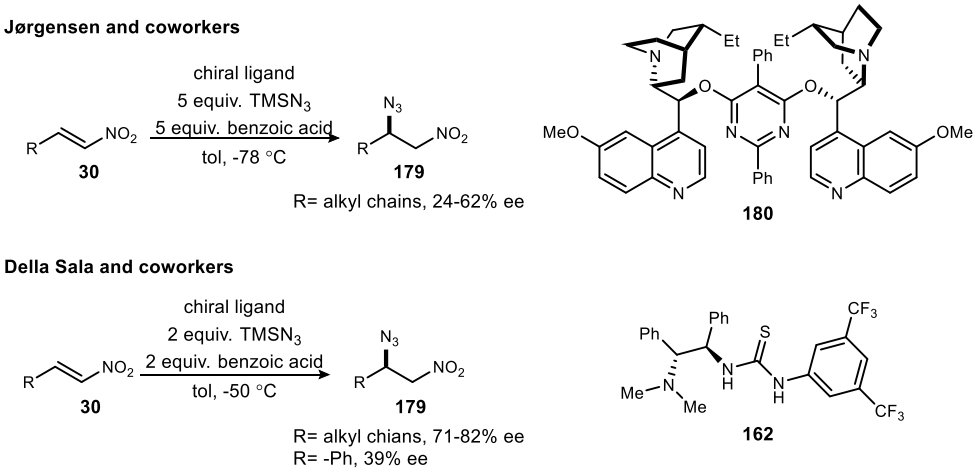

2.1.3 Aryl triflamides as achiral modifiers

When developing bisamidine catalysts for reaction optimization, both the Brønsted basic and acidic portion of the ligands must be considered, owing to their bifunctional nature. It is

[140] Nielsen, M.; Zhuang, W.; Jørgensen, K. A. *Tetrahedron* **2007**, *63*, 5849.
[141] Bellavista, T.; Meninno, S.; Lattanzi, A.; Della Sala, G. *Adv. Synth. Catal.* **2015**, *357*, 3365.

hypothesized, with computational support[22], that the acidic site of the ligand activates the electrophile, enhancing reactivity while controlling facial selectivity. The acidic portion of the ligand is generated by mixing the BAM ligand with a single equivalent of acid, protonating one of the two amidine groups. The 1:1 stoichiometry is an important consideration because nucleophile activation is achieved through the Brønsted basic amidine of the ligand. Importantly, over-protonation of the ligand attenuates (or annihilates) basicity and diminishes catalyst activity and selectivity.[21]

The importance of catalyst basicity on reaction rate has been examined during optimization of a variety of reactions, including the carbamation chemistry described in Chapter 1. Many optimization studies have illustrated the effect that acids have on reactivity and selectivity, but

Table 6: pK_a comparison of common strong acids to aryl triflamides.

Strong acid	pK_a (H_2O)
Tf_2NH	<-14.7
TfOH	-14.7
PhNHTF	4.5
$^3CF_3C_6H_5NHTf$	3.5

the iodolactonization study revealed that ostensibly similar acids (same pKa) could have markedly different selectivities.[19] Though the relationship between counterion and selectivity has been examined in many BAM-catalyzed reactions, most ultimately employ triflimidic acid or triflic acids due to their preparative simplicity. The counterions of these strong acids are considered largely dissociated and thought to have little involvement of the substrate-catalyst complex in the transition state, and therefore little effect on selectivity. However, after observing the effect of weaker acids in previous work[19], it was hypothesized that large achiral acids could have a positive effect on facial selectivity in other reactions. While this effect is not observed in all BAM-catalyzed reactions, it is worthy of exploration because these achiral modifiers serve as an additional variable to explore in catalyst development. We developed a hypothesis that less acidic Brønsted acids, relative to triflimidic acid, could be designed to be electron-deficient hydrogen bond donors while affecting the substrate coordination with their structure. Please note

Table 6 for reported pK_a values of the aforementioned acids.[142,143] A key aspect of this hypothesis is the combination of a chiral neutral ligand (BAM) with an achiral Brønsted acid. *N*-aryl triflamides were identified as potential achiral modifiers for this purpose, and we sought evidence that tied their acidity to activity, and their (achiral) structure to changes in enantioselection.

Trifluoromethanesulfonamides have been used in synthetic, agricultural,[142] and medicinal chemistry.[144] These strong organic acids have been employed extensively in synthetic chemistry, with a prominent role in Brønsted acid catalysis.[145] Another synthetic application of aryl triflamides is Comin's reagent, which is a common triflyl-donating reagent used to prepare vinyl triflates.[146] The therapeutic application of aryl triflamides is attributed to their lipophilicity and ability to hydrogen bond. A few examples of aryl triflamides with biological activity are shown

Figure 56: Application of aryl triflamides in small-molecule therapeutics.

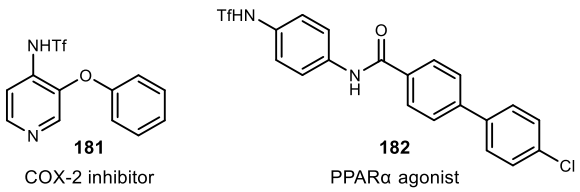

in Figure 56. Compound **181** is a selective COX-2 inhibitor, which may serve as a nonsteroidal anti-inflammatory (NSAID) agent.[147] It was observed that increasing the acidity of the aniline moiety by preparing an aryl triflamide, as opposed to an aryl sulfonamide, the authors were able to selectively inhibit COX-2 over COX-1. This selectivity should reduce side-effects associated with NSAIDs. Compound **182** is a PPARα agonist that may be used to treat issues associated with lipid metabolism.[148] PPARα agonists are used to moderate cholesterol levels in patients.

[142] Trepka, R.; Belisle, J.; Harrington, J. *J. Org. Chem.* **1974**, *39*, 1094.
[143] Trummal, A.; Lipping, L.; Kaljurand, I.; Koppel, I. A.; Leito, I. *The Journal of Physical Chemistry A* **2016**, *120*, 3663.
[144] Shainyan, B. A.; Tolstikova, L. L. *Chem. Rev.* **2013**, *113*, 699.
[145] Cheon, C. H.; Yamamoto, H. *Chem. Commun.* **2011**, *47*, 3043.
[146] Comins, D. L.; Dehghani, A. *Tetrahedron Lett.* **1992**, *33*, 6299.
[147] Julémont, F.; de Leval, X.; Michaux, C.; Damas, J.; Charlier, C.; Durant, F.; Pirotte, B.; Dogné, J.-M. *J. Med. Chem.* **2002**, *45*, 5182.
[148] Faucher, N.; Martres, P.; Laroze, A.; Pineau, O.; Potvain, F.; Grillot, D. *Bioorg. Med. Chem. Lett.* **2008**, *18*, 710.

The application of aryl triflamides as achiral modifiers in enantioselective catalysis is an unprecedented area of study. One parallel to the achiral acid modifier catalyst design can be found in chiral phosphoric acid (CPA) catalysis, particularly those cases that focus on confined cavities.[15] These chiral ligands have been broadly applicable as both organocatalysts[149,150] and as ligands in transition metal catalysis.[151] These ligands are such a successful class of Brønsted acid catalysts because the steric environment around the chiral phosphoric acid framework is highly tunable. Large aromatic ring systems at the 2/2' positions in order to extend the CPA and to confine the pocket. For example, List's dimerized systems create a confined pocket for substrate

Figure 57: Proposed application of aryl triflamides to mirror CPA catalysis.

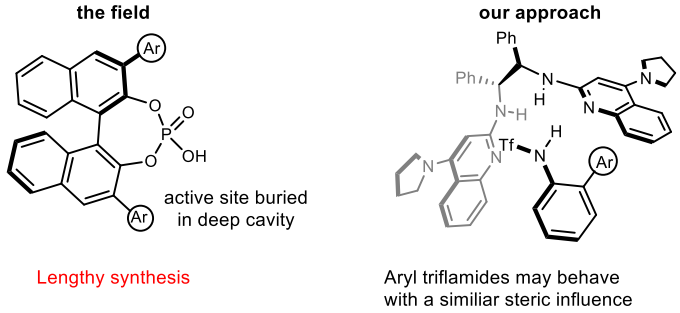

to be activated.[152,153] While this approach was proven to be effective, the preparation of these expansive ligands can be synthetically demanding.[154] If aryl triflamides can effectively achieve a more confined pocket, but using hydrogen bonding to structure it, the preparation and development of organocatalysts would be more efficient. (Figure 57)

Aryl triflamides may serve as a synthetically efficient alternative to these flanking aryl substituents. It is well precedented in BAM catalysis that strong acids serve as proton donors to generate Brønsted acid sites for activation. The resulting amidinium is a potent hydrogen bond donor that may serve to activate a variety of substrates. Because aryl triflamides are less acidic than triflimidic acid, they are not expected to fully dissociate from the ligand. Therefore, they

[149] Uraguchi, D.; Terada, M. *J. Am. Chem. Soc.* **2004**, *126*, 5356.
[150] Riva, R. *Science* **2018**, *361*, 1072.
[151] Rueping, M.; Koenigs, R. M.; Atodiresei, I. *Chem. Eur. J.* **2010**, *16*, 9350.
[152] Čorić, I.; List, B. *Nature* **2012**, *483*, 315.
[153] Tsuji, N.; Kennemur, J. L.; Buyck, T.; Lee, S.; Prévost, S.; Kaib, P. S. J.; Bykov, D.; Farès, C.; List, B. *Science* **2018**, *359*, 1501.
[154] Gatzenmeier, T.; Turberg, M.; Yepes, D.; Xie, Y.; Neese, F.; Bistoni, G.; List, B. *J. Am. Chem. Soc.* **2018**, *140*, 12671.

will flank the BAM ligand pocket through either hydrogen bonding or ionic association. The goal in this work is to design BAM-triflamide combinations that craft the size and shape of the ligand pocket, similar to the phosphoric acid functionality and flanking aryl substituents that are covalently linked in CPA catalysts. This would be a more synthetically tractable approach to catalyst development because rather than undergoing an extensive synthetic sequence to design a tailor-made catalyst, one could use aryl triflamides instead. The broader vision includes adaptation of this strategy to other non-metal and metal-based systems alike, to arrive at simplified catalyst structures. Tools that enable this approach would accelerate catalyst screening and design.

Postdoctoral Scholar Mahesh Vishe prepared and investigated aryl triflamides in a variety of reactions. Unfortunately, he was unable to identify a reaction where they outperformed triflimidic acid. In the course of his research, he was able to obtain two co-crystal structures of aryl triflamides bound to StilbPBAM in a 1:1 molar ratio via X-ray diffraction. (Figure 58) Vishe obtained these crystals from dichloromethane and hexanes. These structures have been informative, showcasing how small modifications to the aryl triflamide scaffold have a significant effect on how the acid coordinates to the BAM ligand. In the first box of Figure 58, the *ortho*-substituted aryl bis(triflamide) coordinates to the BAM ligand through four hydrogen bonds, measuring at 2.04, 2.08, 2.09, and 2.18 Å. The aryl triflamide is tightly bound to the ligand, greatly reducing the size of the ligand pocket. Moving to the *meta*-substituted derivative, as shown in the second box, the aryl triflamide is bound to two BAM ligands. Each triflamide residue is bound to a different ligand molecule via two hydrogen bonds, measuring at 1.96 and 2.18 Å. Modifying the substitution pattern had a profound effect on size of the catalyst pocket in the solid state. Though the aryl bis(triflamide) residues bind to the BAM ligand differently, both structures show a bidentate coordination of the achiral modifier to the chiral ligand. While the size of the catalyst pocket is modified, the orientation of the chiral ligand is largely unchanged, with the dihedral angles in both structures measuring at 59° and 58° respectively. This second example is an excellent illustration of the achiral modifier effect we are hoping to design. One side of the ligand pocket is hindered by an aryl ring, while the other side is open to substrate coordination. This would greatly restrict the rotation of the substrate in the catalyst pocket, and thus affect facial selectivity.

Figure 58: Analysis of BAM·aryl triflamides complexes via XRD.

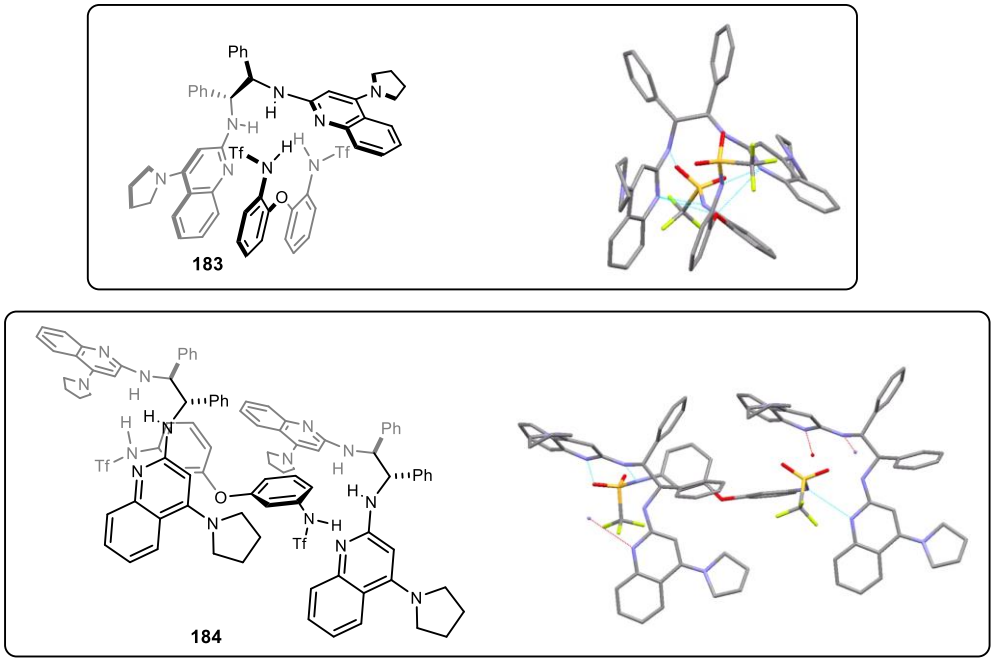

The contents of this chapter will explore the effect of aryl triflamides on the addition of hydrazoic acid to nitroalkenes. In this work, a ligand system which had originally been evaluated as a failure was restored through the application of aryl triflamides. This work illustrates the potential of aryl triflamides as achiral modifiers in BAM catalysis. Given the prevalence of acid salts in organocatalysis broadly, we are optimistic that these aryl triflamides could find applications in other reactions, and more significantly, in other areas of catalysis.

2.2. Development of azide addition to nitroalkenes

2.2.1 Proposal for enantioselective azide addition to nitroalkenes

An unsolved problem in asymmetric catalysis is the lack of methods available to create C-N bonds selectively.[155] There are also few examples that do so using azide as the

[155] Yin, Q.; Shi, Y.; Wang, J.; Zhang, X. *Chem. Soc. Rev.* **2020**, *49*, 6141.

nucleophile.[138,139,156] We propose using BAM catalysis to direct the addition of azide into nitroalkenes enantioselectively. This addition is significant because it will form a C-N bond

Figure 59: Proposed addition of hydrazoic acid to nitroalkenes.

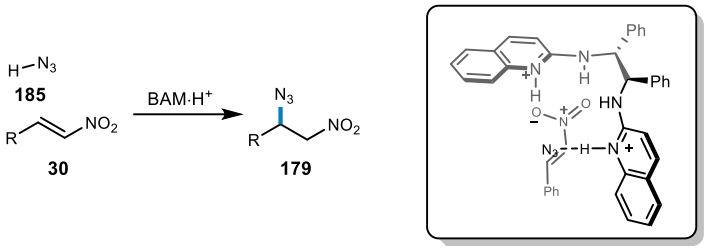

derived stereocenter from intermolecular addition. (Figure 59) Previous work in the field has focused on the addition to β-alkyl nitroalkenes, while the work detailed in this chapter focuses on β-aryl substrates. Because most of our BAM catalysis forms C-O or C-C bonds, it is a notable challenge to develop a catalyst system to direct good nucleophiles, such as azide. This proposal focuses on using this stereoselective addition reaction to make β-substituted nitroalkanes, which in turn are derivatized to a variety of chiral scaffolds, vicinal diamines being a key example. Both benzylic azides and vicinal diamines are common building blocks for the preparation of medicinal compounds, organocatalyst precursors by mild reduction, and ligands for metal complexes.[157,158] An additional utility of azides is that they are precursors to amines.

Figure 60: Reported azide additions to nitroalkenes.

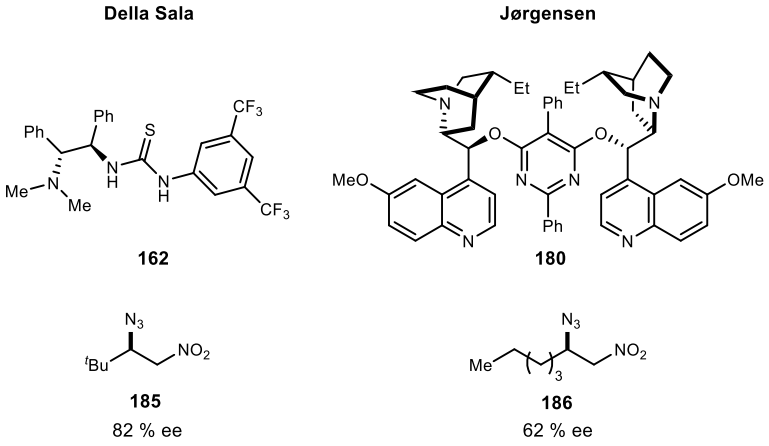

[156] Ding, P.-G.; Hu, X.-S.; Zhou, F.; Zhou, J. *Organic Chemistry Frontiers* **2018**, *5*, 1542.
[157] Lucet, D.; Gall, T. L.; Mioskowski, C. *Angew. Chem. Int. Ed.* **1998**, *37*, 2580.
[158] Kizirian, J.-C. *Chem. Rev.* **2008**, *108*, 140.

The Della Sala group has investigated the addition of azide into nitroalkenes enantioselectively using a secondary amine-thiourea catalyst.[141] They obtained good yields and moderate ee (up to 82% ee) with alkyl substrates. However, nitrostyrene performed poorly in the conditions, the respective product isolated in 39% ee. Prior to Della Sala's work, the Jørgensen group used a cinchona alkaloid catalyst library to direct azide into nitroalkenes with ee ranging from 27-62%.[140] Their results serve as a proof of concept. (Figure 60) A key conclusion from both groups' work was the necessity of a proton source. The catalyst must access the azide though a hydrogen bond interaction in order to control the face of electrophile attack. They proposed that hydrazoic acid is generated in-situ when $TMSN_3$ reacts with the acid source to provide a hydrogen bond donor. The previous work in this field is promising and provides a good starting point for improvement to synthetically useful levels.

The proposed work is premised by two key recent findings in the application of BAM catalysis. (Figure 61) First, Vishe established the possibility of BAM-controlled enantioselection using nitroalkene electrophiles.[32] Second, Struble and coworkers were the first to use BAM catalysis for *N*-cyclization of a urea, thereby achieving control over a nitrogen nucleophile.[29] Until this recent publication, BAM catalysis exclusively catalyzed the formation of C-O or C-C bonds. The organocatalyzed urea cyclization expanded the confines of BAM catalysis, albeit with a very hindered amine and an intramolecular reaction. Using these two findings, we hypothesized that BAM catalysis might be extended to the enantioselective addition of azide to

Figure 61: Recent work in BAM catalysis that include demonstrate a) an asymmetric addition to nitroalkanes and b) preparation of C-N bonds in high ee.

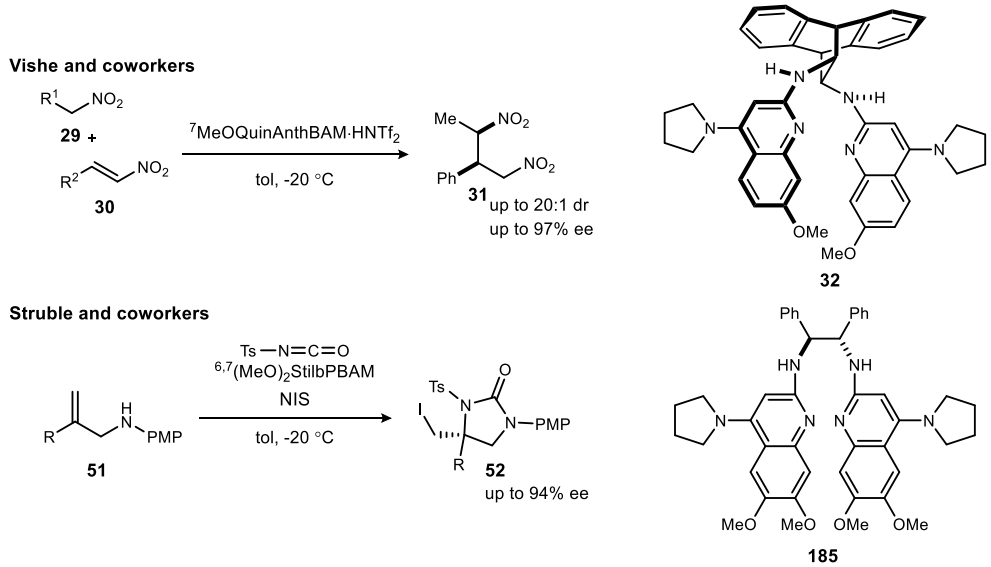

nitroalkenes.

2.2.2 Initial reaction optimization

When the addition of azide into nitroalkenes was first investigated with BAM catalysis, conversion to product was very low. Even with reaction times as long as 6 days, only a 25% yield was observed (Table 7). However, upon addition of 100 mol % of acid, full conversion was achieved, consistent with the generation of HN_3 nucleophile. While the addition of acid is critical for conversion, the product obtained was racemic. Initial work was performed using BAM and AnthBAM derived ligands (see Table 7). Attempts to decrease the substrate-binding pocket size by using a ligand derived from a diamine with a smaller dihedral angle began with StilbPBAM, but gave low ee (9% ee). The absolute configuration of the β-azido nitroalkane was determined using Della Sala's work.[125] This result prompted us to move forward with the stilbene backbone. It was hypothesized that a smaller dihedral angle (i.e. StilbPBAM) furnished the product with some enantioselection because there is a smaller cavity for the presentation of the polar ionic hydrogen bond. This presentation determines which face of the nitroalkene will be attacked by azide.

Table 7: Evaluation of BAM ligands to affect the addition of hydrazoic acid to nitroalkenes.

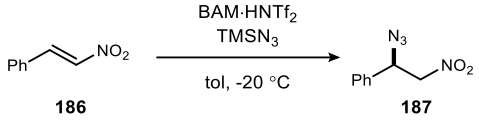

186 **187**

BAM·HNTf$_2$	yield (%)	ee (%)
StilbPBAM	25	9
PBAM	35	0
AnthPBAM	0	-

With StilbPBAM in hand, the catalyst system was further optimized. Noting the necessity of 100 mol % acid addition, a screen was performed to see if these acids had an additional effect on ee. It was found that strong acids, including triflic and triflimidic acid, ablated reactivity. As more acids were investigated, it was observed that acids with a pK_a less than 3 reduced reactivity greatly. It was proposed that reactivity diminished because the BAM ligand was over-protonated,

and the Brønsted basic portion of the ligand was necessary for reactivity. As shown in Table 8, carboxylic acid derivatives were optimal for selectivity. It was observed that phthalic acid was the best acid for both reactivity and selectivity. Notably, when strong acids were employed as the proton source, reactivity was ablated. Additionally, a variety of protic additives were evaluated, however none of them were as successful as the carboxylic acids.

It was encouraging to see selectivity improve with different proton sources, however these results were still insufficient (Table 8). A variety of BAM ligands were evaluated to no avail, selectivity was never observed above 19% ee. We observed that modifications to the Brønsted basic portion of the ligands had a minimal effect on selectivity. It was hypothesized that a more successful catalyst could be designed by modifying the Brønsted acidic site given the effect

Table 8: Evaluation of proton sources in azide addition.

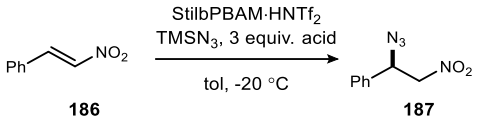

186 187

entry	H^+ source (3 equiv.)	yield (%)	ee (%)
1	acetic acid	96	12
2	benzoic acid	83	3
3	phthalic acid	20	19
4	phthalic acid (1 equiv.)	86	14
5	3,4,5,6-tetrafluorophthalic acid	0	-

different proton sources had on enantioselectivity. We observed that modifications to the Brønsted basic portion of the ligands had a minimal effect on selectivity. It seemed that the only place remaining to explore as a variable was the counterion. As explained earlier, the counterion is normally designed for its ability to dissociate, allowing the substrate to bind for activation. However, we considered an acid design that retained the electron-deficient character, while using a more covalent network to sterically influence substrate-catalyst binding. An acid design was therefore explored that might restrict the size and shape of the ligand pocket. Initial optimization in this azide addition chemistry showed that the stilbene diamine was the most selective, presumably because the smaller cavity is optimal for hydrogen bonding. The size of the cavity could be further reduced if an achiral modifier was tightly bound to the BAM ligand.

We investigated aryl triflamides as a proton source because, in addition to generating hydrazoic acid in-situ, they may further restrict the size and shape of the ligand pocket. Aryl triflamides are similar in acidity to triflic acid and triflimidic acid, which have an established history in BAM catalysis. Unlike these strong acids, aryl triflamides are significantly bigger in size, and we anticipated that the aryl ring could be used to further craft its steric presentation. We proposed that a catalyst prepared from an aryl triflamide may be effective. The conjugate base may remain in the coordination sphere of the BAM ligand, thereby further restricting the size of the ligand pocket, acting as an achiral modifier.

Figure 62: Evaluation of aryl triflamides as proton source.

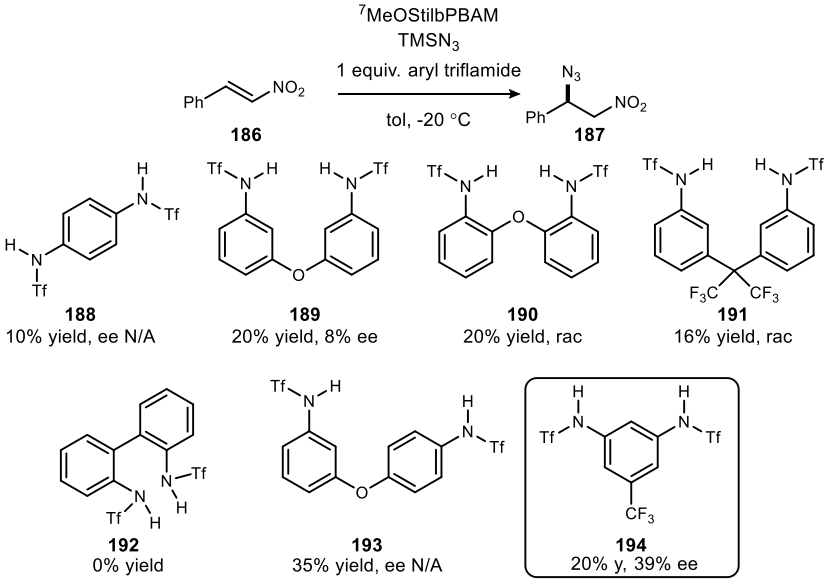

To probe this hypothesis, a variety of aryl triflamides were screened, as shown in Figure 62. When these aryl triflamides were employed as the proton source, reactivity was quite low. The poor reactivity observed with aryl triflamides aligned with initial work, where strong acids reduced ablated reactivity. While none of the biaryl triflamides had an effect on ee, aryl triflamide **194** improved selectivity greatly, up to 39% ee. While 39% is moderate selectivity at best, this was a significant improvement over established selectivity.

It was evident that these aryl triflamides could be applied to this azide addition and have an effect on enantioselectivity. However, the issues with reactivity had to be addressed in order to move forward (Figure 62). Instead of employing the aryl triflamide in stoichiometric quantities, it was proposed that the BAM·triflamide salt may serve as a highly selective catalyst, while

phthalic acid will may serve as a highly reactive proton source to generate hydrazoic acid. This hypothesis was probed with two BAM ligands, and we were delighted to see reactivity and selectivity improve with both cases. The StilbPBAM and ^{7}MeOStilbPBAM ligand salts prepared the β-azido nitroalkane in 65% and 56% ee respectively (Figure 63). These results indicated that modifying the Brønsted acid portion of the catalyst had a profound effect on selectivity. While both examples were only moderately selective, it was encouraging to see that the effect of achiral modifier was consistent with two different ligands. Future work focused on exploring these achiral modifiers further to develop a highly selective reaction.

Figure 63: Evaluation of BAM·aryl triflamide salts.

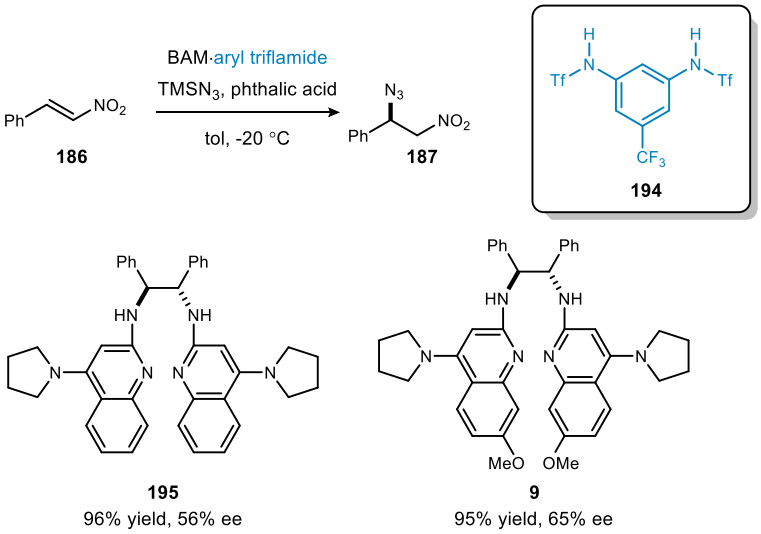

In contrast to all prior work where a monoprotic acid (Tf_2NH, TfOH) was used in combination with the ligand, these *N*-aryl disulfonamides are diprotic acids. All of these initial studies were conducted with catalysts in a 1:1 BAM:aryl bis(triflamide) ratio. It was unclear if the 1:1 ratio would be optimal for reactivity. A 1:1 molar ratio is actually a 1:2 BAM·H^+ ratio, meaning the ligand may be in a doubly protonated state, although this represents the extreme at which a proton is transferred from acid to base. Because the generation of hydrazoic acid was imperative to both reactivity and selectivity, it was proposed that the Brønsted basic portion of the ligand must be maintained for optimal catalysis. To probe this effect, a variety of BAM salts were prepared using StilbPBAM and aryl bis(triflamide) **194**. The optimal ratio for selectivity was confirmed to be a 1:1 molar ratio. Interestingly, when the aryl bis(triflamide) was employed in a

large excess (relative to the BAM ligand), the facial selectivity inverted. While this effect was interesting, selectivity was so low in these conditions that it was not explored further.

Figure 64: The evaluation of BAM·aryl triflamide (1:X) molar ratio on facial selectivity.

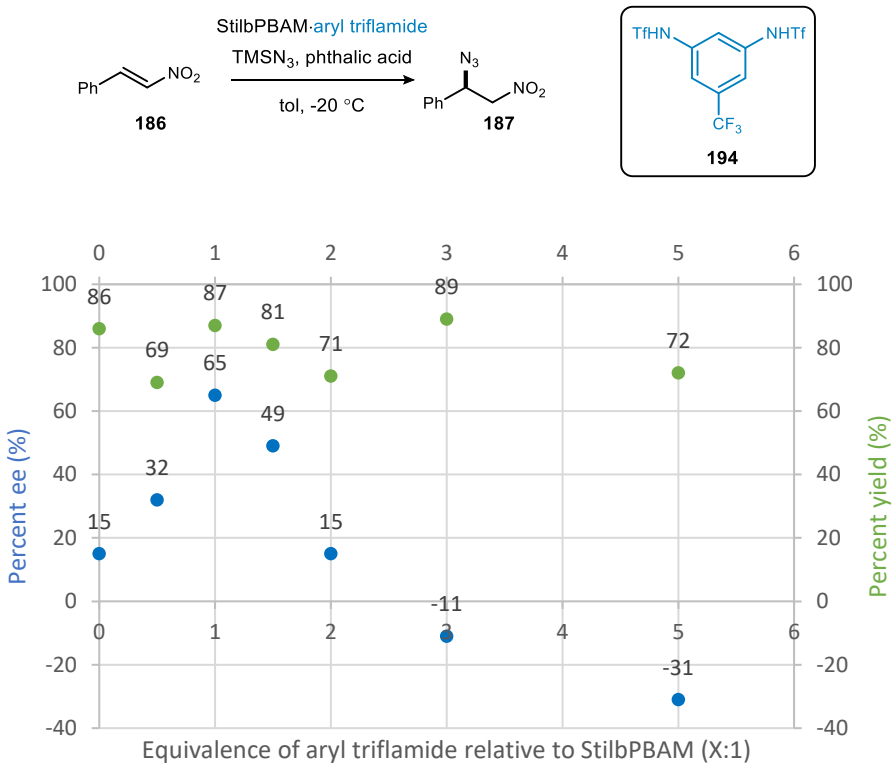

Because hydrazoic acid was generated *in situ*, it was proposed that a different source of azide may have an effect on selectivity (Figure 64). $TMSN_3$ is fully soluble in the reaction conditions, however, most azide salts are minimally soluble. To see if a heterogenous azide salt would affect this chemistry, we evaluated sodium azide and tetrabutyl ammonium azide. Unfortunately, these heterogenous azide sources proved to be significantly less reactive than $TMSN_3$ because of their diminished solubility and were not pursued further.

Investigating the effect of heterogenous azide sources on this chemistry illustrated that solubility may have a significant effect on reaction performance. To investigate this effect further, a solvent screen was performed. Unlike previous examples of BAM catalysis, this reaction is relatively unaffected by a wide range of solvents. In the past, toluene has been the

Table 9: Evaluation of azide sources.

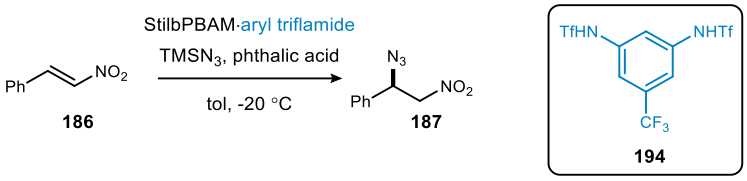

azide source	yield (%)	ee (%)
$TMSN_3$	86	61
NaN_3	9	43
NBu_4N_3	0	-

ideal solvent in BAM catalysis because it does not participate in hydrogen bonding. This is a driving force for nitroalkene to enter catalyst pocket and displace solvent molecules. Aryl triflamide salts of BAM ligands have a different solubility profile and therefore are largely unaffected by polar solvents, with a few exceptions. Both acetonitrile and chloroform performed poorly. It is known that chloroform can react with azide by substitution, which would sequester

Table 10: Evaluation of different solvents on azide additions.

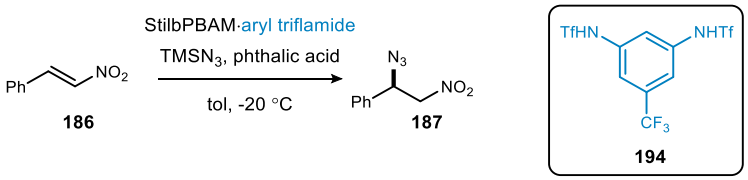

entry	solvent	yield (%)	ee (%)
1	toluene	80	65
2	trifluorotoluene	95	50
3	dichloromethane	83	66
4	chloroform	0	-
5	1:1 dichloromethane/toluene	87	68
6	acetonitrile	55	44
7	diethyl ether	70	62

the azide and prevent any reactivity. Acetonitrile is a polar solvent, which may disfavor the coordination of the nitroalkane to the BAM catalyst. In such a polar solvent system, it was impressive to observe even moderate selectivity. Ethereal and halogenated solvents proved to be effective, which is uncommon in BAM catalysis. While these solvent effects were interesting, no solvent proved to be significantly better than toluene.

As the conditions for this reaction were optimized, it was observed that half an equivalent of phthalic acid (a diacid) was optimal for selectivity, furnishing the nitroalkane in greater than 70% ee. Because modifying the conditions did not have a significant effect on the reaction, ligand design was pursued. It was hypothesized that a more basic BAM ligand would form a shorter hydrogen bond with the aryl triflamide. Coordination of the aryl triflamide to the BAM ligand had a significant effect on selectivity, so strengthening this effect might improve selectivity by creating a 'tighter' pocket. To probe this effect, a variety of BAM ligands were

Figure 65: Evaluation of ligand modifications to affect ee.

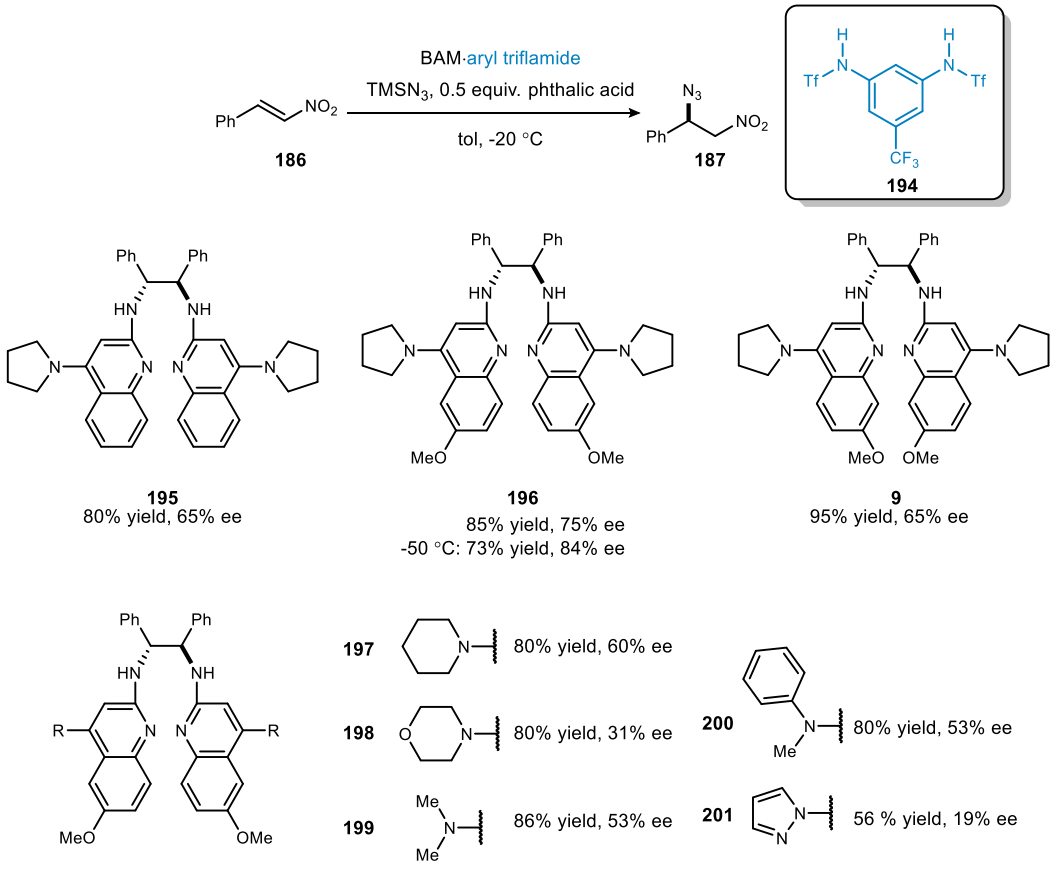

evaluated. As shown in Figure 65, employing a more basic ligand (^{6}MeOStilbPBAM) improved selectivity, consistent with our hypothesis. However, the trend did not hold for ^{7}MeOStilbPBAM. After looking at the crystal structure of the chiral ligand, as shown in Chapter 1, it was observed that the methoxy groups added congestion to the ligand pocket. Though the ligand is more basic, the substituents may block the coordination of the aryl triflamide due to steric effects. To investigate the role of ligand basicity further, substitutions were made at the 4-position. It was proposed that substituents at this position played a significant role in the electronic effects on the ligand, without disturbing the shape of the ligand pocket. Unfortunately, more basic substituents did not have a positive effect on selectivity for reasons that aren't immediately apparent. It is possible that basic heterocycles, though they are more electron rich, may serve as additional sites of hydrogen bonding and thus destabilize aryl triflamide coordination to the BAM ligand. Notably, the reaction temperature could be lowered to -50 °C to bring enantioselectivity up to 84% ee.

Table 11: Summary of procedural modifications to improve ee.

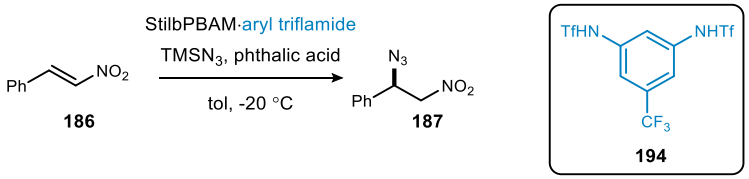

entry	procedural modifications	yield (%)	ee (%)
1	none	95	65
2	^{6}MeOStilbPBAM	82	70
3	phthalic anhydride instead of acid	40	89
4	phthalic acid, $CaCl_2$	85	75
5	**-50 °C**	**73**	**84**
6	1:1 tol/TBME	40	87
7	1:1 tol/CPME	41	87

After many iterations of condition screening and ligand design, selectivity was improved from 65% ee to 84% ee, which is a significant improvement (Table 11). However, increasing selectivity above 84% ee proved to be quite difficult while also maintaining conversion. Various modifications improved selectivity to 89% ee, however, conversion diminished greatly. These modifications included employing phthalic anhydride instead of phthalic acid and using

cyclopentyl methyl ether/toluene solvent mixtures. Phthalic anhydride may serve as a drying agent to generate phthalic acid *in situ*. Unfortunately, other drying agents did not have a similar effect on selectivity. The aryl triflamide salt of ^{6}MeOStilbPBAM was minimally soluble in cyclopentyl methyl ether (CPME), and a remarkable improvement in selectivity was observed with a huge determent to reactivity. A similar effect was observed with *tert*-butyl methyl ether.

These results indicated that in order to develop a highly selective reaction, simply modifying the reaction conditions would not be sufficient. Given the profound effect the aryl triflamide had on selectivity, it was proposed that modifying this scaffold may be the most promising approach to further improving ee. More importantly, modifying the triflamide scaffold presents an opportunity to study these achiral modifiers further.

2.2.3 Application of aryl triflamides as an achiral modifier in BAM catalysis

Aryl triflamide **194** proved to be the most effective acid in the preparation of the BAM catalyst. It was unclear why this specific acid was so effective. To probe this further, a library of aryl triflamides were prepared to study how the substitution of the triflamide ring affected the reaction. By understanding the factors that contributed to acid **194**'s success, we hope to design a

Figure 66: Proposed modifications to aryl triflamides scaffold.

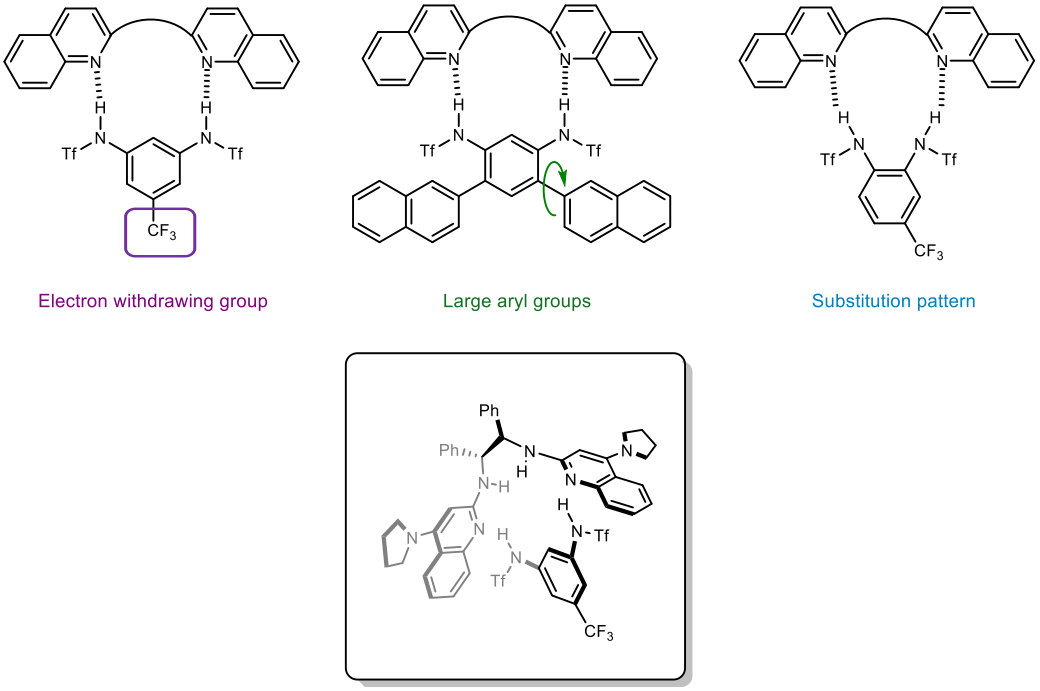

more effective acid. It is hypothesized that two triflamide residues are required because there is a bidentate coordination of the aryl triflamide residue to the amidine portion of the BAM ligand. Based on this hypothesis, we have chosen to investigate three variables in our triflamide scaffold, as depicted in Figure 66.

One of the first areas we hoped to investigate was the acidity of the aryl triflamide residue. The trifluoromethyl group is a withdrawing group that enhances the acidity of the triflamide. As mentioned in Section 2.2.2, we proposed that increasing the basicity of the chiral ligand may strengthen the hydrogen bond to the acid. While this was not always effective, a more acidic triflamide may be a different approach to achieve the same effect. To be clear, there is likely a balance of donating/accepting ability that must be optimized for highest selectivity. The second variable we wanted to pursue was using large aryl rings at the *ortho*-position of the triflamide residue. To stabilize the bidentate coordination of the triflamide residue to the BAM ligand, large aryl groups may restrict the rotation of the C-N. This may ensure the N-H bond is outward facing, toward the ligand and thus enhancing this coordination. The third factor to pursue was the substitution of the aryl ring. Triflamide **194** followed a 1,3,5-substitution motif. It was unclear if this spatial arrangement is matched with the chiral ligand, or if there is flexibility. Moving to a 1,2-diamine scaffold may further restrict the ligand pocket size and thus improve ee. Additionally, it's possible that only one triflamide residue is discretely bound to the BAM ligand. The other triflamide structure may be serving primarily a steric effect, and therefore not contribute significantly to the active catalyst form.

Figure 67: Evaluation of different different aryl bis(triflamide) scaffolds.

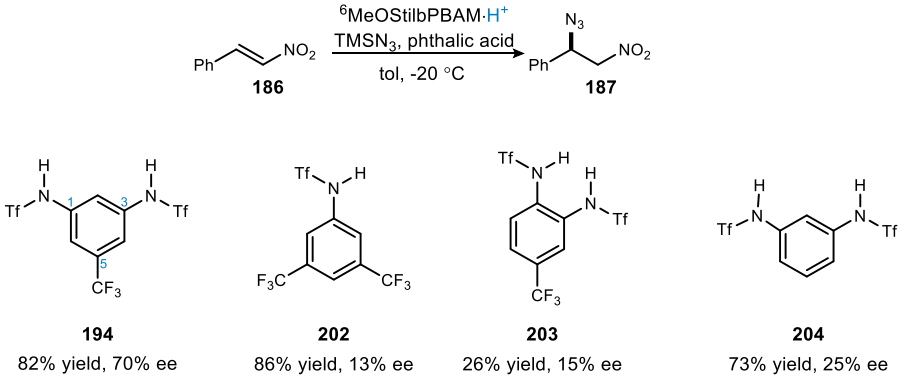

The first variable investigated was the substitution of the aryl triflamide. (Figure 67) The first triflamide that was prepared was **202**, where one of the triflamide residues was replaced with an additional trifluoromethyl group. Though the use of this triflamide provided a catalyst that was reactive, enantioselectivity diminished greatly. Triflimidic acid produced the nitroalkane in similar ee. This suggested that a bidentate coordination of the triflamide residue was important to selectivity. The next triflamide residue that was evaluated was **203** where the special arrangement was evaluated. It was proposed that a 1,2-diamine spatial arrangement may further restrict the ligand pocket size and improve ee accordingly. Triflamide **203** showed poor reactivity, and surprisingly, poor selectivity. This indicated that the spatial arrangement of the triflamide residues must be optimized for the BAM ligand. This effect will be investigated further in section 2.2.8, here aryl triflamides are employed in other reactions. To support this spatial arrangement hypothesis, when BAM ligands were employed with larger dihedral angles, such as PBAM, the biaryl triflamides are more effective than triflamide **194**. Aryl triflamide **204** illustrated how functionality at the 5-position had a significant effect on selectivity. While it is hypothesized that the trifluoromethyl group primarily enhances the acidity of the aryl triflamide, it may also play a structural role and thus contribute to the size and shape of the ligand pocket. This library of aryl triflamides with different substitution patterns was informative and helped us move forward with a hypothesis-driven approach to design achiral modifiers.

The next hypothesis we investigated was using large aryl substituents to restrict the rotation of the C-N bond, but an initial small sample set was not promising in support of this hypothesis. (Figure 68) This small library gave results quite similar to **204**, where the trifluoromethyl group

Figure 68: Evaluation of 4,6-aryl substitutions on aryl triflamide scaffold.

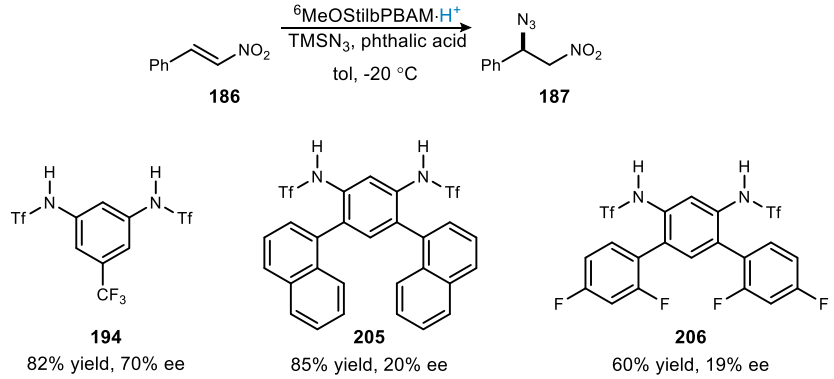

was omitted. These results do support the hypothesis that the acidity of the aryl triflamide residue affects reactivity and selectivity. With these results in hand, we prepared a number of derivatives to probe the effect on acidity and selectivity.

We prepared a few aryl triflamides that were less acidic than triflamide **194**, as shown in Figure 69 Aryl triflamide **204** was already explored in previous works to probe the role of the trifluoromethyl group. To verify that the electron withdrawing nature of the substituent affected selectivity, the aryl sulfonamide derivative **207** was prepared. Sulfonamides are less acidic than triflamides, with pKa values of 8.85 and 4.45 respectively,[142] though very similar in size. Substrate **207** is structurally very similar to triflamide **194**, though selectivity is quite poor when it is applied as a BAM catalyst modifier. With this information, we were confident moving forward that a more acidic triflamide residue should increase selectivity.

Figure 69: Evaluation of eletron-rich aryl triflamide scaffolds.

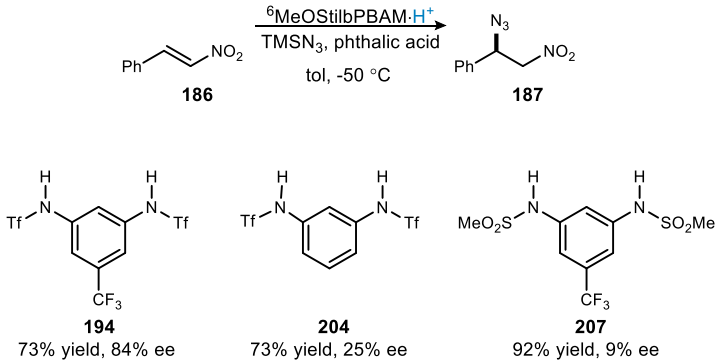

A library of aryl triflamides were prepared that should be more acidic than aryl triflamide **194 (**Figure 70**)**. While most of these derivatives performed fairly well, none of them catalyzed the azide addition with higher facial selectivity than **194**. Some residues were particularly disappointing, such as **208**, **209**, and **210**. The methyl sulfone derivative (**208**), was prepared because sulfone is a more effective withdrawing group than a trifluoromethyl group. To illustrate this effect, the pK_a of $^{p}CF_3C_6H_5NH_2$ is 27.0, while the pKa of $^{p}(MeSO_2)C_6H_5NH_2$ is 25.6.[159] However, the observed selectivity with this triflamide derivative was quite poor. It was hypothesized that the sulfone is a competitive hydrogen bond acceptor with the aryl triflamide residues. Therefore, the proposed bidentate coordination between the amidine residues of the

[159] Bordwell, F. G.; Algrim, D. J. *J. Am. Chem. Soc.* **1988**, *110*, 2964.

chiral ligand and the triflamide residues is affected. Reactivity is still high because the substrate **208** is a strong acid and may serve to prepare the active catalyst. Another surprising result was triflamide **209**, which deviated from the 1,3,5-substitution pattern. Preparing this ligand complex was unusually difficult because the chiral ligand was readily soluble in organic solvent, while the acid was slow to dissolve until it was heated. It is proposed that this poor solubility profile is a result of intramolecular hydrogen bonding between the aryl triflamide and trifluoromethyl groups. This intramolecular hydrogen bonding phenomenon could explain the poor selectivity observed with aryl triflamide **209** because the acid is hydrogen bonding with itself, rather than the BAM ligand. The nitroamine acid **210** deviated from the aryl triflamide scaffold. Because nitroamines are more acidic than triflamides, it was anticipated that it would coordinate well with a BAM ligand to improve ee. However, the observed selectivity was not consistent with this picture. Unlike the sulfonamide functional group, which likely favors *N*-H tautomer, the nitroamine may prefer to bind to ligand amidine as the nitro *O*-H tautomer.

Figure 70: Evaluation of electron-deficient aryl triflamide scaffolds.

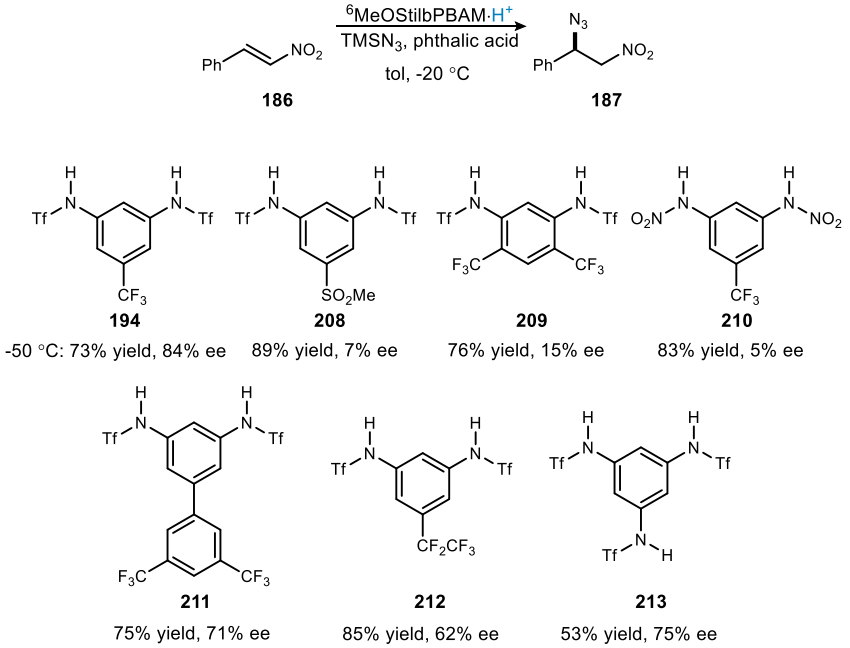

While this selection indicates that optimizing these aryl triflamides is not as straightforward as modifying the pK_a of the structure, this approach to design did yield some other successful derivatives. The biaryl derivative, **211**, was an interesting alternative to **194**. The electron

deficient aryl ring had a similar effect as the trifluoromethyl group. Replacing the trifluoromethyl group with a pentafluoroethyl group did not improve selectivity as expected. The second most selective aryl triflamide derivative was triflamide **213**, with 3 triflamide residues. While selectivity was high, reactivity diminished. This acid was employed as in a 1:1 molar ratio, just like the rest of the library. This is an interesting acid to evaluate because for every two basic sites of the BAM ligand, three acidic protons are available. This may explain the reduced reactivity of this catalyst; if the ligand were to over-protonate, Brønsted base activation of hydrazoic acid would not be possible.

The addition of hydrazoic acid to nitroalkenes has proved to be an interesting reaction to optimize because it has enabled the study of aryl triflamides as achiral modifiers in BAM catalysis. To the best of our knowledge, this is the first design and application of achiral modifiers in organocatalysis. This work illustrated that aryl bis(triflamides) were necessary for high facial selectivity, which indicates that a bidentate coordination of the triflamide is operational in enantiodetermining transition state. Additionally, the acidity of the aryl bis(triflamide) affected enantioselectivity as well. After investigating various derivatives of these aryl bis(triflamides), it was observed that more sterically-robust aryl triflamide derivatives did not significantly affect facial selectivity.

It is important that we develop new approaches for catalysis optimization to enable the rapid development of new enantioselective reactions. Triflic acid is commonly used in organocatalysis with the focus on its dissociated counterion. While this document details the investigation of aryl triflamides in BAM catalysis, it is likely that is approach could be applied more generally to the field of catalysis.

2.2.4 Mechanistic proposal for enantioselection

Initial work in developing conditions for the addition of azide to nitroalkenes indicated that a proton source was necessary for reactivity. It was proposed that hydrazoic acid was generated *in situ* and activated via Brønsted base catalysis. $TMSN_3$ would not be activated in the same manner as hydrazoic acid by the Brønsted basic feature of the chiral catalyst. The nitroalkene, by analogy to BAM catalyzed nitroalkane additions, is activated via Brønsted acid catalysis.[32] The

steps envisioned here involve azide addition to the nitroalkene, protonation of the resulting nitronate by the catalyst, and turnover of the monoprotonated active catalyst. This bifunctional activation of both nucleophile and electrophile is the basic design for stereocontrol within the catalyst's bisamidine pocket. (Figure 71)

Despite these similar catalyst design principles and extensive successful development with BAM enantioselective reaction development, this reaction is unique for its application of aryl triflamides. It is not immediately clear how the aryl triflamide affects the facial selectivity of the azide addition. Shown in Figure 72 are two operating hypotheses. Because the 1,3-bistriflamide regioisomer appears to be critical for enantioselection, we propose that there are two sites of coordination in the reactive transition state. In the first proposal, as depicted in the left box, the aryl triflamide is coordinated to both amidine portions of the chiral ligand. Residing under the ligand pocket, the nitroalkene is unable to flip within the pocket, and is therefore kept in a rigid

Figure 71: Proposed mechanism of BAM catalyzed hydrazoic acid addition to nitroalkenes.

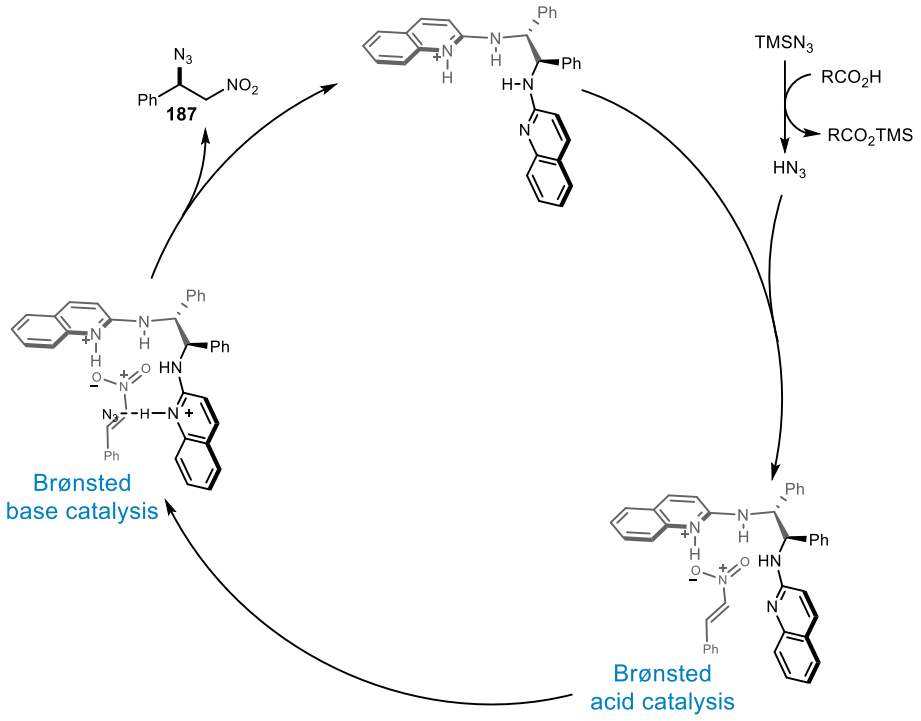

position. This rigidity is responsible for the high degree of electrophile control, and thus the azide may only add to the Re face of the olefin. The other proposed transition state is that the one triflamide donates a proton to the BAM ligand, while the other interacts through a hydrogen

bond. This hypothesis is depicted in the right box. The deprotonated triflamide may serve as a Brønsted base, activating the hydrazoic acid. Both the aryl triflamide and hydrazoic acid are similar in pK_a, which provides a good premise for this proposal.[160]

Figure 72: Proposed models for the formation of the major enantiomer.

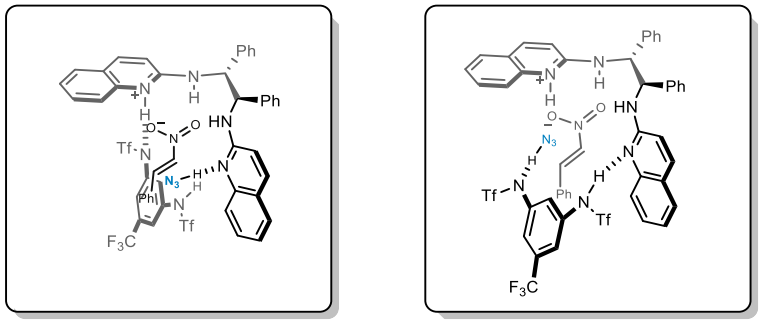

Both of these proposals illustrate why the special arrangement of the bistriflamide has a profound effect on selectivity. In the first proposal there is a matched relationship between the BAM ligand and the aryl triflamide spatially. In the second proposal, the direction of the hydrazoic acid by the aryl triflamide is the source of nucleophile control. As alluded to in earlier discussions, if the bistriflamide spatial arrangement is too close, there may not be enough room for the substrate. There is balance to generating a rigid transition state without preventing reactivity.

2.2.5 Analysis of scope in Michael additions

The substrate scope for this reaction is not complete because optimization for this reaction is ongoing. While 84% ee is a good result, the impact of this chemistry would be more significant if selectivity was greater than 90% ee. Unfortunately, while the test substrate was reactive at reduced temperatures, these low-temperature conditions were not widely applicable for the scope of the chemistry. The scope of this chemistry was relatively small, but a wide tolerance was observed for substrates that varied electronically. (Figure 73) Most important, nitrostyrene derivatives were all fairly well tolerated, producing the nitroalkane in similar facial selectivity as the test substrate (**187**). Notable, both electron rich and electron poor arene rings were tolerated,

[160] Trepka, R.; Belisle, J.; Harrington, J. *J. Org. Chem.* **1974**, *39*, 1094.

though electron deficient arenes proved more reactive. Notably, substrate **216** produced the nitroalkane with slightly diminished selectivity. The reduced facial selectivity may be an issue relating to the sterics of the large aryl ring, which disrupted aryl triflamide coordination. Unfortunately, trisubstituted nitroalkenes were not well tolerated. Additionally, when alkyl-substituted nitroalkanes were employed, selectivity diminished greatly. The aryl ring increases facial differentiation, which supports enantioselectivity.

The substrate scope of this reaction is currently limited – but can be expanded when a more selective catalyst system is developed. While there is still more work to be done, it is important to highlight that the work is a significant improvement over the literature precedent. Initial work published by Jørgensen published a small scope of six substrates, with reported ee's ranging from 24-62% ee.[140] Nitrostyrene derivatives were never investigated, only alkyl-substituted nitroalkenes. While their work is only moderately selective, it is significant because it was the first enantioselective variant of this azide addition to nitroalkenes. The Della Sala lab followed up with their own paper, showcasing a thiourea catalyst.[141] Similarly to Jørgensen, only seven substrates were screened. Alkyl-substituted nitroalkenes were reported in good ee, ranging from 71-82% ee. However, when they applied their conditions to nitrostyrene, the nitroalkane was

Figure 73: Substrate scope of asymmetric azide addition to nitroalkenes.

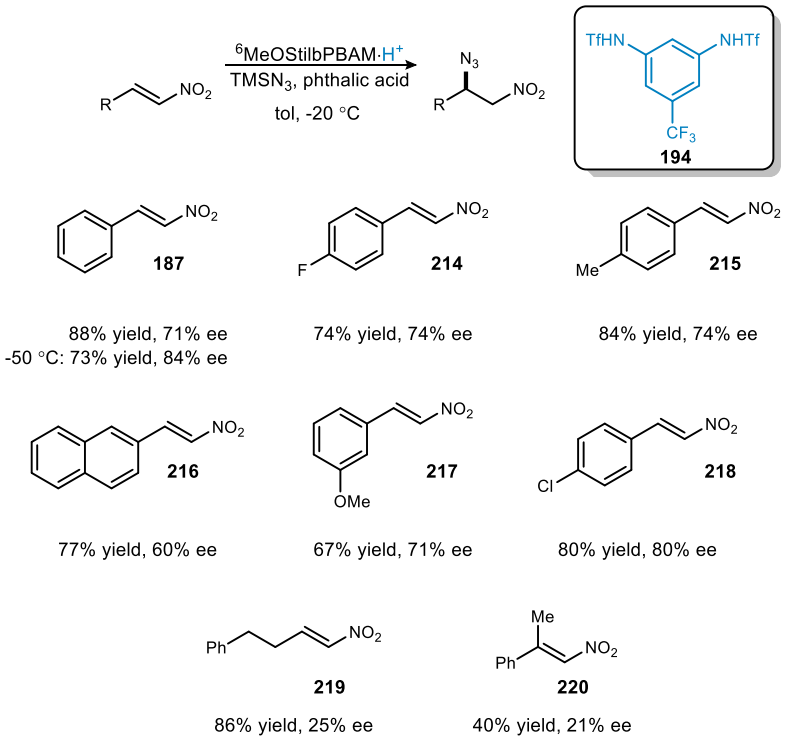

isolated in 39% ee. While the work of Jørgensen showcases good selectivity, a broader substrate scope would have been informative. The scope of this reaction has not been investigated broadly. The work detailed in this chapter addresses an unmet need in the synthetic community, directing the addition of azide to nitrostyrenes in good ee. There is not a highly selective variant of this chemistry published in the literature for these substrates. Using aryl triflamides may prove to be a unique solution to this problem.

2.2.6 Derivation of β-azido nitroalkanes

The preparation of chiral amines is an important area of study given their wide utility in synthetic chemistry. It is well-established that β-azido nitroalkanes can be reduced to chiral diamines.[161] Additionally, the azide may be selectively reduced to furnish the chiral β-amino nitroalkane using sodium borohydride and nickel (II) chloride[162], or via reduction with Lindlar's catalyst. These β-amino nitroalkanes have been successfully used to prepare peptide bonds. UmAS was first reported in 2010[20] and has increased in scope and utility. While there is a myriad of amide bond forming reactions, UmAS provides a unique, powerful alternative.[163] Unlike condensative methods, UmAS proceeds via umpolung reactivity. In basic conditions, α-halo nitroalkanes are used as nucleophiles to engage alkyl amines. These amines are activated by a halonium ion source and are thus electrophilic. The mechanism of UmAS has been investigated in order to further support and clarify steps not specifically addressed in the original proposal.[164,165] Because UmAS mechanistically excludes an active ester intermediate, epimerization through ketene formation or an azlactone intermediate is not possible. This makes UmAS a preferred method for synthesizing acidic amino amides, such as aryl glycine derivatives. Additionally, UmAS does not require the use of coupling reagents or a large excess of reagents, as found in solid-phase peptide synthesis.

[161] Robiette, R.; Tran, T.-V.; Cordi, A.; Tinant, B.; Marchand-Brynaert, J. *Synthesis* **2010**, *2010*, 3138.
[162] Giuliano, R. M.; Deisenroth, T. W. *J. Carbohydr. Chem.* **1987**, *6*, 295.
[163] Pattabiraman, V. R.; Bode, J. W. *Nature* **2011**, *480*, 471.
[164] Shackleford, J. P.; Shen, B.; Johnston, J. N. *Proc. Natl. Acad. Sci. U. S. A.* **2012**, *109*, 44.
[165]Crocker, M. S.; Foy, H.; Tokumaru, K.; Dudding, T.; Pink, M.; Johnston, J. N. *Chem* **2019**, *5*, 1248.

Figure 74: Derivations of β-azido nitroalkanes.

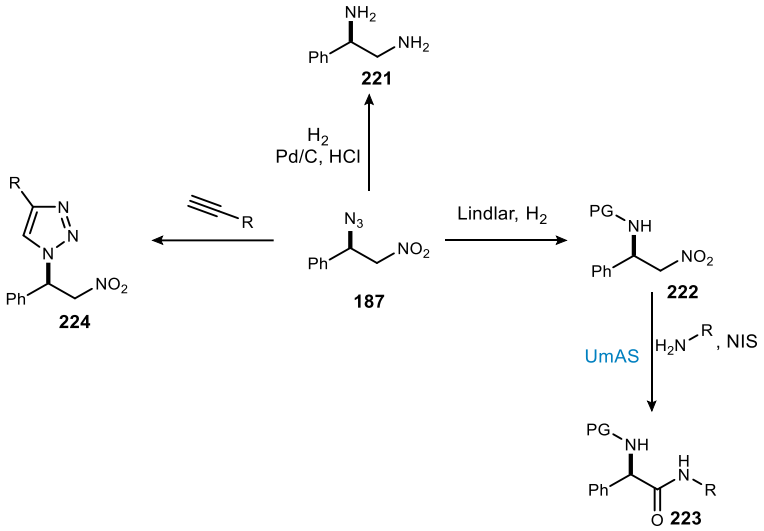

Numerous UmAS conditions have been developed to improve performance in amide bond forming reactions. Initial reports of UmAS were investigated using bromo-nitroalkanes as starting materials. However, Schwieter[166] and Vishe[32] have each developed conditions that generate the halo-nitroalkane *in situ*. Nitroalkanes are reported in the literature ten times more often than bromo-nitroalkanes, making these conditions significantly more impactful. Based on these reactions, we hypothesized that β-azido nitroalkanes would be useful substrates for Umpolung Amide Synthesis. Prior to this proposal, this motif was not considered for the synthesis of amide-bond containing compounds. This approach will expand the utility of β-azido nitroalkanes beyond reductions that give enantioenriched amines, enabling the construction of a range of small molecules with chiral azide functionality.

Chiral azides have found utility in a variety of applications in organic synthesis[156], medicinal chemistry[167], and bioconjugation.[168,169] Huisgen's innovative work in azide cycloaddition chemistry was recently enhanced by others interested in its potential as a bioorthogonal reaction, renewing interest in azide chemistry. Some of the most common contemporary applications of alkyl-azides are in the field of bioconjugation chemistry and the Staudinger ligation. These are often used to tether probes to molecules of interest. In turn, these probes can be used to study proteins. As azides are utilized increasingly in research, it is inevitable that their methods of

[166] Schwieter, K. E.; Shen, B.; Shackleford, J. P.; Leighty, M. W.; Johnston, J. N. *Org. Lett.* **2014**, *16*, 4714.
[167] Debets, M. F.; van Berkel, S. S.; Dommerholt, J.; Dirks, A. J.; Rutjes, F. P. J. T.; van Delft, F. L. *Acc. Chem. Res.* **2011**, *44*, 805.
[168] Schilling, C. I.; Jung, N.; Biskup, M.; Schepers, U.; Bräse, S. *Chem. Soc. Rev.* **2011**, *40*, 4840.
[169] Agard, N. J.; Baskin, J. M.; Prescher, J. A.; Lo, A.; Bertozzi, C. R. *ACS Chem. Biol.* **2006**, *1*, 644.

preparation will need further simplification (i.e. synthesis step count) and higher selectivity (enantiomeric excess (ee) and/or diastereomeric ratio (dr)). Established methods to prepare enantioenriched α-azido amides remain limited and underdeveloped.

Figure 75: Previous work in preparing α-azido amides via UmAS.

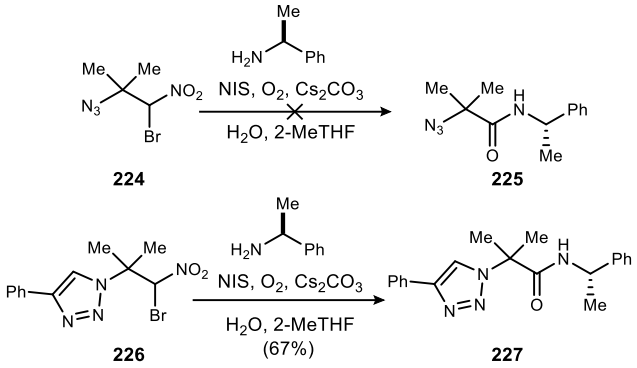

Initial attempts to synthesize α-azido amides are promising. Preliminary results indicate the formation of small amounts of product; however, a considerable number of byproducts are forming as well. While crude NMR indicates the formation of several byproducts yet to be identified, nitrostyrene was clearly formed. Preliminary results from an experiment lacking nitroalkane indicate that many of the byproducts resulted from oxidation of the amine. We hypothesize that this occurs from the halamine intermediate. Typically, the halamine is consumed by the nitronate, however, the β-azido nitronate preferentially reverts to the nitroalkene.

Thus far, the isolation of the desired product from these complex reaction mixtures has not been trivial. While it is not immediately clear what is causing the instability of these β-azido nitroalkanes in UmAS conditions, unpublished work by Tsukanov in our lab observed similar depressed reactivity of β-azido-α-bromo nitroalkanes. However, it was found that after Huisgen cycloaddition with the azide, the α-triazole nitroalkane performed well in UmAS, as shown in Figure 75. Using previous UmAS development as an indicator, identifying the proper oxidant system can be key to desired reactivity. Alternative oxidant systems were investigated, such as DBDMH and urea-hydrogen peroxide. Unfortunately, even after screening a wide variety of amine, oxidants, bases, and solvents, the amide product was never isolated. In all conditions, the primary byproduct was nitrostyrene.

Figure 76: Derivation of β-azido nitroalkenes using thioacid-azide amidation.

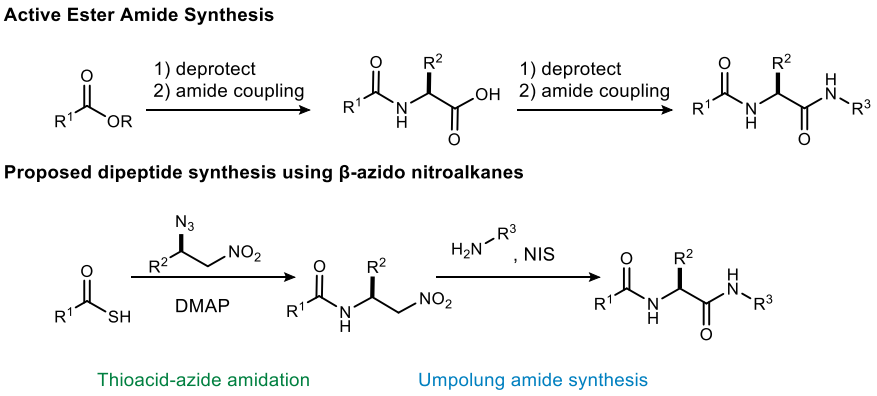

Because UmAS cannot be utilized for the synthesis of α-azido amides at present, it was thought that the azide may be functionalized using Williams' thioacid-azide amidation reaction. Functionalizing the azide with an amide bond should make the subsequent UmAS straightforward to execute because the Johnston lab has successfully used UmAS to synthesize dipeptides previously. The thioacid-azide amidation would be used to attach one amide chain, while UmAS will attach the other. This approach would negate the use of coupling reagents, protecting group manipulations, and other issues commonly found in peptide synthesis, such as epimerization. Preparing dipeptide in this manner would be more efficient than conventional preparations of dipeptides from esters (Figure 76).

Unfortunately, as was observed in the application of β-azido nitroalkanes in UmAS, degradation of the nitroalkane was a huge barrier to reactivity. A variety of conditions were screened, but the nitroalkene was formed in large amounts. The rate of amide bond formation was not competitive with the rate of elimination. Notably, trace amounts of product were observed in ruthenium (III)-promoted conditions.[170] In spite of this positive lead, a Lewis acid could not be identified to increase the rate of amide bond formation.

Some additional work has been done to oxidize the nitroalkane to the carboxylic acid using Nef chemistry.[171] Initial work has yielded trace amounts of product, however, most of the recovered material is the nitroalkene. Unfortunately, Nef reactions are run under basic conditions where

[170] Fazio, F.; Wong, C.-H. *Tetrahedron Lett.* **2003**, *44*, 9083.
[171] Matt, C.; Wagner, A.; Mioskowski, C. *J. Org. Chem.* **1997**, *62*, 234.

several equivalents of $NaNO_2$ are required. This could factor into the decomposition observed in these conditions. When the α-position is activated elimination of the azide occurs.

In spite of many attempts, we were not able to derivatize these β-azido nitroalkanes to amide-bond containing small molecules. This work illustrates how rapidly the elimination of azide is in basic conditions. More specifically, the acidity of the nitroalkane only enhanced the rate of elimination. While disappointing, it is important to note that the preparation of chiral amines is an important area of study it its own right. Chiral amines are widely applicable in a synthetic and medicinal chemistry. The literature indicates that the reduction of these β-azido nitroalkanes is straightforward. The work detailed in this section was hoping to expand, not invent, the utility of this small molecule scaffold.

2.2.7 Synthetic routes to *N*-aryl triflamides

The preparation of *N*-aryl triflamides from aryl amine precursors was straightforward using standard triflation conditions (Figure 77).[172] The yields of these triflation reactions for this library are detailed in the supporting information. When possible, commercially available diamines or nitroarenes were used. This enabled the preparation of a variety of derivatives, including **194**, **188**, **191**, **192**, **202**, **203**, **204**, **207**, and **212**.

Figure 77: Preparation of aryl triflamides.

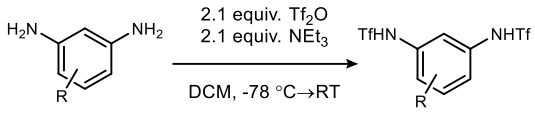

When needed, diamine precursors were preparing through a variety of synthetic transformations. A classic method to prepare aryl amines is a two-step sequence: 1) nitration of the aryl ring, and 2) subsequent reduction of the nitroarene.[173] Nitroarenes can be reduced using standard hydrogenation conditions (H_2, Pd/C), typically in quantitative yields.[174] The nitration of electron-rich aromatic rings is reported as straightforward. However, electron-deficient aromatic

[172] Ma, R.; White, M. C. *J. Am. Chem. Soc.* **2018**, *140*, 3202.
[173] Bonner, T.; Bowyer, F.; Williams, G. *Journal of the Chemical Society (Resumed)* **1953**, 2650.
[174] Tafesh, A. M.; Weiguny, J. *Chem. Rev.* **1996**, *96*, 2035.

rings are significantly less reactive, requiring fuming sulfuric and nitric acid and elevated temperatures for reactivity.[175] Even in these aggressive conditions, conversion was often problematic. Because many of the proposed aryl bis(triflamide) derivatives were prepared from electron-deficient aryl rings, aryl amine precursors were prepared using alternative methods whenever possible.

Figure 78: Preparation of aryl triflamide (**208**) from aryl sulfone.

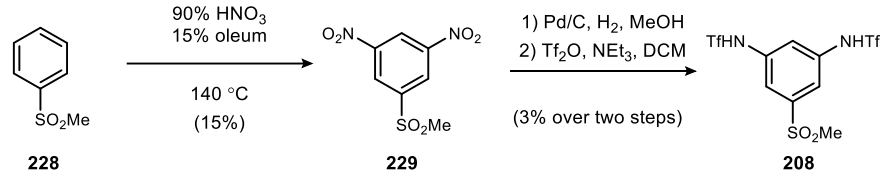

The preparation of derivative **208** was challenging, and alternatives to the nitration conditions could not be identified. As shown in Figure 78, while product was isolated, the overall yield was quite poor. However, with the nitroarene in hand, subsequent reduction was straightforward. Unfortunately, the subsequent triflation was low yielding. While the crude mass was relatively high (>50%), only small amounts of pure material were successfully isolated. Because this aryl triflamide derivative did not prove highly selective in the azide addition to nitroalkenes, this reaction was not optimized further.

Figure 79: Preparation of aryl triflamides (**205**, **206**, and **207**).

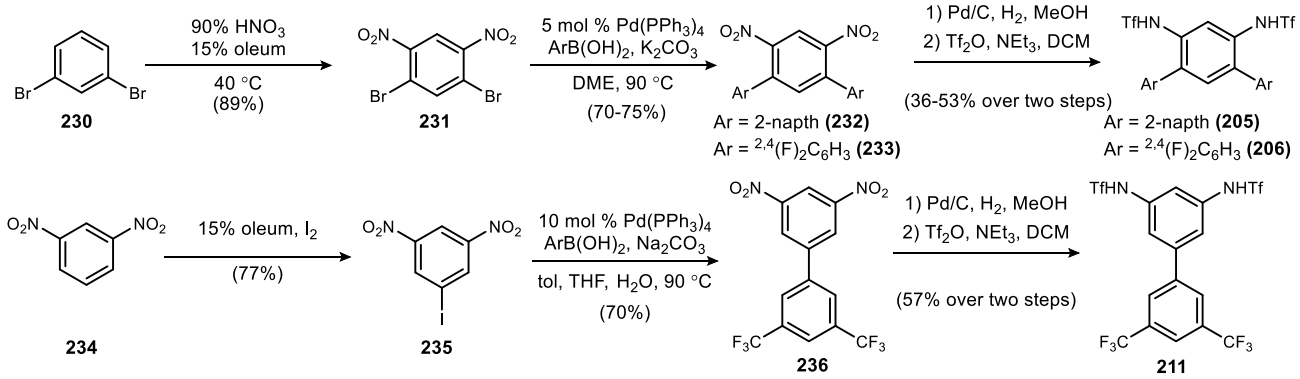

Another class of aryl bis(triflamides) were prepared with aryl substituents. The general approach to access these compounds was to prepare the halogenated nitroarene, followed by a subsequent Suzuki coupling. To prepare aryl bis(triflamides) with 4,6-aryl substitution, 1,3-dibromobenzene was nitrated.[94] Compound **231** was then bis-arylated through a reported Suzuki

[175] Ahmed, H. A. *Bulletin of Faculty of Pharmacy, Cairo University* **2011**, *49*, 25.

coupling.[176] A similar approach was employed to prepare the 1,3,5-substituted scaffold (**211**). Iodination of 1,3-dinitrobenzene prepared the aryl iodide in moderate yields.[177] A similar cross coupling was employed to prepare the intermediate **236**.[178] Intermediates **232, 233,** and **236** were subsequently reduced and triflated for preparation of the respective aryl triflamide.

Preparation of the aryl tris(triflamide), **213**, was achieved through a Schmidt rearrangement, followed by hydrogenation of the nitroarene, and subsequent triflation. (Figure 80)[179] When this acid was initially considered for preparation, the expected precursor was trinitrobenzene. Because trinitrobenzene is a potentially explosive compound, other synthetic preparations were considered. The Schmidt rearrangement proved to be moderately high yielding and the hydrogenation also proceeding smoothly. Unlike previous work, triflation of the 1,3,5-trisaminobenzene intermediate proved low yielding for reasons that are still not immediately clear. The crude NMR did not show clean conversion, which indicates that various regioisomers may have formed with different triflation patterns. This reaction was not optimized further because other aryl triflamide derivatives were more effective achiral modifiers.

Figure 80: Preparation of aryl triflamide **213** via Schmidt rearrangement.

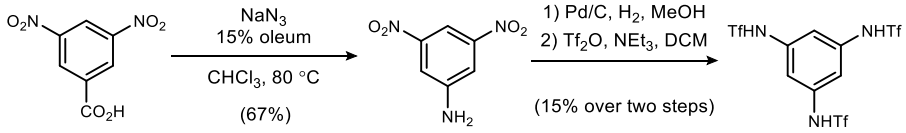

237 **238** **213**

The preparation of aryl bis(triflamide) **209** is dissimilar from previous methods. Rather than preparing the aryl amine for subsequent triflation, a Buchwald-Hartwig coupling was carried out using trifluoromethanesulfonamide. The application of a cross-coupling to prepare an aryl triflamide is not known in the literature, though some work has been done to prepare aryl sulfonamides. [180] The aryl bromide was prepared from 3,5-trifluoroaniline in two steps using a

[176] Luo, D.; Lee, S.; Zheng, B.; Sun, Z.; Zeng, W.; Huang, K.-W.; Furukawa, K.; Kim, D.; Webster, R. D.; Wu, J. *Chem. Sci.* **2014**, *5*, 4944.
[177] Arotsky, J.; Butler, R.; Darby, A. C. *Journal of the Chemical Society C: Organic* **1970**, 1480.
[178] LaLonde, R. L.; Wang, Z. J.; Mba, M.; Lackner, A. D.; Toste, F. D. *Angew. Chem. Int. Ed.* **2010**, *49*, 598.
[179]Caron, K.; Lachapelle, V.; Keillor, J. W. *Org. Biomol. Chem.* **2011**, *9*, 185.
[180] Katz, J. D.; Jewell, J. P.; Guerin, D. J.; Lim, J.; Dinsmore, C. J.; Deshmukh, S. V.; Pan, B.-S.; Marshall, C. G.; Lu, W.; Altman, M. D.; Dahlberg, W. K.; Davis, L.; Falcone, D.; Gabarda, A. E.; Hang, G.; Hatch, H.; Holmes, R.; Kunii, K.; Lumb, K. J.; Lutterbach, B.; Mathvink, R.; Nazef, N.; Patel, S. B.; Qu, X.; Reilly, J. F.; Rickert, K. W.; Rosenstein, C.; Soisson, S. M.; Spencer, K. B.; Szewczak, A. A.; Walker, D.; Wang, W.; Young, J.; Zeng, Q. *J. Med. Chem.* **2011**, *54*, 4092.

reported procedure.[181] The unprecedented Buchwald-Hartwig was successful, albeit low yielding. (Figure 81) The crude NMR showed product, and indiscernible byproduct formation. This reaction was not optimized further because other aryl bis(triflamide) derivatives were more effective achiral modifiers.

Figure 81: Preparation of aryl triflamide via Buchwald-Hartwig coupling.

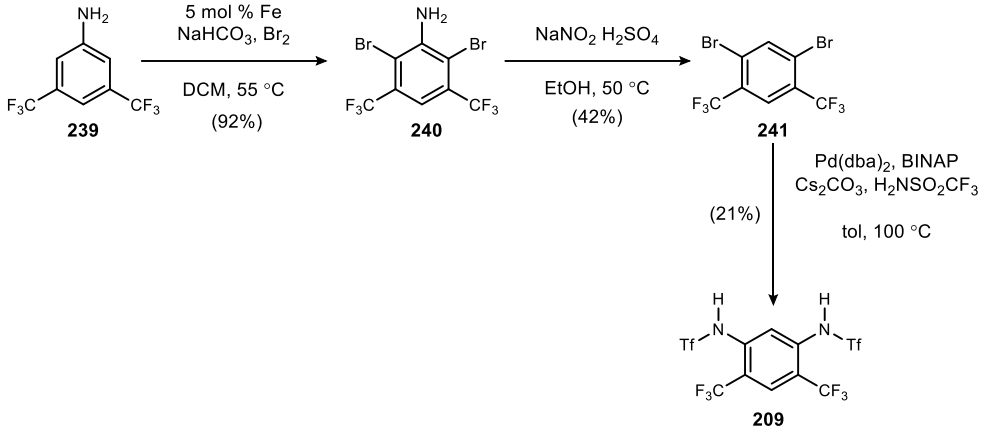

The 1,3-dinitroamine derivative (**210**) was prepared using a commercially available diamine substrate. (Figure 82) The aryl amines were nitrated following a procedure in the literature.[182] The crude NMR showed incomplete conversion, which is a contributing factor to the poor isolated yield. Ultimately, the material was successfully purified via flash chromatography. When applied to the azide addition chemistry, enantioselectivity was poor. For this reason, reaction optimization was not pursued.

Figure 82: Preparation of aryl nitroamine.

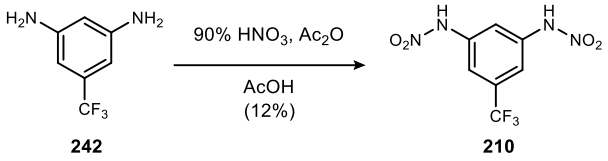

2.2.8 Applications of aryl triflamides in other organocatalyzed reactions

[181] Asmus , S.; Beckendorf, S.; Zurro , M.; Mück-Lichtenfeld, C.; Fröhlich, R.; García Mancheño , O. *Chem. - Asian J.* **2014**, *9*, 2178.
[182] Porcs-Makkay, M.; Mezei, T.; Simig, G. *Org. Process Res. Dev.* **2007**, *11*, 490.

After studying the significant effect of aryl triflamides on the asymmetric azide addition chemistry, it was thought that these achiral modifiers may have a significant impact on other BAM catalyzed reactions. It is evident that a variety of factors contribute to the successful application of achiral modifiers. These factors include the spatial arrangement between the bistriflamide motif, the pK_a of the acid, and the substitution of the aryl ring. In addition, the characteristics of the BAM ligand will also have a significant effect on reactivity and selectivity. We are hopeful that these aryl triflamides will have an effect on a variety of reactions, however, it will be difficult to evaluate such a wide set of parameters. To further study aryl triflamides in BAM catalysis, a small library of catalysts was evaluated in a number of reactions. Some of the reactions chosen had an established history in BAM catalysis. This expedited results because variables such as the BAM ligand, temperature, and solvent were already optimized. The application of the aryl triflamides may serve to improve various aspects of established chemistry, whether that be facial selectivity overall or a few substrates where facial selectivity diminished relative to the rest of the scope. In theory, these aryl triflamides could be used to address weak spots of a scope, which would also be incredibly useful.

One of the first reactions studied was the 6-exo lactonization, as shown in Figure 83.[19] When Dobish first published this work, the effect of achiral acids on selection was studied. However, *N*-aryl triflamides were not established at that time. Because achiral modifiers had a significant effect on selectivity, we hoped to see if the observed trends in the azide addition chemistry

Figure 83: Evaluation of BAM·aryl triflamides on iodolactonization reaction.

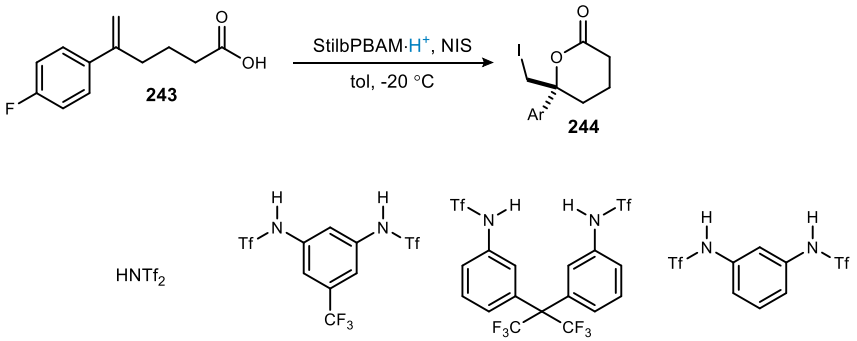

translated well to this lactonization reaction. Even though the stilbene diamine backbone is used in both reactions, the biaryl triflamide (**191**) was the most selective. Additionally, aryl triflamide **194** was outperformed by the less-acidic derivative **204**. This deviates greatly from previous work with aryl triflamides as achiral modifiers. Because triflimidic acid was a more effective acid than aryl triflamides, they were not studied further in this lactonization chemistry.

An additional lactonization reaction that was previously studied is the 6-endo cyclization, as shown in Figure 84. While the observed selectivity in this reaction was good (in the high 80's), it was proposed that aryl triflamides may improve facial selectivity. In previous work, a 1:1 molar ratio of aryl triflamide to BAM ligand was optimal. However, this selectivity was much higher when a 2:1 catalyst was employed. Most of the aryl triflamides furnished the lactone in similar ee, with the exception of **191**. Similar to the previous lactonization reaction, aryl triflamides could be employed but triflimidic acid was a more effective acid for catalyst preparation.

Figure 84: evaluation of BAM·aryl triflamides on 6-endo lactonization

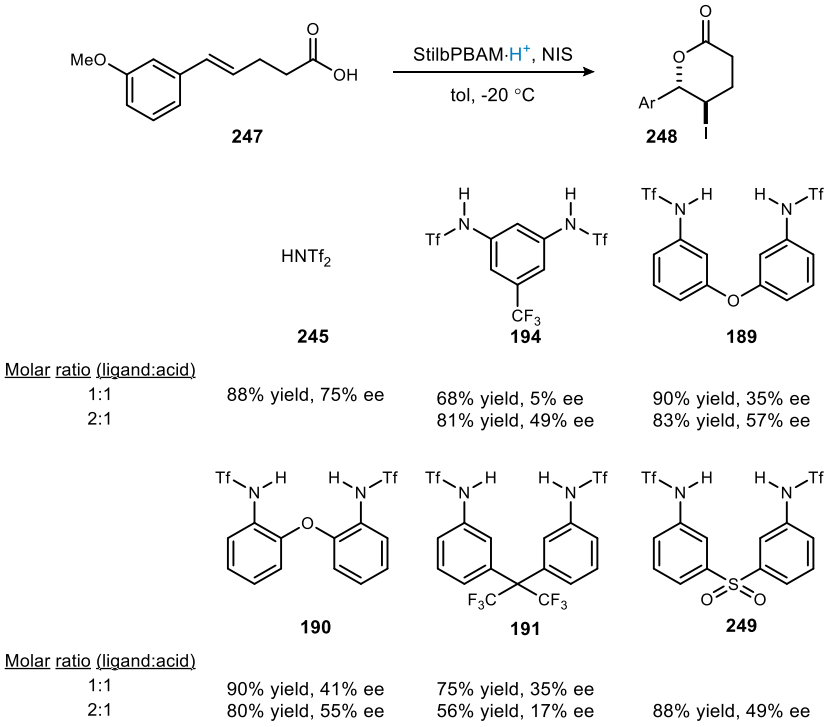

Because BAM catalysis has been successfully applied to aza-Henry chemistry, an asymmetric Strecker reaction was considered for study. (Table 12) BAM catalysis has been applied to the

activation of imines with high success. Additionally, TMSCN is an analogous nucleophile to $TMSN_3$. Triflimidic acid salts of various BAM ligand effected the asymmetric Strecker in high ee, which is impressive for an initial reaction screen. Unfortunately, when aryl triflamide salts were employed as catalysts, reactivity diminished greatly. In these low yield examples, enantioselection was not improved either. For this reason, it was thought that aryl triflamides may not be employable in this reaction. However, it was still intriguing to see BAM catalysis applied to this addition reaction with such high selectivity. This work could serve as a platform for future projects.

Table 12: Evaluation of BAM·aryl triflamides on asymmetric Strecker reaction.

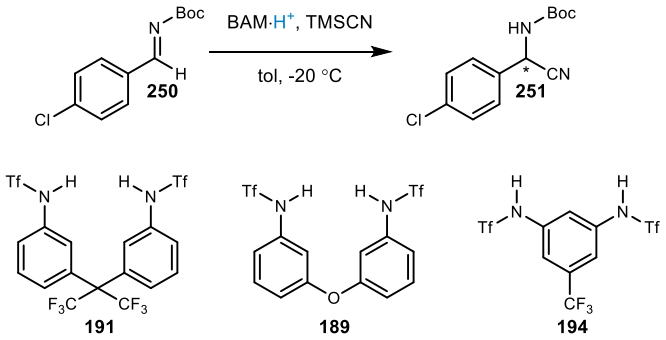

entry	BAM salt	yield (%)	ee (%)
1	StilbPBAM·$HNTf_2$	40	77
2	^{6}MeOStilbPBAM·$HNTf_2$	46	80
3	PBAM·$HNTf_2$	70	82
4	^{6}MeOStilbPBAM·A	Trace	-
5	StilbPBAM·B	17	53
6	StilbPBAM·C	Trace	-
7	PBAM·B	26	79

An additional reaction that was investigated using aryl triflamides was the 7-endo lactonization chemistry developed by Andrew Flach. He was able to isolate the ε-lactone in up to 78% ee. I replicated this work, but used a modified the quench procedure that ultimately improved ee to 85% ee. It was proposed that the application of aryl triflamides may improve selectivity. When aryl triflamides were screened in this chemistry, results were obtained that were comparable to

the triflimidic acid salt. This result indicated that aryl triflamides were not necessarily helpful, but also not detrimental to this lactonization chemistry.

Table 13: Evaluation of BAM·aryl triflamides on 7-exo lactonization.

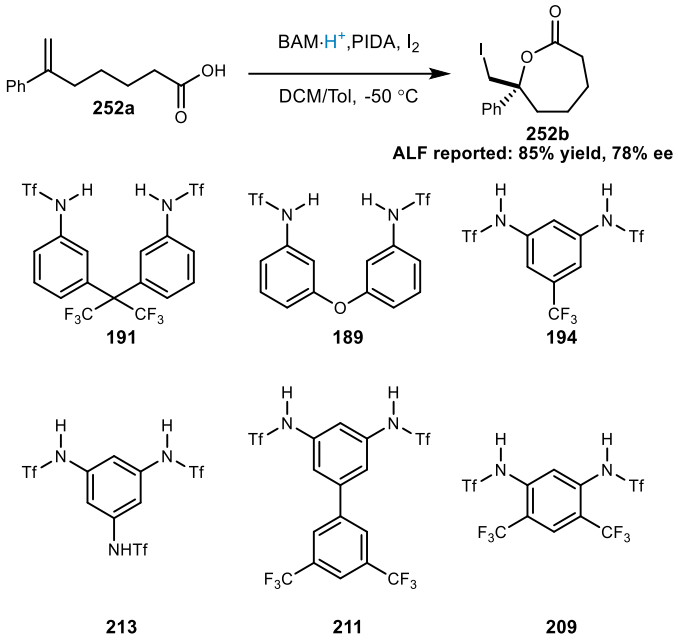

Initial screen			Further work		
BAM salt	**yield (%)**	**ee (%)**	**BAM salt**	**yield (%)**	**ee (%)**
StilbPBAM	33	80	^{6}MeOStilbPBAM	41	84
StilbPBAM·HNTf$_2$	74	85	^{6}MeOStilbPBAM·HNTf$_2$	58	87
StilbPBAM·A	44	80	^{6}MeOStilbPBAM·C	53	80
StilbPBAM·B	44	79	^{6}MeOStilbPBAM·D	56	85
^{6}MeOStilbPBAM·C	67	84	^{6}MeOStilbPBAM·E	61	83
			^{6}MeOStilbPBAM·F	48	67

To explore this potential application further, another aryl triflamide screen was performed using ^{6}MeOStilbPBAM. (Table 13) Because selectivity was largely unaffected by the choice of acid, a free-base BAM ligand was also studied. This second screen illustrated that the nature of the achiral modifier had little effect on selectivity, as the free-base catalyst showed similar facial selectivity as the catalyst salts. In this reaction, the acid was serving primarily as a proton donor, which improved reactivity as opposed to selectivity. It is unclear exactly why *N*-aryl triflamides have no observable effect on this reaction, but the use of PIDA/I$_2$ is quite different (and heterogeneous), generating the possibility that HI or other acid/base might form. While this

lactonization chemistry may not be a suitable application for aryl triflamide catalyst salts, this was still significant work as a project that was thought to produce the lactone in moderate ee was optimized to 87%. This information reignited our effort to optimize the cyclization for 7-membered lactone synthesis, as will be detailed in Chapter 3.

2.2.9 Conclusions

We have developed conditions to prepare enantioenriched β-azido nitroalkanes in up to 84% ee via asymmetric azide addition. These products may serve as precursors to chiral amines, which are commonly used in synthetic and medicinal chemistry. Optimization of this chemistry led to a novel application of aryl triflamides as achiral modifiers in BAM catalysis. This discovery illustrated an untapped area of exploration in organocatalysis. A variety of organocatalysts utilize protonated amines as a Brønsted acid. However, the application of large aryl acids to enhance facial selectivity is a phenomenon that has not been observed previously in this field. Notably, there are examples of achiral modifiers in transition metal catalysis, though it is a developing field.

We have explored the cooperative space of chiral ligand and aryl triflamide design, noting that the two interplay with each other. It was apparent that three factors must be evaluated in aryl triflamide optimization: the special arrangement of the bistriflamide motif, the acidity of the triflamide, and the substitution of the aryl ring. In addition to investigating the asymmetric azide addition, we have investigated aryl triflamides in other reactions. Though a second application of the dramatic effect these aryl triflamides can offer is yet to be discovered, it is already clear that these aryl triflamides can affect both reactivity and selectivity. This indicates that achiral modifiers will be a third variable to pursue in catalyst optimization. This is significant because in order to develop catalysts that are widely applicable, they must be synthetically accessible. These aryl triflamides are a synthetically accessible alternative to ligand design, which lowers the barrier to apply organocatalysis broadly.

2.3 Future directions

Because modifications to the Brønsted acidic site of the BAM catalyst effected enantioselection in azide addition chemistry, it is hypothesized that aryl triflamide design is the optimal design point moving forward. This conclusion is supported by unsuccessful ligand design attempts, as shown in Figure 65. The work reported in this chapter details a moderately selective azide addition to nitrostyrenes, with the limited scope reported in 60-84% ee. For this work to be highly impactful, optimization efforts must be continued. There are a number of aryl triflamide derivatives that may be investigated in the future (Figure 85).

While **208** was not a successful achiral modifier, it was proposed that **253** may address some issues. It was hypothesized that **208** was not coordinated to the BAM ligand via bidentate coordination of the triflamides because the sulfone may participate as a hydrogen bond acceptor. The trifluoromethyl group of **253** would weaken the hydrogen bond between the catalyst and the trifluoromethyl sulfone. This may promote bidentate coordination between the BAM ligand and bis(triflamide), while also enhancing the acidity of the triflamides. It is hypothesized that enhancing this bidentate coordination will improve enantioselection.

The aryl triflamide **211** was a highly reactive and selective achiral modifier, but was not derivatized. This scaffold is amenable to a variety of aryl modifications, some examples being **254** and **255**. Adding more electron withdrawing groups, may increase the acidity of the aryl triflamide and thus improve enantioselection. Additional achiral modifiers we hope to prepare focus on modifying the triflamide directly, as shown in **256**. Various poly-fluorinated sulfonic anhydrides are commercially available. They were not pursued due to their high cost. While reagents to prepare these derivatives may be more expensive than triflic anhydride, they would

Figure 85: Proposed aryl triflamide derivatives for future investigations.

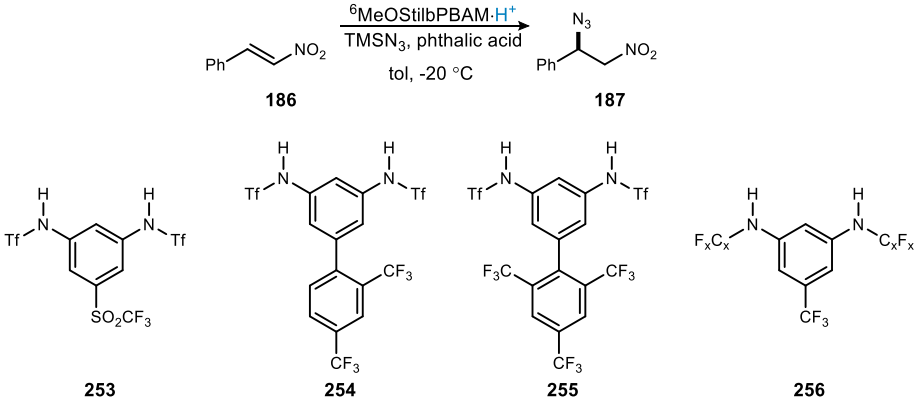

enable the rapid preparation of a variety of derivatives from a single diamine. This is an additional approach to prepare a range of aryl triflamides with different acidities without greatly changing the shape of the scaffold.

We have successfully employed BAM:aryl triflamide catalysts to improve facial selectivity. Future work in the application of aryl triflamides will work beyond BAM catalysis. Strong acids, such as triflic acid, are commonly employed in Lewis acid catalysis and as Brønsted acids in their own right. While aryl triflamides are similar in reactivity to triflic acid, they have a wealth of potential because of their ability to donate protons, hydrogen bond, and take up chemical space. This hypothesis is similar to the fields such as Brønsted acid assisted Lewis acid catalysis and Lewis acid assisted Brønsted acid catalysis.[183] In this area of study, the dimeric acid catalyst is often more reactive and/or more selective through the application of a secondary acid. An analogy can be drawn to the addition of azide to nitroalkenes, where the application of aryl triflamides in BAM catalysis greatly improved enantioselection. While they have been successfully employed in BAM catalysis, their wealth of potential would be applicable in a variety of reactions.

Chapter 3 – optimization of an enantioselective synthesis of ε-lactones from unsaturated acids

3.1 Introduction

A highly enantioselective halolactonization to prepare ε-lactones has been developed that employs a novel phenyliodonium diacetate (PIDA) and iodine oxidant system with a chiral proton catalyst. The preparation of 7-membered lactones is a notable challenge in terms of reactivity, let alone enantioselectivity. When conventional oxidant systems were employed, such as *N*-iodosuccinimide (NIS), reactivity was low. By employing a dual component oxidant system, unsaturated carboxylic acids were converted to *ε*-lactones in high yields and high facial selectivity. (Figure 86)

[183] Yamamoto, H.; Futatsugi, K. *Angew. Chem. Int. Ed.* **2005**, *44*, 1924.

Figure 86: Proposed preparation of ε-lactones via enantioselective halolactonization.

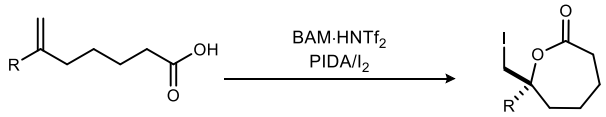

257 **258**

3.1.1 Applications and synthesis of chiral ε-lactones

7-membered lactones are commonly found in a large number of biologically active natural products.[184,185] Some examples of naturally occurring compounds with ε-lactone functionality are briarellin J,[186] prieurianin,[187] and chiisangogen, as shown in Figure 87.[188] While other products in

Figure 87: Naturally occuring compounds containing ε-lactones.

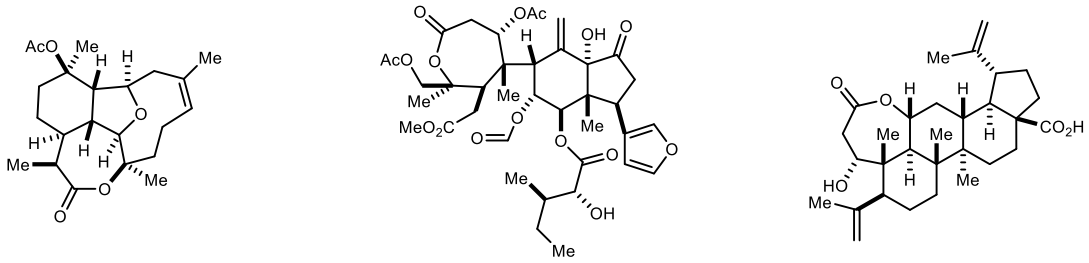

259 briarellin J

260 prieurianin

261 chiisanogenin

the briarellin family showed antimalarial activity, briarellin J was not active.[189] Prieurianin has shown moderate antifeedant activity in cotton bollworm larvae, which feed on a variety of cultivated plants.[190] Chiisangogen has been studied in rat models for its anti-inflammatory effects, with potential as a rheumatoid arthritis therapeutic.[191]

The rigidity and diverse 3D properties of cyclic compounds often improve binding affinity to biological receptors, oral bioavailability, and cell permeability compared to analogous acyclic

[184] Clarke, A. K.; Unsworth, W. P. *Chem. Sci.* **2020**, *11*, 2876.
[185] Hussain, A.; Yousuf, S. K.; Mukherjee, D. *RSC Adv.* **2014**, *4*, 43241.
[186] Crimmins, M. T.; Mans, M. C.; Rodríguez, A. D. *Org. Lett.* **2010**, *12*, 5028.
[187] Tóth, R.; Gerding-Reimers, C.; Deeks, M. J.; Menninger, S.; Gallegos, R. M.; Tonaco, I. A. N.; Hübel, K.; Hussey, P. J.; Waldmann, H.; Coupland, G. *The Plant Journal* **2012**, *71*, 338.
[188] Lee, J. M.; Cho, S.; Lee, M.-H.; Cho, S. H.; Park, C.-G.; Lee, S. *Nat. Prod. Sci.* **2015**, *21*, 82.
[189] Ospina, C. A.; Rodríguez, A. D.; Ortega-Barria, E.; Capson, T. L. *J. Nat. Prod.* **2003**, *66*, 357.
[190] Koul, O.; Daniewski, W. M.; Multani, J. S.; Gumulka, M.; Singh, G. *J. Agric. Food Chem.* **2003**, *51*, 7271.
[191] Jung, H.-J.; Nam, J. H.; Choi, J.; Lee, K.-T.; Park, H.-J. *J. Ethnopharmacol.* **2005**, *97*, 359.

molecules or normal-sized rings.[192,193,194] While ε-lactones show promise in medicinal chemistry, they are underrepresented in the pharmaceutical industry due to synthetic challenges.[195] The preparation of 7-11-membered rings from linear precursors is often challenging because there is a significant entropic barrier.[196] Similar to 5- and 6-membered rings, transannular interactions and strain are additional barriers to cyclization.

The prevailing methods to prepare ε-lactones include ring expansions,[184] ring-closing metathesis,[197] and macrolactonizations.[198] Ring expansions, such as the Baeyer-Villager oxidation, are commonly employed because they circumvent entropic barriers to ring-forming reactions.[199] While these reactions have been successfully employed in the preparation of 7-membered lactones, they are not enantioselective transformations and therefore will not be rigorously outlined in this section.

As described previously in section 1.1.2, organocatalysis is often employed to prepare cyclic lactones enantioselectively. To date, this paradigm has not been expanded to ε-lactones due to reactivity issues. Efforts have been made to prepare 7-membered rings via lactonization,[200,201] though only one enantioselective example has been reported.[202] Tang developed an enantioselective bromoesterification of enynes where NBS is activated by a chiral urea catalyst. (Figure 88) The enyne functionality allows intramolecular cyclization of a carboxylic acid in a 1,4-addition reaction. The 7-membered ring formation is presumably aided by the aryl ring, a feature that conformationally favors cyclization. This approach reduces the entropic barrier to cyclization. At present, there is not an enantioselective cyclization of unsaturated acids to prepare ε-lactones.

---

[192] Romines, K. R.; Watenpaugh, K. D.; Tomich, P. K.; Howe, W. J.; Morris, J. K.; Lovasz, K. D.; Mulichak, A. M.; Finzel, B. C.; Lynn, J. C. *J. Med. Chem.* **1995**, *38*, 1884.
[193] Kopp, F.; Stratton, C. F.; Akella, L. B.; Tan, D. S. *Nat. Chem. Biol.* **2012**, *8*, 358.
[194] Bauer, R. A.; Wenderski, T. A.; Tan, D. S. *Nat. Chem. Biol.* **2013**, *9*, 21.
[195] Illuminati, G.; Mandolini, L. *Acc. Chem. Res.* **1981**, *14*, 95.
[196] Ebine, M.; Suga, Y.; Fuwa, H.; Sasaki, M. *Org. Biomol. Chem.* **2010**, *8*, 39.
[197] Pentzer, E. B.; Gadzikwa, T.; Nguyen, S. T. *Org. Lett.* **2008**, *10*, 5613.
[198] Basabe, P.; Bodero, O.; Marcos, I. S.; Díez, D.; Blanco, A.; de Román, M.; Urones, J. G. *J. Org. Chem.* **2009**, *74*, 7750.
[199] Peris, G.; Miller, S. J. *Org. Lett.* **2008**, *10*, 3049.
[200] Cheng, Y. A.; Chen, T.; Tan, C. K.; Heng, J. J.; Yeung, Y.-Y. *J. Am. Chem. Soc.* **2012**, *134*, 16492.
[201] Simonot, B.; Rousseau, G. *J. Org. Chem.* **1994**, *59*, 5912.
[202] Zhang, W.; Zheng, S.; Liu, N.; Werness, J. B.; Guzei, I. A.; Tang, W. *J. Am. Chem. Soc.* **2010**, *132*, 3664.

Figure 88: Tang's cyclization of enynes to prepare cycloheptanyl esters.

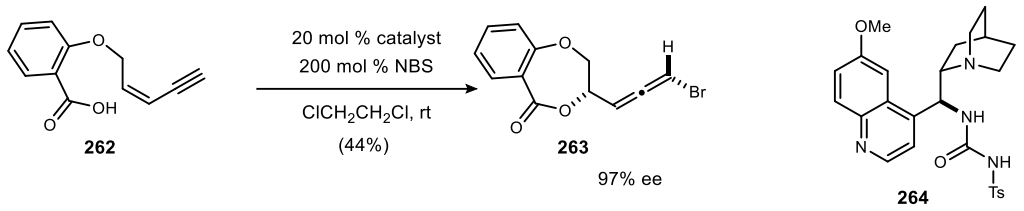

The development of highly selective methods to prepare ε-lactones could offer access to new chemical space. This is particularly important in medicinal chemistry, where it has been shown that limited synthetic methods narrow the chemical shape space in drug development.[4] 7-membered rings are an example of this disparity, where despite improved pharmacodynamic properties, limited synthetic methods have impeded their applications in industry.[184] To help address this, we have successfully developed an enantioselective method to prepare ε-lactones using BAM catalysis.

3.1.2 Mechanistic analysis of PIDA/I_2 as an oxidant system

The dual oxidant system PIDA/I_2, initially investigated by Suarez, has been employed in a variety of reactions, including oxidative decarboxylations[203] 1,5-HAT oxidations,[204] and aromatic halogenations.[205] It was proposed that the active oxidant in these conditions is acetyl hypoiodite, as shown in Figure 89.[206] Several other reagent oxidant combinations with iodine are also thought to generate acetyl hypoiodite in combination, including silver acetate[207], mercuric acetate[208], and lead tetraacetate.[209] While this species has not been successfully isolated, the combination of PIDA/I_2 has been studied to examine this hypothesis. For example, Story and coworkers successfully prepared 2-iodocyclohexyl acetate when PIDA/I_2 was exposed to

[203] Concepcion, J. I.; Francisco, C. G.; Freire, R.; Hernandez, R.; Salazar, J. A.; Suarez, E. *J. Org. Chem.* **1986**, *51*, 402.
[204] Hernández, R.; Rivera, A.; Salazar, J. A.; Suárez, E. *J. Chem. Soc., Chem. Commun.* **1980**, 958.
[205] Barnett, J. R.; Andrews, L. J.; Keefer, R. M. *J. Am. Chem. Soc.* **1972**, *94*, 6129.
[206] Courtneidge, J. L.; Lusztyk, J.; Pagé, D. *Tetrahedron Lett.* **1994**, *35*, 1003.
[207] Wilson, C. V. In *Organic Reactions*, p 332.
[208] Chen, E.; Keefer, R.; Andrews, L. *J. Am. Chem. Soc.* **1967**, *89*, 428.
[209] Heusler, K.; Kalvoda, J. *Angew. Chem. Int. Ed.* **1964**, *3*, 525.

Figure 89: Proposed acetyl hypoiodite formation in PIDA/I_2 oxidant system.

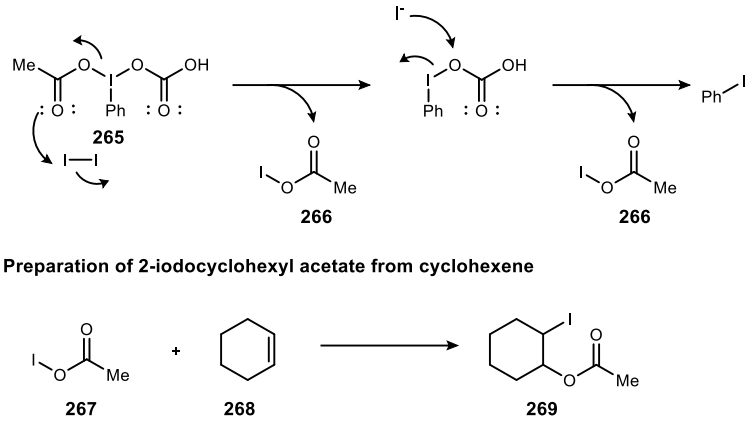

cyclohexene.[210] While this reaction supports the formation of acetyl hypoiodite, additional work has probed the decomposition of acetyl hypoiodite to understand failed isolation experiments.

As shown in Figure 90, it is proposed that isolation issues are linked to the decomposition of acetyl hypoiodite to methyl iodide and carbon dioxide, analogous to the Hundsdiecker reaction.[211] To probe this hypothesis, the thermal decomposition of phenyl diacetate (PIDA) was studied using gas chromatography.[210] It was observed that both methyl iodide and carbon dioxide were produced in 70.4 and 72.5 mol % respectively, relative to one mol of PIDA. In support of this hypothesis, methyl acetate was detected by GC-MS in another study of acetyl hypoiodite decomposition.[206] While acetyl hypoiodite has not been characterized, these decomposition studies support its formation in PIDA/I_2 reactions.

Figure 90: Proposed decomposition of acetyl hypoiodite.

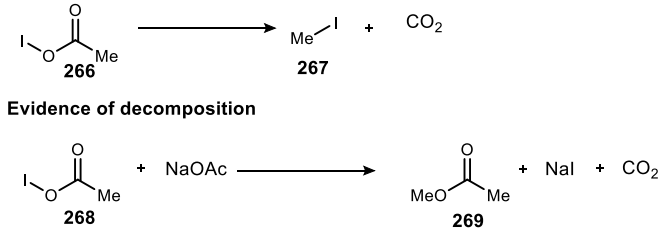

[210] Leffler, J. E.; Story, L. J. *J. Am. Chem. Soc.* **1967**, *89*, 2333.
[211] Hunsdiecker, H.; Hunsdiecker, C. *Berichte der deutschen chemischen Gesellschaft (A and B Series)* **1942**, *75*, 291.

While this oxidant system has been studied extensively, it has primarily been utilized at elevated temperatures or in light-mediated radical reactions.[212] For this reason, it is not clear if acetyl hypoiodite is the active oxidant in other applications. Hypervalent iodine reagents are reported in a variety of enantioselective alkene functionalizations.[213] In many of these reports, chiral iodine (III) catalysts participate in the formation of the halonium ion intermediate.[214,215] While acetyl hypoiodite is reported as a more reactive oxidant, there is precedent that PIDA is the active oxidant in alkene functionalizations. The study of acetyl hypoiodite as an oxidant does not necessarily discredit this alternative hypothesis. For these reasons, the active oxidizing species is still indeterminable in halocyclizations that employ PIDA/I_2.

3.2 Development of an enantioselective lactonization to prepare ε-lactones

3.2.1 Previous work in the preparation of ε-lactones via iodocyclization

The work detailed in this chapter was inspired by previous work to prepare *δ*-lactones using BAM catalysis.[19] In this chemistry, StilbPBAM·$HNTf_2$ furnished the lactone in high ee, and *N*-iodosuccinimide (NIS) proved to be a highly reactive oxidant. However, when these same conditions were employed by Andrew Flach[216] in the preparation of *ε*-lactones, no reactivity was observed. A notable oxidant system that was screened in previous work was PIDA/KI, which furnished the *ε*-lactone in a modest yield (14%). This was significant because it served as a proof of concept that ε-lactones may be prepared using conditions analogous to smaller ring ring-forming reactions. Additionally, this indicated that a hypervalent iodine source may be the key to reactivity in this lactonization. Most halolactonizations are highly specific to a halonium source, with the catalyst presumably activating it directly. Some differences were noted when PIDA/I_2 was employed as a highly reactive and moderately selective oxidant system in slightly modified conditions. Unlike established BAM-catalyzed cyclization, reactivity was poor in toluene.

[212] Giri, R.; Yu, J.-Q. In *Encyclopedia of Reagents for Organic Synthesis*.
[213] Li, X.; Chen, P.; Liu, G. *Beilstein J. Org. Chem.* **2018**, *14*, 1813.
[214] Lee, J. H.; Choi, S.; Hong, K. B. *Molecules* **2019**, *24*, 2634.
[215] Parra, A.; Reboredo, S. *Chem. Eur. J.* **2013**, *19*, 17244.
[216] Flach, A.; Investigation of Counterion Effects in an Organocatalyzed Iodolactonization and Discovery of an Organocatalyzed Iodolactonization to Give 7-Membered Lactones. Vanderbilt University, Nashville, 2017.

However, by employing a 1:1 ratio of toluene/dichloromethane, reactivity was greatly improved while maintaining high facial selectivity. (Figure 91)

Figure 91: Previous work toward the development of enantioselective ε-lactone synthesis.

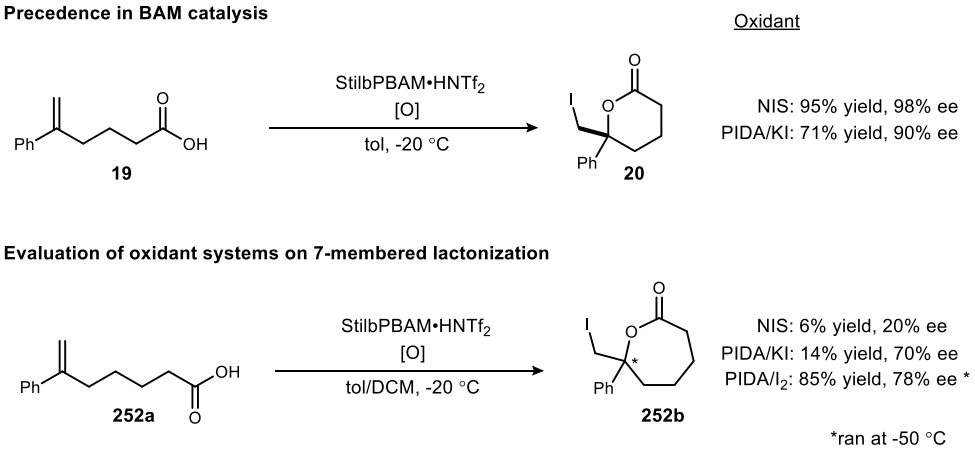

With an effective oxidant system in hand, optimization efforts were continued. However, after investigation of a wide range of variables, a highly selective and high yield reaction was not identified.[216] As noted in Chapter 2, this chemistry was analyzed again as a potential application of aryl triflamides in BAM catalysis. While this reaction was not improved through the application of achiral modifiers, the opportunity to reevaluate this work proved fruitful. The continued optimization of this 7-*exo* addition/lactonization chemistry will be detailed in this chapter.

3.2.2 Continued efforts in the preparation of 7-membered lactones

As briefly described in Chapter 2, modifying the quench procedure had a significant effect on ee. In previous work, the reaction was stopped by passing the crude reaction mixture through a silica plug. The lactone product eluted off silica, while the catalyst and carboxylic acid substrate did not. When this quench was later repeated, it was noted that a large amount of iodine eluted. It was hypothesized that an alternative quench method that efficiently neutralized remaining oxidant may be a more effective procedure. An inefficient quench procedure at elevated temperatures is problematic because the cyclization may proceed at elevated temperatures, which

would occur with lower ee. As illustrated by Table 14, an aqueous sodium thiosulfate quench was more effective and selectivity improved accordingly (entry 2).

With the oxidant system and quench procedure determined, optimization of other variables was pursued (Table 14). By employing a more basic ligand, the reaction time was reduced from three to two days (Table 14, entry 7). Additionally, increasing the concentration had a small improvement on both reactivity and selectivity (Table 14, entries 8 and 9). As observed previously, reactivity was poor when toluene was employed as solvent.

Table 14: Optimization of of BAM catalyzed ε-lactone synthesis.

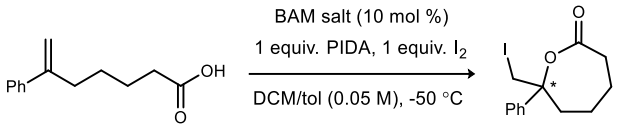

252a **252b**

entry	catalyst	procedural modification	time (h)	NMR yield (%)	ee
1	StilbPBAM·$HNTf_2$	control - SiO_2 quench	72	85	78
2	StilbPBAM·$HNTf_2$	$Na_2S_2O_{3(aq)}$	72	74	85
3	StilbPBAM	-	48	33	80
4	StilbPBAM·AcOH	-	48	33	81
5	StilbPBAM	1 equiv. of NEt_3	48	12	n/a
6	StilbPBAM·$HNTf_2$	toluene (0.2 M)	48	12	93
7	^{6}MeOStilbPBAM·$HNTf_2$	-	48	81	87
8	^{6}MeOStilbPBAM·$HNTf_2$	0.1 M	48	66	87
9	^{6}MeOStilbPBAM·$HNTf_2$	0.075 M	48	70	91
	^{6}MeOStilbPBAM·$HNTf_2$	0.075 M, -40 °C	48	80	83

The free base form of the catalyst furnished the lactone in similar ee to the triflimidic acid salt, though reactivity diminished significantly. Because it is hypothesized that Brønsted acid coordination to the halogen source is necessary for activation, it was proposed that the active catalyst species was actually a salt of the BAM ligand with the unsaturated carboxylic acid. To probe this effect, an acetic acid salt of the BAM ligand was employed, because it is similar in pK_a to the substrate. The StilbPBAM·AcOH catalyst furnished the lactone in similar yield and ee as the free-base example (Table 14, entries 3 and 4). This hypothesis was supported (Table 14,

entry 5) when free base catalyst was evaluated again, with an equivalent of triethylamine. Triethylamine inhibited the formation of a BAM·substrate salt, and therefore the Brønsted acid site was rendered inactive. In this experiment, conversion was poor. These results indicate that the protonation state of the catalyst is associated with turnover and/or reactivity, but little effect on facial selectivity.

Because the protonation state of the catalyst affects reactivity, it is proposed that the mode of activation is similar to previous BAM catalyzed cyclizations (Figure 41). The carboxylic acid is deprotonated by the catalyst, which controls the facial approach of the nucleophile (Brønsted base activation). The protonated site of the ligand hydrogen bonds to the halogenation agent, which provides electrophile control (Brønsted acid activation), as shown in Figure 92. The

Figure 92: Brønsted acid activation in BAM catalysis.

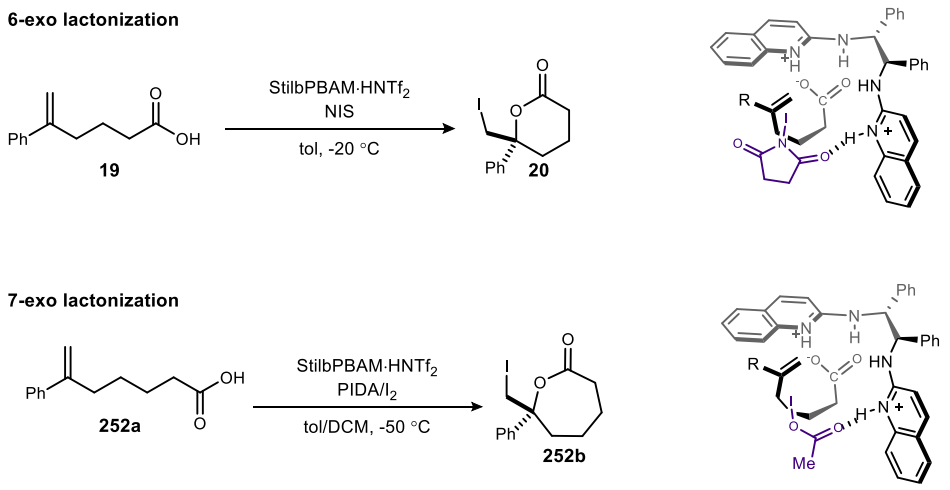

$PIDA/I_2$ oxidant system is capable of forming acetyl hypoiodite *in situ*.[206] Precedent in BAM catalysis indicates that a hydrogen bond acceptor is necessary for facial selectivity.[19] It is proposed that if *O*-iodoacetate is formed, it is a more reactive oxidant than *N*-iodosuccinimide, but still capable of coordinating to the Brønsted acid site of the BAM ligand, which controls alkene activation. As the absolute configuration of the lactone is not currently defined, the facial selectivity illustrated in Figure 92 has not been confirmed. As noted previously, it is possible that acetyl hypoiodite is not the active oxidant in this reaction. In previous work where silver acetate and iodine were employed as a different method to access acetyl hypoiodite, reactivity was poor.[216] For this reason, the nature of the active oxidant in this cyclization is still unclear.

The halolactonization reaction of unsaturated acids is primarily limited to the formation of (β, γ, and δ) lactones. This work employs BAM catalysis to expand this paradigm to include ε-lactones. By modifying the quench procedure and employing a more basic BAM catalyst, this cyclization furnished 7-membered lactones in high ee. A novel oxidant system (PIDA/I_2) proved necessary for conversion, which deviates from previous work in BAM catalysis. With optimization complete, a scope of this chemistry was investigated.

3.2.3 Analysis of scope and limitations BAM-catalyzed lactonization reaction to prepare ε-lactones

Table 15 illustrates the scope of this chemistry. Substituents at the alkene affected reactivity with the preferences for an unhindered π-nucleophile to engage the halogenating agent. As expected, electron donating groups (Table 15, **285b**-**288b**) lead to lactones in high yields and

Figure 93: Evaluation of alkyl substitutions in BAM catalyzed lactonization.

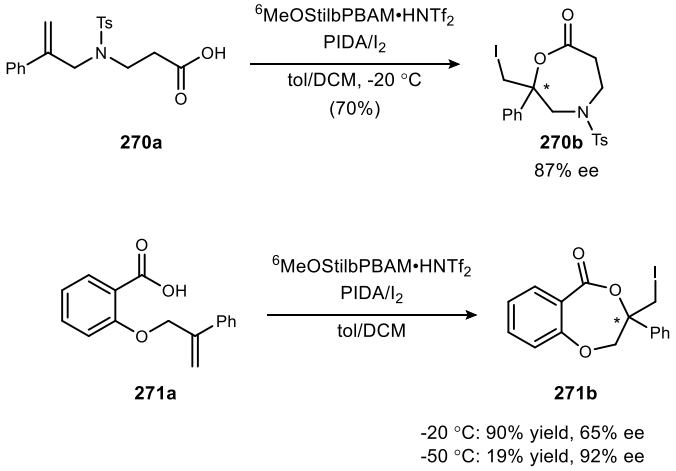

good enantioselectivity (83-90% ee). Highly electron rich *para*-methoxy (**286b**) and sterically demanding 2-napthalene (**277b**) gave the desired product in 49% and 87% ee respectively. Unfortunately, substitution in close proximity to the olefin was not tolerated, as illustrated by substrate **280b**, which was unreactive. Electron deficient aryl rings were prepared in high enantioselectivity (96% ee), but reactivity was poor. Olefins bearing aliphatic substituents, as opposed to styrene derivatives, were converted to desired lactones with moderate selectivity, as

shown with substrate **289b**. This substrate produced the respective lactone in 55% ee. The substrate scope is not yet complete, as evidence by blank entries in the table. Those entries have been left vacant to illustrate current work that is underway. It is anticipated that the substrate scope will be completed very soon.

In addition to modifying substituents of the alkene, substrates were prepared with

Table 15: Substrate scope evaluation of BAM catalyzed lactonization.

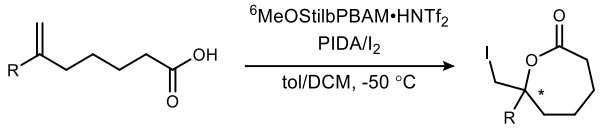

Xa **Xb**

entry	R	product	yield (%)	ee (%)
1	C_6H_5	252b	71	88
2	^2Np	272b	64	87
3	$^pMeC_6H_4$	273b	87	77
4	$^mMeC_6H_4$	274b	76	84
5	$^oMeC_6H_4$	275b	trace	n/a
6	$^pFC_6H_4$	276b	-	-
7	$^mFC_6H_4$	277b	-	-
8	$^pClC_6H_4$	278b	-	-
9	$^mClC_6H_4$	279b	21	96
10	$^pPhC_6H_4$	280b	72	84
11	$^pMeOC_6H_4$	281b	53	49
12	$^mMeOC_6H_4$	282b	63	90
13	$^p(^tBu)C_6H_4$	283b	66	83
14	Me	284b	-	-
15	H	285b	-	-

functionalized alkyl chains as shown in Figure 93. Elevated temperatures were required for reactivity, though selectivity was still quite good (65-87% ee). A surprising drop in ee was observed when substrate **276a** was run at elevated temperatures. Notably, at lower temperatures lactone **276b** was prepared in high enantioselectivity.

3.2.4 Conclusions

In conclusion, we have developed conditions to prepare enantioenriched ε-lactones via BAM catalysis. Optimization of the bisamidine organocatalyst indicated that pK_a had an effect on both reactivity and selectivity, which indicates that the basicity of the catalyst may be tuned to the substrate. Additionally, modifications to the quench procedure had a significant effect on enantioselectivity. As this reaction is not currently reported in the literature, this work illustrates how the paradigm of halocyclization may still be extended to larger ring sizes. The novel application of PIDA/I_2 as an oxidant system may serve as a model for future reaction development in this field.

3.3 Future directions

Future work will focus on completing the substrate scope and showcasing the utility of the cyclization product by derivatizing the scaffold to other small molecules of interest (Figure 94). Derivations of similar scaffolds have been reported previously, which indicates that these proposed reactions should be feasible.[30,60] The halogenated handle may be derivatized via displacement chemistry to incorporate other heteroatoms. This displacement chemistry assumes that the primary halide will be a more reactive electrophile than the ester. The carbonate chemistry is expected to be quite similar to this scaffold, where reduction of the primary halide was carried out in high yield.[30] Lithium aluminum hydride reduction will be investigated to prepare reduced enantioenriched 1,6-diol (**295**).

Employing this lactonization as a method to hydrate olefins enantioselectively would broadly increase the utility of this transformation. Analogous to enantioselective epoxidations or dihydroxylations, this cyclization procedure could be used to functionalize unactivated alkenes. The preparation of chiral tertiary alcohols is a notable synthetic challenge that is addressed by this lactonization reaction. Hydrolysis of the ester with a basic resin should lead to the chiral epoxide **294**. This transformation could also be employed to prepare enantioenriched dihydroxy acids, by opening the chiral epoxide **294** with hydroxide. While ε-lactones have synthetic value in their own right, derivatization of this scaffold would increase the general utility of this reaction.

Figure 94: Proposed derivations of ε-lactones.

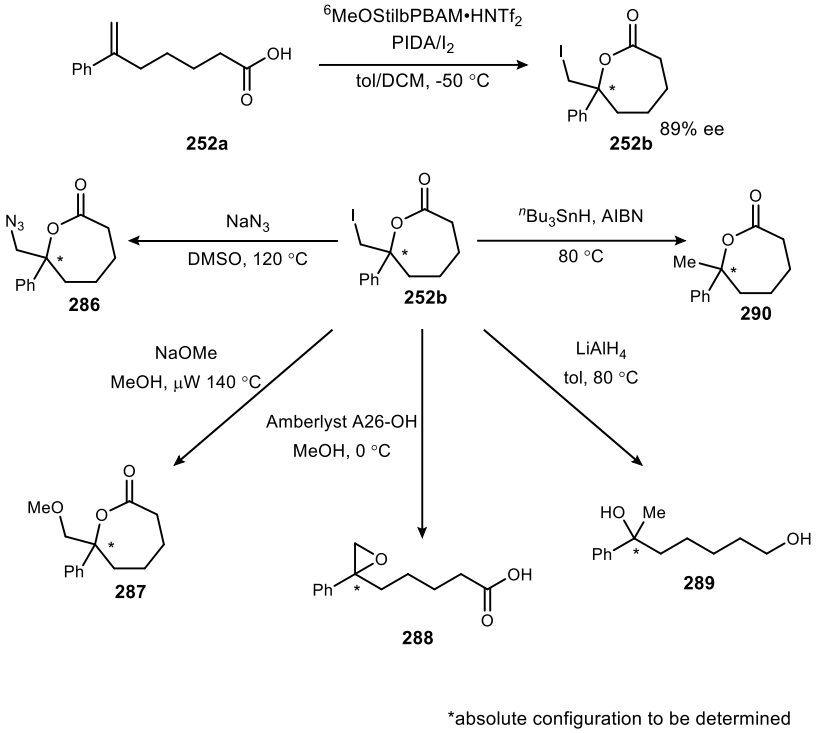

Chapter 4 - experimental appendix

General Procedure for Synthesis of Homoallylic Secondary Amines

Tosylated/mesylated alcohol precursors were prepared according to the known procedure from the corresponding homoallylic alcohols and used immediately due to decomposition.[1]
A flame-dried, round-bottomed flask, equipped with a stir bar and condenser, was charged with the primary amine (10.5 mmol, 5.0 equiv), tosylated alcohol (2.1 mmol, 1.0 equiv) and ethanol (3 mL). The resulting solution was stirred at reflux temperature until TLC showed complete consumption of starting material (12 h). The solution was cooled to room temperature. The reaction mixture was concentrated *in vacuo* to remove ethanol. Flash column chromatography (SiO_2, 10-30% ethyl acetate in hexanes with 0.5% triethylamine) yielded the desired homoallylic disubstituted amine.

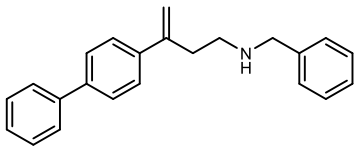

3-([1,1'-Biphenyl]-4-yl)-*N*-benzylbut-3-en-1-amine (134a). The reaction was carried out according to the general procedure, using 3-([1,1'-biphenyl]-4-yl)but-3-en-1-yl 4-methylbenzenesulfonate (309 mg, 81.7 µmol) and benzyl amine (437 mg, 4.09 mmol). The crude material was separated by silica gel chromatography (SiO_2, 20-50% ethyl acetate in hexanes with 0.5% triethylamine) to afford a yellow oil (109 mg, 43%). IR (film) 3308, 3057, 3018, 2938, 2824, 1676, 1601, 1487 cm^{-1}; R_f = 0.1 (50% EtOAc/hexanes); ^1H NMR (400 MHz, $CDCl_3$) δ 7.61 (m, 2H), 7.57 (dt, *J*=8.4, 2.0 Hz, 2H), 7.49 (m, 2H), 7.44 (dt, *J* = 7.9, 1.6 Hz, 2H), 7.37-7.29 (m, 2H), 7.27 (d, *J*=2.8 Hz, 2H), 7.26-7.20 (m, 2H), 5.40 (d, *J*=1.4 Hz, 1H), 5.14 (d, *J*=1.1 Hz, 1H), 3.79 (s, 2H), 2.79 (t, *J*=3.3 Hz, 4H); ^{13}C NMR (150 MHz, $CDCl_3$) ppm 145.9, 140.8, 140.5, 139.7, 128.9, 128.5, 128.2, 127.5, 127.2, 127.12, 127.10, 127.0, 126.7, 113.9, 53.9, 47.8, 35.8; HRMS (ESI): Exact mass calcd for $C_{23}H_{24}N$ $[M+H]^+$ 314.1903, found 314.1919.

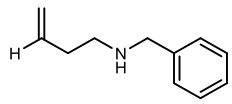

N-benzylbut-3-en-1-amine (143a). A 25-mL round-bottomed flasked was charged with benzyl amine (1.0 mL, 9.5 mmol), Cs_2CO_3 (1.49 g, 4.58 mmol), and DMF (13.5 mL) and stirred at room temperature for 30 m. To the white suspension, 4-bromobut-1-ene (0.93 mL, 4.58 mmol) was added in one portion. After 24 hours, the reaction was filtered and concentrated. The residue was taken up in ethyl acetate and washed with NaOH (1 M). The combined organic layer was washed with brine, dried with $MgSO_4$, and concentrated. Flash column chromatography (SiO_2, 10% ethyl acetate in hexanes) of the residue yielded an orange oil (471 mg, 64%). IR (film) 3308, 3065, 3028, 2924, 2844, 1674, 1643 cm^{-1}; R_f = 0.2 (30% EtOAc/hexanes); ^1H NMR (400 MHz, $CDCl_3$) δ 7.26 (d, *J* = 1.7 Hz, 2H), 7.20 (s, 3H), 5.74 (ddt *J* = 17.2, 10.2, 6.9 Hz, 1H), 5.03 (ddd, *J* = 17.1, 3.4, 1.6 Hz, 2H), 4.98 (ddt, *J* = 10.2, 1.7, 0.8 Hz, 1H), 3.74 (s, 2H), 2.65 (t, *J* = 6.8 Hz, 2H), 2.32 (ddt, *J* = 13.7, 6.8, 1.3 Hz, 2H); ^{13}C NMR (100 MHz, $CDCl_3$) ppm 136.5, 128.5, 128.2, 127.0, 116.4, 54.0, 48.4, 34.3; HRMS (ESI): Exact mass calcd for $C_{11}H_{16}N$ $[M+H]^+$ 162.1277, found 162.1283.

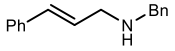

(E)-N-benzyl-3-phenylprop-2-en-1-amine (S1). The reaction was carried out according to the general procedure, using cinnamyl methanesulfonate (789 mg, 3.7 mmol) and benzyl amine (1.6 mL, 15 mmol). The crude material was separated by silica gel chromatography (SiO_2, 10-30% ethyl acetate in hexanes with 0.5% triethylamine) to afford a

[1] Haung, Q.; Fazio, A.; Dai, G.; Campo, M.A.; Larock, R.C. *J. Am. Chem. Soc.* **2004**, 126, 7460-7461.

yellow oil (286 mg, 35%). IR (film) 3026, 2920, 2806, 2359, 2335, 1554, 1535, 1492, 1451 cm^{-1}; R_f = 0.2 (30% EtOAc/hexanes); ^1H NMR (400 MHz, $CDCl_3$) δ 7.37 (t, *J* = 1.5 Hz, 1H), 7.36 (br s, 2H), 7.35 (s, 1H), 7.33 (d, *J* = 1.1 Hz, 2H), 7.32, (br s, 1H), 7.30 (br s, 1H), 7.28-7.26 (m, 1H), 7.23-7.19 (m, 1H), 6.54 (d, *J* = 15.9 Hz, 1H), 6.32 (ddd, *J* = 15.9, 6.3, 6.3, 1H), 3.84 (s, 2H), 3.44 (dd, *J* = 6.3, 1.4 Hz, 2H), ^{13}C NMR (100 MHz, $CDCl_3$) ppm 140.4, 137.3, 131.51, 128.7, 128.6, 128.6, 128.3, 127.5, 127.1, 126.4, 53.5, 51.4; HRMS (ESI): Exact mass calculated for $C_{16}H_{17}N$ $[M+H]^+$ 224.1395, found 224.1434.

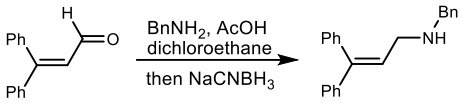

N-benzyl-3,3-diphenylprop-2-en-1-amine (S2). A flame dried 15-mL, round bottomed flask, equipped with a stir bar was charged with 3,3-diphenylacrylaldehyde (250 mg, 1.2 mol), benzyl amine (0.14 mL, 1.2 mol), acetic acid (70 µL, 1.2 mmol), and dichloroethane (4.3 mL). The mixture was allowed to stir at room temperature for 10 m, then sodium cyanoborohydride (356 mg, 1.7 mmol) was added. The reaction was monitored by TLC and after four hours was quenched with sat. $NaHCO_{3(aq)}$. The mixture was transferred to the separatory funnel and was extracted with ethyl acetate. The combined organic layers were dried with $MgSO_4$ and concentrated. Flash column chromatography (SiO_2, 10-30% ethyl acetate in hexanes) of the residue yielded a colorless oil (160 mg, 45%). IR (film) 3329, 3036, 3026, 2913, 2845, 2399, 1668, 1598 cm^{-1}; R_f = 0.1 (30% EtOAc/hexanes); ^1H NMR (400 MHz, $CDCl_3$) δ 7.37-7.33 (m, 3H), 7.31 (s, 1H), 7.29 (d, *J* = 1.2 Hz, 1H), 7.28-7.26 (m, 3H), 7.25 (dd, *J* = 4.5, 1.2 Hz, 3H), 7.24 (dd, *J* = 2.5, 2.5 Hz, 1H), 7.16 (ddd, *J* = 6.0, 1.7, 1.7 Hz, 2H), 6.20 (dd, *J* = 6.9, 6.9 Hz, 1H), 3.74 (s, 2H), 3.35 (d, *J* = 6.9 Hz, 2H); ^{13}C NMR (100 MHz, $CDCl_3$) ppm 143.7, 142.3, 140.3, 139.7, 129.9, 128.5, 128.3, 128.2, 127.8, 127.5, 127.4, 127.3, 127.0, 53.6, 48.2; HRMS (ESI): Exact mass calcd for $C_{22}H_{21}N$ $[M+H]^+$ 300.1708, found 300.1747.

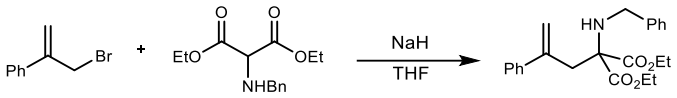

Diethyl 2-(benzylamino)-2-(2-phenylallyl)malonate (S3). A 50-mL, round-bottomed flask equipped with a stir bar was charged with diethyl 2-(benzylamino)malonate (500 mg, 1.88 mmol) and THF (20 mL). NaH (90 mg, 37.6 mmol) was added slowly at 0 ºC, then the reaction was heated to 80 ºC. (3-Bromoprop-1-en-2-yl)benzene (445 mg, 2.26 mmol) was added dropwise. The reaction mixture was stirred for 2 h, cooled to rt, quenched with satd aq NH_4Cl, and extracted with ethyl acetate. The combined organic layers were dried ($MgSO_4$), filtered, and concentrated. Flash column chromatography (SiO_2, 10-30% ethyl acetate in hexanes) of the residue yielded a clear oil (389 mg, 55%). IR (film) 3448, 3059, 3028, 2982, 2935, 2846, 1734, 1628 cm^{-1}; R_f = 0.6 (20% EtOAc/hexanes); ^1H NMR (400 MHz, $CDCl_3$) δ 7.36-7.24 (m, 2H), 7.27 (m, 2H), 7.26 (m, 3H), 7.25 (m, 3H), 5.47 (s, 1H), 5.42 (s, 1H), 4.30 (s, 1H), 4.21 (q, *J* = 7.1 Hz, 2H), 3.90 (s, 2H), 3.75 (s, 2H), 1.53 (s, 2H), 1.27 (t, *J* = 7.1 Hz, 6H); ^{13}C NMR (100 MHz, $CDCl_3$) ppm 168.3, 145.4, 139.9, 139.0, 129.2, 128.3, 128.1, 127.6, 127.3, 126.8, 116.1, 65.2, 61.3, 55.7, 55.6, 14.3; HRMS (ESI): Exact mass calcd for $C_{23}H_{28}NO_4$ $[M+H]^+$ 382.2013, found 382.2013.

General Procedure for Enantioselective Carbamations

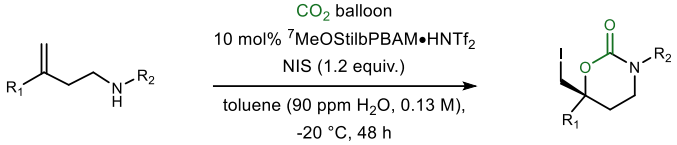

To an oven-dried vial equipped with a stir bar was added ^{7}MeOStilbPBAM•HNTf$_2$ (12.0 mg, 12.6 μmol), the amine (126 μmol), and a wet solution of toluene (90 ppm, 1 mL)[2]. The reaction mixture was stirred at 750 RPM at 25 °C for 15 minutes under CO_2 atmosphere (balloon) and then cooled to -20 °C. NIS (34.0 mg, 151 μmol) was added after 1 hour.[3] The reaction mixture was stirred without light for 48 h (unless noted otherwise) under CO_2 (balloon). The mixture was treated with 20% aq sodium thiosulfate (4 mL). The aqueous layer was extracted twice with ethyl acetate and the organic layers were combined, dried over magnesium sulfate and concentrated. Flash column chromatography (SiO_2, 5-10-30% ethyl acetate in hexanes) yielded the desired product.

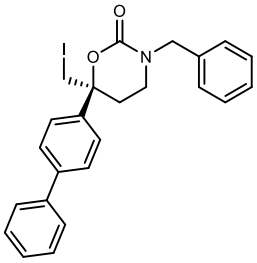

(*S*)-6-([1,1'-Biphenyl]-4-yl)-3-benzyl-6-(iodomethyl)-1,3-oxazinan-2-one (134b). The reaction was carried out over 48 h according to the general procedure, using 3-([1,1'-biphenyl]-4-yl)-N-benzylbut-3-en-1-amine (39.0 mg, 126 μmol) and (*S,S*)-^{7}MeOStilBPBAM·HNTf$_2$. The crude material was separated by silica gel chromatography (SiO_2, 5-30% ethyl acetate in hexanes) to afford a yellow solid (46.6 mg, 77%) that was determined to be 91% ee by chiral HPLC (Chiralpak AD-H: 20% IPA/hexanes, 1.0 mL/min: t_r(major) = 20.7 min, t_r(minor) = 22.8 min)). Mp 100-103 °C; $[\alpha]_D^{20}$ +39.3 (*c* 1.00, $CHCl_3$); R_f = 0.3 (30% EtOAc/hexanes); IR (film) 3034, 2916, 1692, 1485, 1445 cm^{-1}; ^{1}H NMR (400 MHz, $CDCl_3$) δ 7.61 (dd, *J* = 8.0, 8.0 Hz, 4H), 7.47 (m, 4H), 7.38 (m, 1H), 7.16 (dd, *J* = 3.1, 3.1 Hz, 3H), 7.00 (d, *J* = 1.8 Hz, 1H), 6.99 (t, *J* = 3.6 Hz, 1H), 4.59 (d, *J* = 15.1 Hz, 1H), 4.40 (d, *J* = 15.1 Hz, 1H), 3.60 (d, *J* = 11.0 Hz, 1H), 3.53 (d, *J* = 11.4 Hz, 1H), 3.07 (ddd, *J* = 11.9, 6.1, 1.8 Hz, 1H), 2.90 (ddd, *J* = 17.7, 17.7, 5.1 Hz, 1H), 2.55 (ddd, *J* = 20.0, 20.0, 6.0 Hz, 1H), 2.45 (ddd, *J* = 13.9, 5.3, 2.2 Hz, 1H); ^{13}C NMR (150 MHz, $CDCl_3$) ppm 153.1, 141.7, 140.2, 137.9, 136.2, 129.0, 128.6, 127.9, 127.8, 127.7, 127.6, 127.2, 125.8, 81.1, 52.4, 41.8, 20.8, 15.8; HRMS (ESI): Exact mass calcd for $C_{24}H_{23}INO_2$ -[M+H]$^+$ 484.0768, found 484.0804.

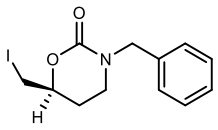

(S)-3-benzyl-6-(iodomethyl)-1,3-oxazinan-2-one (143b). The reaction was carried out over 5 days according to the general procedureusing *N*-benzylbut-3-en-1-amine (20.3 mg, 126 μmol). The crude material was purified by silica gel chromatography (SiO_2, 5-30% ethyl acetate in hexanes) to afford a yellow oil (17.8 mg, 43%) that was determined to be 13% ee by chiral HPLC (Chiralcel IA: 15% IPA/hexanes, 1.0 mL/min, t_r(major) = 19.0 min, t_r(minor) = 16.5 min). $[\alpha]_D^{20}$ +6.7 (*c* 1.00, $CHCl_3$); R_f = 0.2 (30% EtOAc/hexanes); IR (film) 3027, 2924, 1691, 1489 cm^{-1}; ^{1}H NMR (400 MHz, $CDCl_3$) δ 7.30 (dd, *J* = 7.0, 7.0 Hz, 2H), 7.27 (d, *J* = 7.0 Hz, 1H), 7.24 (s, 1H), 7.22 (s, 1H), 4.66 (d, *J* = 14.8 Hz, 1H), 4.49 (d, *J* = 14.9 Hz, 1H), 4.24 (dddd, *J* = 10.2, 7.6, 4.6, 2.7 Hz, 1H), 3.37 (dd, *J* = 10.5, 4.3 Hz, 1H), 3.23 (ddd, *J* = 11.4, 11.4, 5.1 Hz, 1H), 3.19 (dd, *J* = 10.5, 7.9 Hz, 1H),

[2] In order to prepare a 90 ppm solution of wet toluene, 2.7 μL of water was added to 30 mL of dry toluene. Amount of water in solution was constant for at least 6 weeks when maintained properly in a sealed flask.
[3] It is important to stir substrate vigorously, without material adhering to the sides of the glass.

3.15 (ddd, *J* = 12.0, 6.1, 2.8 Hz, 1H), 2.23 (dddd, *J* = 13.8, 5.1, 2.6, 2.6 Hz, 1H), 1.83 (dddd, *J* = 13.8, 10.6, 10.6, 5.9 Hz, 1H); ^{13}C NMR (150 MHz, $CDCl_3$) ppm 153.1, 136.5, 128.9, 128.2, 128.0, 76.1, 52.7, 43.2, 27.3, 5.46; HRMS (ESI): Exact mass calcd for $C_{12}H_{15}INO_2$ $[M+H]^+$ 332.0103, found 332.0142.

Synthesis of a Selective σ1 Ligand

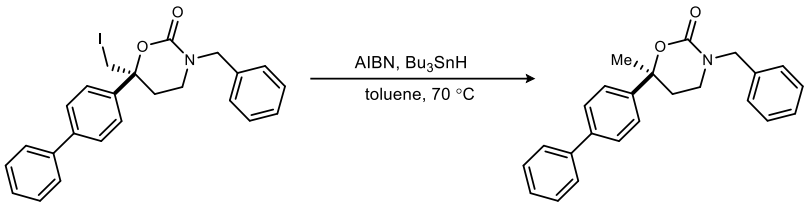

(*S*)-6-([1,1'-Biphenyl]-4-yl)-3-benzyl-6-methyl-1,3-oxazinan-2-one (149a). To a microwave vial equipped with a stir bar was added (*S*)-6-([1,1'-biphenyl]-4-yl)-3-benzyl-6-(iodomethyl)-1,3-oxazinan-2-one (104.1 mg, 220 μmol, 89% ee), tributyltin hydride (105 μL, 390 μmol) and anhydrous toluene (1 mL). The reaction mixture was degassed and warmed to 80 °C. Once warmed, a solution of AIBN (30 mg, 180 μmol) and toluene (1 mL) was added in portions until full conversion was observed. The reaction mixture was cooled to ambient temperature, concentrated to an oil, and purified by silica gel chromatography (SiO_2, 5-30% ethyl acetate in hexanes) to afford a pale yellow amorphous solid (63.3 mg, 82%) that was determined to be 84% ee by chiral HPLC (Chiralpak AD-H: 15% IPA/hexanes, 1.0 mL/min: t_r(minor) = 16.0 min, t_r(major) = 17.5 min)). $[\alpha]_D^{20}$ +28.2 (*c* 1.00, $CHCl_3$); R_f = 0.3 (30% EtOAc/hexanes); IR (film) 2924, 2855, 1690, 1488, 1449 cm^{-1}; ^{1}H NMR (400 MHz, $CDCl_3$) δ ^{1}H NMR (400 MHz, $CDCl_3$) δ 7.59 (d, *J* = 8.0 Hz, 4H), 7.46 (dd, *J* = 7.4, 7.4 Hz, 2H), 7.43 (d, *J* = 8.5 Hz, 2H), 7.37 (t, *J* = 7.2 Hz, 1H), 7.20 (dd, *J* = 5.1, 1.7 Hz, 3H), 7.07 (m, 2H), 4.56 (d, *J* = 15.1 Hz, 1H), 4.48 (d, *J* = 15.1 Hz, 1H), 3.06 (ddd, *J* = 11.8, 5.8, 3.3 Hz, 1H), 2.90 (ddd, *J* = 17.2, 17.2, 5.1 Hz, 1H), 2.40 (ddd, *J* = 13.8, 5.0, 3.3 Hz, 1H), 2.23 (ddd, *J* = 14.0, 11.1, 6.0 Hz, 1H), 1.70 (s, 3H); ^{13}C NMR (150 MHz, $CDCl_3$) ppm 153.9, 142.4, 140.6, 140.5, 136.5, 129.0, 128.6, 127.8, 127.59, 127.57, 127.2, 124.9, 81.8, 52.4, 41.9, 32.9, 30.5, 29.8; HRMS (ESI): Exact mass calcd for $C_{24}H_{24}NO_2$ $[M+H]^+$ 358.1802, found 358.1800.

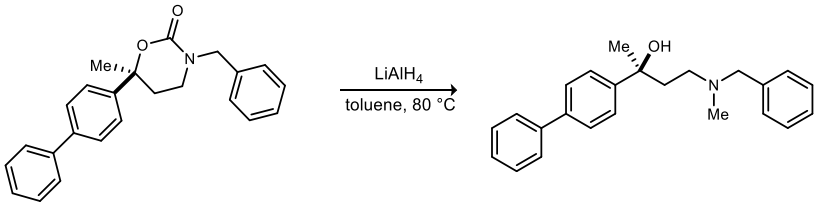

(*S*)-2-([1,1'-Biphenyl]-4-yl)-4-(benzyl(methyl)amino)butan-2-ol (149b). To a microwave vial equipped with a stir bar was added $LiAlH_4$ (8.0 mg, 500 μmol), (*S*)-6-([1,1'-biphenyl]-4-yl)-3-benzyl-6-methyl-1,3-oxazinan-2-one (55.3 mg, 150 μmol, 84% ee) and anhydrous toluene (2.7 mL). The reaction mixture was stirred at 80 °C (preheated oil bath) for 12 h. The mixture was then cooled to room temperature and treated with Rochelle's salt solution (2 mL). The aqueous layer

was extracted twice with CH_2Cl_2 and the organic layers were combined, dried, and concentrated. The desired product was a yellow-tinted amorphous solid (49.9 mg, 92%) that was determined to be 84% ee by chiral HPLC (Chiralpak AD: 4% EtOH/hexanes, 1.0 mL/min: t_r(minor) = 8.1 min, t_r(major) = 9.4 min). $[\alpha]_D^{20}$ -24.4 (*c* 1.0, $CHCl_3$); R_f = 0.1 (30% EtOAc/hexanes); IR (film) 3271, 3029, 3085, 2923, 2851, 1603, 1553, 1485 cm^{-1}; ^1H NMR (400 MHz, $CDCl_3$) δ ^1H NMR (400 MHz, $CDCl_3$) δ 7.62 (d, *J* = 6.9 Hz, 2H), 7.56 (d, *J* = 8.5 Hz, 2H), 7.51 (d, *J* = 8.3 Hz, 2H), 7.44 (dd, *J* = 7.6, 7.6 Hz, 3H), 7.34 (dd, *J* = 7.0, 7.0 Hz, 3H), 7.32 (dd, *J* = 4.1, 4.1 Hz, 2H), 7.30 (m, 1H), 3.56 (d, *J* = 12.7 Hz, 1H), 3.34 (d, *J* = 12.5 Hz, 1H), 2.49 (m, 2H), 2.17 (s, 3H), 2.17 (m, 1H), 1.95 (ddd, *J* = 14.6, 4.5, 3.2 Hz, 1H), 1.55 (s, 3H); ^{13}C NMR (150 MHz, $CDCl_3$) ppm 147.7, 141.1, 139.1, 129.7, 128.9, 128.7, 127.9, 127.2, 127.1, 126.8, 125.6, 75.7, 62.5, 54.7, 41.6, 38.1, 31.6, 29.8; HRMS (ESI): Exact mass calcd $C_{24}H_{28}NO$ for $[M+H]^+$ 346.2165, found 346.2192.

X-ray Struction of 7MeOStilbPBAM (10)

A single crystal of purified ligand **10** was grown by the vapor-diffusion method in dichloromethane under hexanes atmosphere, and was analyzed by X-ray crystallography.

Details of crystallographic refinement for 10.

A suitable crystal was selected for analysis and mounted in a polyimide loop. All measurements were made on a Rigaku Oxford Diffraction Supernova EosS2 CCD with filtered Cu-Kα radiation at a temperature of 100 K. Using Olex2[1], the structure was solved with the ShelXT structure solution program using Direct Methods and refined with the ShelXL refinement package using Least Squares minimization.[2]

Table 1. Crystal data and structure refinement for 7c.

Empirical formula	$C_{42}H_{44}N_6O_2 \cdot 3(CH_2Cl_2)$	
Formula weight	919.61	
Temperature	100.01(10) K	
Wavelength	1.54184 Å	
Crystal system	Orthorhombic	
Space group	$P2_12_12_1$	
Unit cell dimensions	a = 14.5500(3) Å	α = 90°
	b = 24.8696(5) Å	β = 90°
	c = 25.0479(5) Å	γ = 90°
Volume	9063.7(3) $Å^3$	
Z	8	
Density (calculated)	1.348 Mg/m^3	
Absorption coefficient	3.810 mm^{-1}	
F(000)	3840	
Crystal size	0.333 x 0.271 x 0.15 mm^3	
Theta range for data collection	2.504 to 63.674°.	
Index ranges	-13<=h<=16, -25<=k<=28, -29<=l<=29	
Reflections collected	44220	
Independent reflections	14841 [R(int) = 0.0486]	
Completeness to theta = 63.674°	99.8 %	
Absorption correction	Gaussian	
Max. and min. transmission	1.000 and 0.413	
Refinement method	Full-matrix least-squares on F^2	
Data / restraints / parameters	14841 / 0 / 1067	
Goodness-of-fit on F^2	1.066	
Final R indices [I>2sigma(I)]	R1 = 0.0908, wR2 = 0.2480	
R indices (all data)	R1 = 0.0969, wR2 = 0.2570	
Absolute structure parameter (Flack)	0.020(6)	
Largest diff. peak and hole	1.109 and -0.944 $e/Å^{-3}$	

Table 2. Atomic coordinates (x 10^5) and equivalent isotropic displacement parameters ($Å^2$x 10^4) for 7c. U(eq) is defined as one third of the trace of the orthogonalized U^{ij} tensor.

	x	y	z	U(eq)
Cl(1A)	40297(19)	56461(11)	16010(10)	598(6)
Cl(2A)	36260(19)	53725(10)	27127(10)	591(6)
C(1A)	44560(70)	56120(40)	22560(40)	570(20)
Cl(1G)	28520(30)	66817(15)	7950(20)	1032(14)
Cl(2G)	32850(30)	77924(14)	10515(19)	1031(14)
C(1G)	34500(90)	71270(50)	12320(60)	770(40)
Cl(1F)	95580(20)	82417(12)	32498(14)	759(8)
Cl(2F)	106720(20)	73188(13)	35553(15)	783(9)
C(1F)	96170(80)	75470(50)	32810(60)	710(30)
Cl(1C)	20210(30)	62940(20)	22530(40)	1530(30)
Cl(2C)	12560(30)	73388(12)	20425(15)	796(9)
C(1C)	11460(120)	66450(70)	22020(110)	1180(70)
Cl(1D)	85440(20)	96783(14)	-2336(16)	820(9)
Cl(2D)	67300(20)	92925(19)	331(18)	949(11)
C(1D)	76590(100)	96830(50)	2290(50)	720(30)
Cl(1E)	73228(19)	89038(11)	46381(11)	627(6)
Cl(2E)	90361(19)	83198(14)	47761(15)	765(9)
C(1E)	79290(90)	83170(50)	44750(60)	730(30)
O(1)	104820(60)	56460(40)	43840(30)	680(20)
O(2)	27420(50)	69490(30)	37150(20)	479(15)
N(1)	90190(40)	62390(30)	27840(20)	295(13)
N(2)	102390(50)	49910(30)	18830(30)	416(16)
N(3)	82920(40)	65290(20)	20290(20)	276(12)
N(4)	64440(40)	67040(30)	18970(20)	300(12)
N(5)	52920(40)	68190(20)	25070(20)	277(12)
N(6)	48210(50)	83780(30)	18810(30)	337(13)
C(1)	88410(50)	61560(30)	22620(30)	300(15)
C(2)	92060(50)	57270(30)	19640(30)	314(15)
C(3)	98260(50)	53730(30)	21910(30)	333(16)
C(4)	99910(50)	54300(30)	27600(30)	318(15)
C(5)	95790(50)	58700(30)	30250(30)	333(16)
C(6)	97460(60)	59490(40)	35770(30)	391(17)
C(7)	102710(60)	55870(40)	38580(30)	480(20)
C(8)	106490(70)	51350(40)	36100(40)	540(20)
C(9)	105120(70)	50600(40)	30720(40)	470(20)
C(10)	100970(90)	60990(70)	46540(40)	770(40)
C(11)	111490(80)	47420(50)	19840(50)	630(30)
C(12)	115410(90)	46420(60)	14470(50)	740(40)
C(13)	106960(90)	45560(50)	10940(40)	660(30)
C(14)	100480(60)	49850(40)	12990(30)	450(20)
C(15)	78990(50)	64680(30)	15030(30)	273(14)
C(16)	70650(50)	68540(30)	14670(30)	269(14)
C(17)	85990(50)	65480(30)	10580(30)	305(15)
C(18)	85410(60)	62590(40)	5880(30)	398(18)
C(19)	91940(70)	63240(40)	1850(40)	540(20)
C(20)	99310(70)	66600(50)	2670(40)	550(30)
C(21)	100070(60)	69480(40)	7360(40)	480(20)
C(22)	93400(60)	68950(30)	11310(30)	373(17)
C(23)	66080(50)	68560(30)	9300(30)	290(15)
C(24)	69370(50)	71810(30)	5150(30)	367(17)

C(25)	65140(70)	71820(40)	250(40)	490(20)
C(26)	57460(80)	68800(40)	-670(40)	530(20)
C(27)	53950(70)	65620(40)	3400(40)	500(20)
C(28)	58290(60)	65580(30)	8290(30)	398(18)
C(29)	57710(50)	70240(30)	21010(30)	256(13)
C(30)	56200(50)	75390(30)	18900(30)	275(14)
C(31)	49430(50)	78740(30)	21010(30)	279(14)
C(32)	43840(50)	76610(30)	25270(30)	285(14)
C(33)	45970(50)	71280(30)	27070(30)	295(15)
C(34)	40580(50)	68950(30)	31170(30)	330(15)
C(35)	33270(60)	71510(30)	33310(30)	358(16)
C(36)	30870(70)	76720(40)	31520(30)	470(20)
C(37)	36120(70)	79090(40)	27670(30)	427(19)
C(38)	28670(80)	64020(50)	38640(40)	590(30)
C(39)	42720(80)	88240(40)	20820(60)	660(30)
C(40)	47030(90)	93130(50)	18220(50)	670(30)
C(41)	49830(90)	90900(40)	12860(40)	580(30)
C(42)	53440(70)	85270(30)	14070(30)	412(19)
O(1B)	84290(40)	88230(20)	12440(20)	426(13)
O(2B)	67710(40)	47490(30)	4430(20)	431(13)
N(1B)	77690(40)	75380(20)	26290(20)	285(12)
N(2B)	58740(50)	85930(30)	33660(30)	348(14)
N(3B)	74420(40)	69120(20)	32730(20)	290(12)
N(4B)	66030(40)	59370(20)	30080(20)	299(13)
N(5B)	66900(40)	55340(20)	21940(20)	285(12)
N(6B)	82160(50)	42670(30)	28650(30)	409(15)
C(1B)	72890(50)	74180(30)	30630(30)	270(14)
C(2B)	66550(50)	77650(30)	33120(30)	290(14)
C(3B)	65270(50)	82850(30)	31220(30)	307(15)
C(4B)	70680(50)	84450(30)	26670(30)	303(15)
C(5B)	76400(50)	80590(30)	24290(30)	322(15)
C(6B)	81210(50)	81730(30)	19550(30)	323(15)
C(7B)	80240(60)	86780(30)	17200(30)	380(17)
C(8B)	74780(60)	90680(30)	19570(30)	383(17)
C(9B)	70180(60)	89560(30)	24090(30)	373(17)
C(10B)	87940(70)	84080(40)	9310(30)	510(20)
C(11B)	57960(60)	91770(30)	33620(30)	378(17)
C(12B)	51940(60)	92940(40)	38470(30)	410(18)
C(13B)	45850(60)	88080(40)	38900(30)	410(18)
C(14B)	52440(60)	83520(30)	37700(30)	389(17)
C(15B)	68150(50)	66560(30)	36430(30)	289(14)
C(16B)	69010(50)	60410(30)	35580(30)	278(14)
C(17B)	69890(60)	68170(30)	42220(30)	337(16)
C(18B)	62650(70)	69180(40)	45590(40)	470(20)
C(19B)	64120(80)	70580(50)	50880(40)	590(30)
C(20B)	73120(90)	70890(40)	52820(30)	560(30)
C(21B)	80310(80)	69890(40)	49540(40)	500(20)
C(22B)	78770(60)	68540(30)	44230(30)	403(18)
C(23B)	63610(50)	57180(30)	39620(30)	302(15)
C(24B)	67700(60)	55160(30)	44150(30)	376(17)
C(25B)	62650(70)	52340(40)	47940(30)	470(20)
C(26B)	53360(70)	51680(30)	47330(30)	440(20)
C(27B)	49080(60)	53800(30)	42870(30)	393(17)
C(28B)	54040(50)	56530(30)	39100(30)	335(15)
C(29B)	69160(50)	55170(30)	27070(30)	266(14)
C(30B)	74330(50)	50950(30)	29340(30)	318(15)

C(31B)	77530(50)	46730(30)	26260(30)	313(15)
C(32B)	75420(50)	46840(30)	20640(30)	317(15)
C(33B)	70010(50)	51220(30)	18670(30)	274(14)
C(34B)	67530(50)	51540(30)	13260(30)	320(15)
C(35B)	70080(50)	47680(30)	9690(30)	364(17)
C(36B)	75460(60)	43270(30)	11490(30)	386(17)
C(37B)	77910(50)	42890(30)	16670(30)	364(16)
C(38B)	62440(70)	51820(40)	2490(30)	470(20)
C(39B)	88880(60)	38940(40)	26190(40)	450(20)
C(40B)	94990(80)	37130(40)	30810(40)	570(20)
C(41B)	88410(80)	37510(50)	35630(40)	580(30)
C(42B)	83240(70)	42620(40)	34550(30)	470(20)

Table 3. Bond lengths [Å] for 10.

Cl(1A)-C(1A)	1.756(11)	C(8)-H(8)	0.9300
Cl(2A)-C(1A)	1.766(12)	C(8)-C(9)	1.374(13)
C(1A)-H(1AA)	0.9700	C(9)-H(9)	0.9300
C(1A)-H(1AB)	0.9700	C(10)-H(10A)	0.9600
Cl(1G)-C(1G)	1.785(13)	C(10)-H(10B)	0.9600
Cl(2G)-C(1G)	1.732(14)	C(10)-H(10C)	0.9600
C(1G)-H(1GA)	0.9700	C(11)-H(11A)	0.9700
C(1G)-H(1GB)	0.9700	C(11)-H(11B)	0.9700
Cl(1F)-C(1F)	1.732(12)	C(11)-C(12)	1.482(17)
Cl(2F)-C(1F)	1.775(12)	C(12)-H(12A)	0.9700
C(1F)-H(1FA)	0.9700	C(12)-H(12B)	0.9700
C(1F)-H(1FB)	0.9700	C(12)-C(13)	1.529(17)
Cl(1C)-C(1C)	1.549(19)	C(13)-H(13A)	0.9700
Cl(2C)-C(1C)	1.779(16)	C(13)-H(13B)	0.9700
C(1C)-H(1CA)	0.9700	C(13)-C(14)	1.512(13)
C(1C)-H(1CB)	0.9700	C(14)-H(14A)	0.9700
Cl(1D)-C(1D)	1.732(15)	C(14)-H(14B)	0.9700
Cl(2D)-C(1D)	1.735(14)	C(15)-H(15)	0.9800
C(1D)-H(1DA)	0.9700	C(15)-C(16)	1.551(9)
C(1D)-H(1DB)	0.9700	C(15)-C(17)	1.522(10)
Cl(1E)-C(1E)	1.752(14)	C(16)-H(16)	0.9800
Cl(2E)-C(1E)	1.779(13)	C(16)-C(23)	1.499(10)
C(1E)-H(1EA)	0.9700	C(17)-C(18)	1.382(12)
C(1E)-H(1EB)	0.9700	C(17)-C(22)	1.394(12)
O(1)-C(7)	1.362(11)	C(18)-H(18)	0.9300
O(1)-C(10)	1.428(16)	C(18)-C(19)	1.396(13)
O(2)-C(35)	1.379(10)	C(19)-H(19)	0.9300
O(2)-C(38)	1.422(13)	C(19)-C(20)	1.374(16)
N(1)-C(1)	1.348(10)	C(20)-H(20)	0.9300
N(1)-C(5)	1.368(10)	C(20)-C(21)	1.381(16)
N(2)-C(3)	1.362(11)	C(21)-H(21)	0.9300
N(2)-C(11)	1.484(11)	C(21)-C(22)	1.391(12)
N(2)-C(14)	1.489(11)	C(22)-H(22)	0.9300
N(3)-H(3)	0.8600	C(23)-C(24)	1.401(11)
N(3)-C(1)	1.358(10)	C(23)-C(28)	1.377(12)
N(3)-C(15)	1.444(9)	C(24)-H(24)	0.9300
N(4)-H(4)	0.8600	C(24)-C(25)	1.372(13)
N(4)-C(16)	1.455(9)	C(25)-H(25)	0.9300
N(4)-C(29)	1.361(10)	C(25)-C(26)	1.367(16)
N(5)-C(29)	1.333(10)	C(26)-H(26)	0.9300
N(5)-C(33)	1.365(10)	C(26)-C(27)	1.389(15)
N(6)-C(31)	1.379(10)	C(27)-H(27)	0.9300
N(6)-C(39)	1.456(12)	C(27)-C(28)	1.378(12)
N(6)-C(42)	1.459(11)	C(28)-H(28)	0.9300
C(1)-C(2)	1.406(11)	C(29)-C(30)	1.403(10)
C(2)-H(2)	0.9300	C(30)-H(30)	0.9300
C(2)-C(3)	1.384(11)	C(30)-C(31)	1.395(11)
C(3)-C(4)	1.452(11)	C(31)-C(32)	1.441(11)
C(4)-C(5)	1.413(11)	C(32)-C(33)	1.436(10)
C(4)-C(9)	1.425(11)	C(32)-C(37)	1.415(11)
C(5)-C(6)	1.417(11)	C(33)-C(34)	1.415(11)
C(6)-H(6)	0.9300	C(34)-H(34)	0.9300
C(6)-C(7)	1.375(12)	C(34)-C(35)	1.351(11)
C(7)-C(8)	1.397(15)	C(35)-C(36)	1.414(13)

C(36)-H(36)	0.9300	C(12B)-H(12C)	0.9700
C(36)-C(37)	1.364(13)	C(12B)-H(12D)	0.9700
C(37)-H(37)	0.9300	C(12B)-C(13B)	1.502(13)
C(38)-H(38A)	0.9600	C(13B)-H(13C)	0.9700
C(38)-H(38B)	0.9600	C(13B)-H(13D)	0.9700
C(38)-H(38C)	0.9600	C(13B)-C(14B)	1.516(12)
C(39)-H(39A)	0.9700	C(14B)-H(14C)	0.9700
C(39)-H(39B)	0.9700	C(14B)-H(14D)	0.9700
C(39)-C(40)	1.516(16)	C(15B)-H(15B)	0.9800
C(40)-H(40A)	0.9700	C(15B)-C(16B)	1.549(10)
C(40)-H(40B)	0.9700	C(15B)-C(17B)	1.526(10)
C(40)-C(41)	1.508(17)	C(16B)-H(16B)	0.9800
C(41)-H(41A)	0.9700	C(16B)-C(23B)	1.511(10)
C(41)-H(41B)	0.9700	C(17B)-C(18B)	1.372(13)
C(41)-C(42)	1.527(12)	C(17B)-C(22B)	1.390(13)
C(42)-H(42A)	0.9700	C(18B)-H(18B)	0.9300
C(42)-H(42B)	0.9700	C(18B)-C(19B)	1.386(13)
O(1B)-C(7B)	1.377(10)	C(19B)-H(19B)	0.9300
O(1B)-C(10B)	1.402(13)	C(19B)-C(20B)	1.398(18)
O(2B)-C(35B)	1.362(10)	C(20B)-H(20B)	0.9300
O(2B)-C(38B)	1.409(12)	C(20B)-C(21B)	1.354(16)
N(1B)-C(1B)	1.325(10)	C(21B)-H(21B)	0.9300
N(1B)-C(5B)	1.401(10)	C(21B)-C(22B)	1.391(12)
N(2B)-C(3B)	1.365(10)	C(22B)-H(22B)	0.9300
N(2B)-C(11B)	1.457(10)	C(23B)-C(24B)	1.376(11)
N(2B)-C(14B)	1.492(11)	C(23B)-C(28B)	1.407(11)
N(3B)-H(3B)	0.8600	C(24B)-H(24B)	0.9300
N(3B)-C(1B)	1.383(9)	C(24B)-C(25B)	1.390(12)
N(3B)-C(15B)	1.449(9)	C(25B)-H(25B)	0.9300
N(4B)-H(4B)	0.8600	C(25B)-C(26B)	1.370(14)
N(4B)-C(16B)	1.467(9)	C(26B)-H(26B)	0.9300
N(4B)-C(29B)	1.368(9)	C(26B)-C(27B)	1.383(13)
N(5B)-C(29B)	1.326(10)	C(27B)-H(27B)	0.9300
N(5B)-C(33B)	1.388(9)	C(27B)-C(28B)	1.370(12)
N(6B)-C(31B)	1.355(10)	C(28B)-H(28B)	0.9300
N(6B)-C(39B)	1.479(11)	C(29B)-C(30B)	1.412(10)
N(6B)-C(42B)	1.488(11)	C(30B)-H(30B)	0.9300
C(1B)-C(2B)	1.407(11)	C(30B)-C(31B)	1.382(11)
C(2B)-H(2B)	0.9300	C(31B)-C(32B)	1.439(11)
C(2B)-C(3B)	1.391(11)	C(32B)-C(33B)	1.433(11)
C(3B)-C(4B)	1.442(11)	C(32B)-C(37B)	1.445(11)
C(4B)-C(5B)	1.405(11)	C(33B)-C(34B)	1.403(11)
C(4B)-C(9B)	1.426(11)	C(34B)-H(34B)	0.9300
C(5B)-C(6B)	1.408(11)	C(34B)-C(35B)	1.364(11)
C(6B)-H(6B)	0.9300	C(35B)-C(36B)	1.421(12)
C(6B)-C(7B)	1.394(12)	C(36B)-H(36B)	0.9300
C(7B)-C(8B)	1.387(13)	C(36B)-C(37B)	1.348(12)
C(8B)-H(8B)	0.9300	C(37B)-H(37B)	0.9300
C(8B)-C(9B)	1.345(12)	C(38B)-H(38D)	0.9600
C(9B)-H(9B)	0.9300	C(38B)-H(38E)	0.9600
C(10B)-H(10D)	0.9600	C(38B)-H(38F)	0.9600
C(10B)-H(10E)	0.9600	C(39B)-H(39C)	0.9700
C(10B)-H(10F)	0.9600	C(39B)-H(39D)	0.9700
C(11B)-H(11C)	0.9700	C(39B)-C(40B)	1.528(13)
C(11B)-H(11D)	0.9700	C(40B)-H(40C)	0.9700
C(11B)-C(12B)	1.526(12)	C(40B)-H(40D)	0.9700

C(40B)-C(41B)	1.543(16)
C(41B)-H(41C)	0.9700
C(41B)-H(41D)	0.9700
C(41B)-C(42B)	1.500(13)
C(42B)-H(42C)	0.9700
C(42B)-H(42D)	0.970

Table 4. Anisotropic displacement parameters ($Å^2 x\ 10^4$) for 10. The anisotropic displacement factor exponent takes the form: $-2\pi^2[\ h^2\ a^{*2}U^{11} + ... + 2\ h\ k\ a^*\ b^*\ U^{12}\ ]$

	U^{11}	U^{22}	U^{33}	U^{23}	U^{13}	U^{12}
Cl(1A)	649(14)	496(13)	651(14)	32(11)	30(11)	33(11)
Cl(2A)	736(15)	387(12)	648(13)	2(10)	1(12)	-128(11)
C(1A)	530(50)	460(50)	730(60)	-160(50)	-20(50)	-40(40)
Cl(1G)	1080(30)	593(18)	1420(30)	-260(20)	-640(30)	159(18)
Cl(2G)	1200(30)	607(19)	1290(30)	117(19)	-680(30)	-249(19)
C(1G)	660(70)	640(70)	1000(90)	-20(60)	-340(70)	30(60)
Cl(1F)	837(19)	545(15)	900(20)	-11(14)	-160(16)	-82(14)
Cl(2F)	658(16)	658(17)	1030(20)	10(16)	-361(16)	-45(14)
C(1F)	620(60)	520(60)	980(90)	110(60)	-280(60)	-100(50)
Cl(1C)	710(20)	880(30)	2990(90)	650(40)	330(40)	160(20)
Cl(2C)	900(20)	470(15)	1020(20)	-14(14)	-202(17)	-83(14)
C(1C)	940(110)	600(90)	2000(200)	180(110)	360(130)	-180(80)
Cl(1D)	727(17)	631(17)	1100(20)	-192(16)	214(17)	-138(15)
Cl(2D)	607(16)	1010(30)	1230(30)	-210(20)	179(18)	33(17)
C(1D)	940(90)	580(70)	630(60)	-90(50)	-120(60)	10(60)
Cl(1E)	637(14)	582(15)	662(14)	76(11)	-27(11)	78(12)
Cl(2E)	532(14)	778(19)	990(20)	292(16)	-160(14)	-24(13)
C(1E)	740(70)	500(60)	960(90)	50(60)	-160(70)	10(60)
O(1)	750(50)	910(60)	380(30)	110(30)	-70(30)	400(40)
O(2)	520(30)	480(40)	440(30)	80(30)	180(30)	140(30)
N(1)	300(30)	300(30)	280(30)	50(20)	-20(20)	10(30)
N(2)	420(40)	390(40)	440(30)	-60(30)	-140(30)	160(30)
N(3)	300(30)	210(30)	320(30)	0(20)	-20(20)	80(20)
N(4)	340(30)	260(30)	300(30)	70(20)	30(20)	-10(20)
N(5)	300(30)	250(30)	280(30)	-20(20)	20(20)	20(20)
N(6)	420(30)	250(30)	340(30)	10(20)	-20(30)	100(30)
C(1)	250(30)	290(40)	350(30)	70(30)	10(30)	-20(30)
C(2)	300(30)	290(40)	360(40)	20(30)	-40(30)	40(30)
C(3)	300(40)	310(40)	390(40)	10(30)	0(30)	70(30)
C(4)	320(40)	290(40)	350(40)	30(30)	-20(30)	80(30)
C(5)	340(40)	340(40)	320(40)	40(30)	-10(30)	60(30)
C(6)	410(40)	420(40)	340(40)	-20(30)	-50(30)	80(40)
C(7)	490(50)	590(60)	350(40)	90(40)	-70(40)	180(40)
C(8)	620(60)	540(60)	460(50)	130(40)	-170(40)	190(50)
C(9)	540(50)	420(50)	450(40)	50(40)	-90(40)	150(40)
C(10)	740(70)	1330(120)	240(40)	-80(50)	-150(40)	400(80)
C(11)	590(60)	570(60)	720(60)	-130(50)	-170(50)	400(50)
C(12)	670(70)	940(90)	620(60)	-150(60)	-110(50)	490(70)
C(13)	770(70)	650(70)	550(50)	-130(50)	-140(50)	330(60)
C(14)	470(50)	490(50)	400(40)	-100(40)	-100(40)	250(40)
C(15)	280(30)	210(30)	330(30)	10(30)	30(30)	60(30)
C(16)	250(30)	180(30)	370(30)	30(30)	30(30)	40(30)
C(17)	310(30)	300(40)	310(30)	90(30)	0(30)	70(30)
C(18)	360(40)	470(50)	360(40)	-40(30)	30(30)	40(40)
C(19)	660(60)	560(60)	380(40)	-70(40)	90(40)	140(50)
C(20)	570(60)	590(60)	510(50)	130(40)	250(40)	120(50)
C(21)	430(50)	460(50)	570(50)	120(40)	120(40)	-40(40)
C(22)	390(40)	310(40)	410(40)	50(30)	80(30)	20(30)
C(23)	320(40)	230(30)	320(30)	-30(30)	20(30)	110(30)
C(24)	340(40)	390(40)	380(40)	60(30)	-10(30)	0(30)
C(25)	550(50)	560(60)	370(40)	160(40)	50(40)	160(40)

C(26)	700(60)	490(50)	410(40)	-70(40)	-150(40)	60(50)
C(27)	660(60)	320(40)	540(50)	0(40)	-260(40)	-50(40)
C(28)	500(50)	270(40)	420(40)	30(30)	-80(40)	30(30)
C(29)	290(30)	170(30)	300(30)	-50(30)	-40(30)	20(30)
C(30)	320(30)	210(30)	290(30)	20(30)	-60(30)	40(30)
C(31)	340(40)	180(30)	320(30)	-10(30)	-70(30)	20(30)
C(32)	290(40)	270(40)	300(30)	-30(30)	-60(30)	30(30)
C(33)	340(40)	240(30)	310(30)	-40(30)	-40(30)	30(30)
C(34)	380(40)	270(40)	330(30)	0(30)	30(30)	10(30)
C(35)	390(40)	330(40)	350(40)	-30(30)	30(30)	40(30)
C(36)	530(50)	500(50)	370(40)	10(40)	130(40)	200(40)
C(37)	570(50)	320(40)	390(40)	30(30)	80(40)	210(40)
C(38)	670(60)	560(60)	550(50)	150(50)	260(50)	80(50)
C(39)	640(60)	290(50)	1050(80)	160(50)	330(60)	190(50)
C(40)	730(70)	390(50)	900(80)	-20(50)	-50(60)	60(50)
C(41)	960(80)	250(40)	520(50)	90(40)	60(50)	180(50)
C(42)	630(50)	230(40)	380(40)	60(30)	-10(40)	50(40)
O(1B)	520(30)	360(30)	390(30)	90(20)	90(20)	-90(30)
O(2B)	530(30)	410(30)	350(30)	-80(20)	20(20)	-20(30)
N(1B)	330(30)	220(30)	300(30)	20(20)	0(20)	10(20)
N(2B)	400(30)	250(30)	390(30)	0(30)	10(30)	30(30)
N(3B)	340(30)	200(30)	330(30)	40(20)	20(20)	30(20)
N(4B)	390(30)	220(30)	300(30)	0(20)	10(20)	70(20)
N(5B)	360(30)	180(30)	310(30)	-30(20)	50(20)	20(20)
N(6B)	470(40)	290(30)	470(40)	50(30)	0(30)	80(30)
C(1B)	320(30)	190(30)	300(30)	0(30)	-30(30)	-40(30)
C(2B)	360(40)	260(40)	250(30)	30(30)	-30(30)	0(30)
C(3B)	350(40)	220(30)	350(30)	-60(30)	-40(30)	20(30)
C(4B)	310(30)	220(30)	390(40)	-20(30)	-70(30)	-10(30)
C(5B)	320(40)	250(40)	390(40)	40(30)	-20(30)	-50(30)
C(6B)	380(40)	230(40)	360(40)	40(30)	-60(30)	-40(30)
C(7B)	430(40)	350(40)	360(40)	10(30)	-50(30)	-120(30)
C(8B)	450(40)	250(40)	450(40)	60(30)	-60(30)	-70(30)
C(9B)	460(40)	270(40)	390(40)	40(30)	-30(30)	0(30)
C(10B)	610(60)	550(60)	380(40)	110(40)	100(40)	-140(50)
C(11B)	420(40)	240(40)	470(40)	-30(30)	-30(30)	40(30)
C(12B)	450(40)	360(40)	420(40)	-10(30)	-20(30)	90(40)
C(13B)	370(40)	440(50)	410(40)	-20(30)	20(30)	70(40)
C(14B)	450(40)	350(40)	360(40)	-30(30)	50(30)	-40(40)
C(15B)	360(40)	250(40)	260(30)	-10(30)	0(30)	-30(30)
C(16B)	330(40)	230(30)	270(30)	10(30)	-30(30)	20(30)
C(17B)	500(40)	200(30)	310(40)	0(30)	0(30)	-60(30)
C(18B)	580(50)	440(50)	400(40)	-70(40)	70(40)	-130(40)
C(19B)	820(70)	650(70)	310(40)	-160(40)	210(50)	-170(60)
C(20B)	990(80)	420(50)	280(40)	-40(30)	-40(50)	-200(50)
C(21B)	750(60)	370(50)	390(40)	0(30)	-240(40)	-40(40)
C(22B)	490(50)	310(40)	400(40)	20(30)	-110(40)	40(40)
C(23B)	410(40)	180(30)	320(30)	-40(30)	10(30)	-40(30)
C(24B)	450(40)	350(40)	320(40)	70(30)	-70(30)	-120(30)
C(25B)	600(50)	470(50)	340(40)	150(30)	-70(40)	-180(40)
C(26B)	590(50)	320(40)	410(40)	-40(30)	120(40)	-110(40)
C(27B)	360(40)	330(40)	490(40)	-50(30)	100(30)	-10(30)
C(28B)	380(40)	250(40)	380(40)	0(30)	-40(30)	20(30)
C(29B)	280(30)	190(30)	320(30)	10(30)	30(30)	0(30)
C(30B)	350(40)	270(40)	330(30)	40(30)	-10(30)	-20(30)
C(31B)	310(30)	190(30)	440(40)	20(30)	40(30)	50(30)
C(32B)	280(30)	250(40)	420(40)	-40(30)	60(30)	-20(30)
C(33B)	270(30)	200(30)	350(30)	-20(30)	20(30)	-10(30)
C(34B)	340(40)	260(40)	360(40)	-40(30)	20(30)	-10(30)

C(35B)	330(40)	300(40)	460(40)	-100(30)	20(30)	-70(30)
C(36B)	380(40)	340(40)	440(40)	-140(30)	50(30)	20(30)
C(37B)	350(40)	240(40)	500(40)	-50(30)	20(30)	90(30)
C(38B)	610(50)	470(50)	330(40)	-50(30)	-20(40)	0(40)
C(39B)	470(50)	350(40)	540(50)	-10(40)	-80(40)	120(40)
C(40B)	600(60)	430(50)	680(60)	30(40)	-100(50)	200(40)
C(41B)	760(70)	500(60)	490(50)	100(40)	-80(50)	140(50)
C(42B)	610(50)	390(50)	400(40)	40(30)	-60(40)	150(40)

Table 5. Hydrogen coordinates (x 10^4) and isotropic displacement parameters ($Å^2$x 10^3) for 10.

	x	y	z	U(eq)
H(1AA)	4656	5967	2367	68
H(1AB)	4986	5376	2264	68
H(1GA)	3233	7073	1595	92
H(1GB)	4101	7045	1223	92
H(1FA)	9546	7400	2924	85
H(1FB)	9113	7414	3497	85
H(1CA)	816	6620	2537	142
H(1CB)	759	6482	1931	142
H(1DA)	7454	10050	282	86
H(1DB)	7889	9551	568	86
H(1EA)	7993	8292	4090	88
H(1EB)	7587	8006	4597	88
H(3)	8171	6818	2204	33
H(4)	6508	6389	2034	36
H(2)	9029	5681	1610	38
H(6)	9500	6247	3749	47
H(8)	10989	4888	3806	65
H(9)	10766	4760	2908	57
H(10A)	10216	6419	4451	115
H(10B)	10371	6133	5001	115
H(10C)	9446	6051	4691	115
H(11A)	11539	4983	2188	75
H(11B)	11082	4407	2180	75
H(12A)	11931	4326	1448	89
H(12B)	11897	4949	1326	89
H(13A)	10841	4610	720	79
H(13B)	10441	4199	1142	79
H(14A)	10181	5331	1138	54
H(14B)	9413	4890	1227	54
H(15)	7665	6099	1475	33
H(16)	7286	7219	1538	32
H(18)	8060	6018	539	48
H(19)	9131	6142	-137	64
H(20)	10381	6693	5	66
H(21)	10503	7178	788	58
H(22)	9390	7092	1445	45
H(24)	7448	7398	572	44
H(25)	6756	7391	-248	59
H(26)	5460	6888	-400	64
H(27)	4872	6354	284	61
H(28)	5588	6346	1101	48
H(30)	5977	7658	1606	33
H(34)	4212	6555	3243	40
H(36)	2580	7849	3293	56
H(37)	3454	8253	2655	51
H(38A)	2839	6179	3551	89
H(38B)	2392	6297	4108	89
H(38C)	3456	6359	4032	89
H(39A)	4309	8847	2468	79
H(39B)	3633	8786	1978	79
H(40A)	4262	9603	1784	81
H(40B)	5231	9440	2022	81
H(41A)	5458	9310	1125	69

H(41B)	4461	9074	1046	69
H(42A)	5223	8282	1113	49
H(42B)	5999	8532	1479	49
H(3B)	7930	6741	3179	35
H(4B)	6210	6153	2868	36
H(2B)	6319	7645	3605	35
H(6B)	8499	7915	1800	39
H(8B)	7431	9407	1803	46
H(9B)	6652	9222	2560	45
H(10D)	8996	8551	595	77
H(10E)	8330	8140	870	77
H(10F)	9305	8248	1113	77
H(11C)	5507	9303	3036	45
H(11D)	6394	9346	3398	45
H(12C)	5564	9338	4166	49
H(12D)	4833	9618	3793	49
H(13C)	4090	8822	3632	49
H(13D)	4327	8775	4246	49
H(14C)	5577	8243	4088	47
H(14D)	4922	8043	3625	47
H(15B)	6188	6764	3549	35
H(16B)	7550	5942	3589	33
H(18B)	5667	6893	4431	57
H(19B)	5917	7131	5312	71
H(20B)	7416	7179	5638	68
H(21B)	8628	7011	5084	60
H(22B)	8374	6786	4199	48
H(24B)	7396	5568	4468	45
H(25B)	6559	5090	5091	56
H(26B)	4997	4982	4988	53
H(27B)	4278	5337	4244	47
H(28B)	5105	5798	3615	40
H(30B)	7560	5100	3298	38
H(34B)	6407	5445	1209	38
H(36B)	7730	4063	908	46
H(37B)	8137	3993	1773	44
H(38D)	6165	5145	-130	70
H(38E)	6554	5514	325	70
H(38F)	5653	5182	420	70
H(39C)	9247	4076	2348	55
H(39D)	8578	3590	2458	55
H(40C)	10024	3950	3125	69
H(40D)	9715	3348	3029	69
H(41C)	8429	3445	3575	70
H(41D)	9178	3772	3896	70
H(42C)	7731	4259	3632	56
H(42D)	8670	4572	3576	56

Catalyst Synthesis

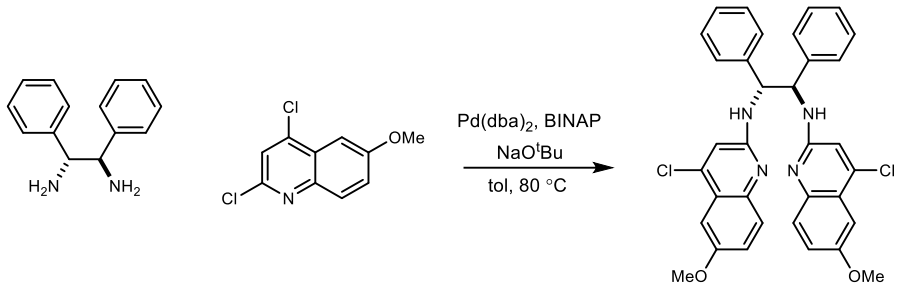

^{4}Cl-^{6}MeOStilb-BAM or (1R,2R)-N1,N2-bis(4-chloro-6-methoxyquinolin-2-yl)-1,2-diphenylethane-1,2-diamine (S4). A 25-mL, round-bottomed flask equipped with a stir bar was charged with (+)-(1*R*, 2*R*)-1,2-diphenylethylenediamine (500 mg, 2.4 mmol), $Pd(dba)_2$ (20 mg, 35 μmol), *rac*-BINAP (44 mg, 70 μmol), sodium *tert*-butoxide (565 mg, 5.8 mmol), and 2,4-dichloro-6-methoxylquinoline (1.1 g, 4.7 mmol). The reaction vessel was placed under an argon atmosphere, toluene (16 mL) was dispensed into the flask. The reaction vessel was evacuated and backfilled with argon gas three times. The round-bottomed flask was placed into an oil bath heated to 80 °C with stirring. The reaction was monitored by TLC and after 4 h nearly complete conversion was observed. The reaction was cooled to 25 °C, diluted with ethyl acetate, and filtered through a plug of Celite. Flash column chromatography (SiO_2, 15-35% ethyl acetate in hexanes) of the residue yielded a pale yellow solid (912 mg, 65%). $[\alpha]_D^{20}$ -4.1 (*c* 1.0, $CHCl_3$); R_f = 0.7 (30% EtOAc/hexanes); mp 201-205 °C; IR (film) 3241, 3062, 3027, 1600, 1491 cm^{-1}; ^{1}H NMR (400 MHz, DMSO-d_6) δ 7.79 (br d, *J* = 7.16 Hz, 2H), 7.45 (d, *J* = 9.0 Hz, 2H), 7.30 (br s, 2H), 7.29 (br s, 2H), 7.21 (dd, *J* = 8.9, 2.7 Hz, 2H), 7.18 (d, *J* = 2.7 Hz, 2H), 7.14 (dd, *J* = 7.5, 7.5 Hz, 4H), 7.04 (dd, *J* = 7.7, 7.7 Hz, 2H), 7.02 (s, 2H), 5.54 (dd, *J* = 12.6, 7.7 Hz, 2H), 3.81 (s, 6H). ^{13}C NMR (100 MHz, DMSO-d_6) ppm 154.9, 154.6, 143.6, 141.7, 139.5, 127.9, 127.7, 127.6, 126.5, 121.6, 120.8, 112.3, 102.6, 59.3, 55.3; HRMS (ESI): Exact mass calcd for $C_{34}H_{29}Cl_2N_4O_2$ $[M+H]^+$ 595.1662, found 595.1662.

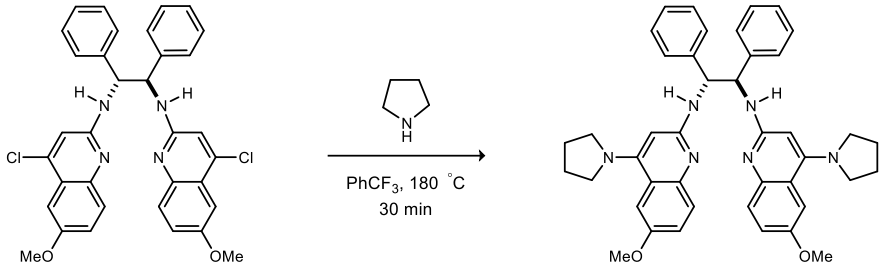

^{6}MeOStilbPBAM or (1R,2R)-N1,N2-bis(6-methoxy-4-(pyrrolidin-1-yl)quinolin-2-yl)-1,2-diphenylethane-1,2-diamine (196). A 2-5 mL microwave vial equipped with a stir bar was charged with ^{4}Cl-^{6}MeOStilb-BAM (444 mg, 750 μmol), pyrrolidine (300 μL, 3.4 mmol), and trifluoromethylbenzene (2.5 mL). The vial was sealed, and the suspension was heated with stirring at 180 °C in the microwave for 30 m. The reaction mixture was diluted with dichloromethane and transferred to a round-bottomed flask for evaporation. The resulting solid was dissolved in dichloromethane and stirred with 5 M NaOH (~20 mL) overnight. The contents of the flask were then transferred to a separatory funnel where the aqueous layer was extract with DCM. The resulting organic layer was dried and concentrated to provide a light brown powder. The solid was then recrystallized from hexanes and dichloromethane to provide a light yellow solid (260 mg, 53%). Mp 162-166 °C; $[\alpha]_D^{20}$ +62.4 (*c* 1.00, $CHCl_3$); R_f = 0.1 (10% MeOH/DCM); IR (film) 3255, 2965, 1648, 1587, 1456 cm^{-1}; ^{1}H NMR (400 MHz, $CDCl_3$) δ 7.63 (d, *J* =8.5 Hz, 2H), 7.31 (d, *J* = 2.80 Hz, 2H), 7.28 (s, 2H), 7.26 (s, 2H), 7.19 (d, *J* = 6.8 Hz, 2H), 7.17 (d, *J* = 7.4 Hz, 2H), 7.15 (d, *J* = 2.8 Hz, 2H), 7.12 (d, *J* = 2.8 Hz, 2H), 5.90 (br s, 2H), 5.55 (br s, 2H), 5.51 (br s, 2H), 3.84 (s,

6H), 3.36 (br s, 4H), 3.25 (br s, 4H), 1.88 (br s, 8H); ^{13}C NMR (150 MHz, $CDCl_3$) ppm 156.9, 152.7, 144.9, 141.5, 128.1, 128.0 (2C), 127.6, 127.0, 118.6, 106.5, 92.15, 77.4, 62.6, 55.8, 51.4, 25.7; HRMS (ESI): Exact mass calcd for $C_{42}H_{45}N_6O_2$ $[M+H]^+$ 665.3500, found 665.3593.

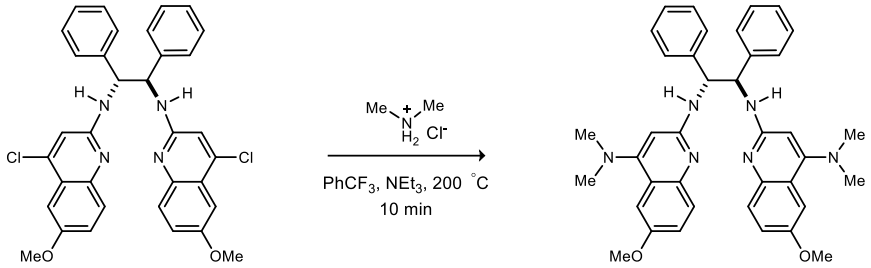

***N*2,*N*2'-((1*R*,2*R*)-1,2-Diphenylethane-1,2-diyl)bis(6-methoxy-*N*4,*N*4-dimethylquinoline-2,4-diamine) (199).** A 2-5 mL microwave vial equipped with a stir bar was charged with ^{4}Cl^{6}MeOStilb-BAM (200 mg, 340 μmol), $Me_2NH{\cdot}HCl$ (368 μL, 3.4 mmol), triethylamine (745 μL, 5.4 mmol) and trifluoromethylbenzene (1 mL). The vial was sealed, and the suspension was heated with stirring at 200 °C in the microwave for 10 m. After cooling, the reaction mixture was diluted with dichloromethane and transferred to a round-bottomed flask for evaporation. The resulting solid was dissolved in dichloromethane and stirred with 4 M aq NaOH (~10 mL) for 5 h. The contents of the flask were then transferred to a separatory funnel where the aqueous layer was extracted with dichloromethane. The resulting organic layer was dried and concentrated to provide a light brown foam (177 mg, 87%). $[\alpha]_D^{20}$ +42.2 (*c* 1.00, $CHCl_3$); R_f = 0.1 (10% MeOH/DCM); IR (film) 3244, 2941, 2789, 1597, 1527, 1490 cm^{-1}; ^{1}H NMR (400 MHz, $CDCl_3$) δ 7.67 (d, *J* = 9.8 Hz, 2H), 7.24 (d, *J* = 7.2 Hz, 4H), 7.21 (d, *J* = 7.1 Hz, 2H), 7.20-7.13 (m, 8H), 6.10 (s, 2H), 5.79 (s, 2H), 5.60 (br s, 2H), 3.87 (s, 6H), 2.69 (s, 12H); ^{13}C NMR (100 MHz, $CDCl_3$) ppm 157.3, 156.8, 153.7, 144.5, 141.3, 128.1 (2C), 127.90 (2C), 127.0, 119.5, 104.5, 98.6, 62.6, 55.6, 43.3; HRMS (ESI): Exact mass calcd for $C_{38}H_{41}N_6O_2$ $[M+H]^+$ 613.3286, found 613.3292.

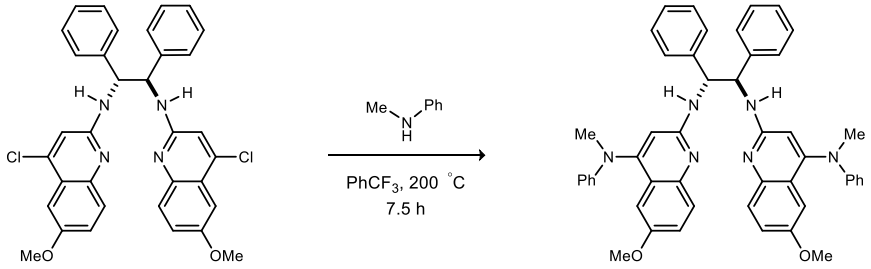

***N*2,*N*2'-((1*R*,2*R*)-1,2-Diphenylethane-1,2-diyl)bis(6-methoxy-*N*4-methyl-*N*4-phenylquinoline-2,4-diamine) (200).** A 2-5 mL microwave vial equipped with a stir bar was charged with ^{4}Cl^{6}MeOStilb-BAM (200 mg, 340 μmol), *N*-Me-aniline (1.45 mL, 13.4 mmol), and trifluoromethylbenzene (2 mL). The vial was sealed, and the suspension was heated with stirring at 200 °C in the microwave for 7.5 h. The reaction mixture was diluted with dichloromethane and transferred to a round-bottomed flask for evaporation. The resulting solid was dissolved in dichloromethane and stirred with 4 M aq NaOH (~10 mL) for 5 h. The contents of the flask were then transferred to a separatory funnel where the aqueous layer was extracted with DCM. The resulting organic layer was dried and concentrated to provide a light brown powder. The crude material was separated by silica gel chromatography (2% methanol in dichloromethane) to afford an off-white solid (77 mg, 30%). Mp 126-129 °C; $[\alpha]_D^{20}$ +23.6 (*c* 1.00, $CHCl_3$); R_f = 0.3 (10% MeOH/DCM); IR (film) 3390, 3250, 3061, 3030, 3002, 2951, 2831, 1600, 1519,

1493 cm^{-1}; ^1H NMR (400 MHz, $CDCl_3$) δ 7.65 (d, *J* = 9.0 Hz, 2H), 7.29 (d, *J* = 7.2 Hz, 4H), 7.23-7.18 (m, 4H), 7.18-7.15 (m, 4H), 7.15-7.12 (m, 4H), 7.09 (dd, *J* = 9.1, 2.9 Hz, 2H), 6.85 (dd, *J* = 7.4, 7.4 Hz, 2H), 6.77 (s, 2H), 6.75 (d, *J* = 3.4 Hz, 2H), 6.25 (s, 2H), 6.18 (br s, 2H), 5.59 (br d, *J* = 2.4 Hz, 2H), 3.53 (s, 6H), 3.20 (s, 6H); ^{13}C NMR (150 MHz, $CDCl_3$) ppm 156.6, 154.4, 153.5, 149.6, 145.0, 141.0, 129.2, 128.4, 128.3, 128.0, 127.4, 120.8, 120.7, 118.7, 112.3, 105.8, 104.0, 62.3, 55.3, 41.2; HRMS (ESI): Exact mass calcd for $C_{48}H_{45}N_6O_2$ $[M+H]^+$ 737.3599, found 737.3604.

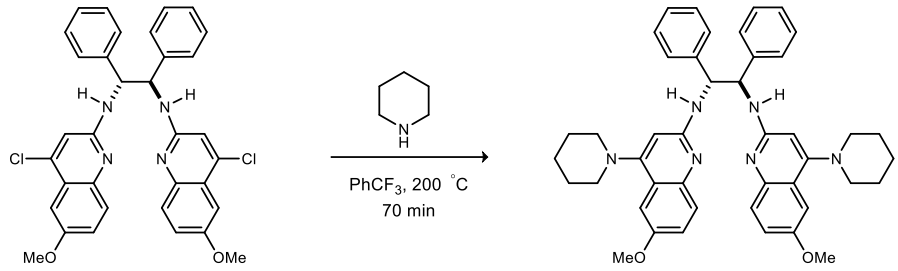

***N*2,*N*2'-((1*R*,2*R*)-1,2-Diphenylethane-1,2-diyl)bis(6-methoxy-*N*4-methyl-*N*4-phenylquinoline-2,4-diamine) (197).** A 2-5 mL microwave vial equipped with a stir bar was charged with $^4Cl^6$MeOStilb-BAM (200 mg, 340 μmol), piperidine (700 μL, 6.8 mmol), and trifluoromethylbenzene (2 mL). The vial was sealed, and the suspension was heated with stirring at 200 °C in the microwave for 70 min. The reaction mixture was diluted with dichloromethane and transferred to a round-bottomed flask for evaporation. The resulting solid was dissolved in dichloromethane and stirred with 5 M aq NaOH (~10 mL) overnight. The contents of the flask were then transferred to a separatory funnel where the aqueous layer was extracted with dichloromethane. The resulting organic layer was dried and concentrated to provide a light brown powder. The crude material was separated by silica gel chromatography (0-5% methanol in dichloromethane) to afford an off-white solid (203 mg, 88%). Mp 135-142 °C; $[\alpha]_D^{20}$ +27.4 (*c* 1.00, $CHCl_3$); R_f = 0.2 (10% MeOH/DCM); IR (film) 3245, 3028, 2934, 2851, 1600, 1525, 1494, 1459 cm^{-1}; ^1H NMR (400 MHz, $CDCl_3$) δ 7.68 (d, *J* = 9.0 Hz, 2H), 7.31 (d, *J* = 7.2 Hz, 4H), 7.23-7.20 (m, 4H), 7.18-7.17 (m, 2H), 7.16 (m, 2H), 7.12 (dr d, *J* = 2.5 Hz, 2H), 6.05 (br s, 2H), 5.75 (s, 2H), 5.63 (s, 2H), 3.88 (s, 6H), 2.88 (br s, 4H), 2.71 (br s, 4H), 1.71 (br s, 8H), 1.58 (dd, *J* = 11.3, 6.3 Hz, 4H); ^{13}C NMR (150 MHz, $CDCl_3$) ppm 157.8, 156.8, 154.2, 144.5, 141.4, 128.31, 128.30, 128.0, 127.2, 120.3, 119.6, 103.7, 99.9, 62.4, 55.5, 53.2, 26.2, 24.6; HRMS (ESI): Exact mass calcd for $C_{44}H_{49}N_6O_2$ $[M+H]^+$ 693.3912, found 693.3918.

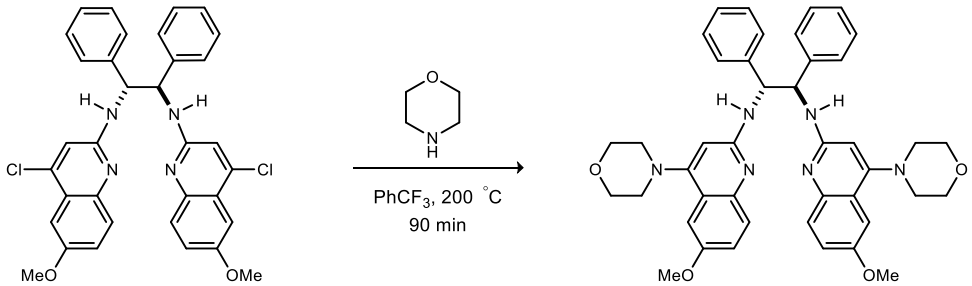

(1*R*,2*R*)-*N*1,*N*2-bis(6-Methoxy-4-morpholinoquinolin-2-yl)-1,2-diphenylethane-1,2-diamine (198). A 2-5 mL microwave vial equipped with a stir bar was charged with $^4Cl^6$MeOStilb-BAM (200 mg, 340 μmol), morpholine (600 μL, 6.7 mmol), and trifluoromethylbenzene (2 mL). The vial was sealed, and the suspension was heated with stirring at 200 °C in the microwave for 90 min. The reaction mixture was diluted with dichloromethane and transferred to a round-bottomed flask for evaporation. The resulting solid was dissolved in dichloromethane and stirred with 5 M aq NaOH (~10 mL) overnight. The contents of the flask were then transferred to a separatory funnel where the aqueous layer was extracted with dichloromethane. The resulting

organic layer was dried and concentrated to provide a light brown powder. The crude material was separated by silica gel chromatography (0-5% methanol in dichloromethane) to afford an off-white solid (164 mg, 70%). Mp 147-153 °C; $[\alpha]_D^{20}$ +28.0 (*c* 1.00, $CHCl_3$); R_f = 0.2 (10% MeOH/DCM); IR (film) 3238, 2959, 2847, 1601, 1528, 1493 cm^{-1}; ^1H NMR (400 MHz, $CDCl_3$) δ 7.70 (d, *J* = 9.4 Hz, 2H), 7.30 (d, *J* = 7.1 Hz, 4H), 7.23-7.19 (m, 4H), 7.19-7.13 (m, 4H), 7.11 (d, *J* = 2.6 Hz, 2H), 6.14 (br s, 2H), 5.80 (s, 2H), 5.62 (s, 2H), 3.86 (s, 6H), 3.84-3.82 (m, 8H), 2.97-2.94 (m, 4H), 2.79-2.75 (m, 4H); ^{13}C NMR (150 MHz, $CDCl_3$) ppm 156.7, 156.4, 154.4, 144.6, 141.1, 128.37, 128.36, 128.0, 127.3, 119.8, 119.6, 103.7, 100.1, 67.0, 62.6, 55.6, 52.2; HRMS (ESI): Exact mass calcd for $C_{42}H_{45}N_6O_4$ $[M+H]^+$ 697.3497, found 697.3502.

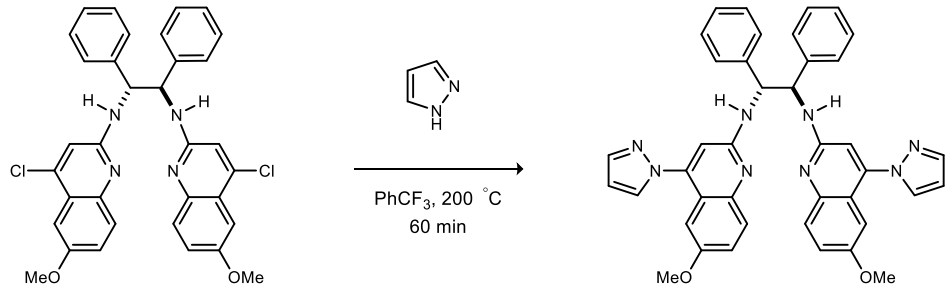

(1*R*,2*R*)-*N*1,*N*2-bis(6-Methoxy-4-(1H-pyrazol-1-yl)quinolin-2-yl)-1,2-diphenylethane-1,2-diamine (201). A 2-5 mL microwave vial equipped with a stir bar was charged with $^4Cl^6MeO$Stilb-BAM (200 mg, 340 μmol), pyrazole (114 mg, 1.7 mmol), and trifluoromethylbenzene (2 mL). The vial was sealed, and the suspension was heated with stirring at 200 °C in the microwave for 60 min. The reaction mixture was diluted with dichloromethane and transferred to a round-bottomed flask for evaporation. The resulting solid was dissolved in dichloromethane and stirred with 5 M aq NaOH (~10 mL) overnight. The contents of the flask were then transferred to a separatory funnel where the aqueous layer was extracted with dichloromethane. The resulting organic layer was dried and concentrated to provide a light brown powder. The crude material was separated by silica gel chromatography (10-50% ethyl acetate in hexanes) to afford an off-white solid (196 mg, 89%). Mp 135-140 °C; $[\alpha]_D^{20}$ +18.1 (*c* 1.00, $CHCl_3$); R_f = 0.2 (50% EtOAc/hex); IR (film) 3266, 3030, 3002, 3935, 2833, 1611, 1517, 1452 cm^{-1}; ^1H NMR (400 MHz, $CDCl_3$) δ 7.78 (d, *J* = 1.6 Hz, 2H), 7.72 (d, *J* = 8.9 Hz, 2H), 7.67 (d, *J* = 1.4 Hz, 2H), 7.29-7.26 (m, 4H), 7.23 (dd, *J* = 5.3, 2.9 Hz, 4H), 7.23-7.21 (m, 2H), 7.20-7.18 (m, 2H), 7.18-7.15 (m, 2H), 6.56 (s, 2H), 6.48 (dd, *J* = 2.1, 2.1 Hz, 2H), 6.19 (s, 2H), 5.66 (s, 2H), 3.79 (s, 6H); ^{13}C NMR (150 MHz, $CDCl_3$) ppm 155.5, 155.4, 145.1, 144.6, 141.7, 140.4, 130.9, 128.4, 128.2, 128.0, 127.6, 121.9, 119.0, 107.3, 105.3, 103.1, 62.0, 55.6; HRMS (ESI): Exact mass calcd for $C_{40}H_{35}N_8O_2$ $[M+H]^+$ 659.2877, found 659.2881.

General Procedure for the Triflation of Aryl Amines

To an oven-dried flask was added the aryl amine, triethylamine, and dichloromethane under an argon atmosphere. The reaction mixture was cooled to -78 ºC, then trifluoromethane sulfonic anhydride was added dropwise. The mixture was allowed to stir for a few minutes before it was warmed to room temperature. The reaction was monitored by TLC and once the starting material was consumed (reaction times were typically 24-48 hours), the mixture was concentrated under reduced pressure, and then dissolved in ethyl acetate and transferred to a separatory funnel. The organic layer was washed with 1 M HCl and the aqueous layer was extracted with ethyl acetate. The organic layers with combined, dried, filtered, and concentrated. The reaction mixture was then purified by SiO_2

chromatography (EtOAc in Hex). If chromatography did not sufficiently purify the aryl triflimide, the crude mixture was recrystallized from boiling chloroform.

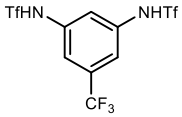

N,N'-(5-(trifluoromethyl)-1,3-phenylene)bis(1,1,1-trifluoromethanesulfonamide) (194). The reaction was carried out according to the general procedure, 3,5-diaminobenzotrifluoride (260 mg, 1.47 mmol), triethylamine (450 µL, 3.10 mmol), and trifluoromethane sulfonic anhydride (530 µL, 3.10 mmol). The crude material was separated by silica gel chromatography (SiO_2, 20-50 % ethyl acetate in hexanes) to afford a white solid (577 mg, 90 %). Mp 133-135 °C; IR (film) 3274, 3057, 1619, 1426 cm^{-1}; R_f = 0.25 (30 % EtOAc/hexanes); ^1H NMR (400 MHz, $(CD_3)_2CO$) δ 10.75 (br s, 2H), 7.76 (t, *J* = 1.8 Hz, 1H), 7.63 (d, *J* = 1.3 Hz, 2H); ^{13}C NMR (100 MHz, $(CD_3)_2CO$) ppm 138.3, 133.3, (q, *J* = 33.0 Hz), 122.6, 120.8 (q, *J* = 320.1 Hz), 119.3, 117.1 (q, *J* = 3.7 Hz); ^{19}F NMR (282 MHz, $(CD_3)_2CO$) ppm -63.8, -77.0; HRMS (ESI): Exact mass calcd for $C_9H_5F_9N_2O_4S_2$ $[M]^+$ 439.9542, found 439.9548. MV-1-031

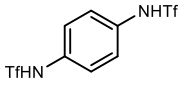

N,N'-(1,4-phenylene)bis(1,1,1-trifluoromethanesulfonamide) (188). The reaction was carried out according to the general procedure, benzene-1,4-diamine (300 mg, 2.77 mmol), triethylamine (813 µL, 5.83 mmol), and trifluoromethane sulfonic anhydride (984 µL, 5.83 mmol). The crude material was separated by silica gel chromatography (SiO_2, 5-20 % ethyl acetate in hexanes) to afford a brown solid (308 mg, 31 %). Mp 194-196 °C; IR (film) 3071, 1694, 1462 cm^{-1}; R_f = 0.6 (30 % EtOAc/hexanes); ^1H NMR (400 MHz, $(CD_3)_2CO$) δ 10.34 (br s, 2H), 7.47 (s, 4H); ^{13}C NMR (100 MHz, $(CD_3)_2CO$) ppm 134.4, 125.1, 120.9 (q, *J* = 320.5 Hz) ^{19}F NMR (282 MHz, $(CD_3)_2CO$) ppm -76.8 HRMS (ESI): Exact mass calcd for $C_8H_6F_9N_2O_4S_2$ $[M]^+$ 371.9668, found 371.9667. MV-1-019

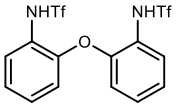

N,N'-(oxybis(2,1-phenylene))bis(1,1,1-trifluoromethanesulfonamide) (190). The reaction was carried out according to the general procedure, 2,2'-oxydianiline (300 mg, 1.49 mmol), triethylamine (439 µL, 3.10 mmol), and trifluoromethane sulfonic anhydride (531 µL, 3.10 mmol). The crude material was separated by silica gel chromatography (SiO_2, 5-25 % ethyl acetate in hexanes) to afford an off-white solid (553 mg, 80 %). Mp 118-120 °C; IR (film) 3281, 1596, 1498 cm^{-1}; R_f = 0.3 (30 % EtOAc/hexanes); ^1H NMR (400 MHz, $CDCl_3$) δ 7.62 (dd, *J* = 7.9, 1.7 Hz, 2H), 7.50 (br s, 2H), 7.25 (ddd, *J* = 7.8, 7.8, 1.8 Hz, 2H), 7.21 (ddd, *J* = 7.7, 7.7, 1.6 Hz, 2H), 6.90 (dd, *J* = 8.1, 1.5 Hz, 2H); ^{13}C NMR (100 MHz, $CDCl_3$) ppm 148.0, 128.6, 125.5, 125.4, 125.1, 121.4, 118.2; ^{19}F NMR (282 MHz, $CDCl_3$) ppm -75.8 HRMS (ESI): Exact mass calcd for $C_{14}H_{10}F_6N_2O_5S_2$ $[M]^+$ 463.9930, found 463.9916. MV-1-068

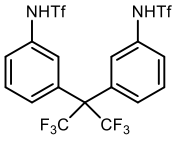

N,N'-((perfluoropropane-2,2-diyl)bis(1,1,1-trifluoromethanesulfonamide) (191). The reaction was carried out according to the general procedure, 3,3'-(perfluoropropane-2,2-diyl)diamine (200 mg, 0.60 mmol), triethylamine (175 µL, 1.26 mmol), and trifluoromethane sulfonic anhydride (212 µL, 1.26 mmol, 4.09 mmol). The crude material was separated by silica gel chromatography (SiO_2, 5-25 % ethyl acetate in hexanes to afford a white solid (251 mg, 70 %). Mp 133-135 °C; IR (film) 3283, 1602, 1419 cm^{-1}; R_f = 0.3 (30 % EtOAc/hexanes); ^1H NMR (400 MHz, $(CD_3)_2CO$) δ 10.35 (br s, 2H), 7.62 (dd, *J* = 7.9, 7.8 Hz, 2H), 7.57 (ddd, *J* = 8.1, 1.6, 1.6 Hz, 2H), 7.44 (br s, 2H), 7.39 (br d, *J* = 7.6 Hz, 2H); ^{13}C NMR (100 MHz, $(CD_3)_2CO$) ppm 136.3, 134.9, 130.8, 129.0, 126.3, 125.2, 124.6, 123.5 120.8 (q, *J* = 321 Hz); ^{19}F NMR (282 MHz, $(CD_3)_2CO$) ppm -64.3, -76.8 HRMS (ESI): Exact mass calcd for $C_{17}H_{10}F_{12}N_2O_4S_2$ $[M]^+$ 597.9885, found 597.9885. MV-1-178

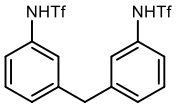

N,N'-(methylenebis(3,1)-phenylene))bis(1,1,1-trifluoromethanesulfonamide) (S5). The reaction was carried out according to the general procedure, 3,3'-methylenedianiline (130 mg, 0.65 mmol), triethylamine (192 µL, 1.38 mmol), and trifluoromethane sulfonic anhydride (233 µL, 1.38 mmol). The crude material was separated by silica gel chromatography (SiO_2, 0-20% ethyl acetate in hexanes) to afford a white solid (121 mg, 40 %). Mp 144-146 °C; IR (film) 3266, 1596, 1417cm^{-1}; R_f = 0.6 (30 % EtOAc/hexanes); ^{1}H NMR (400 MHz, $(CD_3)_2CO$) δ 10.25 (br s, 2H), 7.37 (m, 2H), 7.26 (br s, 2H), 7.25-7.23 (m, 2H), 7.21 (br d, *J* = 7.5 Hz, 2H), 4.10 (s, 2H); ^{13}C NMR (100 MHz, $(CD_3)_2CO$) ppm 143.3, 136.0, 130.5, 128.3, 124.4, 121.8, 120.9 (q, *J* = 323.5 Hz), 41.6; ^{19}F NMR (282 MHz, $(CD_3)_2CO$) ppm -76.7 HRMS (ESI): Exact mass calcd for $C_{15}H_{12}F_6N_2O_4S_2$ $[M]^+$ 462.0137, found 462.0128. MV-1-142

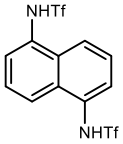

N,N'-(naphthalene-1,5-diyl)bis(1,1,1-trifluoromethanesulfonamide) (S6). The reaction was carried out according to the general procedure, napthalene-1,5-diamine (300 mg, 1.90 mmol), triethylamine (551 µL, 3.98 mmol), and trifluoromethane sulfonic anhydride (672 µL, 3.98 mmol). The crude material was separated by silica gel chromatography (SiO_2, 5-30 % ethyl acetate in hexanes to afford a brown solid (80 mg, 10%). Mp > 250°C; IR (film) 3283, 1602 cm^{-1}; R_f = 0.4 (30 % EtOAc/hexanes); ^{1}H NMR (400 MHz, $(CD_3)_2CO$) δ 10.52 (br s, 2H), 8.37-8.33 (m, 2H), 7.79 (d, *J* = 1.2 Hz, 2H), 7.78 (br s, 2H); ^{13}C NMR (100 MHz, $(CD_3)_2CO$) ppm 132.3, 131.3, 127.7, 127.6, 124.3, 121.0 (q, *J* = 319.7 Hz); ^{19}F NMR (282 MHz, $(CD_3)_2CO$) ppm -77.0 HRMS (ESI): Exact mass calcd for $C_{12}H_8F_6N_2O_4S_2$ $[M]^+$ 421.9824, found 421.9811. MV-1-189

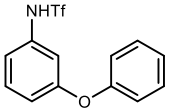

1,1,1-trifluoro-N-(3-phenoxyphenyl)methanesulfonamide (S7). The reaction was carried out according to the general procedure, 3-phenoxyaniline (300 mg, 1.62 mmol), triethylamine (131 µL, 1.78 mmol), and trifluoromethane sulfonic anhydride (300 µL, 1.78 mmol). The crude material was separated by silica gel chromatography (SiO_2, 2-5 % ethyl acetate in hexanes) to afford a colorless liquid (396 mg, 77%). IR (film) 3287, 1592, 1485 cm^{-1}; R_f = 0.6 (30% EtOAc/hexanes); ^{1}H NMR (400 MHz, $CDCl_3$) δ 7.40-7.35 (m, 2H), 7.32 (m, 1H), 7.17 (dddd, *J* = 11.2, 11.2, 1.1, 1.1 Hz, 2H), 7.05 (dd, *J* = 3.1, 2.1 Hz, 1H), 7.02 (m, 1H), 7.00-6.98 (m, 1H), 6.92 (br d, *J* = 1.4 Hz), 6.92-6.90 (m, 1H), (N-H peak not observed); ^{13}C NMR (100 MHz, $CDCl_3$) ppm 158.6, 156.1, 135.0, 130.8, 130.1, 124.3, 119.7 (q, *J* = 320.7 Hz), 119.5, 117.6, 117.3, 113.4; ^{19}F NMR (282 MHz, $CDCl_3$) ppm -76.8 HRMS (ESI): Exact mass calcd for $C_{13}H_{10}F_3NO_3S$ $[M]^+$ 317.0328, found 317.0319. MV-1-194

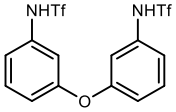

N,N'-(oxybis(3,1-phenylene))bis(1,1,1-trifluoromethanesulfonamide) (189). The reaction was carried out according to the general procedure, 3,3'-oxydianiline (300 mg, 1.49 mmol), triethylamine (439 µL, 3.15 mmol), and trifluoromethane sulfonic anhydride (531 µL, 3.15 mmol). The crude material was separated by silica gel chromatography (SiO_2, 20-50 % ethyl acetate in hexanes) to afford a crystalline white solid (595 mg, 86%). IR (film) 3286, 1597, 1487, 1418 cm^{-1}; R_f = 0.6 (30 % EtOAc/hexanes); ^{1}H NMR (400 MHz, $CDCl_3$) δ 7.37 (dd, *J* = 7.8, 7.8 Hz, 2H), 7.04 (br d, *J* = 8.4 Hz, 2H), 6.95-6.94 (m, 4H), 6.81 (br s, 2H); ^{13}C NMR (100 MHz, $CDCl_3$) ppm 157.4, 135.3, 131.1, 119.8, (q, *J* = 320.7 Hz), 118.5, 117.9, 114.0; ^{19}F NMR (282 MHz, $CDCl_3$) ppm -75.3 HRMS (ESI): Exact mass calcd for $C_{14}H_{10}F_6N_2O_5S_2$ $[M]^+$ 463.9930, found 463.9919. MV-1-246

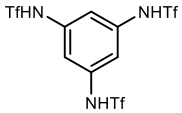

N,N',N''-(benzene-1,3,5-triyl)tris(1,1,1-trifluoromethanesulfonamide) (213). The reaction was carried out according to the general procedure, benzene-1,3,5-triamine (100 mg, 0.81 mmol) triethylamine (360 µL, 2.6 mmol), and trifluoromethane sulfonic anhydride (450 µL, 2.6 mmol). The crude material dissolved in ethyl acetate and washed with 1 M K_2CO_3. The aqueous layer was acidified and extracted with ethyl acetate to afford a pale pink solid (40 mg, 20%). IR (film) 3272, 3082, 1685, 1614, 1513 cm^{-1}; R_f = 0.4 (30 % EtOAc/hexanes); ^{1}H NMR (400 MHz, $(CD_3)_2CO$) δ 10.63 (br s, 3H), 7.38 (s, 3H); ^{13}C NMR (100 MHz, $(CD_3)_2CO$) ppm 138.2, 120.8 (q, *J* = 322.4 Hz), 113.4; ^{19}F NMR

(282 MHz, $(CD_3)_2CO$) ppm -76.9 HRMS (ESI): Exact mass calcd for $C_9H_5F_9N_3O_6S_3$ $[M]^+$ 517.9202, found 517.9193.

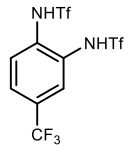

N,N'-(4-(trifluoromethyl)-1,2-phenylene)bis(1,1,1-trifluoromethanesulfonamide) (203). The reaction was carried out according to the general procedure, 4,5-diaminobenzotrifluoride (300 mg, 1.7 mmol) triethylamine (500 µL, 3.6 mmol), and trifluoromethane sulfonic anhydride (600 µL, 3.6 mmol). The crude material was separated by silica gel chromatography (SiO_2, 20-50 % ethyl acetate in hexanes) to afford a pink solid (425 mg, 57%). IR (film) 3288, 1621, 1521, 1456 cm^{-1}; R_f = 0.2 (30 % EtOAc/hexanes); ^1H NMR (400 MHz, $(CD_3)_2CO$) δ 10.33 (br s, 2H), 7.93 (dd, *J* = 8.7, 1.6 Hz, 1H), 7.88-7.84 (m, 2H); ^{13}C NMR (150 MHz, $(CD_3)_2CO$) ppm 135.7, 131.36, 130.9 (q, *J* = 33.5 Hz), 128.8, 127.4 (dd, 7.8, 3.2 Hz), 126.1, 124.2 (q, *J* = 271.5 Hz), 120.7 (dq, *J* = 321.8, 6.4 Hz) ; ^{19}F NMR (282 MHz, $(CD_3)_2CO$) ppm -63.47, -76.93, -77.06; HRMS (ESI): Exact mass calcd for $C_9H_4F_9N_2O_4S_2$ $[M-H]^-$ 438.9474, found 438.9474.

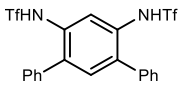

N,N'-([1,1':3',1''-Terphenyl]-4',6'-diyl)bis(1,1,1-trifluoromethanesulfonamide) (S8). The reaction was carried out according to the general procedure, [1,1':3',1"-terphenyl]-4',6'-diamine (85 mg, 330 µmol), triethylamine (95 µL, 690 mmol), and trifluoromethane sulfonic anhydride (117 µL, 690 µmol). The crude material was separated by silica gel chromatography (20-50% ethyl acetate in hexanes) to afford a pink wax (91 mg, 53%). IR (film) 3298, 3067, 1693, 1514, 1484 cm^{-1}; R_f = 0.2 (30 % EtOAc/hex); ^1H NMR (400 MHz, $(CD_3)_2CO$) δ 9.61 (br s, 2H), 7.71 (s, 1H), 7.55-7.51 (m, 3H), 7.53 (s, 1H), 7.51-7.46 (m, 5H), 7.46-7.41 (m, 2H); ^{13}C NMR (100 MHz, $(CD_3)_2CO$) ppm 141.0, 138.0, 134.7, 132.0, 130.4, 129.4, 129.1, 128.0, 120.6 (q, *J* = 321.6 Hz); ^{19}F NMR (282 MHz, $(CD_3)_2CO$) ppm -77.81; HRMS (ESI): Exact mass calcd for $C_{20}H_{14}F_6N_2O_4S_2Na$ $[M+Na]^+$ 547.0191, found 547.0195.

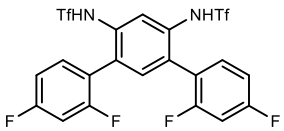

N,N'-(2,2'',4,4''-Tetrafluoro-[1,1':3',1''-terphenyl]-4',6'-diyl)bis(1,1,1-trifluoromethanesulfonamide) (206). The reaction was carried out according to the general procedure, 2,2",4,4"-tetrafluoro-[1,1':3',1"-terphenyl]-4',6'-diamine (85 mg, 330 µmol), triethylamine (365 µL, 2.6 mmol), and trifluoromethane sulfonic anhydride (435 µL, 2.6 mmol). The crude material was separated by silica gel chromatography (20-50% ethyl acetate in hexanes) to afford a pink wax (265 mg, 36%). IR (film) 3282, 3092, 1692, 1515, 1491 cm^{-1}; R_f = 0.2 (30 % EtOAc/hex); ^1H NMR (400 MHz, $(CD_3)_2CO$) δ 9.85 (br s, 2H), 7.76 (s, 1H), 7.58-7.54 (m, 2H). 7.54 (s, 1H), 7.20-7.13 (m, 4H); ^{13}C NMR (150 MHz, $(CD_3)_2CO$) ppm 164.4 (dd, *J* = 248.2, 11.6 Hz), 161.34 (dd, *J* = 250.4, 13.8 Hz), 136.3, 134.9, 134.8 (q, *J* = 4.8 Hz), 134.0, 126.8, 122.3, 122.2 (d, *J* = 3.3 Hz), 113.1 (*J* = 21.6, 3.9 Hz), 105.5 (dd, *J* = 26.0, 26.0 Hz); ^{19}F NMR (282 MHz, $(CD_3)_2CO$) ppm -77.68; HRMS (ESI): Exact mass calcd for $C_{20}H_9F_{10}N_2O_4S_2$ $[M-H]^-$ 594.9850, found 594.9839.

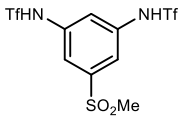

N,N'-(5-(methylsulfonyl)-1,3-phenylene)bis(1,1,1-trifluoromethanesulfonamide) (208). The reaction was carried out according to the general procedure, the corresponding diamine (180 mg, 96 µmol), triethylamine (382 µL, 2.0 mmol), and trifluoromethane sulfonic anhydride (340 µL, 2.0 mmol). The crude material was separated by silica gel chromatography (30-100% ethyl acetate in hexanes) to afford impure material. This material was then dissolved in $CHCl_3$ and Et2O and the impurities precipitated out of solution upon addition of hexanes. The filtrate was then concentrated and purified by silica gel chromatography (0.5%-5% MeOH/DCM) to give a brown wax (13.6 mg, 3%). IR (film) 3500, 3077, 2928, 2852, 1694, 1612 cm^{-1}; R_f = 0.1 (10 % MeOH/DCM); ^1H NMR (400 MHz, $(CD_3)_2CO$) δ N-H peak not detected, 7.41 (d, J = 1.8 Hz, 2H), 7.38 (t, *J* = 2.0 Hz, 1H), 3.04 (s, 3H); ^{13}C NMR (100 MHz, $(CD_3)_2CO$) ppm 144.6, 142.8, 122.1 (q, J = 326.0 Hz), 122.0, 116.1, 44.3; ^{19}F NMR (282 MHz, $(CD_3)_2CO$) ppm -77.15; HRMS (ESI): Exact mass calcd for $C_9H_7F_6N_2O_6S_3$ $[M-H]^-$ 448.9376, found 448.9315.

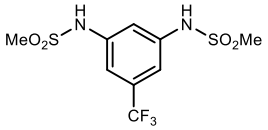

N,N'-(5-(trifluoromethyl)-1,3-phenylene)dimethanesulfonamide (207). The reaction was carried out according to the general procedure, the corresponding diamine (300 mg, 170 µmol), triethylamine (498 µL, 3.6 mmol), and methane sulfonic anhydride (327 mg, 3.6 mmol). The crude material was separated by silica gel chromatography (10-25% ethyl acetate in hexanes) to afford impure material. This material was recrystallized in chloroform to give a light brown wax (69 mg, 12%). IR (film) 3262, 1702, 1613, 1487 cm^{-1}; R_f = 0.2 (30 % EA/Hex); ^1H NMR (400 MHz, $(CD_3)_2CO$) δ 9.03 (br s, 2H), 7.57 (t, *J* = 1.6 Hz, 1H), 7.38 (d, *J* = 1.6 Hz, 2H), 3.11 (s, 3H); ^{13}C NMR (100 MHz, $(CD_3)_2CO$) ppm 141.0, 132.5 (q, *J* = 32.4 Hz), 124.23 (q, *J* = 271.9 Hz), 113.4, 111.3 (q, *J* = 4.1 Hz), 39.5; ^{19}F NMR (282 MHz, $(CD_3)_2CO$) ppm -63.52; HRMS (ESI): Exact mass calcd for $C_9H_{11}F_3N_2O_4S_2Na$ $[M+Na]^+$ 335.0009, found 355.0006.

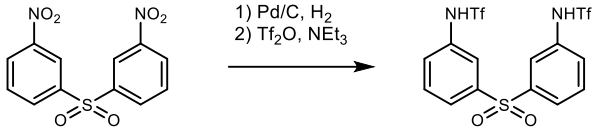

N,N'-(sulfonylbis(3,1-phenylene))bis(1,1,1-trifluoromethanesulfonamide) (S9). A 15 mL RBF was charged with nitroarene (142 mg, 0.46 mmol), Pd/C (30 mg, 20% by weight), and ethyl acetate (8 mL). The reaction was purged and refilled three times with argon, and then hydrogen gas. The reaction was monitored by TLC, full conversion was observed after 4 h. The flask was purged with argon, and then passed through celite with ethyl acetate. The crude material was then carried forward crude.

The triflation reaction reaction was carried out according to the general procedure, using crude 3,3'-sulfonyldianiline, triethylamine (106 µL, 76 µmol), and trifluoromethane sulfonic anhydride (127 µL, 76 µmol). The crude material was separated by silica gel chromatography (SiO_2, 20-50 % ethyl acetate in hexanes) to afford a white wax (59 mg, 36%). IR (film) 3104, 3085, 2822, 1474, 1449 cm^{-1}; R_f = 0.2 (50% EtOAc/hexanes); ^1H NMR (400 MHz, $(CD_3)_2CO$) δ N-H peak not detected, 8.42 (ddd, *J* = 7.9, 1.6, 1.1 Hz, 2H), 8.33 (dd, *J* = 1.8, 1.8 Hz, 2H), 8.12 (dd, *J* = 8.0, 1.3 Hz, 2H), 8.01 (dd, *J* = 8.1, 8.1 Hz, 2H); ^{13}C NMR (100 MHz, $(CD_3)_2CO$) ppm 142.9, 136.7, 132.9, 132.2, 131.8, 130.4, 119.2, (q, *J* = 324.4 Hz); ^{19}F NMR (282 MHz, $(CD_3)_2CO$) ppm -71.9 HRMS (ESI): Exact mass calcd for $C_{14}H_9F_6N_2O_5S_2$ $[M-H]^-$ 510.9532, found 510.9495.

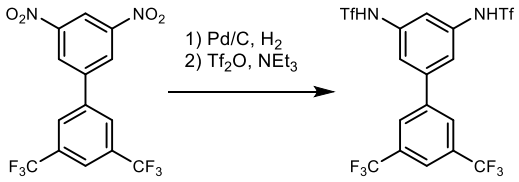

N,N'-(3',5'-bis(trifluoromethyl)-[1,1'-biphenyl]-3,5-diyl)bis(1,1,1-trifluoromethanesulfonamide) (211). A 15 mL RBF was charged with nitroarene (115 mg, 0.30 mmol), Pd/C (58 mg, 50% by weight), and methanol (5 mL). The reaction was purged and refilled three times with argon, and then hydrogen gas. The reaction was monitored by TLC, full conversion was observed after 6 h. The flask was purged with argon, and then passed through celite with ethyl acetate. The crude material was then carried forward crude.

The triflation reaction was carried out according to the general procedure, using the crude diamine, triethylamine (86 µL, 62 µmol), and trifluoromethane sulfonic anhydride (104 µL, 62 µmol). The crude material was separated by silica gel chromatography (SiO_2, 5-25% ethyl acetate in hexanes) to afford a white wax (97 mg, 57%). IR (film) 3281, 3265, 3014, 2974, 1603, 1515, 1484 cm^{-1}; R_f = 0.3 (50 % EtOAc/hexanes); ^1H NMR (400 MHz, $(CD_3)_2CO$) δ 10.57 (br s, 2H), 8.28 (br s, 2H), 8.17 (br s, 1H), 7.26 (d, *J* = 2.2 Hz, 2H), 7.62 (t, *J* = 1.8 Hz, 1H); ^{13}C NMR (100 MHz, $(CD_3)_2CO$) ppm 142.4, 141.6, 138.03, 137.97, 133.0 (q, *J* = 33.1 Hz), 128.7 (q, *J* = 4.1 Hz), 123.0 (q, *J* = 4.1 Hz), 121.0 (q, *J* = 322.1 Hz), 120.7, 117.1; ^{19}F NMR (282 MHz, $(CD_3)_2CO$) ppm -63.4, -76.9; HRMS (ESI): Exact mass calcd for $C_{16}H_8F_{12}N_2O_4S_2$ $[M]^+$ 583.9734, found 583.9738.

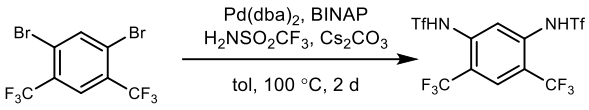

N,N'-(4,6-bis(trifluoromethyl)-1,3-phenylene)bis(1,1,1-trifluoromethanesulfonamide) (209). A 50-mL, round-bottomed flask equipped with a stir bar was charged with 1,5-dibromo-2,4-bis(trifluoromethyl)benzene (300 mg, 0.8 mmol), $Pd(dba)_2$ (74 mg, 80 μmol), *rac*-BINAP (100 mg, 160 μmol), and cesium carbonate (1.57 g, 4.8 mmol). The reaction vessel was placed under an argon atmosphere, toluene (5.5 mL) was dispensed into the flask. The reaction vessel was evacuated and backfilled with argon gas three times. The round-bottomed flask was placed into an oil bath heated to 100 °C with stirring. The reaction was monitored by LR-MS and after 2 d nearly complete conversion was observed. The reaction was cooled to 0 °C and quenched with 1 M HCl. The aqueous layer was extracted with ethyl acetate, dried, and concentrated. Flash column chromatography (SiO_2, 20-50% ethyl acetate in hexanes), followed by reverse phase chromatography (C18, 0-70% acetonitrile/water with 0.1% TFA) to yield a pale pink solid (86 mg, 21%). Mp 194-198 °C; IR (film) 3268, 3014, 2974, 1671, 1587, 1518 cm^{-1}; R_f = 0.1 (100 % EtOAc); ^1H NMR (400 MHz, $(CD_3)_2CO$) δ 8.05 (s, 1H), 7.72 (s, 1H); ^{13}C NMR (150 MHz, $(CD_3)_2CO$) ppm 160.6 (q, *J* = 35.4 Hz), 125.1 (dq, *J* = 5.5, 5.5 Hz), 124.0 (q, *J* = 271.6 Hz), 123.9, 121.1 (q, *J* = 323.6 Hz), 118.2 (q, *J* = 30.2 Hz); ^{19}F NMR (282 MHz, $(CD_3)_2CO$) ppm -60.3 (q, *J* = 2.7 Hz), -75.8 (q, *J* = 2.7 Hz); HRMS (ESI): Exact mass calcd for $C_{10}H_3F_{12}N_2O_4S_2$ $[M-H]^-$ 506.9348, found 506.9340.

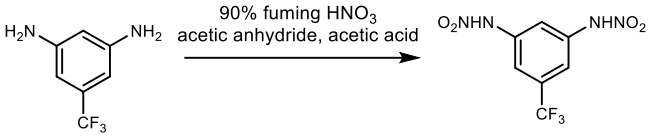

N,N'-(5-(trifluoromethyl)-1,3-phenylene)dinitramide (210). A 25-mL, round-bottomed flask equipped with a stir bar was charged with the diamine (500 mg, 2.8 mmol), and acetic acid (5 mL). Fuming nitric acid (0.6 mL, 14.1 mmol), then acetic anhydride (0.6 mL, 14.1 mmol) was added dropwise. The heterogeneous mixture was stirred at room temperature for one hour, and then poured over ice. The aqueous layer was extracted with ethyl acetate, dried, and concentrated. Flash column chromatography (SiO_2, 20-75% ethyl acetate in hexanes yielded a red solid (57 mg, 8%). Mp 138-141 °C; IR (film) 3266, 3014, 2974, 1671, 1589 cm^{-1}; R_f = 0.1 (50 % EtOAc/Hex); ^1H NMR (400 MHz, $(CD_3)_2CO$) δ N-H peak not detected, 7.98 (br s, 1H), 7.80 (br s, 2H); ^{13}C NMR (150 MHz, $(CD_3)_2CO$) ppm 138.6, 132.2 (q, *J* = 33.1 Hz), 124.2 (q, *J* = 272.0 Hz), 118.4, 116.7 (q, *J* = 3.7 Hz); ^{19}F NMR (282 MHz, $(CD_3)_2CO$) ppm -63.6); HRMS (ESI): Exact mass calcd for $C_7H_4F_3N_4O_4$ $[M-H]^-$ 265.0190, found 265.0184.

Triflamide precursors

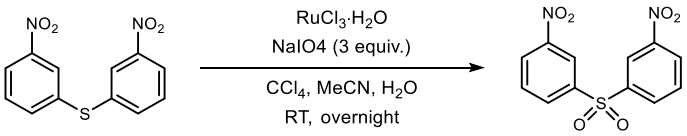

3,3'-sulfonylbis(nitrobenzene) (S10). A 100 mL round-bottomed flask equipped with a stir bar was charged with sulfane (976 mg, 3.50 mmol) and carbon tetrachloride (9 mL), acetonitrile (9 mL), and water (18 mL). The suspension was mixed at room temperature prior to $RuCl_3·H_2O$ (40 mg, 180 μmol) addition. After 5 min, sodium

periodate (2.26 g, 10.6 mmol) was added in one portion. The suspension was allowed to stir overnight. The reaction mixture was diluted with water and transferred to a separatory funnel where the aqueous layer was extracted with ethyl acetate. The resulting organic layer was dried and concentrated to provide a pale yellow wax (627 mg, 59%).R_f = 0.2 (50% EtOAc/hex); IR (film) 3076, 2929, 1694, 1589, 1473 cm^{-1}; ^1H NMR (400 MHz, $CDCl_3$) δ 8.89 (dd, *J* = 1.9, 1.9 Hz, 2H), 8.48 (ddd, *J* = 8.2, 2.1, 1.0 Hz, 2H), 8.33 (ddd, *J* = 7.9, 1.6, 1.0 Hz, 2H), 7.81 (dd, *J* = 8.0, 8.0 Hz, 2H);^{13}C NMR (100 MHz, $(CD_3)_2CO$) ppm 143.5, 137.4, 133.5, 132.9, 132.4, 131.06; HRMS (ESI): Exact mass calcd for $C_{12}H_9N_2O_6S$ $[M+H]^+$ 309.0176, found 309.0131.

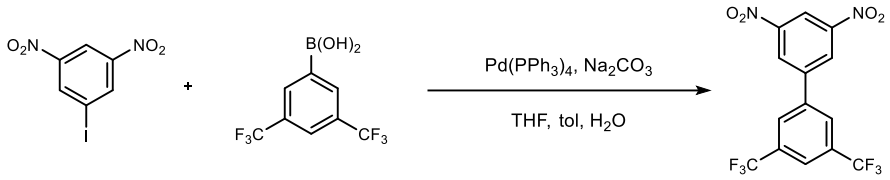

3,5-dinitro-3',5'-bis(trifluoromethyl)-1,1'-biphenyl (236). A flame-dried 10 mL round-bottomed flask equipped with a stir bar was charged with $Pd(PPh_3)_4$ (60 mg, 50 µmol), the aryl halide (150 mg, 0.50 mmol), the boronic acid (195 mg, 0.75 mmol), and sodium carbonate (130 mg, 125 mmol). The reaction vessel was placed under an argon atmosphere, toluene (10 mL), tetrahydrofuran (10 mL), and water (5 mL) were dispensed into the flask. The round-bottomed flask was placed into an oil bath heated to 85 °C with stirring overnight. The reaction was cooled to 25 °C, then diluted with ethyl acetate and water. The aqueous layer was extracted with ethyl acetate and the combined organic layers are dried and concentrated. Flash column chromatography (SiO_2, 0-5% diethyl ether in hexanes) of the residue yielded a pale-yellow wax (122 mg, 63%). R_f = 0.2 (10% EtOAc/hex); IR (film) 3095, 3014, 2974, 1544, 1479 cm^{-1}; ^1H NMR (400 MHz, $CDCl_3$) δ 9.12 (t, *J* = 2.1 Hz, 1H), 8.82 (d, *J* = 2.2 Hz, 2H), 8.14 (br s, 2H), 8.05 (br s, 1H);^{13}C NMR (100 MHz, $CDCl_3$)) ppm 149.4, 141.8, 138.8, 133.4 (q, *J* = 33.9 Hz), 127.7 (q, *J* = 3.6 Hz), 127.4, 123.6 (dq, *J* = 3.6, 3.9 Hz), 123.0 (q, *J* =273.0), 118.8; ^{19}F NMR (282 MHz, $CDCl_3$) ppm -62.9); HRMS (ESI): Exact mass calcd for $C_{14}H_6F_6N_2O_4$ $[M]^+$ 380.0232, found 380.0239.

General procedure for azide addition into nitroolefins

To an oven-dried vial equipped with a stir bar was added ^{6}MeOStilbPBAM•**X** (11.0 mg, 10.0 µmol), phthalic acid (8.3 mg, 50.0 µmol), Na_2SO_4 (60 mg, 42 µmol), and toluene (3 mL). The reaction mixture was stirred for 5 minutes before $TMSN_3$ (40 µL, 300 µmol) was added and then cooled to -20 °C. The nitroolefin (100 µmol) was added after 1 hour. The reaction mixture was stirred without light for 48 under Ar (balloon). The mixture was cooled to -78 ºC before it was flushed through a silica plug using 10 % ethyl acetate in hexanes to yield the desired product.

General procedure for the synthesis of 6-aryl heptanoic acids[3]

A flame-dried round-bottomed flask equipped with a stir bar was charged with $Pd(PPh_3)_4$, hept-6-ynoic acid, the aryl boronic acid, and freshly distilled 1,4-dioxane. The resulting mixture was treated with acetic acid under an argon atmosphere. Argon was bubbled through the reaction mixture for 15 min while stirring at room temperature. The round-bottomed flask was placed in an oil bath overnight at 105 °C. The reaction mixture was concentrated *in vacuo* and the crude material was dissolved in ethyl acetate. The organic layer was washed with 1 M HCl, dried, and concentrated. Flash column chromatography of the residue yielded the 6-aryl heptanoic acid.

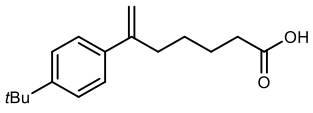

6-(4-(tert-butyl)phenyl)hept-6-enoic acid (288a). The reaction was carried out according to the general procedure, using $Pd(PPh_3)_4$ (55 mg, 48 µmol), hept-6-ynoic acid (200 mg, 1.6 mmol), the aryl boronic acid (338 mg, 1.9 mmol), acetic acid (9 µL, 0.16 mmol), and 1,4-dioxane (6 mL).The crude material was separated by silica

gel chromatography (SiO_2, 5-15% ethyl acetate in hexanes) to afford a yellow oil (138 mg, 35%). IR (film) 3082, 3032, 2960, 2866, 1725, 1625, 1513, 1462 cm^{-1}; R_f = 0.5 (30% EtOAc/hexanes); ^1H NMR (400 MHz, $CDCl_3$) δ 7.33 (br s, 4H), 5.27 (d, *J* = 1.1 Hz, 1H), 5.02 (d, *J* = 1.1 Hz, 1H), 2.52 (t, *J* = 7.4 Hz, 2H), 2.36 (t, *J* = 7.4 Hz, 2H), 1.70 (tt, *J* = 11.4, 7.7 Hz, 2H), 1.53 (tt, *J* = 11.5, 7.7 Hz), 1.32 (s, 9H); ^{13}C NMR (150 MHz, $CDCl_3$) ppm 179.8, 150.5, 147.7, 138.1, 125.8, 125.3, 111.9, 35.0, 34.6, 33.9, 31.4, 27.7, 24.4; HRMS (ESI): Exact mass calcd for $C_{17}H_{23}O_2$ $[M-H]^-$ 259.1704, found 259.1697.

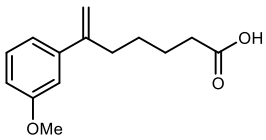

6-(3-methoxyphenyl)hept-6-enoic acid (287a). The reaction was carried out according to the general procedure, using $Pd(PPh_3)_4$ (55 mg, 48 µmol), hept-6-ynoic acid (200 mg, 1.6 mmol), the aryl boronic acid (290 mg, 1.9 mmol), acetic acid (9 µL, 0.16 mmol), and 1,4-dioxane (6 mL).The crude material was separated by silica gel chromatography (SiO_2, 5-15% ethyl acetate in hexanes) to afford a yellow oil (133 mg, 36%). IR (film) 3078, 2936, 2864, 2672, 1706, 1597, 1576, 1487 cm^{-1}; R_f = 0.4 (30% EtOAc/hexanes); ^1H NMR (400 MHz, $CDCl_3$) δ 7.23 (d, *J* = 7.8 Hz, 1H), 6.98 (ddd, *J* = 7.7, 1.2, 0.9 Hz, 1H), 6.92 (dd, *J* = 2.3, 1.8 Hz, 1H), 6.82 (ddd, *J* = 8.2, 2.6, 0.7 Hz, 1H), 5.27 (d, *J* = 1.4 Hz, 1H), 5.06 (d, *J* = 1.2 Hz, 1H), 3.82 (s, 3H), 2.51 (t, *J* =. 7.2 Hz, 2H), 2.35 (t, *J* = 7.5 Hz, 2H), 1.68 (tt, *J* = 11.4, 7.6 Hz, 2H), 1.52 (tt, *J* = 11.2, 7.6 Hz, 2H); ^{13}C NMR (150 MHz, $CDCl_3$) ppm 180.3, 159.6, 148.0, 142.8, 129.3, 118.8, 112.8, 112.7, 112.2, 55.3, 35.1, 34.0, 27.6, 24.3; HRMS (ESI): Exact mass calcd for $C_{14}H_{18}O_3$ $[M-H]^-$ 233.1183, found 233.1178.

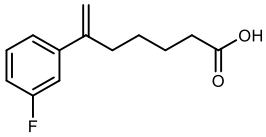

6-(3-fluorophenyl)hept-6-enoic acid (282a). The reaction was carried out according to the general procedure, using $Pd(PPh_3)_4$ (77 mg, 70 µmol), hept-6-ynoic acid (282 mg, 2.2 mmol), the aryl boronic acid (373 mg, 2.7 mmol), acetic acid (13 µL, 0.22 mmol), and 1,4-dioxane (9 mL).The crude material was separated by silica gel chromatography (SiO_2, 5-15% ethyl acetate in hexanes) to afford a yellow oil (208 mg, 42%). IR (film) 3080, 2933, 2865, 2672, 1707, 1621, 1580, 1487 cm^{-1}; R_f = 0.4 (30% EtOAc/hexanes);^1H NMR (400 MHz, $CDCl_3$) δ 7.28 (dt, *J* = 7.9, 6.0 Hz, 1H), 7.16 (ddd, *J* = 7.8, 1.2, 0.9 Hz, 1H), 7.08 (ddd, *J* = 10.6, 2.2, 2.0 Hz, 1H), 6.95 (ddd, *J* = 8.3, 2.5, 0.7 Hz, 1H), 5.29 (br s, 1H), 5.10 (d, *J* = 1.2 Hz, 1H), 2.50 (t, *J* = 7.5 Hz, 2H), 2.35(t, *J* = 7.5 Hz, 2H), 1.68 (tt, *J* = 11.5, 7.7 Hz, 2H), 1.51 (tt, *J* = 11.1, 7.6 Hz, 2H); ^{13}C NMR (150 MHz, $CDCl_3$) ppm 180.4, 163.0 (d, *J* = 244.3 Hz), 146.9 (d, *J* = 2.2 Hz), 143.5 (d, *J* = 6.6 Hz), 129.8 (d, *J* = 8.8 Hz), 121.8 (d, *J* = 2.2 Hz), 114.2 (d, *J* = 21.0 Hz), 113.5, 113.1 (d, *J* = 23.2 Hz), 34.8, 33.9, 27.5, 24.2; ^{19}F NMR (282 MHz, $CDCl_3$) ppm -113.5); HRMS (ESI): Exact mass calcd for $C_{13}H_{15}FO_2$[M-H]$^-$ 221.0983, found 221.0979.

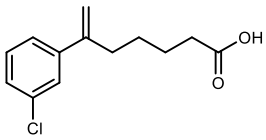

6-(3-chlorophenyl)hept-6-enoic acid (284a). The reaction was carried out according to the general procedure, using $Pd(PPh_3)_4$ (110 mg, 95 µmol), hept-6-ynoic acid (400 mg, 3.2 mmol), the aryl boronic acid (595 mg, 3.8 mmol), acetic acid (18 µL, 0.32 mmol), and 1,4-dioxane (12 mL).The crude material was separated by silica gel chromatography (SiO_2, 5-15% ethyl acetate in hexanes) to afford a yellow oil (208 mg, 42%). IR (film) 3062, 2933, 2864, 2672, 1706, 1592, 1562, 1475 cm^{-1}; R_f = 0.4 (30% EtOAc/hexanes); ^1H NMR (400 MHz, $CDCl_3$) δ 7.36 (m, 1H), 7.26-7.23 (m, 4H), 5.28 (br s, 1H), 5.10 (d, *J* = 1.1 Hz, 1H), 2.49 (t, *J* = 7.6 Hz, 2H), 2.35 (t, *J* = 7.4 Hz, 2H), 1.86 (tt, *J* = 11.4, 7.6 Hz, 2H), 1.50 (tt, *J* = 11.2, 7.6 Hz, 2H); ^{13}C NMR (150 MHz, $CDCl_3$) ppm 180.4, 146.7, 143.0, 134.2, 129.5, 127.4, 126.2, 124.2, 113.6, 34.7, 33.8, 27.3, 24.1; HRMS (ESI): Exact mass calcd for $C_{13}H_{15}ClO_2$ $[M-H]^-$ 237.0688, found 237.0682.

References

[1] Dolomanov, O. V.; Bourhis, L. J.; Gildea, R. J.; Howard, J. A. K.; Puschmann, H., *J. Appl. Crystallogr.* **2009,** *42* (2), 339-341.
[2] Sheldrick, G., *Acta Crystallographica Section A* **2008,** *64* (1), 112-122.
[3] Oh, C.; Jung, H.; Kim, K.; Kim, N.; *Angew. Chem. Int. Ed.*, **2003**, 42, No.7, 805-808.

Spectral data and HPLC traces

Figure 1. ^{1}H NMR (400 MHz, $CDCl_3$) of **134a**

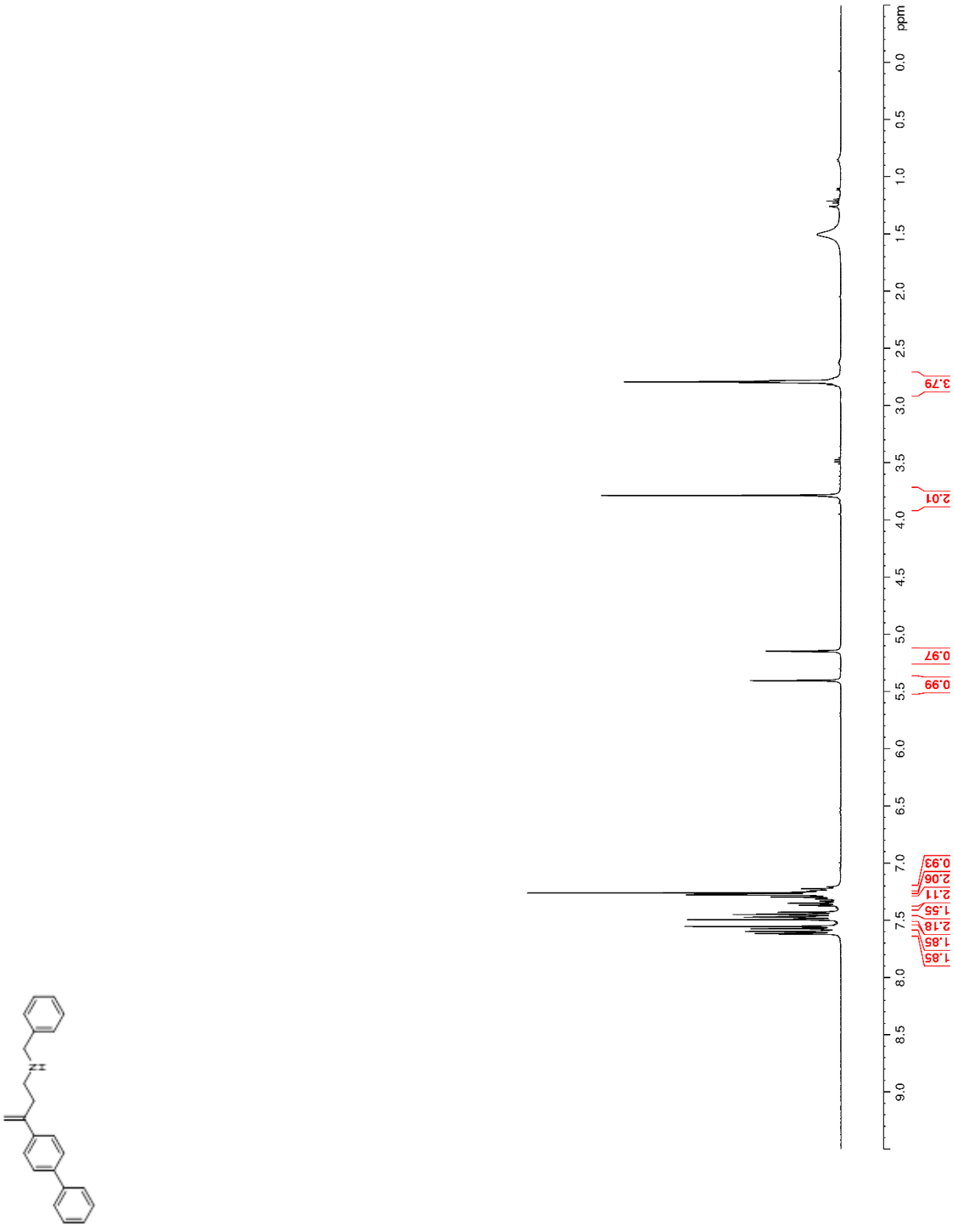

Figure 2. ^{13}C NMR (150 MHz, $CDCl_3$) of **134a**

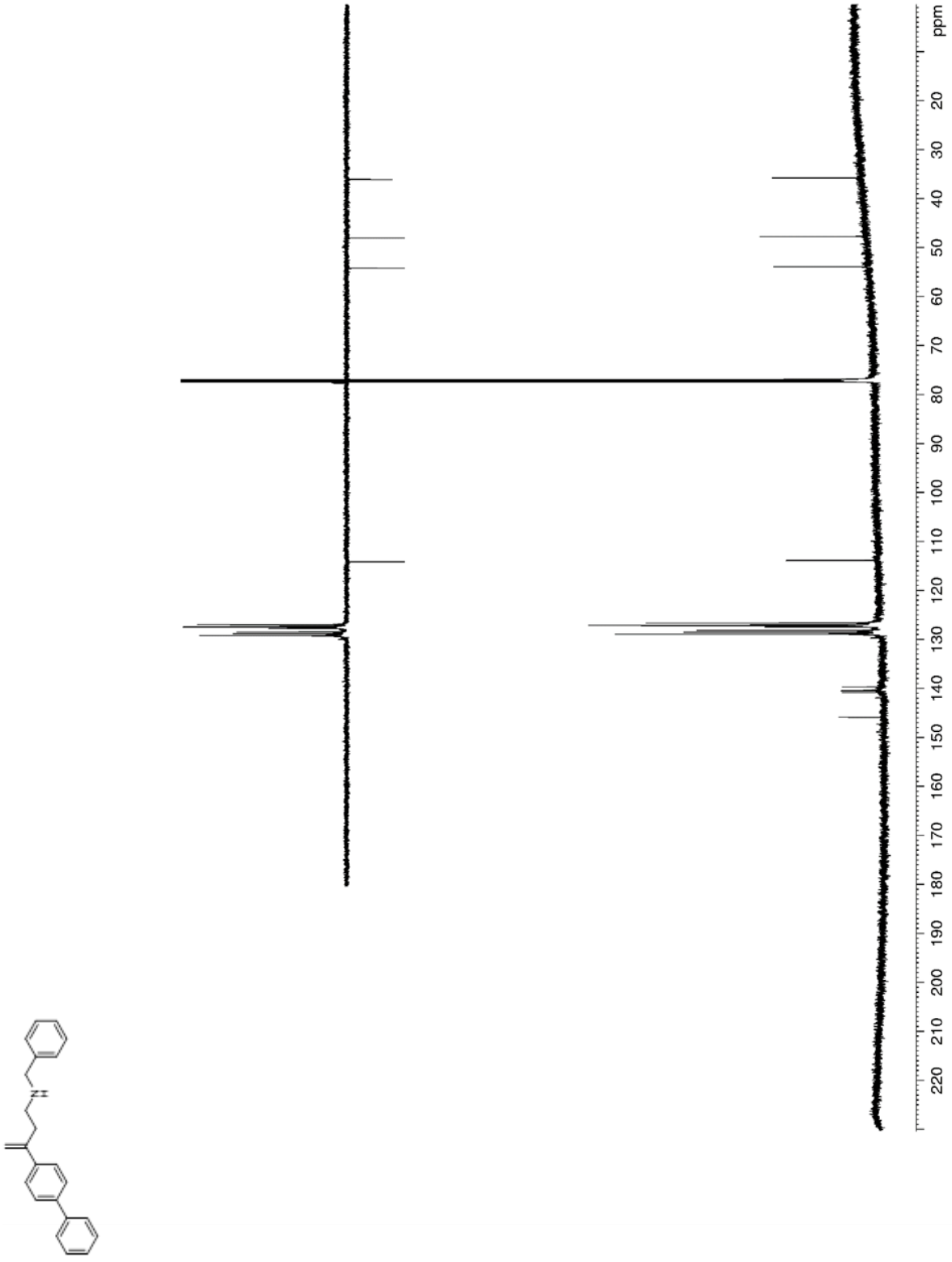

Figure 3. ^{1}H NMR (400 MHz, $CDCl_3$) of **143a**

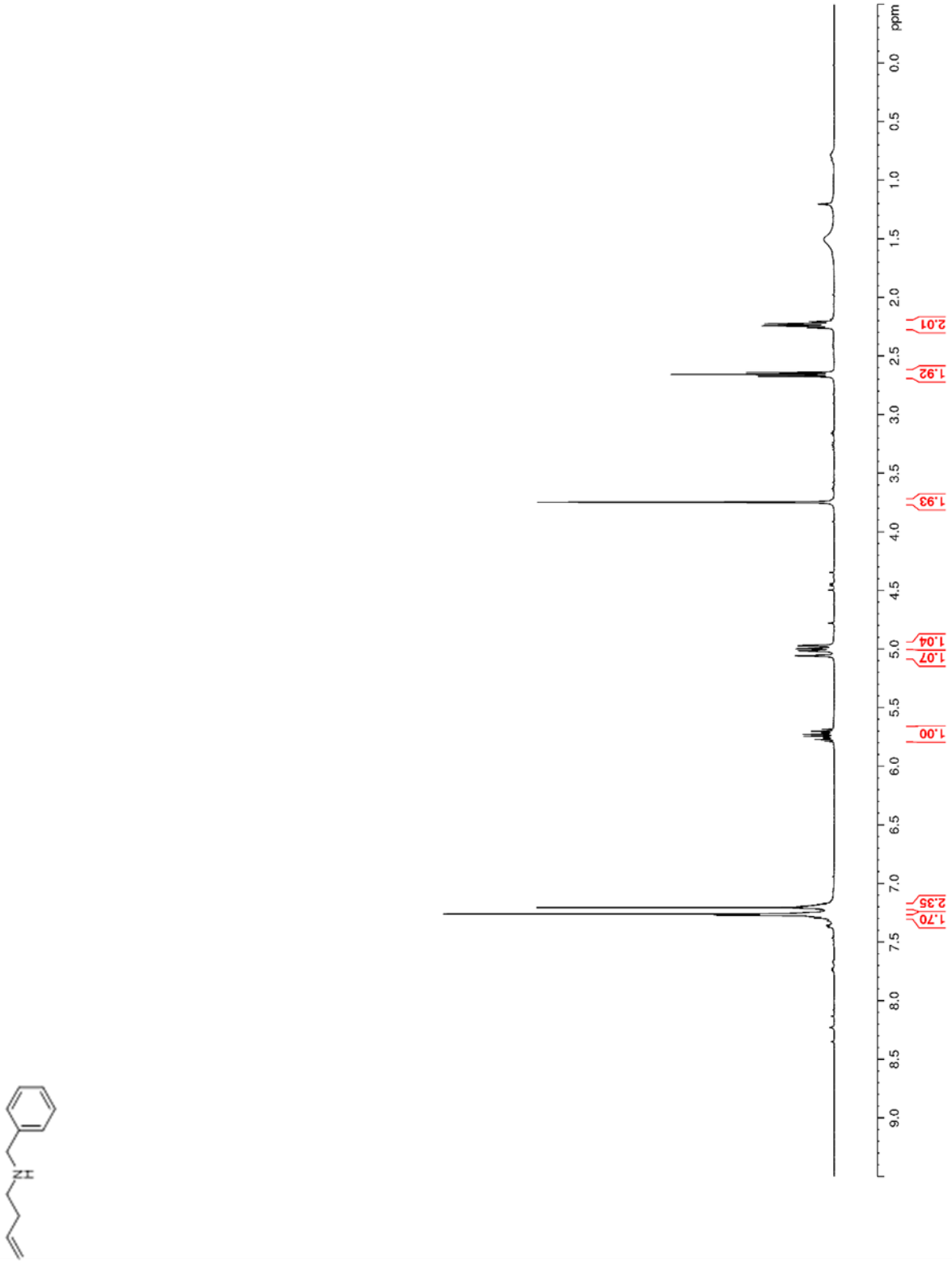

Figure 4. ^{13}C NMR (150 MHz, $CDCl_3$) of **143a**

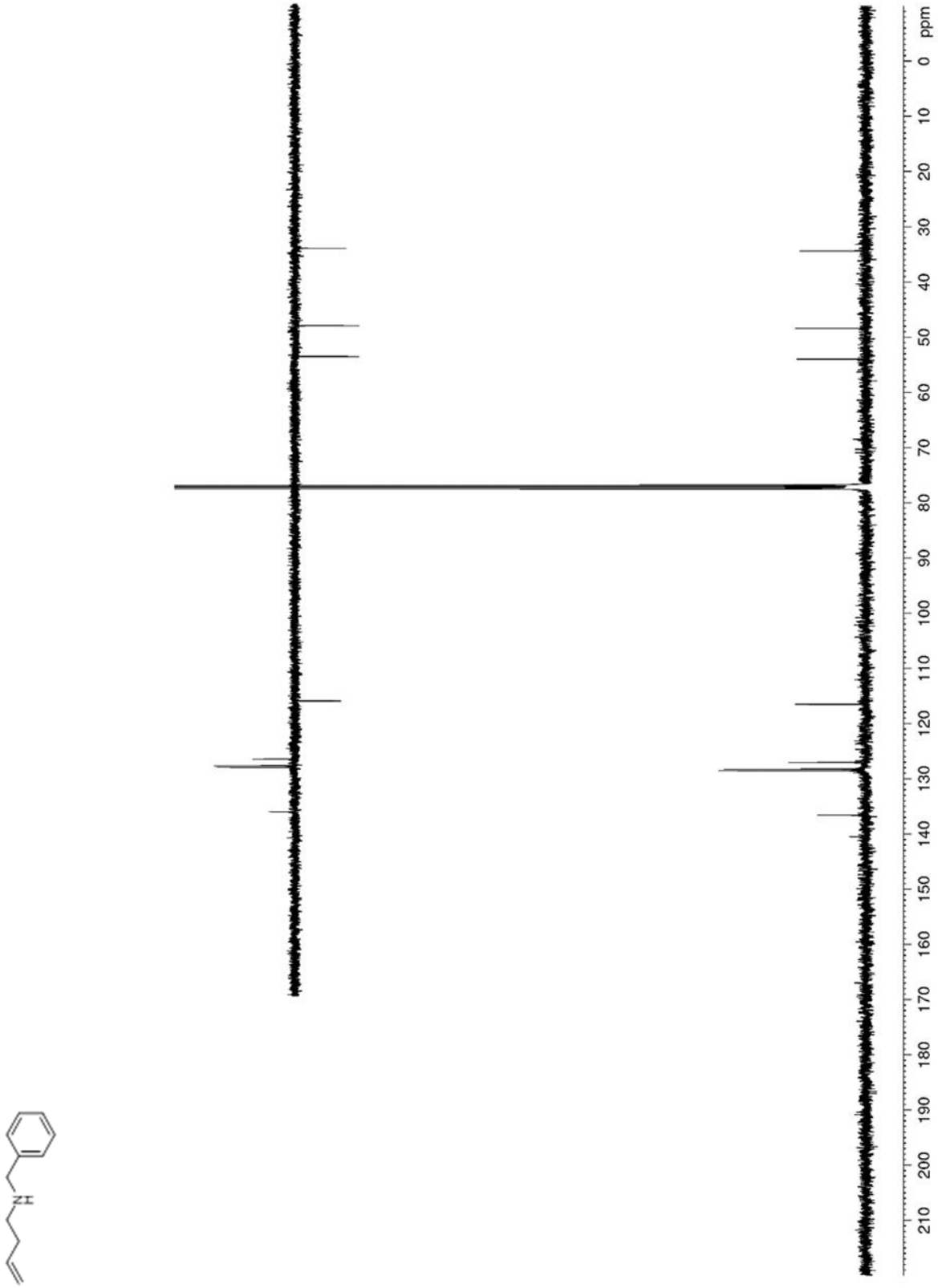

Figure 5. ^{1}H NMR (400 MHz, $CDCl_3$) of **S1**

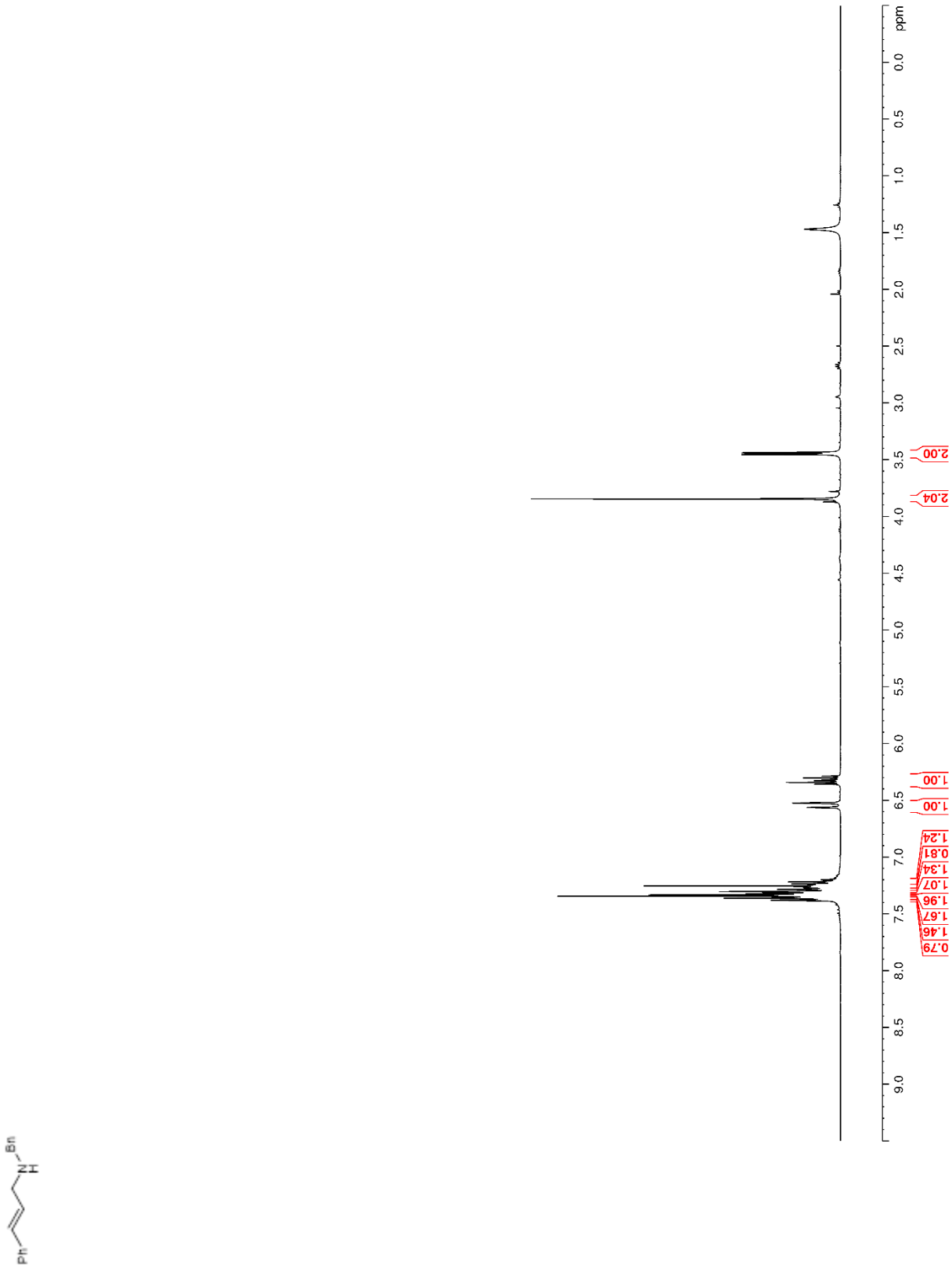

Figure 6. ^{13}C NMR (100 MHz, $CDCl_3$) of **S1**

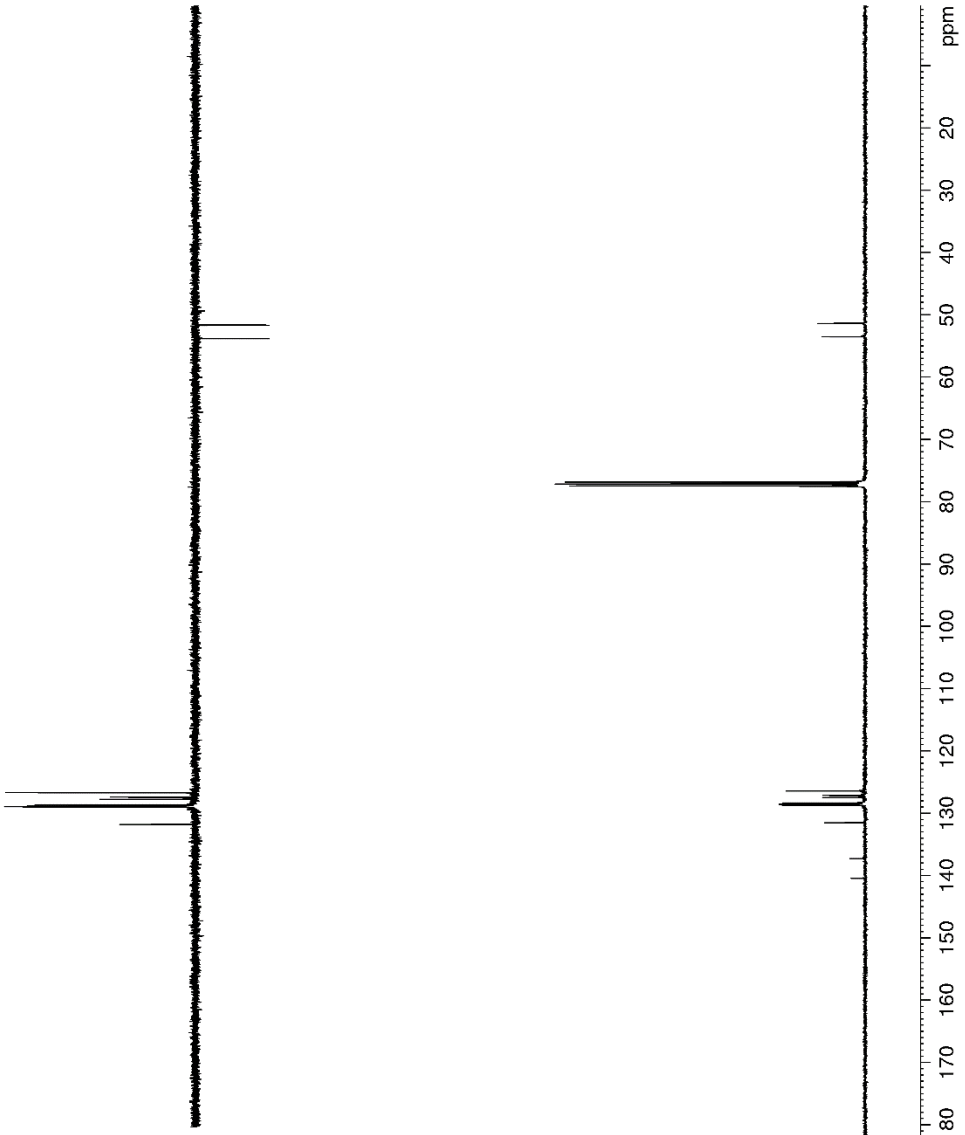

Figure 7. ^{1}H NMR (400 MHz, $CDCl_3$) of **S2**

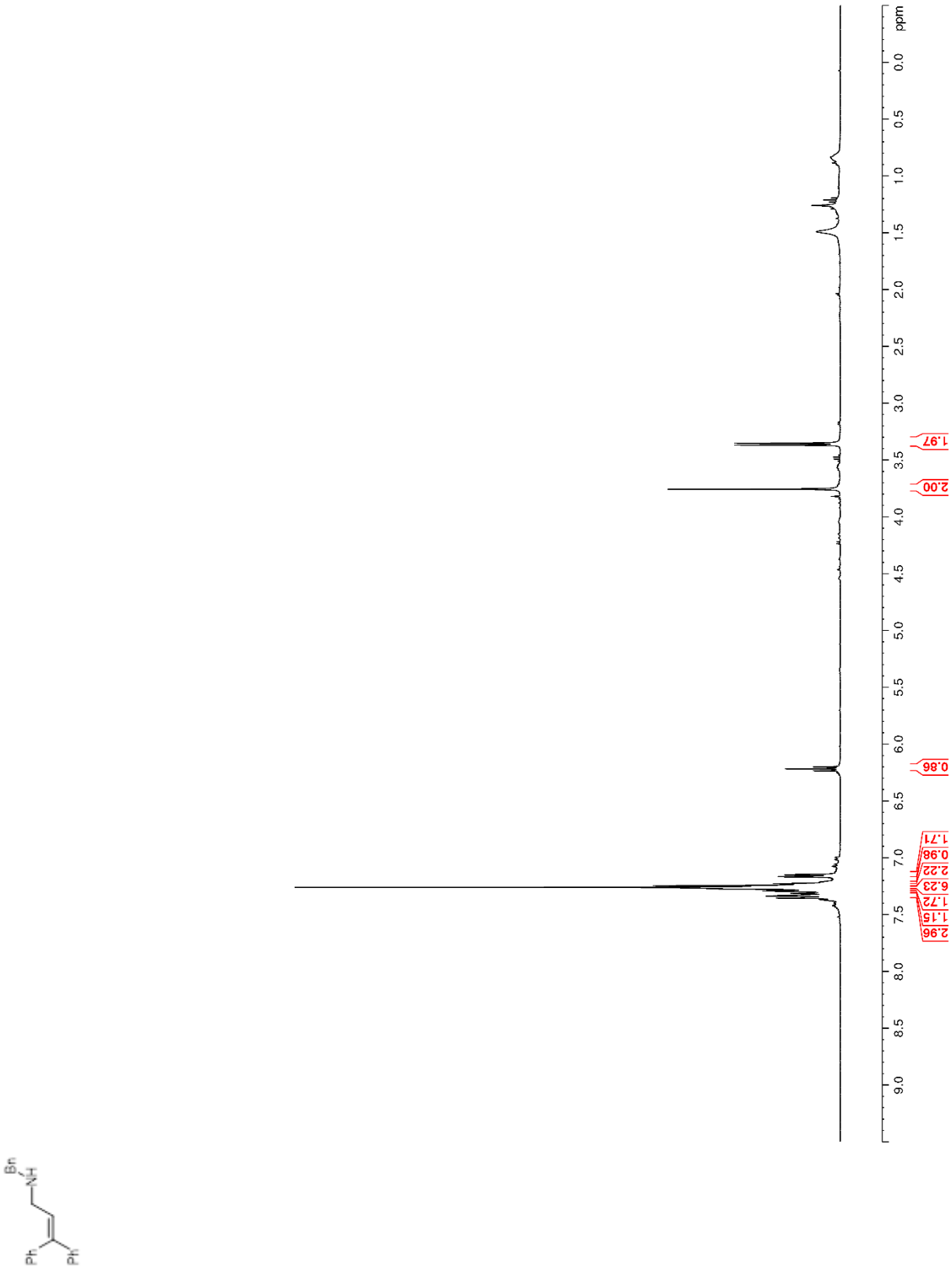

Figure 8. ^{13}C NMR (100 MHz, $CDCl_3$) of **S2**

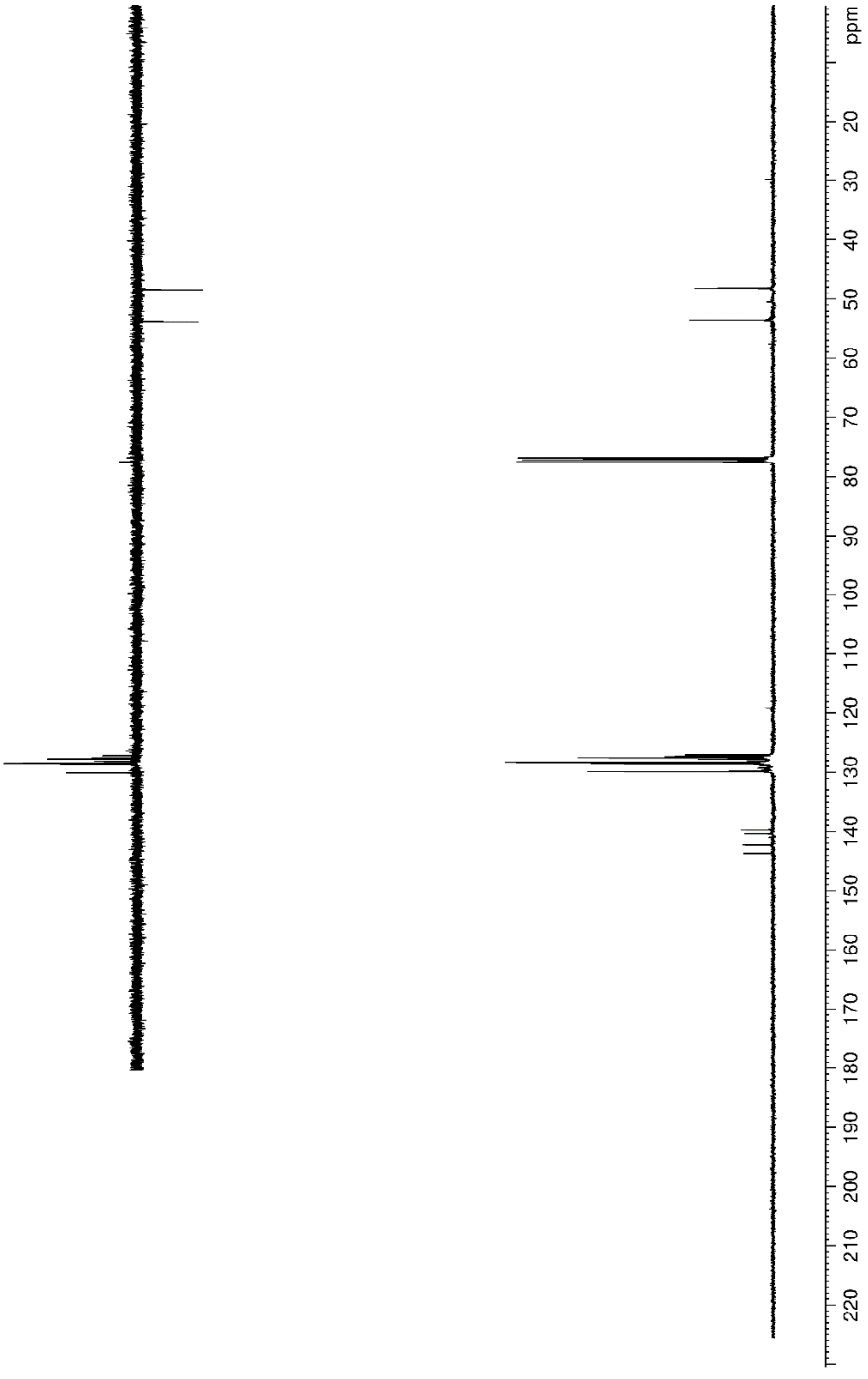

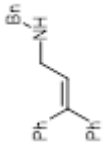

Figure 9. ^{1}H NMR (400 MHz, $CDCl_3$) of **S3**

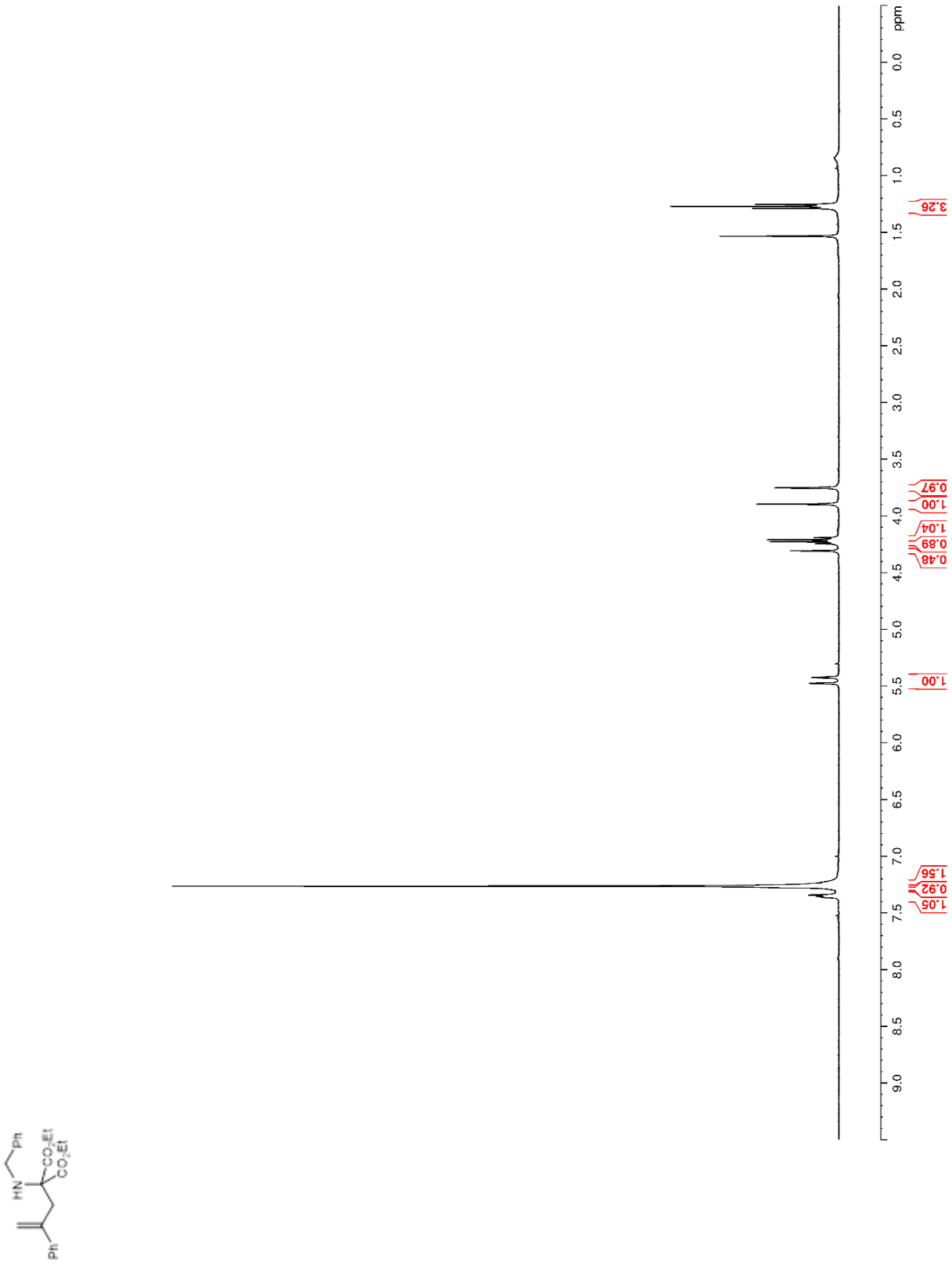

Figure 10. ^{13}C NMR (100 MHz, $CDCl_3$) of **S3**

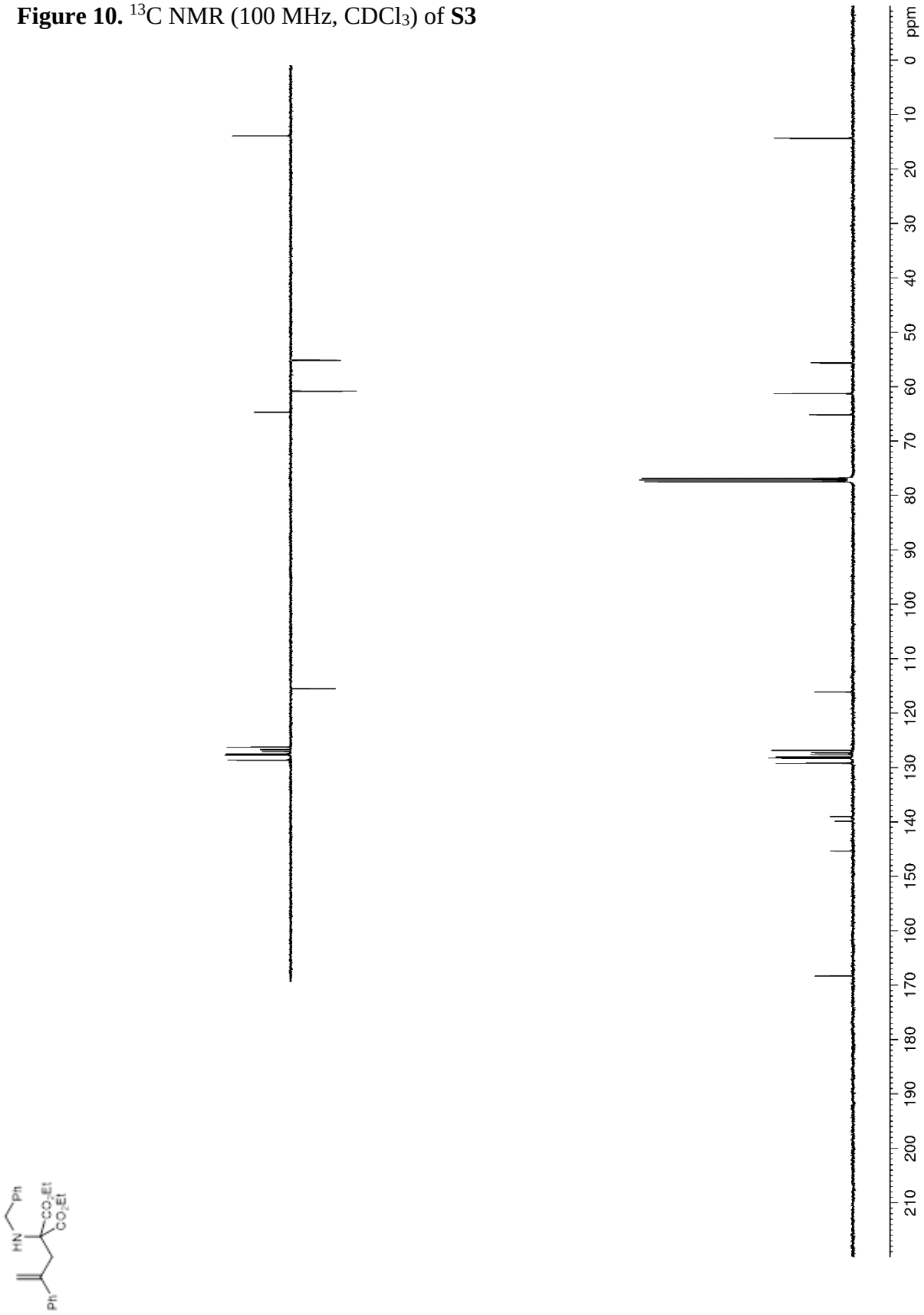

Figure 11. ^{1}H NMR (400 MHz, $CDCl_3$) of **134b**

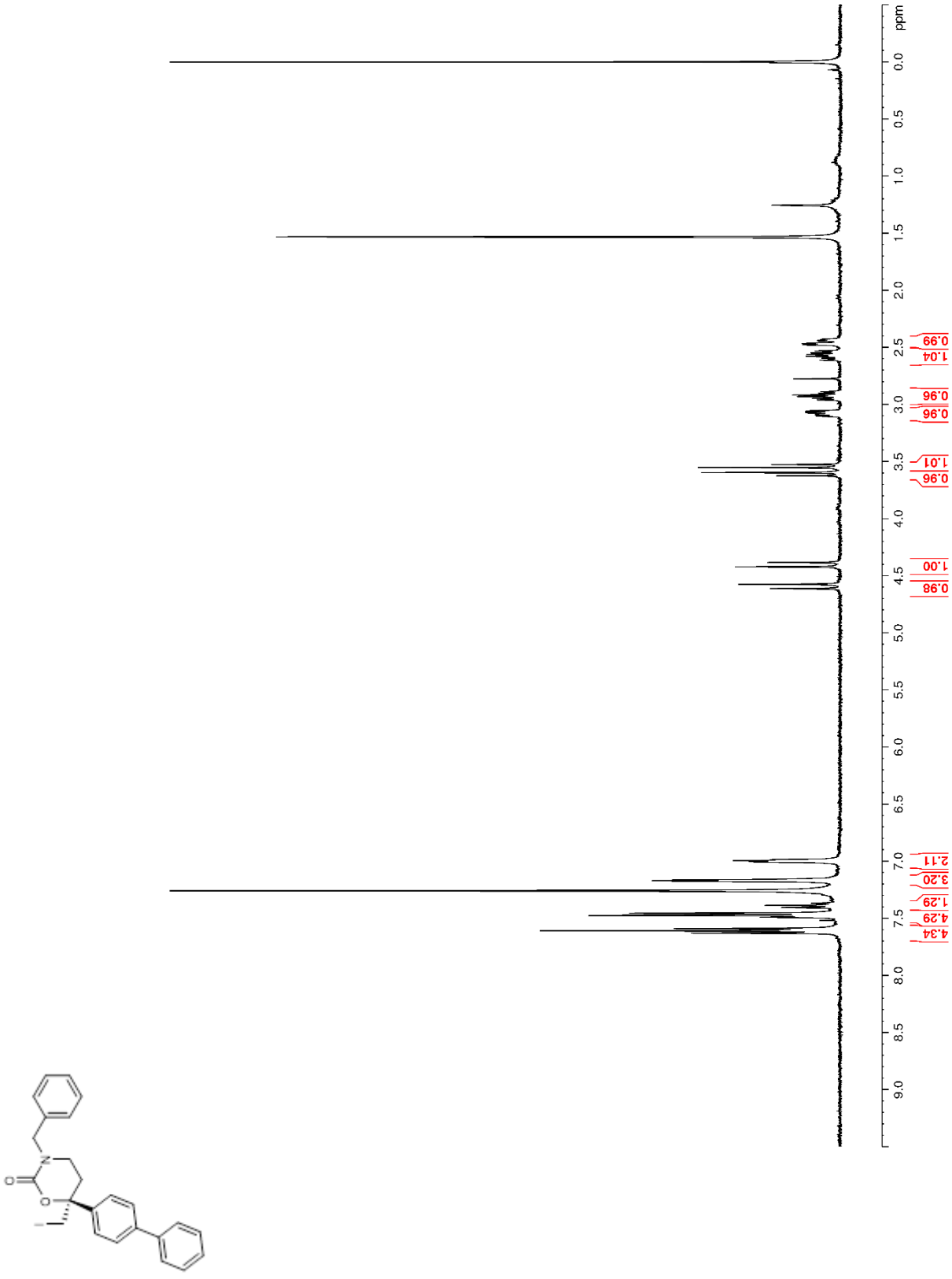

Figure 12. ^{13}C NMR (100 MHz, $CDCl_3$) of **134b**

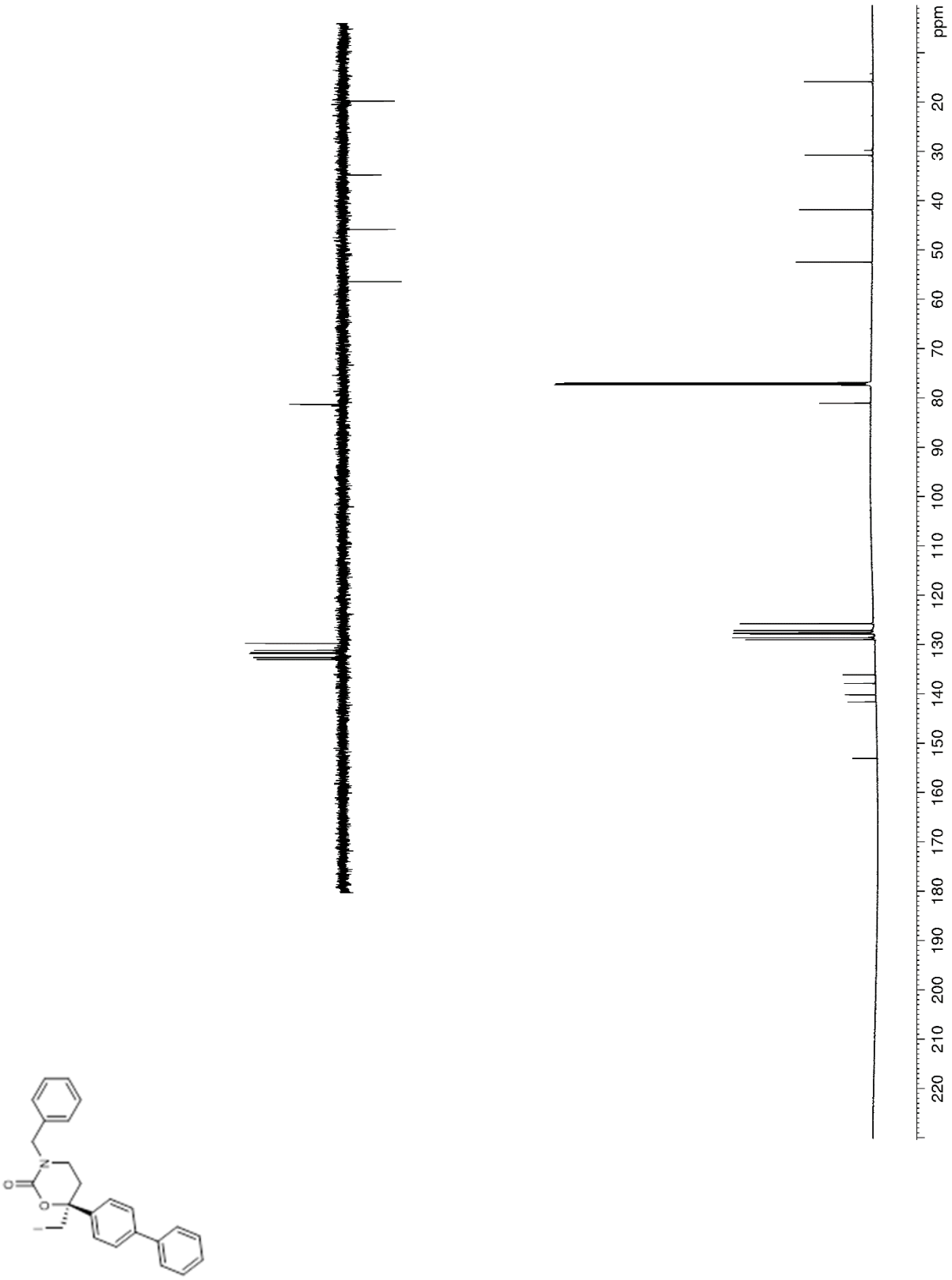

Figure 13. ^{1}H NMR (400 MHz, $CDCl_3$) of **143b**

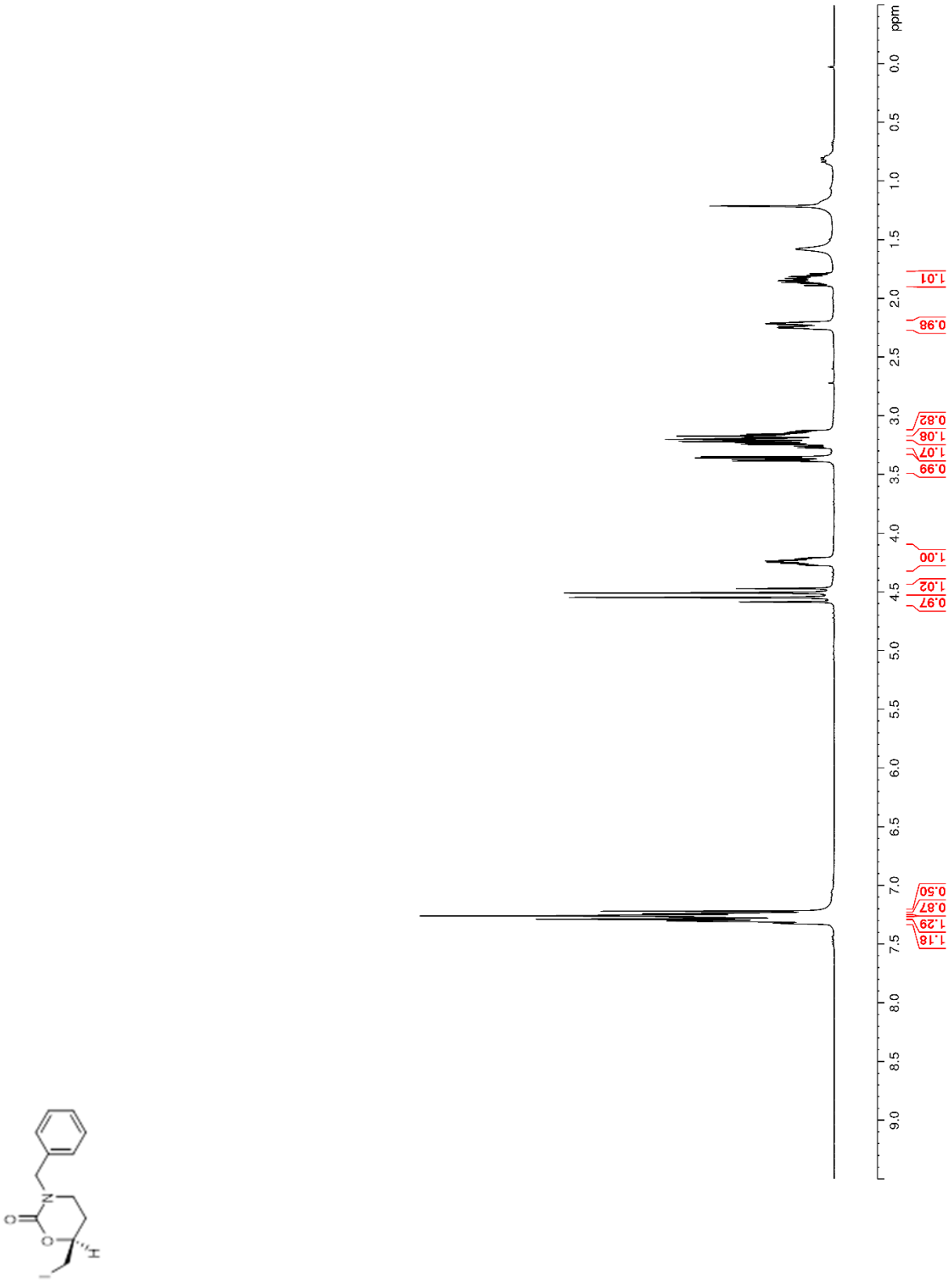

Figure 14. ^{13}C NMR (100 MHz, $CDCl_3$) of **143b**

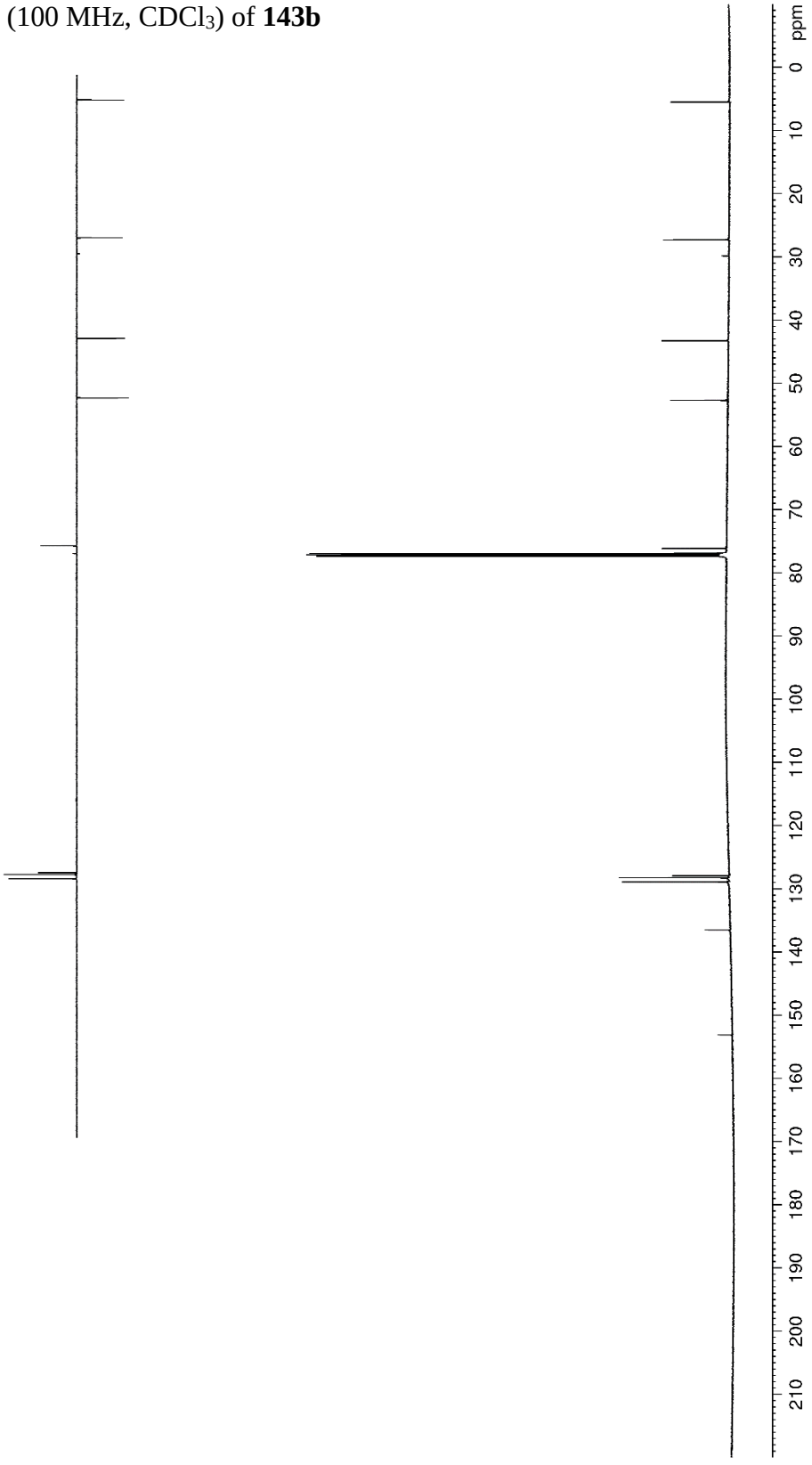

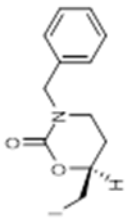

Figure 15. ^{1}H NMR (600 MHz, $CDCl_3$) of **149a**

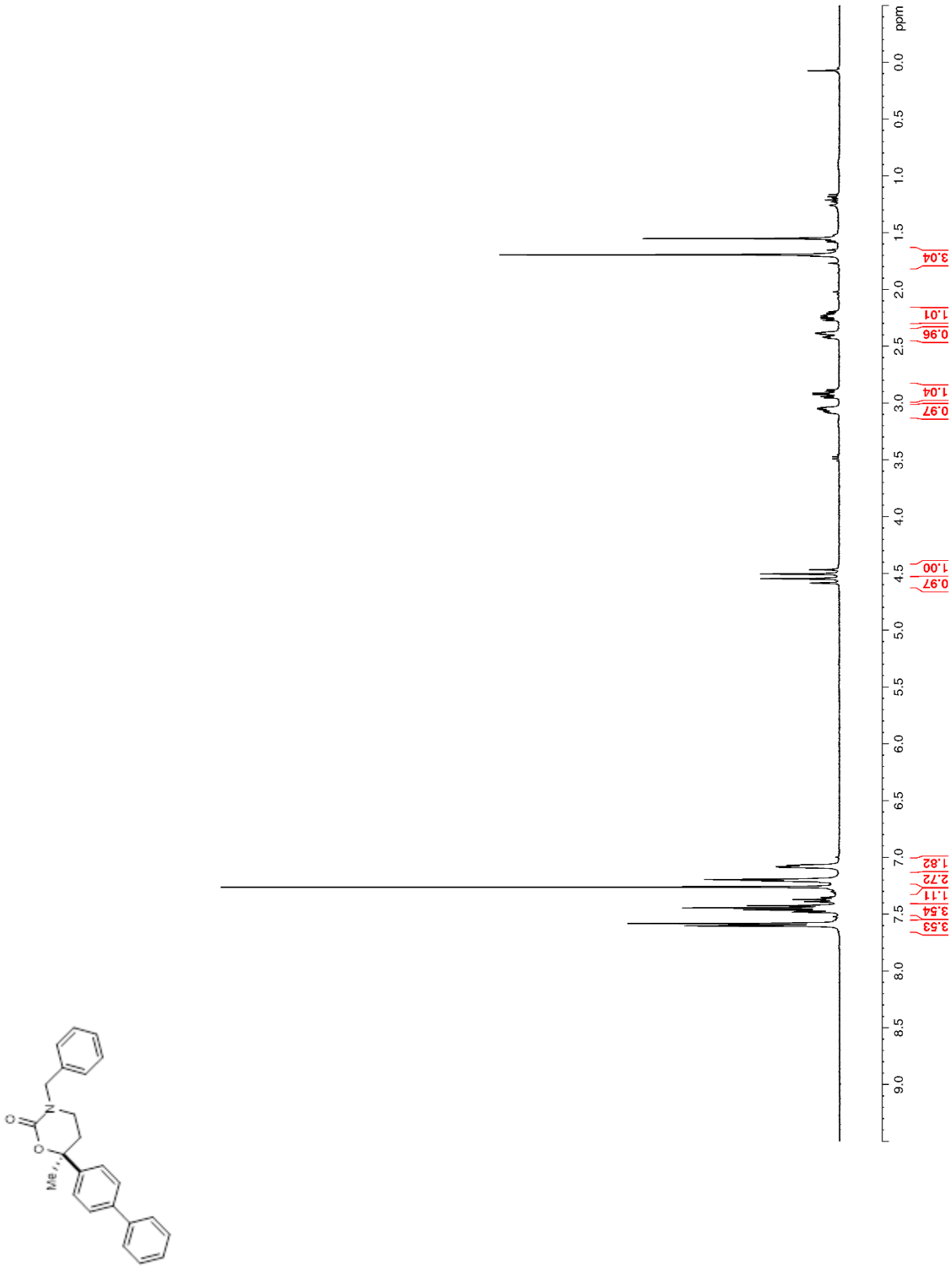

Figure 16. ^{13}C NMR (150 MHz, $CDCl_3$) of **149a**

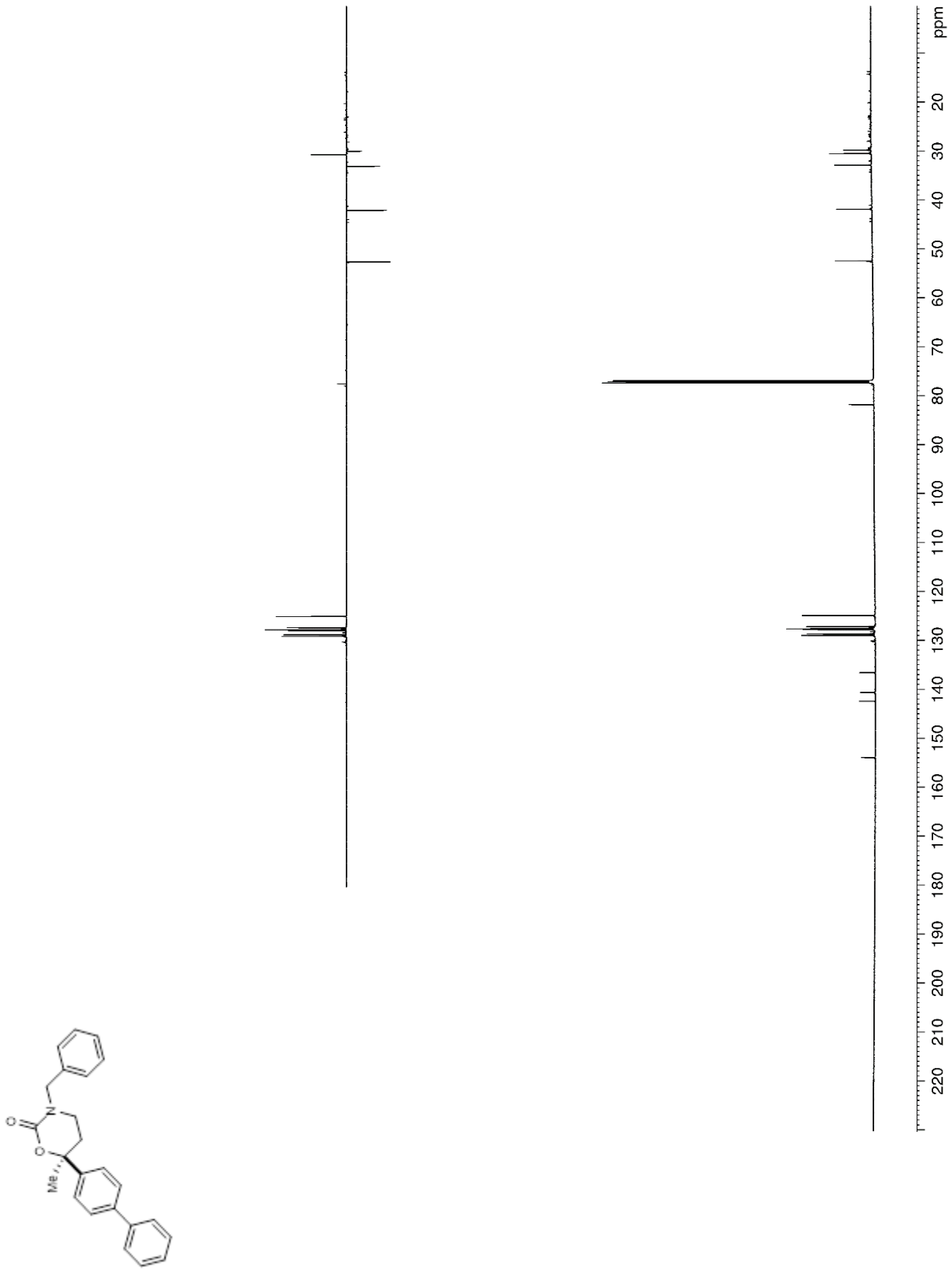

Figure 17. ^{1}H NMR (600 MHz, $CDCl_3$) of **149b**

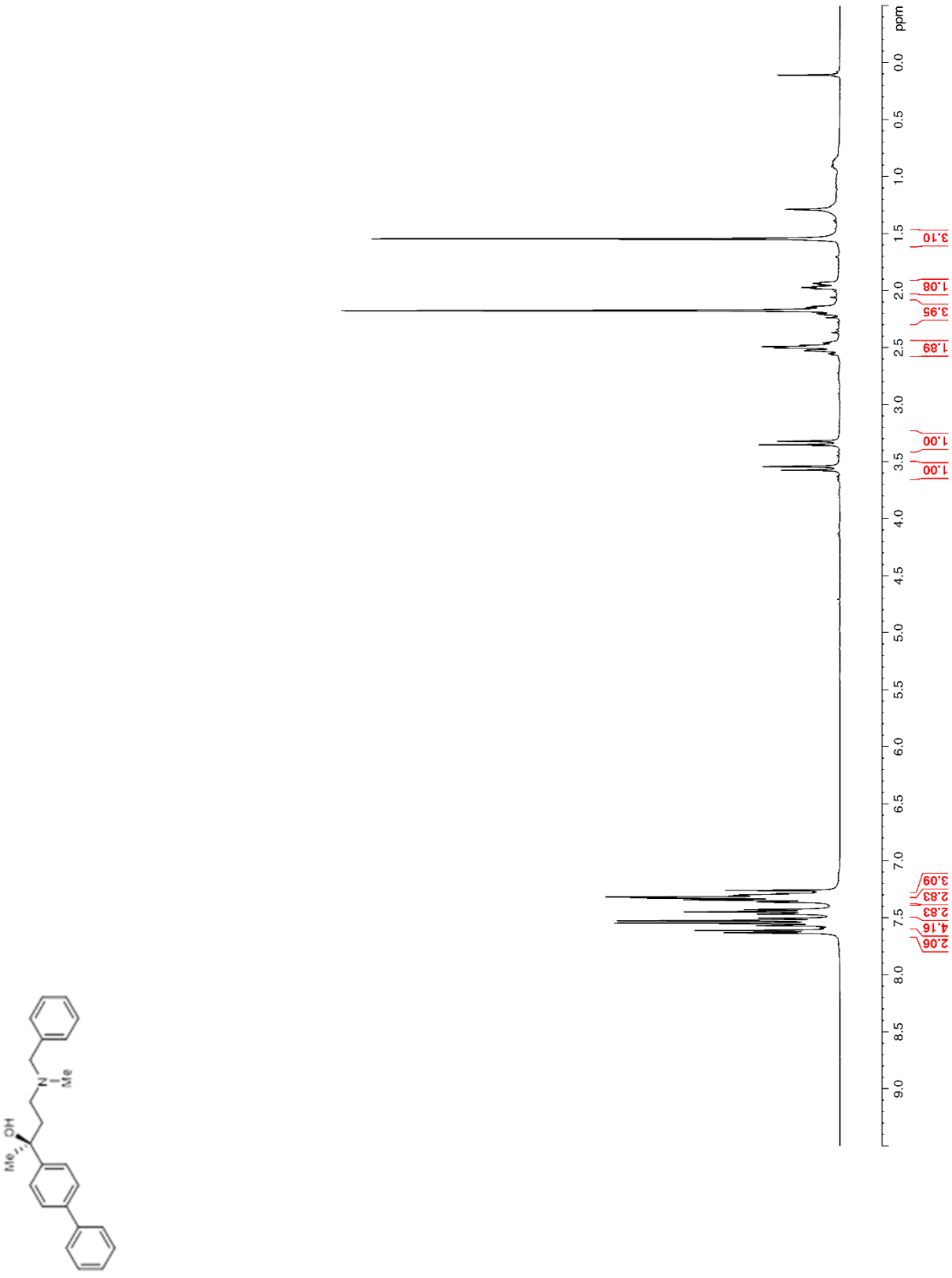

Figure 18. ^{13}C NMR (150 MHz, $CDCl_3$) of **149b**

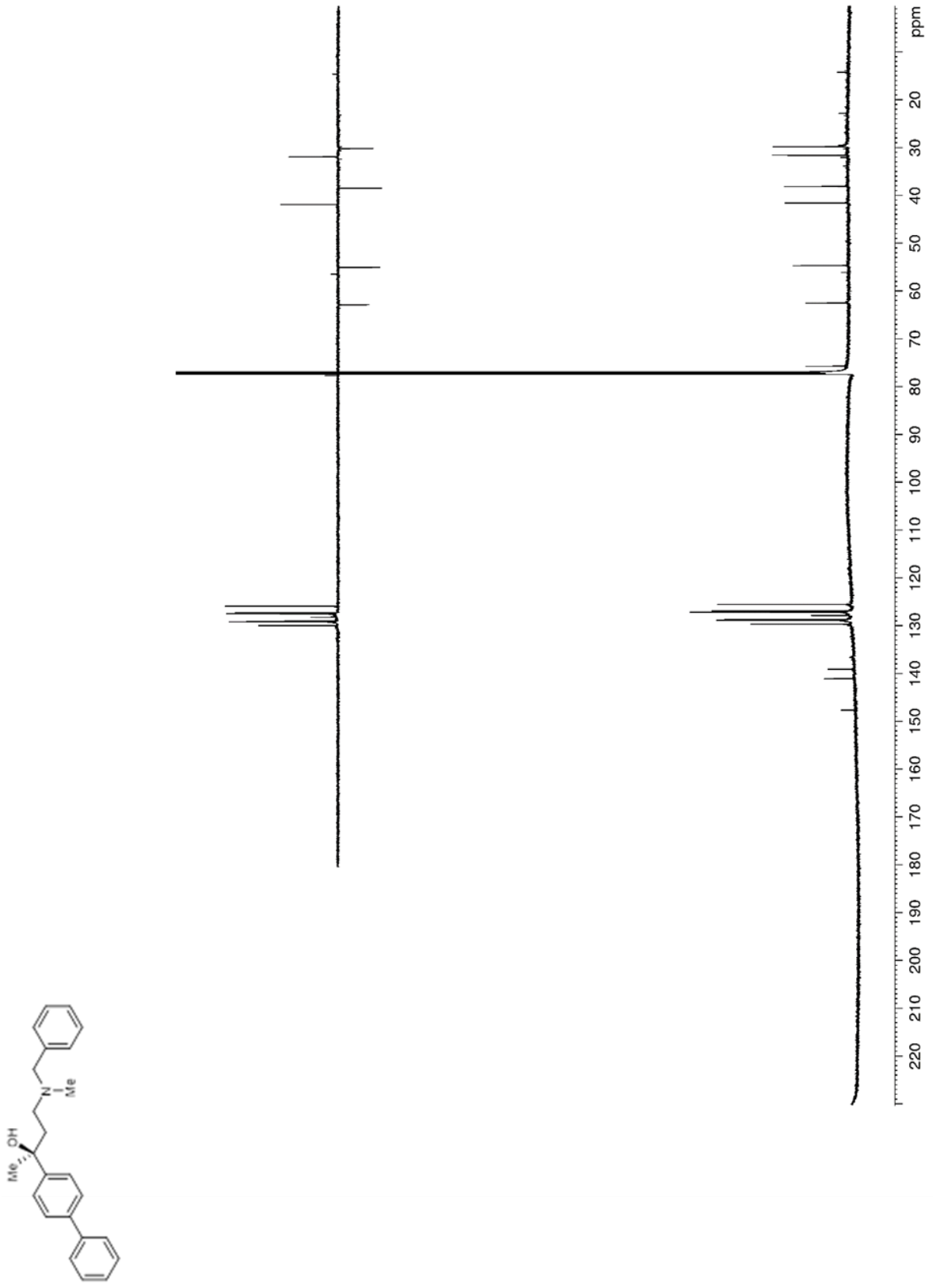

Figure 19. HPLC trace of **134b**

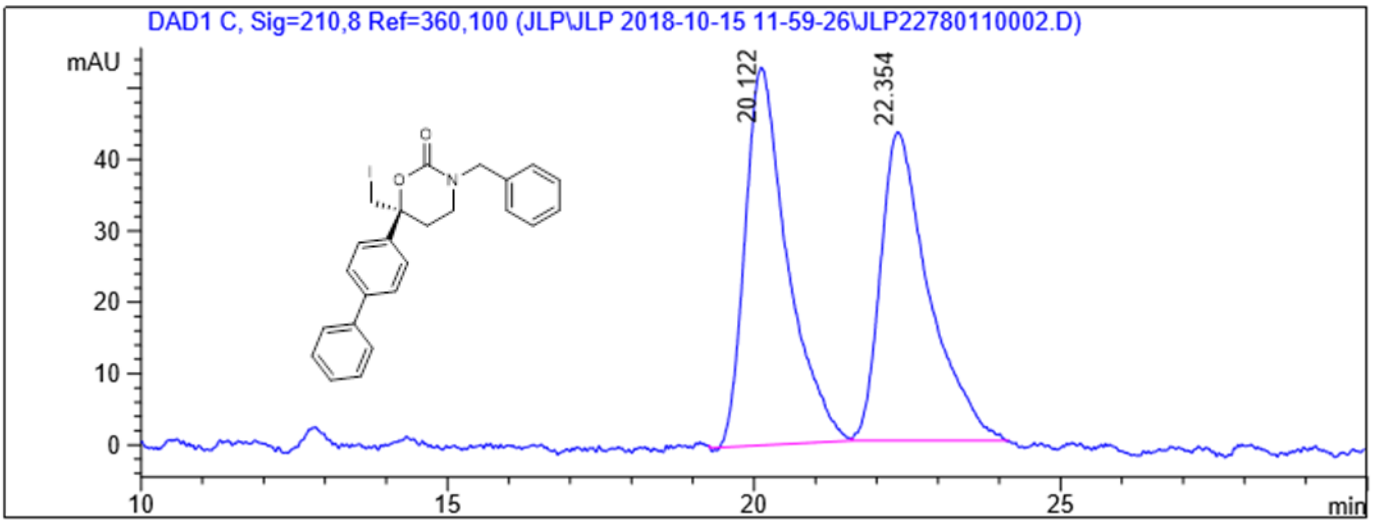

Meas.RT min	Area	Width min	Area %
20.12	2542.1	0.800	51.6
22.35	2382.9	0.918	48.4

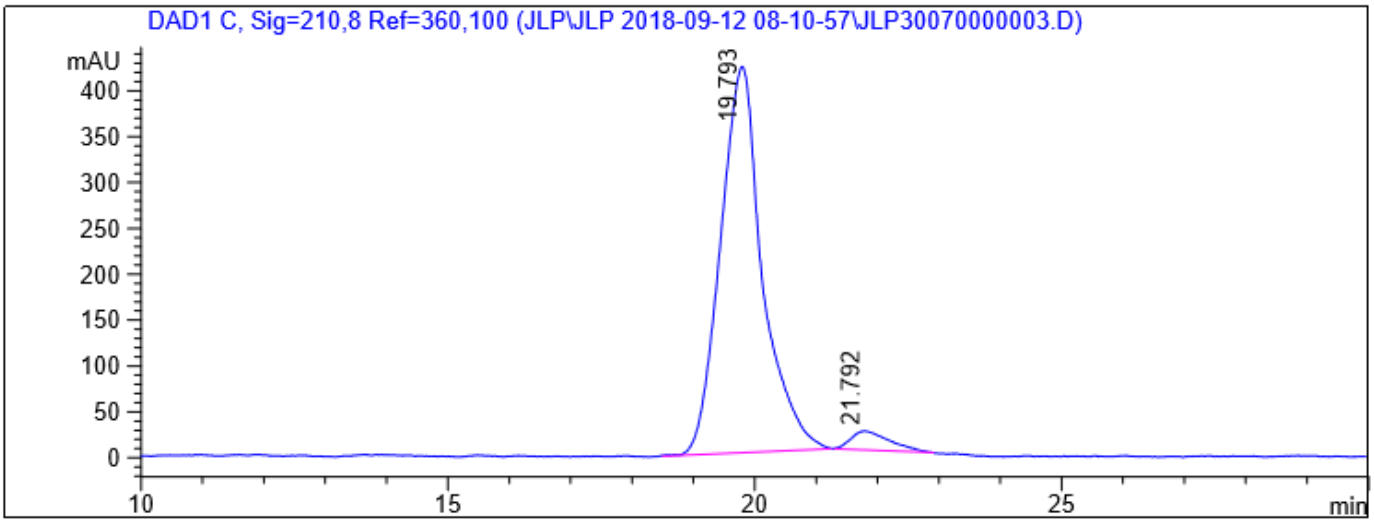

Meas.RT min	Area	Width min	Area %
19.79	20006.1	0.792	95.7
21.79	897.2	0.731	4.3

Figure 20. HPLC trace of **143b**

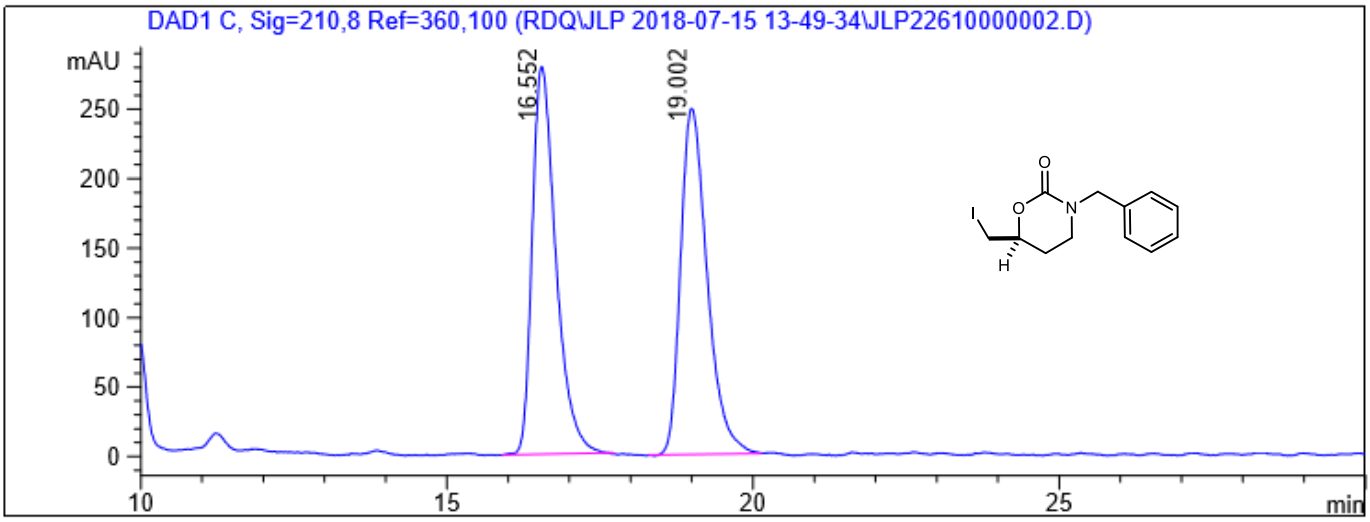

Meas.RT min	Area	Width min	Area %
16.55	7494.8	0.448	49.9
19.00	7514.1	0.503	50.1

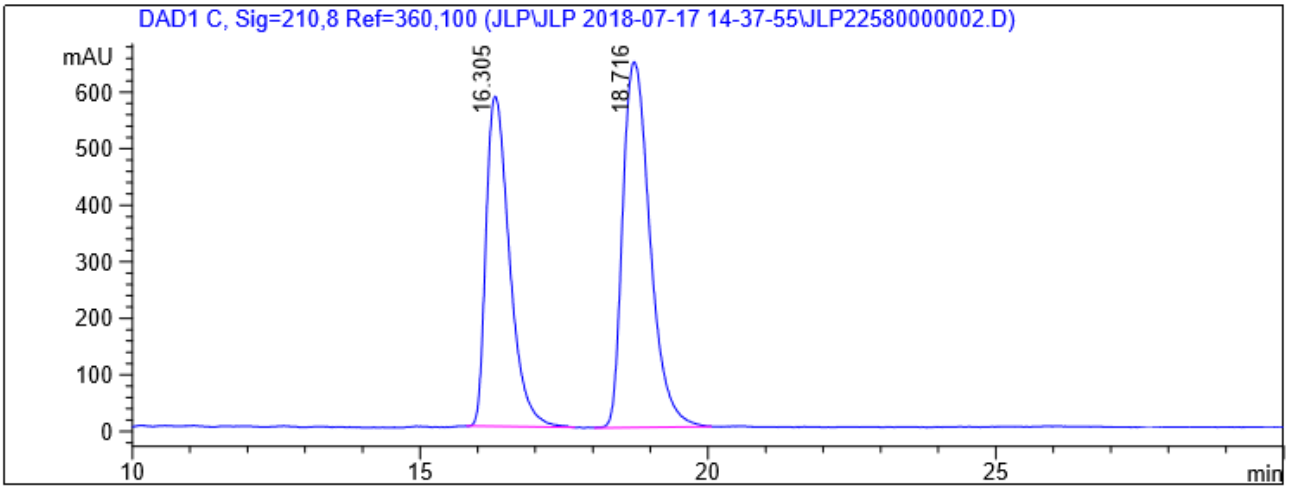

Meas.RT min	Area	Width min	Area %
16.31	16556.8	0.473	43.6
18.72	21402.4	0.551	56.4

Figure 21. HPLC trace of **149a**

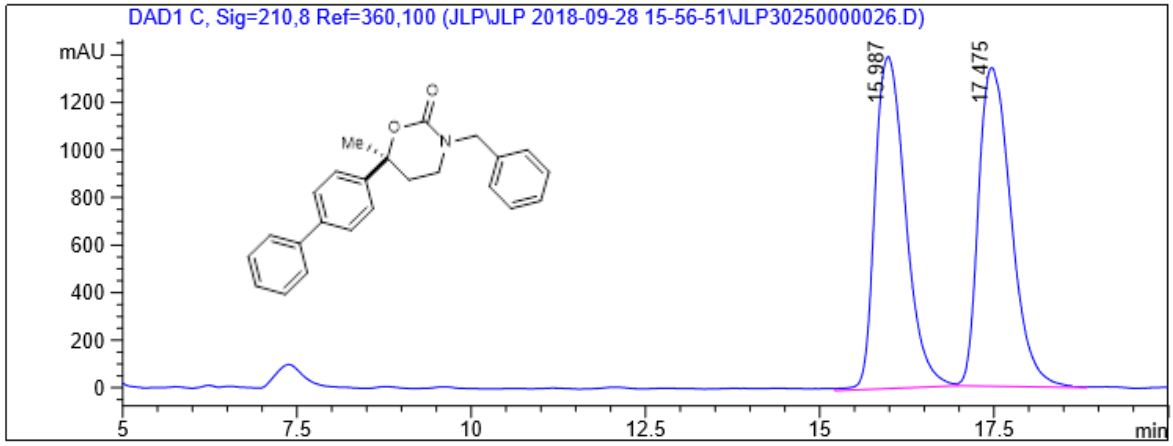

Meas.RT min	Area	Width min	Area %
15.99	42664.6	0.509	49.5
17.48	43593.3	0.542	50.5

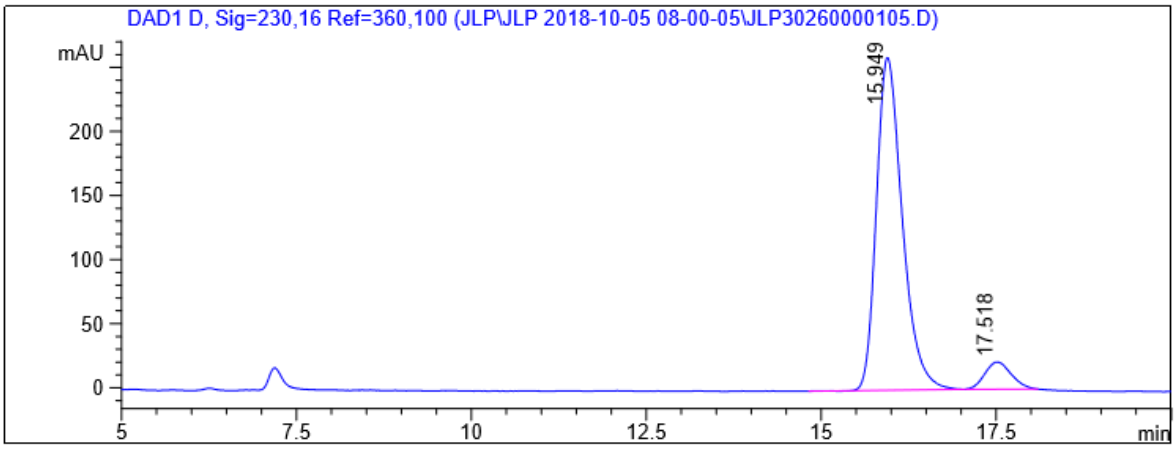

Meas.RT min	Area	Width min	Area %
15.95	6678.6	0.429	92.3
17.52	559.1	0.440	7.7

Figure 22. HPLC trace of **149b**

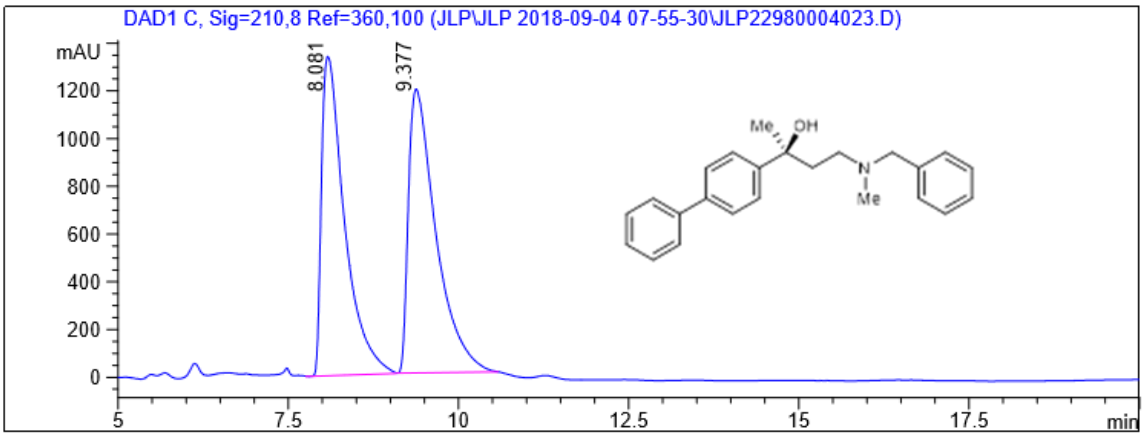

Meas.RT min	Area	Width min	Area %
8.08	31527.3	0.393	48.6
9.38	33409.8	0.468	51.4

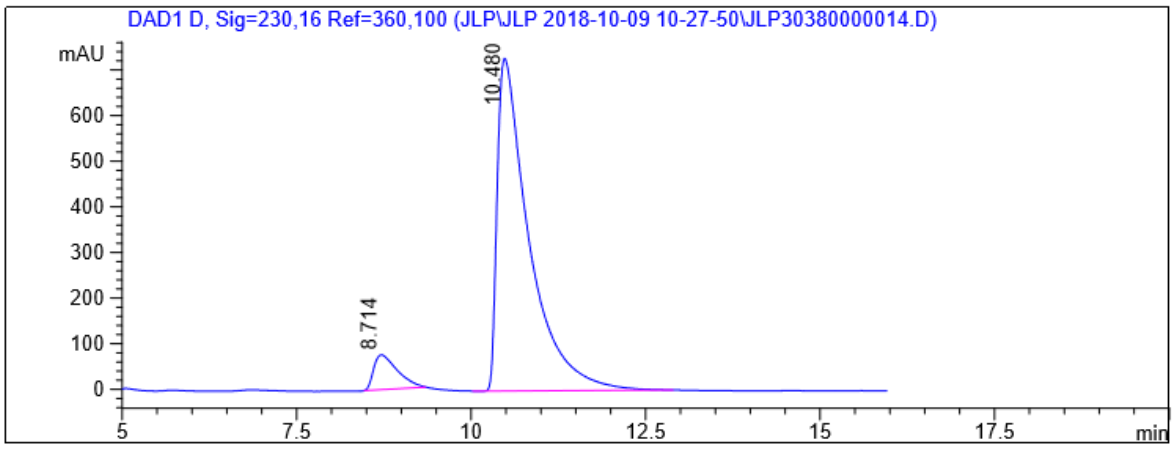

Meas.RT min	Area	Width min	Area %
8.71	1783.2	0.391	7.2
10.48	23134.0	0.529	92.8

Figure 23. ^{1}H NMR (400 MHz, d^{6}-DMSO) of **S4**

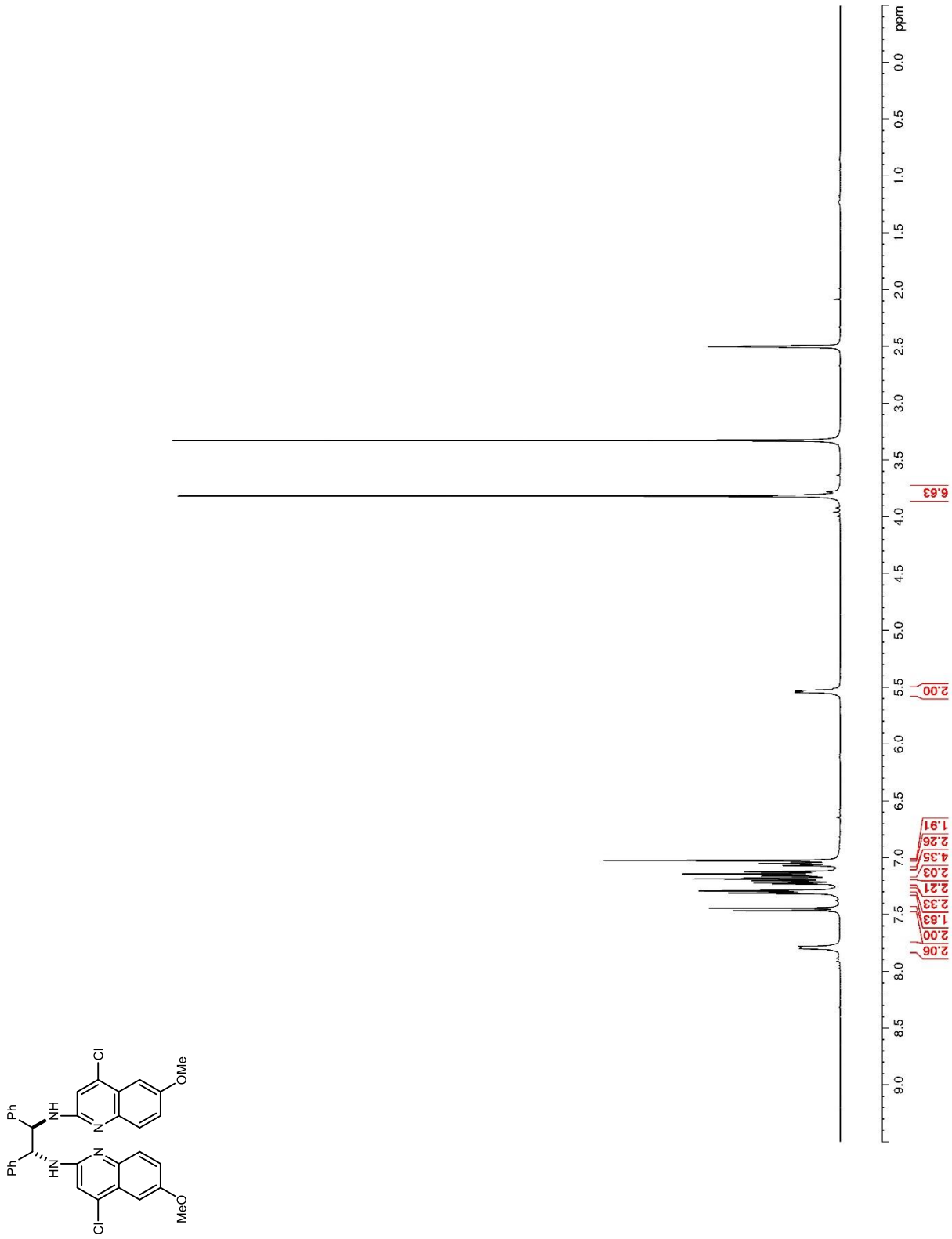

Figure 24. ^{13}C NMR (150 MHz, d^6-DMSO) of **S4**

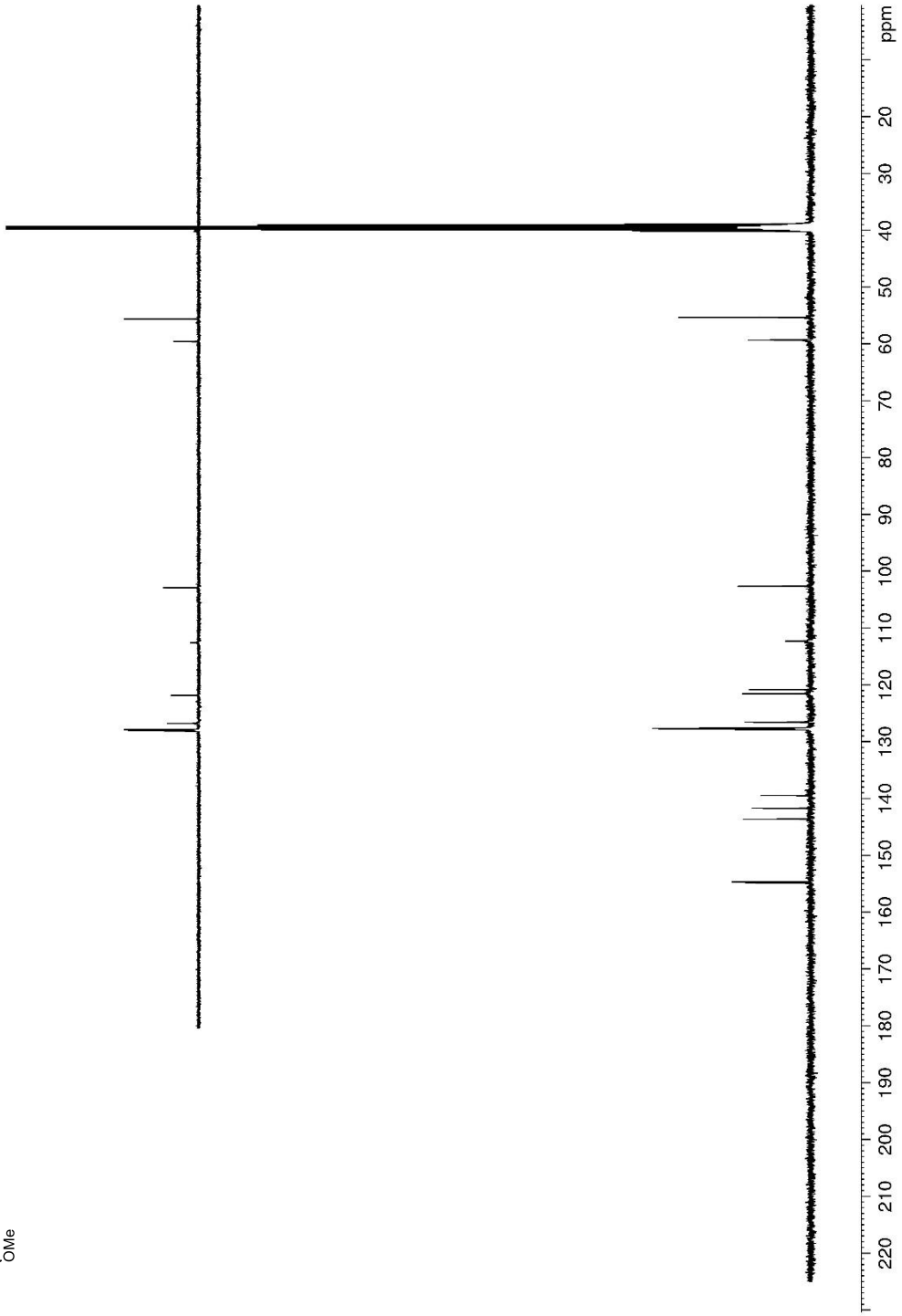

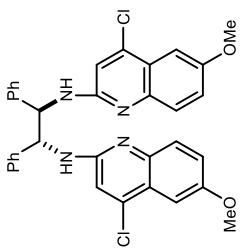

Figure 25. ^{1}H NMR (600 MHz, $CDCl_3$) of **196**

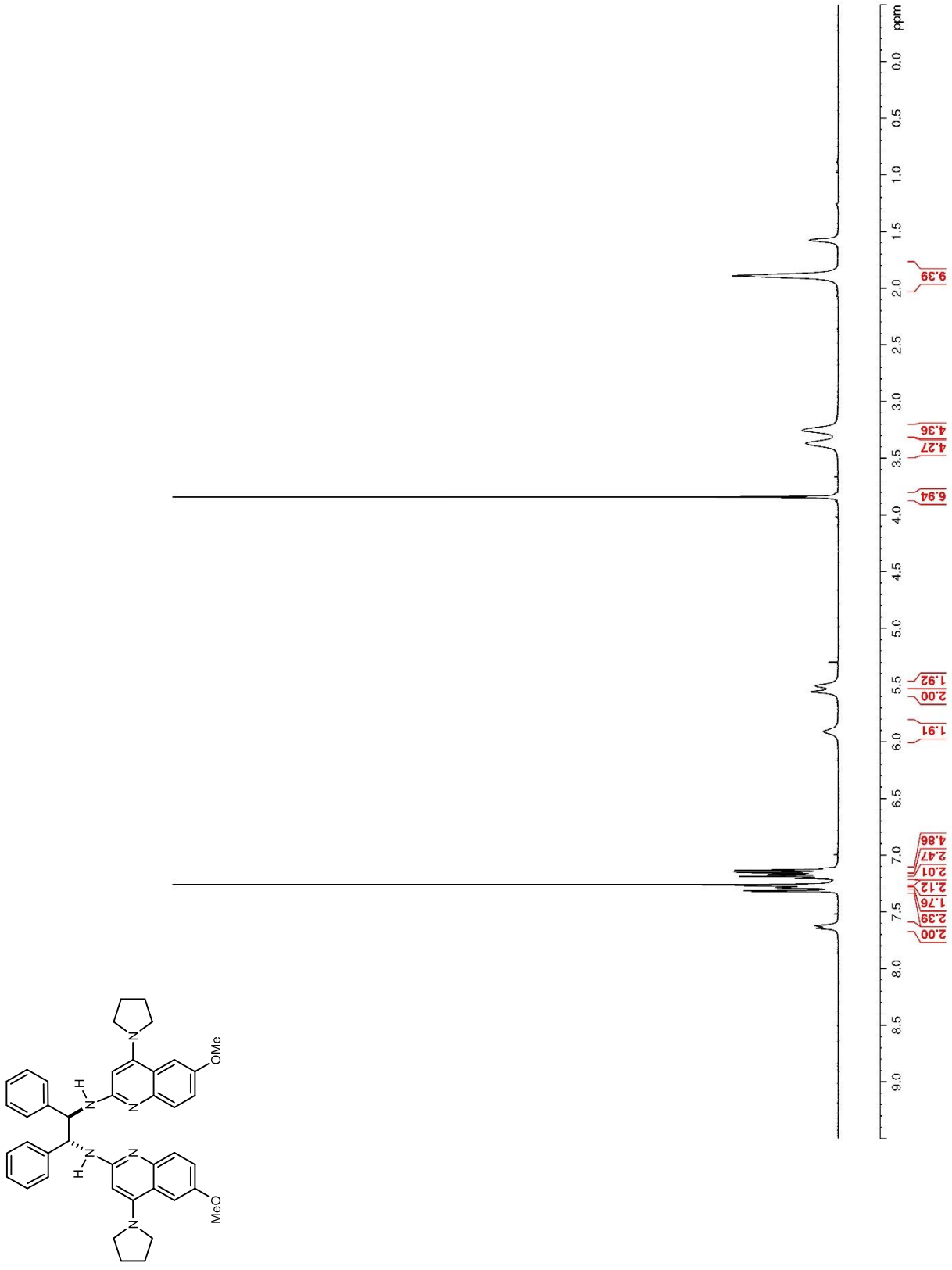

Figure 26. ^{13}C NMR (150 MHz, $CDCl_3$) of **196**

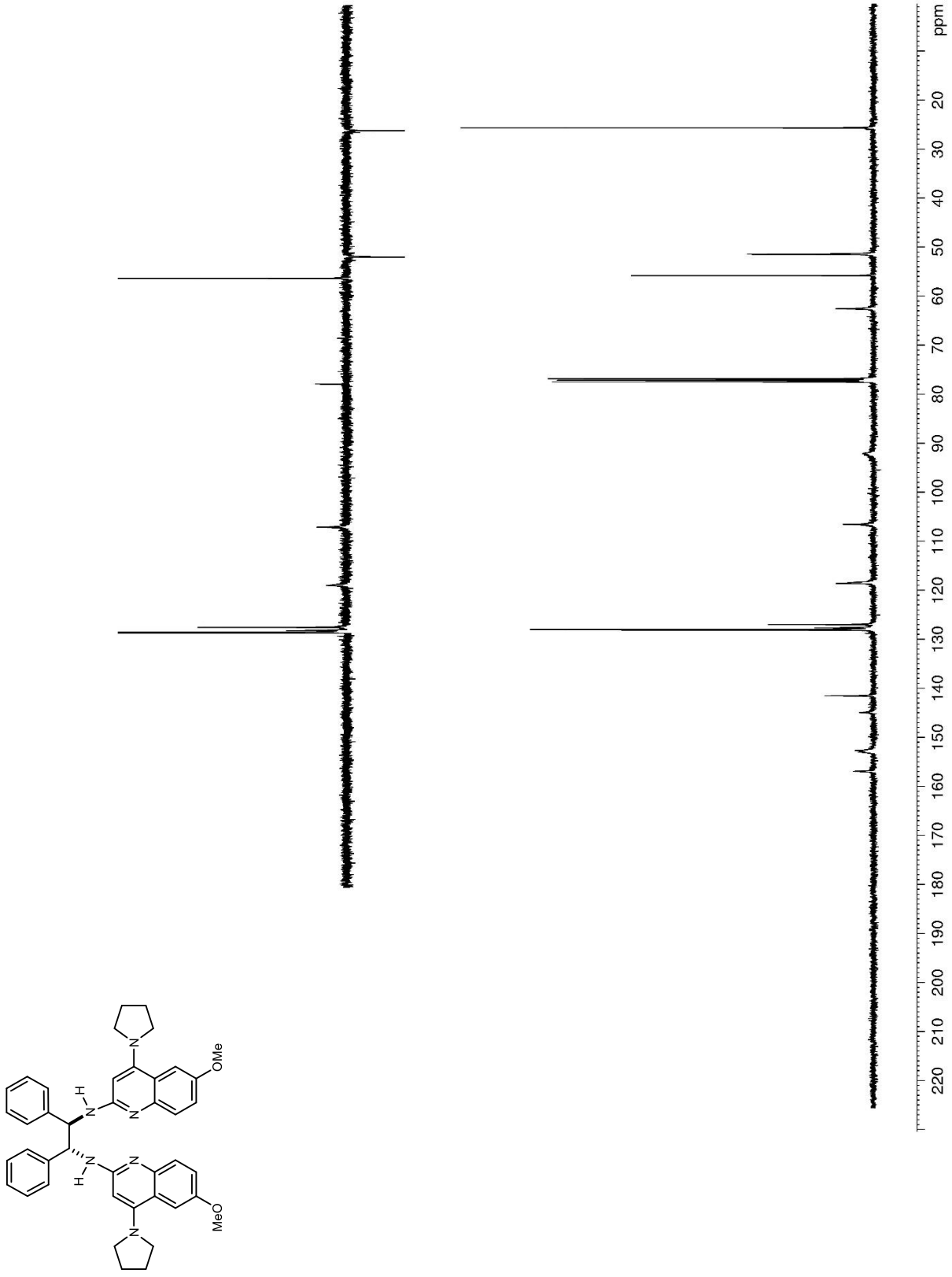

Figure 27. ^{1}H NMR (400 MHz, $CDCl_3$) of **199**

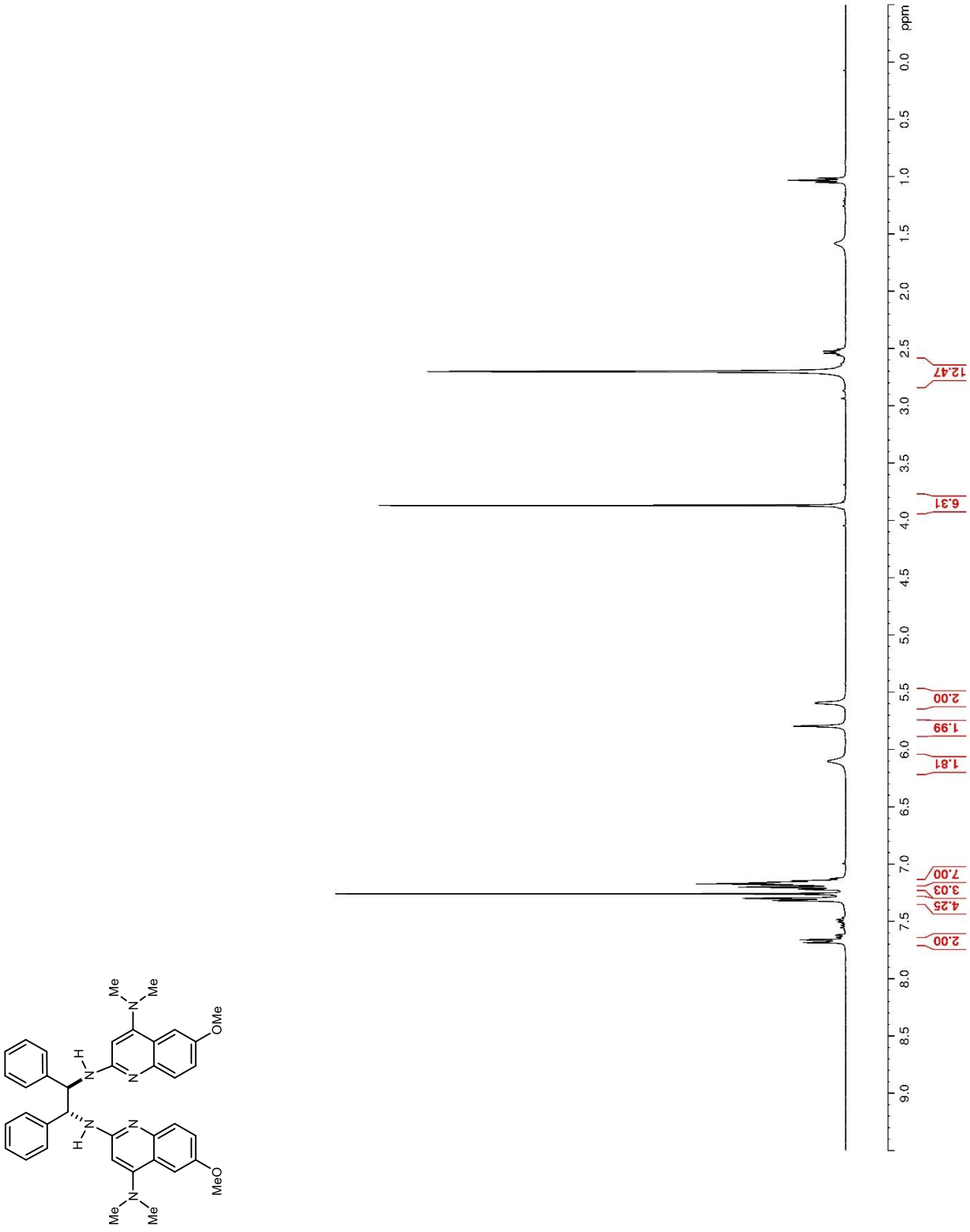

Figure 28. ^{13}C NMR (100 MHz, $CDCl_3$) of **199**

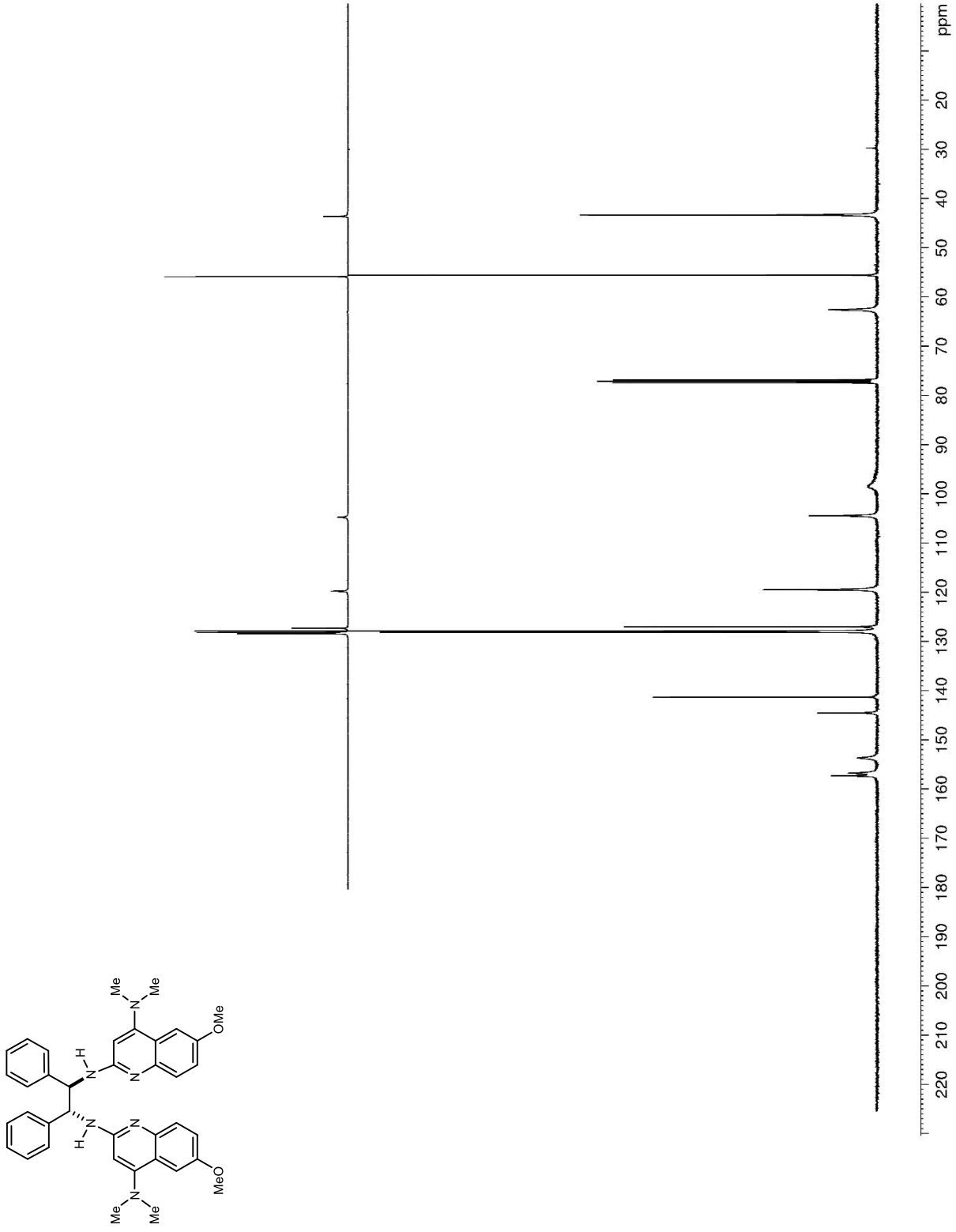

Figure 29. ^{1}H NMR (400 MHz, $CDCl_3$) of **200**

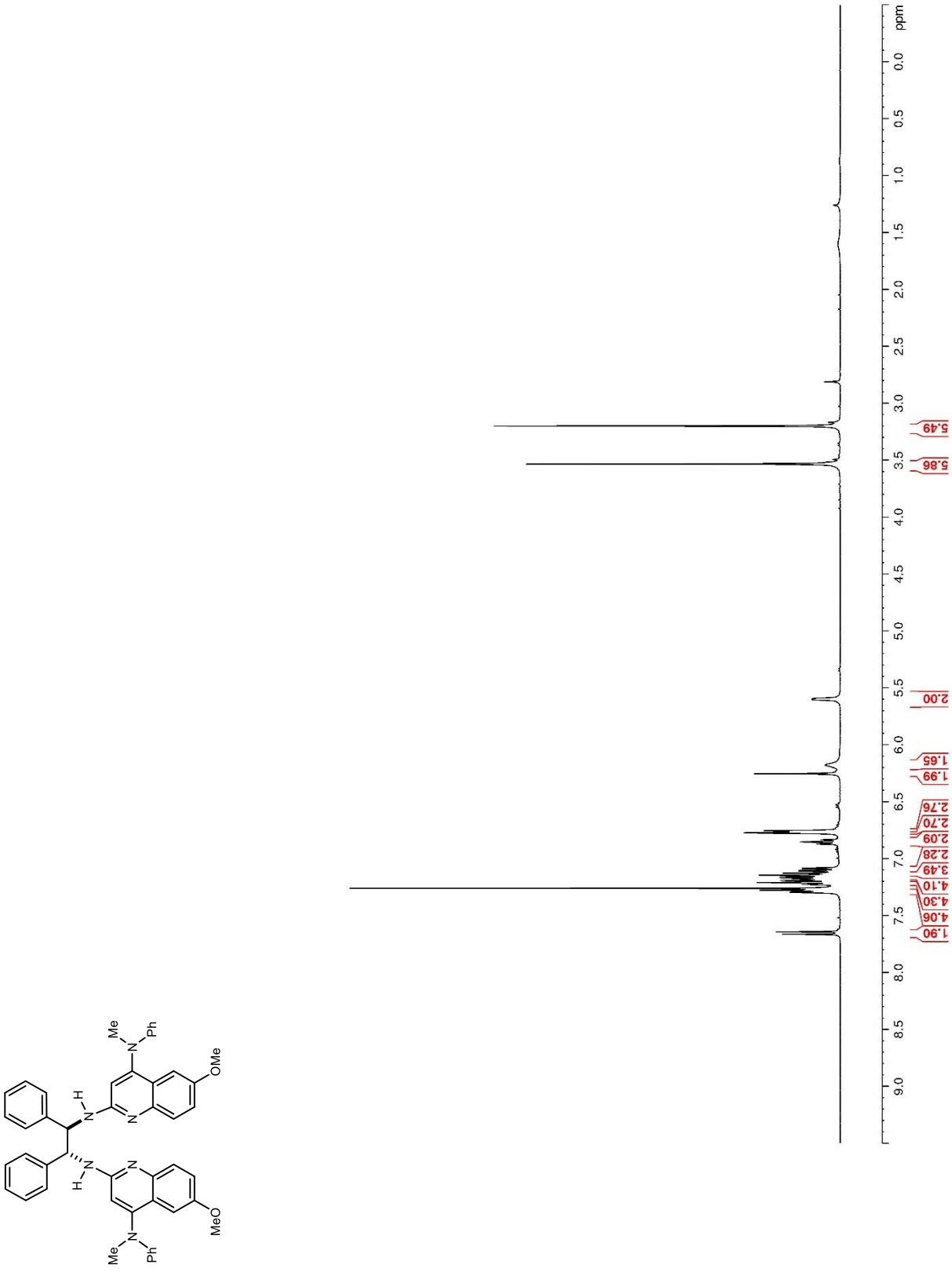

Figure 30. ^{13}C NMR (150 MHz, $CDCl_3$) of **200**

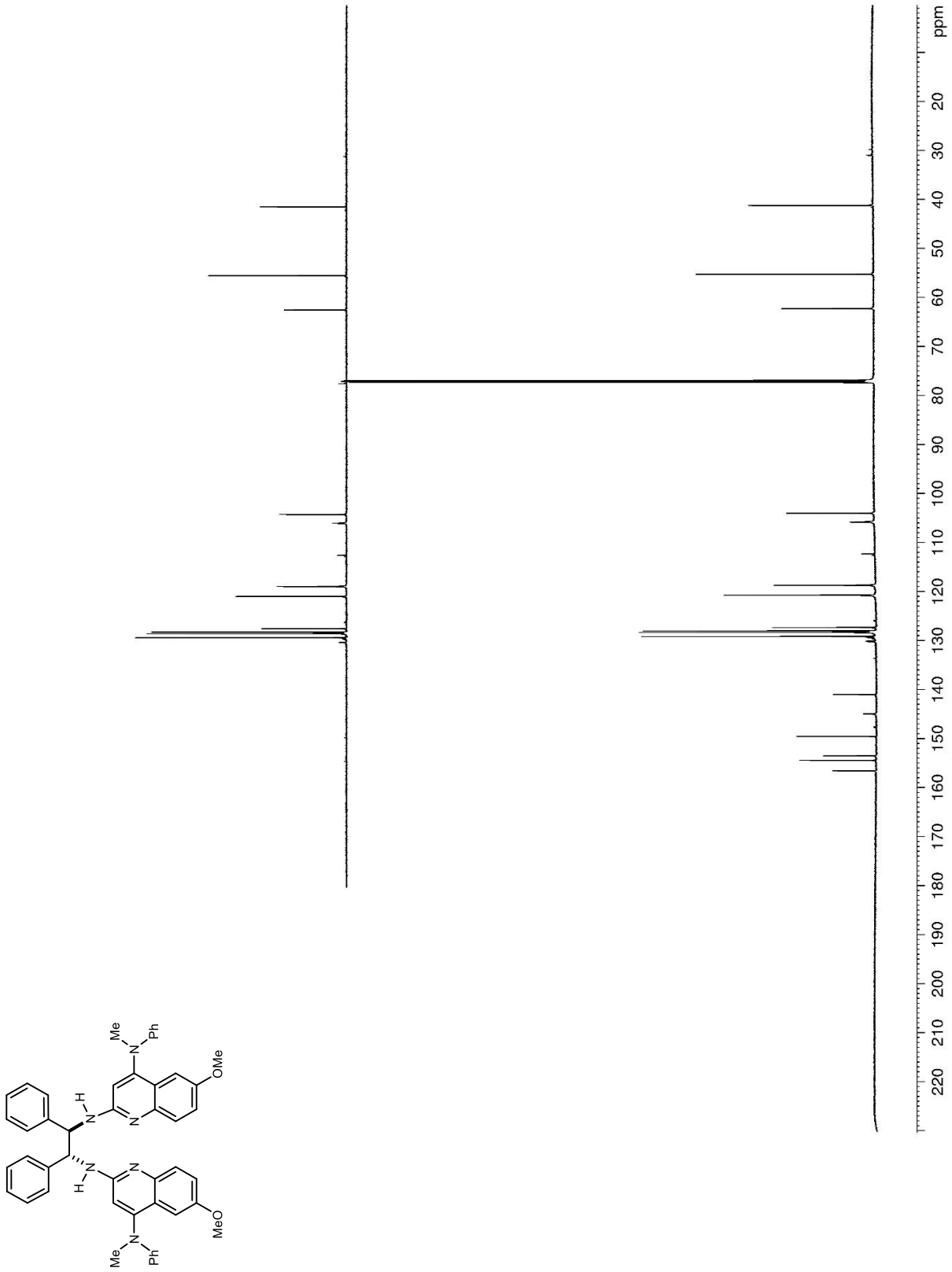

Figure 31. ^{1}H NMR (400 MHz, $CDCl_3$) of **197**

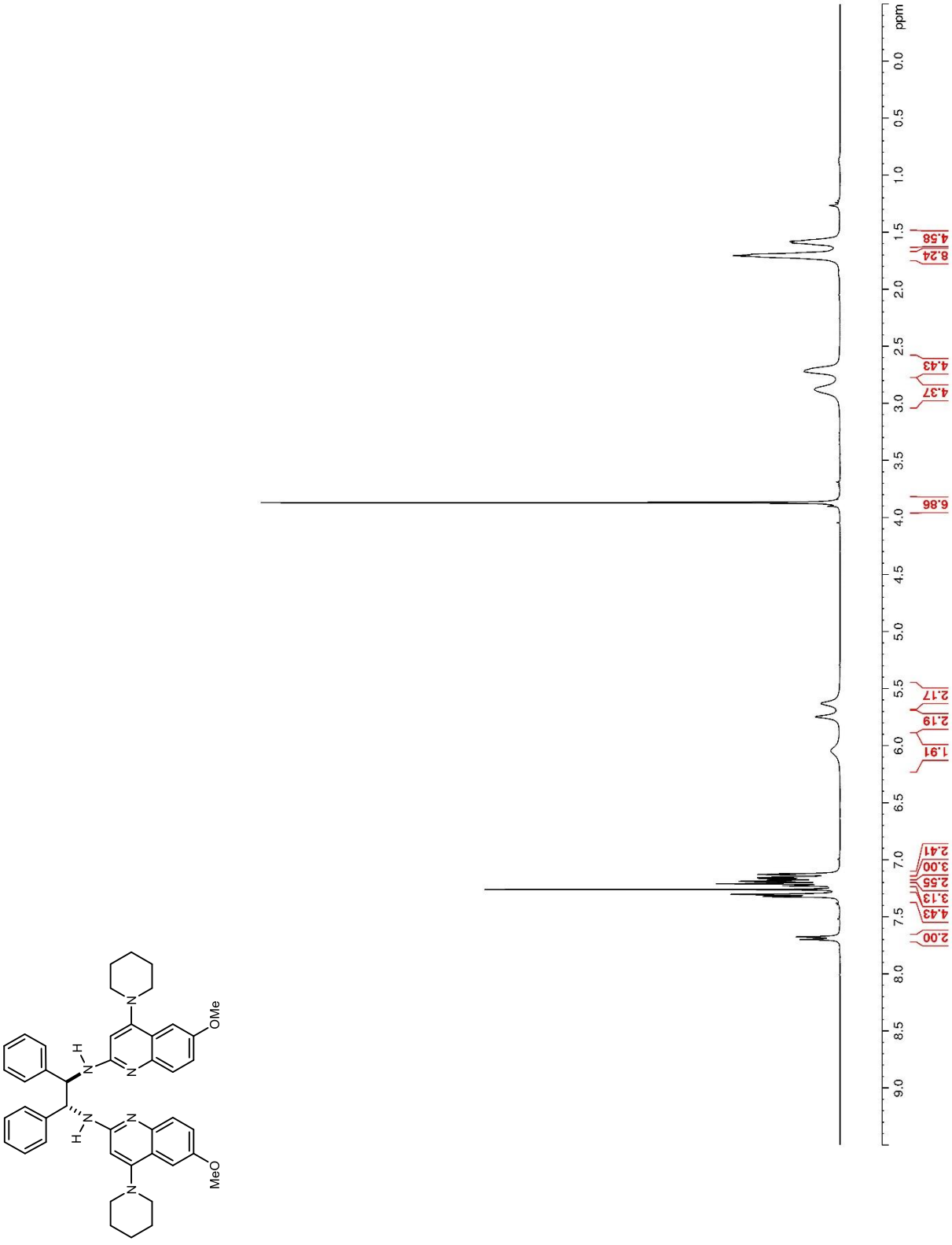

Figure 32. ^{13}C NMR (150 MHz, $CDCl_3$) of **197**

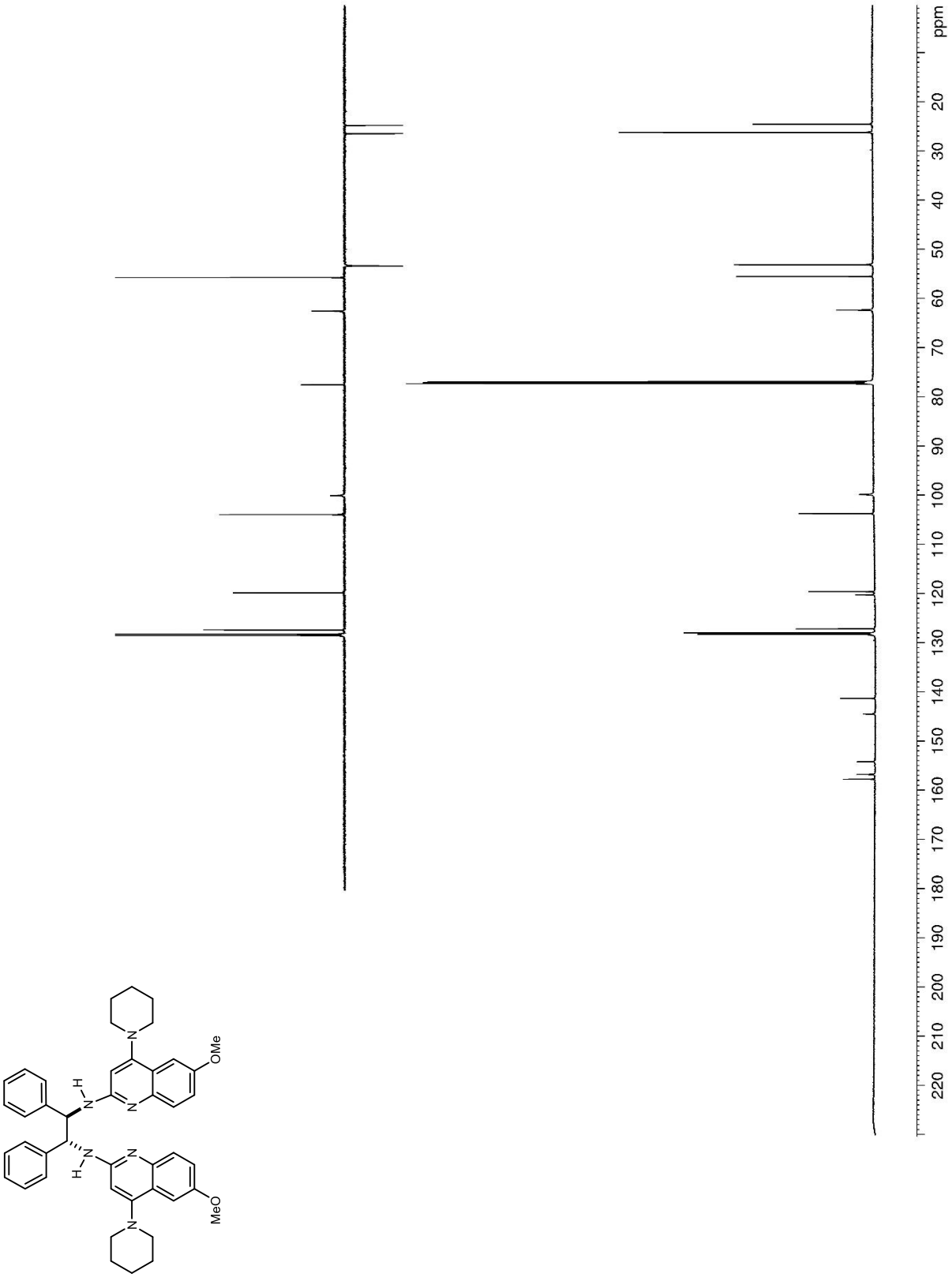

Figure 33. ^{1}H NMR (400 MHz, $CDCl_3$) of **198**

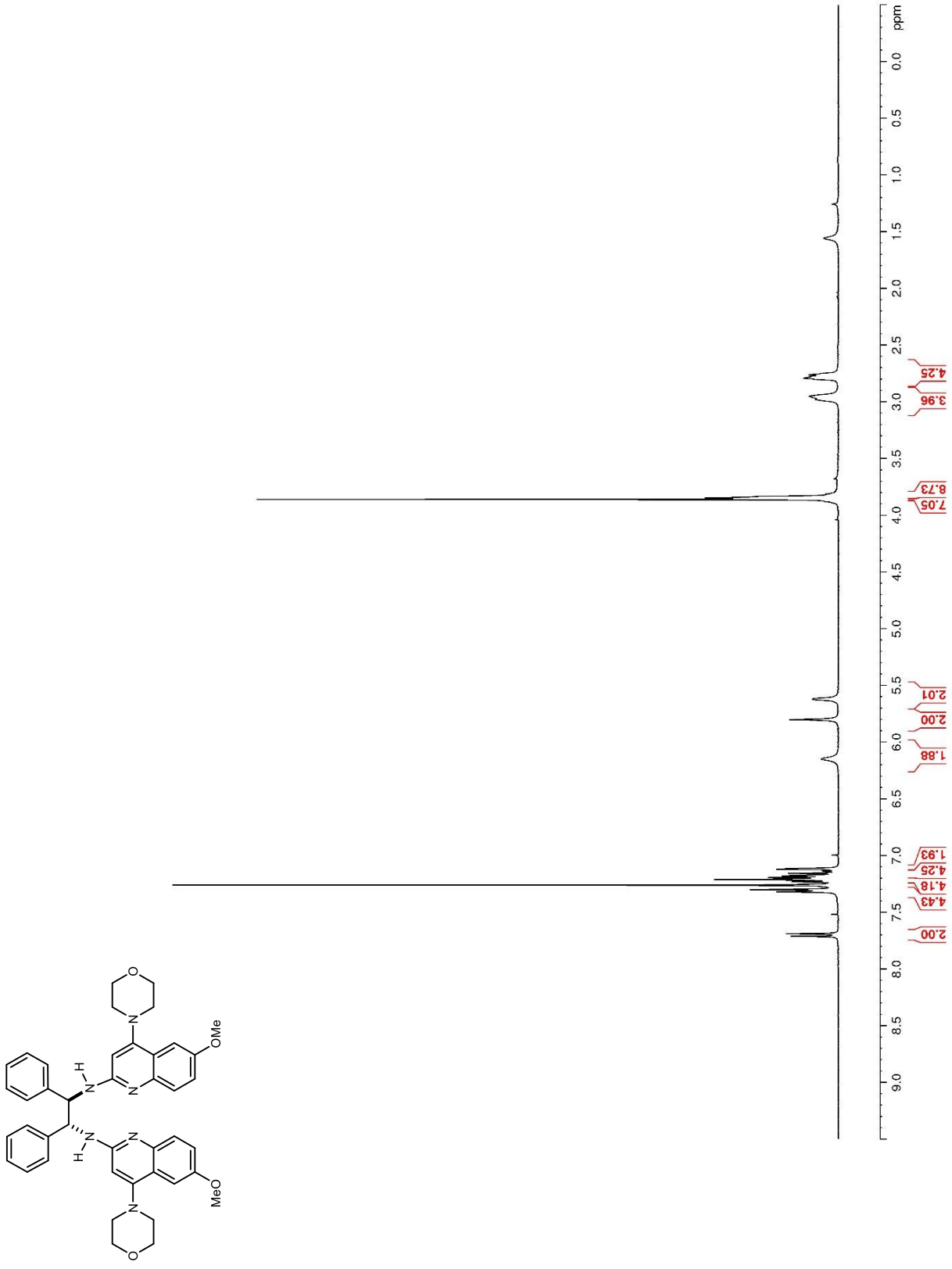

Figure 34. ^{13}C NMR (150 MHz, $CDCl_3$) of **198**

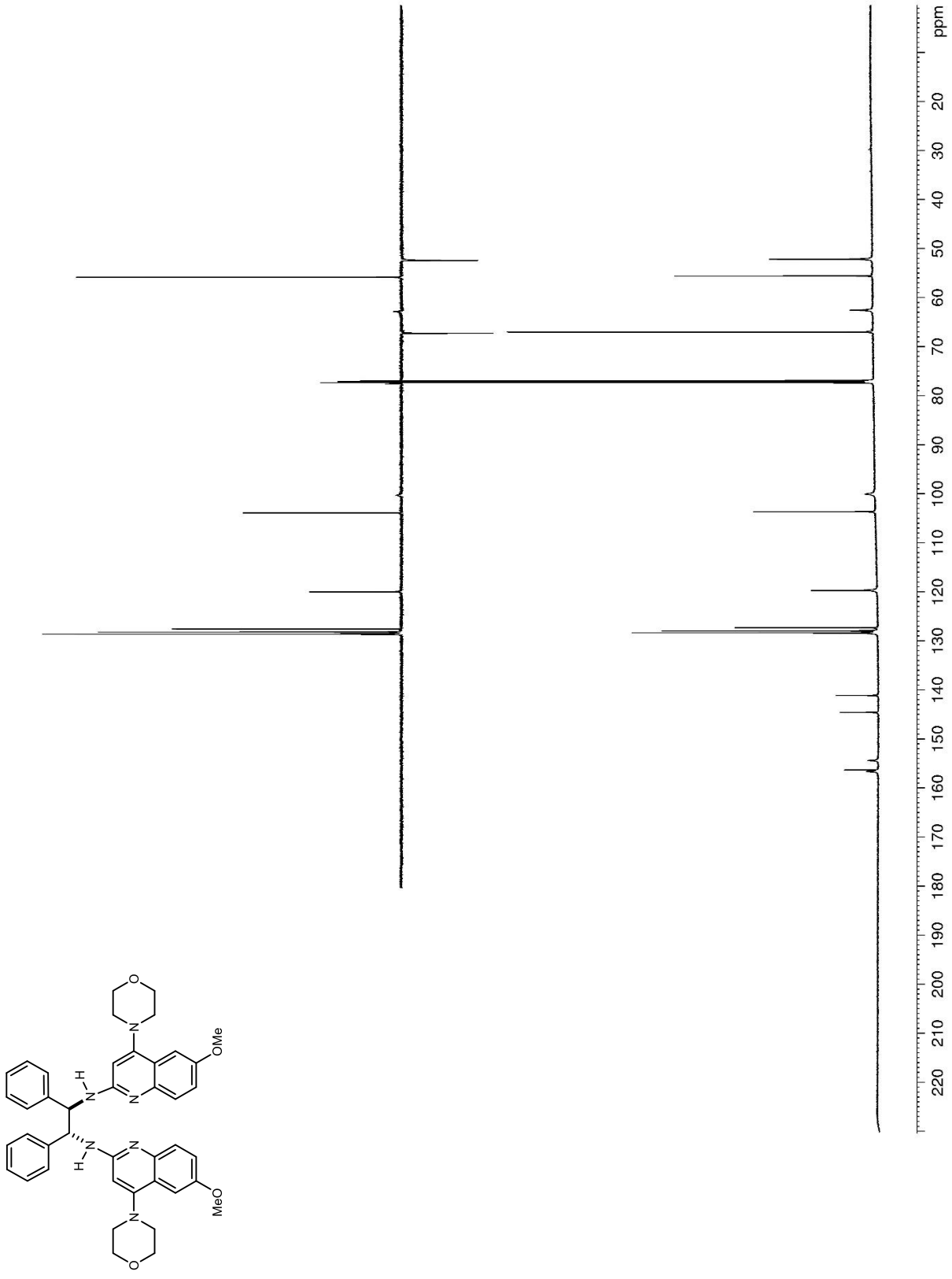

Figure 35. ^{1}H NMR (400 MHz, $CDCl_3$) of **201**

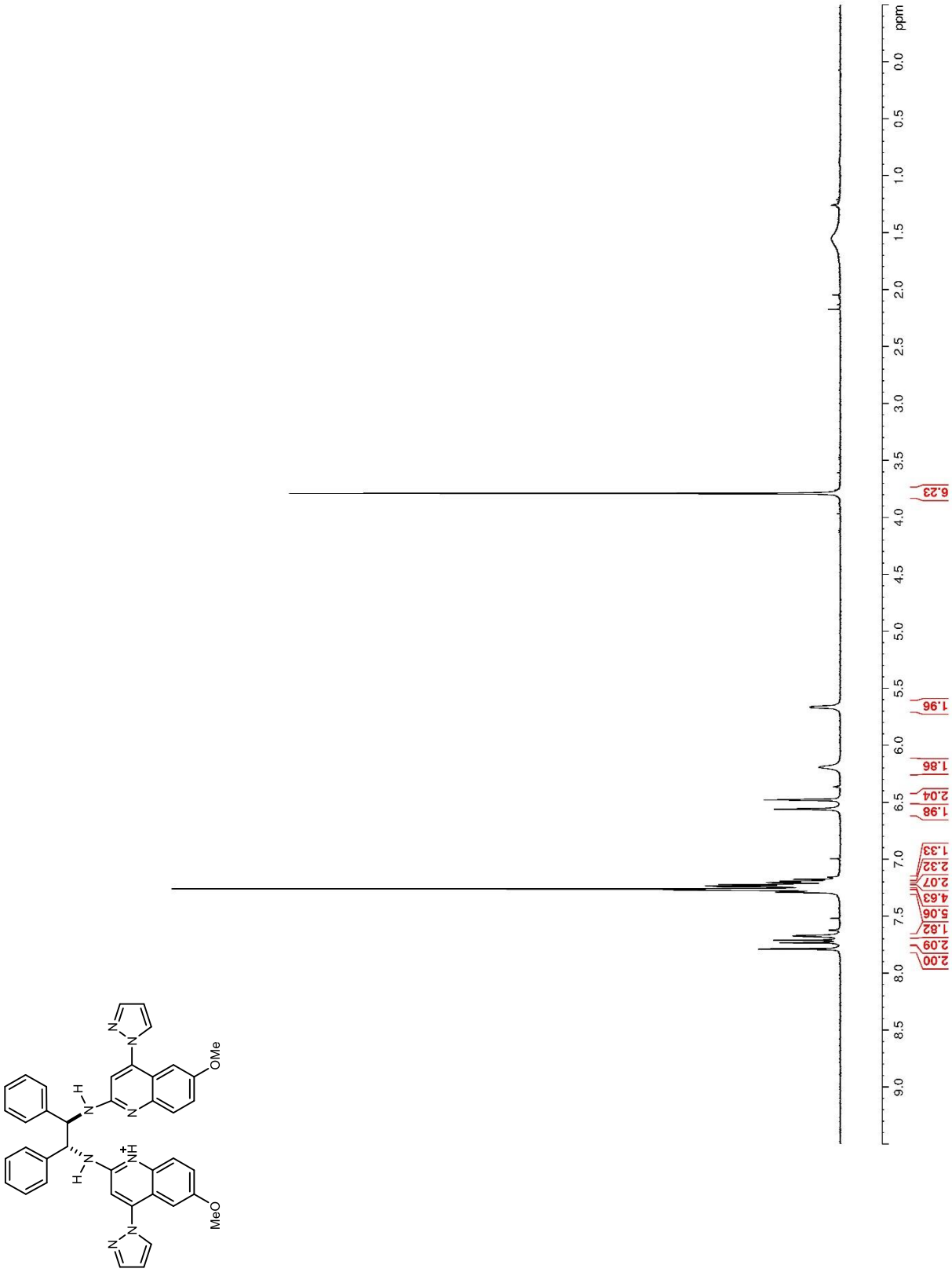

Figure 36. ^{13}C NMR (150 MHz, $CDCl_3$) of **201**

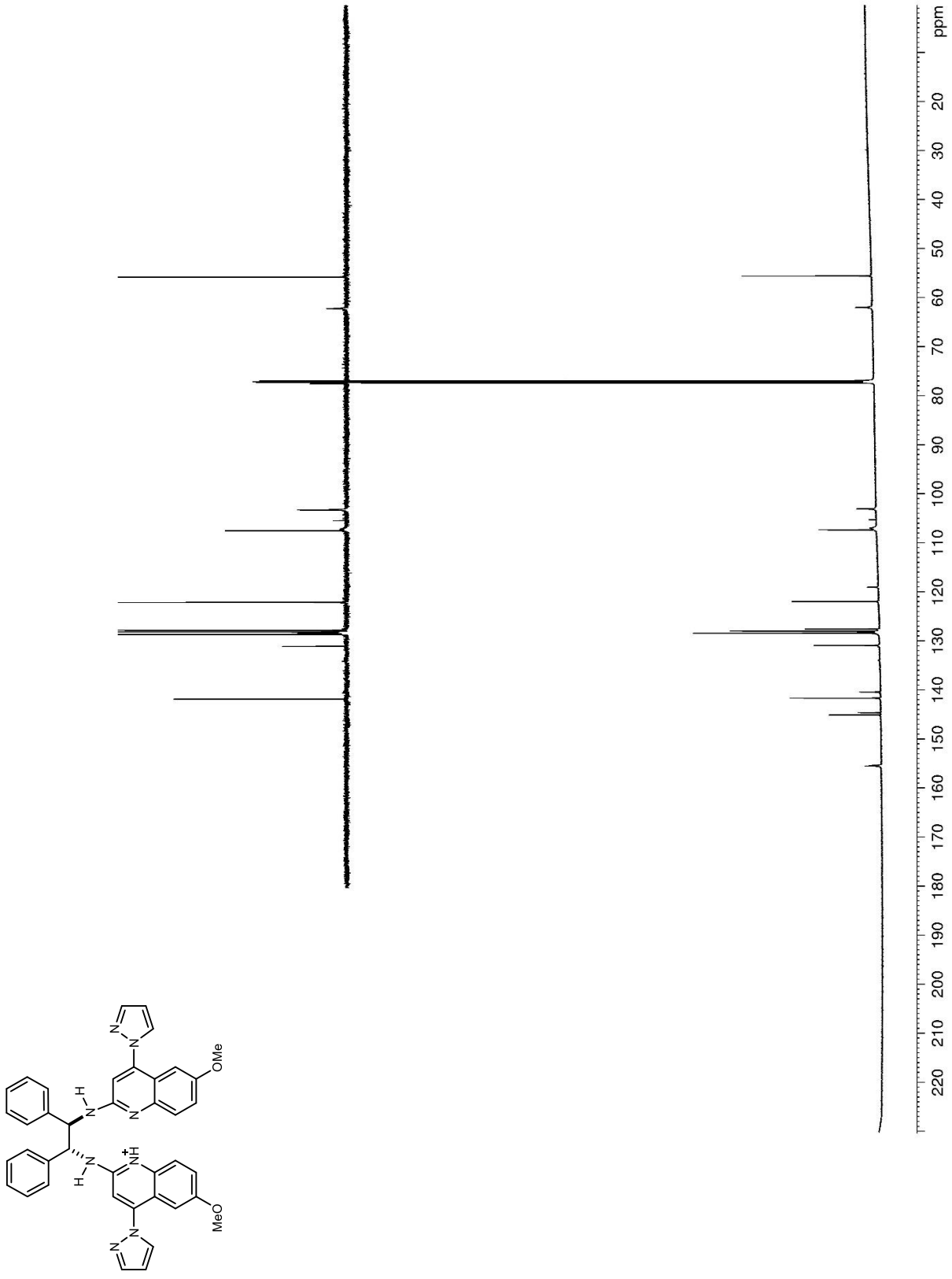

Figure 37. ^{1}H NMR (400 MHz, $CDCl_3$) of **194**

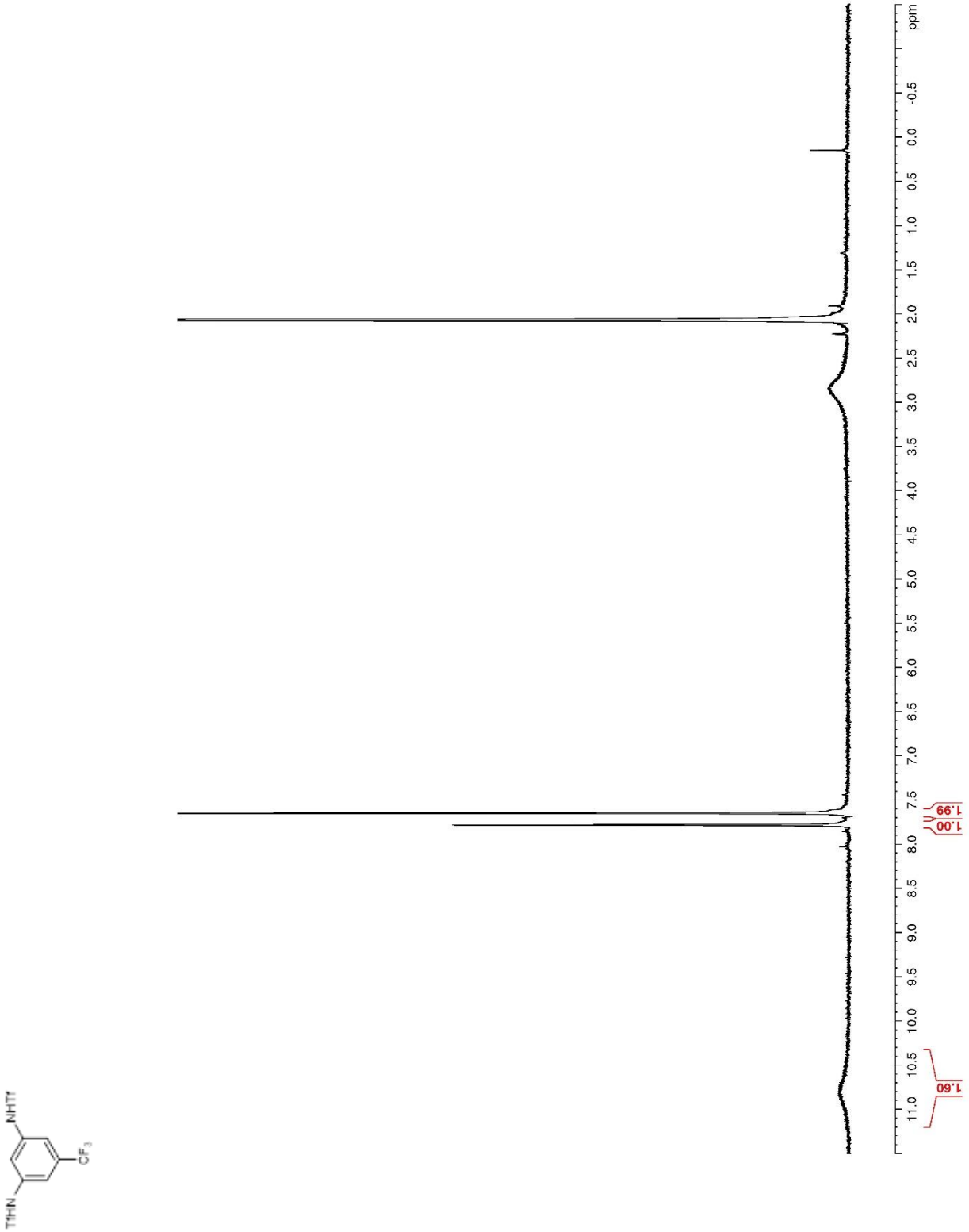

Figure 38. ^{13}C NMR (100 MHz, $CDCl_3$) of **194**

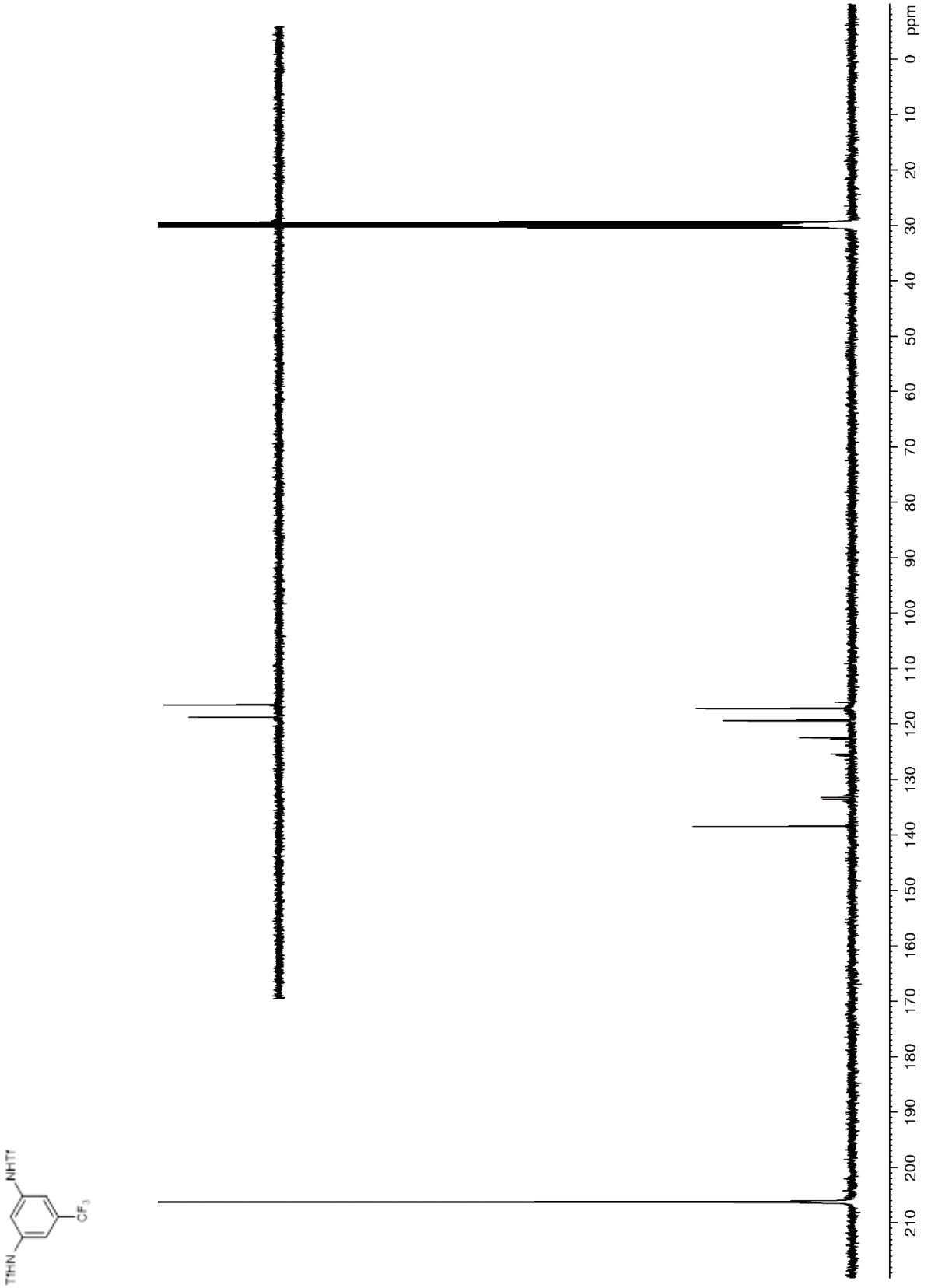

Figure 39. ^{19}F NMR (282 MHz, $(CD_3)_2CO$) of **194**

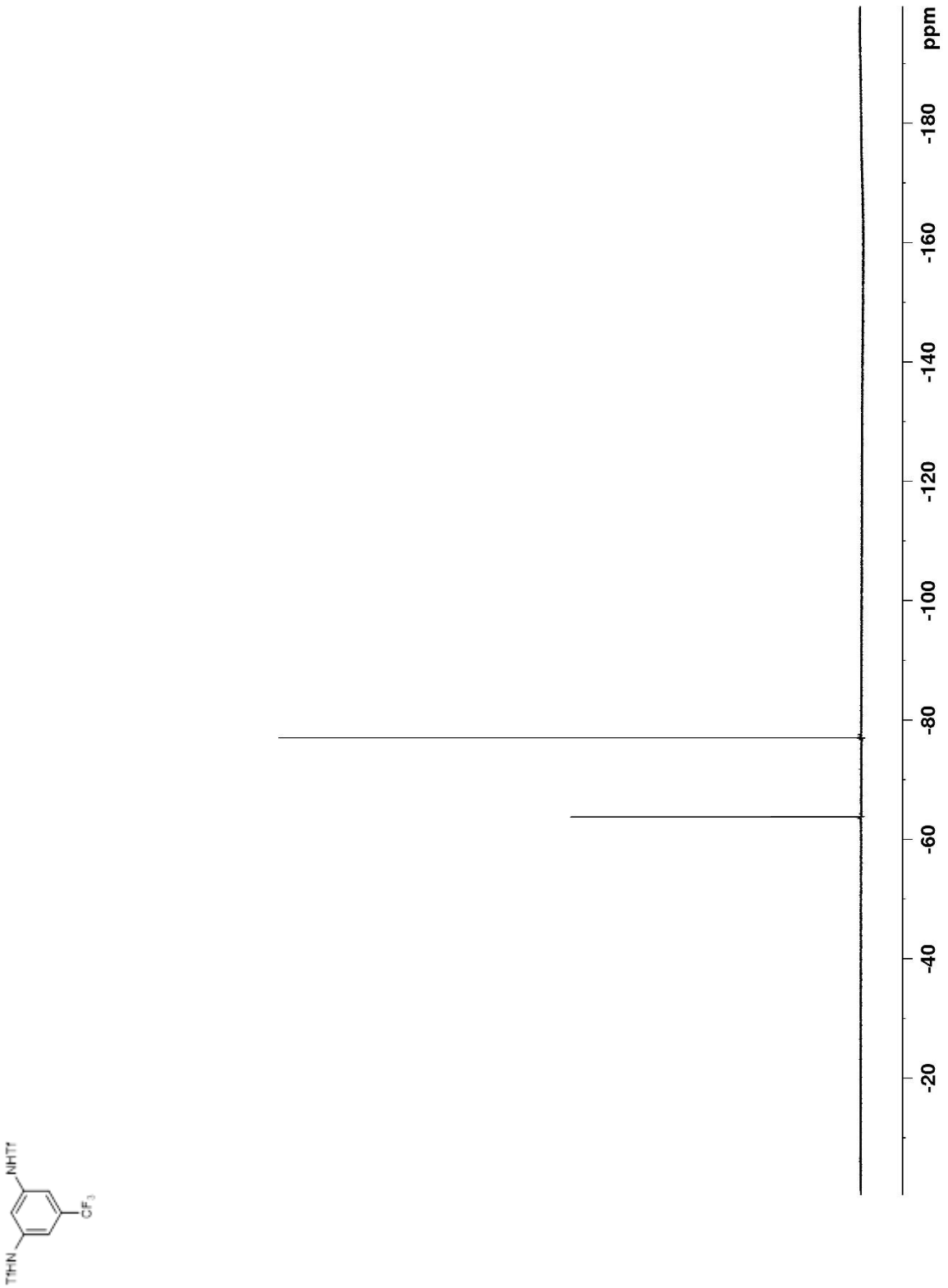

Figure 40. ^{1}H NMR (400 MHz, $CDCl_3$) of **188**

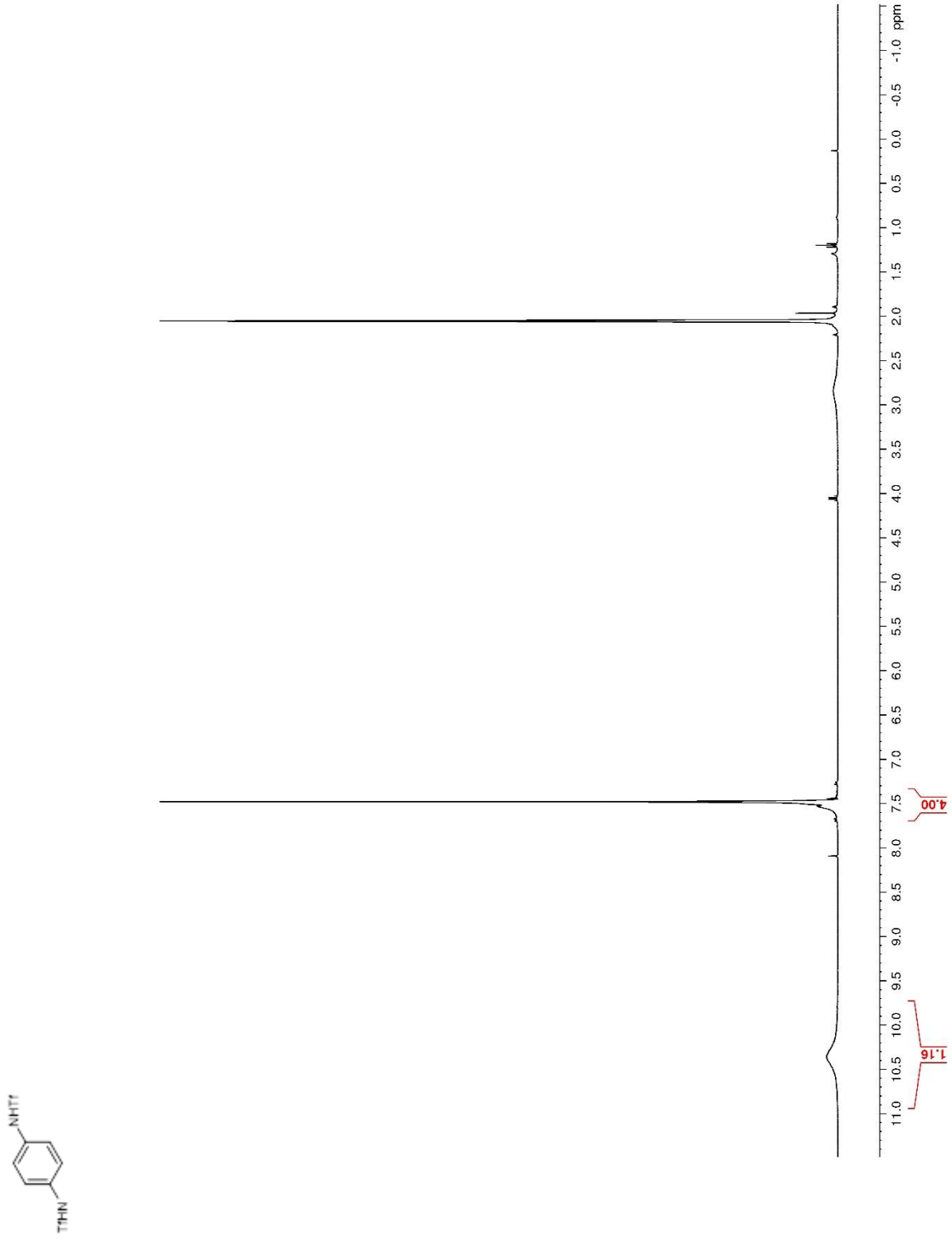

Figure 41. ^{13}C NMR (100 MHz, $CDCl_3$) of **188**

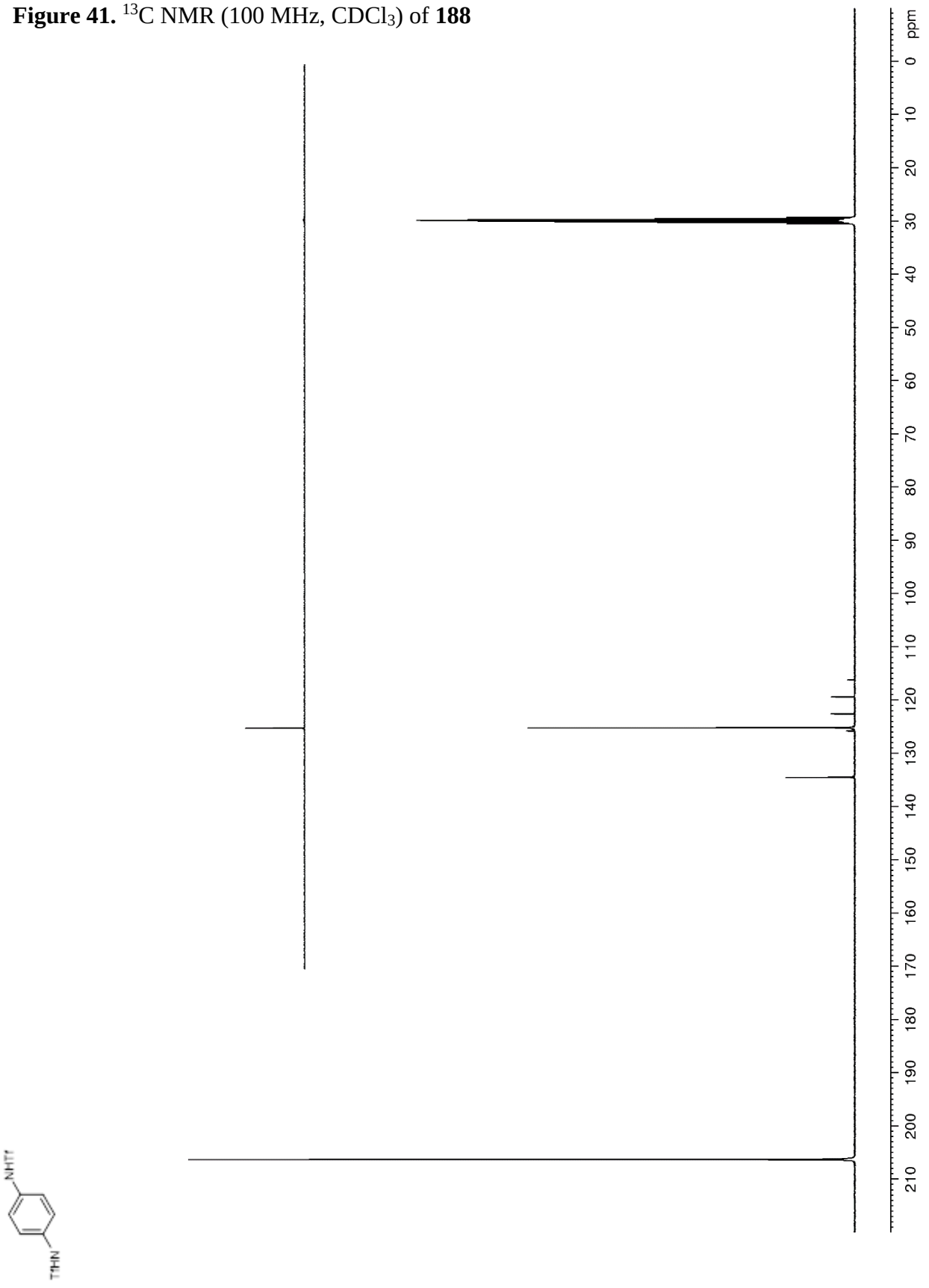

Figure 42. ^{19}F NMR (282 MHz, $(CD_3)_2CO$) of **188**

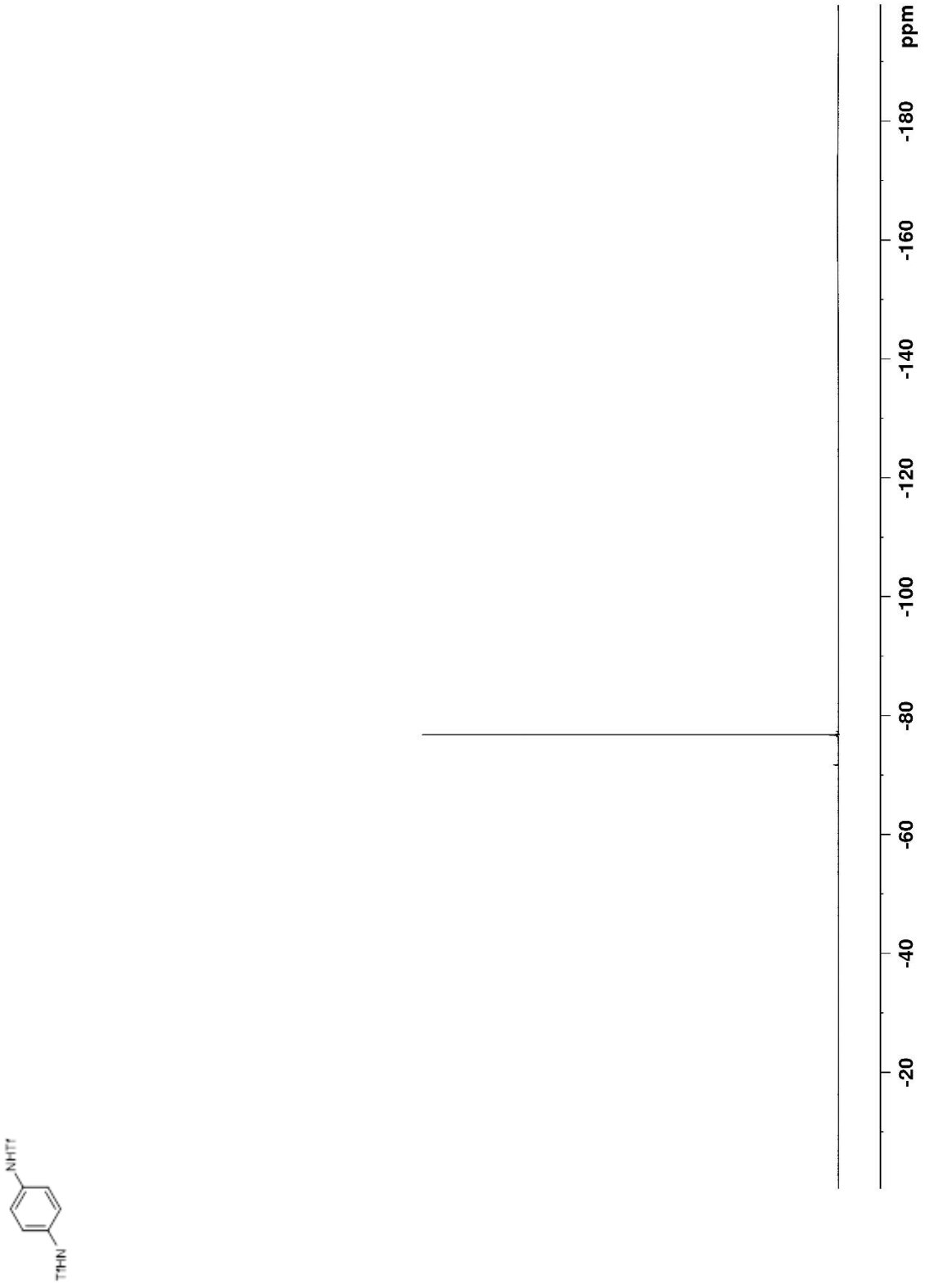

Figure 43. ^{1}H NMR (400 MHz, $CDCl_3$) of **190**

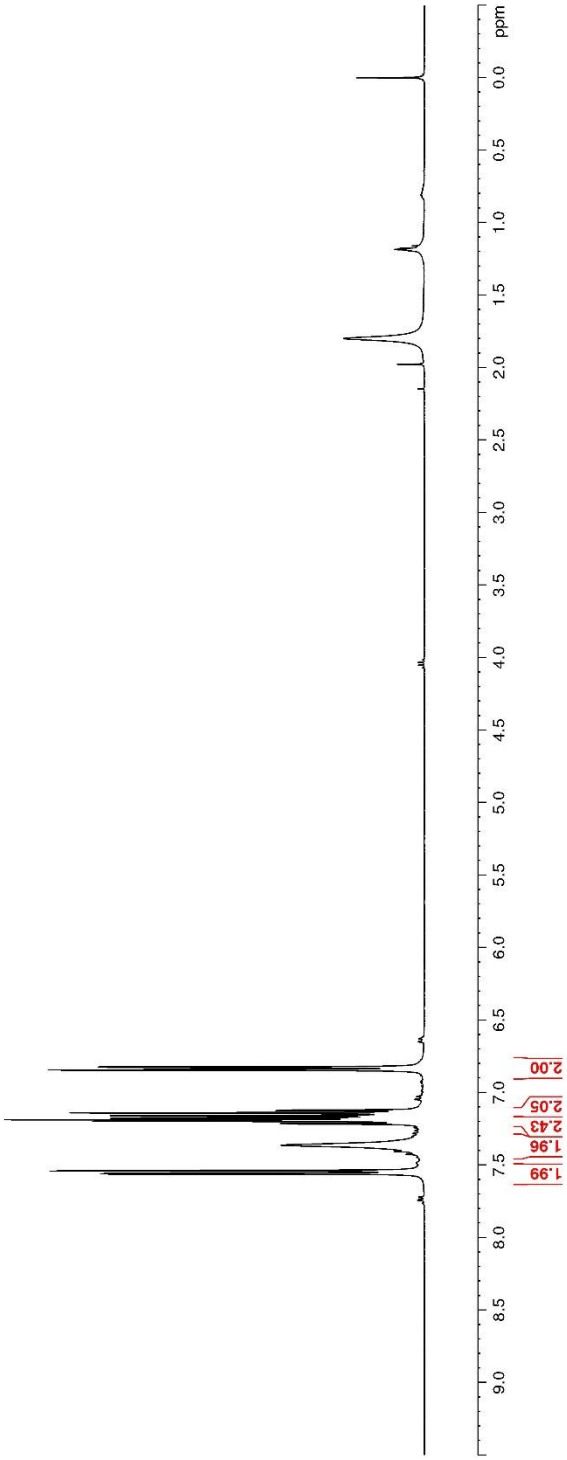

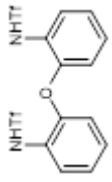

Figure 44. ^{13}C NMR (100 MHz, $CDCl_3$) of **190**

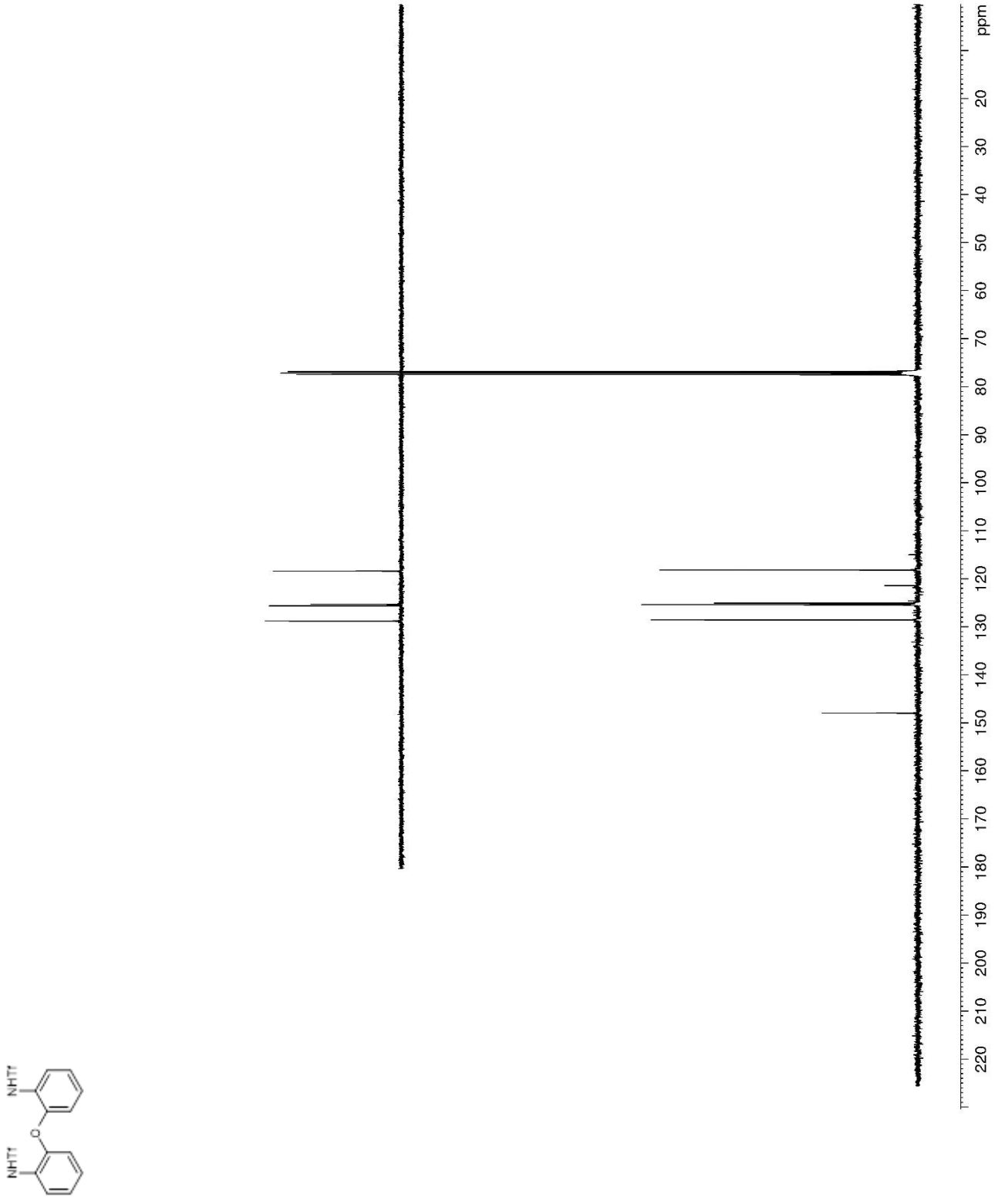

Figure 45. ^{19}F NMR (282 MHz, $CDCl_3$) of **190**

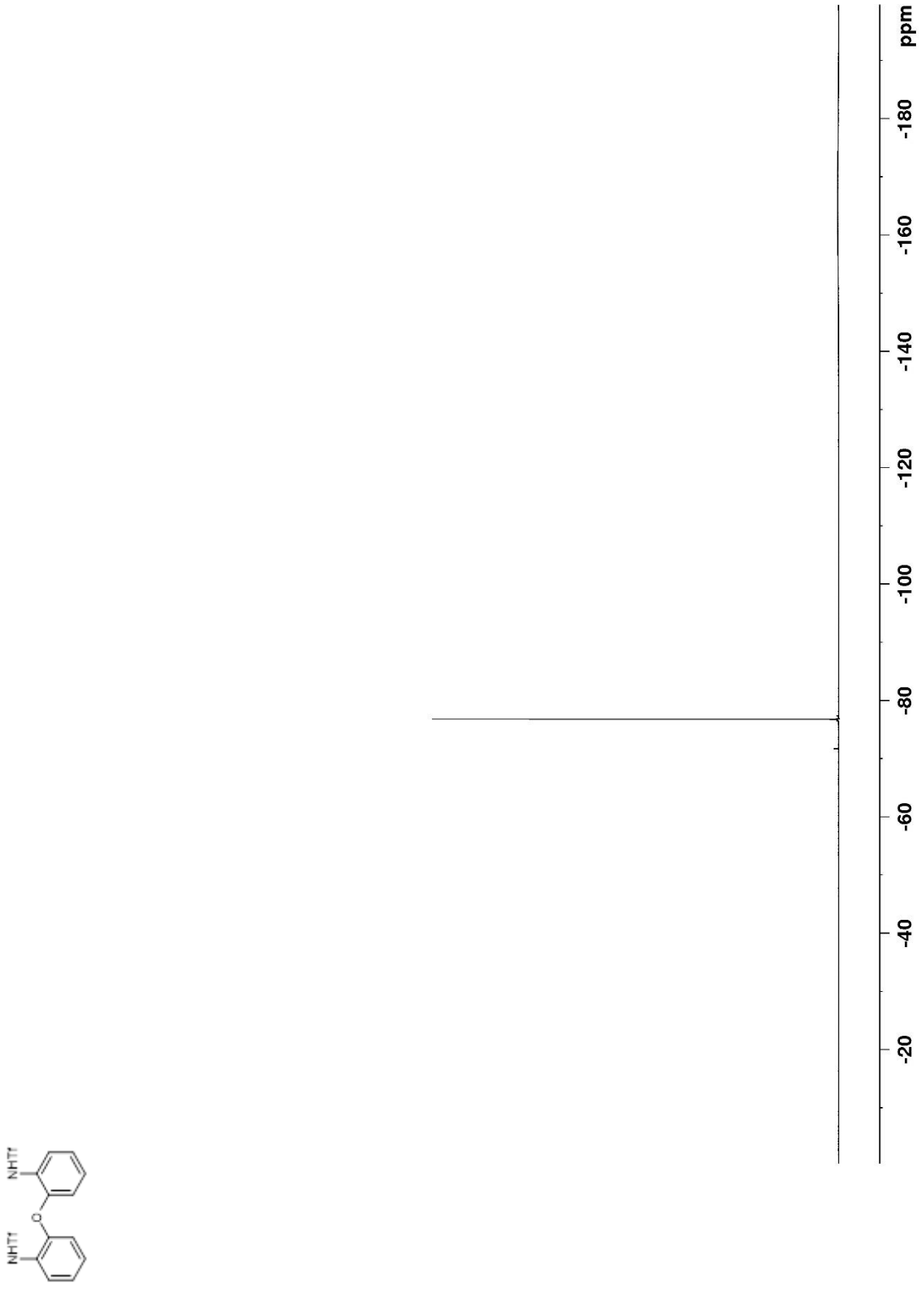

Figure 46. ^{1}H NMR (400 MHz**, (**$(CD_3)_2CO$) of **191**

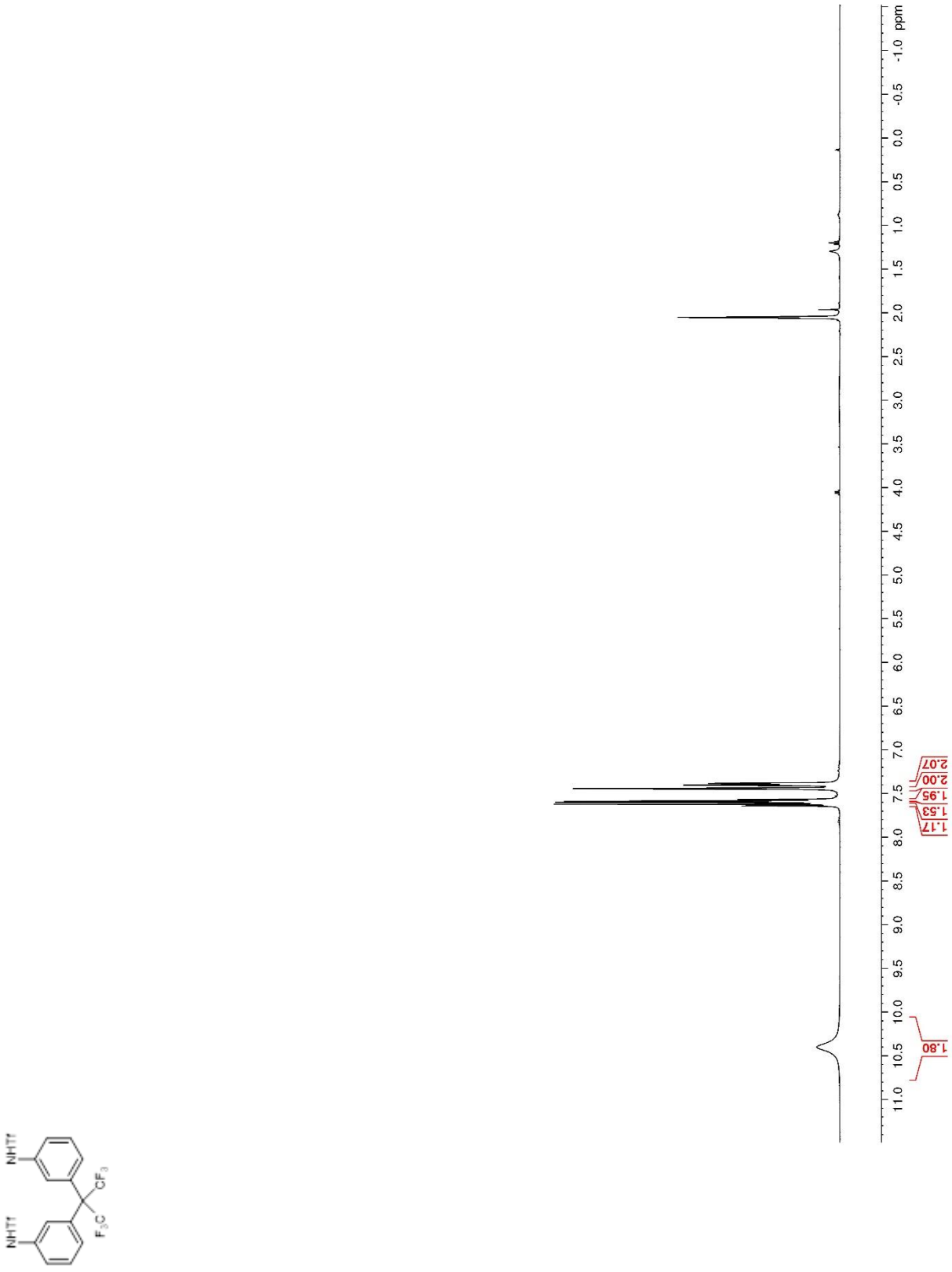

Figure 47. ^{13}C NMR (100 MHz, $(CD_3)_2CO$) of **191**

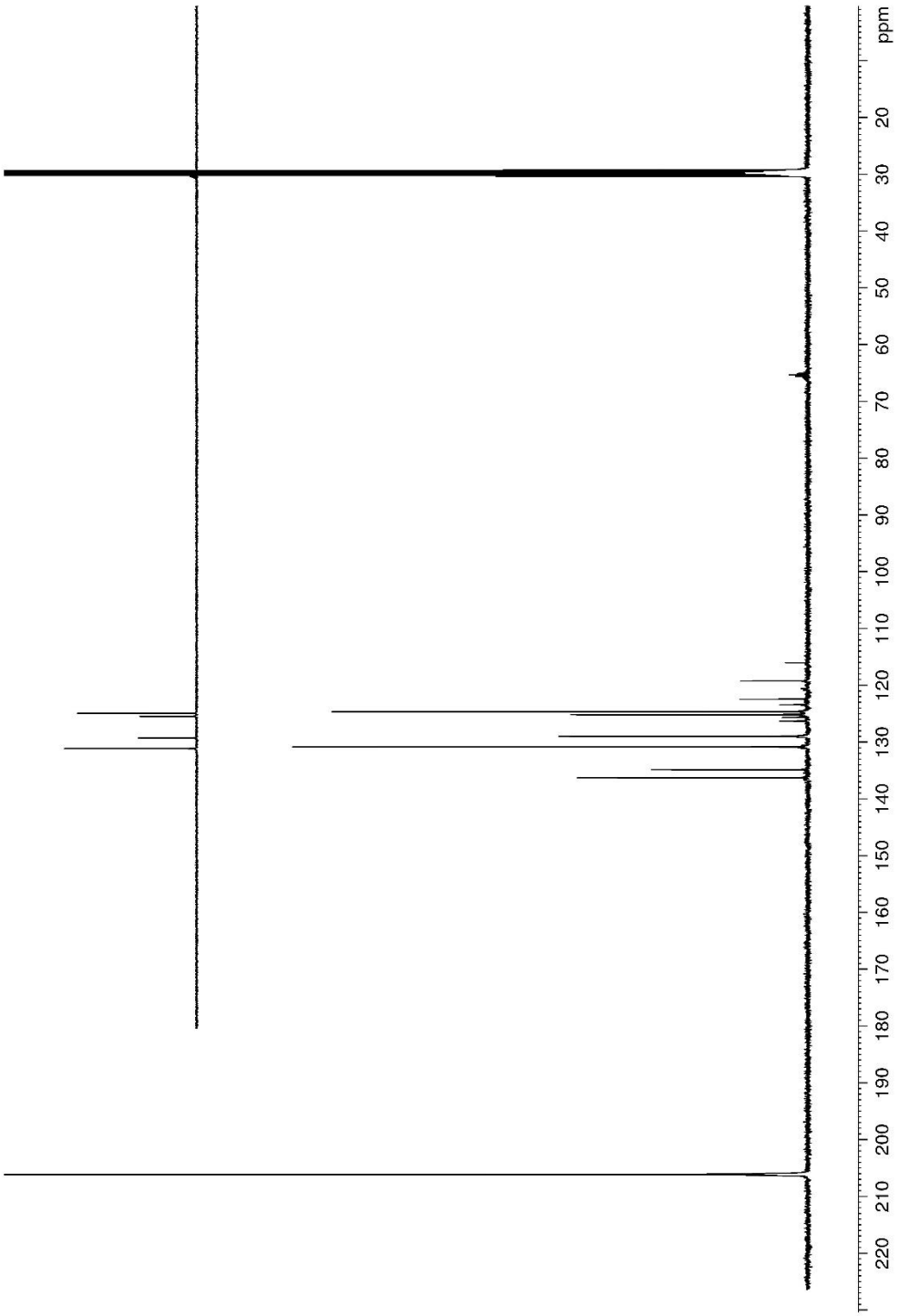

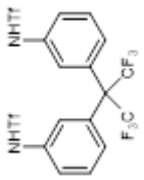

Figure 48. ^{19}F NMR (282 MHz, $(CD_3)_2CO$) of **191**

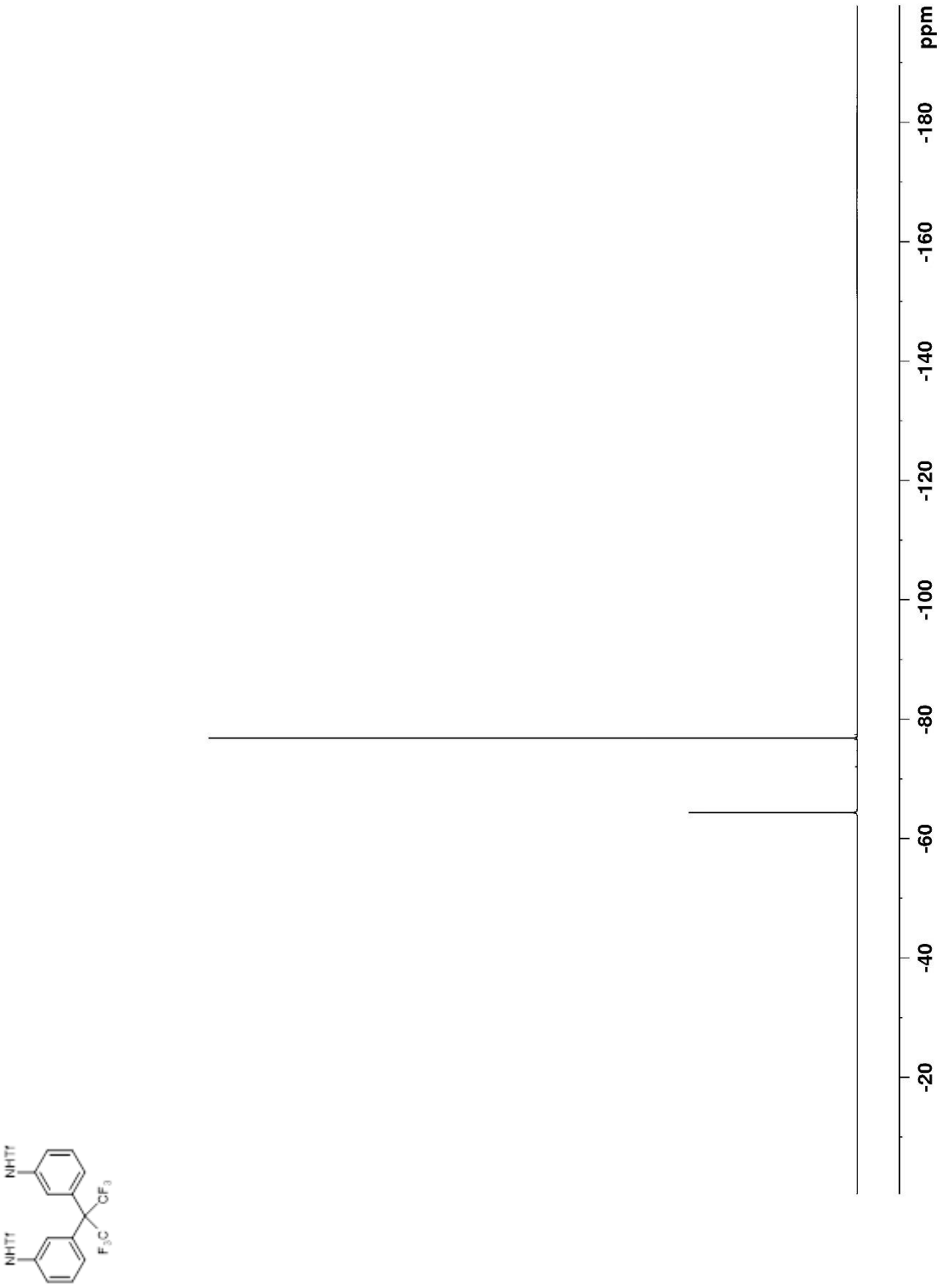

Figure 49. ^{1}H NMR (400 MHz**, (**$CD_3)_2CO$) of **S5**

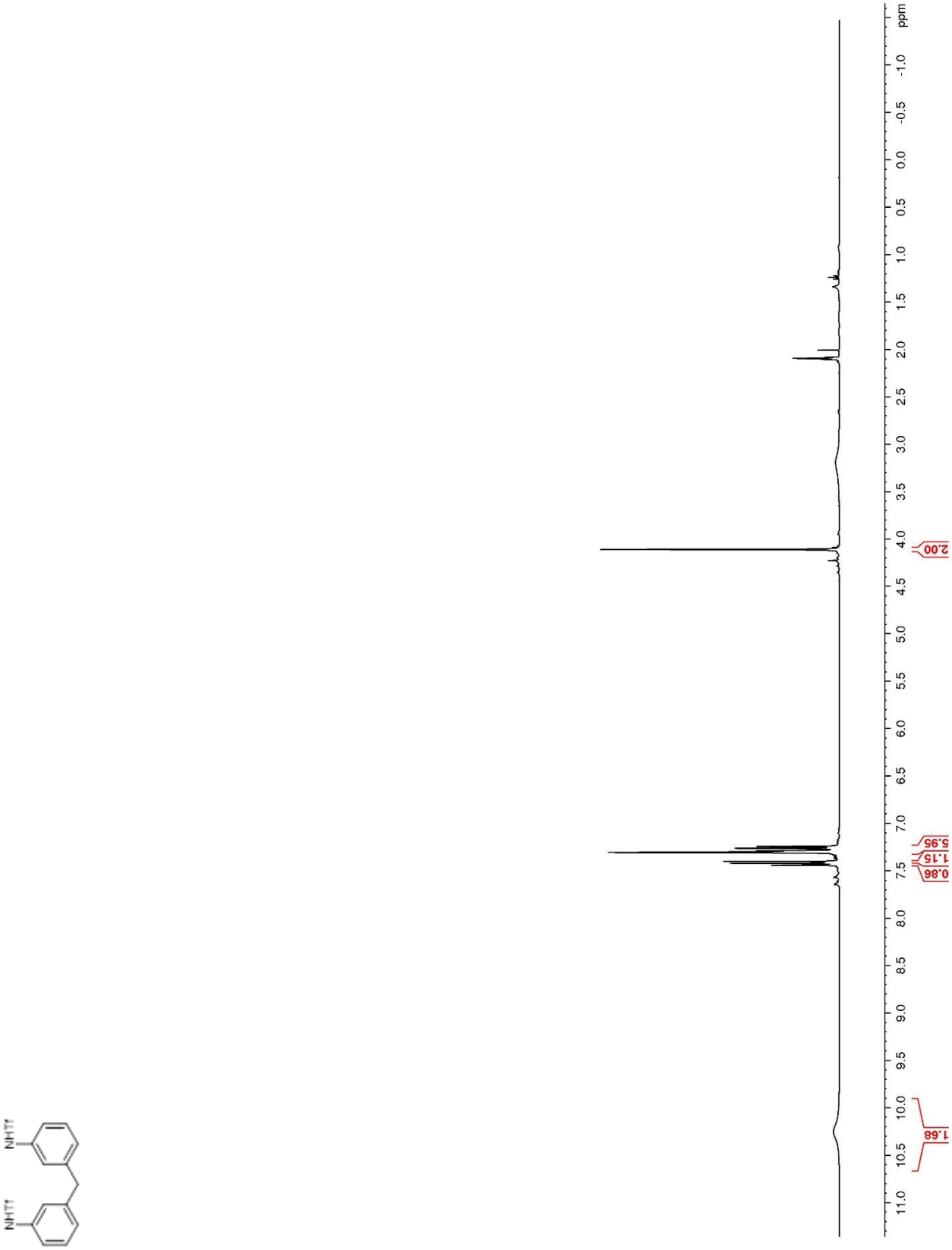

Figure 50. ^{13}C NMR (100 MHz, $(CD_3)_2CO$) of **S5**

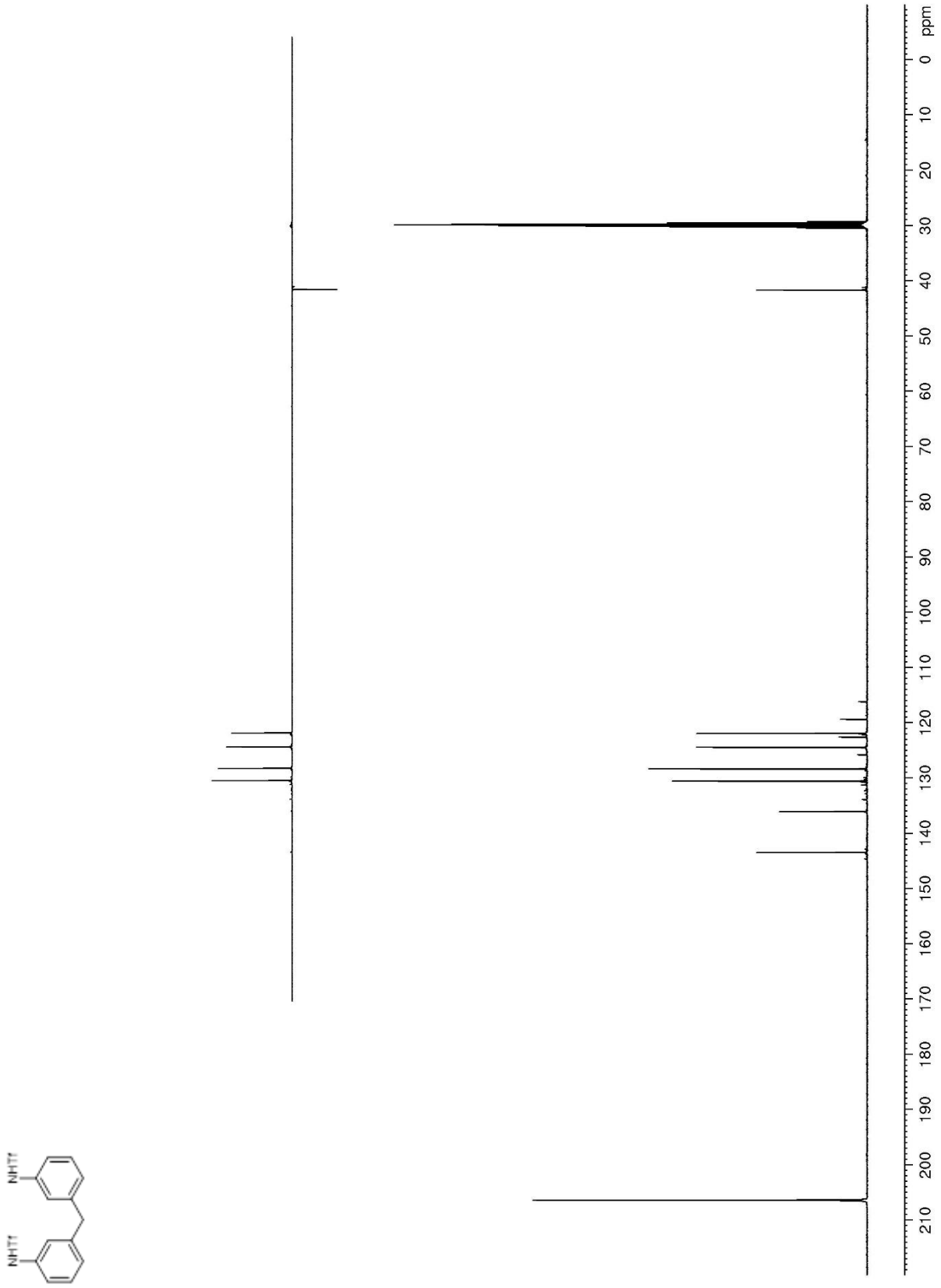

Figure 51. ^{19}F NMR (282 MHz, $(CD_3)_2CO$) of **S5**

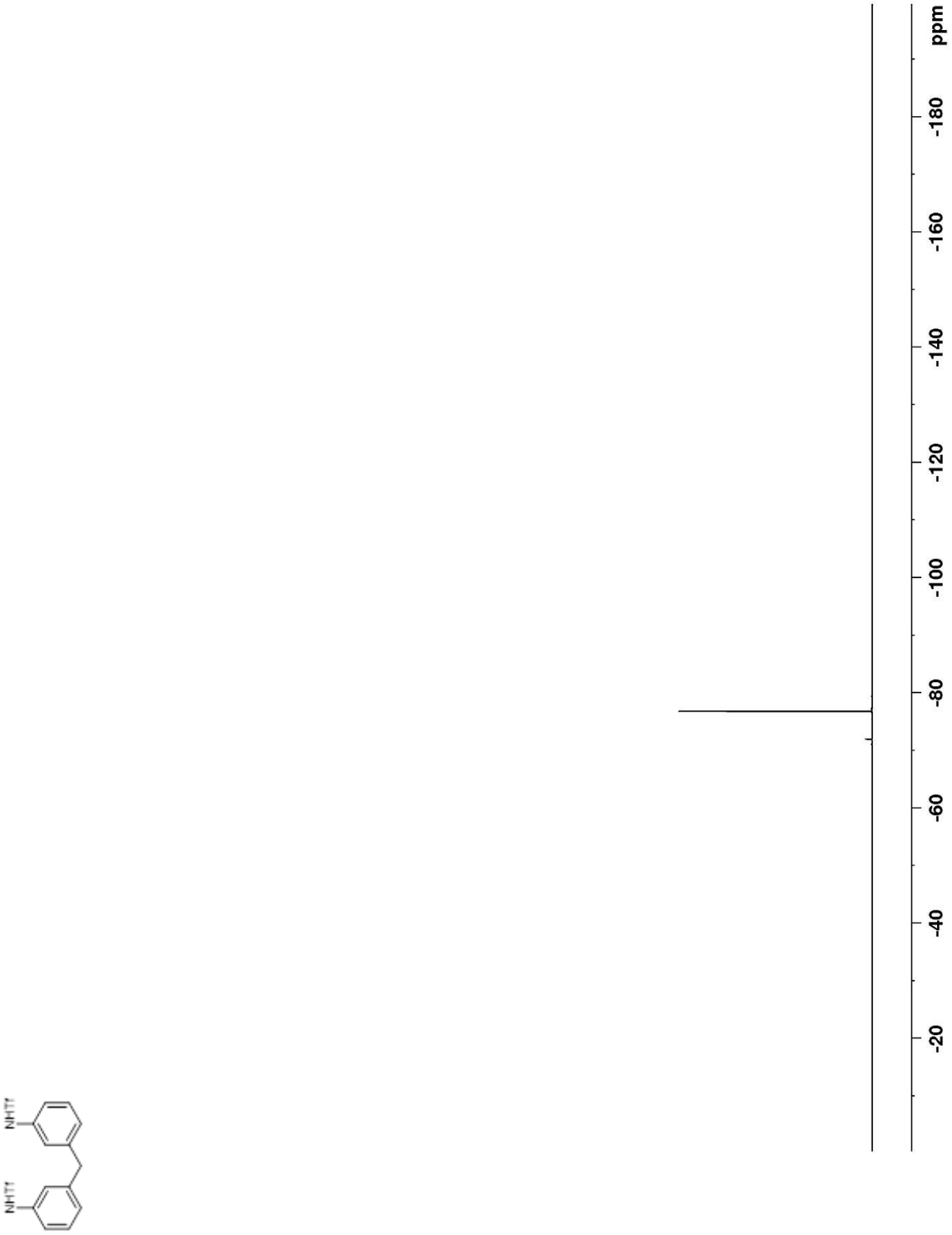

Figure 52. ^{1}H NMR (400 MHz, **(**$CD_3)_2CO$) of **S6**

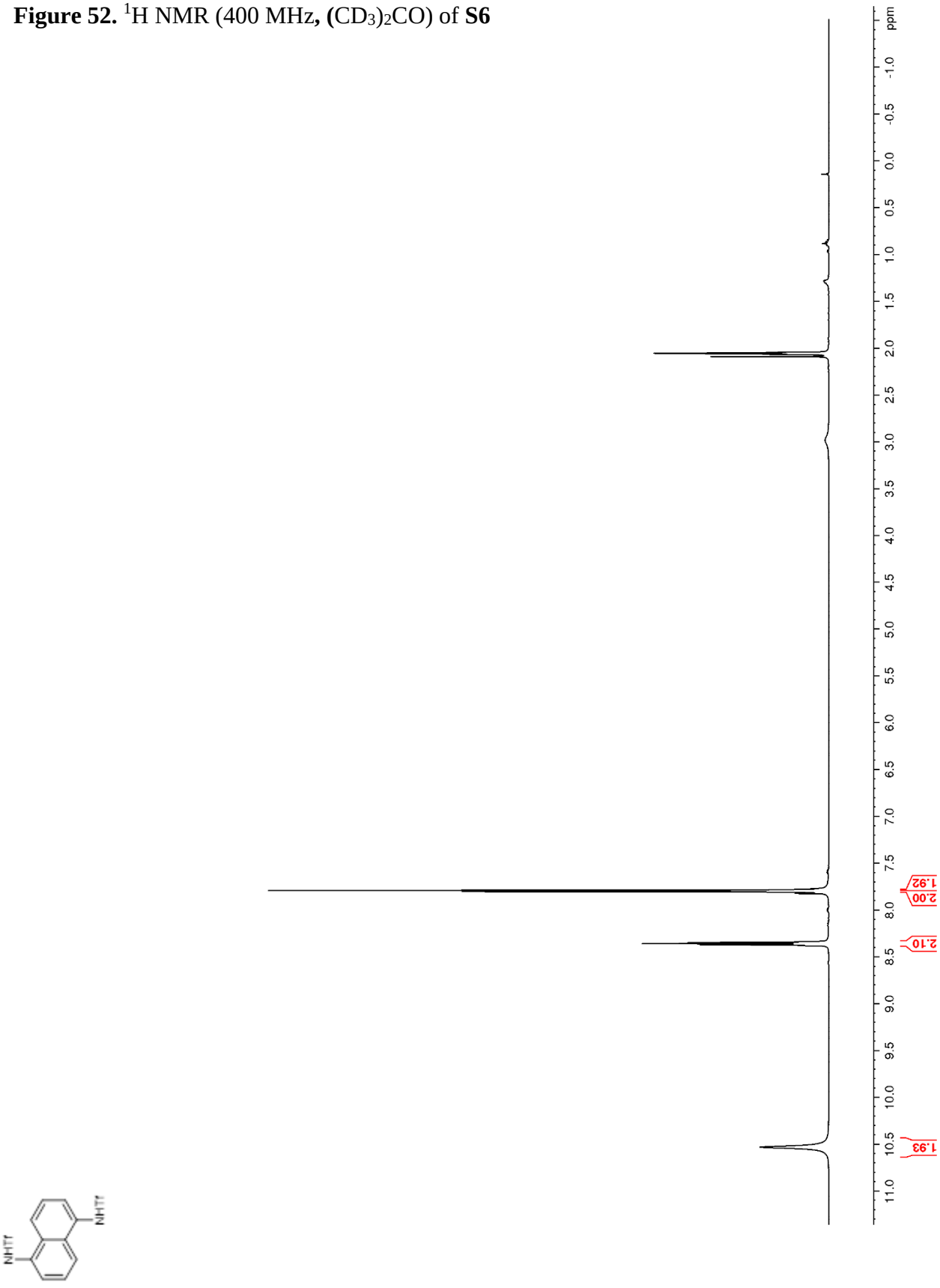

Figure 53. ^{13}C NMR (100 MHz, $(CD_3)_2CO$) of **S6**

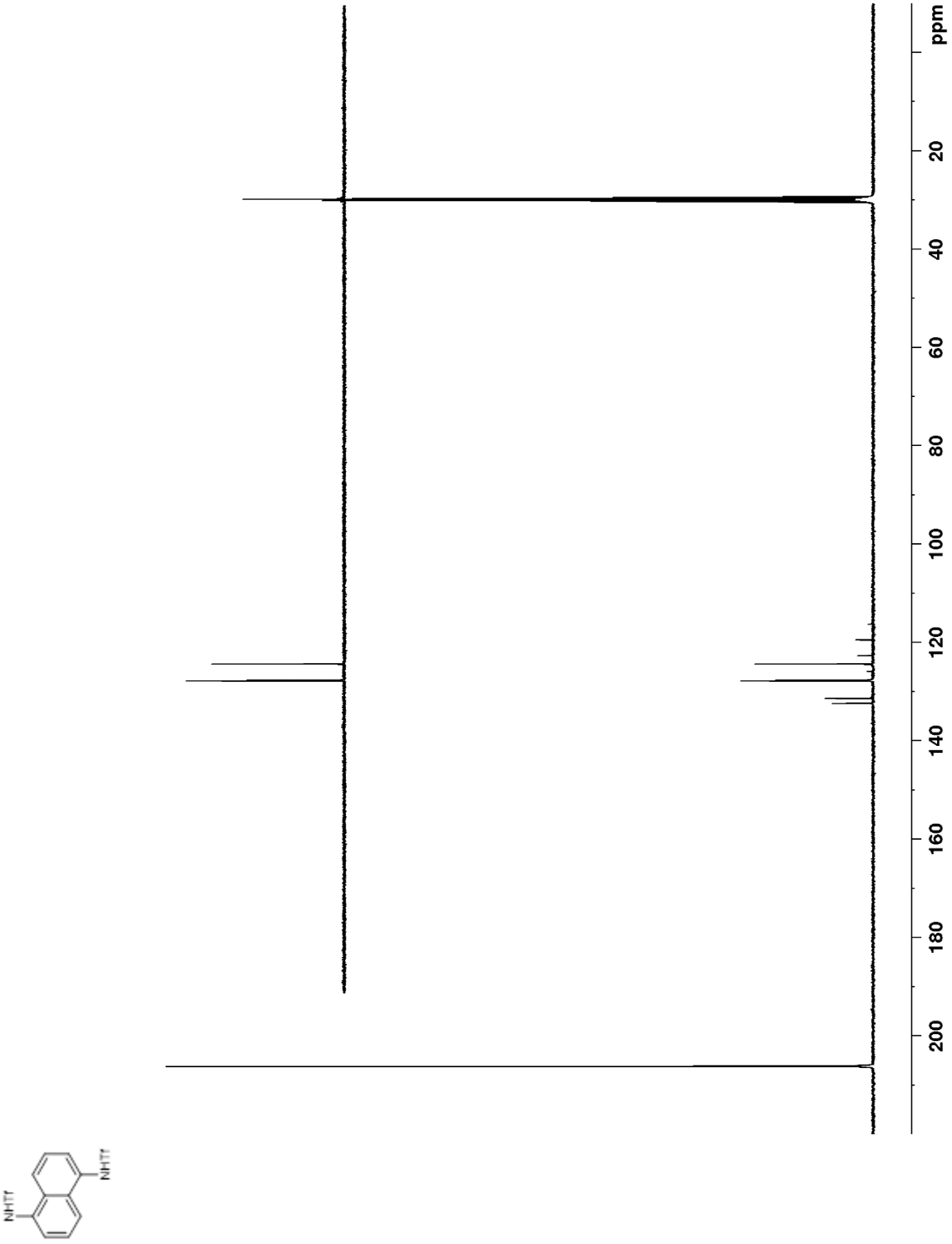

Figure 54. ^{19}F NMR (282 MHz, $(CD_3)_2CO$) of **S6**

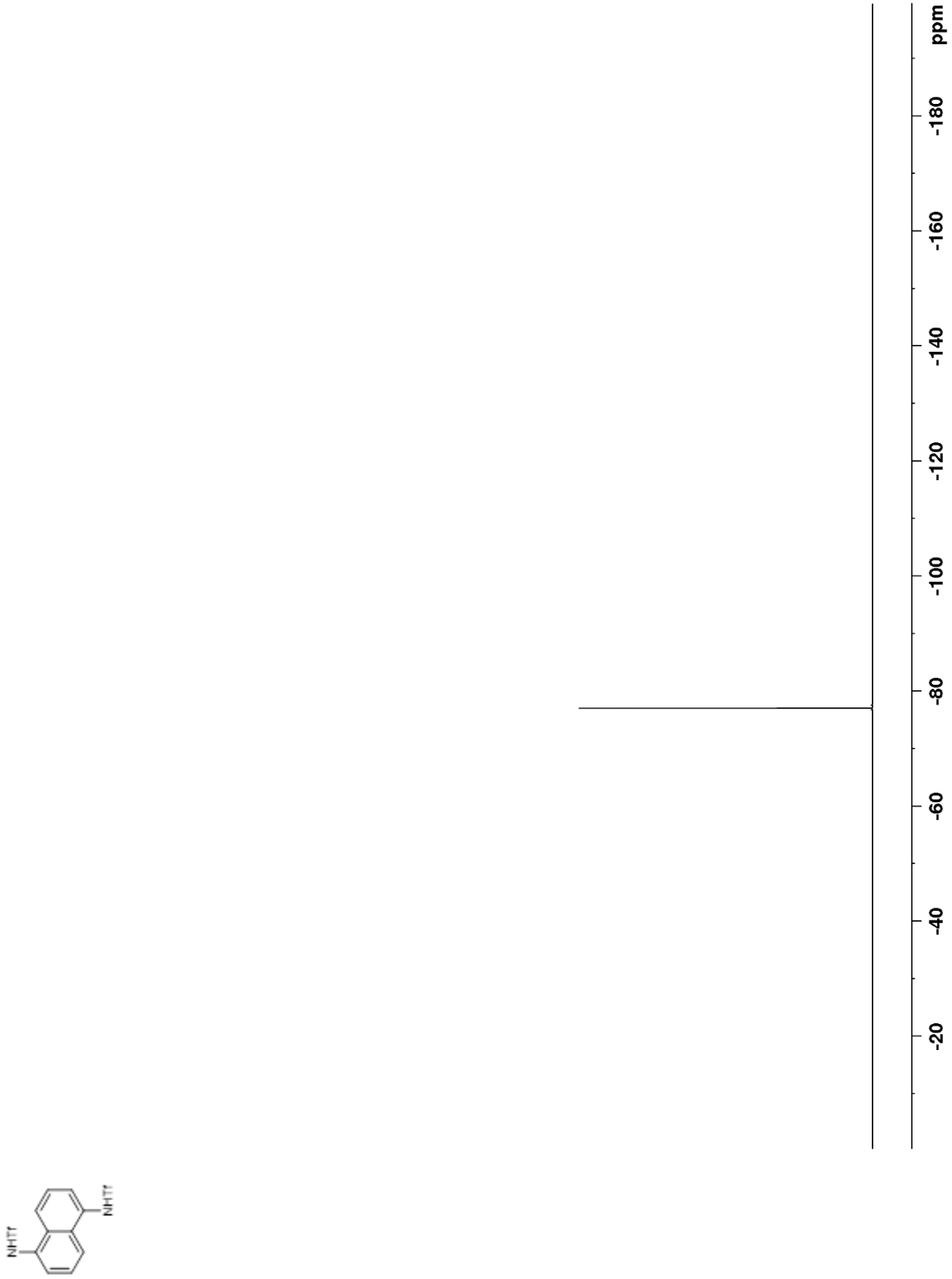

Figure 55. ^{1}H NMR (400 MHz**,** $CDCl_3$) of **S7**

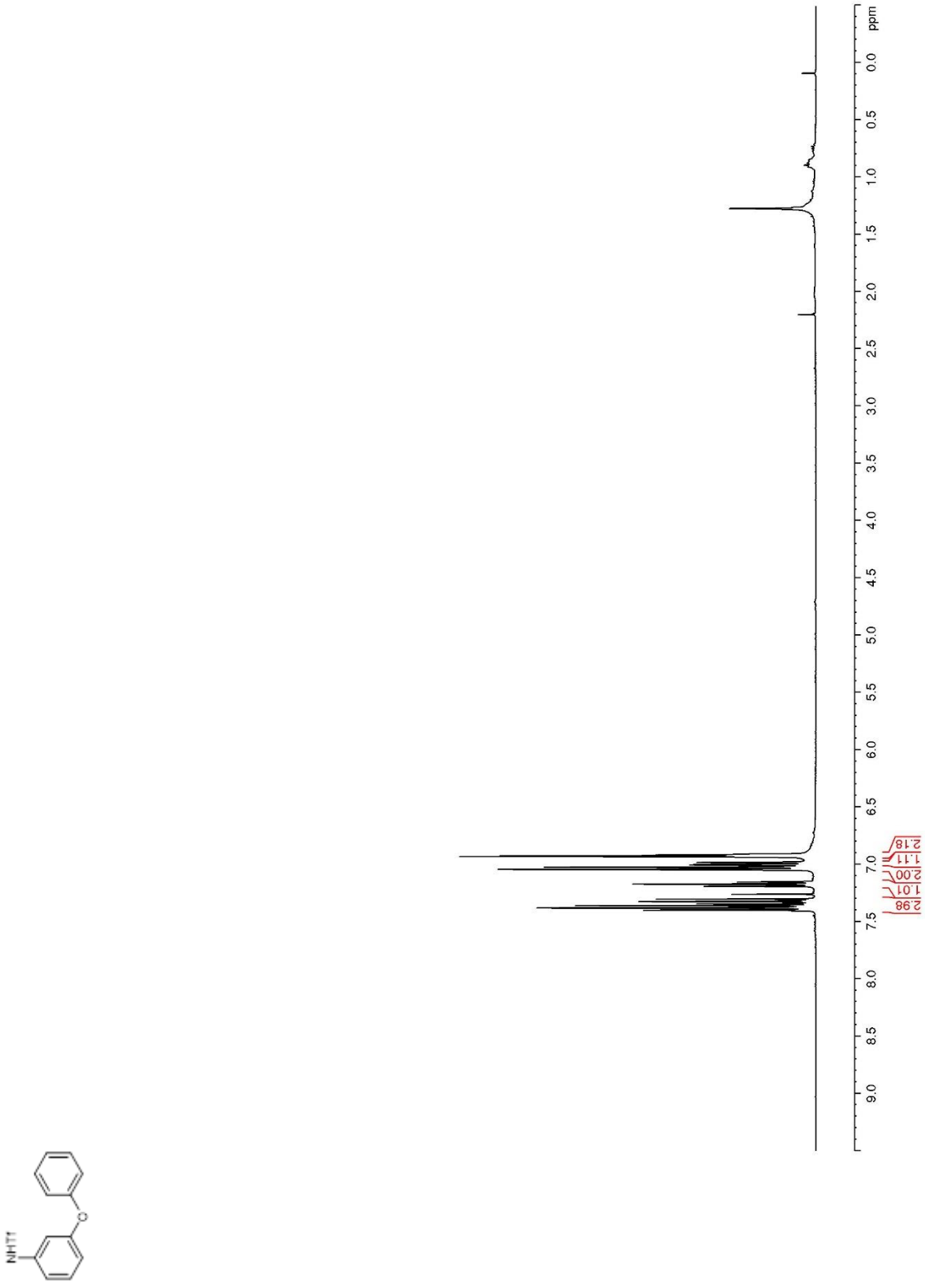

Figure 56. ^{13}C NMR (100 MHz, $CDCl_3$) of **S7**

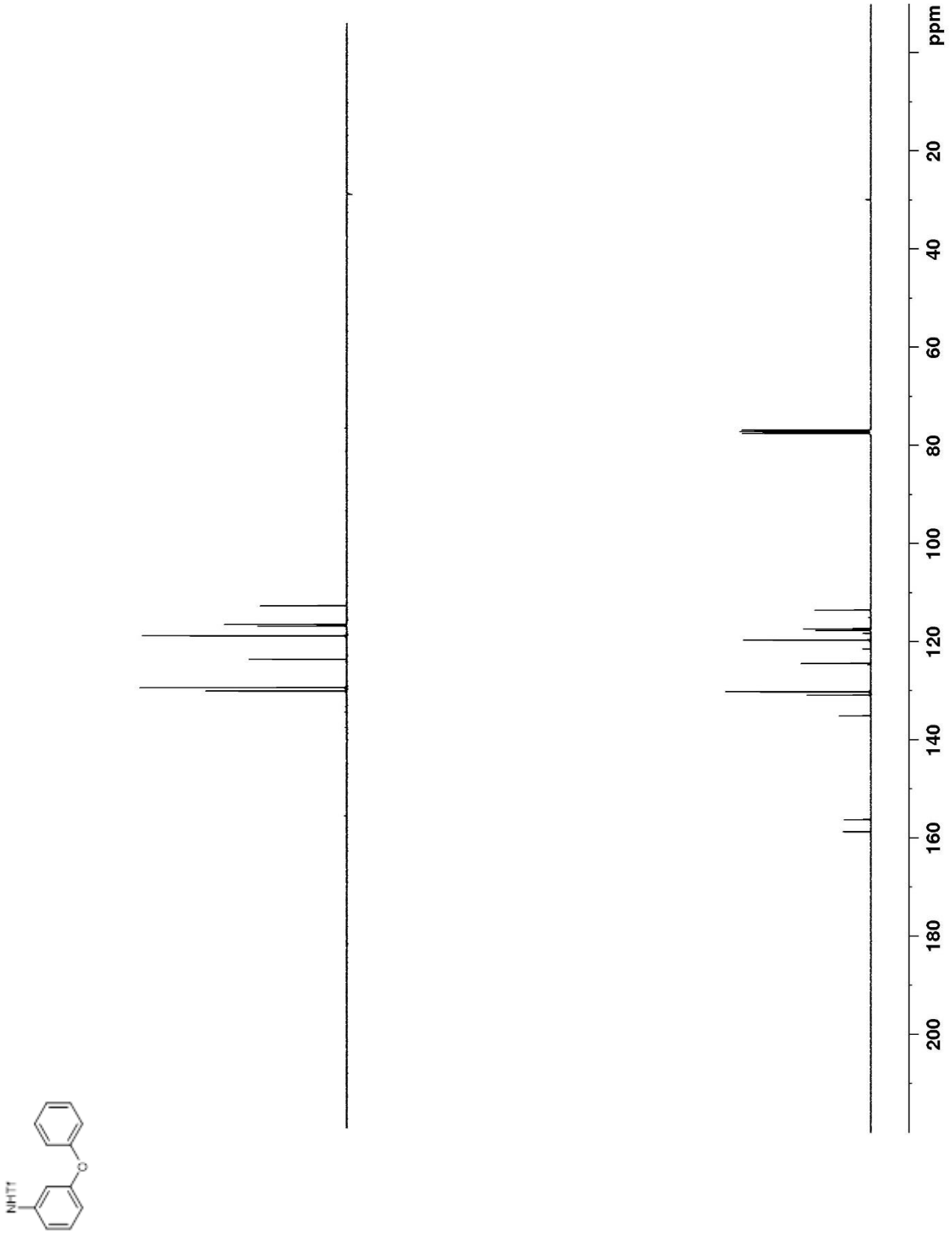

Figure 57. ^{19}F NMR (282 MHz, $CDCl_3$) of **S7**

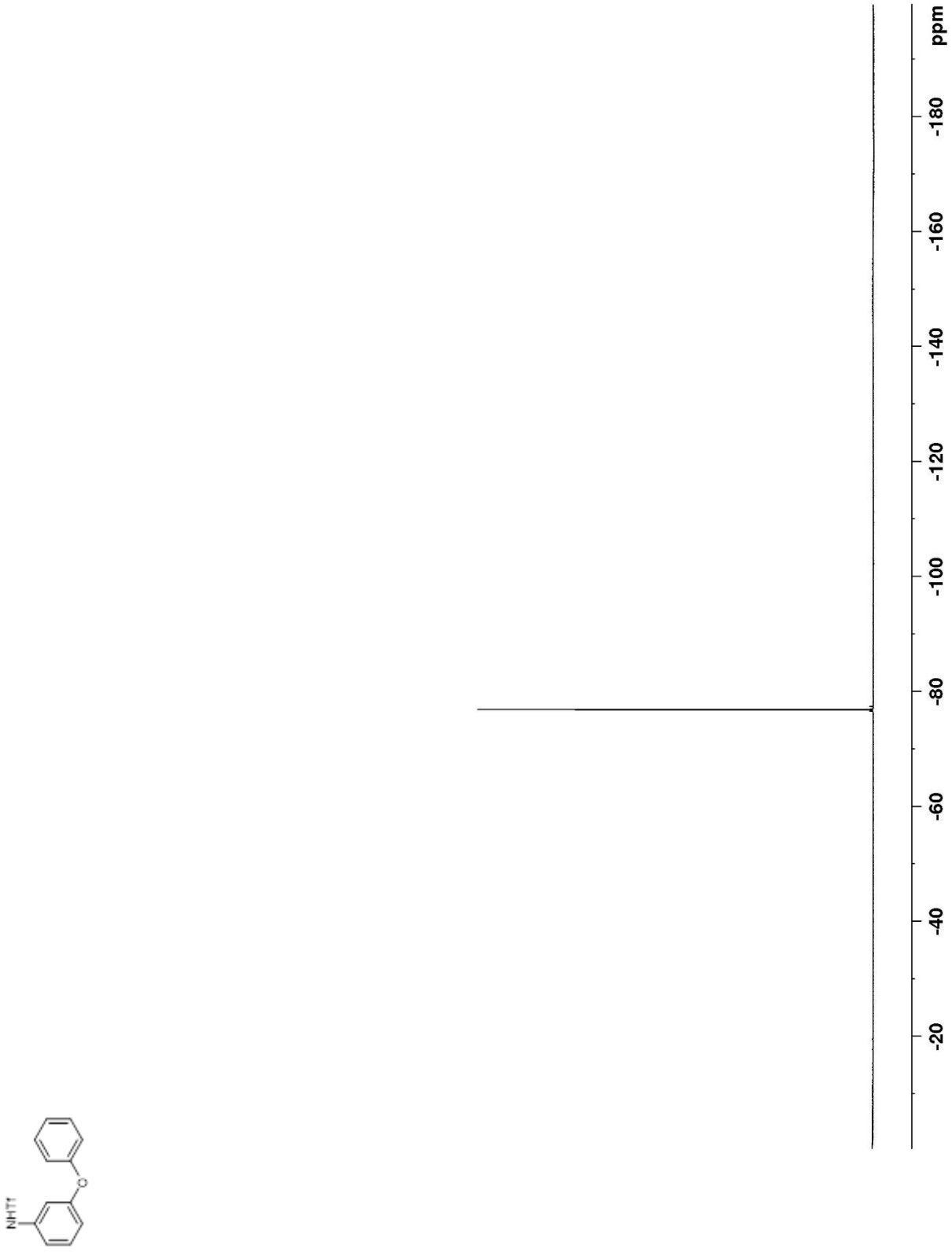

Figure 58. ^{1}H NMR (400 MHz**,** $CDCl_3$) of **189**

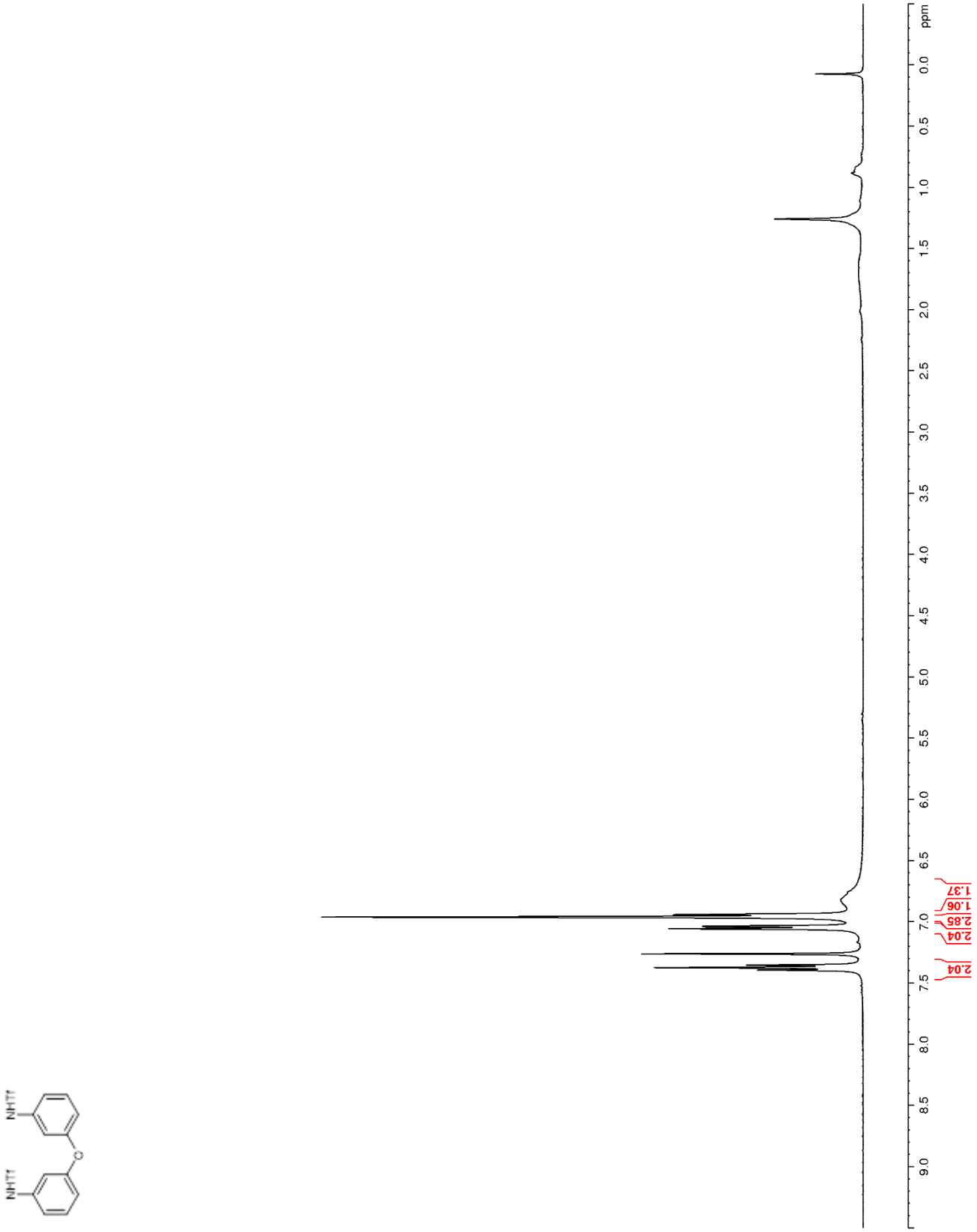

Figure 59. ^{13}C NMR (100 MHz, $CDCl_3$) of **189**

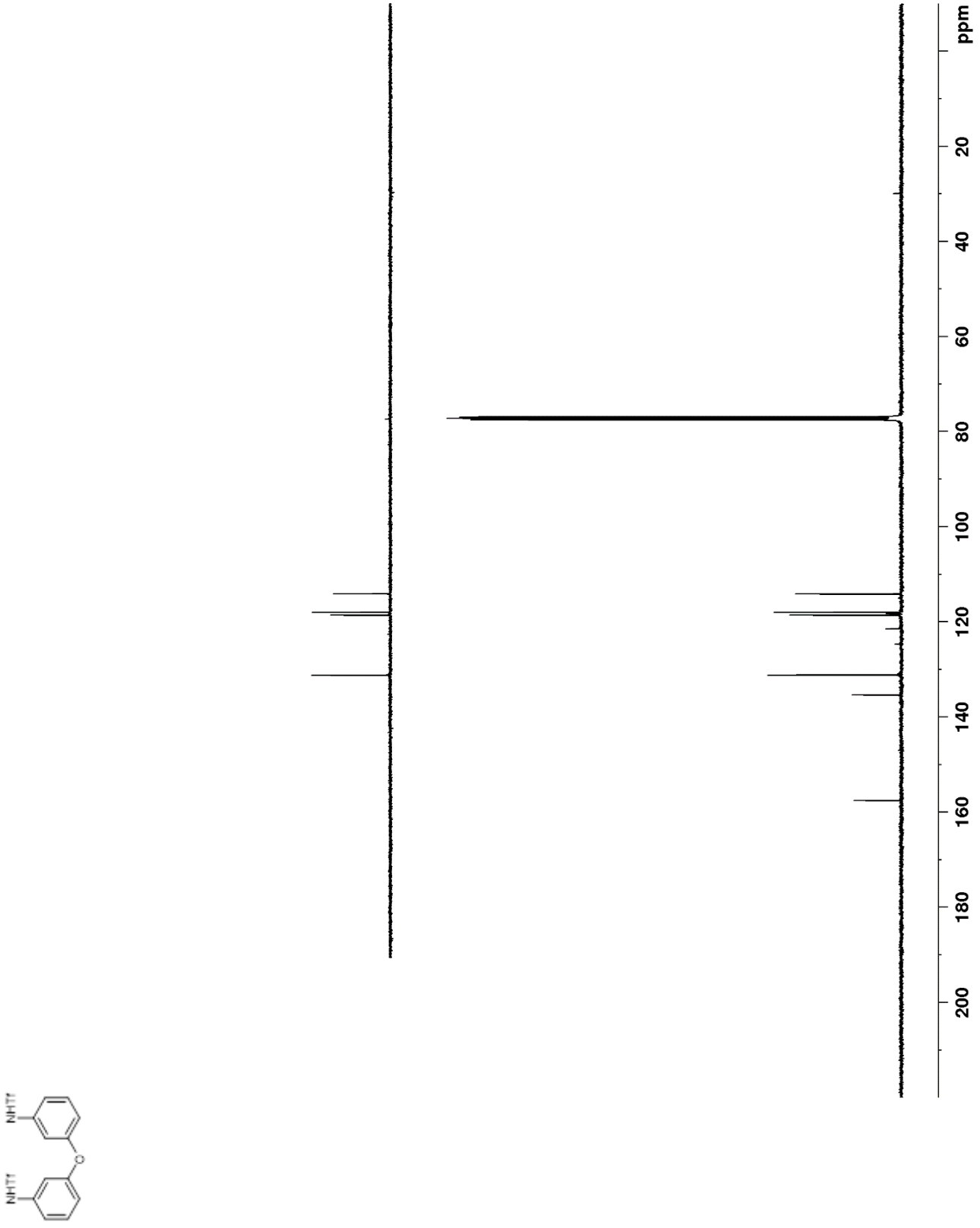

Figure 60. ^{19}F NMR (282 MHz, $CDCl_3$) of **189**

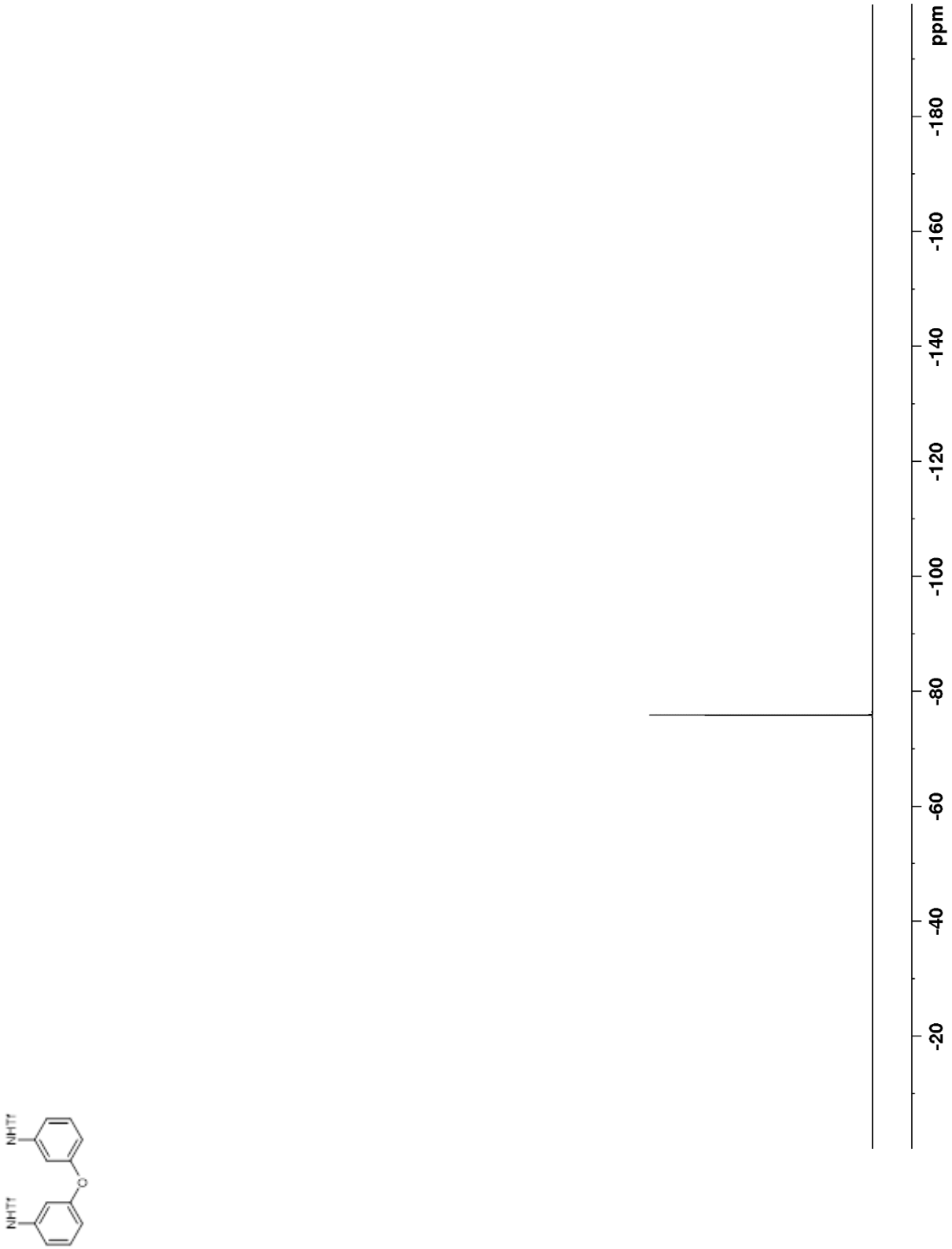

Figure 61. ^{1}H NMR (400 MHz**, (**$(CD_3)_2CO$) of **213**

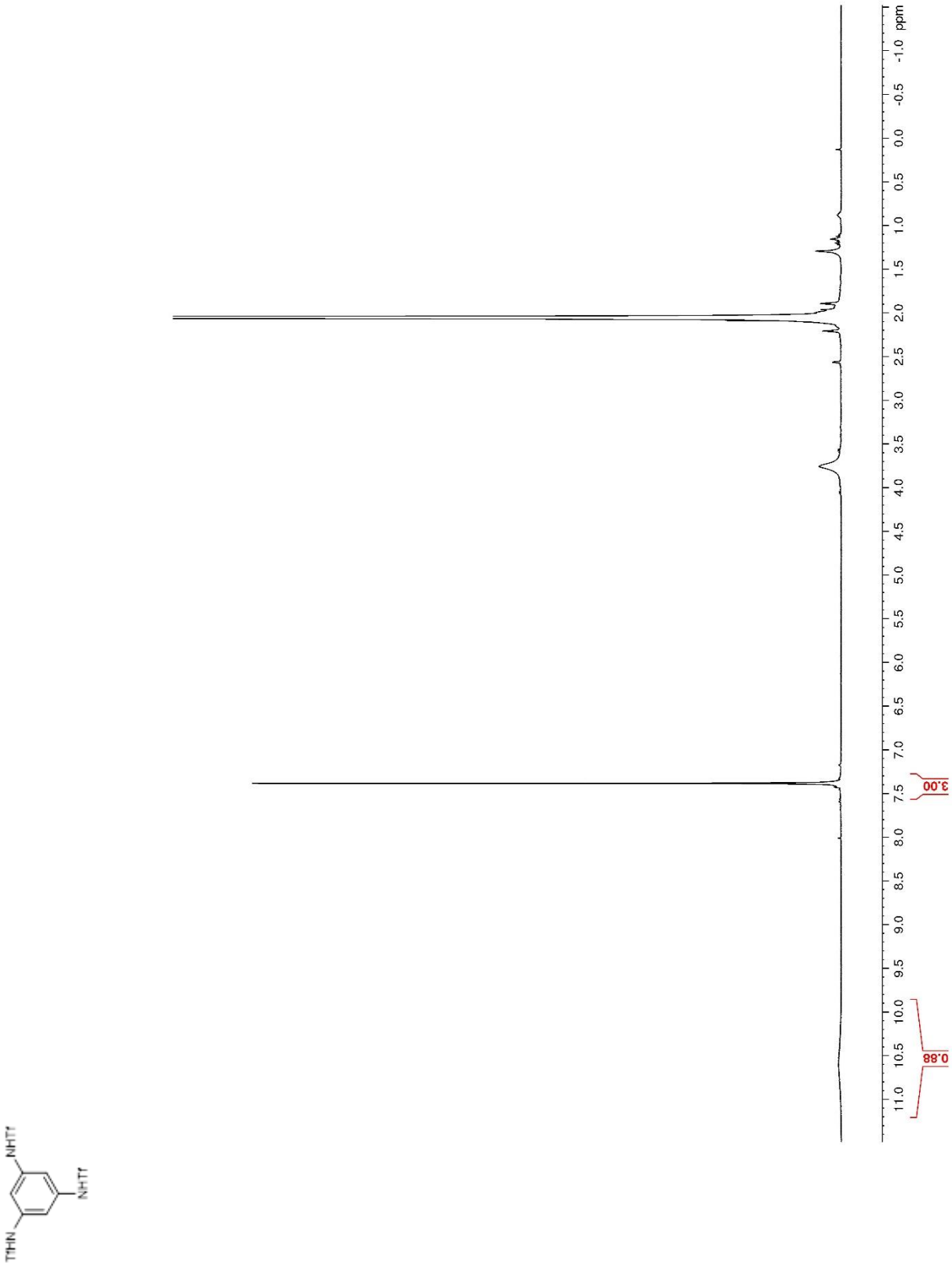

Figure 62. ^{13}C NMR (150 MHz, $(CD_3)_2CO$) of **213**

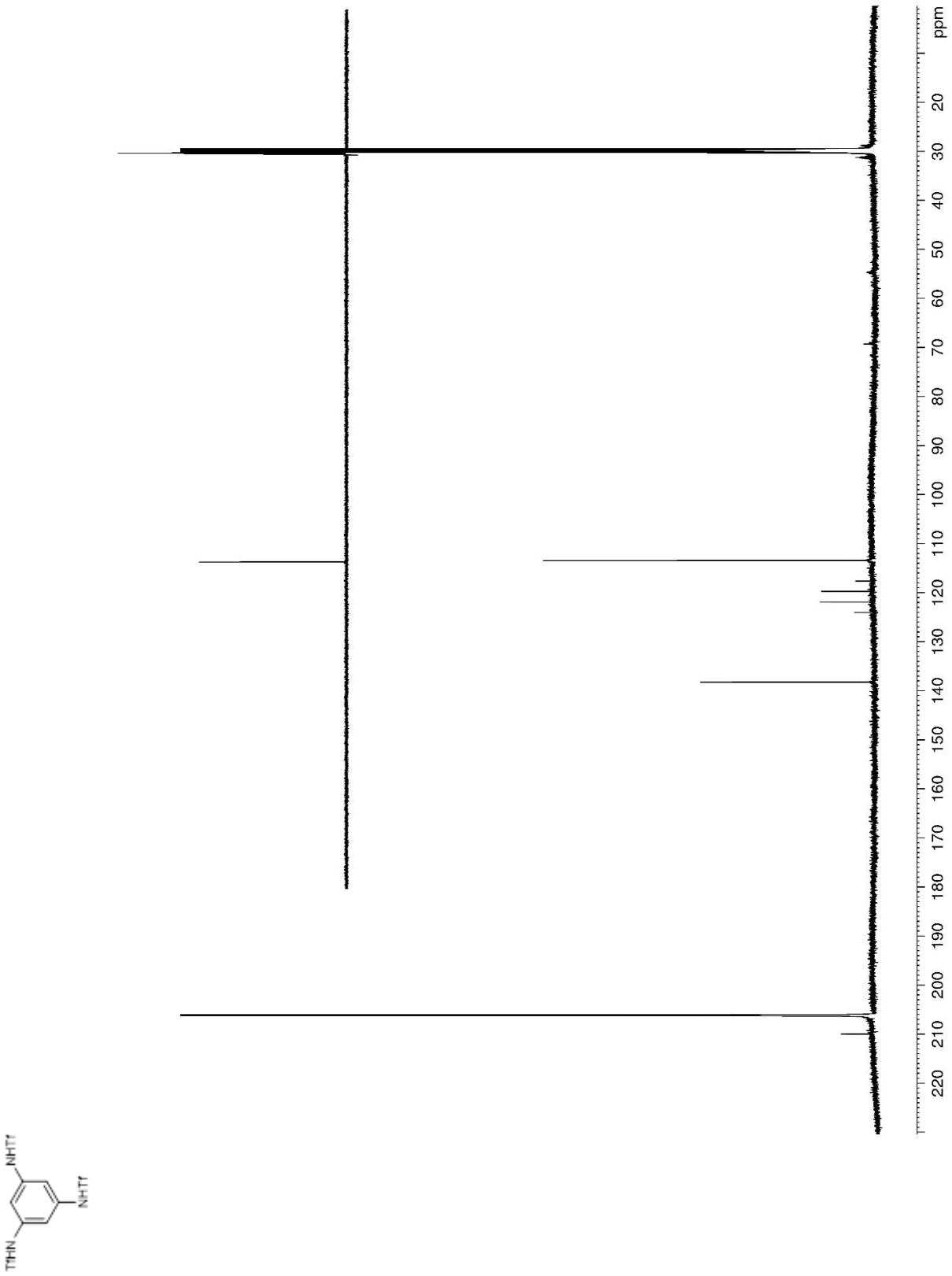

Figure 63. ^{19}F NMR (282 MHz, $(CD_3)_2CO$) of **213**

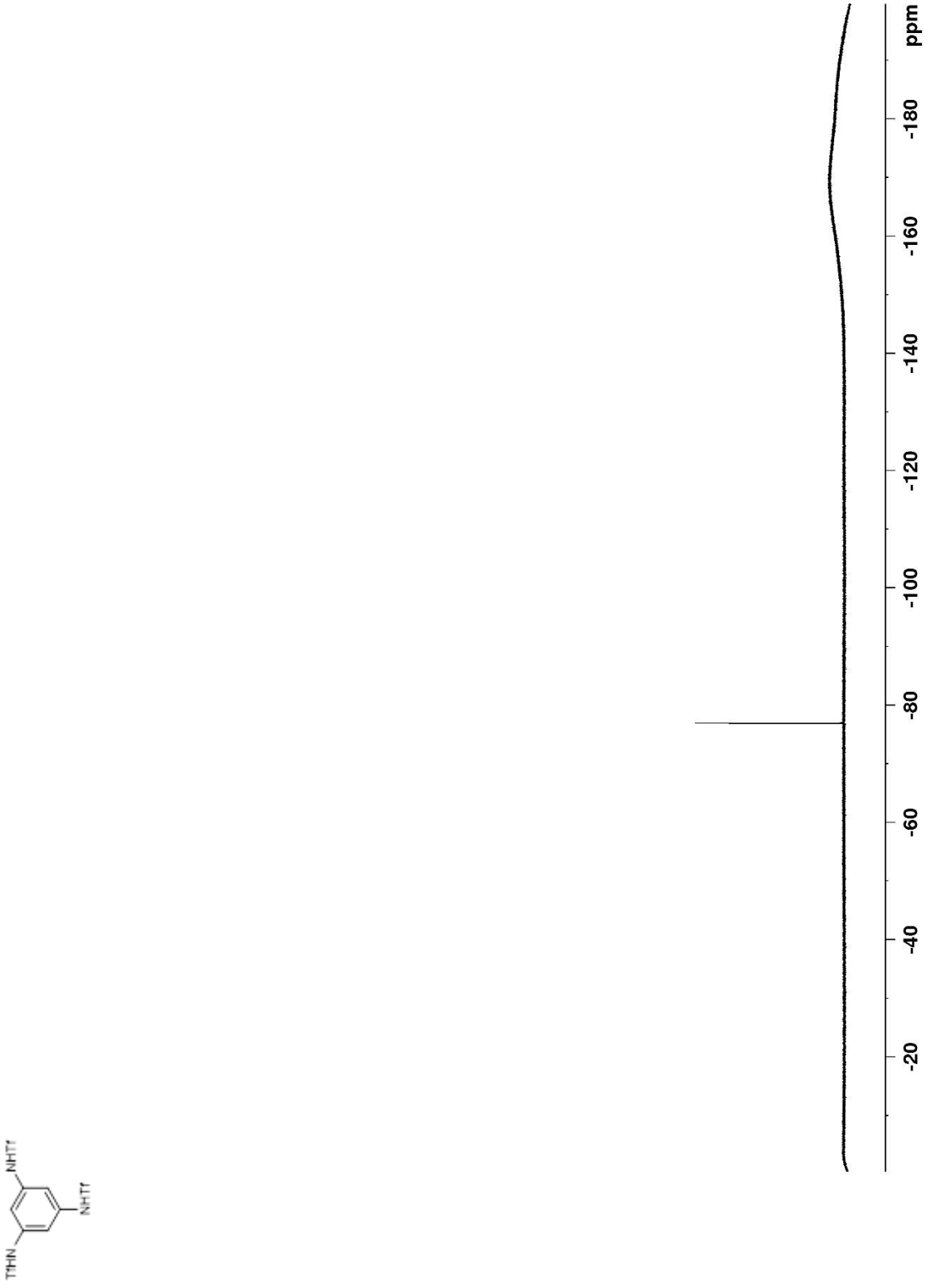

Figure 64. ^{1}H NMR (400 MHz**, (**$(CD_3)_2CO$) of **203**

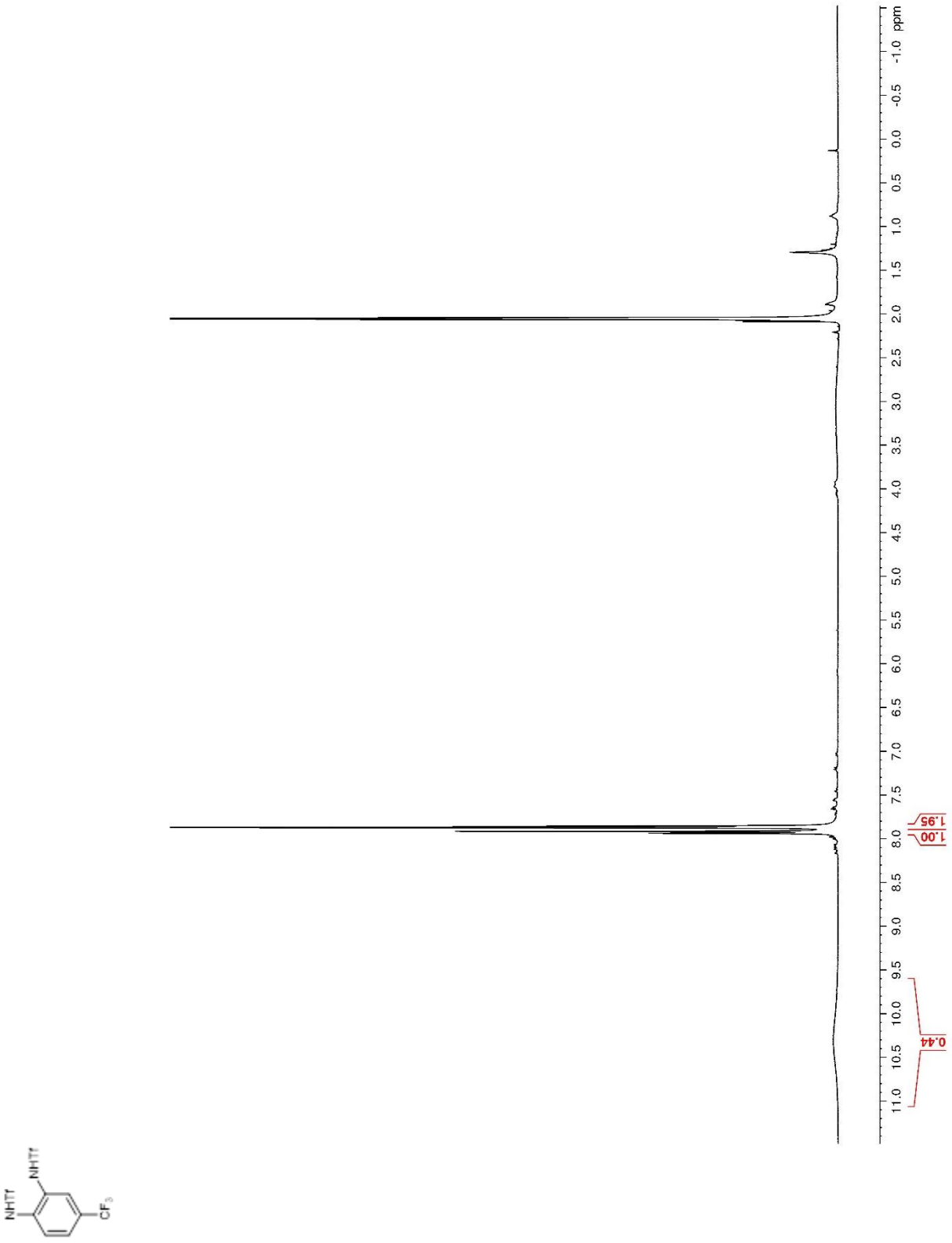

Figure 65. ^{13}C NMR (150 MHz, $(CD_3)_2CO$) of **203**

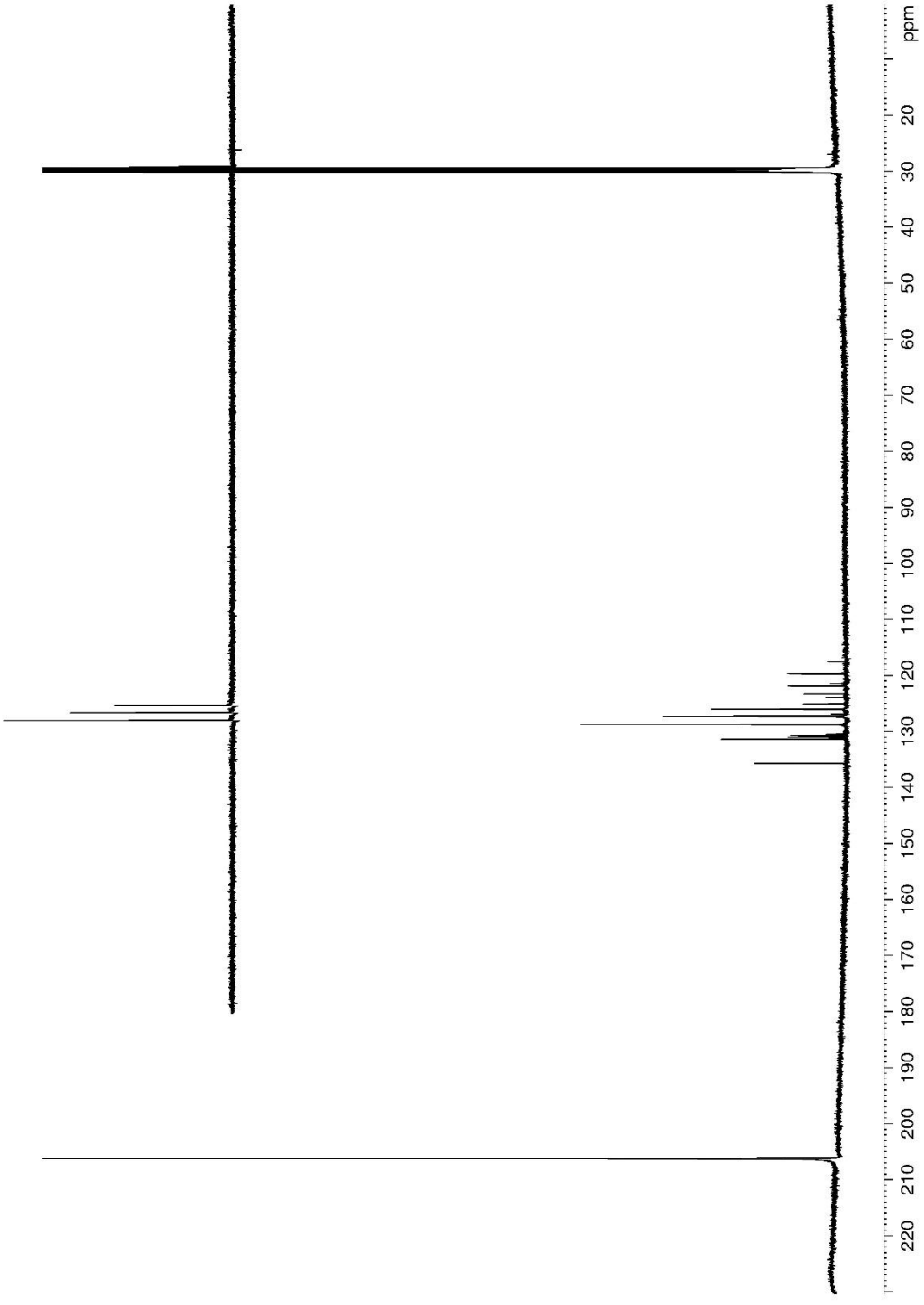

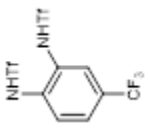

Figure 66. ^{19}F NMR (282 MHz, $(CD_3)_2CO$) of **203**

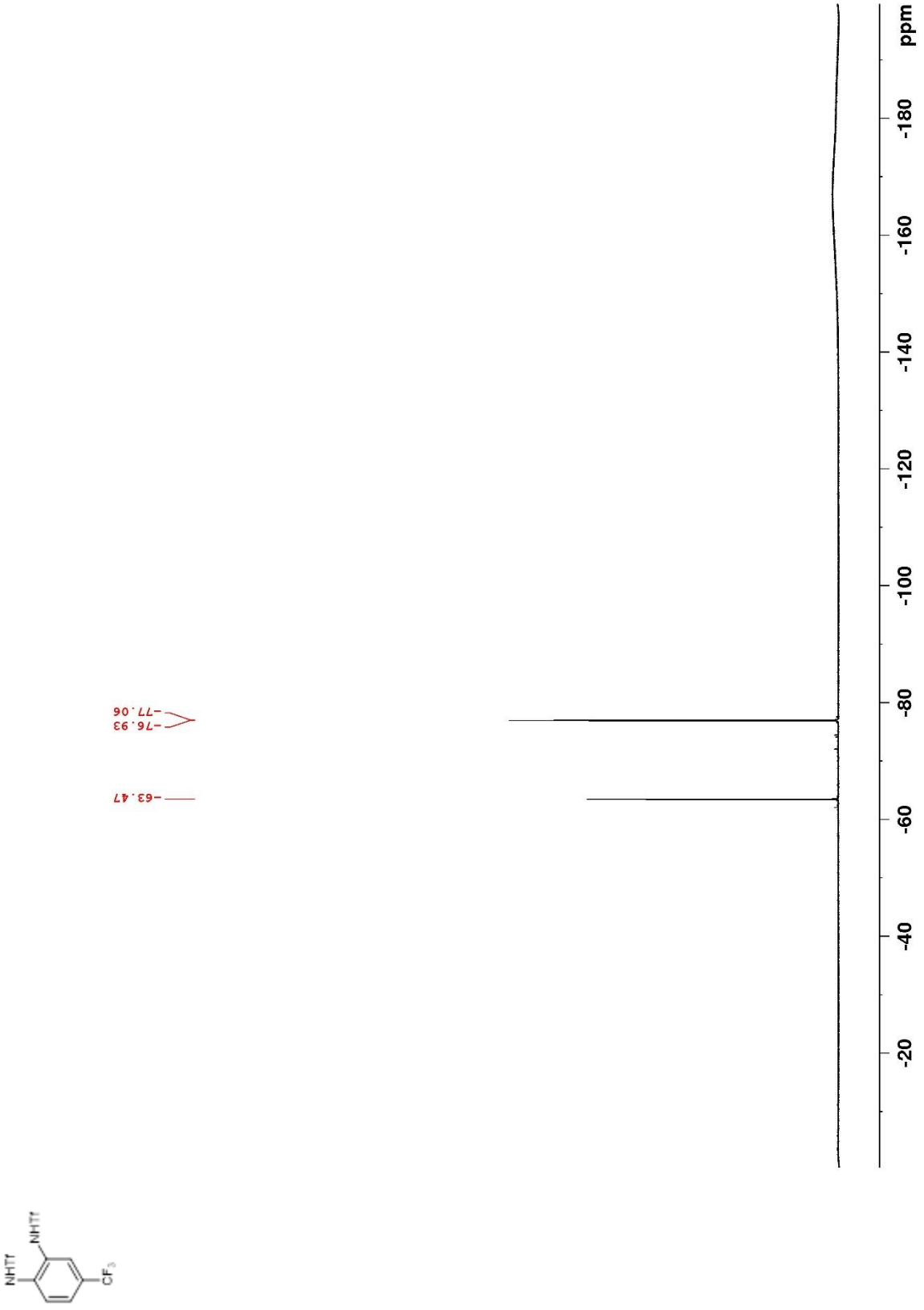

Figure 67. ^{1}H NMR (400 MHz, $(CD_3)_2CO$) of **S8**

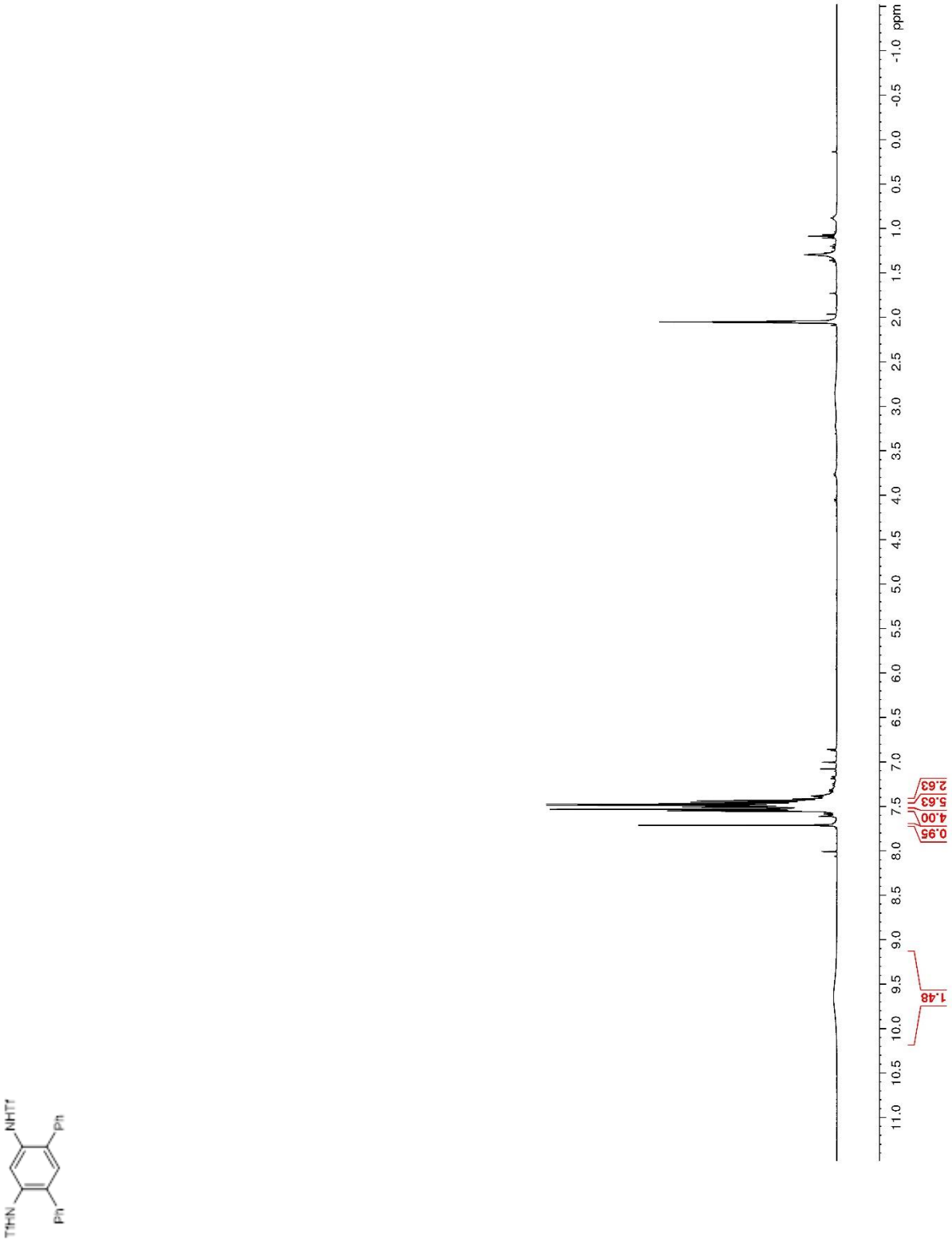

Figure 68. ^{13}C NMR (100 MHz, $(CD_3)_2CO$) of **S8**

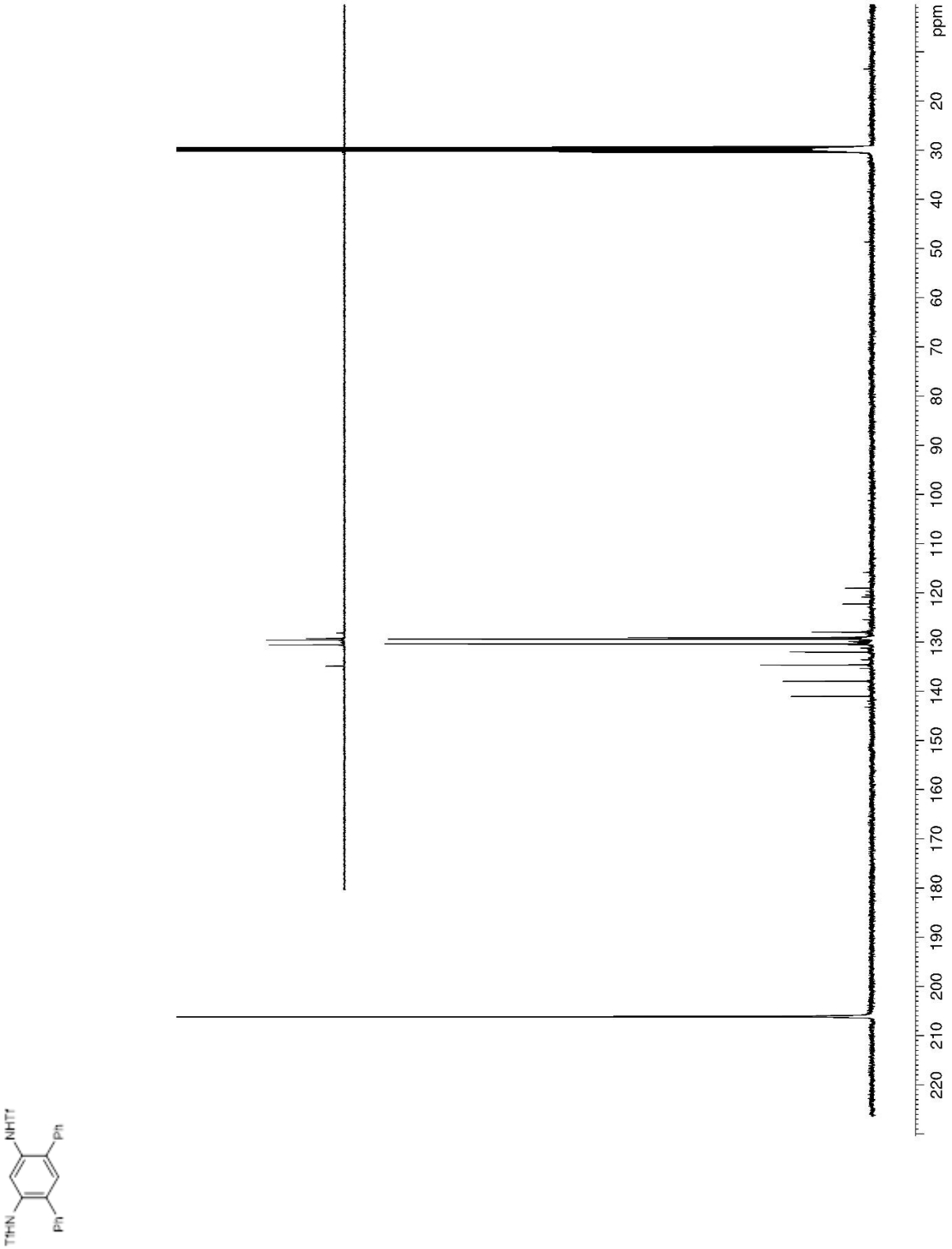

Figure 69. ^{19}F NMR (282 MHz, $(CD_3)_2CO$) of **S8**

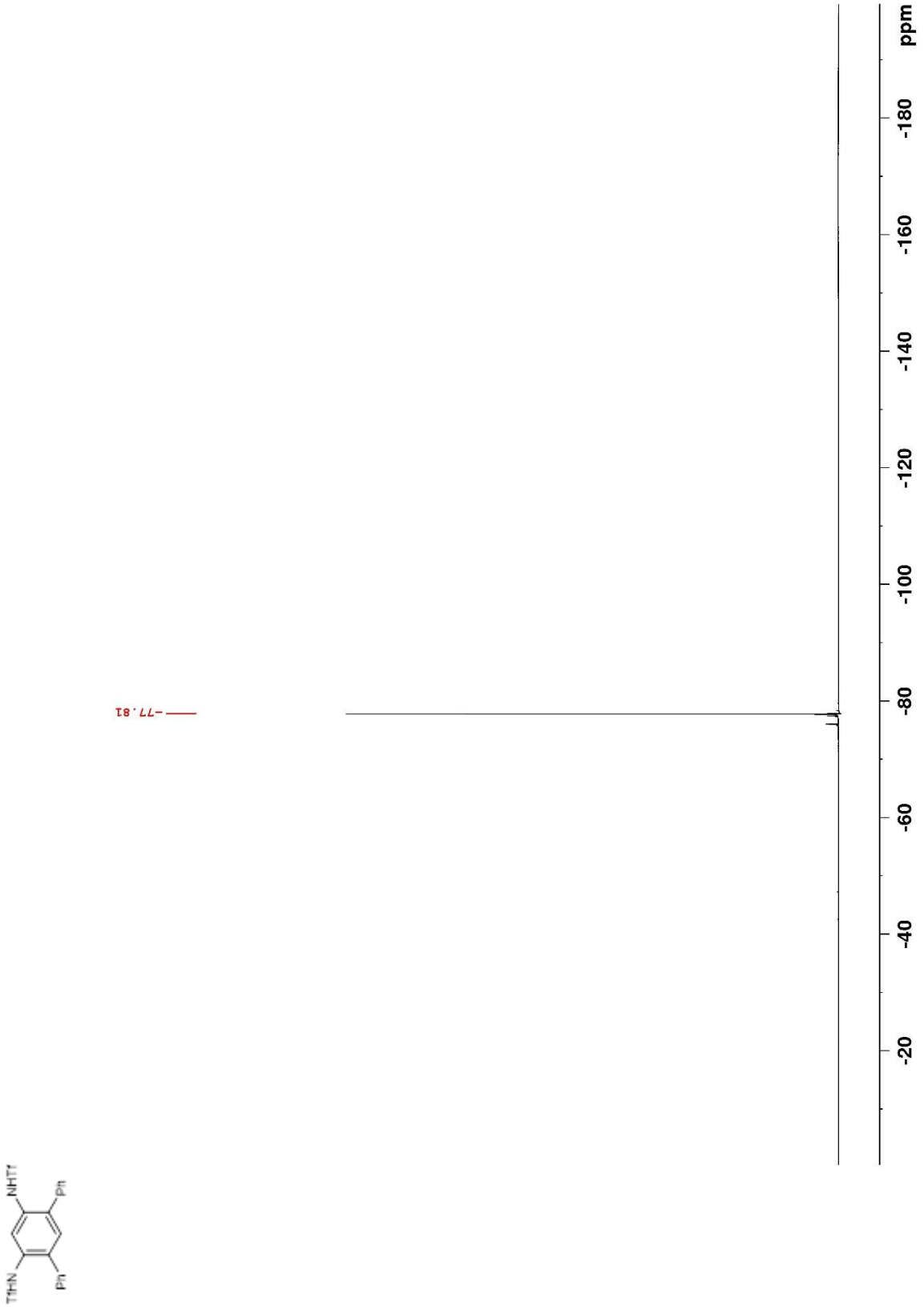

Figure 70. ^{1}H NMR (400 MHz, $(CD_3)_2CO$) of **206**

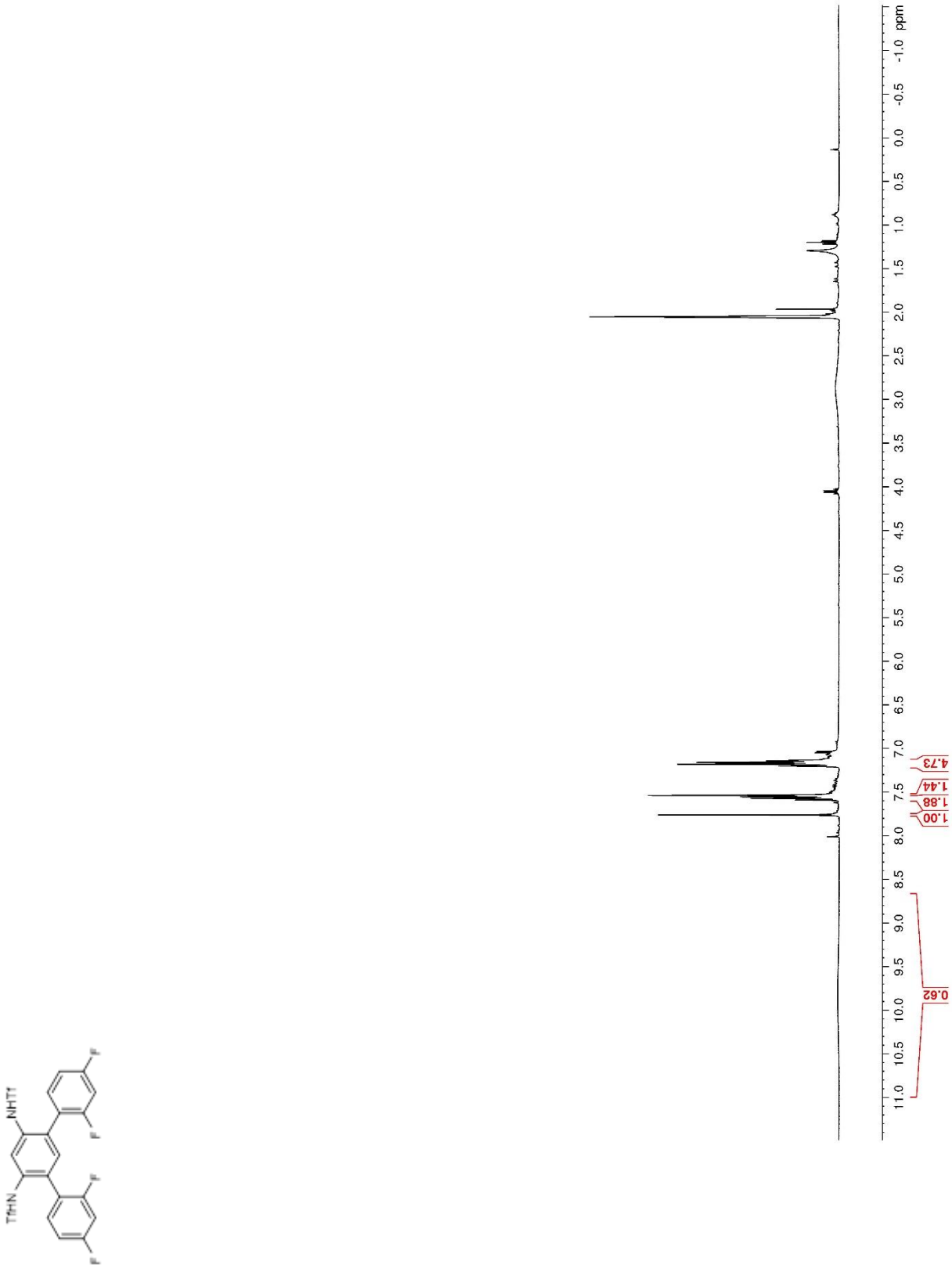

Figure 71. ^{13}C NMR (150 MHz, $(CD_3)_2CO$) of **206**

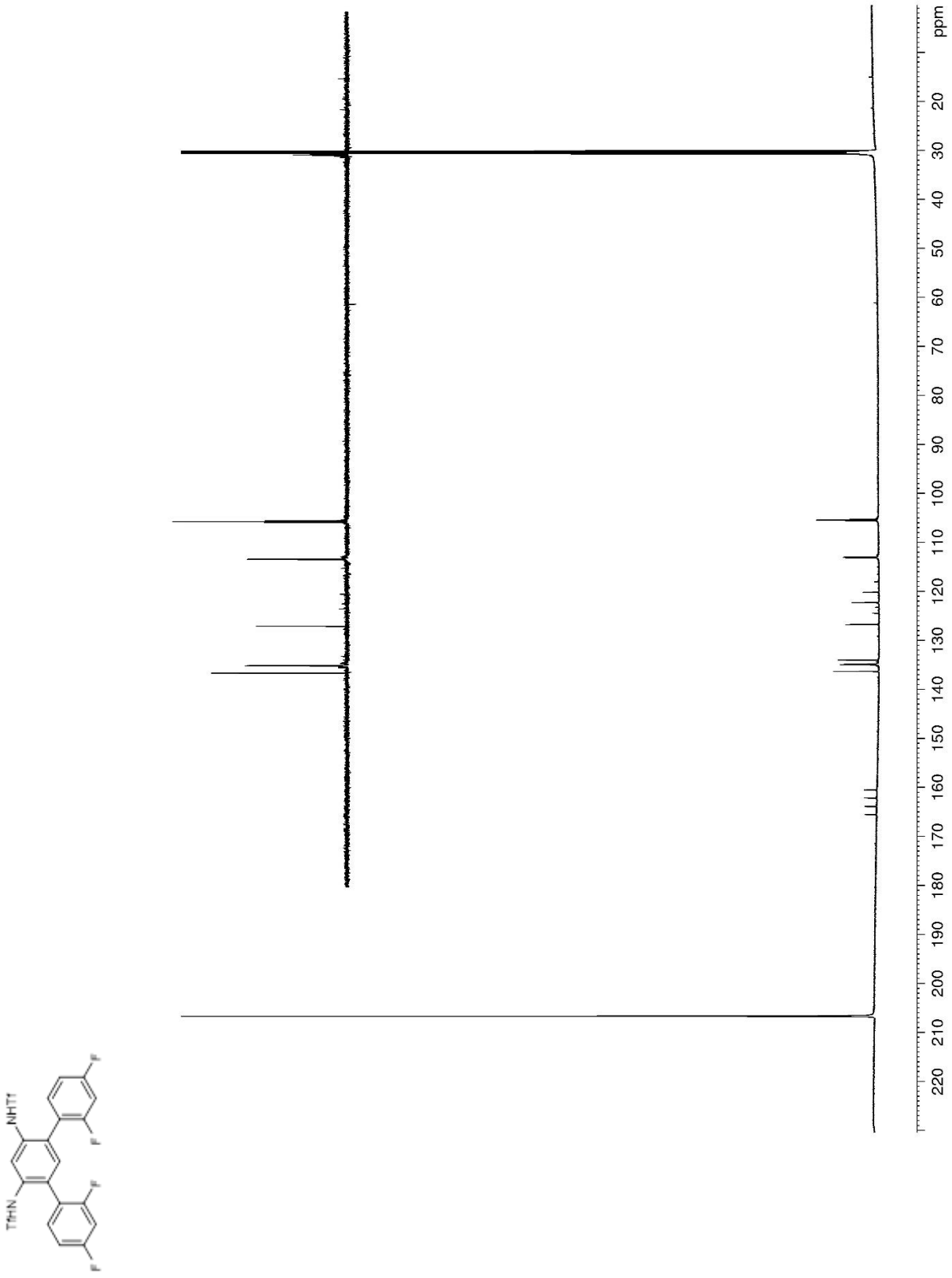

Figure 72. ^{19}F NMR (282 MHz, $(CD_3)_2CO$) of **206**

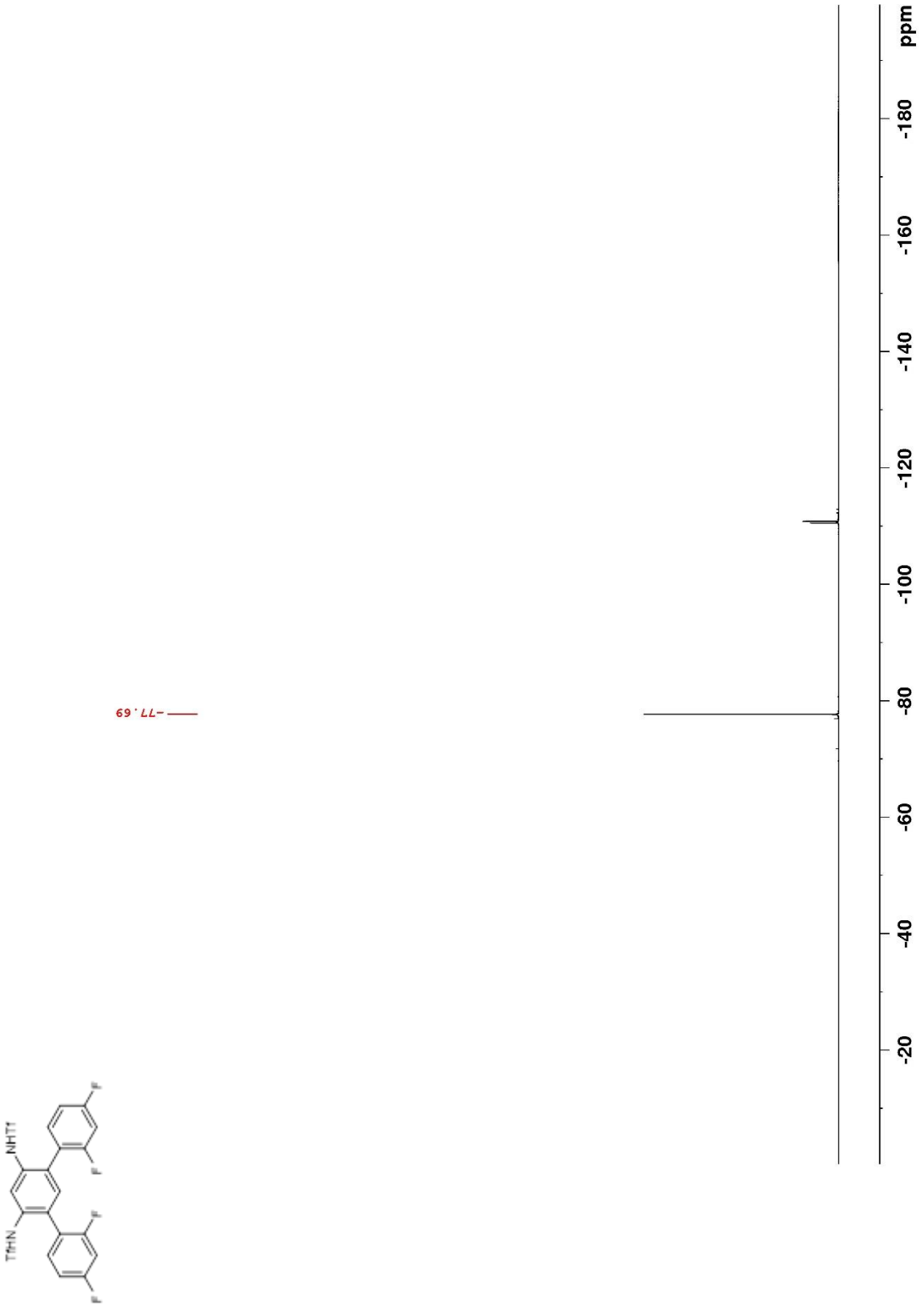

Figure 73. ^{1}H NMR (400 MHz, $(CD_3)_2CO$) of **208**

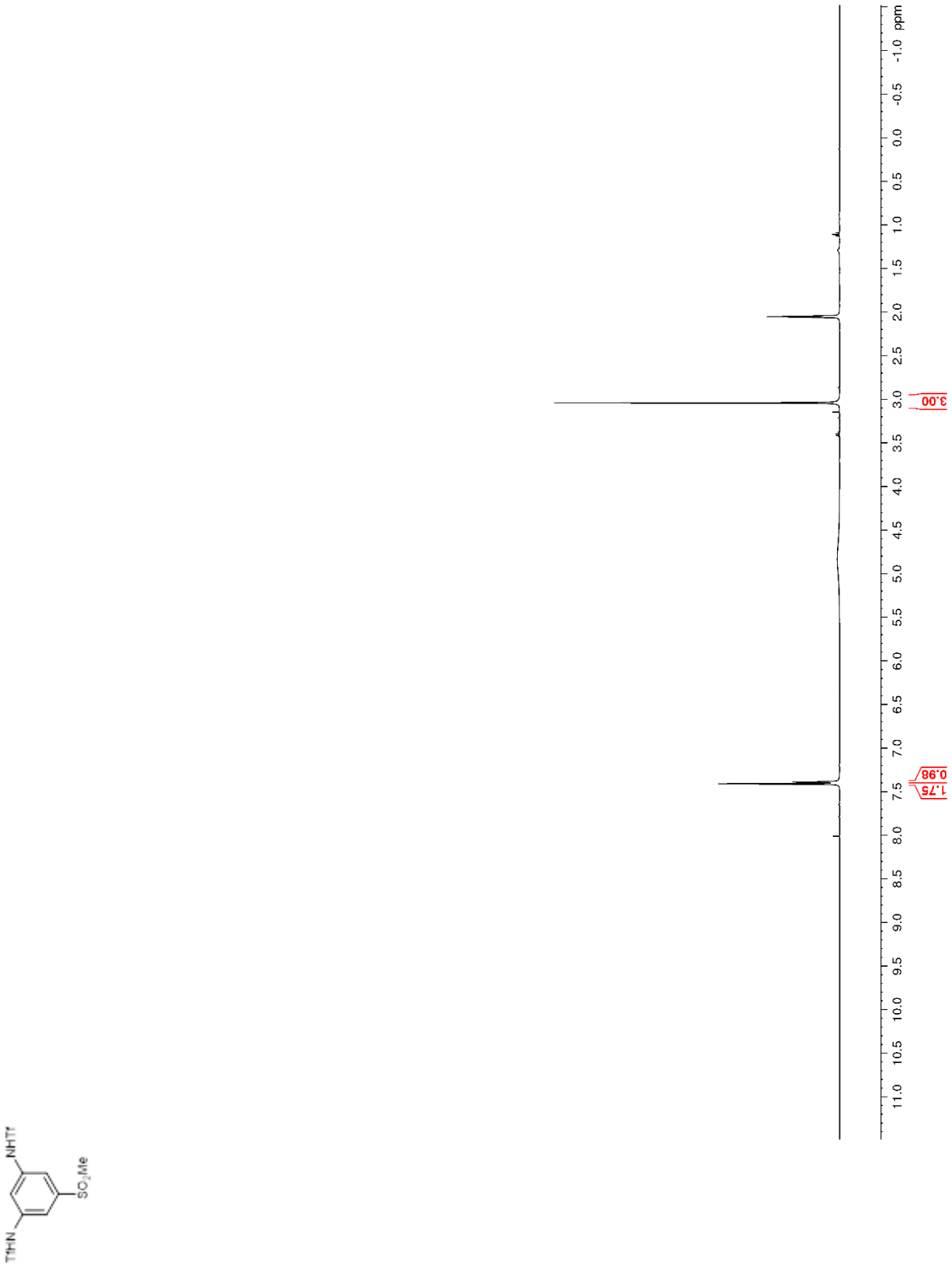

Figure 74. ^{13}C NMR (100 MHz, $(CD_3)_2CO$) of **208**

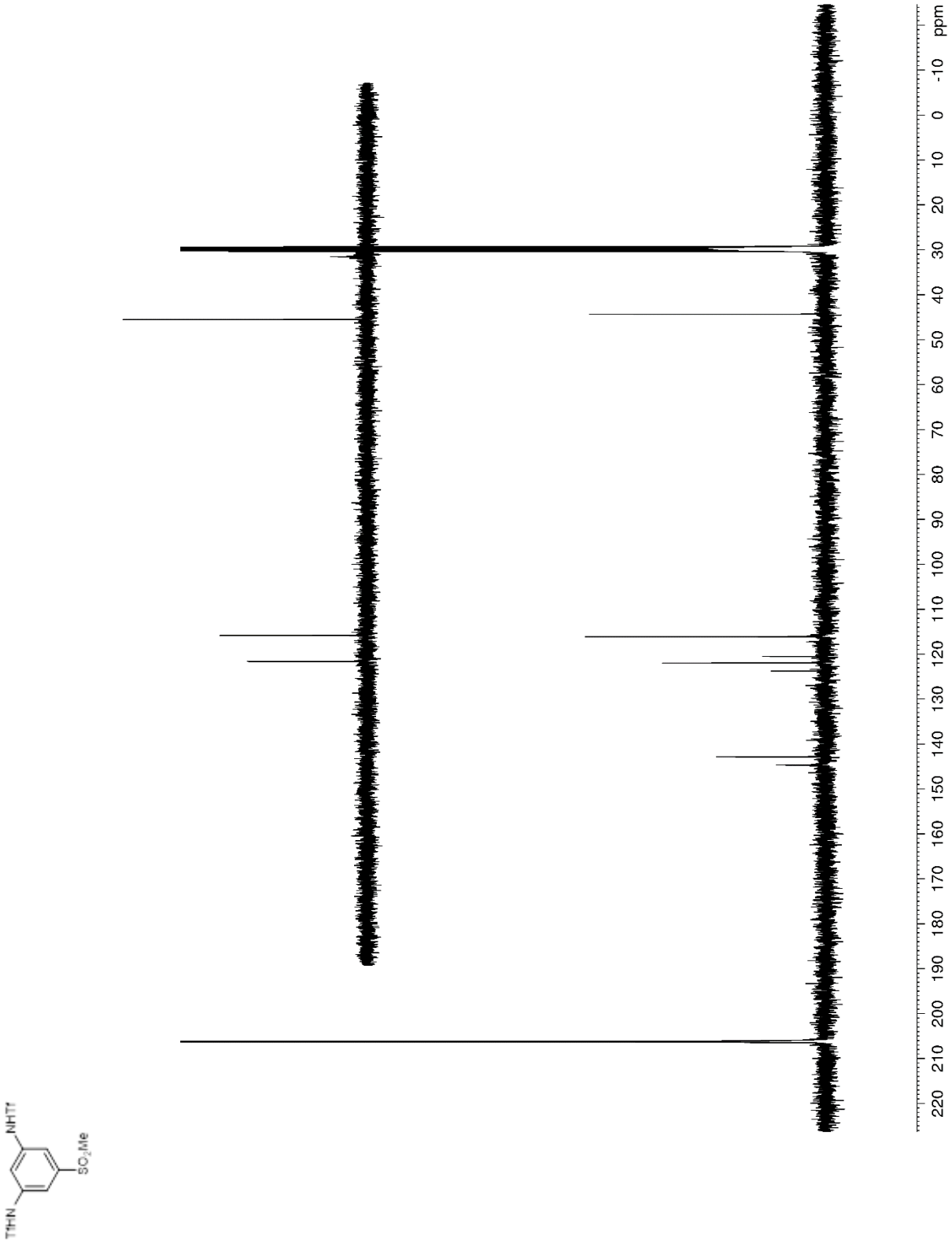

Figure 75. ^{19}F NMR (282 MHz, $(CD_3)_2CO$) of **208**

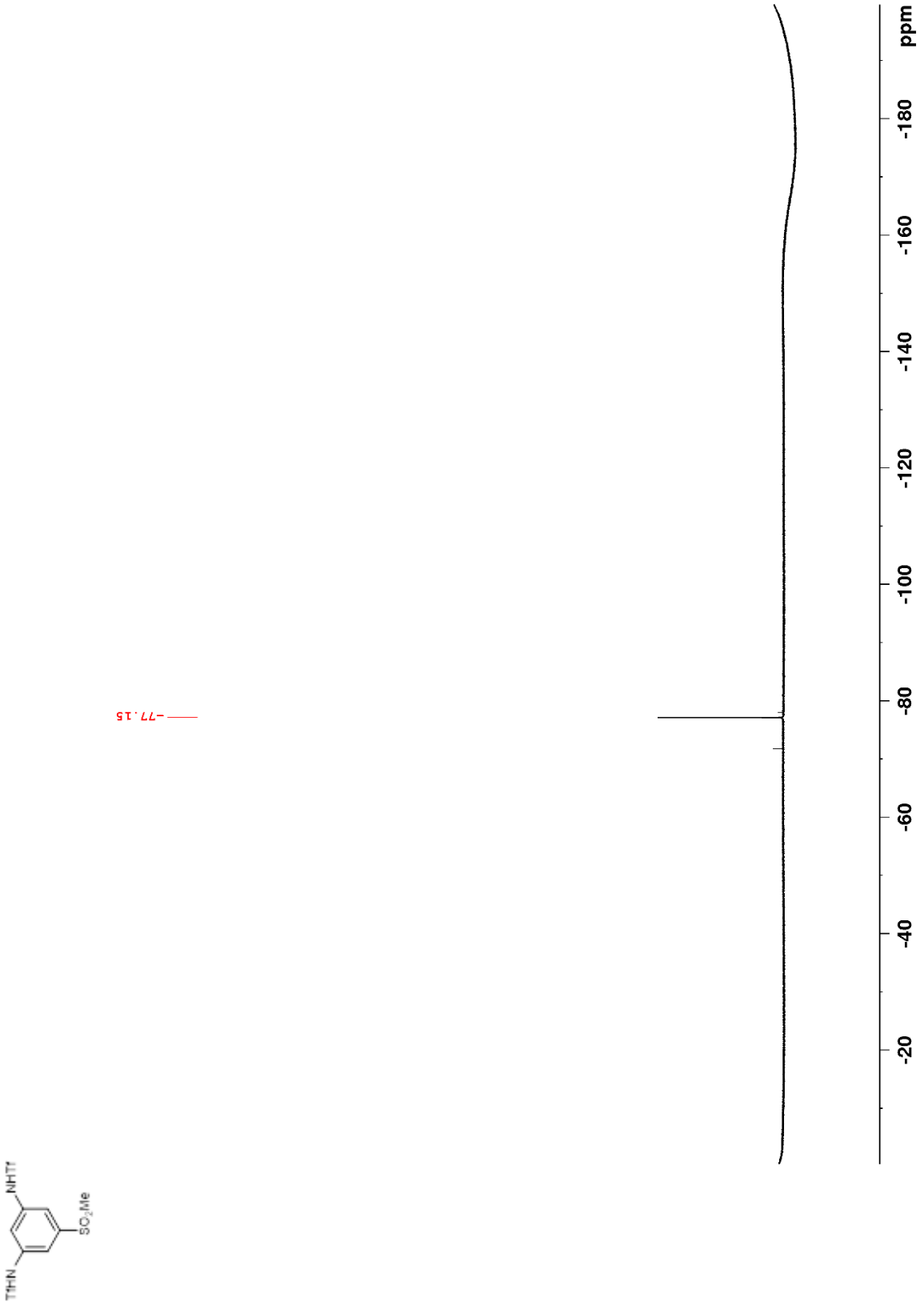

Figure 76. ^{1}H NMR (400 MHz, $(CD_3)_2CO$) of **207**

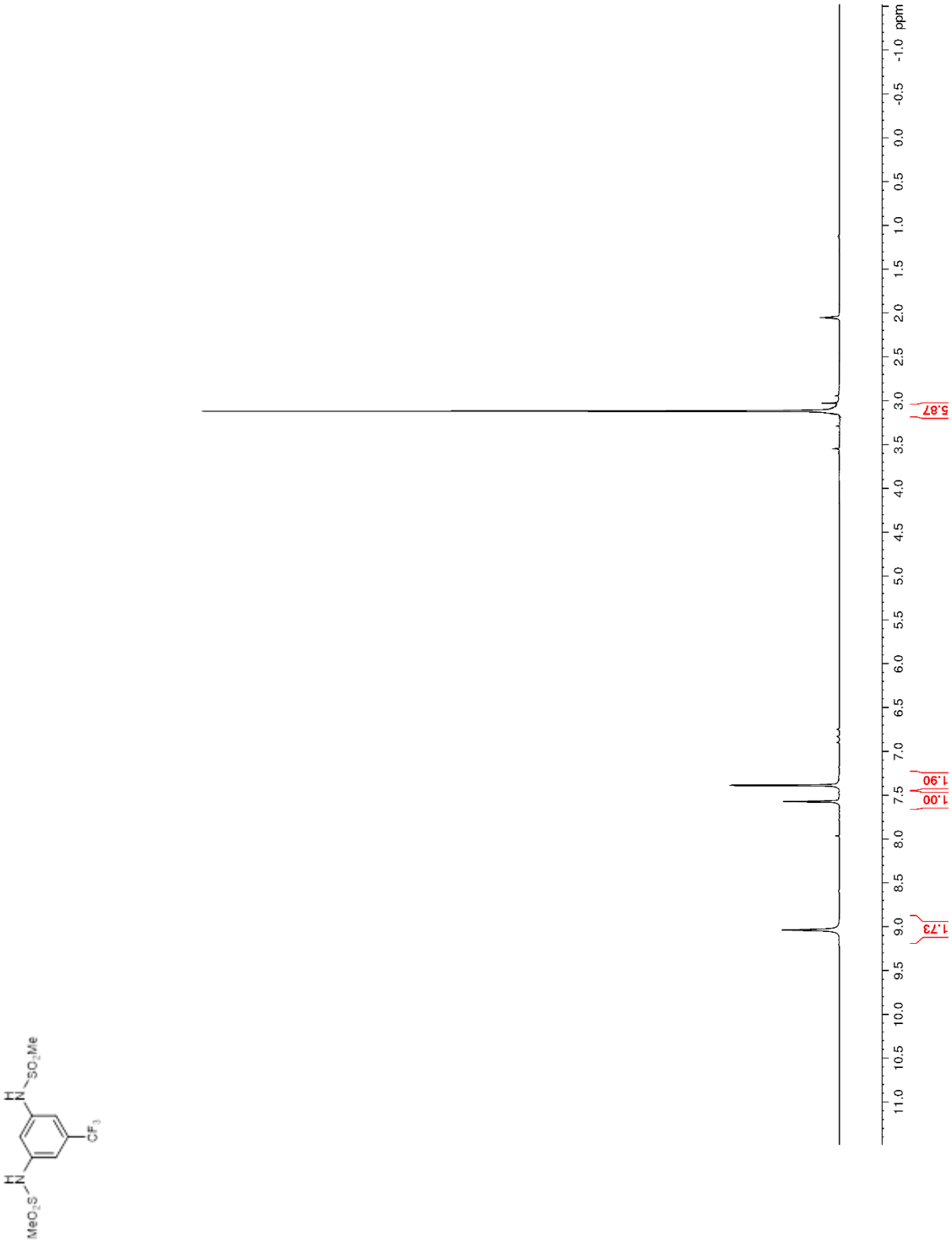

Figure 77. ^{13}C NMR (100 MHz, $(CD_3)_2CO$) of **207**

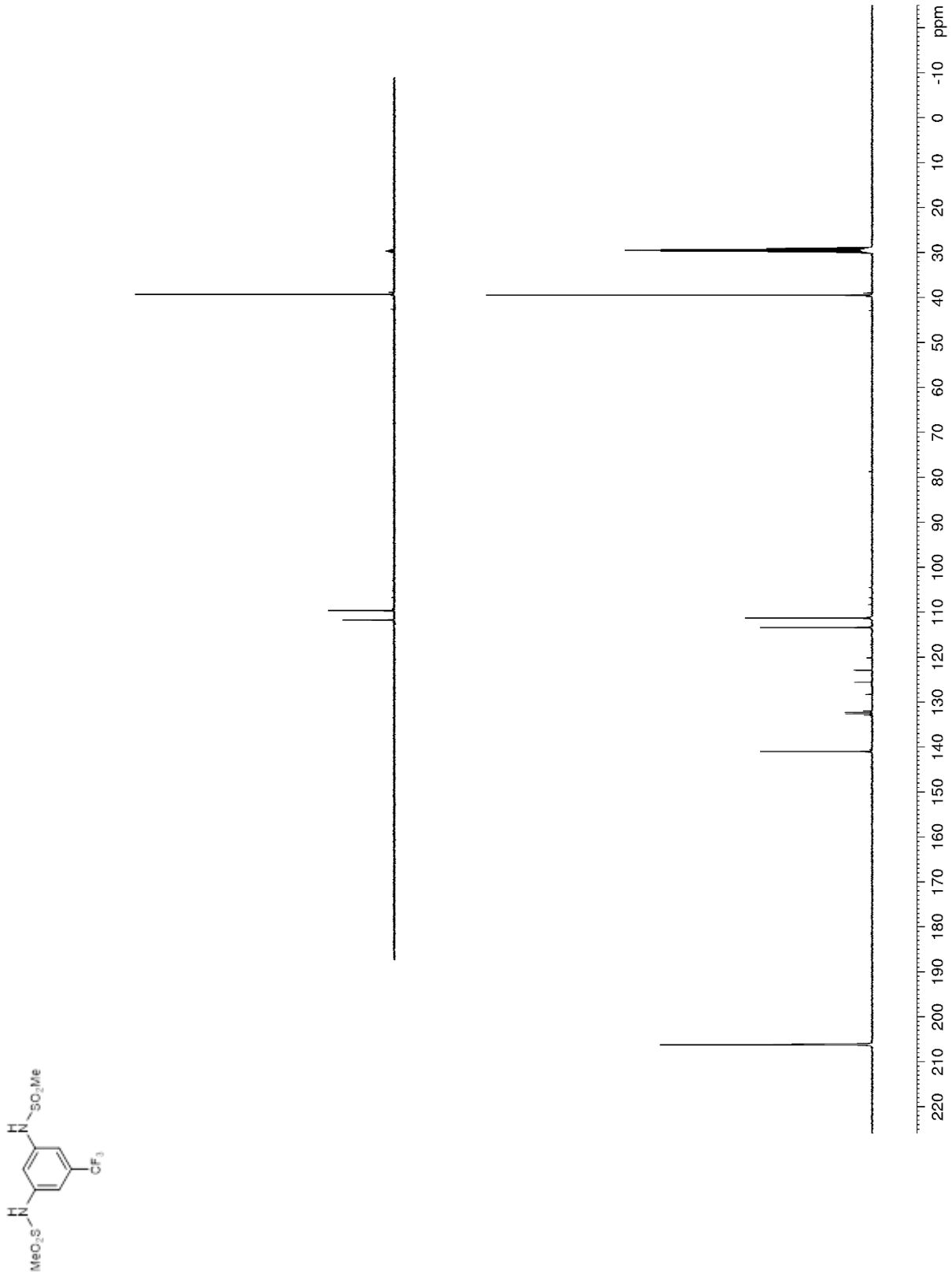

Figure 78. ^{19}F NMR (282 MHz, $(CD_3)_2CO$) of **207**

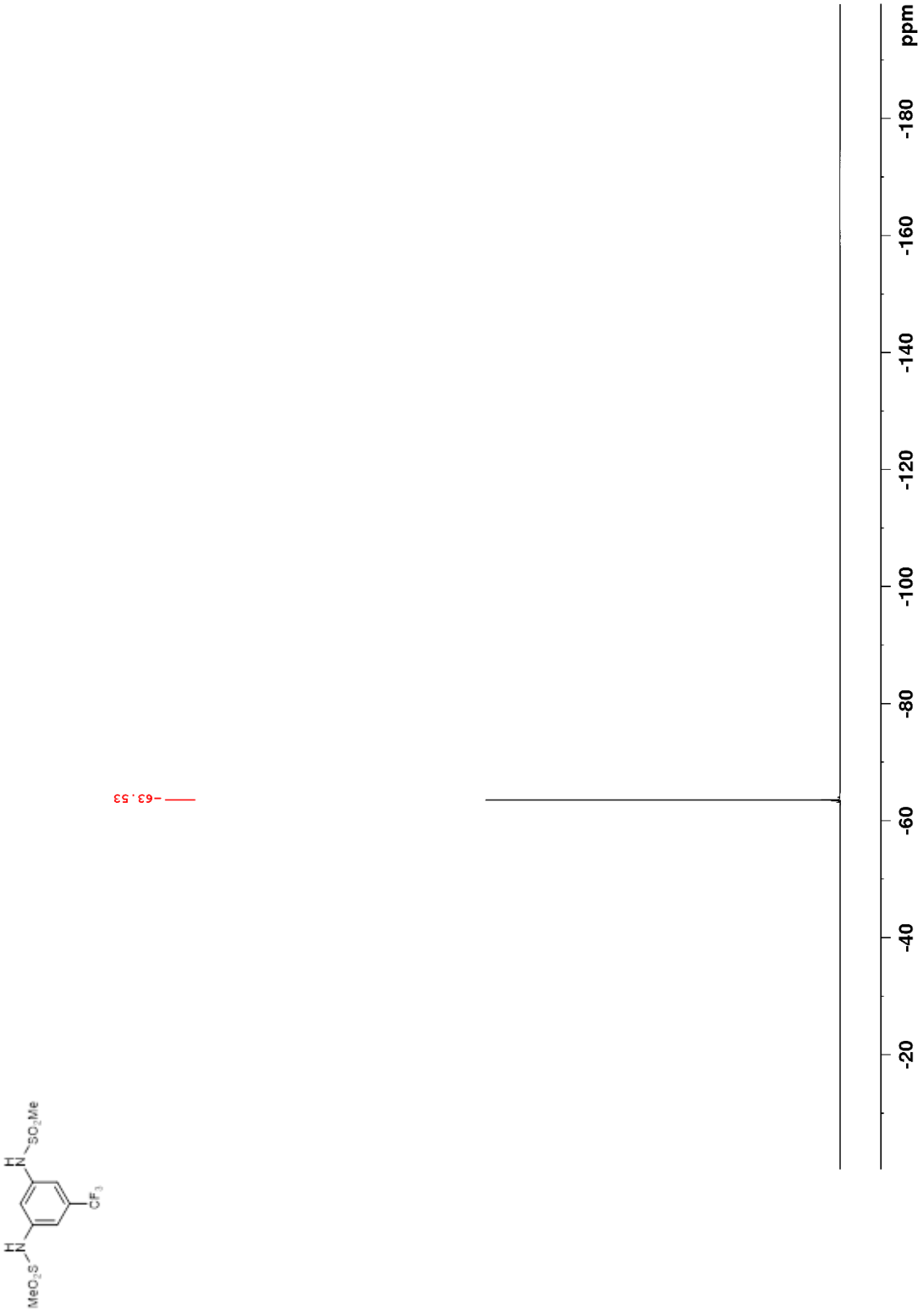

Figure 79. ^{1}H NMR (400 MHz, $(CD_3)_2CO$) of **S9**

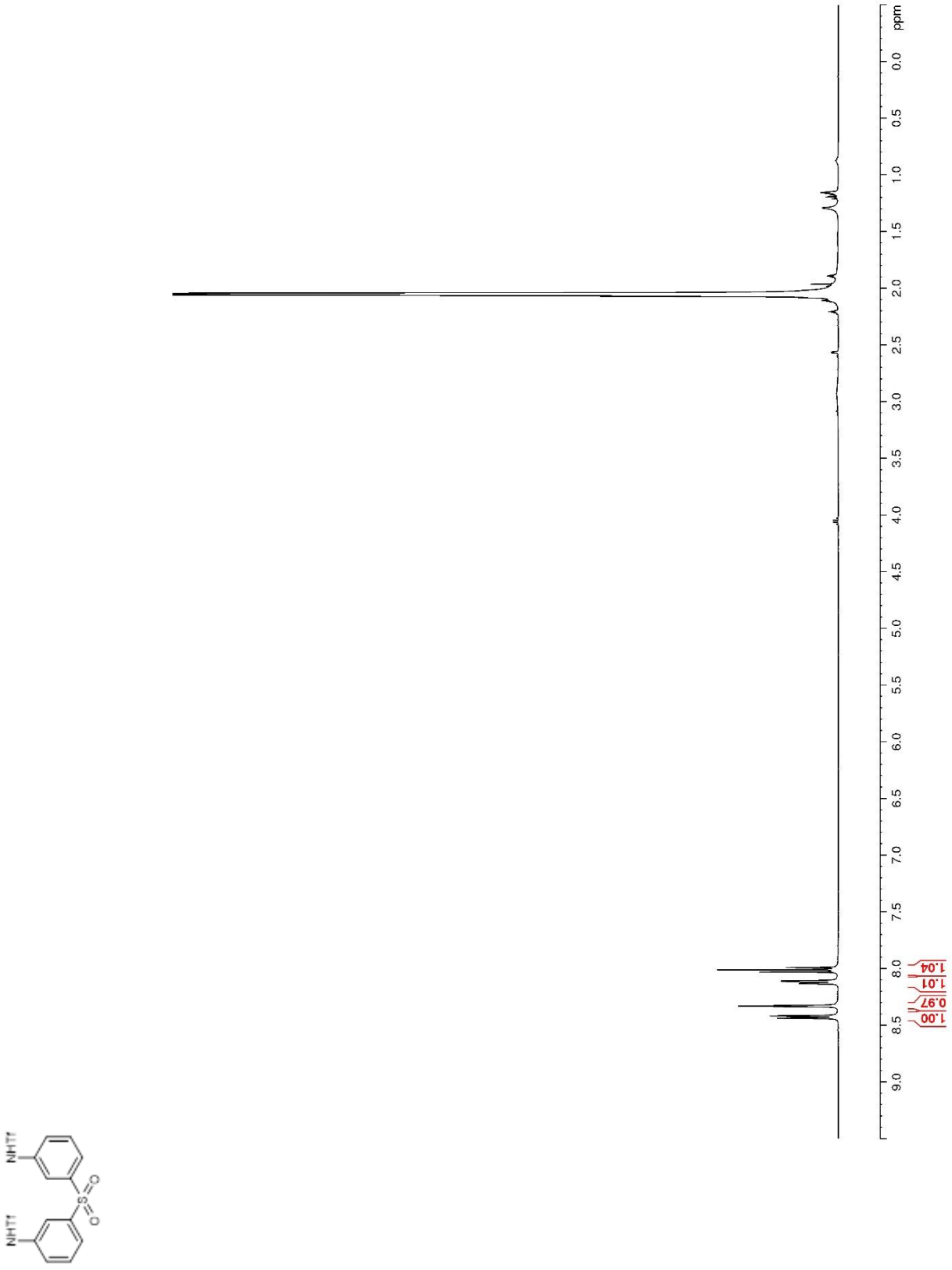

Figure 80. ^{13}C NMR (100 MHz, $(CD_3)_2CO$) of **S9**

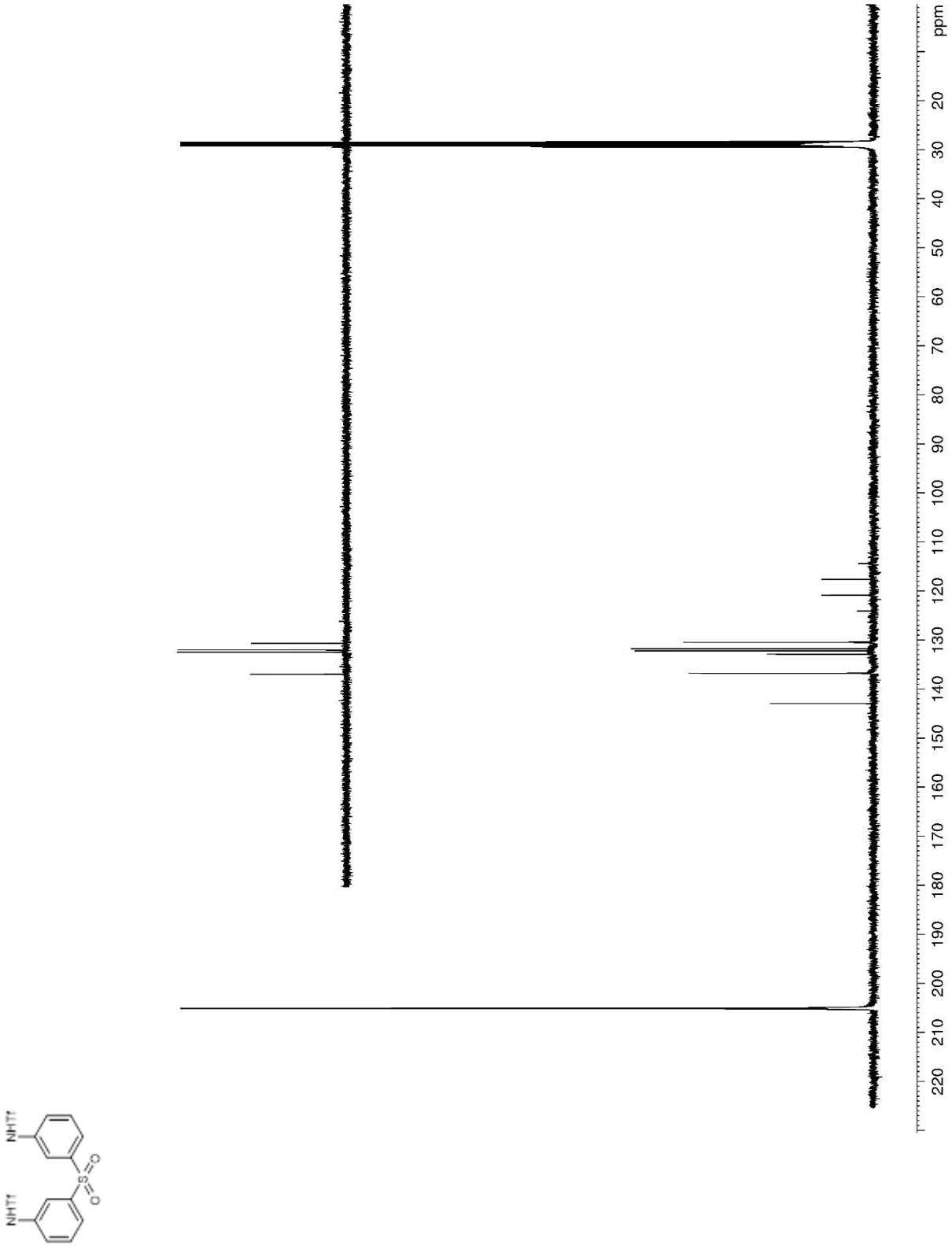

Figure 81. ^{19}F NMR (282 MHz, $(CD_3)_2CO$) of **S9**

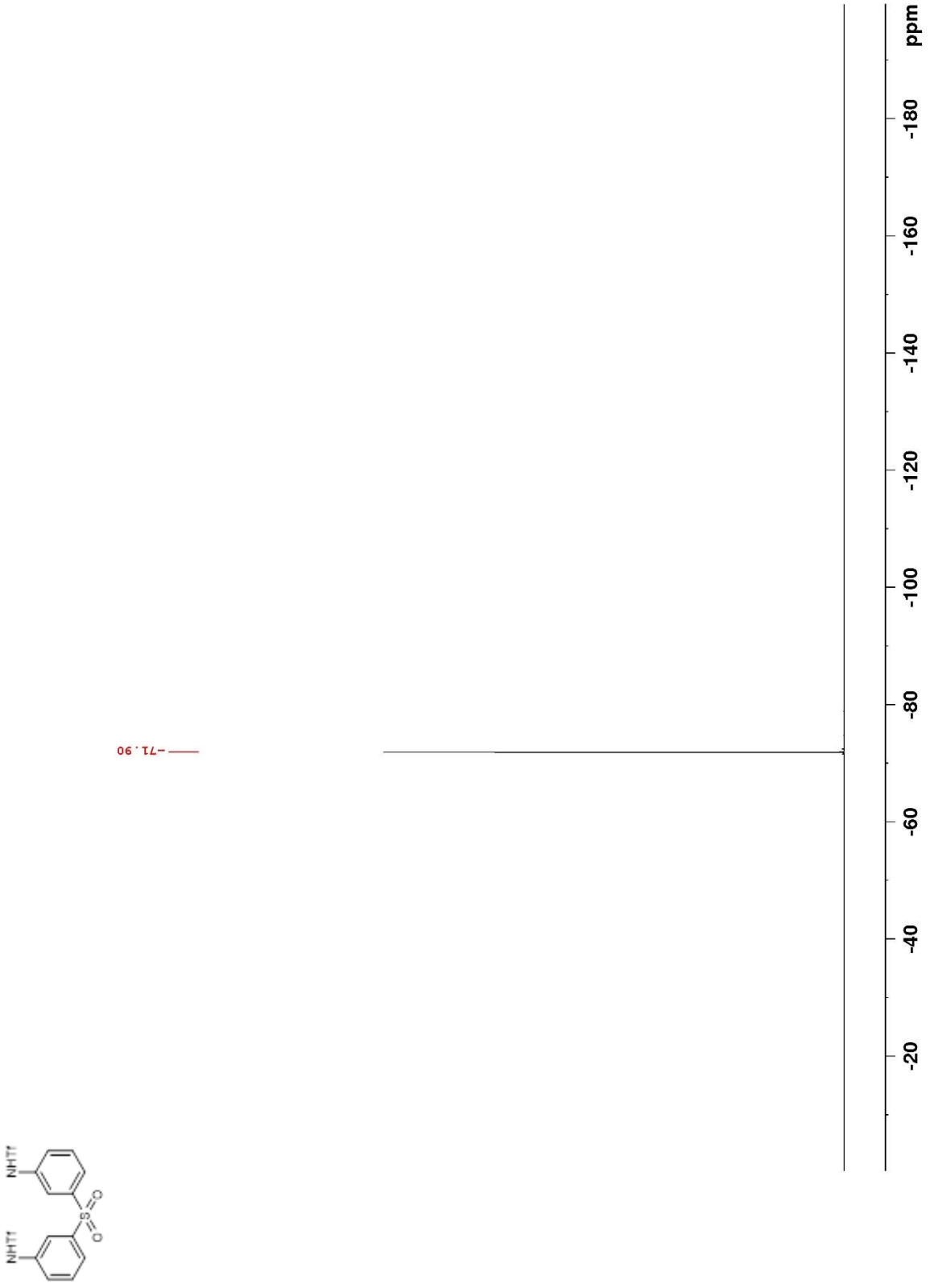

Figure 82. ^{1}H NMR (400 MHz, $(CD_3)_2CO$) of **211**

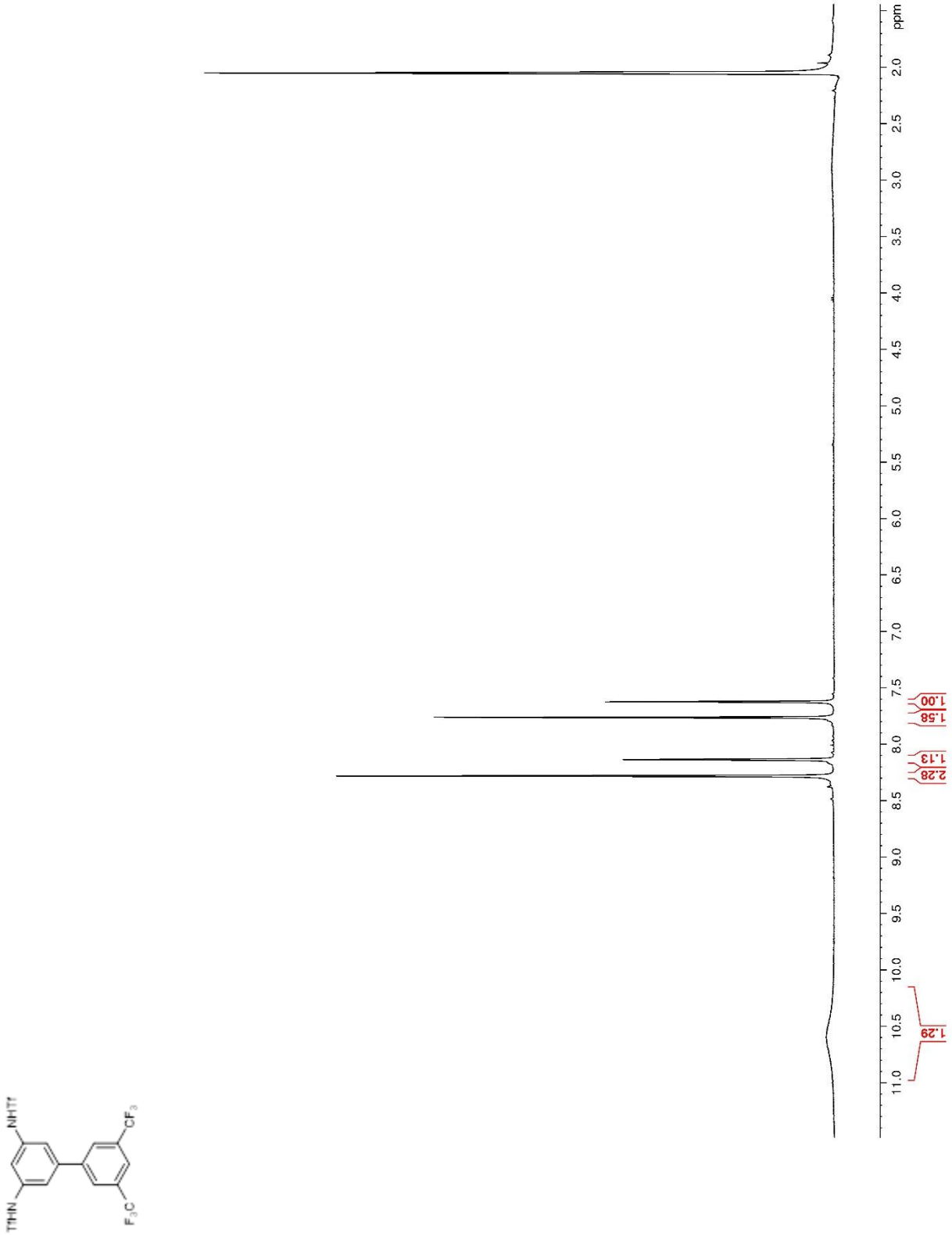

Figure 83. ^{13}C NMR (100 MHz, $(CD_3)_2CO$) of **211**

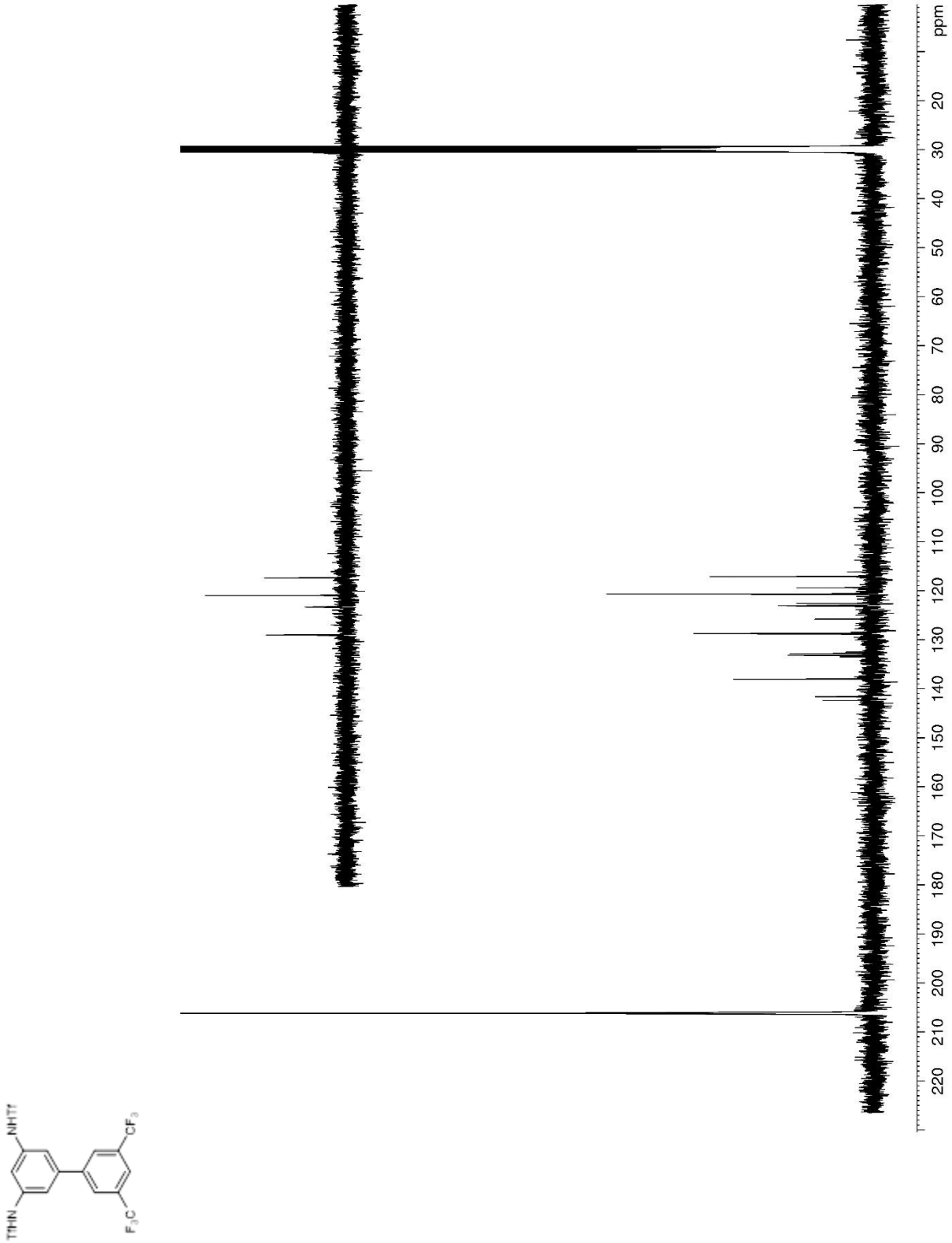

Figure 84. ^{19}F NMR (282 MHz, $(CD_3)_2CO$) of **211**

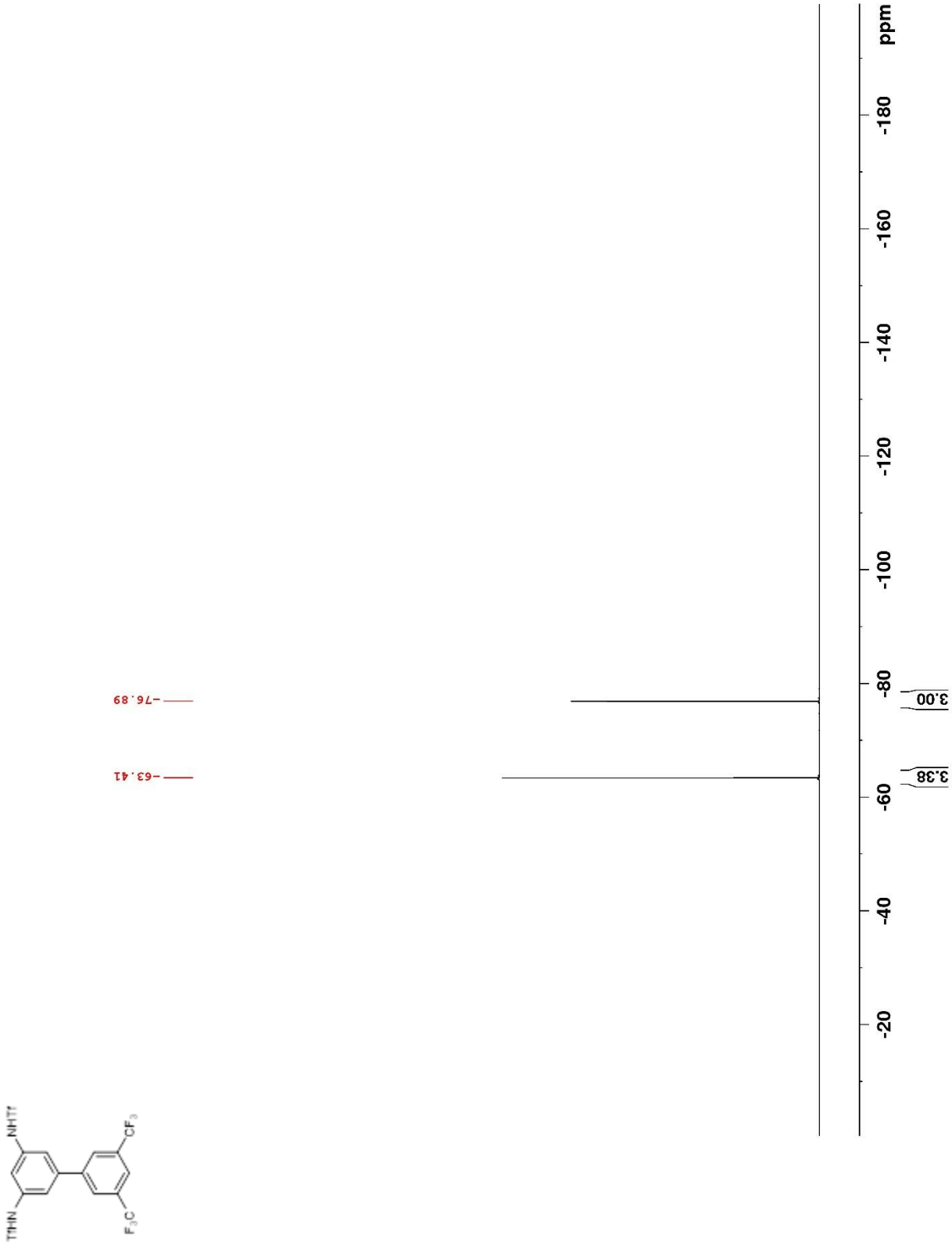

Figure 85. ^{1}H NMR (400 MHz, $(CD_3)_2CO$) of **209**

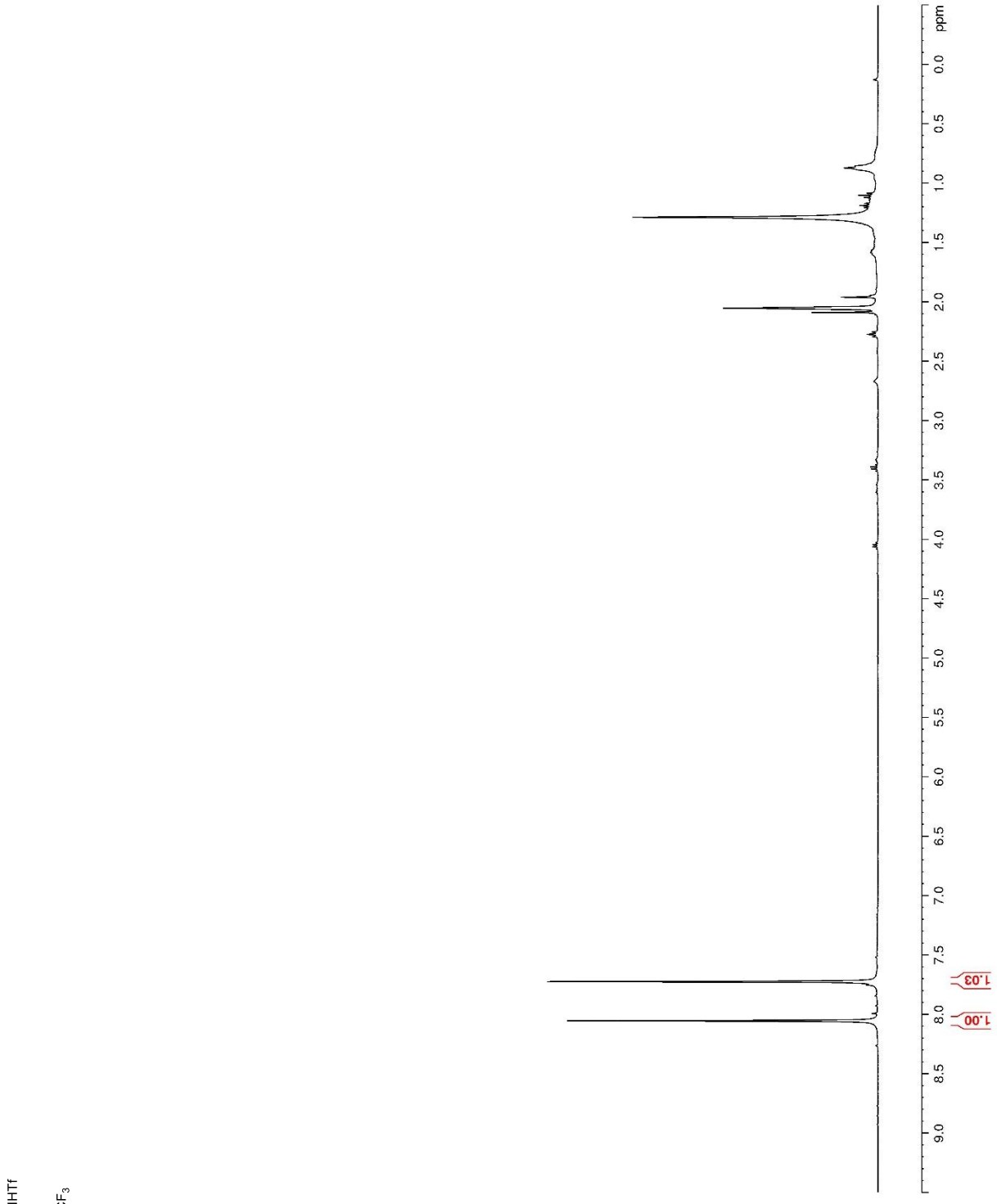

Figure 86. ^{13}C NMR (100 MHz, $(CD_3)_2CO$) of **209**

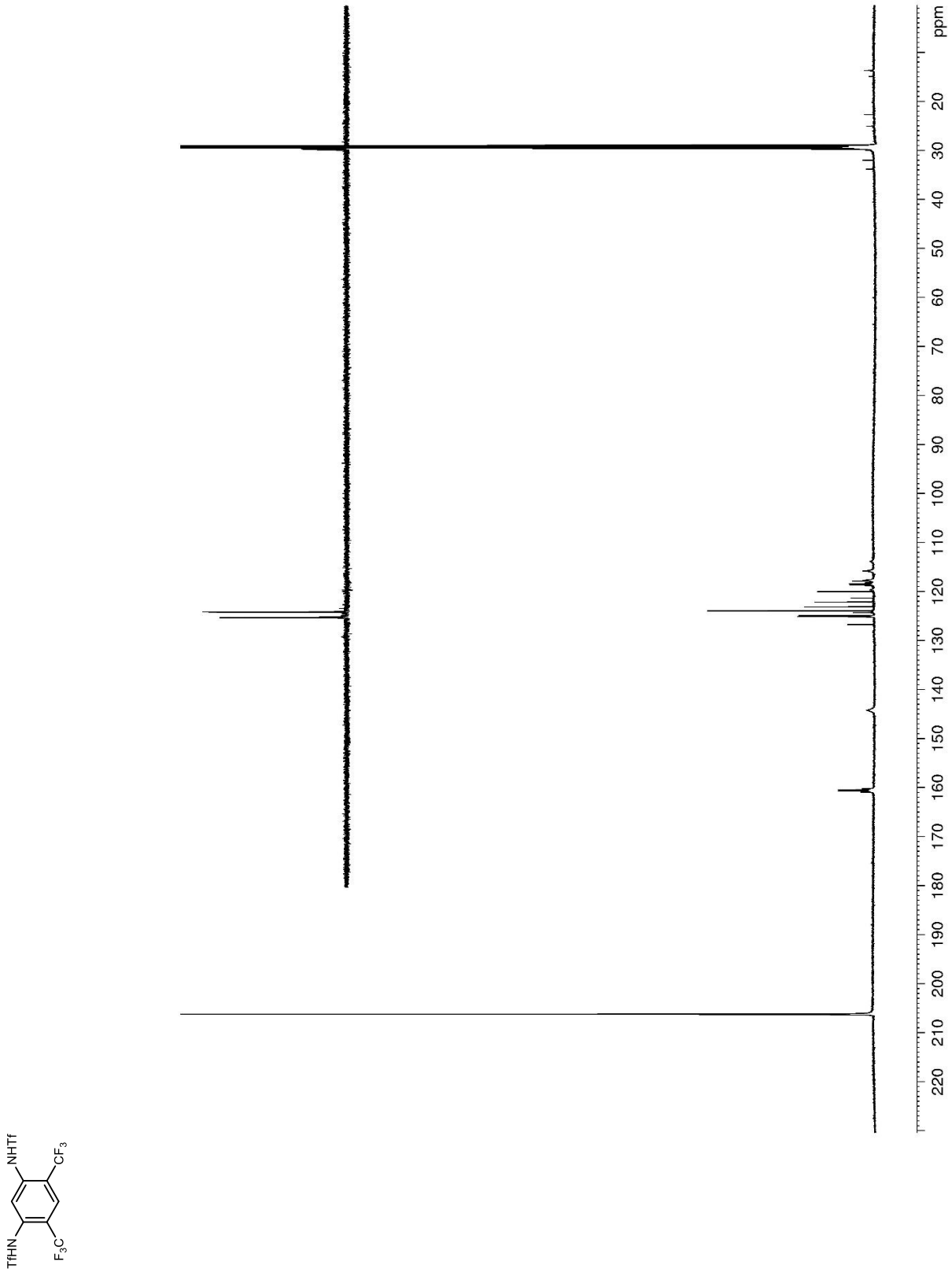

Figure 87. ^{19}F NMR (282 MHz, $(CD_3)_2CO$) of **209**

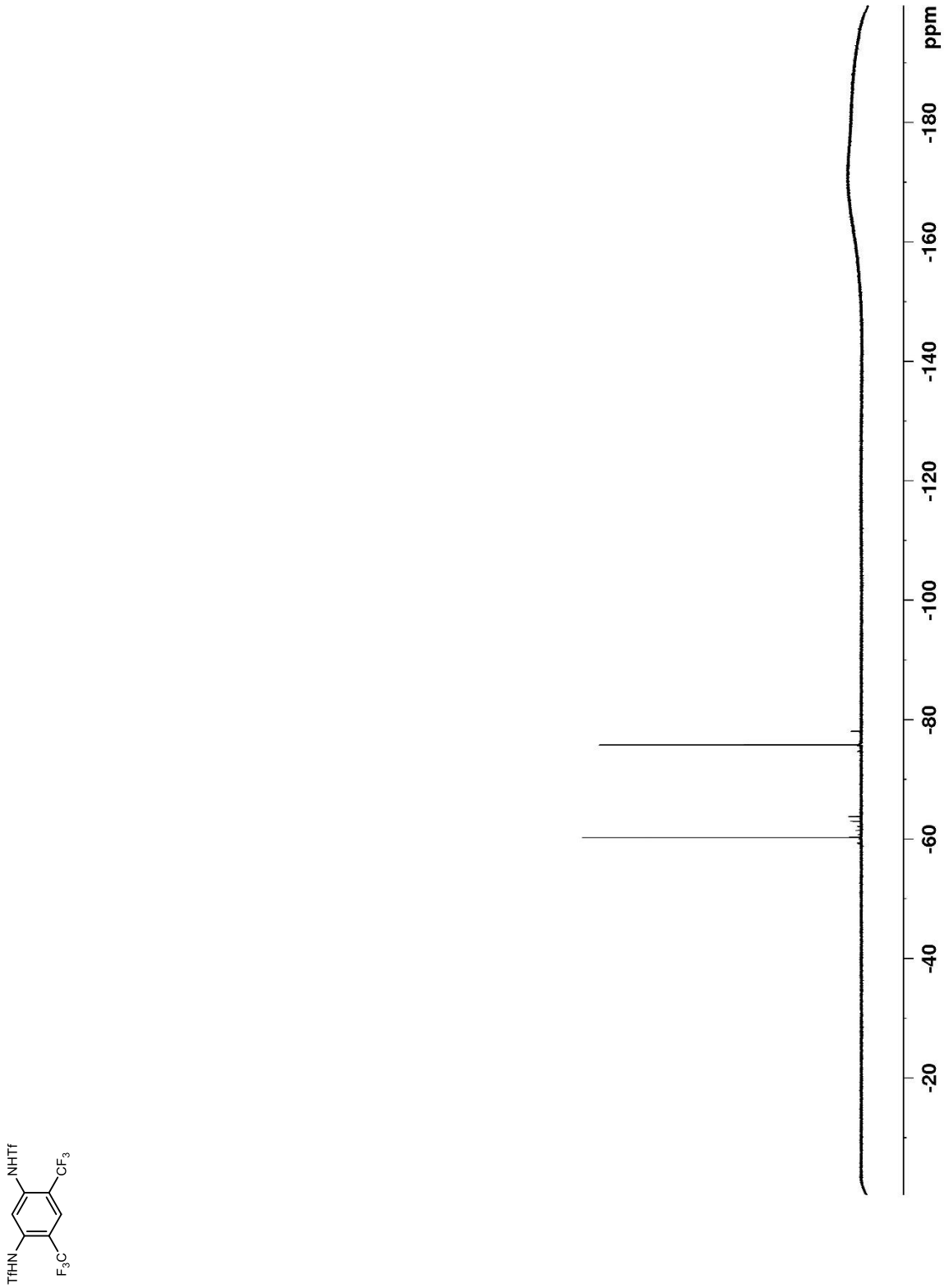

Figure 88. ^{1}H NMR (400 MHz, $(CD_3)_2CO$) of **210**

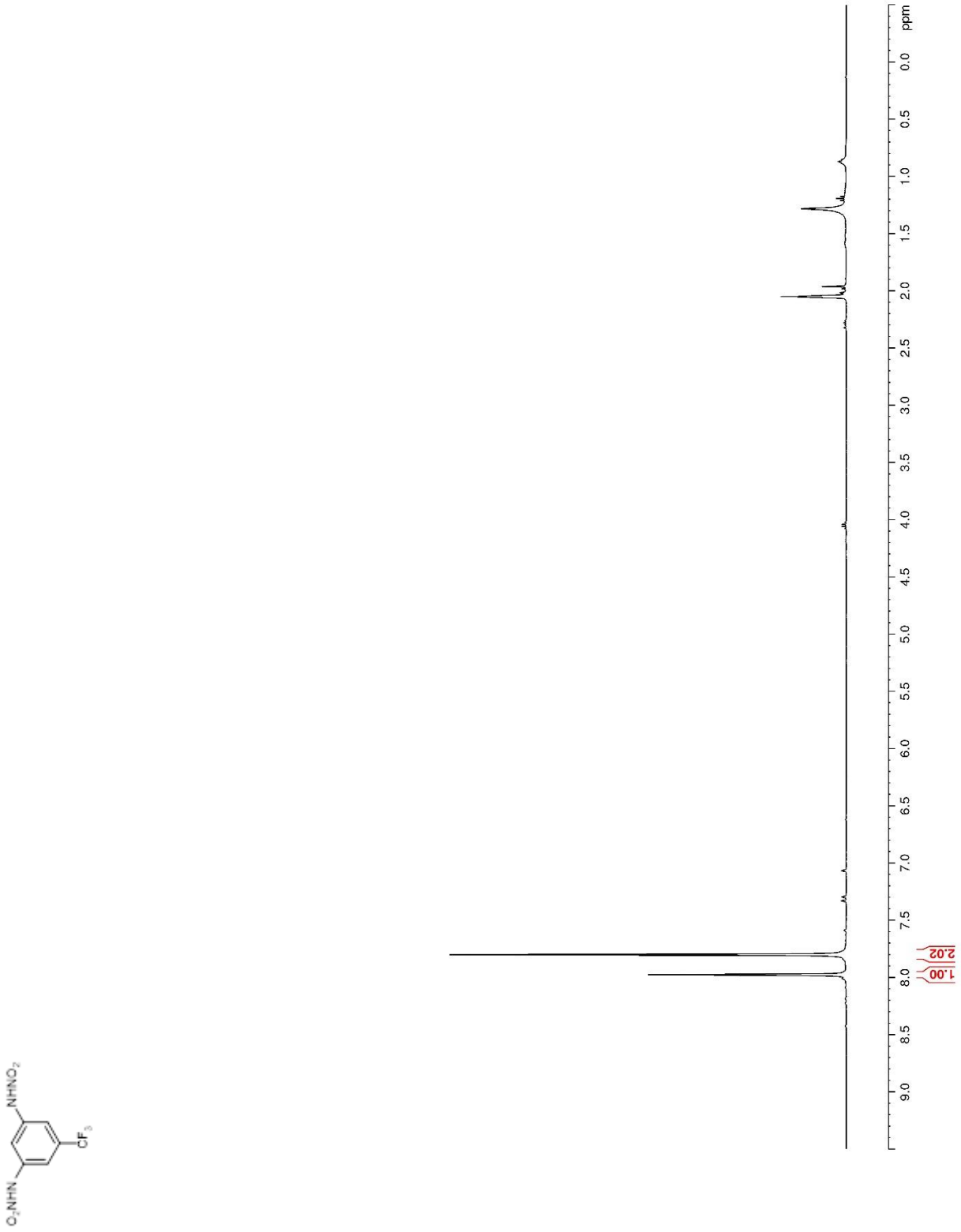

Figure 89. ^{13}C NMR (150 MHz, $(CD_3)_2CO$) of **210**

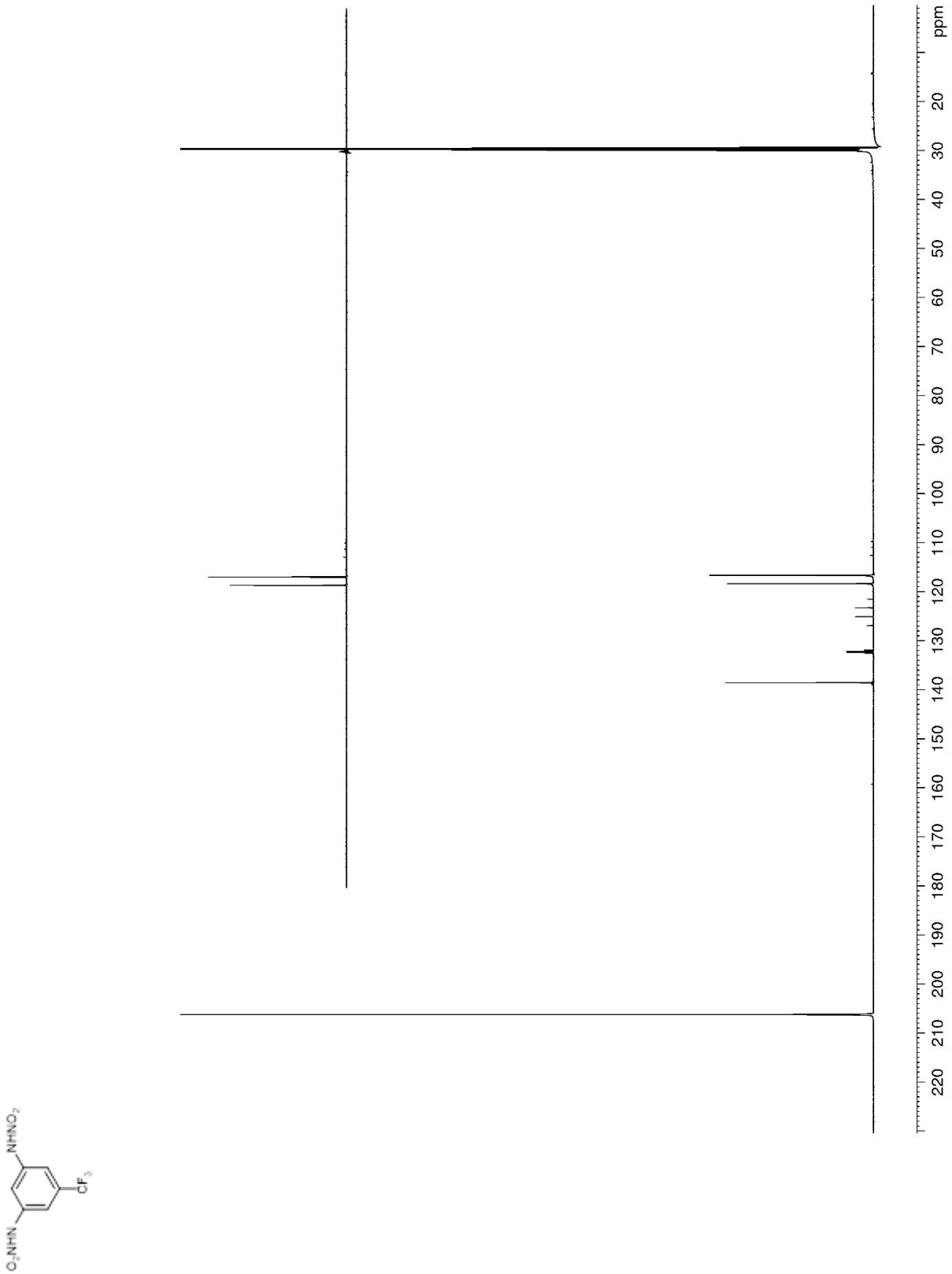

Figure 90. ^{19}F NMR (282 MHz, $(CD_3)_2CO$) of **210**

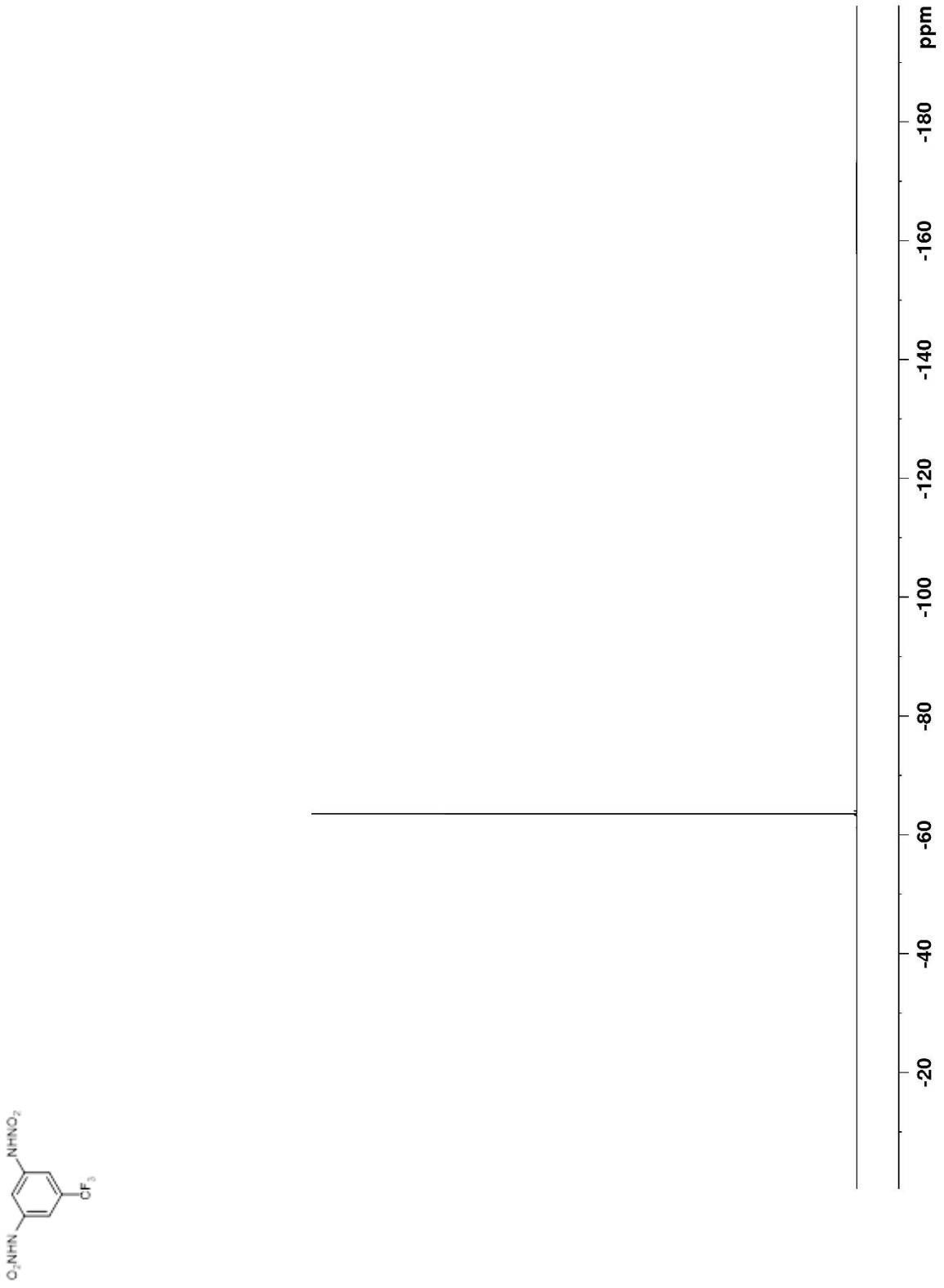

Figure 91. ^{1}H NMR (**400 MHz,** $(CD_3)_2CO$) of **207**

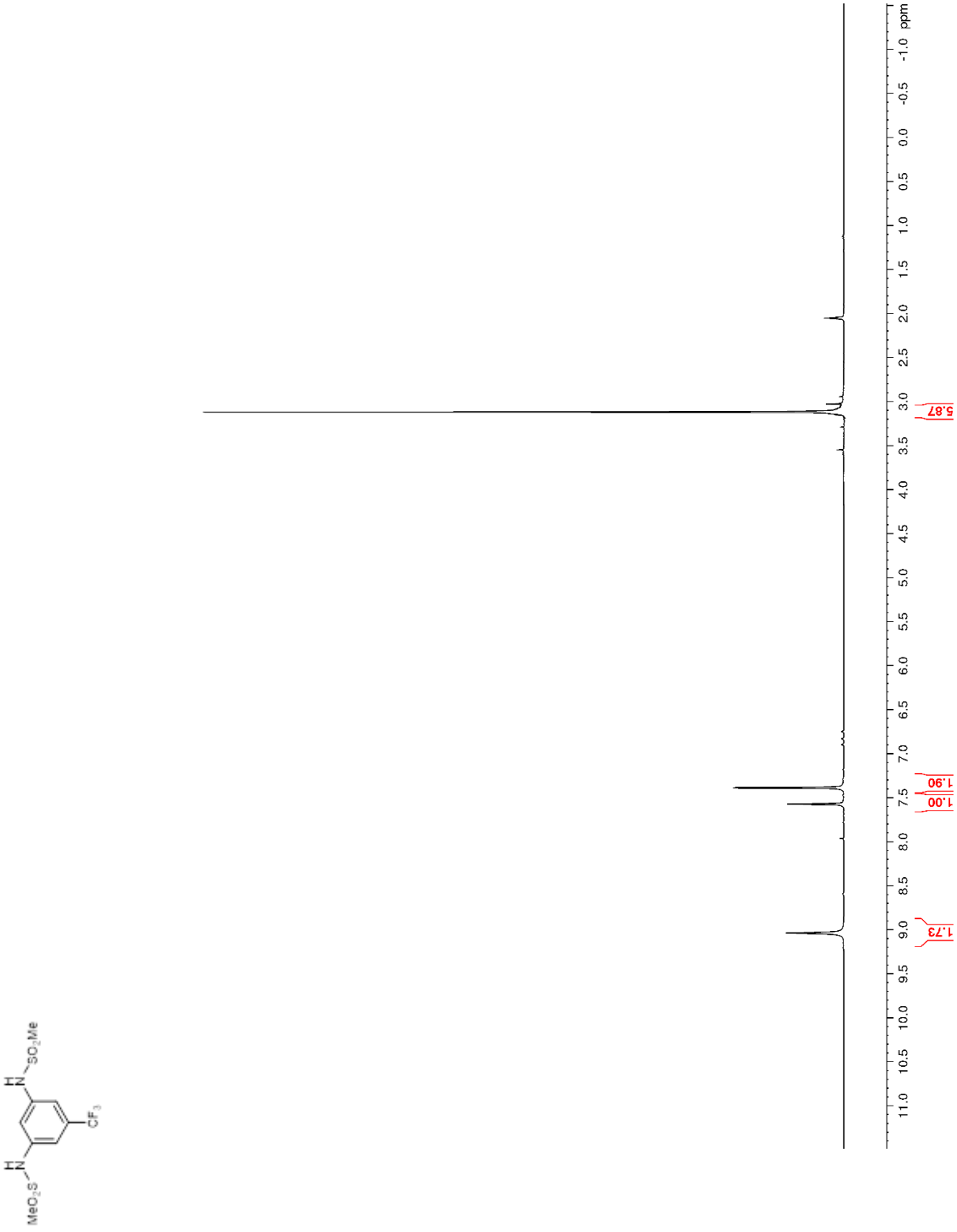

Figure 92. ^{13}C NMR (**150 MHz,** $(CD_3)_2CO$) of **207**

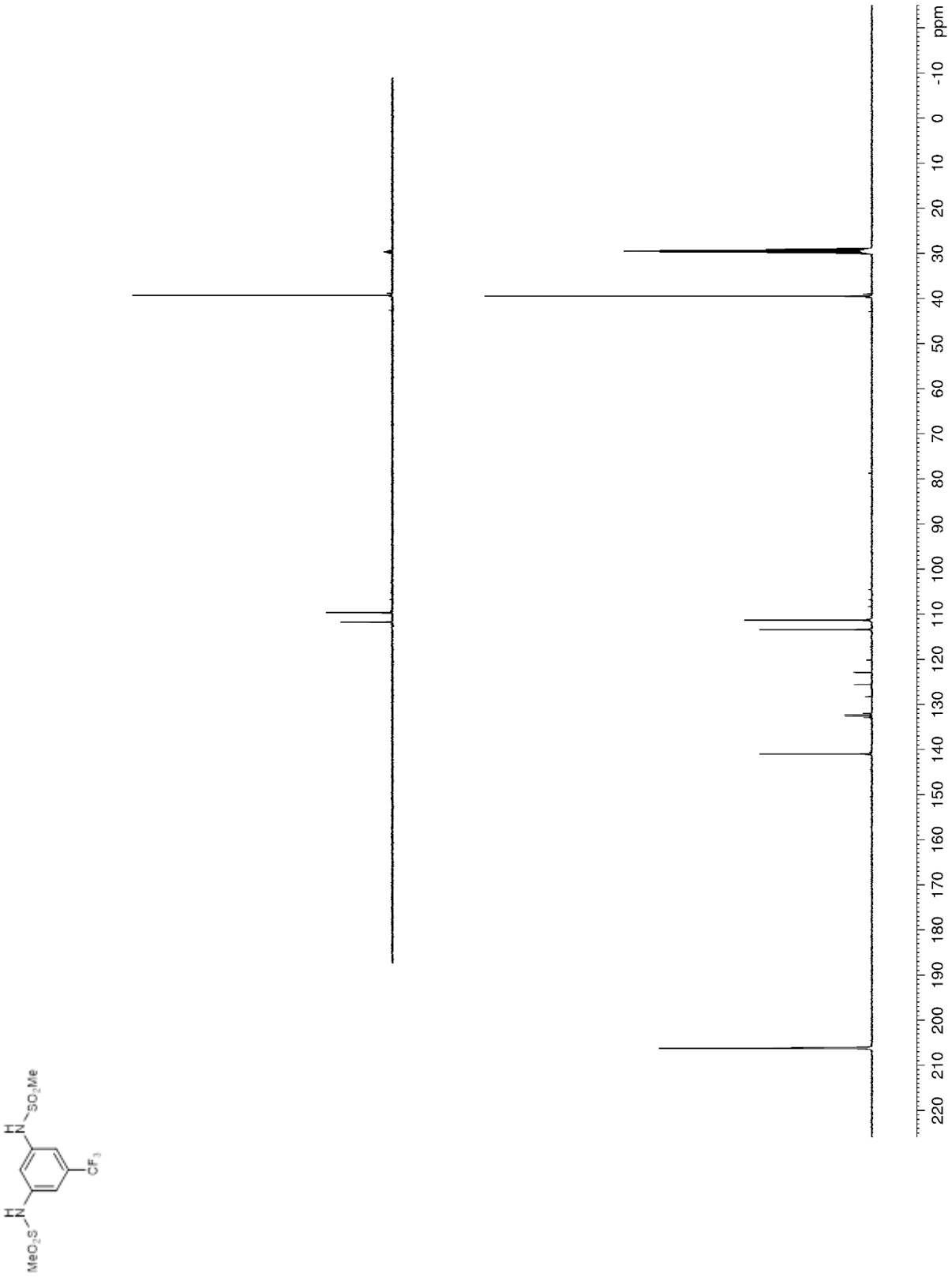

Figure 93. ^{19}F NMR (282 MHz, $(CD_3)_2CO$) of **207**

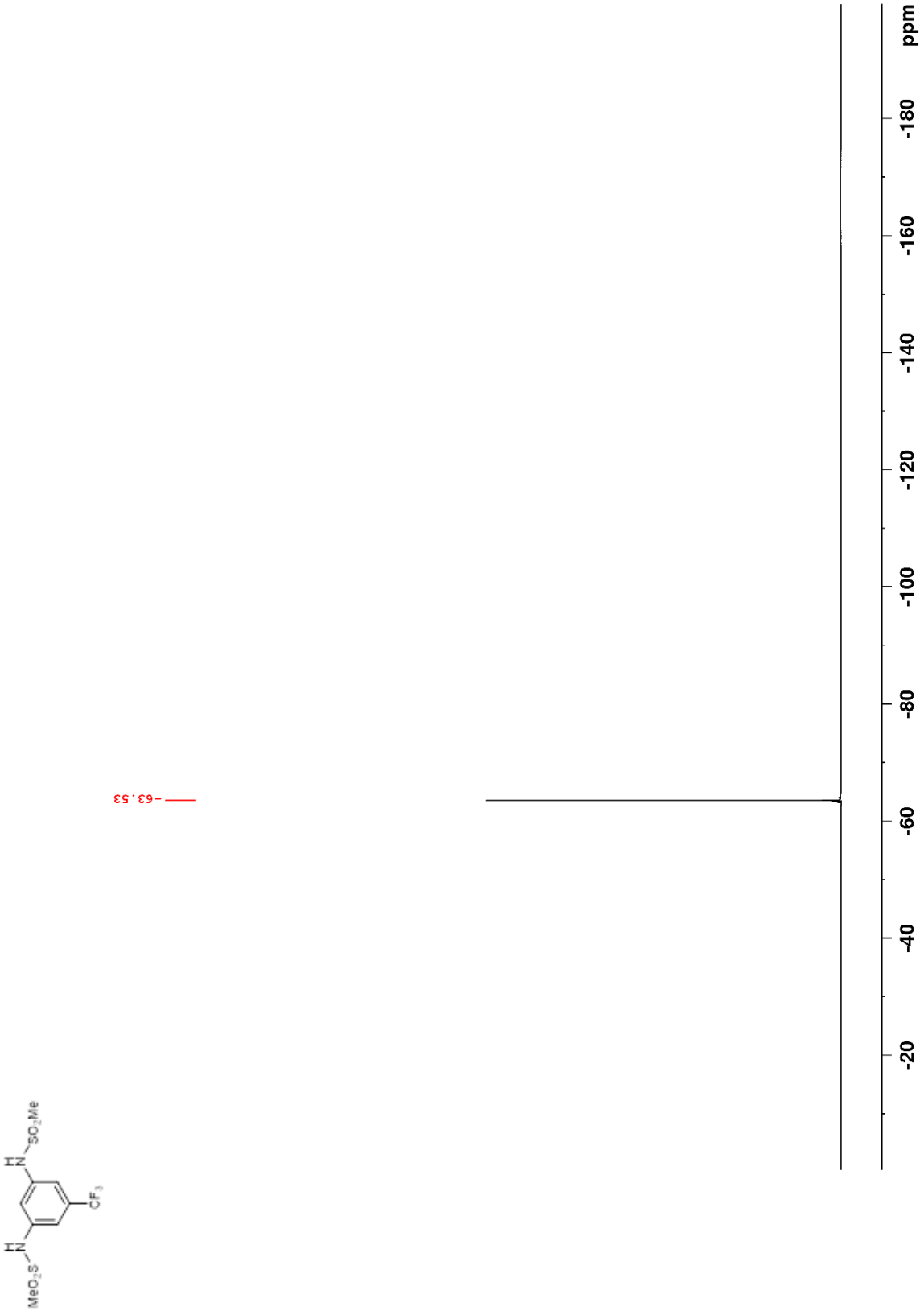

Figure 94. ^{1}H NMR (400 MHz, ($CDCl_3$) of **S10**

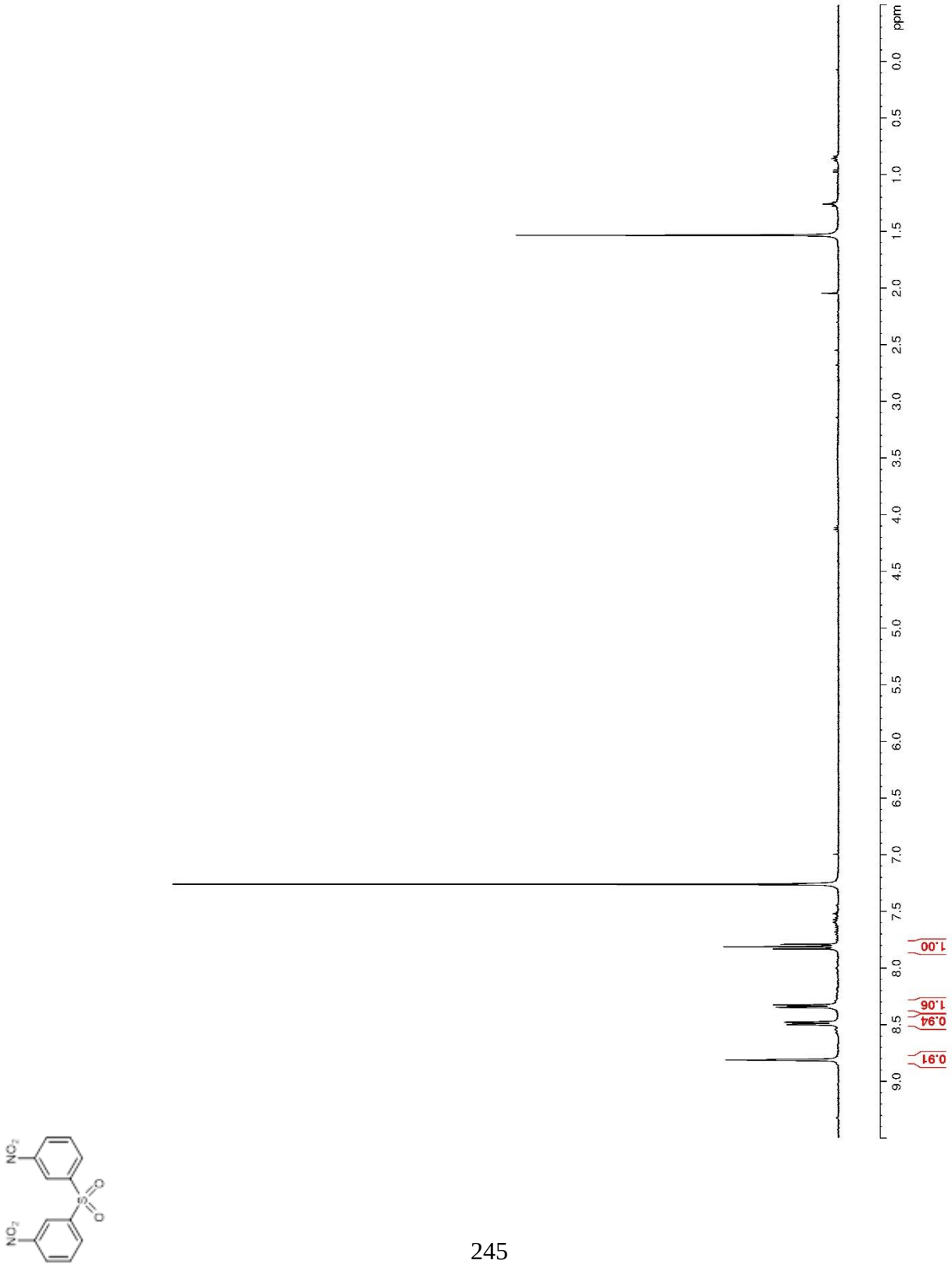

Figure 95. ^{13}C NMR (100 MHz, $(CD_3)_2CO$) of **S10**

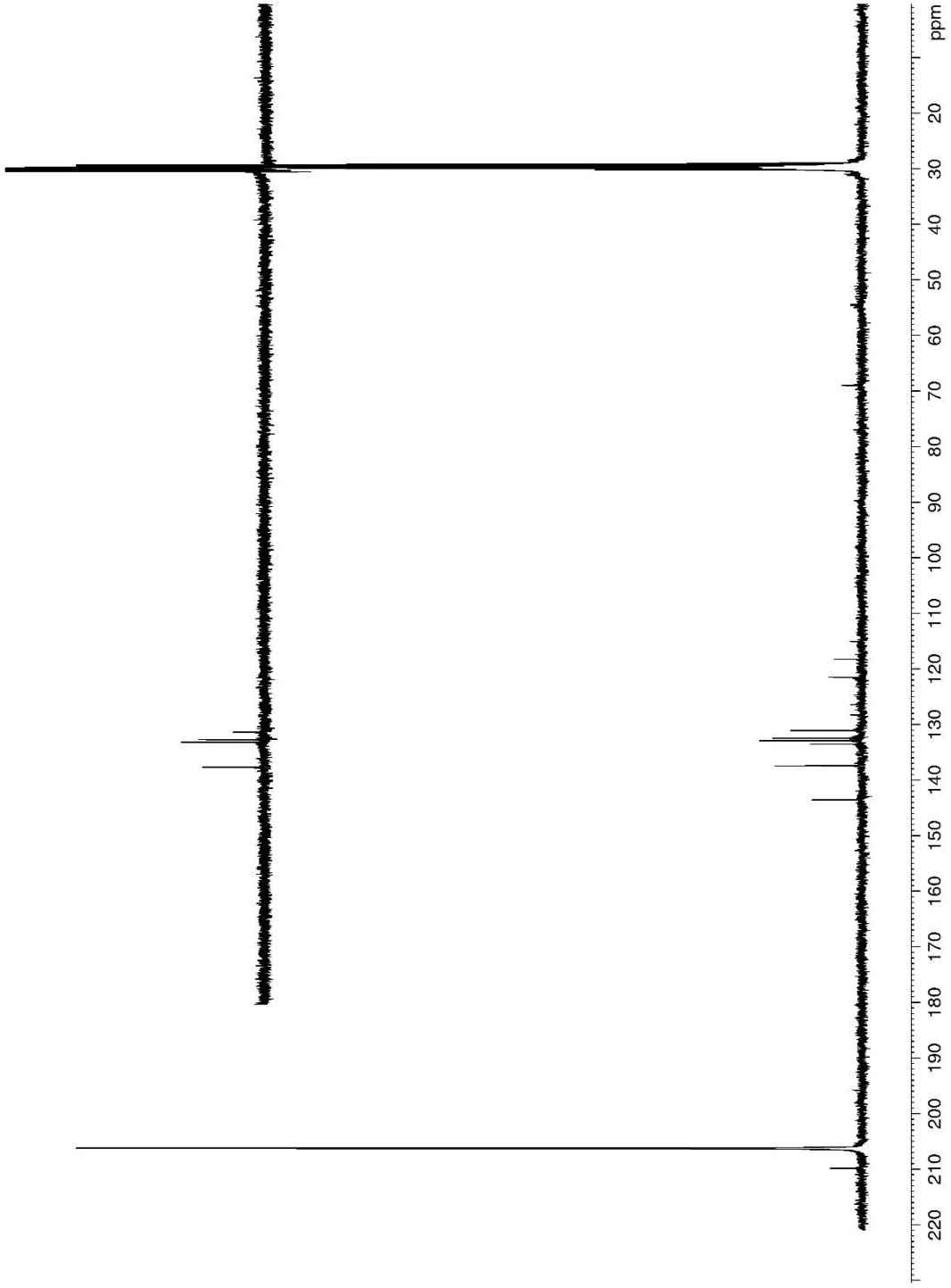

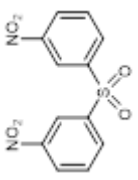

Figure 96. ^{1}H NMR (400 MHz, $CDCl_3$) of **236**

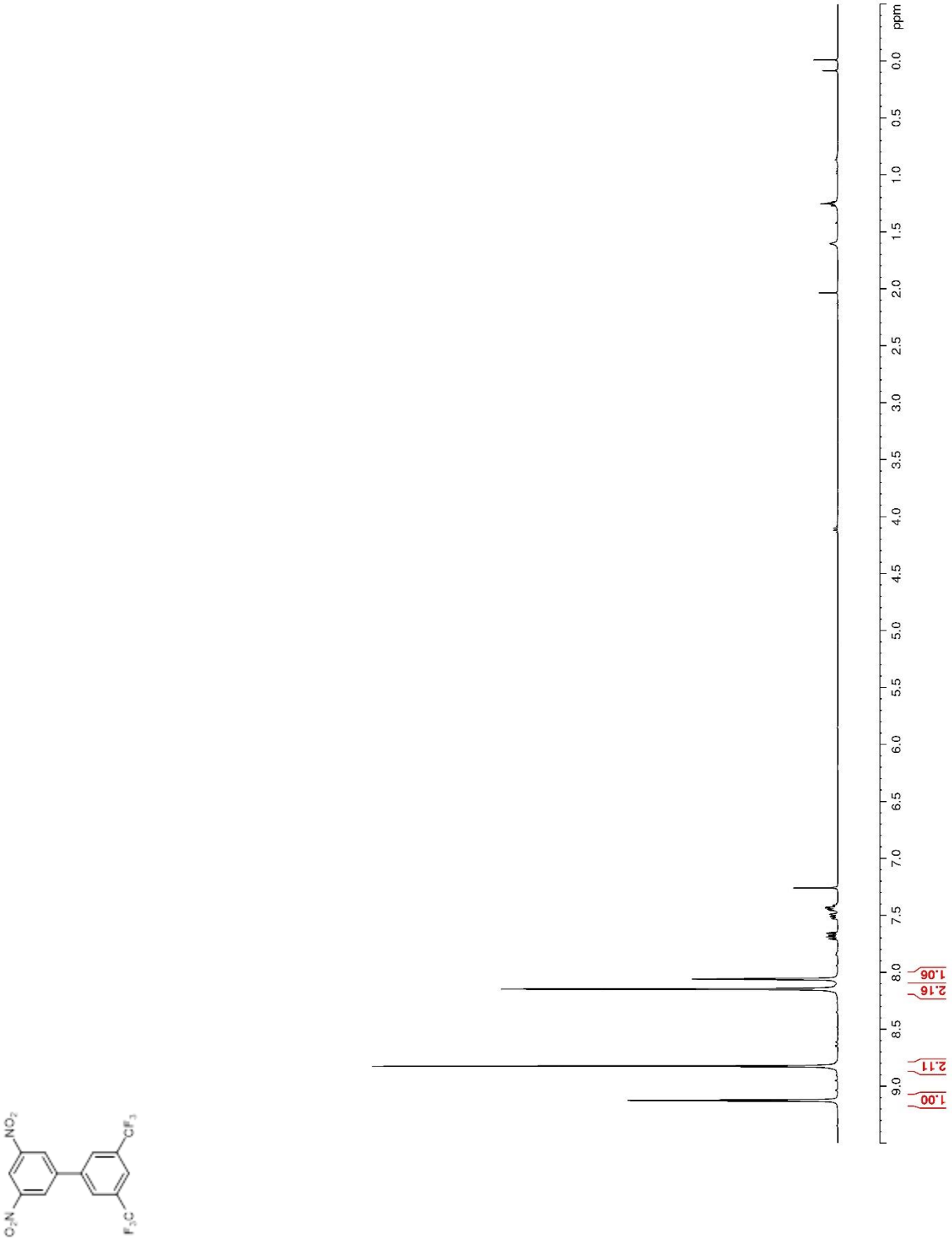

Figure 97. ^{13}C NMR (100 MHz, $CDCl_3$) of **236**

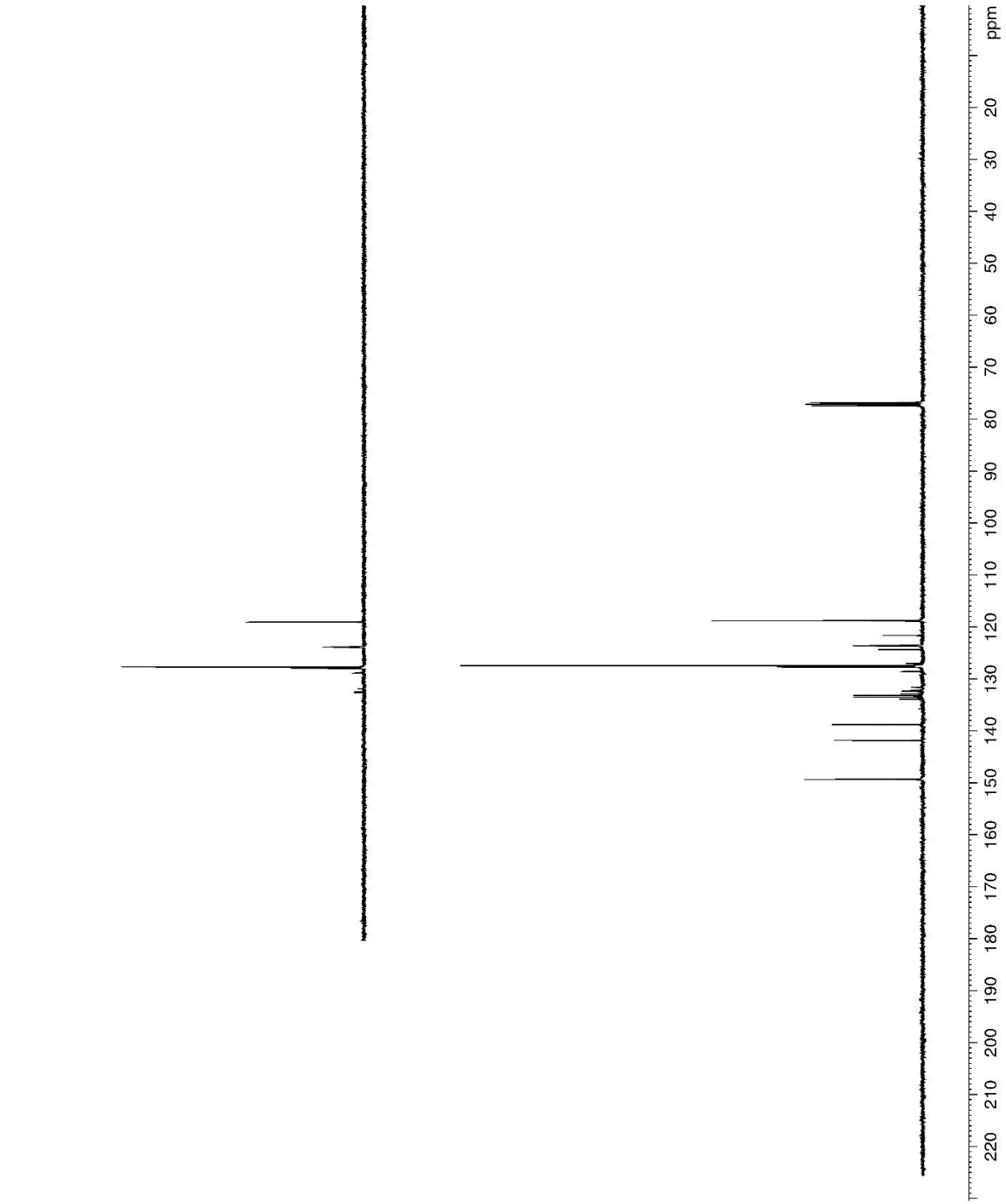

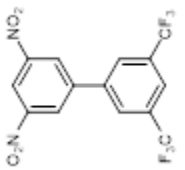

Figure 98. ^{19}F NMR (282 MHz, $CDCl_3$) of **236**

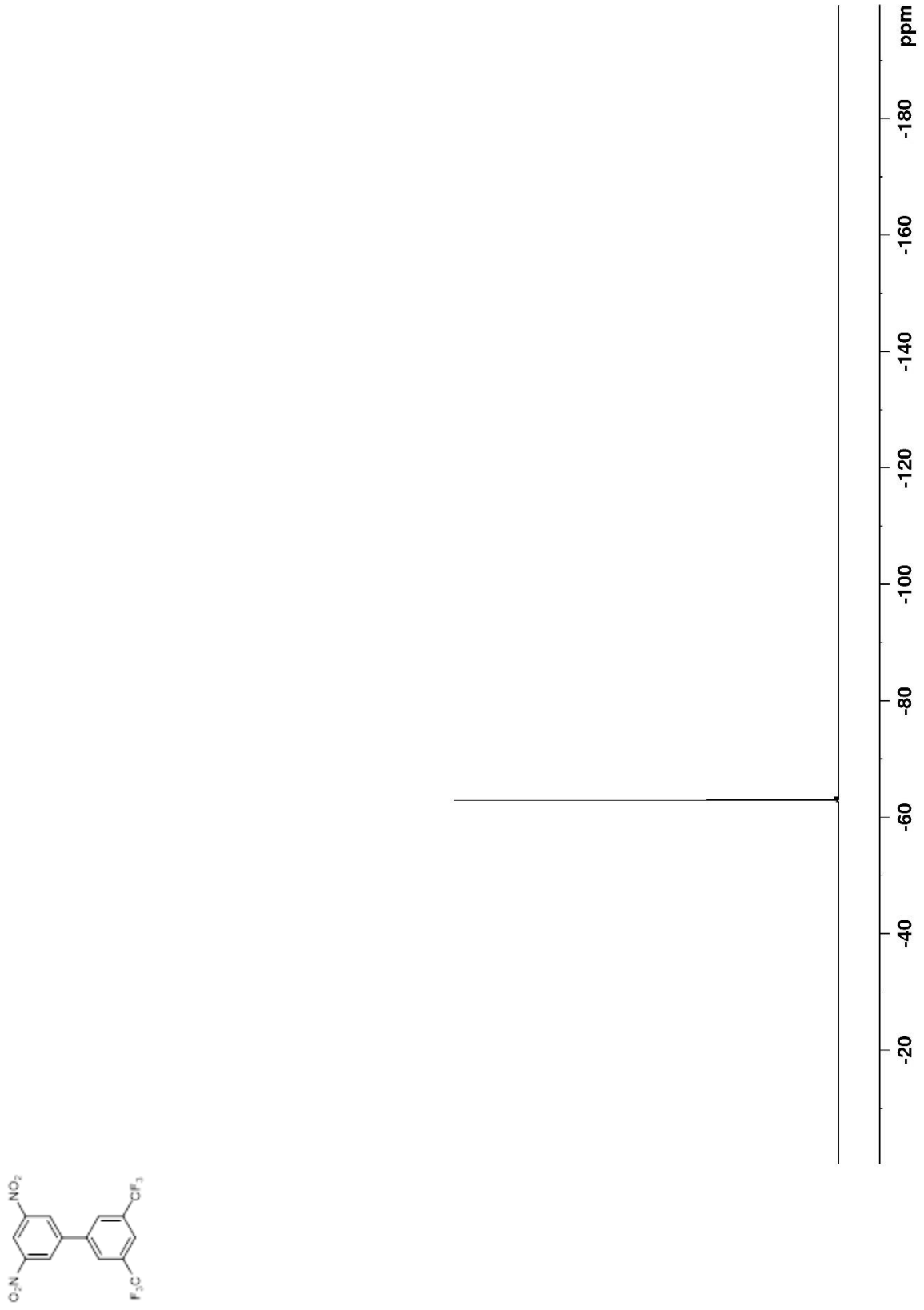

Figure 99. ^{1}H NMR (400 MHz, $CDCl_3$) of **283a**

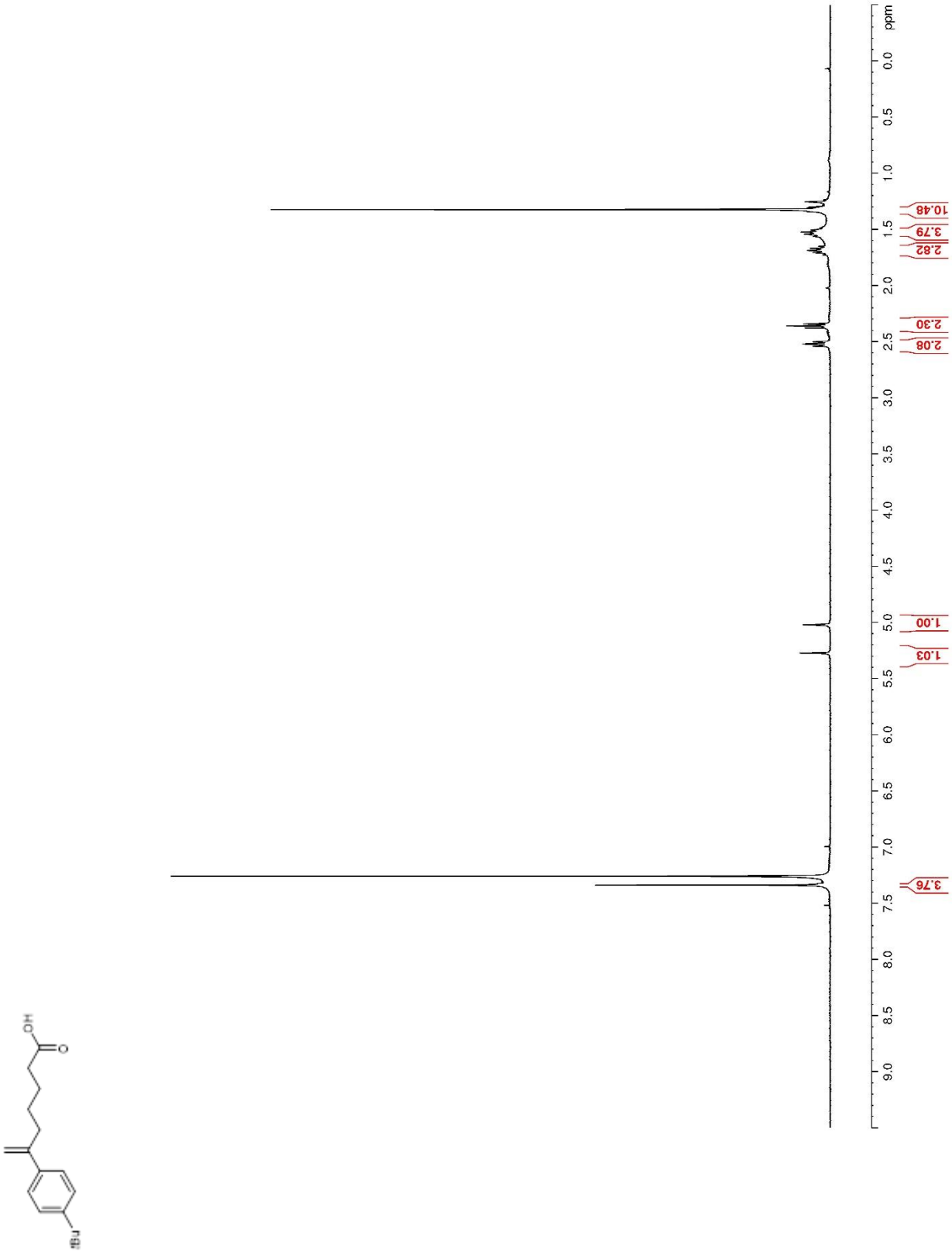

Figure 100. ^{13}C NMR (150 MHz, $CDCl_3$) of **283a**

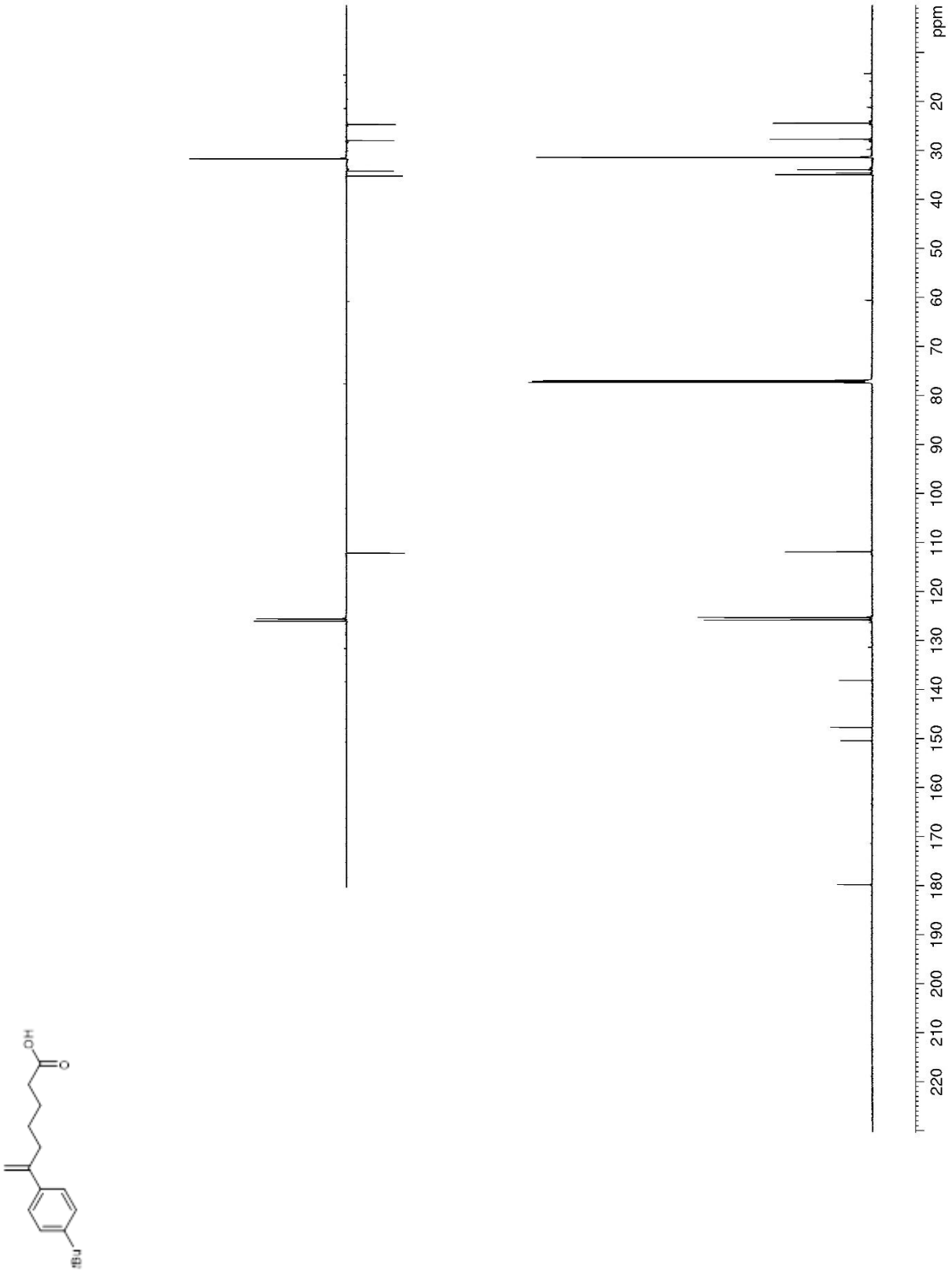

Figure 101. ^{1}H NMR (400 MHz, $CDCl_3$) of **282a**

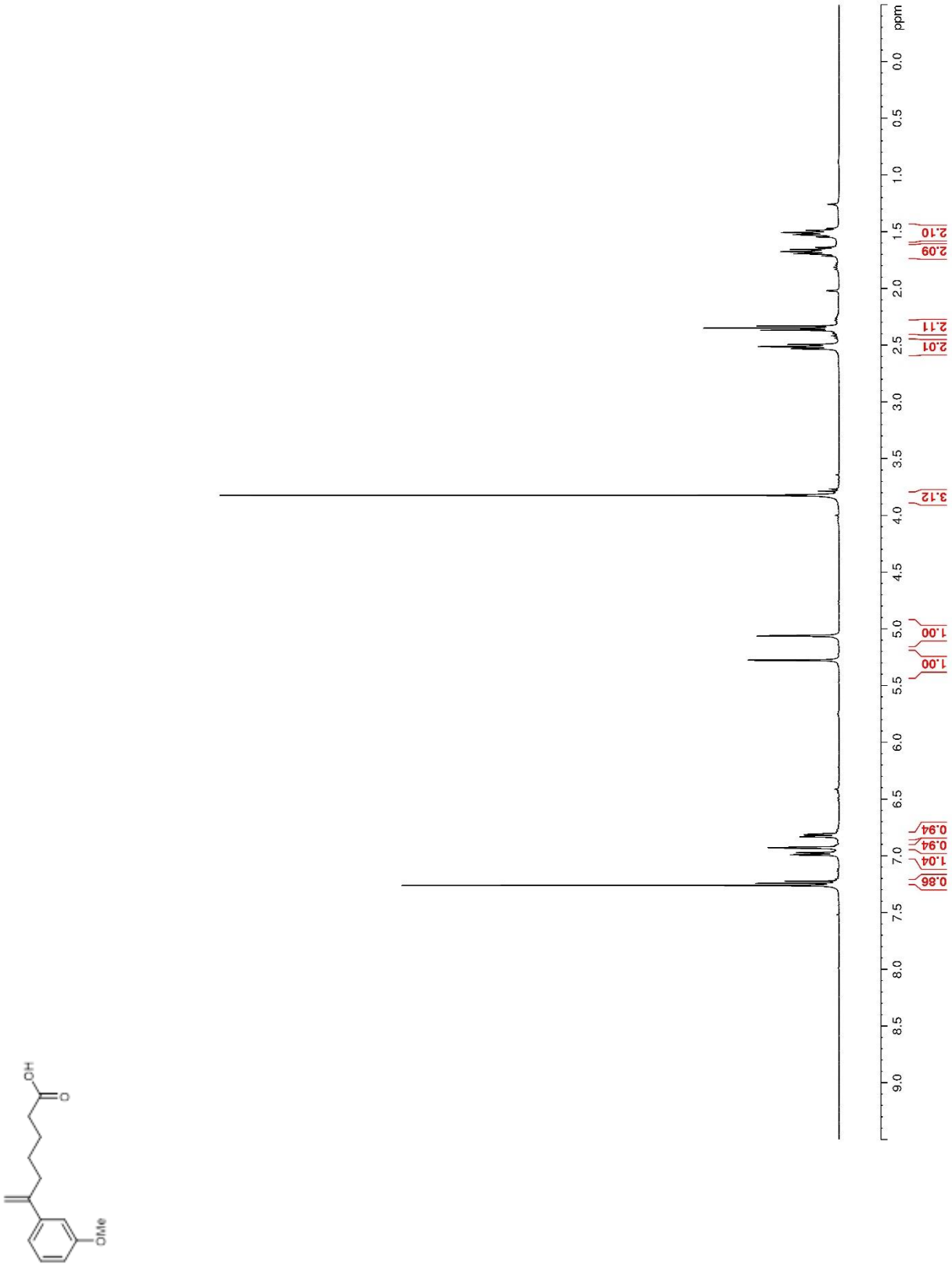

Figure 102. ^{13}C NMR (150 MHz, $CDCl_3$) of **282a**

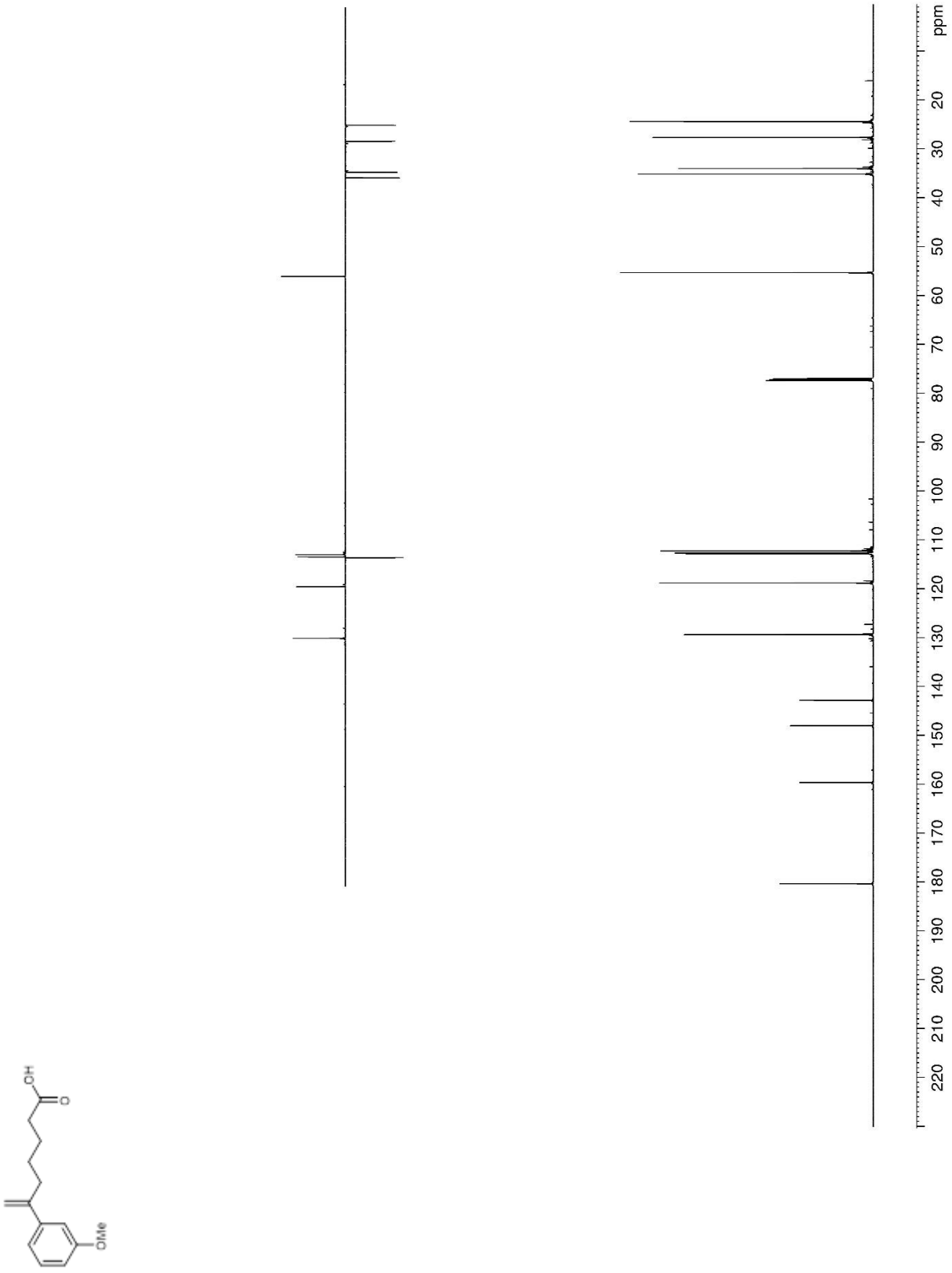

Figure 103. ^{1}H NMR (400 MHz**,** $CDCl_3$) of **277a**

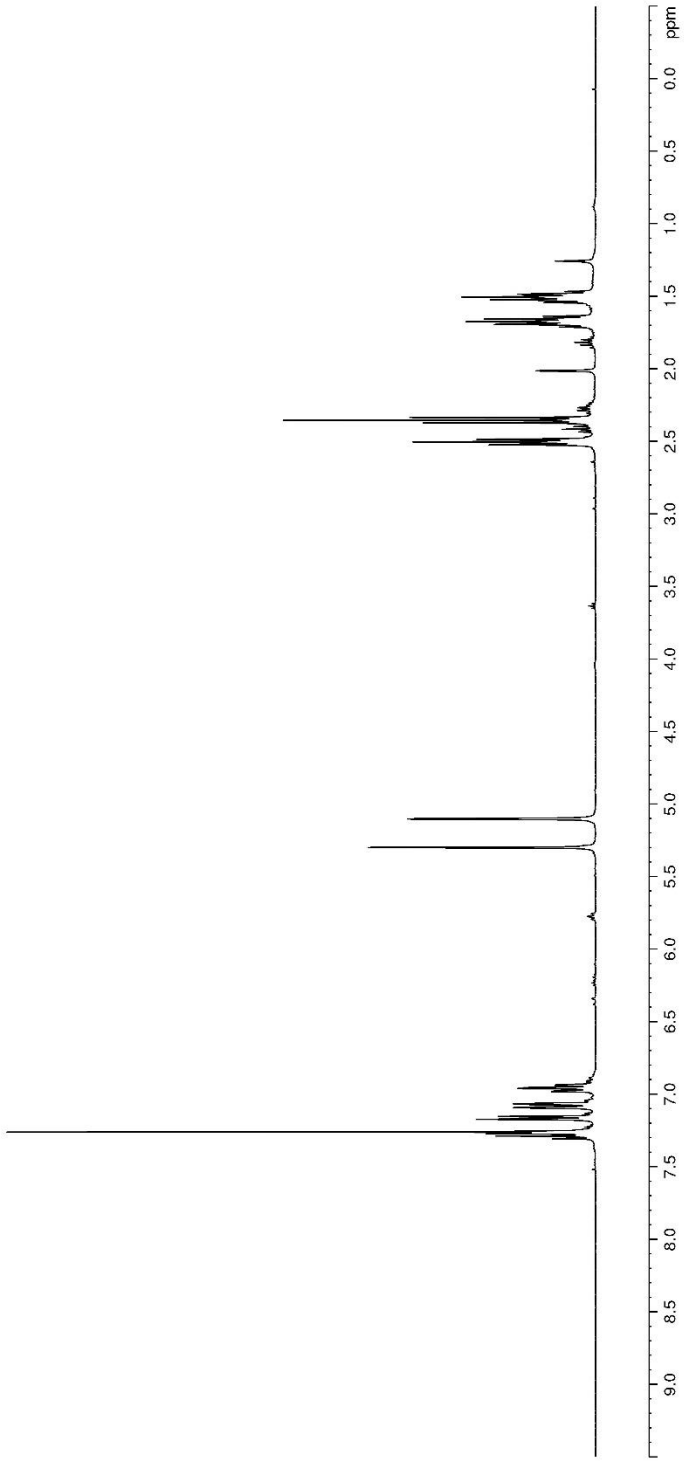

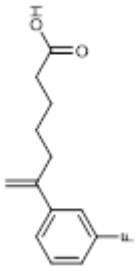

Figure 104. ^{13}C NMR (150 MHz**,** $CDCl_3$) of **277a**

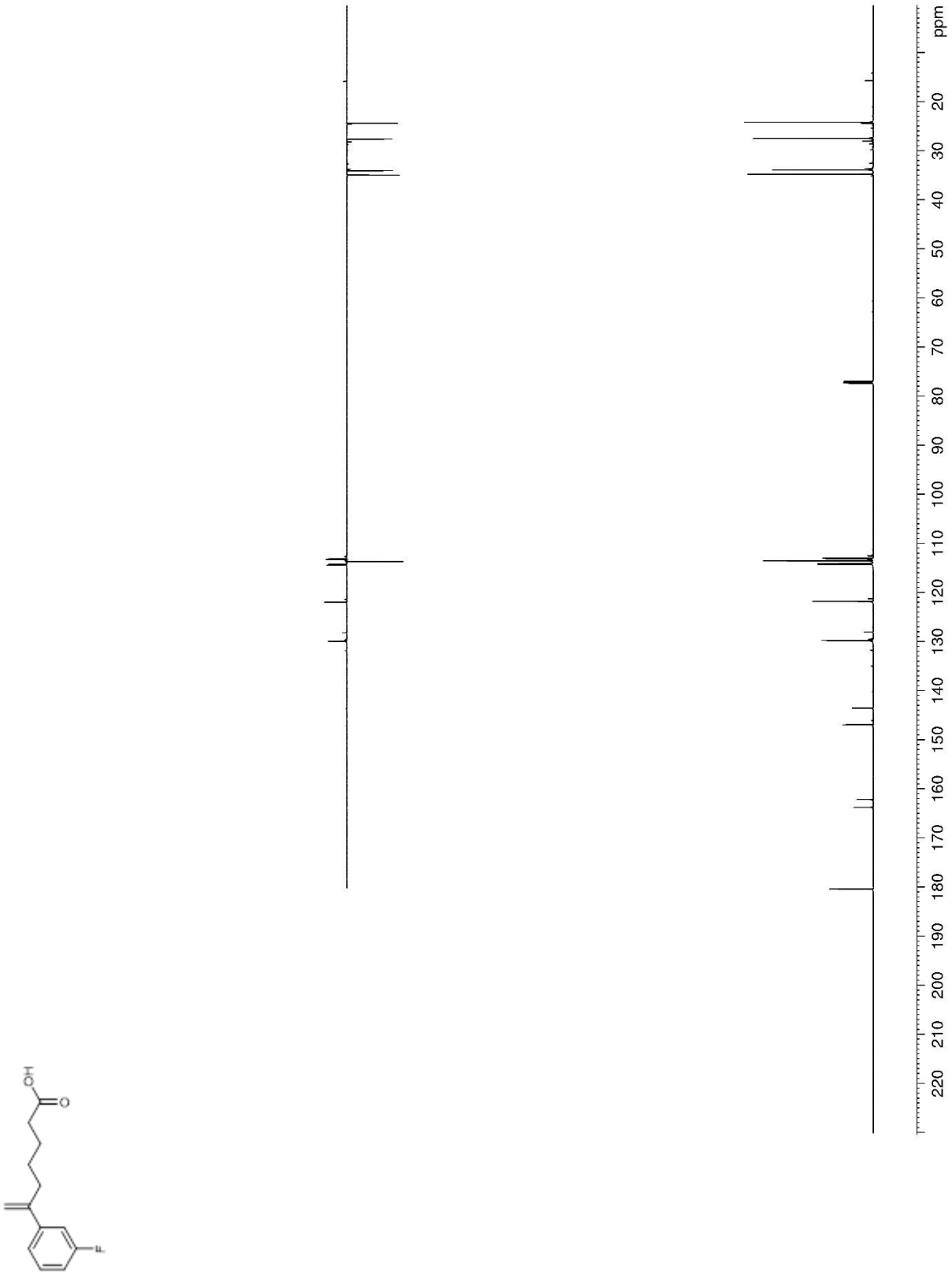

Figure 105. ^{19}F NMR (282 MHz, $CDCl_3$) of **277a**

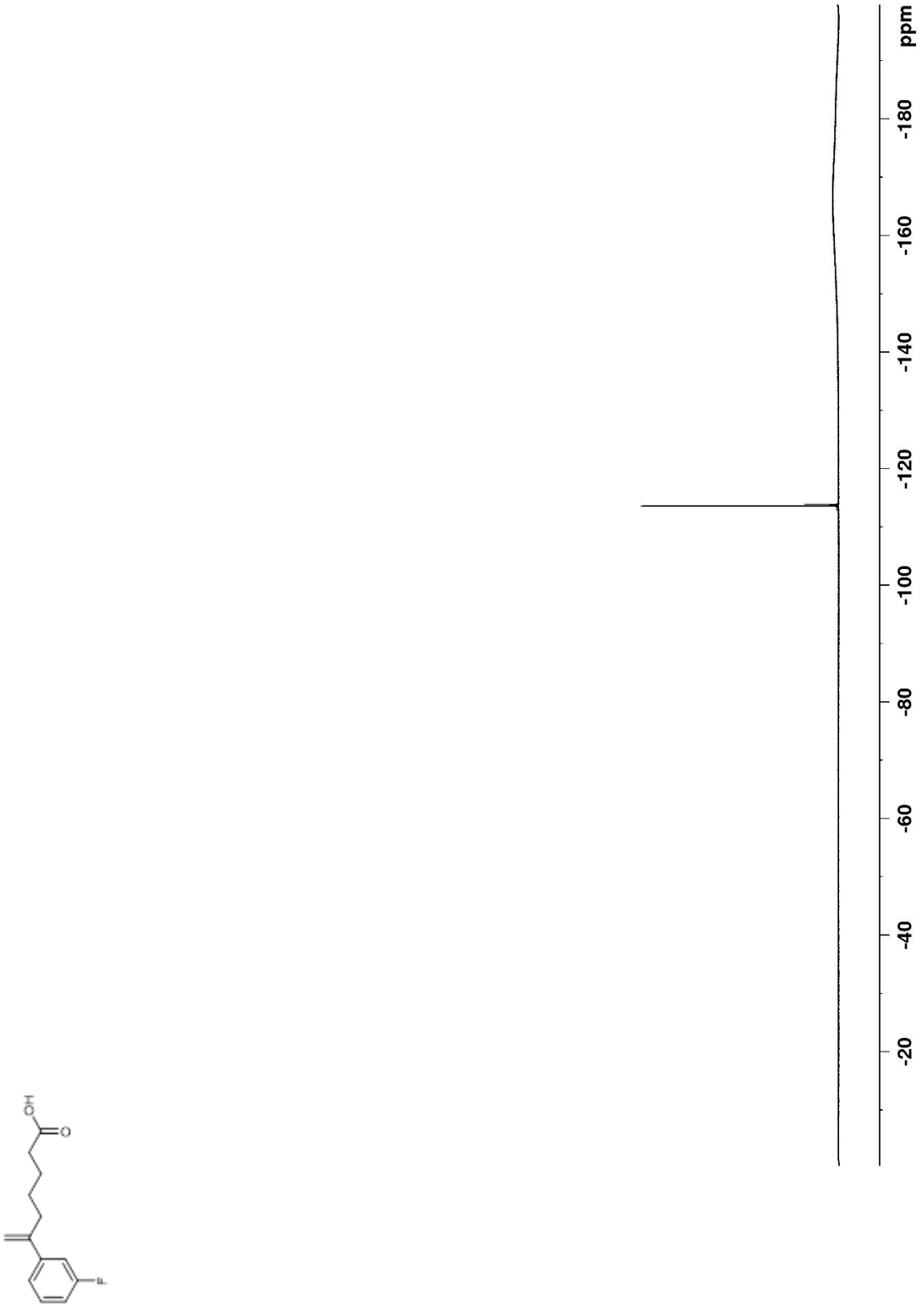

Figure 106. ^{1}H NMR (400 MHz, $CDCl_3$) of **279a**

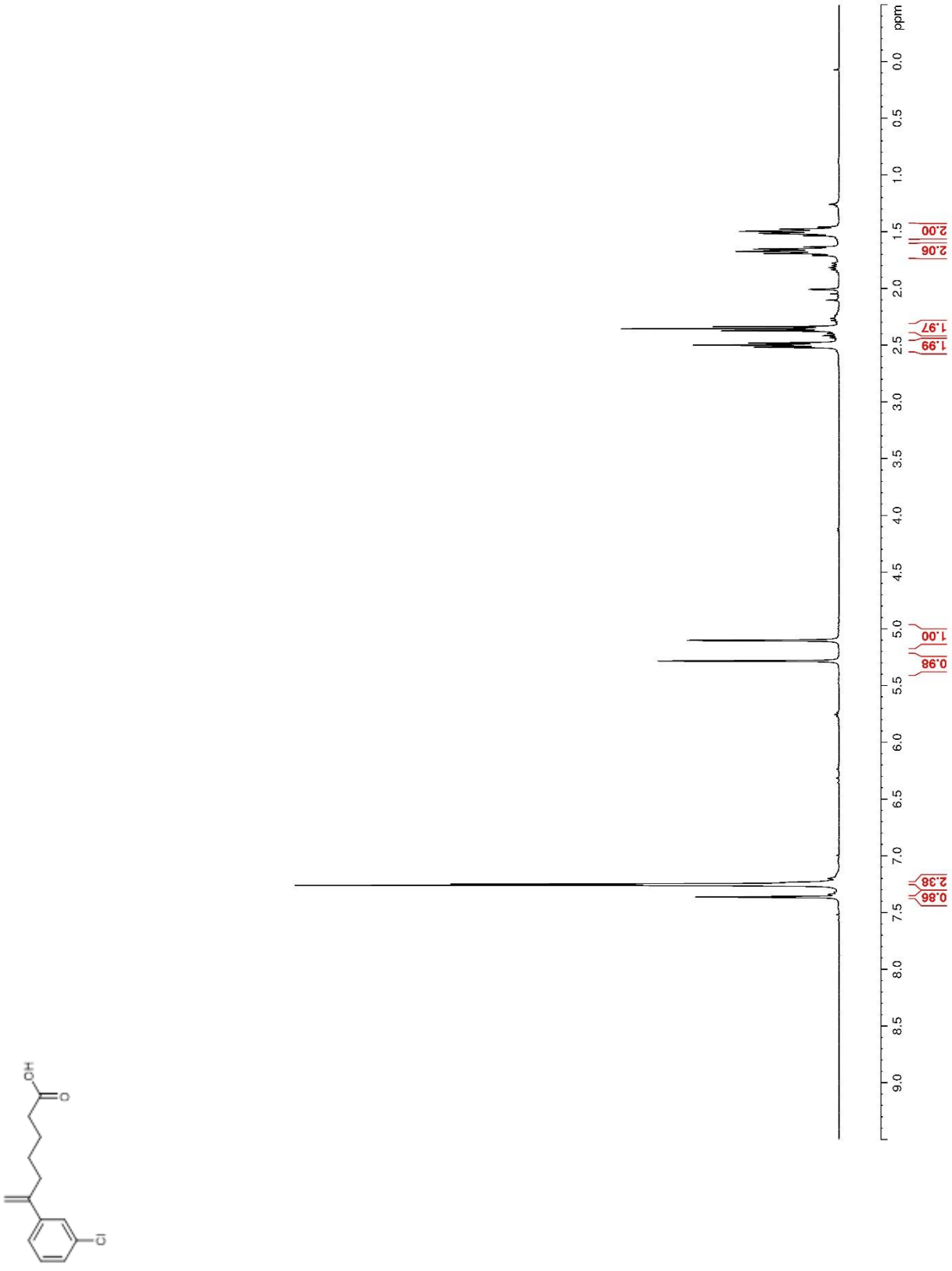

Figure 107. ^{13}C NMR (150 MHz, $CDCl_3$) of **279a**